Acoustic Diffusion and Scattering Coefficients for Room Surfaces

Tristan John Hargreaves

Telford Research Institute

Department of Acoustics and Audio Engineering

University of Salford, Salford, UK

Submitted in partial fulfilment of the requirements of the Degree of Doctor of Philosophy, August 2000

TABLE OF CONTENTS

LIST OF FIGURES

LIST OF TABLES

ACKNOWLEDGMENTS

The research presented in this thesis would not have been possible without the assistance of the following craftsmen:

David Stevens

Lionel Bailey

Joe Riley

Thankyou very much gentlemen, I hope you enjoyed it as much as I did!

In addition to my supervisor, Dr Trevor Cox, I would also like to thank:

Dr Peter D'Antonio and all the staff at RPG.

Vanessa - you can have your spare room back now.

My parents - I'll get a proper job now.

Christine at Multimetals.

Julie Gerrard at British Vita.

Michael Bolger at Altair Engineering.

Everyone at the University who has helped me over the years, especially Geoff, Roger and John. And no thanks to those who didn't.

ABSTRACT

This project concerns quantifying the diffuseness of sound reflections from surfaces by means of a diffusion coefficient. Although it is now acknowledged that diffuse reflections are important in determining sound fields within rooms, no standardised diffusion coefficient currently exists. Definition of a universal coefficient would permit comparison of different surfaces and aid the understanding of diffusion. It would also benefit diffuser designers and room acoustic computer modellers. Previously proposed diffusion parameters for room surfaces are investigated and new ones developed.

One approach is to parameterise the uniformity of the scattered energy measured as a polar response; a number of such parameters have been previously published. These are appraised using measured and predicted 2D and 3D polar responses for a diverse range of sample surfaces. The situations in which the parameters succeed and fail are discussed and it is demonstrated that none is ideal. A new polar response coefficient, superior to those previously published, is presented. This satisfies many criteria of the ideal diffusion measure and is likely to be standardised by the Audio Engineering Society. It is shown that the application of all polar response diffusion parameters is, however, limited.

Two recently proposed alternative approaches to evaluating a scattering coefficient, which involve measuring the invariance of the energy reflected from a surface to its orientation, are discussed. One of these is a free field technique and the other requires reverberant conditions. Practical analysis shows that the reverberation chamber method is superior. It is likely to be standardised by ISO.

An empirical reverberation chamber technique is also investigated, as is the possibility of quantifying the diffusion efficacy of surfaces from their effect on sound field diffuseness. Both of these approaches require further research.

It is concluded that to provide maximum benefit, the choice of diffusion coefficient is application dependent.

1 INTRODUCTION.

1.1 Why is a measure for quantifying diffusion required?

Diffuse reflections can play a key role in determining the sound field within an enclosed space, what is often referred to as the 'acoustic'. The principal objective of the research presented in this thesis was to develop a parameter which quantifies the efficacy of room surfaces in diffusing the sound energy they reflect.

In simple room acoustics it is often assumed that Snell's law applies and reflections are specular, i.e. the angle of incidence equals the angle of reflection. In practice however, a proportion of the reflected energy is scattered into directions other than the specular and this proportion can be large, particularly if the wavelength of the sound is similar to a dimension of the reflecting surface. This scattering of the reflected energy into a multitude of directions is diffusion.

Diffusion is of particular importance in acoustically critical spaces designed for quality music or clear speech such as concert halls, lecture theatres and underground stations. For many years, interest in the role of diffusion, particularly in auditoria, listening rooms and studios, has been increasing and it has recently been shown that its correct use in performance spaces may enhance the acoustic for both the audience and musicians[1].

Although the importance of diffusion from surfaces is now generally acknowledged, no standard or accepted parameter for quantifying it currently exists.

Without a numerical measure of the degree of diffusion, it is difficult to compare the performance of different architectural surfaces or develop design specifications for specialist diffusers. Furthermore, it is hoped that a diffusion parameter will improve the understanding of diffuse reflection phenomena among practitioners in both the acoustics and building industries and contribute to the future design and construction of rooms with better acoustics.

One tool for assisting with the acoustic design of rooms which has been developed extensively over the past few years are computer-based geometric room acoustic prediction models. Such models are still being refined and a recent round-robin test[2] showed that the common feature of those which gave the most accurate sound field predictions was the inclusion of some form of diffusion modelling. Diffusion is usually implemented in these prediction models by assigning to each surface some value quantifying their diffusion efficacy. The problem is that at present these values have to be chosen empirically[3] because there are no clear relationships between the physical properties of a surface and the diffusion coefficients adopted by the models. For this reason, a diffusion coefficient which could readily be measured or predicted for any surface would also be of great interest to developers of geometric room acoustic prediction models.

1.2 Properties of the ideal diffusion coefficient.

In order to appraise the various existing diffusion coefficients found in literature and develop superior ones, it was necessary to have a set of criteria against which coefficients could be evaluated. At the outset of this research it was therefore decided that the ideal diffusion coefficient would:

- Have a solid physical foundation, be clear in definition and concept, and related to the current role of diffusion in room acoustics.

The coefficient should be defined in such a manner that values of it are not just of academic interest but practically useful to the acoustic community.

- Consistently evaluate and rank diffusion efficacy.

If the definition of the coefficient is flawed then it will fail in certain circumstances; its value will not correctly indicate the diffusion efficacy of the surface. Establishing whether or not a coefficient is flawed requires a combination of philosophical thought experiments and the calculation of coefficient values for a wide variety of surfaces.

- Be bounded.

The coefficient should be bounded, preferably between zero and unity, by the conceptual limiting cases of no diffusion and total diffusion. The physical realisation of these limits depends on the definition of the coefficient but no diffusion usually corresponds to the reflection being purely specular.

In addition, practical values of the coefficient should ideally be spread over its entire range; effective diffusers should have values close to unity and poor ones values close to zero.

- Apply to all of the different geometries of surfaces encountered in rooms.

Room surfaces to which diffusion coefficient values may need to be assigned can be divided into three loose categories:

- Isolated articles in free space, such as suspended diffusers/reflectors and some structural pillars.

- Large rough surfaces, such as walls covered with relief decoration, coffered ceilings and the audience.

- Articles mounted on or recessed into a large plane surface, such as sculptured areas and half-pillars on otherwise flat walls.

- Be straightforward to measure and predict.

In order for a diffusion coefficient to be accepted by the wider acoustic community, its value must be obtainable by a simple procedure. If it is not, or is perceived to be not, then practitioners may judge that the difficulties of obtaining the coefficient value for a surface outweigh the benefits of knowing it. Therefore if possible, the coefficient should be measurable using standard facilities and predictable using established, validated methods.

These criteria are strict constraints and therefore difficult to satisfy. If analogous criteria were formulated for the ideal absorption coefficient then Sabine's coefficient, the principal measure of absorption used throughout the 20th century, would fall a long way short of satisfying them.

1.3 Introduction to diffusion measurement.

A variety of methods for quantifying the diffusion efficacy of surfaces have been proposed in the last few years, the reason for this diversity of approaches is that there are many ways of describing how diffusers behave. However, every one of these methods can be classified as belonging to one of two groups, depending upon the conditions in which the measurement is performed: free field or reverberation chamber.

The free field methods can be laborious if the diffusion coefficient for more than a single angle of sound incidence is required because they generally require a large number of individual measurements to be made but they are straightforward to predict. The reverberation chamber methods, on the other hand, yield a random incidence diffusion coefficient value directly but prediction is difficult.

There exists an analogy here with the absorption coefficient. The two standard techniques for measuring the absorption coefficient of a material are the impedance tube[4,5] and reverberation room[6]. The former enables the absorption coefficient at a particular angle of incidence to be obtained, a quantity which can in fact be calculated if certain physical properties of the material are known. The result of the reverberation chamber method is a random incidence absorption coefficient which cannot easily be predicted. Which value is the more useful depends upon the application to which the absorbent material is being put. It seems also that the appropriate method for measuring the diffusion coefficient is application dependent also.

1.4 Free field methods for quantifying diffusion.

The most popular current approach to quantifying diffusion, if this is measured by the number of publications referring to it, is to examine the polar response, the spatial distribution of the reflected energy. Just as the polar response of a loudspeaker shows how directional it is, so the polar response of a surface shows how much of the reflected energy is scattered into different directions. For reasons of simplicity, most of the literature refers to scattering in only a single plane as opposed to three dimensions. Various methods for condensing this data into a diffusion coefficient have been suggested but many of these exhibit only subtle differences and therefore most of them can be classified as being based on one of three concepts: standard deviation[7-13], directivity[14,15] and specular zone[16].

To appraise these coefficients, polar responses of a wide variety of surfaces were required and previous work has used both measurement and prediction to produce these. Cox and Lam[17-19] have shown that accurate predictions of single-plane scattering can be made using boundary element methods (BEM) but measured data should also be used. An established facility[11] for measuring single-plane scattering exists at RPG Diffusor Systems Inc. in Maryland, USA and an overview of this system is given in Section 2.4. RPG Diffusor Systems Inc. collaborated with the University of Salford on this research, a major aspect of the collaboration being the measurement of numerous polar responses.

Standard deviation type diffusion coefficients are reviewed in Section 3.4, their foundation is the standard deviation of the sound pressure level (SPL) polar response. The standard deviation of the scattered energy has also been used to quantify diffusion, the resulting parameters are very similar to the directivity type diffusion coefficients discussed in Section 3.5. These compare the fraction of the total scattered energy at each measurement point to the reciprocal of the number of measurement directions. Both standard deviation and directivity type diffusion coefficients implicitly assume that complete diffusion equates to a uniform polar response. This is not necessarily the case and the concept of complete diffusion is addressed in Section 3.2. Section 3.6 examines specular zone type diffusion

coefficients which quantify diffusion from the proportion of the reflected energy scattered in non-specular directions.

One original aim of this research was to investigate whether these existing methods could be extended from single-plane diffusion to three dimensions. To accomplish this, three-dimensional polar responses of surfaces showing how the reflected energy is scattered into half-space were required. These can be predicted without undue difficulty using BEM as detailed in Section 2.5 but understandably take longer than single-plane predictions. To accurately measure half-space polar responses in an acceptably short length of time is a challenging task and required the design and construction of a new specialist system, described in Section 2.9. Not only is the measurement and prediction of half-space polar responses more complex and time consuming but there are additional factors to consider as explained in Section 3.11.

The only published method specifically for quantifying diffusion from the three-dimensional polar response is that proposed by Angus[20] which utilises surface spherical harmonics. This does not require measurement of the entire polar response and is discussed in Section 3.7.

Although using the polar response to quantify diffusion is a popular suggestion, analysis of the published coefficients reveals that they all fall short of the ideal. However, the philosophy is valid and this body of work provided a foundation for new research with the aim of devising a better diffusion coefficient of this type.

Some possibilities for new diffusion coefficients which were investigated during this research but dismissed are outlined in Section 3.8. One particular measure which expresses the percentage of directions into which most of the reflected energy is scattered is discussed more thoroughly because it appeared to have fewer failings than other parameters. However, although this measure is derived from a cogent concept, rigorous testing using practical polar responses revealed that in a few circumstances it fails to evaluate diffusion correctly.

In Section 3.9, a novel diffusion coefficient developed during the research which is superior to current polar response parameters because it satisfies more of the ideal criteria is described and its advantages and limitations are discussed. This measure has its origins in the autocorrelation function and is likely to be standardised by the Audio Engineering Society[21].

Reducing the polar response of a surface to a single figure of merit is not the only published free field method for quantifying scattering, another is that suggested by Mommertz and Vorländer[22] which is considered in Chapter 4. This method gauges diffusion from the invariance of the scattered pressure measured at the specular reflection position to movement of the surface. Various aspects of this method were investigated in detail. To assist with the appraisal, measurements and/or predictions of the diffusion efficacy of several different surfaces were performed using this method and the results compared to their polar response parameter values.

For all of these free field methods, the value of the diffusion coefficient is dependent upon the distances of the source and receivers from the sample surface unless they are situated in the far field. As discussed in Sections 2.7 and 2.8, this causes problems with measurements unless either the sample is small, for example an individual reflector, or scale model techniques are employed because the size of the measurement facility required becomes unfeasibly large.

1.5 Reverberation chamber methods for quantifying diffusion.

Reverberation chamber methods for quantifying diffusion do not suffer from the problem outlined above and several have been suggested in literature[22-24] although none is in common use.

The most widely known reverberation chamber method for quantifying diffusion is that suggested by Mommertz and Vorländer[22] which is described and evaluated in Chapter 5. This shares conceptual similarities with their free field approach but requires instead diffuse field conditions and involves examining the invariance of

the impulse response to movement of the surface to determine its random incidence scattering coefficient. Various aspects of the procedure have been practically investigated and it has been used to measure the diffusion efficacy of several surfaces to enable comparison with other methods. Evaluation of this method was particularly important because it will probably be incorporated into an ISO standard[25].

A second reverberation chamber technique for quantifying diffusion is that proposed by Lam and Pantelides[23] which is discussed in Chapter 6. This method examines how the replacement of a plane boundary with the sample surface changes the reverberation time of a non-diffuse space; a reverberation chamber with one absorptive wall. A geometric room acoustic computer model of the space is constructed and random incidence absorption and diffusion coefficients are assigned to each surface. The diffusion coefficient of the sample surface is determined empirically by adjusting its value in the model until the predicted reverberation time is the same as that measured. To evaluate this method, measurements of several surfaces at approximately 1:2 scale were made using a real reverberation chamber, the first time that this has been done as previous work was confined to 1:50 scale models.

A variation on Lam's method is suggested in Chapter 7. This determines the diffusion coefficient of the sample surface not by comparing the measured reverberation time with that predicted by a computer model but by ascertaining where it lies in the range between the maximum and minimum practically achievable values.

Other methods for quantifying the diffusion efficacy of a surface by measuring its effect on certain parameters of a non-diffuse space are also described in Chapter 7. These involve examination of the changes in: the spatial variation of reverberation time, the spatial variation of sound pressure level and the linearity of the reverberant level decay.

1.6 Subjective aspects of diffusion.

One question beyond the scope of this research is how any of these objective measures relate to the subjective impression of diffusion. It would be useful to know whether any of the diffusion parameters are a linear perceptual scale and the value of the difference limen for diffusion. Lee[26] has performed some subjective experiments and these are briefly discussed in Section 7.3, along with the related concepts of quantifying diffusion in the time domain by examination of the impulse response and frequency domain from comb filtering effects.

1.7 Evaluation of the research.

The most effective measures for quantifying diffusion which have been either reviewed or proposed during the research are brought together and compared in Chapter 8. The fact that different applications currently require different information from a diffusion coefficient is discussed, along with the implications of this for the development of a universal parameter. Also discussed is whether the information required from diffusion coefficients will change in the future, particularly in relation to the potential for increasing the complexity of computer models as technology advances.

1.8 Conclusions.

The conclusions of the research are presented in Chapter 9.

2. MEASUREMENT AND PREDICTION OF POLAR RESPONSES.

2.1 Introduction.

One of the most important considerations when appraising all diffusion parameters, both those published in the literature and those developed during the course of this research, is whether they evaluate diffusion properly. To ascertain this for the case of parameters which quantify the diffusion efficacy of surfaces from the shape of their polar response, polar responses of a wide variety of different surfaces are required.

In this chapter, the sample surfaces employed for this purpose are described and the reasons why measurement and prediction are important and complementary methodologies for obtaining their polar responses are briefly discussed. Two measurement facilities are described, an existing one for measuring single-plane polar responses and a new system designed and constructed at the University of Salford for measuring three-dimensional scattering into half-space. The BEMs used to predict polar responses are also outlined, as are some far-reaching practical considerations relevant to both measurements and predictions.

2.2 Importance of both measurements and predictions.

Appraising diffusion coefficients using measured data carries more weight than using data obtained solely from computer models because it demonstrates their practical as opposed to theoretical merit. This is important because in order for a diffusion coefficient to be accepted by the acoustic community, it is necessary to show that the coefficient correctly evaluates the diffusion efficacy of a wide variety of real-life surfaces. Additionally, although polar responses of simple, rigid, surfaces can be readily predicted using BEMs as discussed in Section 2.5, predicting polar responses of more geometrically complex surfaces and those with areas of non-zero admittance, particularly if the areas of non-zero admittance are not locally reacting and especially in three dimensions, is a time consuming process. For such surfaces, measurements are required to verify the predictions,

especially if a new prediction method is used.

However once a method for predicting the polar response of a particular surface or type of surfaces has been validated, further investigation, for example the effect on the polar response of changing the angle of incidence or the distance of the receivers from the surface, is usually more straightforward using predictions than measurements.

2.3 The sample surfaces: descriptions and reasons for their use.

2.3.1 Introduction.

In order for this research to be as comprehensive as possible, the set of test samples included standard geometric shapes, surfaces found in performance spaces and commercial products designed to produce diffusion. Many of the geometric samples are popular design choices but their primary purpose was to provide polar responses with particular shapes or characteristics to use as test cases for assessing diffusion parameters.

Amongst the samples are both good and poor diffusers, shapes which redirect rather than scatter the reflected energy, surfaces with periodic and random topography, samples which produce diffusion in a single plane rather than three dimensions and surfaces which are diffusing as a result of variations in their impedance as opposed to their shape.

Most of the samples are 1:5 scale models because there is a practical upper limit on the size of samples for which meaningful polar responses can be obtained. The reason this limit exists, and the problems it causes, are discussed in detail in Section 2.8.1.

For samples 2.3.3 to 2.3.7, the polar response was measured in only a single plane, using the system at RPG Diffusor Systems Inc. described in Section 2.4. The reason for this was that many aspects of quantifying diffusion from polar

responses could be satisfactorily investigated using these single-plane responses. All of these samples have an axis along which their cross-section is invariant; the polar response was measured in the plane perpendicular to this axis.

For samples 2.3.8 to 2.3.13, the three-dimensional polar response was measured using the system described in Section 2.9 which was designed and constructed at the University of Salford specifically for this purpose, as part of this research. Some of the samples were also measured at RPG, chiefly to verify that the Salford measurement system was producing the correct results. Measurement at RPG was only possible for those samples which have one or more planes of symmetry; the polar response in one of these planes can be measured if the sample is sectioned along it.

2.3.2 **Plane**.

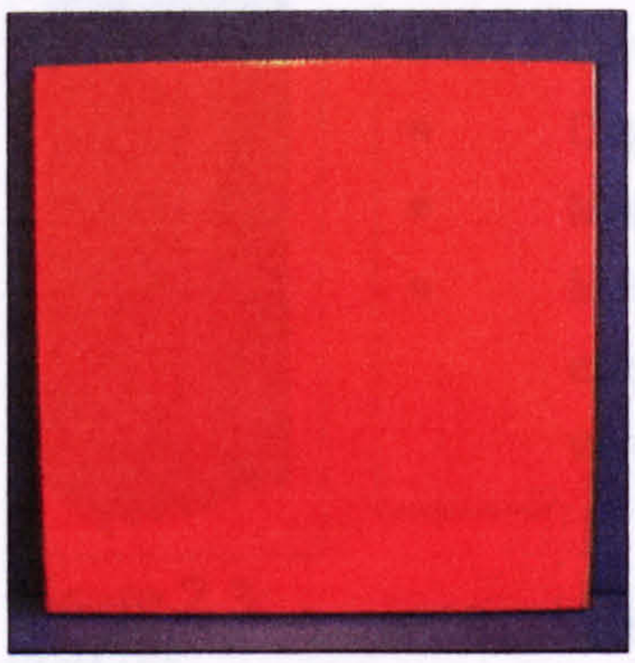

Figure 2.1: Plane.

A rigid plane is the simplest surface and known to be a poor diffuser unless small in comparison to a wavelength[27]. Its featureless topography results in simple specular reflections except at frequencies where diffraction due to the similarity between its dimensions and the wavelength occurs.

Various shapes and sizes of plane surfaces were used as references and for the purpose of determining to what extent the diffusion produced by other surfaces resulted from their topography and how much was due simply to their finite size.

2.3.3 **Semicylinder**.

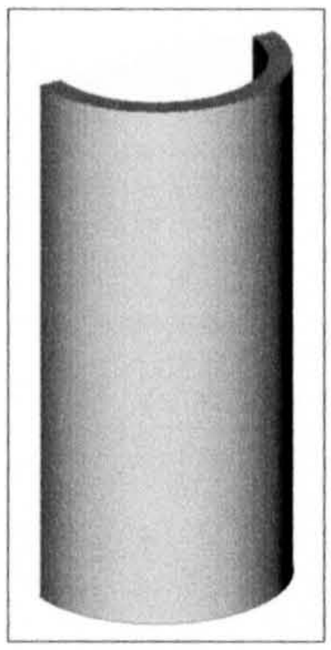

Figure 2.2: Semicylinder

- Diameter = 110mm.
- Length = 300mm.
- Material: Extruded high density plastic.

A convex semicylindrical shell was included in the set of samples because this shape has been shown to be an effective diffuser over a wide range of frequencies for sound incident perpendicular to its axis[12]. In addition to measuring the polar response of a single unit, arrays of various numbers of adjacent semicylinders were used to investigate the scattering from periodic surfaces.

2.3.4 **Quadratic Residue Diffusor (QRD™)**.

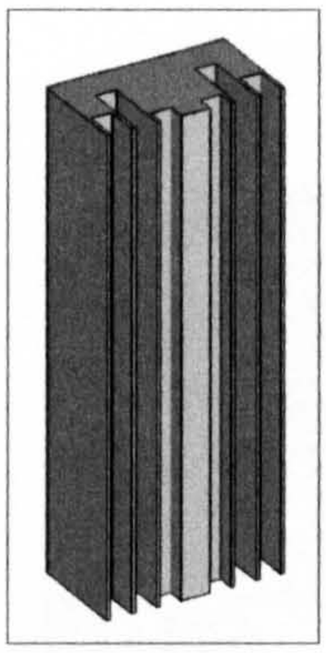

Figure 2.3: QRD™.

- Width = 102mm.
- Length = 300mm.
- Depth = 60mm.
- Max. well depth = 40mm.
- Material: Sandwich construction of metal and varnished wood.

The QRD is probably the best known example of the many specialist diffusers which have been developed over recent years from Schroeder's seminal papers on using mathematical number theory sequences to achieve diffusion[28-34]. Details concerning their design will not be repeated here as this is discussed in many publications, eg. D'Antonio[35]. Numerous types of QRDs are available; this research utilised a 1:5 scale model of a single-period QRD with seven wells as shown in Figure 2.3.

2.3.5 **Triangular prism**.

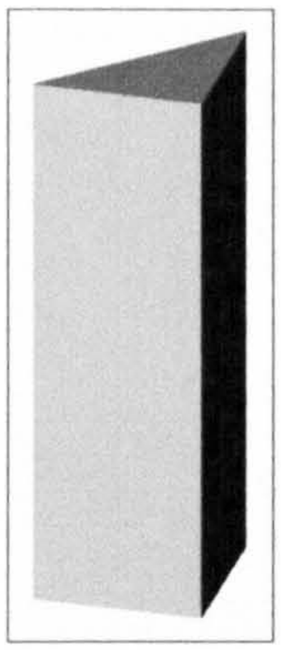

- Width = 108mm.
- Length = 300mm.
- Depth = 54mm.
- Cross-section is a right-angled isosceles triangle.

Figure 2.4: Triangular prism.

This sample was used because it was reasoned that at mid to high frequencies the polar response would show redirection from the plane surfaces of the prism rather than scattering of the reflected energy and therefore provide an interesting test case for diffusion coefficients. Whether or not a surface which redirects the reflected energy as opposed to scattering it can be called a diffuser is discussed in Section 3.6.3.

2.3.6 **Concave prism**.

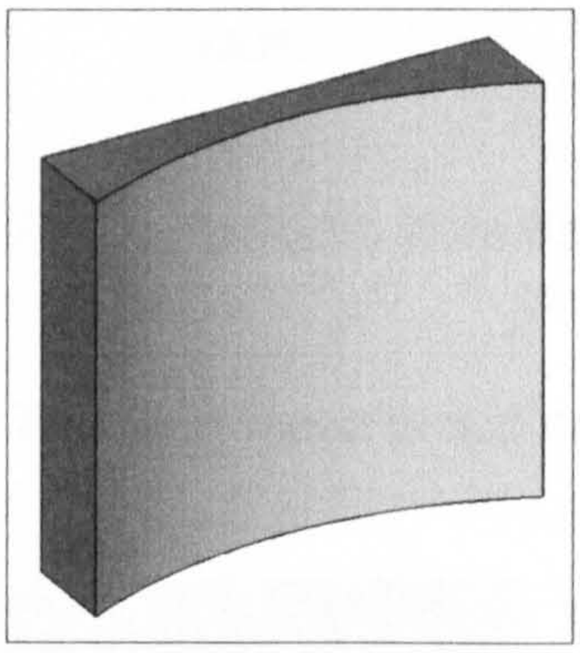

- Width = 300mm.
- Length = 300mm.
- Depth ≈ 35mm.
- Material: Nylon 66.
- Produced by CNC machining.

Figure 2.5: Concave prism.

This sample was designed specifically for the measurement system at RPG; its profile is part of an ellipse which has as its foci the normal incidence source and receiver positions. The purpose of this sample was to provide a polar response showing worse diffusion for normal incidence than the equivalent sized plane surface by focussing the specular reflection to the normal microphone.

2.3.7 **Seating**.

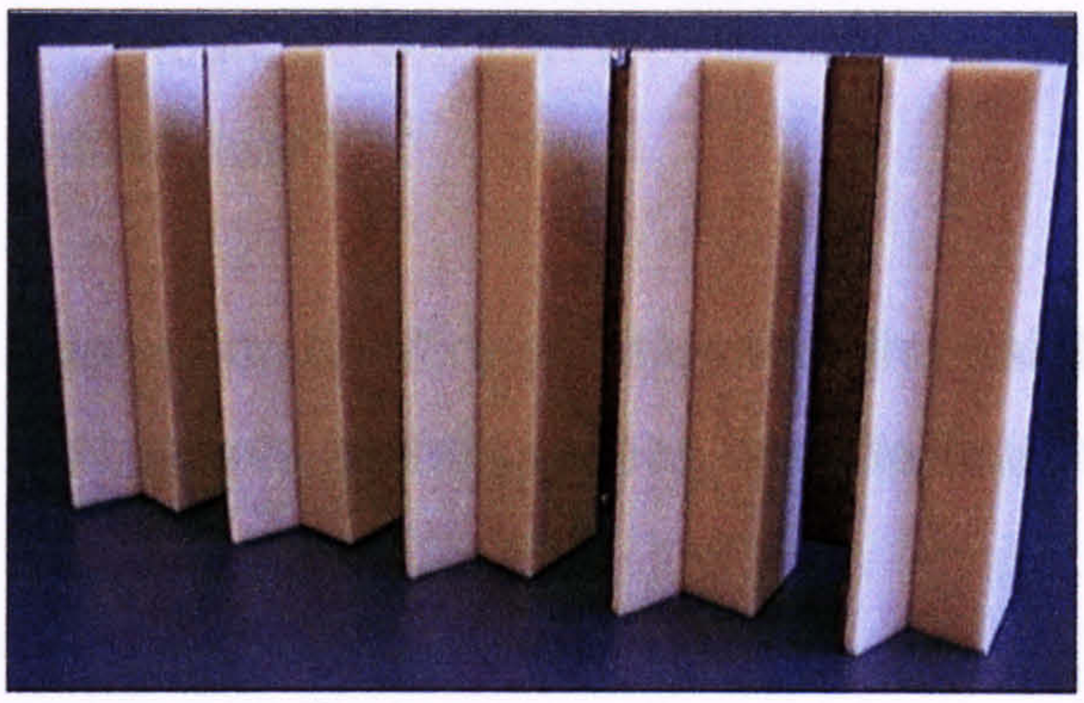

Figure 2.6: Seating.

- Width = 570mm.
- Length = 300mm.
- Depth ≈ 135mm.
- Material: Seats are 30kgm^{-3} open-cell foam mounted on 3mm varnished plywood. Base is varnished 25mm MDF.

This sample is a simple model of five rows of upholstered seating with the seat cushions in the folded-up position and the seat backs at an angle of 70° to the floor. It was intended to be representative of a surface commonly encountered in performance spaces rather than produce a particular polar response. The foam used for the seats is the same type as that used by Davies[36] in his scale models of seating for the investigation of seat-dip attenuation.

2.3.8 **Periodic hemispheres**.

This is in fact a group of four samples as shown Figure 2.7.

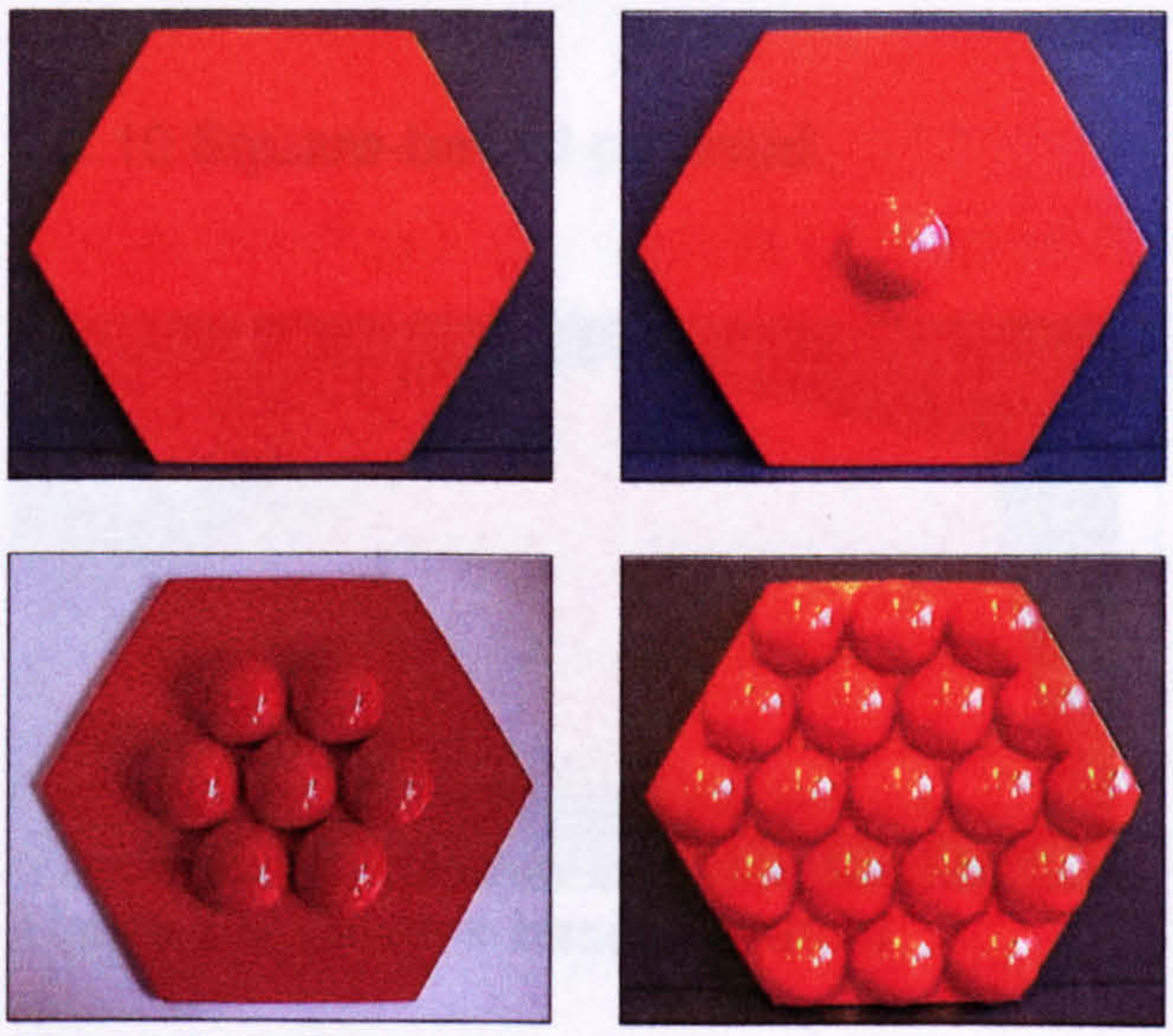

Figure 2.7: Periodic hemispheres.

- Width of base ≈ 340mm AF.
- Depth = 50mm.
- Diameter of hemispheres = 75mm.
- Material: Hemispheres are solid moulded plaster which is sealed and then painted to give a reflective finish. Bases are 12.5mm painted plywood.

The purpose of these samples was to investigate how the three-dimensional polar response of a surface known to be a poor diffuser changed as it was covered with a periodic arrangement of elements which are known to be effective scatterers individually[37].

Absorption coefficient values for the painted plaster are given in Section 2.3.14. Full details of the process used to manufacture all the plaster samples can be found in Appendix A.

2.3.9 **Cone**.

- Diameter = 300mm.
- Depth = 70mm.
- Material: Solid plaster mounted on a 12.5mm plywood base then sealed and painted.

Figure 2.8: Right circular cone.

In common with the triangular prism described in Section 2.3.5, the purpose of this sample was to redirect rather than scatter the reflected energy. However in this case the redirection is into three dimensions as opposed to a single plane.

2.3.10 **Square-based pyramid**.

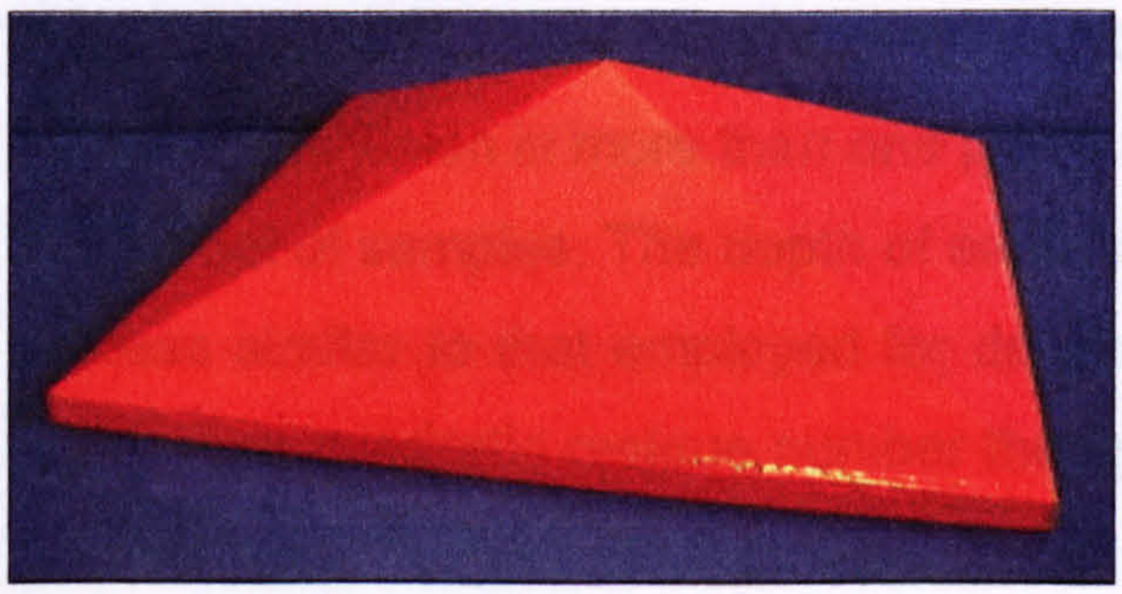

- Width = 300mm.
- Length = 300mm.
- Depth = 70mm.
- Material: Solid plaster mounted on a 12.5mm plywood base then sealed and painted.

Figure 2.9: Square-based pyramid.

This sample is similar to the cone described above; it has the same dimensions, is made from the same material and is also designed to redirect rather than scatter

the reflected energy. Furthermore, if this sample were cut in half parallel to one of the sides of its square base, the shape of the face revealed would be identical to that which would result if the cone were sectioned in a similar manner.

The implication of this is that the single plane scattering in the plane of the cut would be very similar However, despite the similarities it was expected that the three-dimensional polar responses would be quite different because this sample comprises four distinct plane surfaces whereas the cone is one continuous surface. The purpose of the square-based pyramid was therefore to assist with the decision as to whether single-plane polar responses are sufficent to reliably quantify diffusion or whether measurements in three dimensions are required.

2.3.11 **Skyline®**.

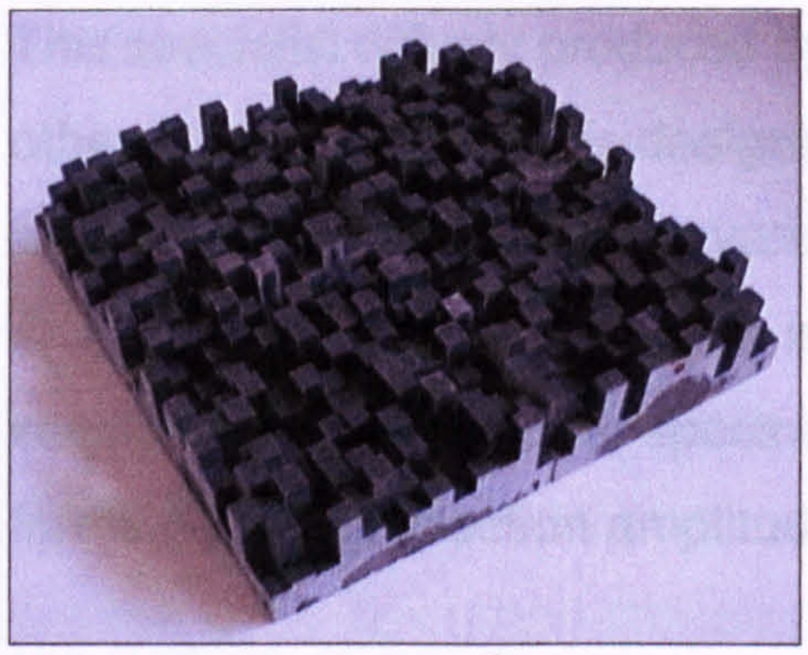

- Width = 110mm (each unit).
- Length = 110mm (each unit).
- Depth = 45mm.
- Material: The actual product is moulded from either polystyrene or glass fibre but the 1:5 scale models measured are constructed from short lengths of high density plastic bar glued together.

Figure 2.10: Skyline® (four units).

The Skyline® is a commercial product of RPG Diffusor Systems Inc. and is so-called because its shape bears some resemblance to a city skyline. It is designed to produce diffusion in more than one plane and this was the reason for including it in the set of samples. The depth of each 'well' is determined by a mathematical process similar to that employed for designing QRDs except that primitive root rather than quadratic residue number theory is used[30].

To increase the sample area, with the objective of increasing the level of the reflected sound, the three-dimensional polar response measurements utilised four identically orientated units in a 2×2 arrangement. Only two units were required for

the measurement at RPG Diffusor Systems Inc. because the sample is effectively reflected in the hard floor as explained in Section 2.4.2.

2.3.12 **Binary Amplitude Diffsorbor™ (BAD™ Panel)**.

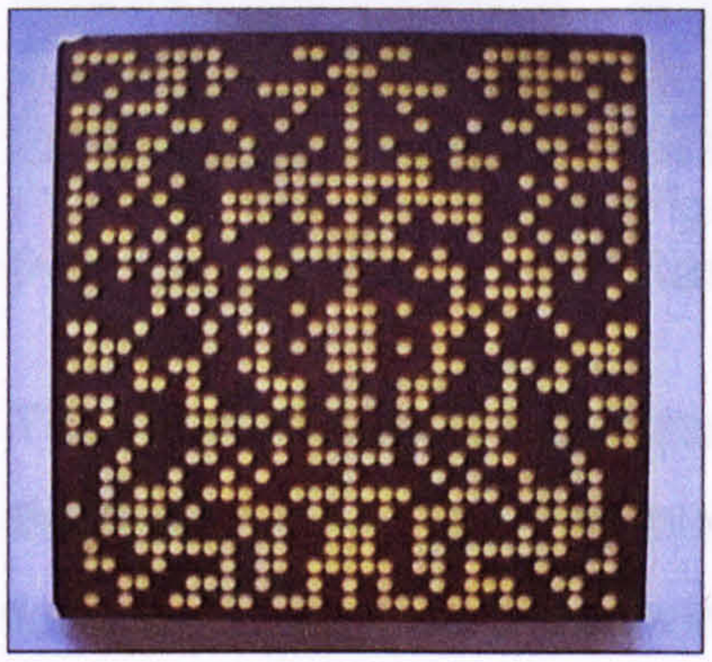

Figure 2.11: BAD™ Panel.

- Width = 600mm.
- Length = 600mm.
- Depth = 50mm.
- Material: A block of fibrous absorbent with a piece of melamised paper, perforated with a pattern of 16mm diameter holes, attached to the exposed face. A thin acoustically transparent fabric encloses the unit to prevent the escape of fibres.

This specialist diffuser produced by RPG Diffusor Systems Inc. differs from all the other samples in that it is designed to provide absorption in addition to diffusion and the diffusion results from variations in its surface impedance, not its physical shape[38]. The pattern of holes is based on a two-dimensional optimal binary sequence with a flat power spectrum and the resulting variable impedance surface forms a binary reflection amplitude grating as suggested by Angus[39,40].

Because of the difficulties involved in scaling absorption and the fact that its size was not prohibitive, the actual product was used as the sample rather than a 1:5 scale model.

2.3.13 **Periodic and Random Battens**.

These samples both comprise fifteen parallel battens, as shown in Figure 2.12 on the following page. The salient difference between them is that in one case the battens are arranged in a simple periodic manner whereas in the other their arrangement was determined by chance, producing a surface with random binary topography (in one direction).

Figure 2.12a:
Periodic battens.

Figure 2.12b:
Random battens.

- Width = 560mm.
- Length = 600mm.
- Depth ≈ 30mm.
- Cross-section of battens = 18mm.
- Material: Battens are varnished hardwood. Base is varnished 12.5mm plywood.

The randomness of the latter case contrasts with all the other samples; this was the reason for its use. The purpose of the periodic sample was to act as a control for the random one, allowing the effect on the polar response and diffusion coefficient values of simply rearranging the battens to be isolated. It was expected that any effect would be larger in the plane perpendicular to the battens than that parallel to them.

2.3.14 **Absorption coefficient of the plaster samples.**

To verify that the painted and sealed plaster is highly reflective, its absorption coefficient was measured. High reflectivity is desirable because the more reflective a sample is, the larger the proportion of the incident energy reflected in any particular direction and the easier it is to extract this reflected energy from the measurements; the signal to noise ratio is effectively increased.

The absorption coefficient was measured using the standard impedance tube technique[4] and a Brüel & Kjær Standing Wave Apparatus, Type 4002. This apparatus utilises two tubes of different dimensions, enabling absorption coefficient measurements to be made over a wider range of frequencies than would be possible with a single tube. The results for a 50mm thickness of sealed and painted plaster, prepared as described in Appendix A, are shown in Figure 2.13.

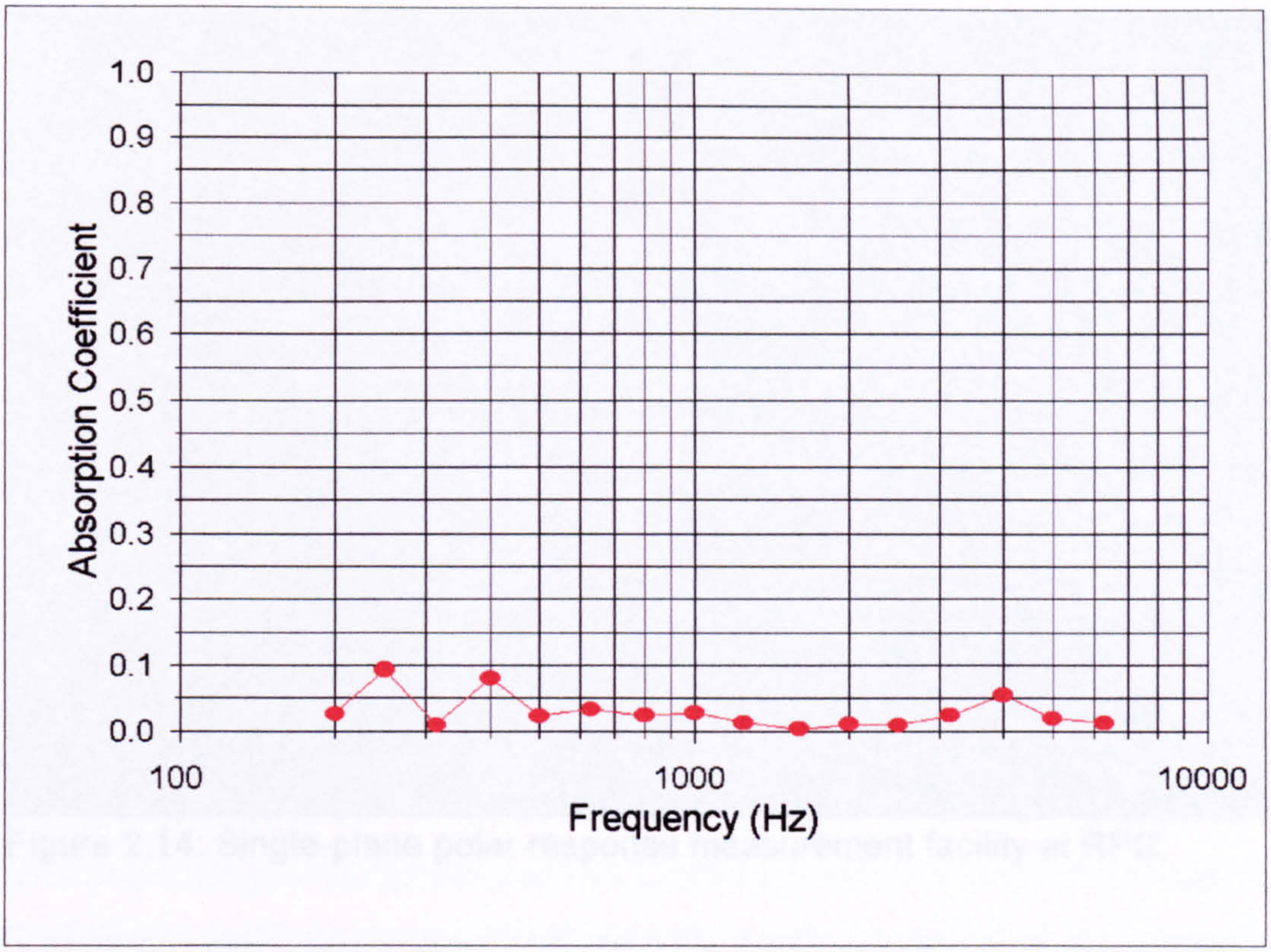

Figure 2.13: Absorption coefficient of sealed painted plaster (50mm thick).

These results confirmed that there was nothing unexpected about the absorption characteristics of the plaster samples.

2.4 **Measurement facility at RPG Diffusor Systems Inc.**

2.4.1 **Introduction.**

For several years, RPG have operated a facility for making measurements of single-plane scattering. Only a synopsis of their system will be included here because a detailed description is given by D'Antonio[11].

2.4.2 **Geometry.**

Figure 2.14 shows the arrangement of the sample, source and receivers, which are situated on a hard floor in what can be referred to as a Reflection Free Zone (RFZ); the walls and ceiling of the room are far enough away for reflections from them not to interfere with the measurement. The sample is placed at a point which

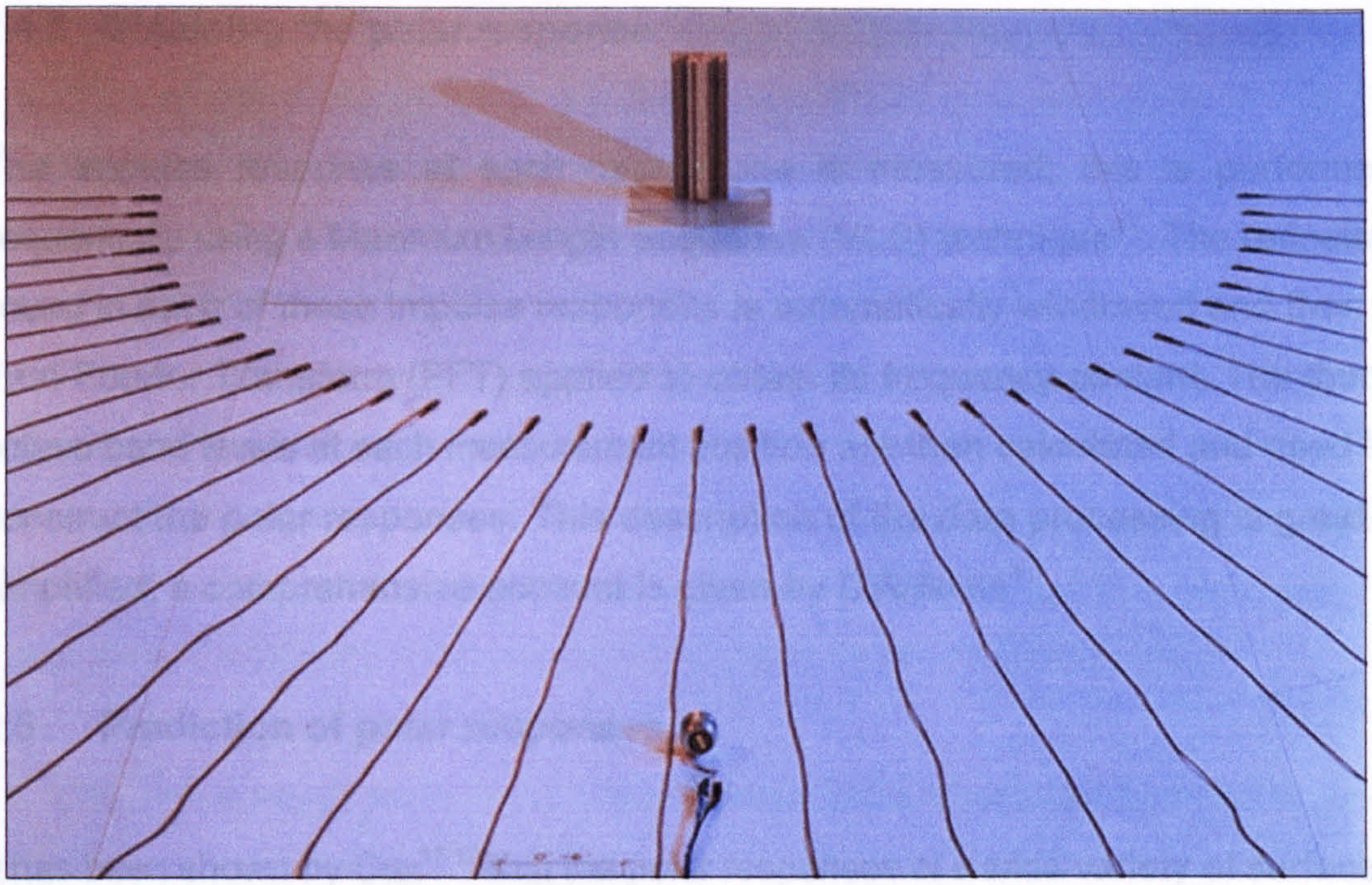

Figure 2.14: Single-plane polar response measurement facility at RPG.

is the centre of two concentric semicircles in the plane of the floor. The inner semicircle is 2m in diameter and has thirty-seven microphones spaced at 5° intervals around it. The source is placed on the outer 4m diameter semicircle at whatever angle of incidence is desired. The measurements are made in 1:5 scale for the reasons discussed in Section 2.7, this means that the 20kHz upper frequency limit corresponds to a limit of 4kHz in full scale.

In this system, the sample, source and receivers are reflected in the floor. To obtain the best quality measurements, the source and receivers must be physically as close to the floor as possible. The polar response can only be measured in a plane of symmetry of the sample; for measurement the sample must be cut in half so that this and the floor are co-planar, i.e. so that the physical half and its reflection in the floor re-form the complete sample. For samples which have a cross-section that is invariant along the axis perpendicular to the measurement plane, this sectioning is not necessary. In these cases the sample should theoretically be infinite in extent to remove the effect of its ends on the scattering but in practice it has been found that any additional height above 300mm does not significantly affect the results.

2.4.3 Obtaining the polar response.

The impulse response at each microphone is measured; this is performed sequentially using a Maximum Length Sequence (MLS) technique[41]. The reflected sound in each of these impulse responses is automatically windowed and then a Fast Fourier Transform (FFT) applied to obtain its frequency content. The third-octave band levels at each measurement position are then calculated and used to construct the polar responses. This description of the data processing is greatly simplified; a comprehensive account is given by D'Antonio[11].

2.5 Prediction of polar responses.

It has been shown by Cox[17-19] that the polar responses of a wide variety of surfaces can be accurately predicted using BEMs. Cox's work includes detailed descriptions of predicting scattering using BEMs, therefore only an outline of the process is given here.

Prediction of a polar response using BEMs involves formulating the pressures at the receiver points as a combination of the pressure direct from the source and a surface integral of the pressure and its derivative over the surface of the sample. The sample surface is discretised into small elements across which it is approximated that the pressure is constant. In order for this approximation to hold true, the elements must be significantly smaller than the wavelength of the highest frequency of interest. Simultaneous equations are then set up for the surface pressures using the Helmholtz-Kirchhoff integral equation[17]. Solving these equations gives the surface pressure on each element but precautions are necessary to ensure unique solutions[42]. Once the surface pressures are known, the receiver point pressures can be calculated by numerical integration of the Helmholtz-Kirchhoff integral equation.

Initially, predicted polar responses required for this research were generated using a two-dimensional BEM formulation. However, this model was developed specifically to predict the scattering from samples with a uniform cross-section and

is strictly two-dimensional, the sample is reduced to its footprint. Although this is satisfactory for samples such as the semicylinder and triangular prism, to accurately predict the scattering from samples which do not have a uniform cross-section, a model which includes the third dimension is required, even to predict single plane scattering. The simplest method of modelling diffusers which comprise a number of wells separated by thin fins, such as QRDs, is to represent them as cuboids with a variable admittance on the front face. These front face admittances are calculated assuming that plane waves propagate up and down the wells, inducing a phase change with no absorption. For this to be true it is necessary to assume hard surfaces, local reaction and small radiation admittance.

An alternative approach is to use a collocated BEM where the formulation is in terms of pressure differences across each element and this has also been implemented by Cox[18]. When a sample is broken down into a set of thin panel elements, all surfaces can be modelled including thin fins but the prediction time becomes long for large complicated surfaces.

These two-dimensional BEM models have been extended to predict three-dimensional scattering but further work is required to reduce the computation time. Since the development of prediction models was not a principal aim of this research, it was decided to use the commercial SYSNOISE Rev 5.3A analysis solver developed by LMS Numerical Technologies N.V. for any predictions involving a third dimension. The three-dimensional meshes of samples required by SYSNOISE were prepared in NASTRAN format using Altair Engineering Inc.'s HyperMesh® 3.0 finite element pre-processor.

2.6 **Comparison of measured and predicted single-plane polar responses.**

Figures 2.15 to 2.20 show, for comparison, both measured and predicted single-plane, normal incidence, polar responses of a variety of samples. Because the predicted responses are evaluated at single frequencies, in some cases they contain large numbers of maxima and minima. These local variations are absent from the measurements as a result of the third-octave smoothing. It is evident that

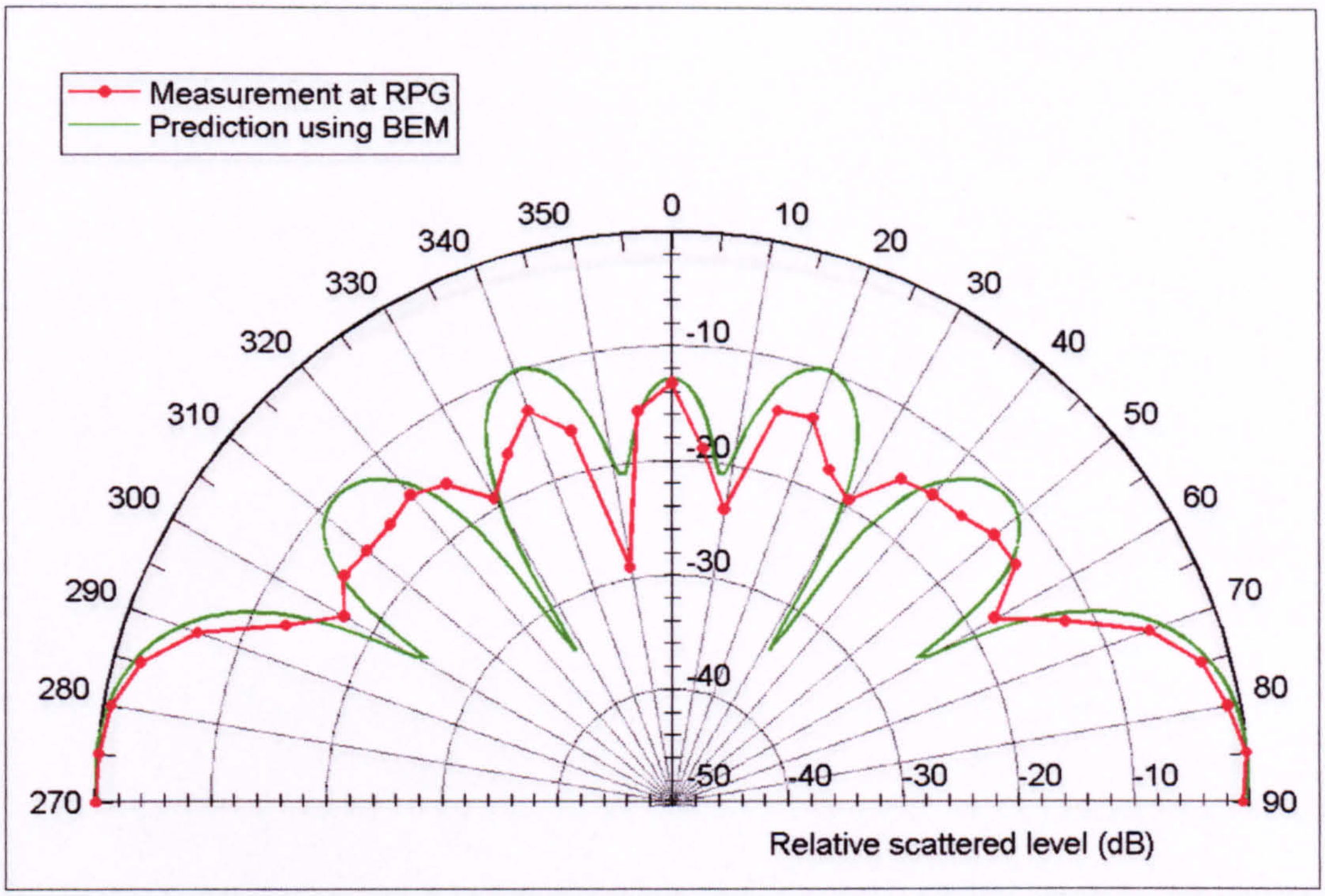

Figure 2.15: Comparison of the 2kHz measured polar response of the triangular prism with a prediction obtained using a two-dimensional BEM model.

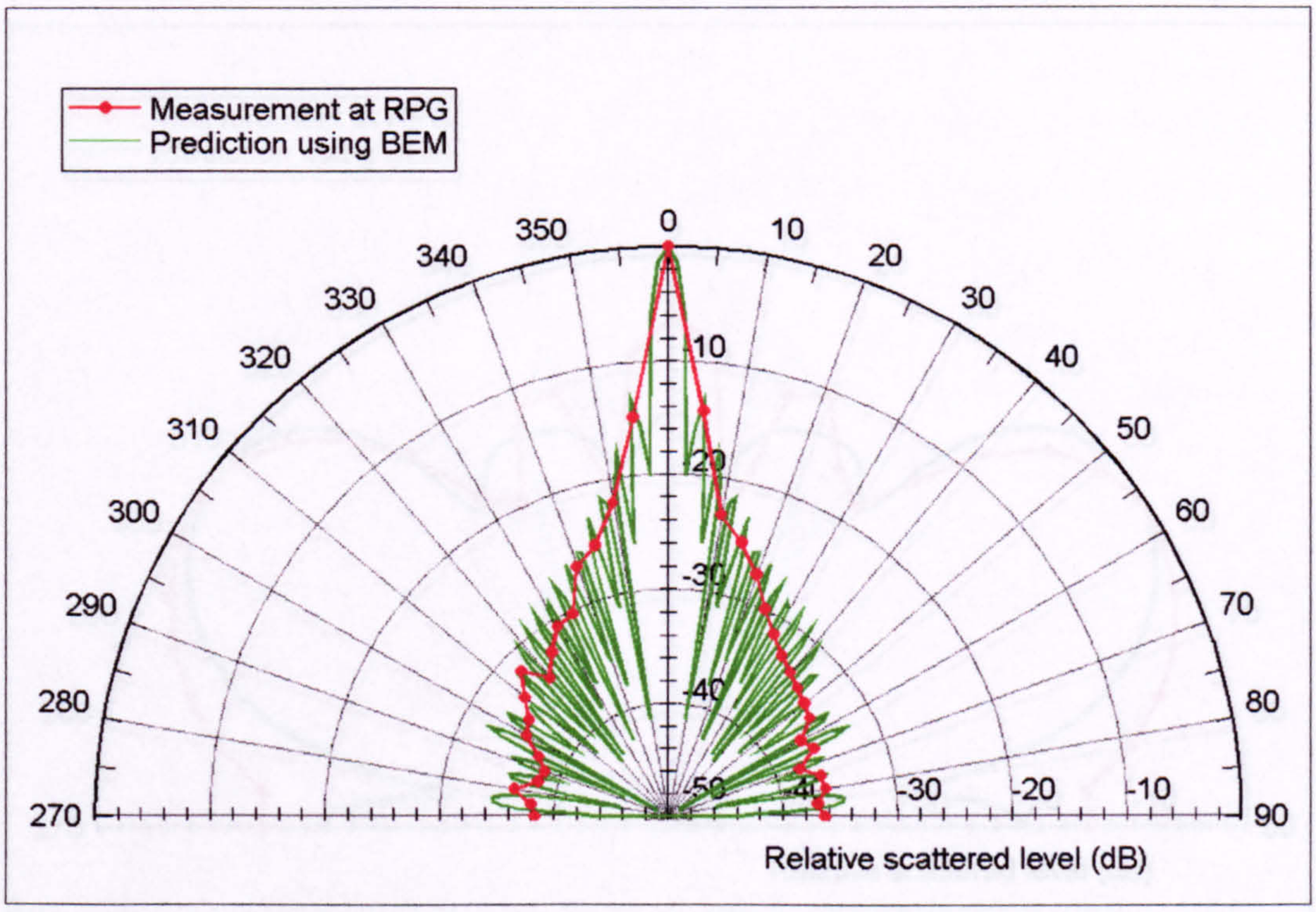

Figure 2.16: Comparison of the 4kHz measured polar response of the concave prism with a prediction obtained using a two-dimensional BEM model.

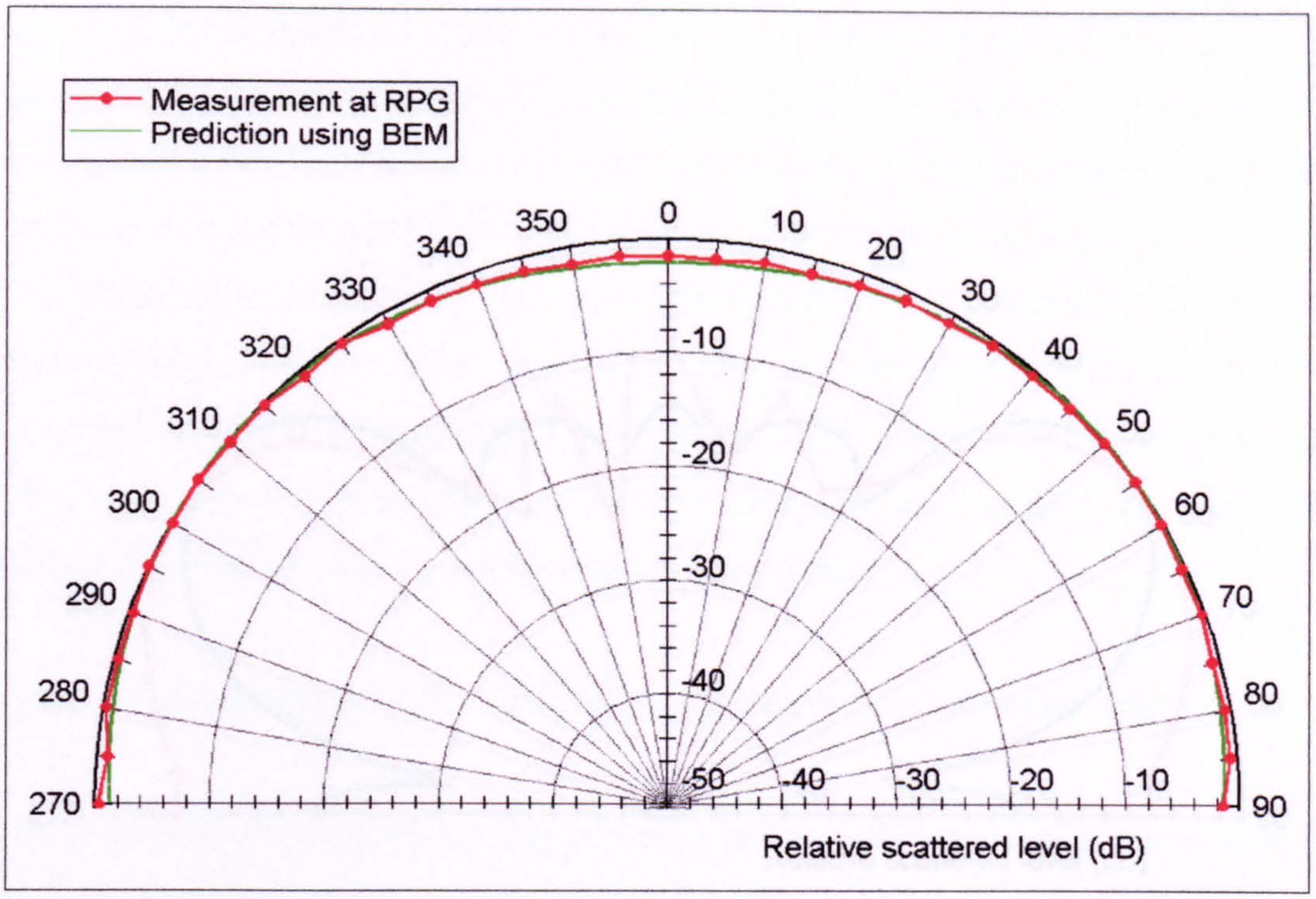

Figure 2.17: Comparison of the 500Hz measured polar response of the semicylinder with a prediction obtained using a two-dimensional BEM model.

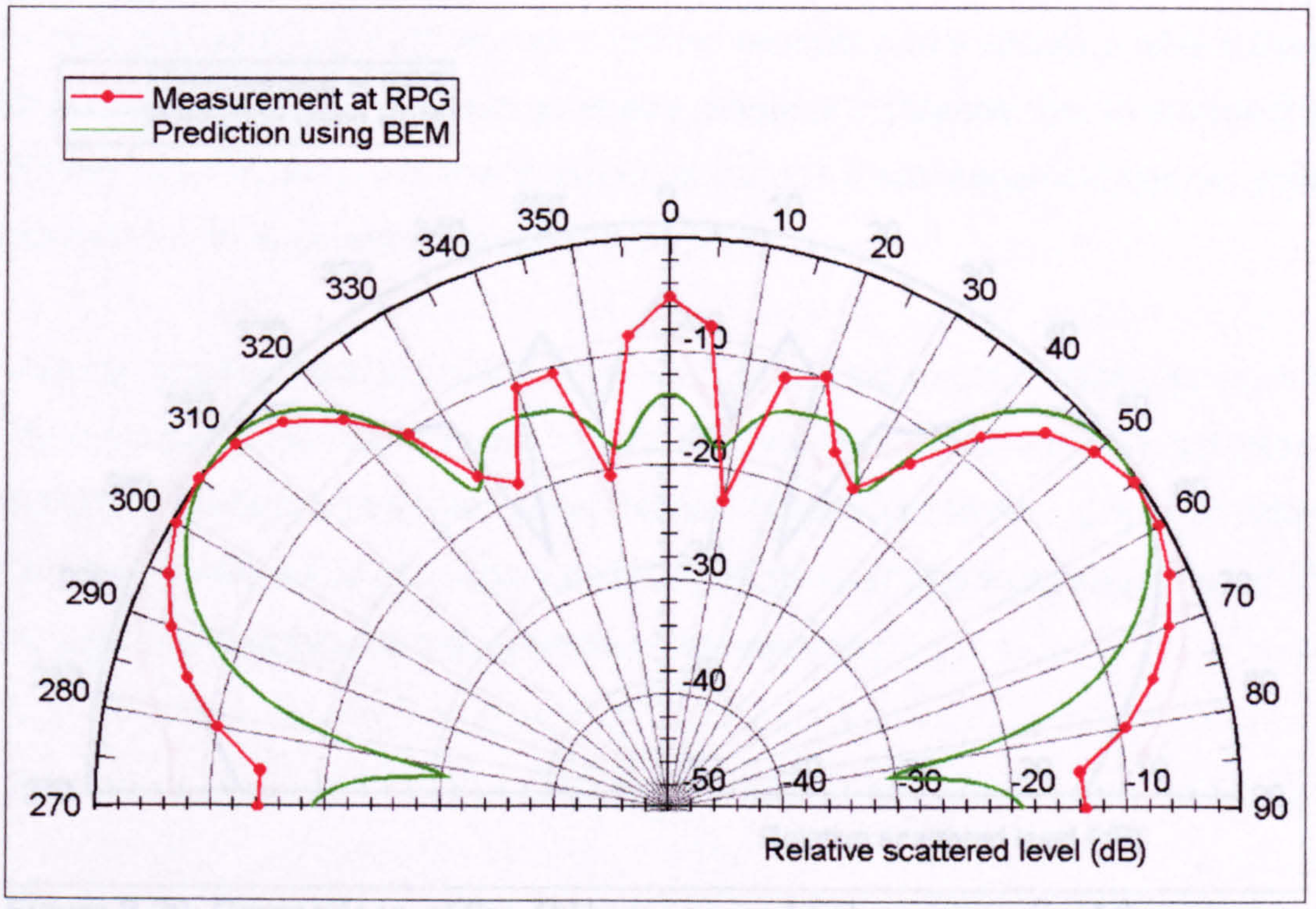

Figure 2.18: Comparison of the 1kHz measured polar response of the cone with a prediction obtained using a two-dimensional BEM model.

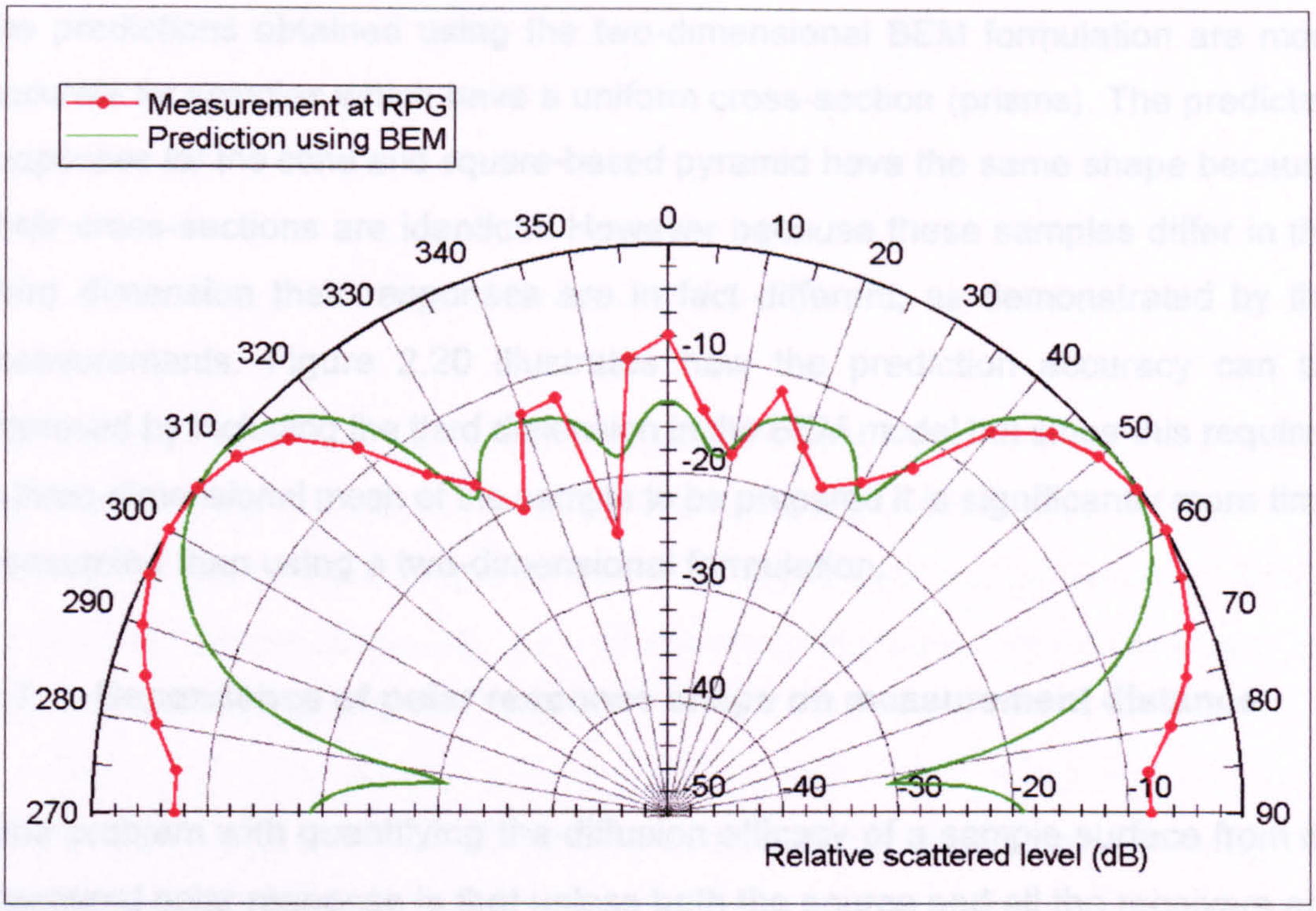

Figure 2.19: Comparison of the 1kHz measured polar response of the square-based pyramid with a prediction obtained using a two-dimensional BEM model.

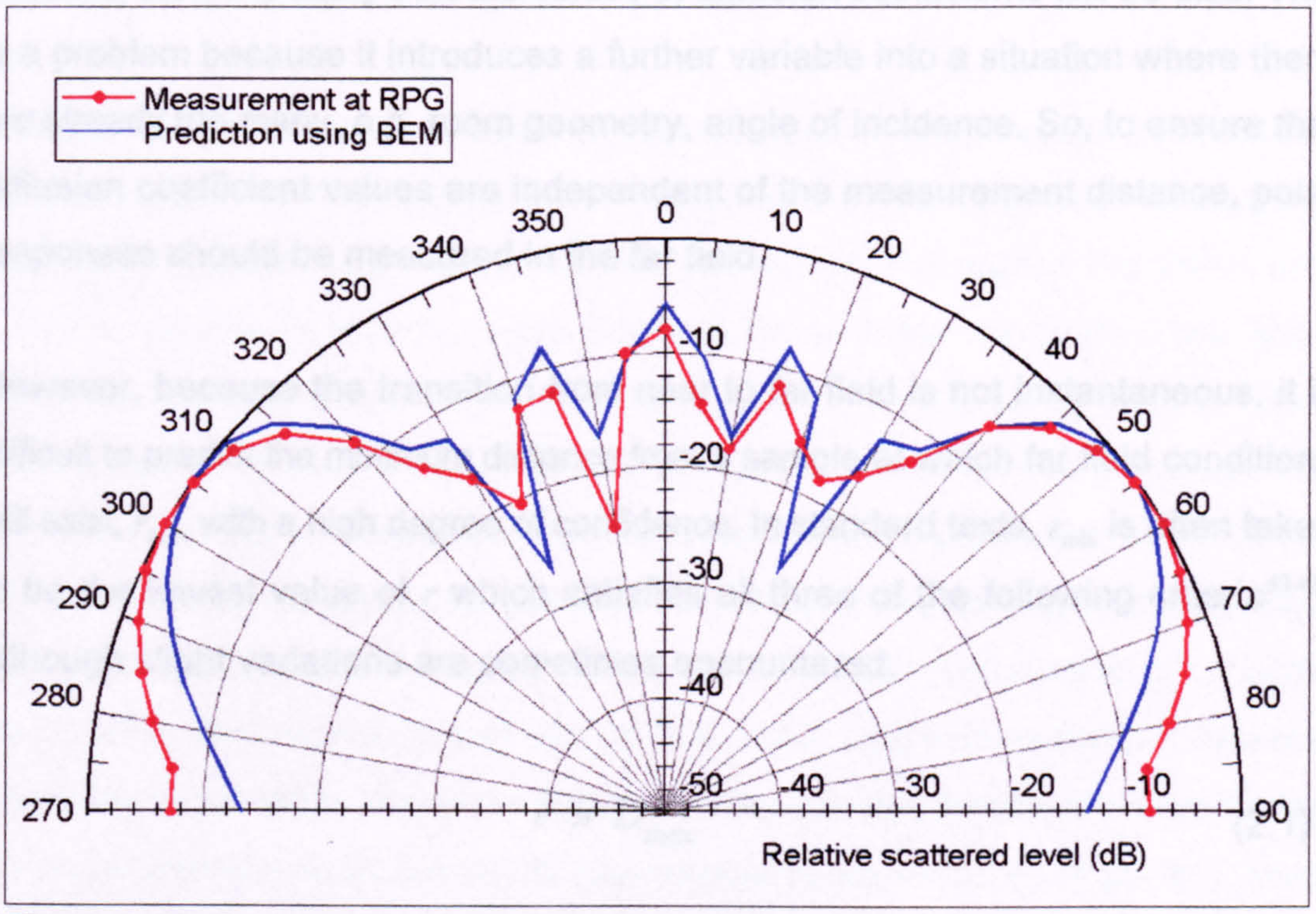

Figure 2.20: Comparison of the 1kHz measured polar response of the square-based pyramid with a prediction obtained using a three-dimensional BEM model.

the predictions obtained using the two-dimensional BEM formulation are most accurate for samples which have a uniform cross-section (prisms). The predicted responses for the cone and square-based pyramid have the same shape because their cross-sections are identical. However because these samples differ in the third dimension their responses are in fact different, as demonstrated by the measurements. Figure 2.20 illustrates how the prediction accuracy can be improved by including the third dimension in the BEM model but since this requires a three-dimensional mesh of the sample to be prepared it is significantly more time consuming than using a two-dimensional formulation.

2.7 Dependence of polar response shape on measurement distance.

One problem with quantifying the diffusion efficacy of a sample surface from its measured polar response is that unless both the source and all the receivers are in the far field, the shape of the response depends on their distance from the sample. If the shape of the polar response is dependent on the measurement distance then it is likely that the values of diffusion coefficients will be also. This is a problem because it introduces a further variable into a situation where there are already too many, e.g. room geometry, angle of incidence. So, to ensure that diffusion coefficient values are independent of the measurement distance, polar responses should be measured in the far field.

However, because the transition from near to far field is not instantaneous, it is difficult to predict the minimum distance from a sample at which far field conditions will exist, r_{min}, with a high degree of confidence. In standard texts, r_{min} is often taken to be the lowest value of r which satisfies all three of the following criteria[43-45], although slight variations are sometimes encountered.

$$r \gg D_{max} \tag{2.1}$$

$$r \gg \frac{\lambda}{2\pi} \tag{2.2}$$

$$r \gg \frac{D_{\max}^{\ 2}}{\lambda} \tag{2.3}$$

where:

D_{max} = maximum dimension of sample, λ = wavelength

Strictly speaking, these criteria refer to normal incidence; the near field may extend significantly further for oblique sources and receivers. Furthermore, the near field is really only well defined for places where coherent interference happens. Where destructive interference occurs, such as close to a minimum in the polar response, the near field can extend to infinity[46].

Examination of (2.1), (2.2) and (2.3) readily shows that attempting to solve the problem of diffusion coefficient values being distance-dependent by measuring polar responses in the far field unfortunately creates a further problem; for many surfaces the source and receiver distances necessary are too large for the measurement to be accommodated in most test facilities.

A partial solution to this is to make the measurements in model scale; this involves decreasing the size of the sample and increasing the frequency commensurately. The benefit is that $r_{\min}$ is reduced by the scale factor. The reason that this is only a partial solution is that there are practical limits on the maximum scale factor which can be used. One of these is that as a result of the frequency scaling, either the equivalent full-scale measurement bandwidth must be reduced or transducers operating at ultrasonic frequencies are required. A second practical problem is that the absorption of the scaled sample, including viscous boundary layer effects, must be the same at the scaled frequencies as that of the full-size surface at full-scale frequencies. This becomes more difficult to achieve as the scale factor increases. The scale factor of five chosen by RPG is therefore a compromise, any smaller and the measurement distances would have remained impractically large, any larger and the reduction in bandwidth would have been unacceptable.

2.8 Other practical considerations when measuring polar responses.

2.8.1 Determining suitable dimensions for test samples.

To assist with deciding the dimensions of the test samples described in Section 2.3, the maximum size (width) of sample which could be measured at RPG in the far field was estimated using (2.1) and (2.3). Letting r be equal to the sample to receiver distance of 1m and interpreting "much greater than" as "a factor of three or more greater than", as is usual in acoustics[43,45], revealed that if the measurements were to remain in the far field up to 20kHz then (2.3) is the more restrictive criterion, determining that D_{max} must be less than approximately 8cm. It should be noted that (2.2) is nothing to do with sample size, it simply gives a lower limit for frequency as a function of r. In the case of the RPG measurement system this limit is approximately 160Hz or 32Hz full-scale. This is lower than any frequency of interest in this research and therefore of no consequence.

Although the maximum width of sample which can be measured in the far field calculated using the above criteria is 8cm, all of the test samples described in Section 2.3 are wider. There are several reasons for this. Firstly, Kinsler and Frey[44] present a slightly different version of (2.3), which gives a larger value of D_{max} for any given measurement distance and frequency:

$$r_{min} \sim \frac{1}{4}\frac{D_{max}^{\,2}}{\lambda} \qquad (2.4)$$

This expression is derived geometrically from the assumption that the far field begins at a point on the acoustic axis where the distances from all points on the sample differ by no more than about one half-wavelength. Using (2.4), the limiting value obtained for D_{max} is about 26cm, much larger than the 8cm obtained from (2.3) and close to the limit of 30cm or so given by (2.1).

A second reason is that for the purposes of this research it was not actually necessary for the measurements to be made in the far field because their function

was to provide a comprehensive set of polar responses to use as a tool for investigating diffusion coefficients, not to formally quantify the diffusion efficacy of the surfaces. However, it was necessary for each of the measured polar responses to at least exhibit the same characteristics, e.g. re-direction, specular reflection, as the corresponding far field case, even if their shapes were not identical. Unless this were so, the response would not be representative of the sample surface measured and so could not be used to determine the ability or otherwise of a diffusion coefficient to correctly quantify the diffusion produced by that particular type of surface.

Finally, many of the samples were designed for use with the new system for measuring three-dimensional scattering described in Section 2.9 and it was known from the outset of this research that the sample to receiver distance of this new system would be 50-100% larger than at RPG, enabling larger samples to be measured. It is advantageous to use as large a sample as possible because the larger the sample, the greater the proportion of the energy emitted by the source that is reflected, increasing the signal to noise ratio of the measurement.

Because of the large difference in the values of D_{max} given by (2.3) and (2.4), they were of limited use in obtaining a reliable estimate of the maximum width of sample which could be measured at RPG, even though it was not essential that the measurements were made in the far field. Therefore an empirical approach to the problem was employed instead. The normal incidence single-plane polar responses which would be measured at both RPG and in the far field were predicted at 20kHz for plane samples of various width. Figures 2.21 to 2.25 compare the responses obtained in the two cases for sample widths ranging from 10cm to 50cm. Plane surfaces were used for this investigation because their polar response changes shape radically with measurement distance and so provides if not the worst case, an example close to it. The reason why the polar response of plane surfaces is so dependent on the measurement distance and the implications of this for quantifying diffusion are discussed in Section 3.3. The polar responses were predicted at 20kHz because it is the highest frequency used at RPG and, as stated in Section 2.7, the extent of the near field increases with frequency.

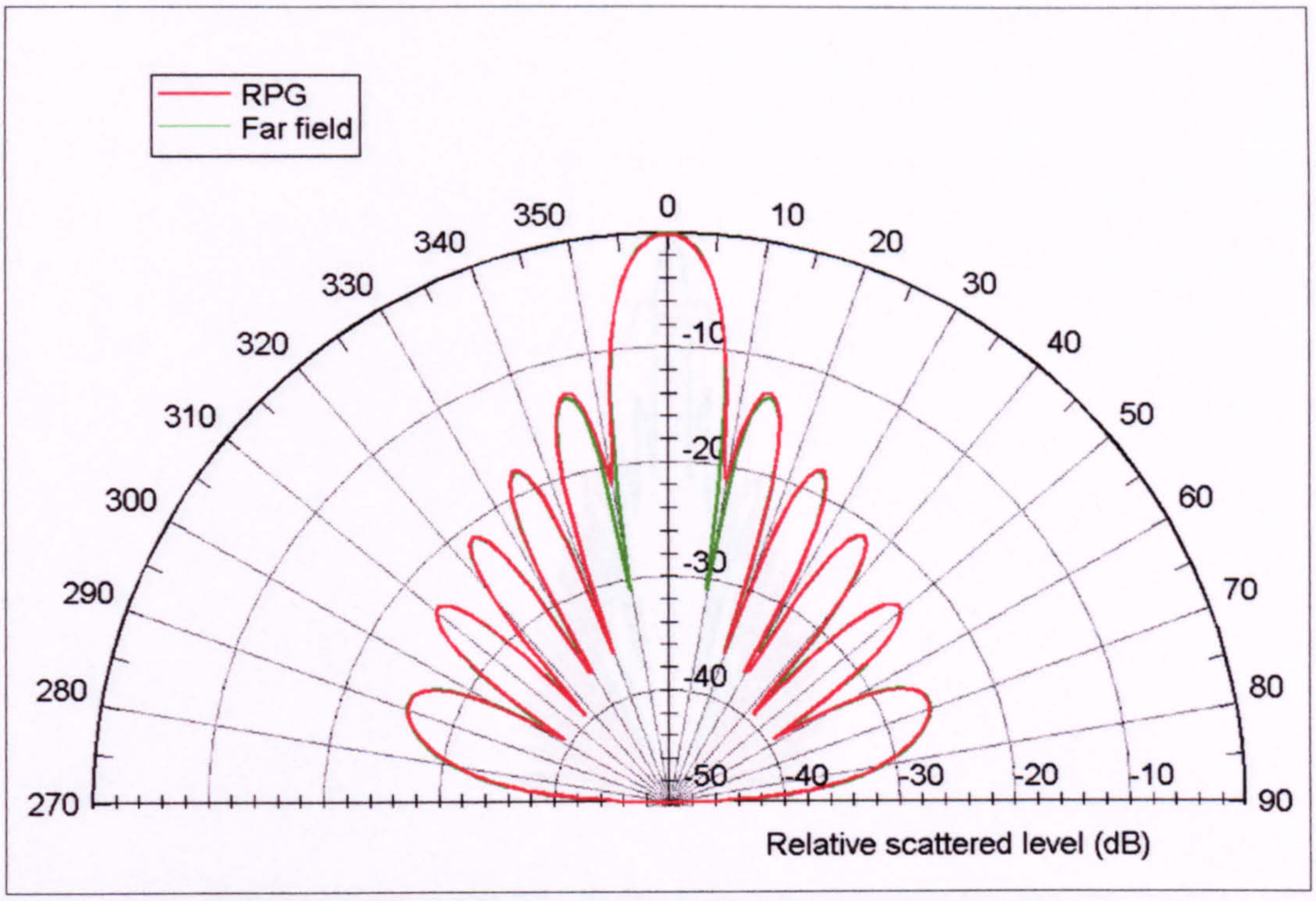

Figure 2.21: Predicted polar responses of 0.1m plane sample.

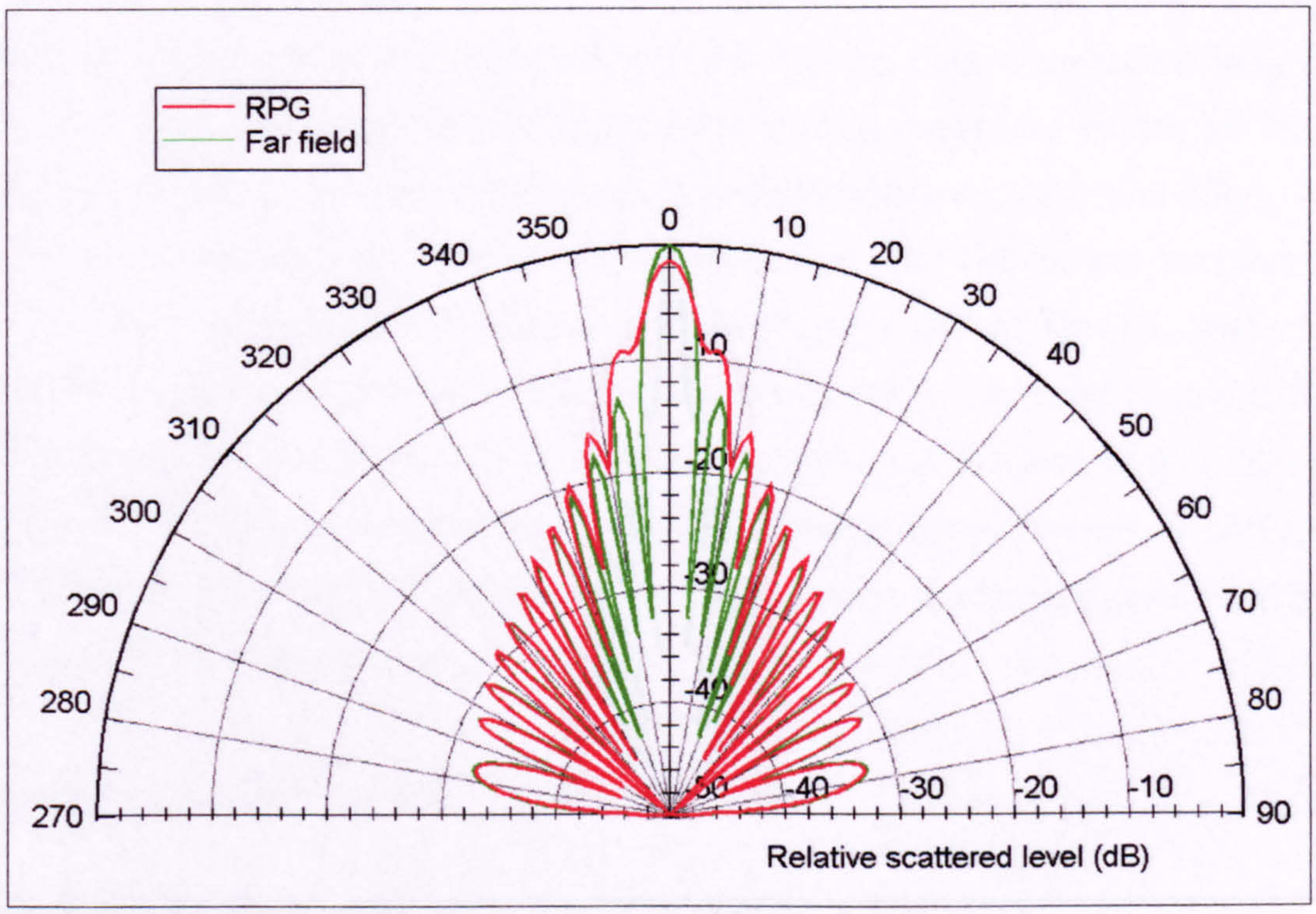

Figure 2.22: Predicted polar responses of 0.2m plane sample.

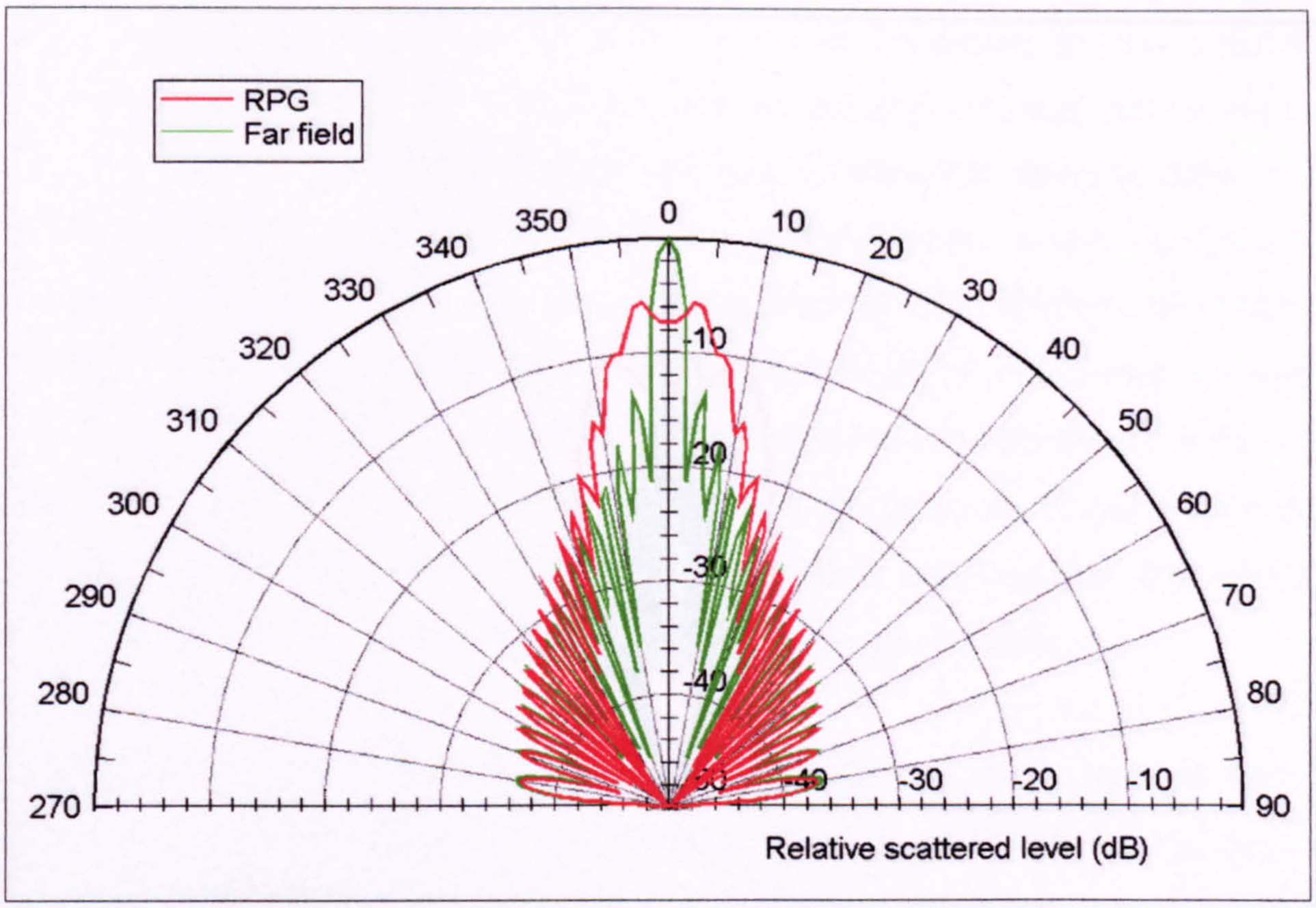

Figure 2.23: Predicted polar responses of 0.3m plane sample.

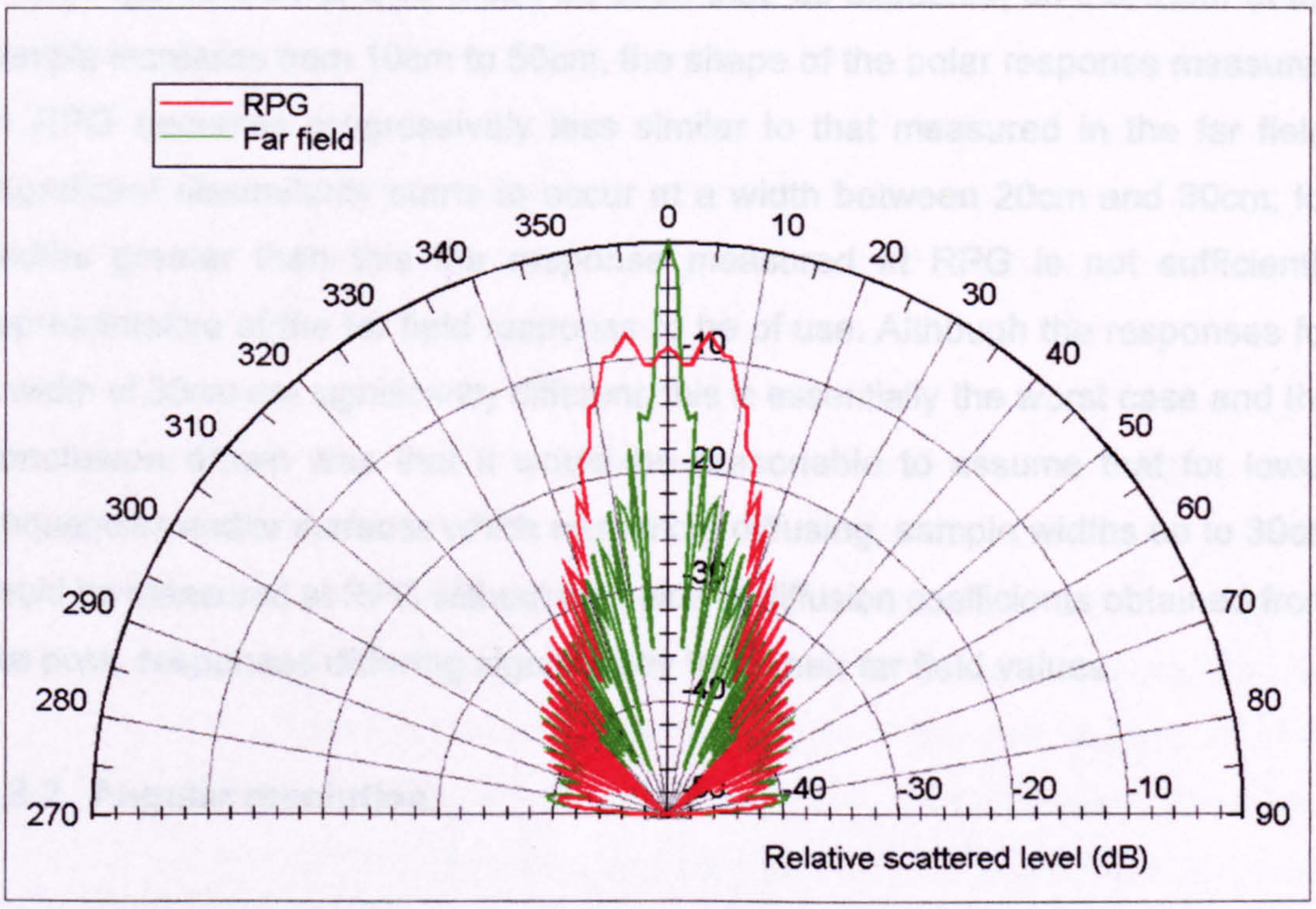

Figure 2.24: Predicted polar responses of 0.4m plane sample.

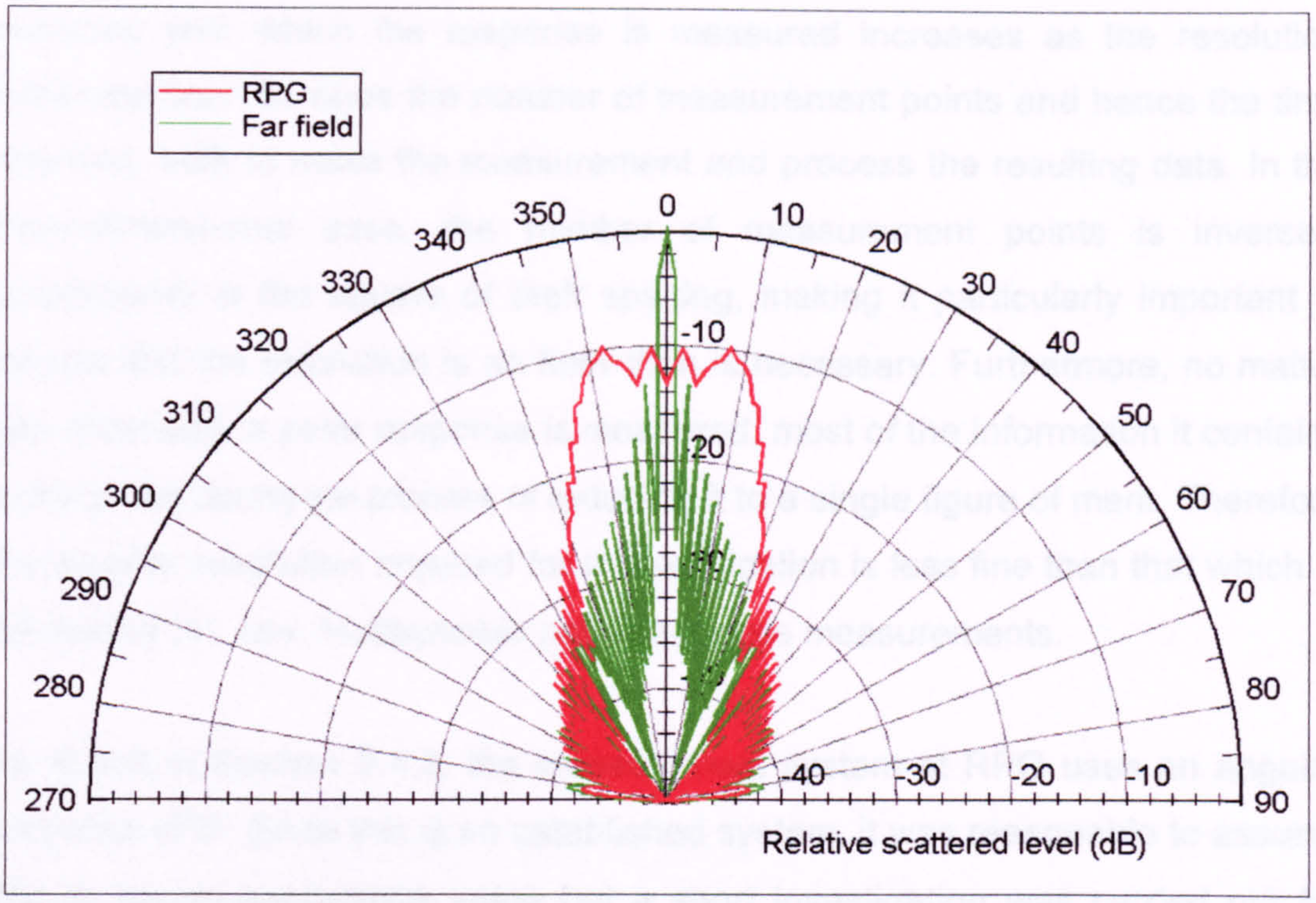

Figure 2.25: Predicted polar responses of 0.5m plane sample.

From Figures 2.21 to 2.25 it can be seen that, as expected, as the width of the sample increases from 10cm to 50cm, the shape of the polar response measured at RPG becomes progressively less similar to that measured in the far field. Significant dissimilarity starts to occur at a width between 20cm and 30cm; for widths greater than this the response measured at RPG is not sufficiently representative of the far field response to be of use. Although the responses for a width of 30cm are significantly different, this is essentially the worst case and the conclusion drawn was that it would be reasonable to assume that for lower frequencies and/or surfaces which were more diffusing, sample widths up to 30cm could be measured at RPG without the value of diffusion coefficients obtained from the polar responses differing significantly from their far field values.

2.8.2 **Angular resolution**.

An important parameter which must be considered when measuring polar responses is the angular spacing between individual measurement points. Determining this angular resolution involves compromise because although the

accuracy with which the response is measured increases as the resolution becomes finer, so does the number of measurement points and hence the time required, both to make the measurement and process the resulting data. In the three-dimensional case, the number of measurement points is inversely proportional to the square of their spacing, making it particularly important to ensure that the resolution is no finer than is necessary. Furthermore, no matter how accurately a polar response is measured, most of the information it contains is discarded during the process of reducing it to a single figure of merit. Therefore the angular resolution required for this application is less fine than that which is necessary for, say, loudspeaker polar response measurements.

As stated in Section 2.4.2, the measurement system at RPG uses an angular resolution of 5°. Since this is an established system, it was reasonable to assume this to be an appropriate value but a short investigation was carried out for verification purposes nevertheless. The normal incidence 20kHz polar responses, as measured at RPG, of a plane and a semicylinder were predicted using an angular resolution of 1°. The standard deviations of the sets of predicted levels comprising these responses were then calculated because, as stated in Section 1.4 and discussed in detail in Section 3.4, previous work has used this as the basis of simple diffusion coefficients. The standard deviations were then re-calculated using every other point in the responses, then every third one and so on to enable diffusion to be plotted as a function of angular resolution.

The reason for using both a plane and a semicylindrical sample for this investigation was that previous work has shown their polar responses to be very different[47]; one exhibits a specular reflection whereas the other shows essentially even scattering. The benefit of this is that it provides confidence in generalising the results because the shape of the polar responses of the vast majority of other surfaces will lie somewhere between these extremes. The polar responses were predicted at the highest RPG measurement frequency because this is the worst case; the number of maxima and minima is greatest, hence so is the chance of the diffusion parameter being affected by the angular resolution. Figure 2.26 shows, for both samples, the effect of the angular resolution on the diffusion parameter.

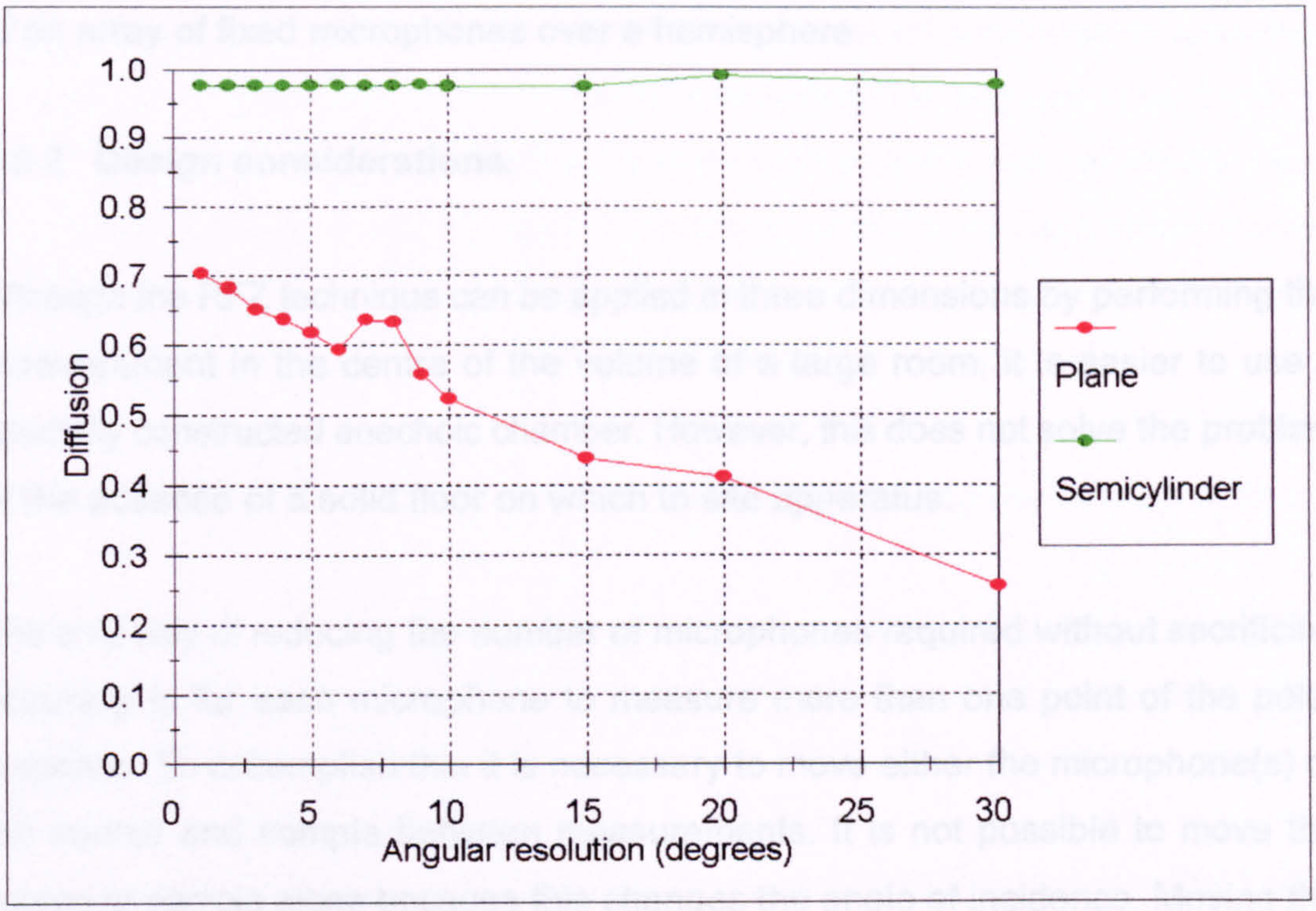

Figure 2.26: Effect of the angular resolution on a simple diffusion parameter.

The salient result is that even in worst-case conditions, this calculated value of diffusion changes by less than 10% as the angular resolution is decreased from 1° to 5°. This indicated that 5° would indeed be a sensible initial value; for most samples a finer resolution would greatly increase the number of measurement points but produce no significant increase in accuracy. However, the diffusion parameter used here is far from ideal and as new measures were developed during the course of the research, a check was made that 5° was still an appropriate angular resolution to be using.

2.9 **A new automated system for measuring three-dimensional polar responses**.

2.9.1 **Introduction**.

Extending the measurement of scattering from a single plane to three-dimensional half-space is theoretically simple but in practise requires a much more complex system. There are two principal causes of this increased complexity; the need for anechoic conditions to be extended to three dimensions and the prohibitive cost

of an array of fixed microphones over a hemisphere.

2.9.2 **Design considerations.**

Although the RFZ technique can be applied in three dimensions by performing the measurement in the centre of the volume of a large room, it is easier to use a specially constructed anechoic chamber. However, this does not solve the problem of the absence of a solid floor on which to site apparatus.

The only way of reducing the number of microphones required without sacrificing accuracy is for each microphone to measure more than one point of the polar response. To accomplish this it is necessary to move either the microphone(s) or the source and sample between measurements. It is not possible to move the source or sample alone because this changes the angle of incidence. Moving the microphone(s) is the more straightforward of the two options and was therefore the approach chosen. Cost dictated that a single microphone was used.

The simplest method of measuring half-space polar responses using a single microphone is for the microphone to traverse the surface of an imaginary hemisphere centred on the sample and measure the scattered pressure at a number of points spaced equally in angle. As discussed in Section 2.8.2, investigations concluded that an angular resolution of 5°, the value used at RPG, would also be suitable for three-dimensional measurements. It was further decided that this new system would share the same scale factor as that used at RPG, enabling the same samples to be measured using both systems. This was cost-effective and permitted the use of single-plane polar response measurements obtained at RPG to validate those obtained using the new apparatus.

The target measurement bandwidth was approximately 500Hz to 40kHz, which is double that of the RPG system and corresponds to 125Hz to 8kHz full-scale. Using this range of frequencies, extending to the ultrasonic, placed demanding constraints on the design of the measurement system. Not only were transducers which operated over this wide bandwidth required but any reflective object in the

sound field significant in size in comparison to a wavelength could potentially produce unwanted reflections; at 40kHz a wavelength is approximately 9mm. To reduce the probability of problematic reflections occurring, it was decided to cover the structures holding the sample and source in position with absorbent material and attempt to support and move the microphone without presenting an obstruction of more than a few millimetres to the sound incident on the sample.

2.9.3 **Structure for supporting the sample and moving the microphone**.

The apparatus designed and constructed for moving the microphone and supporting the sample is shown in Figure 2.27; the absorbent covers have been removed for clarity.

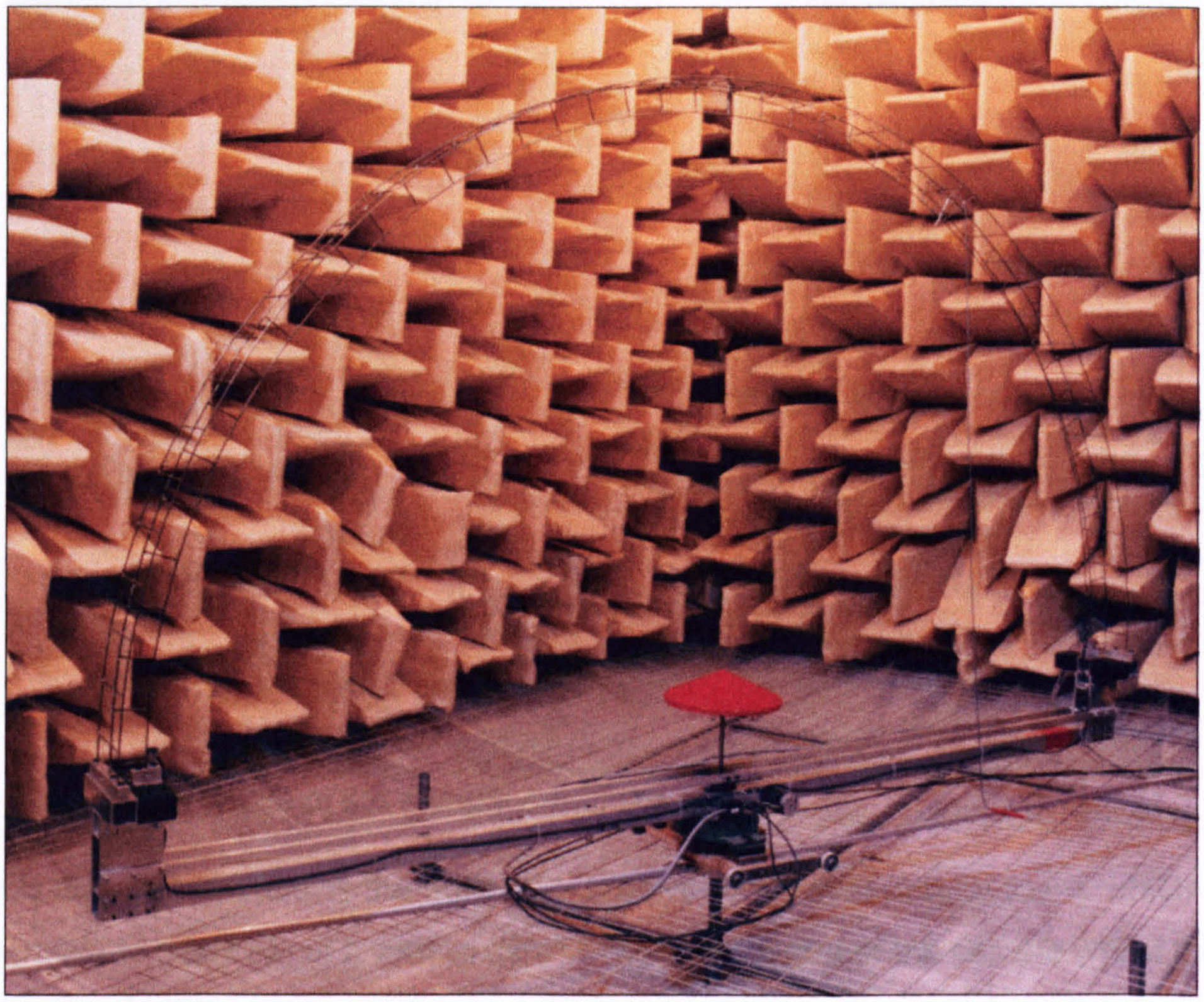

Figure 2.27: Apparatus for supporting the sample and moving the microphone over the surface of a hemisphere.

The sample - in this case the cone - is attached to a horizontal plate supported at

its centre by a vertical metal rod. This rod passes through a bearing situated on top of the middle of the horizontal beam forming the base of the semicircle, the beam itself and also the centre of the turntable to which the beam is attached as shown in Figure 2.28. Both the rod and the turntable are fixed to a medium-density fibreboard (MDF) base plate which supports the entire apparatus and is mounted atop a pole which is attached to the structural floor of the chamber.

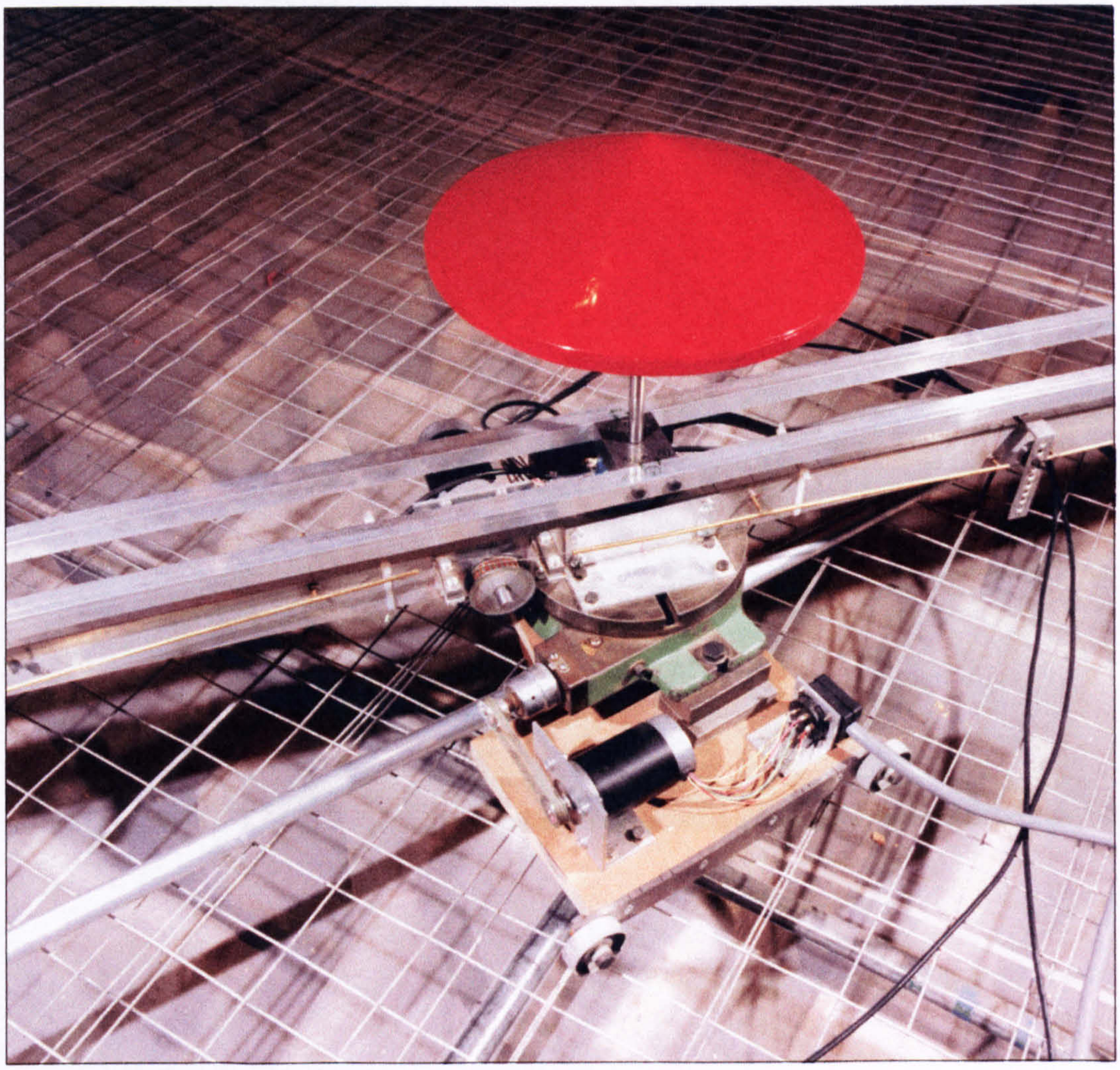

Figure 2.28: Detail of the sample mounting.

This arrangement allows the horizontal beam and the semicircular frame which it supports to rotate about a vertical axis through the centre of the sample whilst the sample itself remains stationary. When it rotates, the semicircular frame circumscribes a hemisphere with a radius of 1.5m centred on the sample and can therefore be used to position a microphone at the necessary points to measure the half-space polar response of the sample.

So as to present the minimum obstruction to the incident sound, the semicircular frame has a lattice construction of 4mm diameter steel rod. To provide sufficient rigidity a T-shaped cross-section is used and, as shown in Figure 2.29, the three extremities of the T double as rails on which a wire-frame trolley carrying the microphone and preamplifier runs.

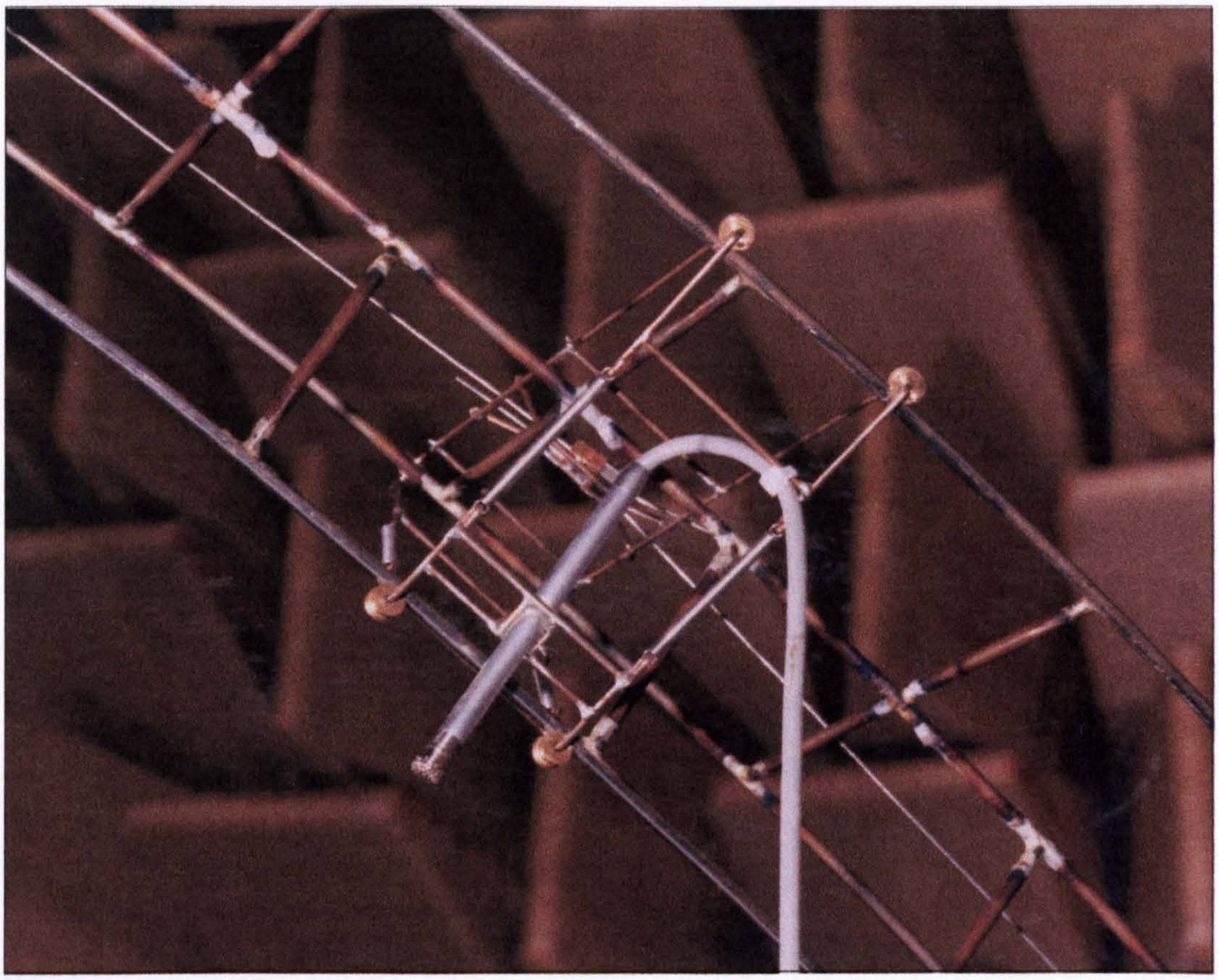

Figure 2.29: Microphone trolley.

2.9.4 **Microphone**.

The microphone and preamplifier are both ¼″ Brüel & Kjær units, types 4135 and 2670 respectively. These have a usable frequency response to in excess of 40kHz and are physically small. Figure 2.29 shows that the microphone is mounted radially and therefore points towards the centre of the sample whatever its elevation or azimuth. As a consequence, the directivity of the microphone - which may be significant at the higher measurement frequencies - does not need to be considered; a further advantage over a Cartesian positioning system.

2.9.5 **Structure for supporting the source**.

The source is mounted on a second, larger, semicircular frame centred on the sample as shown in Figure 2.30.

Figure 2.30: Complete apparatus for measuring three-dimensional polar responses.

This larger semicircle is 6m in diameter and fabricated from aluminium. To hold it in position in the anechoic chamber, it is suspended at its apex from the structural ceiling and supported at its ends by the wire mesh floor. Aluminium was used because the semicircle needs to be sufficiently rigid to accurately position the source but light enough that it does not distort under its own weight. The advantages of mounting the source on this semicircle instead of a simple stand are that changing the angle of incidence is straightforward, the axis of the source

2.9.5 **Structure for supporting the source**.

The source is mounted on a second, larger, semicircular frame centred on the sample as shown in Figure 2.30.

Figure 2.30: Complete apparatus for measuring three-dimensional polar responses.

This larger semicircle is 6m in diameter and fabricated from aluminium. To hold it in position in the anechoic chamber, it is suspended at its apex from the structural ceiling and supported at its ends by the wire mesh floor. Aluminium was used because the semicircle needs to be sufficiently rigid to accurately position the source but light enough that it does not distort under its own weight. The advantages of mounting the source on this semicircle instead of a simple stand are that changing the angle of incidence is straightforward, the axis of the source

always points towards the sample and the source to sample distance is fixed.

2.9.6 **Source**.

The source is a Visonik 6003 two-way ported loudspeaker which comprises a Vifa D20TD-47 tweeter and a Visonik T100.25.164 woofer. This unit was chosen because the manufacturer states that the frequency response extends to beyond 30kHz and it is physically small. A two-way loudspeaker is not ideal for this application because the angle of incidence is to some extent frequency dependent and thus difficult to define precisely. However a commercially available single transducer or co-axial combination with an operating range of 500Hz to 40kHz could not be identified. The possibility of using a ribbon or plasma loudspeaker was investigated but nothing operating down to the 500Hz region that is not prohibitively large exists at the present time. The port in the rear of the loudspeaker was blocked with Blu-Tack® to prevent any sound emanating from it and confusing the measurement. The purpose of the port is to extend the low frequency response and this is of no concern in this application.

To verify that the source operated satisfactorily over the frequency range stated by the manufacturer, its sensitivity was measured as a function of frequency using standard techniques[48], the microphone being aligned with the centre of the front face of the loudspeaker.

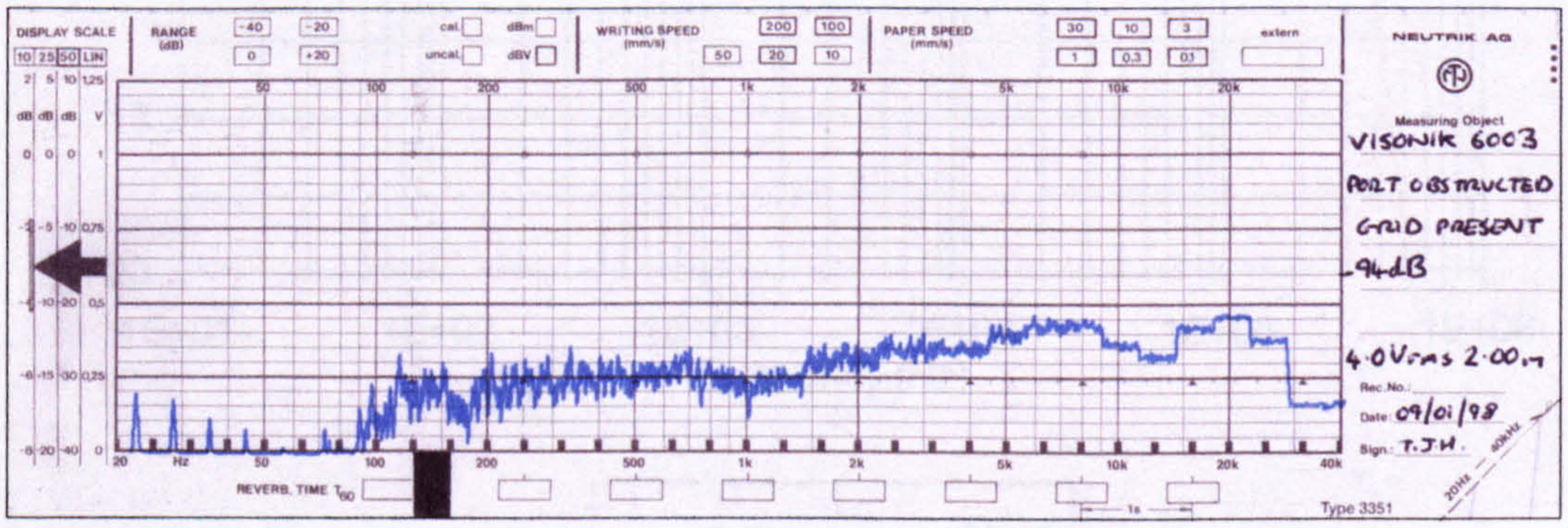

Figure 2.31: Frequency response of the Visonik 6003 loudspeaker.

Figure 2.31 shows the result and it can be seen that although the frequency response does extend to beyond 30kHz, there is a decrease in sensitivity of almost

10dB between the 25kHz and 31.5kHz third-octave bands. Consequently the measurement bandwidth was slightly less than desired.

2.9.7 **Power amplifier**.

A specialist power amplifier, designed and constructed at the University of Salford for previous research, was used to drive the source. Although it was known that this amplifier had an essentially flat frequency response to beyond 20kHz, the exact shape of its response at higher frequencies was unknown. For this reason the response was measured using standard techniques[49] with a 10Ω resistive dummy load connected and output levels of 0dB and +20dB. Figure 2.32 shows the results and it can be seen that the response is flat to frequencies beyond the point where the sensitivity of the source rolls off. Note that the +20dB trace is terminated at 50kHz because above this frequency, at this output level, distortion resulting from slew-rate limiting occurred.

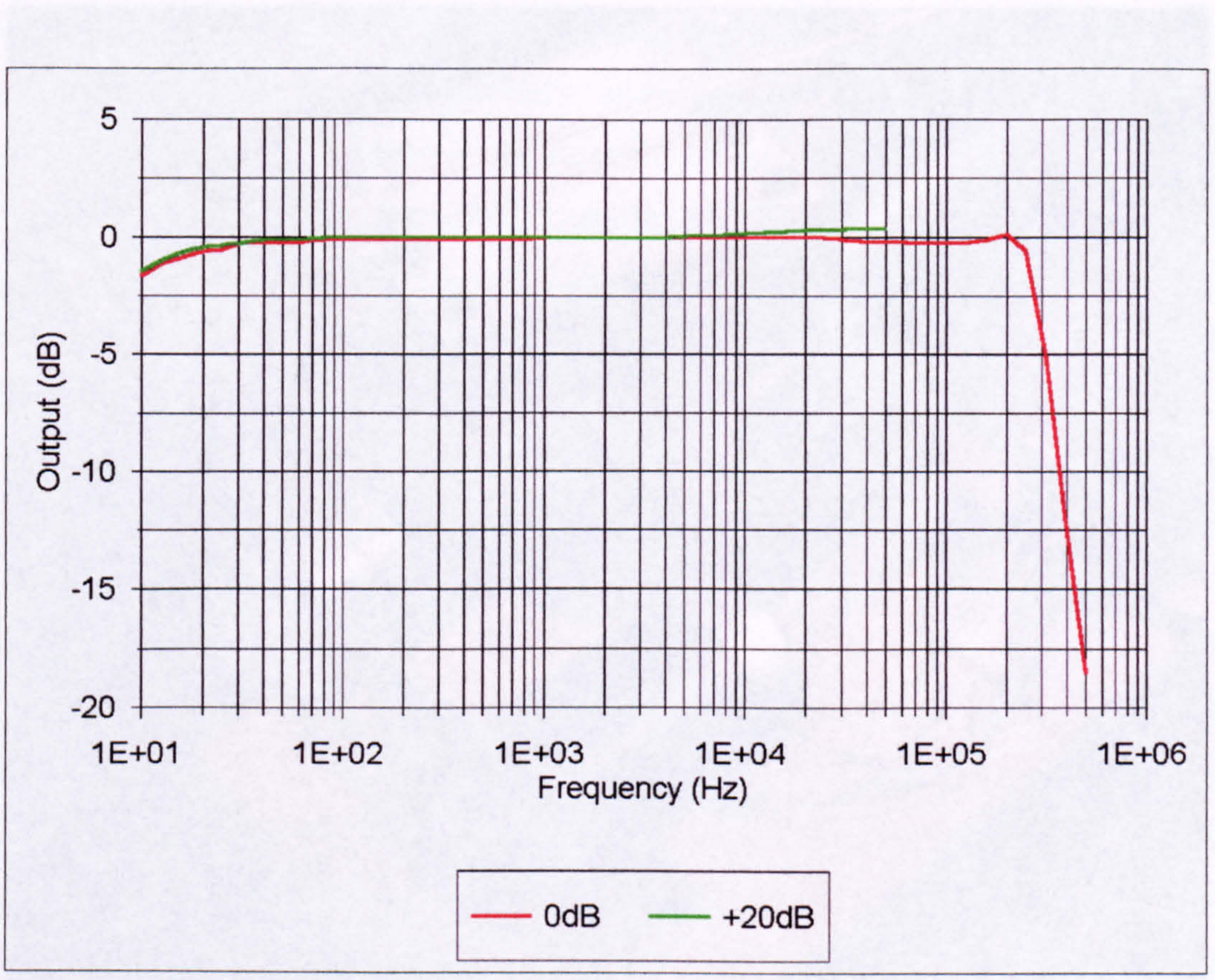

Figure 2.32: Frequency response of power amplifier.

2.9.8 **Automating movement of the microphone**.

Although the half-space polar response could be measured manually using the apparatus shown in Figure 2.30 it would be a very laborious task because the microphone would have to be moved to a new position between each measurement. To overcome this problem the microphone is moved automatically between measurements by a computer controlled electro-mechanical system.

The microphone trolley is attached to a continuous loop of thin steel cable which runs around the outside of the semicircular frame and along the side of the horizontal beam, where it is contained within a tube to prevent excessive vibration. Close to where the beam is attached to the turntable, the cable is wound around a pulley which is driven directly by a stepper motor. Both pulley and stepper motor can be seen in the top left of Figure 2.33.

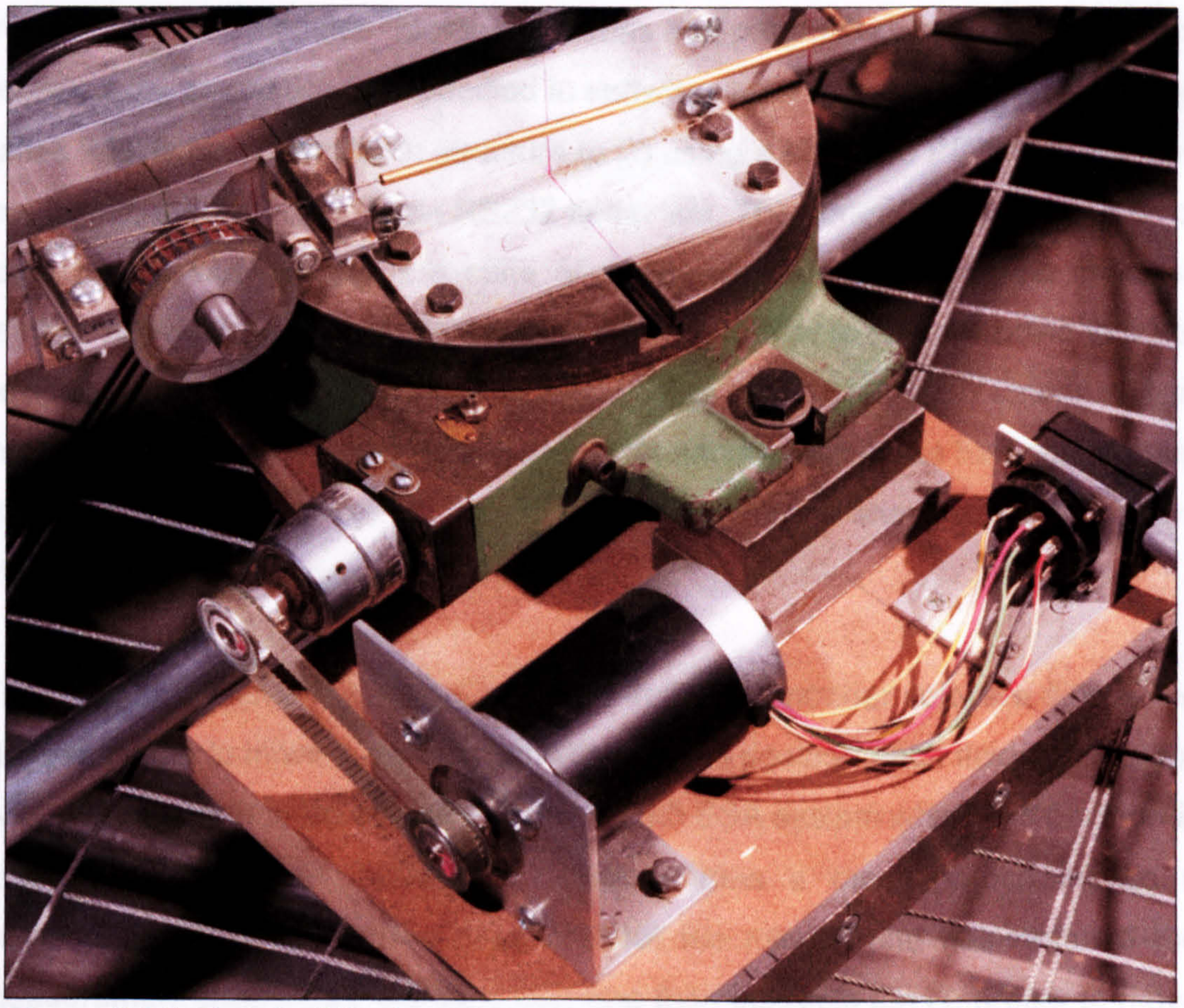

Figure 2.33: Detail of the two stepper motors and drive mechanisms.

The required tension and number of turns on the pulley to ensure that there was sufficient friction that the cable did not slip but instead caused the microphone trolley to traverse the semicircular frame when the stepper motor operated were determined by experiment. The diameter of the pulley is such that one revolution changes the angle of elevation of the microphone by approximately 5°.

The azimuthal position of the microphone is controlled by a second stepper motor which can be seen in the foreground of Figure 2.33. This motor drives the turntable and thus rotates the whole semicircular frame around the sample. The turntable is driven via a toothed belt and a 120:1 reduction gearbox so one revolution of the stepper motor corresponds to a change in azimuth of exactly 3°.

2.9.9 **Control and measurement system**.

To control the stepper motors, a programmable two-axis controller was assembled from commercial modules. Motor operations and parameters such as start, stop, acceleration, speed etc are specified in software written in a high level language called RSL (which is similar in structure to C) using a standard PC text editor and loaded into the controller via an RS232 serial link. The controller has a number of logic inputs and outputs, the state of which can be examined and changed respectively by the software. This enables the controller to be connected to other devices and for this application it was interfaced to a MLSSA measurement system installed on a PC to enable fully automated measurements of the half-space polar response to be performed. Figure 2.34 on the next page shows a block diagram of the entire measurement system.

The basic operation of the control system is that the controller software directs the stepper motors to move the microphone to the next position each time the MLSSA system instructs it to do so and informs the MLSSA system when this position is reached. The MLSSA system concurrently runs a macro which makes a measurement each time it is informed that the microphone has reached the measurement position by the controller and then instructs the controller to move the microphone to the next position when the measurement is finished and the

results saved. This process continues automatically until a pre-determined number of measurements have been made. Measurement of the full half-space polar response at an angular resolution of 5° takes just less than 2½ hours.

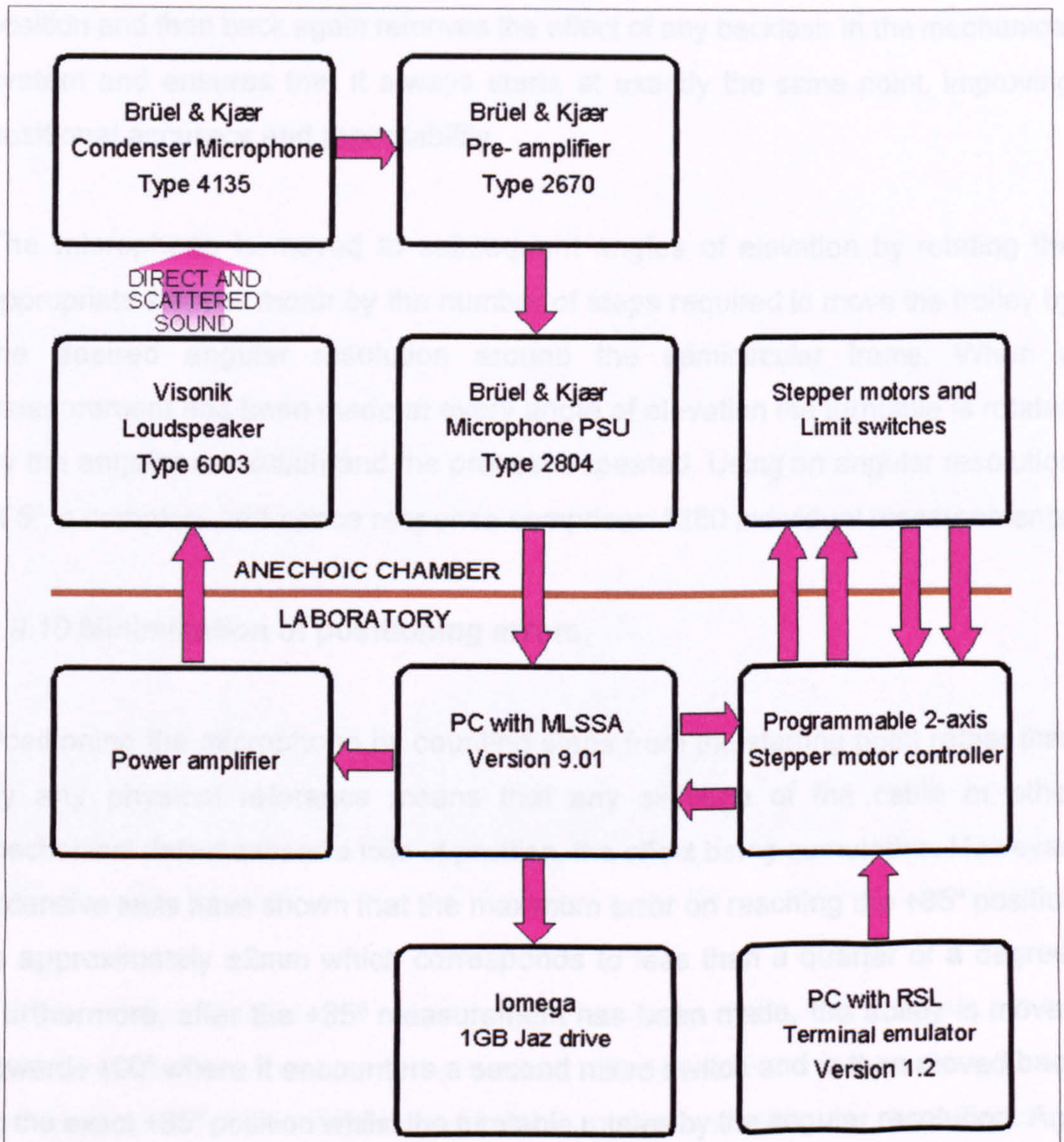

Figure 2.34: Block diagram of the complete system for measuring three-dimensional polar responses.

The first measurement position is at an angle of 85° from the sample normal rather than 90° because compromises made when practical difficulties were encountered during construction of the semicircular frame resulted in the microphone trolley being unable to reach the ±90° positions but this is not considered a significant shortcoming. To reach this first position, the controller moves the trolley at

speed towards -90° but a short distance after passing -85° the trolley operates a micro switch connected to the controller. This causes the trolley to stop before being moved back a fixed number of steps so that the microphone comes to rest at the -85° position. This process of moving the microphone beyond the desired position and then back again removes the effect of any backlash in the mechanical system and ensures that it always starts at exactly the same point, improving positional accuracy and repeatability.

The microphone is moved to subsequent angles of elevation by rotating the appropriate stepper motor by the number of steps required to move the trolley by the desired angular resolution around the semicircular frame. When a measurement has been made at every angle of elevation the turntable is rotated by the angular resolution and the process repeated. Using an angular resolution of 5°, a complete half-space response comprises 1260 individual measurements.

2.9.10 **Minimisation of positioning errors**.

Positioning the microphone by counting steps from the starting point rather than by any physical reference means that any slippage of the cable or other mechanical defect causes a loss of position, the effect being cumulative. However, extensive tests have shown that the maximum error on reaching the +85° position is approximately ±2mm which corresponds to less than a quarter of a degree. Furthermore, after the +85° measurement has been made, the trolley is moved towards +90° where it encounters a second micro switch and is then moved back to the exact +85° position whilst the turntable rotates by the angular resolution. Any positional error in elevation which has accumulated is therefore eliminated each time the microphone is moved to a new angle of azimuth.

The azimuthal position is also determined by counting steps but since the rotation is unidirectional and drive is via a toothed belt, position cannot be lost unless the belt jumps a tooth or the motor stalls and loses one or more steps. The belt tension and motor current required to ensure that this did not happen were determined by experiment.

2.9.11 **Absorbent covers**.

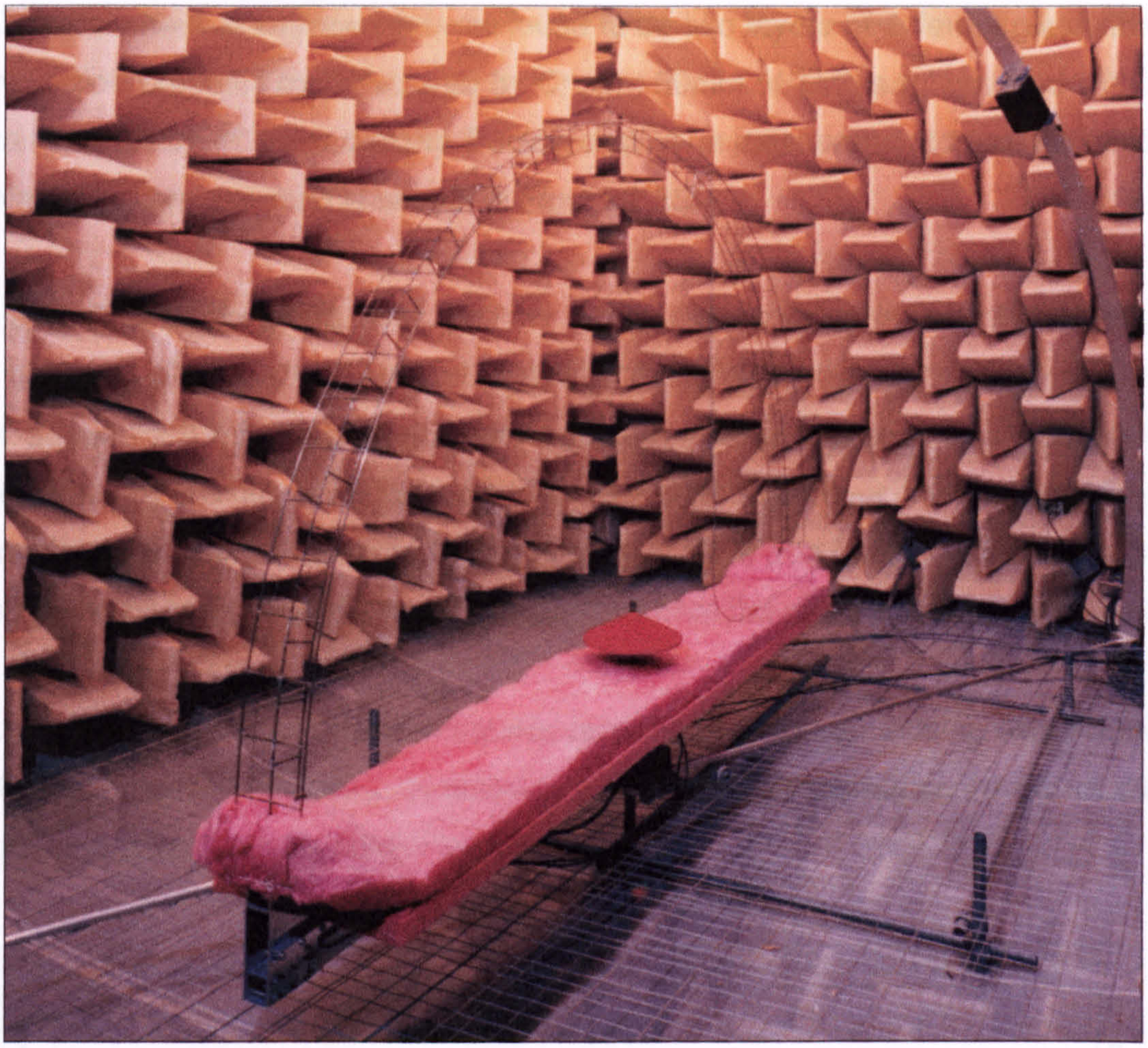

Figure 2.35: Absorbent cover in position on microphone positioning apparatus.

Experimental measurements of scattering performed whilst optimising the control system revealed the presence of unwanted reflections. This was not unexpected and from examination of their arrival times it was concluded that they originated from either the horizontal beam or the base-plate below. This area of the apparatus was therefore covered with an 80mm layer of a specialist open celled acoustic foam called PYROSORB-S which, according to literature provided by the supplier, has an absorption coefficient measured to BS EN 20354 close to unity above the 125Hz octave band. However, although this treatment did reduce the magnitude of the reflections it was not as effective as expected. Alternative absorptive treatments were tried experimentally, there appearing to be little correlation between their BS EN 20354 absorption coefficients and the amount by

which the magnitude of the unwanted reflections was reduced.

The most effective arrangement was found to be two layers of different glass fibre insulation products manufactured by Crown; 50mm of 'Dritherm' covered with a nominal 60mm of lower density 'Factoryclad'. The measurement apparatus with this glass fibre attached is shown in Figure 2.35.

2.9.12 **Data processing**.

In Section 2.9.2 it is stated that the half-space polar response of a sample is obtained by making a large number of measurements over the surface of an imaginary hemisphere centred on the sample. This is true but the polar response is not measured directly, it must be extracted from the raw measurement data.

At each microphone position an impulse response is measured using established MLS techniques[41]. Figure 2.36 shows a typical impulse response; the direct and reflected sound can be readily identified.

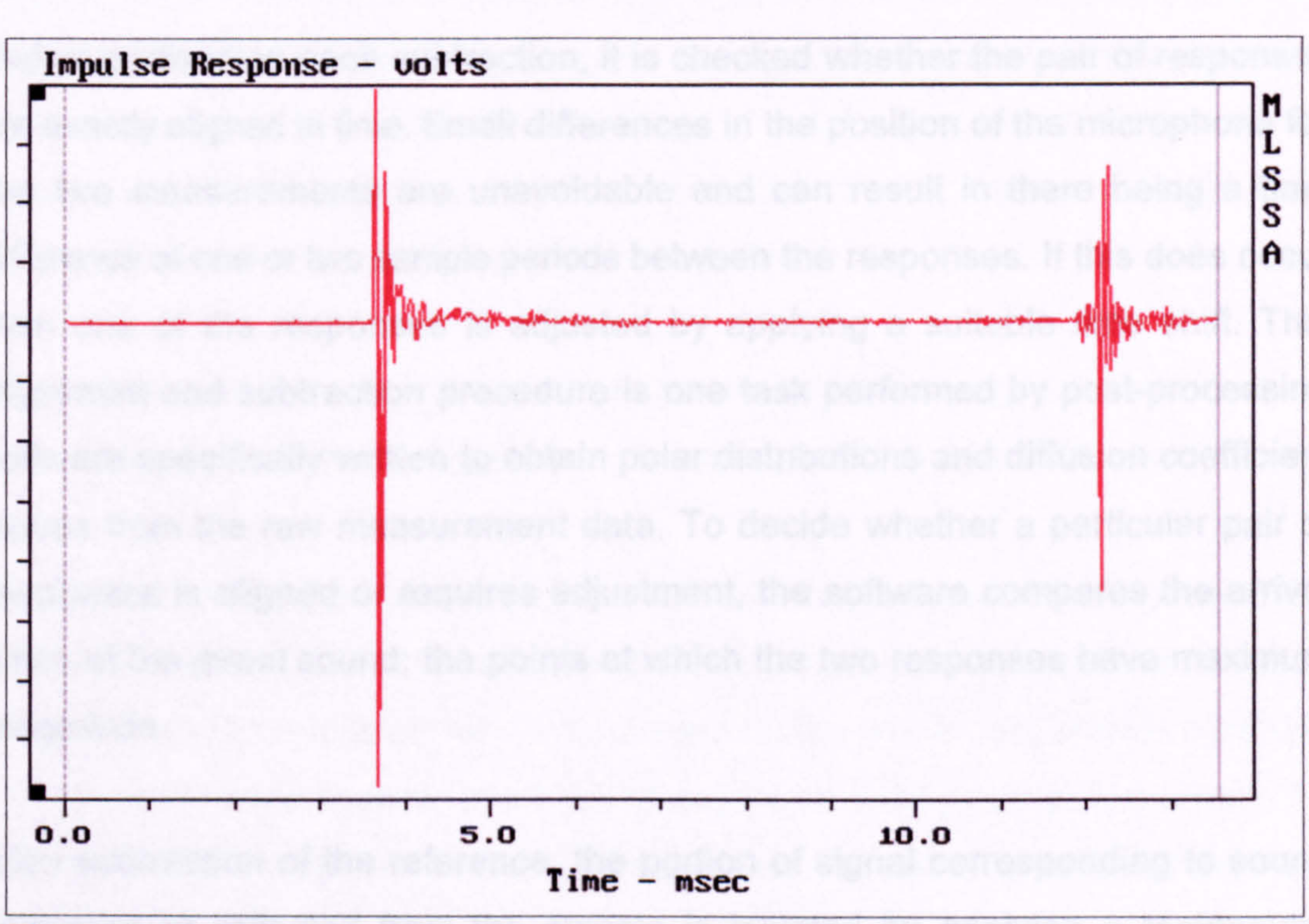

Figure 2.36: Typical impulse response measured using MLSSA.

The length of MLS stimulus used was 65536 points and a 4096 point impulse response was calculated. The sampling frequency was 75.47kHz, permitting calculation of the polar response up to the 25kHz third-octave band. Once the impulse response has been calculated, it is saved to disk as a binary file with a unique filename for post-processing and the microphone moved to the next position.

Although theoretically the polar response can be extracted directly from the set of measured impulse responses, in practise the signal to noise ratio is too low for quality results to be obtained, especially at angles where little energy is scattered. The signal to noise ratio is greatly increased and hence much better results obtained if a second set of impulse responses are measured without the sample present and these reference measurements subtracted from the original set before further processing. The reason for this is that although most of the apparatus is covered with fibrous absorbent, some low-level reflections are still observed in the impulse responses and these are removed by the subtraction because they occur whether or not the sample is present.

Before performing each subtraction, it is checked whether the pair of responses are exactly aligned in time. Small differences in the position of the microphone for the two measurements are unavoidable and can result in there being a time difference of one or two sample periods between the responses. If this does occur then one of the responses is adjusted by applying a suitable time shift. This alignment and subtraction procedure is one task performed by post-processing software specifically written to obtain polar distributions and diffusion coefficient values from the raw measurement data. To decide whether a particular pair of responses is aligned or requires adjustment, the software compares the arrival times of the direct sound; the points at which the two responses have maximum magnitude.

After subtraction of the reference, the portion of signal corresponding to sound scattered or reflected from the sample is isolated by applying a rectangular window. The beginning of this window can be calculated from geometrical

considerations but the end is more difficult to determine because sound can be reflected from one part of the sample to another before propagating to the microphone. For this reason the window was defined manually for each sample by inspection of the impulse responses.

After windowing and appending padding zeros if necessary to fill the analysis frame, a 1024-point FFT is applied to the signal to obtain its power spectrum. This gives results at 512 real frequencies with a resolution of approximately 15Hz full-scale. From these results, third-octave band levels are calculated. The polar response at any particular third-octave band can then be constructed from the appropriate band levels calculated at each measurement position.

2.9.13 **Signal to noise ratio.**

Defining the signal to noise ratio of the measurement as the difference between the pressure measured at a point with and without the sample present, a maximum broadband value of 55dB was achieved when measuring the normal reflection from a plane sample. The optimum source level was determined by experiment; it was found that increasing the level increased the signal to noise ratio to its maximum value but beyond this a significant amount of noise materialized in the impulse responses. The likely source of this noise is distortion in the loudspeaker, MLS measurements being particularly sensitive to this[50].

2.10 **Comparison of polar responses measured using the new Salford system with both measurements made at RPG and BEM predictions.**

Figures 2.37 and 2.38 show two typical but differently shaped single-plane polar responses measured at both Salford and RPG. In both cases the results obtained using the different measurement systems are on the whole very similar, although in Figure 2.37 some disparity is evident at angles close to grazing. The reason for this discrepancy could be that at low frequencies the distance between the base of the sample and the absorbent attached to the apparatus, shown in Figure 2.35, is too small in comparison to a wavelength. This distance is less than intended

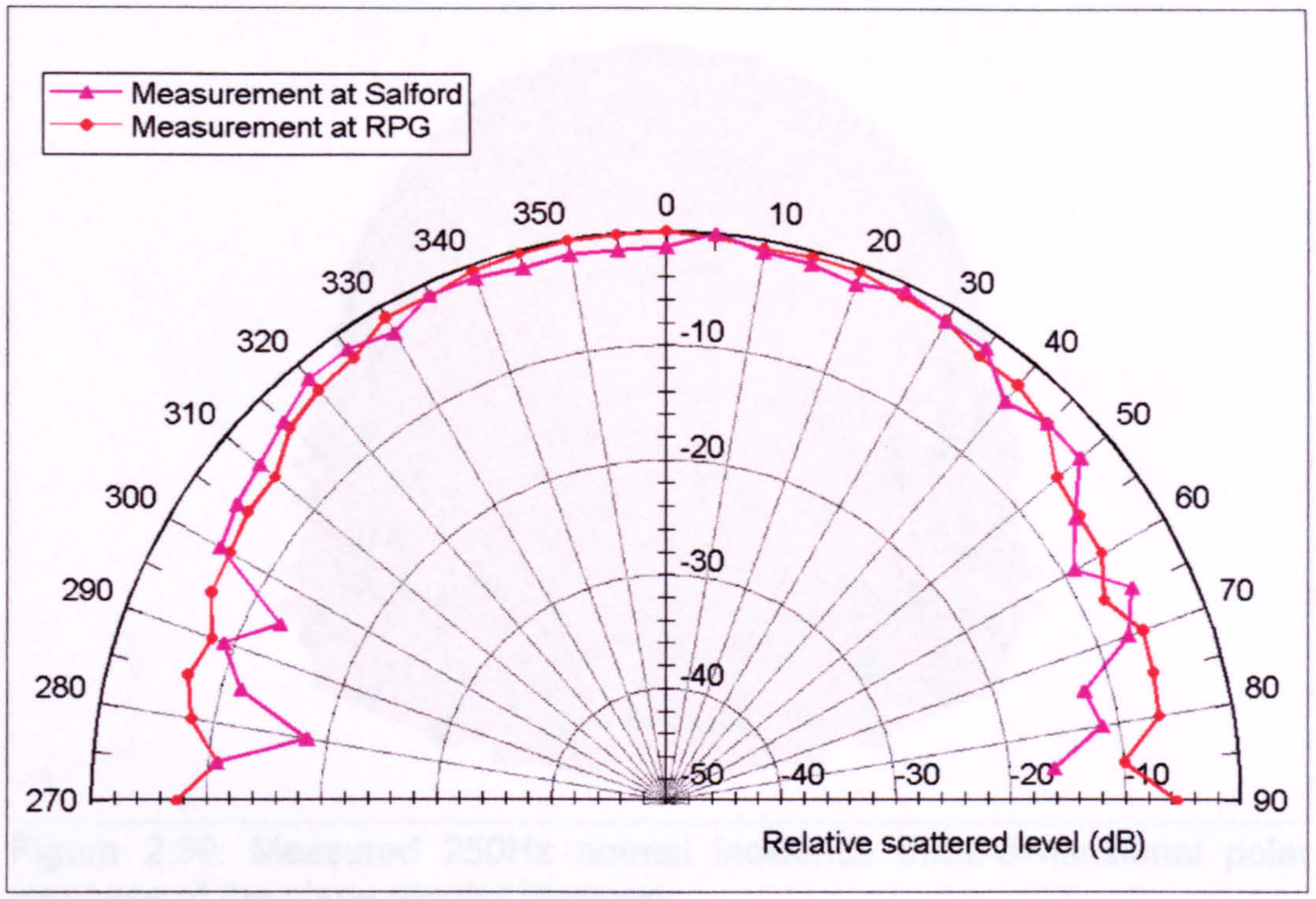

Figure 2.37: Comparison of the 250Hz normal incidence, single-plane, polar responses of the square-based pyramid measured at RPG and Salford.

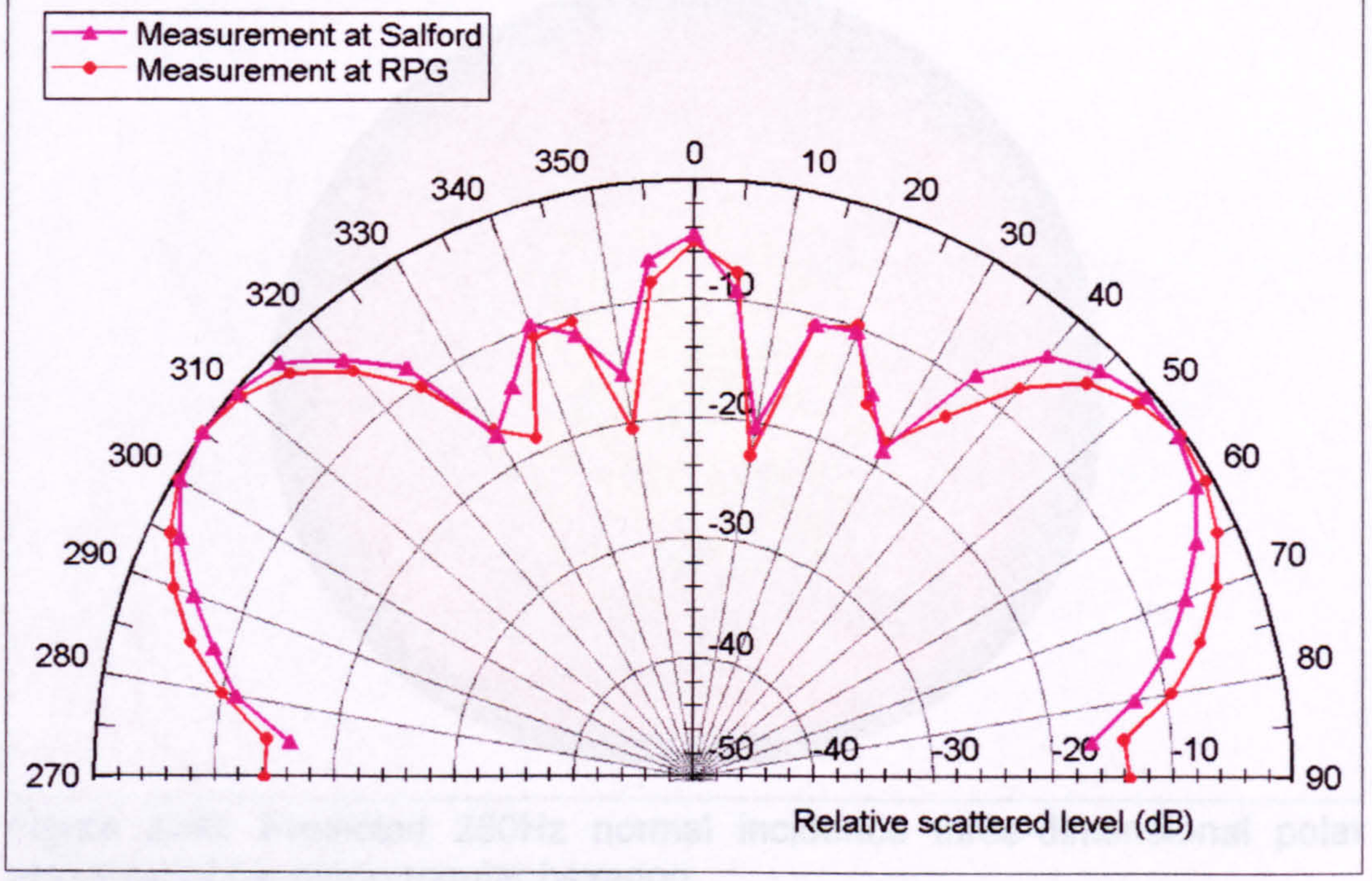

Figure 2.38: Comparison of the 1kHz normal incidence, single-plane, polar responses of the cone measured at RPG and Salford.

Figure 2.39: Measured 250Hz normal incidence three-dimensional polar response of the plane regular hexagon.

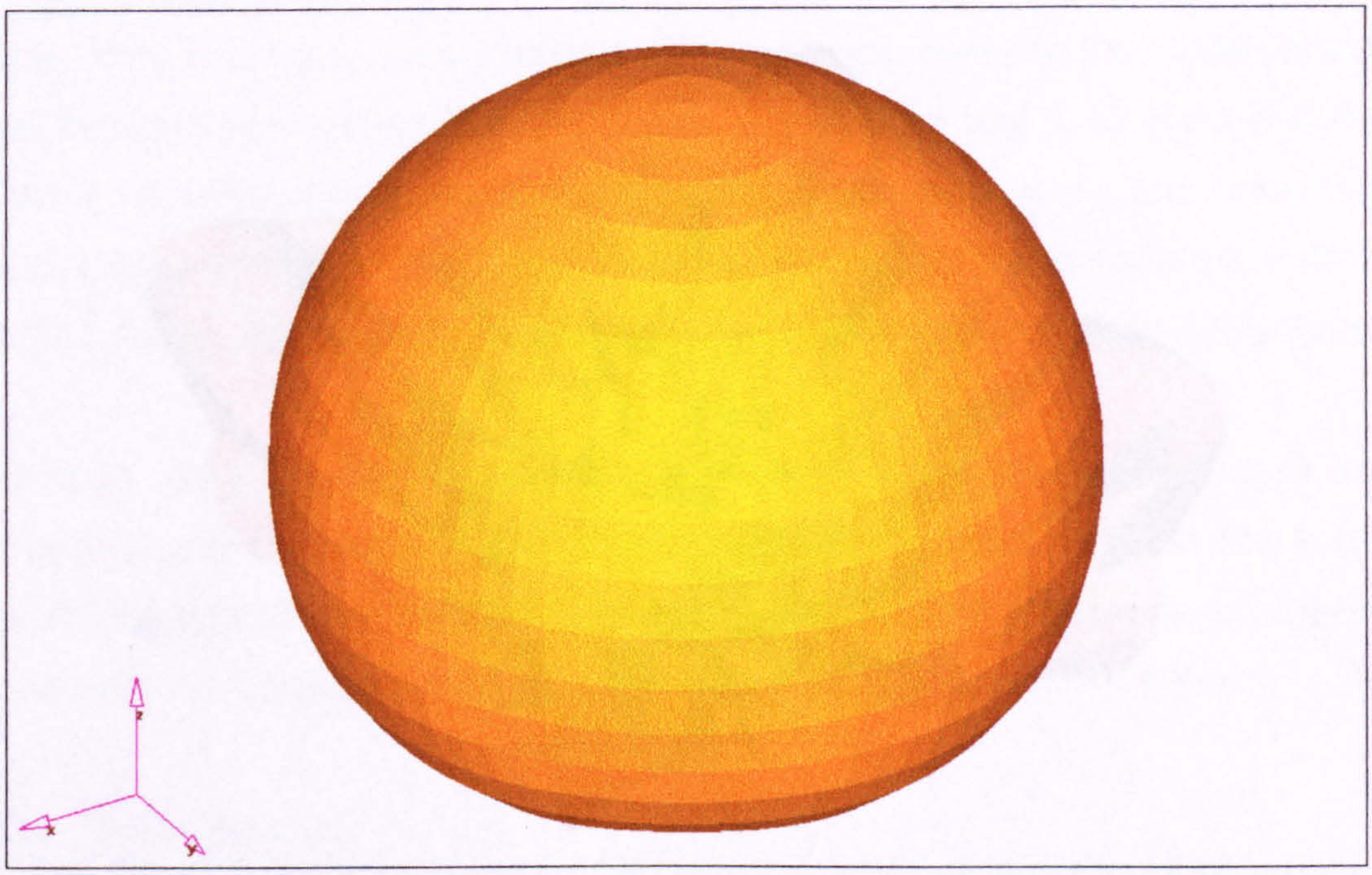

Figure 2.40: Predicted 250Hz normal incidence three-dimensional polar response of the plane regular hexagon.

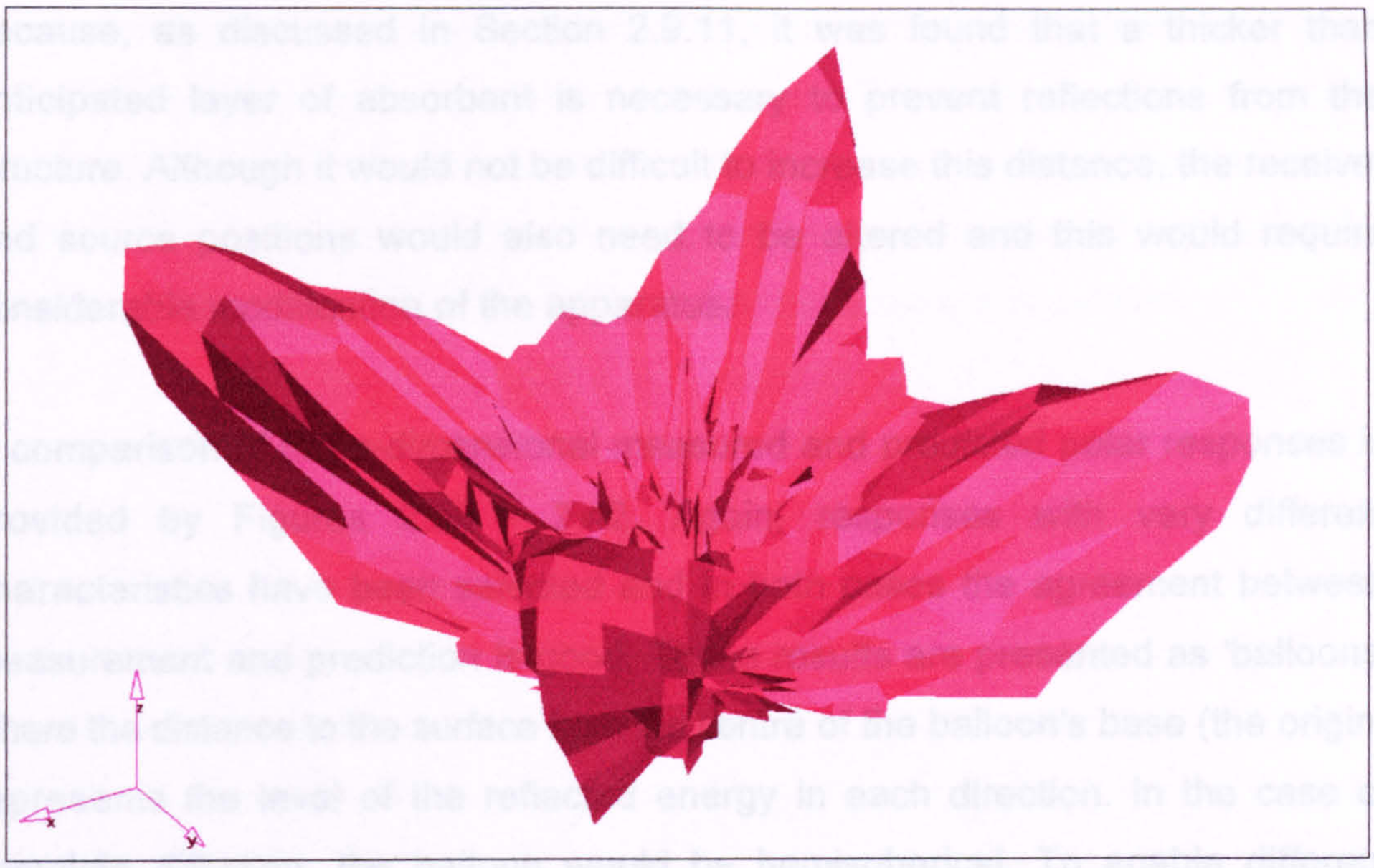

Figure 2.41: Measured 2kHz normal incidence three-dimensional polar response of the square-based pyramid.

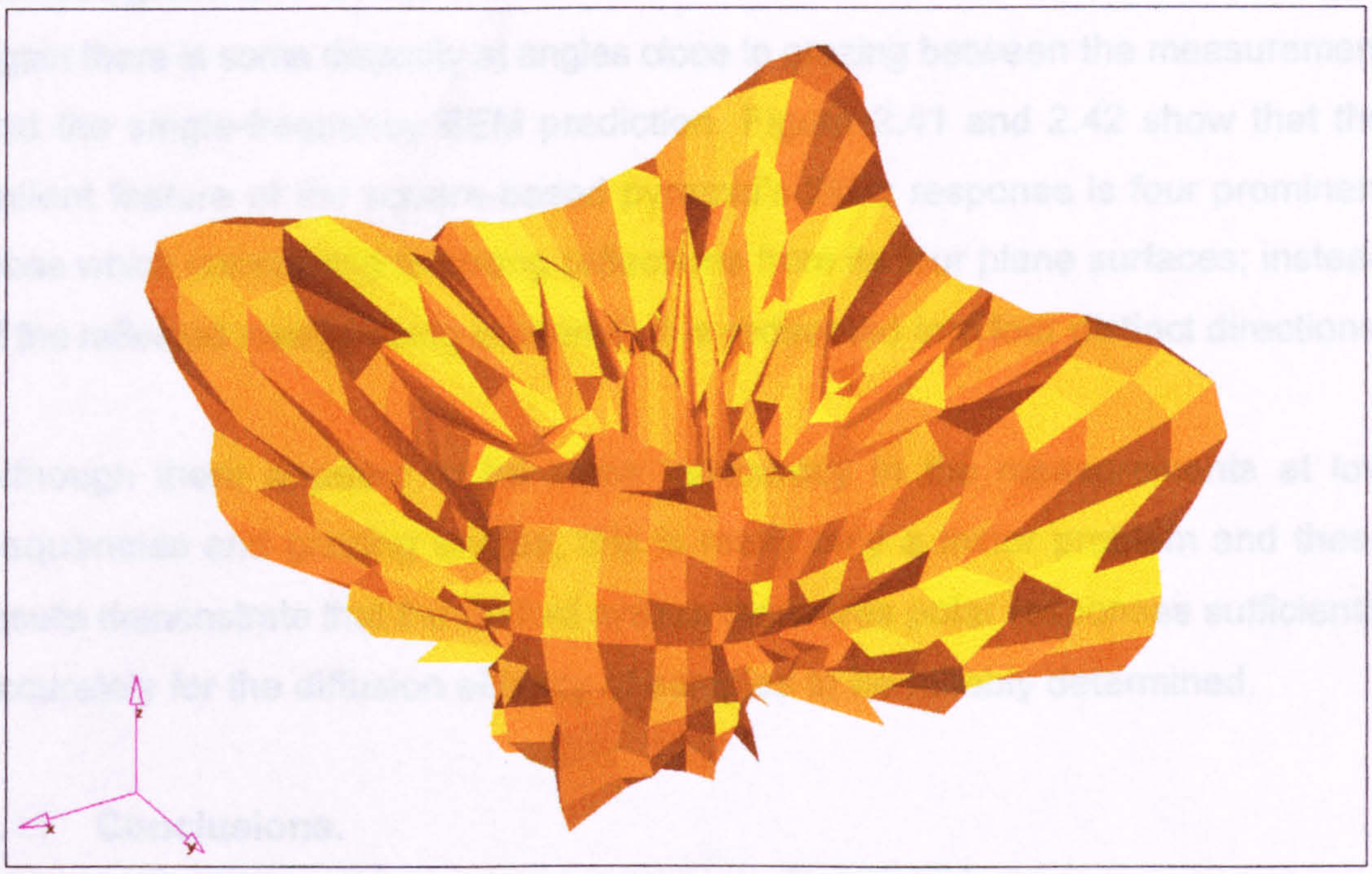

Figure 2.42: Predicted 2kHz normal incidence three-dimensional polar response of the square-based pyramid.

because, as discussed in Section 2.9.11, it was found that a thicker than anticipated layer of absorbent is necessary to prevent reflections from the structure. Although it would not be difficult to increase this distance, the receiver and source positions would also need to be altered and this would require considerable modification of the apparatus.

A comparison of three-dimensional measured and predicted polar responses is provided by Figures 2.39 - 2.42. Again, responses with very different characteristics have been selected and in both cases the agreement between measurement and prediction is good. These results are presented as 'balloons' where the distance to the surface from the centre of the balloon's base (the origin) represents the level of the reflected energy in each direction. In the case of complete diffusion, the balloon would be hemispherical. To enable different responses to be compared, the maximum distance between the origin and the surface corresponds to 50dB in all cases. Figures 2.39 and 2.40 show that for a plane surface similar in size to a wavelength the reflected level is independent of azimuth, greatest in the normal direction and decreases with decreasing elevation. Again there is some disparity at angles close to grazing between the measurement and the single-frequency BEM prediction. Figure 2.41 and 2.42 show that the salient feature of the square-based pyramid's 2kHz response is four prominent lobes which correspond to strong reflections from its four plane surfaces; instead of the reflected energy being scattered, it is redirected into four distinct directions.

Although there appears to be some inaccuracy in the measurements at low frequencies and grazing angles, this is really only a minor problem and these results demonstrate that the Salford system measures polar responses sufficiently accurately for the diffusion efficacy of samples to be reliably determined.

2.11 Conclusions.

In this chapter the techniques employed during the research for measuring and predicting polar responses, along with the sample surfaces measured, have been described. A new automated system for measuring polar responses in three-

dimensions has been discussed in detail. A selection of measurements have been presented and shown to agree with predictions. The problem of the response shape depending on the measurement distance except in the far field has been outlined. This is discussed further in Chapter 3, where methods of evaluating the diffusion efficacy of samples from their polar response are examined.

3. CHARACTERISING DIFFUSION FROM POLAR RESPONSES.

3.1 Introduction.

This chapter investigates how polar responses, obtained using the measurement or prediction techniques discussed in Chapter 2, can be used to evaluate the diffusion efficacy of surfaces. The most common approach is to examine the similarity between the shape of the response and that corresponding to complete diffusion. After discussing the response shape which best represents complete diffusion, a number of previously published diffusion parameters are described and appraised. Measured and predicted results are used to demonstrate the situations in which these parameters can be most successfully applied and those in which they fail. New polar response diffusion parameters formulated during the course of this research are also presented. It is demonstrated that one of these original parameters, which is based on the concept of autocorrelation, is superior to those previously published. To simplify presentation, most of the discussions are illustrated using single-plane responses but in general they extend to three-dimensions. Issues specific to quantifying diffusion from three-dimensional responses are addressed in Section 3.11, again using measured and predicted results. Also examined in this chapter are the practical limitations of using polar responses to quantify diffusion, particular attention being given to the consequences of the response shape varying with the source and receiver distances.

3.2 Defining complete and zero diffusion in terms of polar response shape.

3.2.1 Introduction.

If polar responses are to be used to quantify diffusion, then it is necessary to establish the connection between their shape and the diffusion efficacy of the surfaces to which they relate. Only when this has been established is it possible to define parameters which evaluate diffusion by reducing the polar response to

a single figure of merit. A first step is to determine the response shapes corresponding to complete and zero diffusion. When considering the propagation of sound in enclosed spaces, analogies are sometimes drawn with optics, the movement of energy around the space being modelled using the concept of rays[51]. The optical definition of complete diffusion is the case where the energy in an incident light ray is scattered in accordance with Lambert's cosine law[27]. This definition has been carried over into acoustics by being implemented in many ray-tracing computer models.

3.2.2 **Lambert's cosine law**.

Suppose that an elemental area, dS, of a rough surface is esonified by a bundle of parallel or nearly parallel rays which make an angle θ_o to its normal, as illustrated in Figure 3.1.

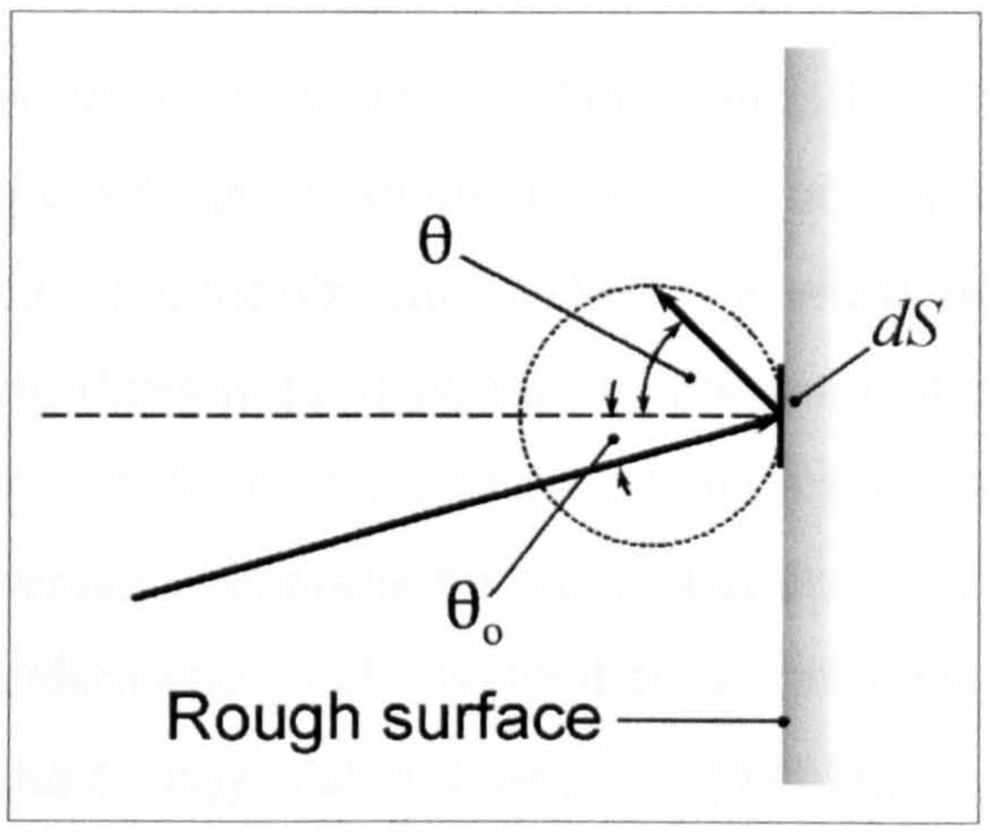

Figure 3.1: Reflection from a rough surface according to Lambert's law.

Lambert's cosine law states that if the intensity of these rays is I_o then the intensity of the scattered sound will be given by:

$$I(r,\theta) = I_o dS \frac{\cos\theta \cos\theta_o}{\pi r^2} = B_o dS \frac{\cos\theta}{\pi r^2} \qquad (3.1)$$

where:

θ = Angle between the scattering direction and the surface normal

r = Distance from the reflecting area element dS

B_o is known as the 'irradiation strength', it is the energy incident on unit area of the surface per second.

The problem with Lambert's law is that it only applies to the case of incoherent point scattering, whereas in room acoustics wavelengths can be large and surfaces are finite. These conditions result in coherent wave behaviour, the pressure in the reflected sound field being determined by interference effects. If the reflections were not coherent then profiled diffusers based on wells, such as those described by Schroeder[30], would not work.

In an enclosure in which there exists a diffuse field, then above the Schroeder frequency[52], the energy reflected from any point on a boundary surface, averaged over time, does obey Lambert's law. It has therefore been suggested that Lambertian scattering does indeed equate to complete diffusion, as has been assumed in computer models. This is despite the fact that each individual reflection in a reverberation chamber with plane surfaces is specular and it is only because the time-averaged incident energy at any point on a surface is Lambertian that the time-averaged reflected energy is also. Modern applications of specialist diffusion often have the aim of reducing the prominence of first-order specular reflections by scattering this energy into other directions; the promotion of a Lambertian diffuse field is therefore not a primary concern. To establish the degree to which this objective is accomplished, it is necessary to examine the polar response of the surface as a whole, not just reflections at various points on it.

3.2.3 **Complete diffusion.**

If the purpose of diffusion is generally to reduce the prominence of specular reflections then a logical conclusion is that complete diffusion is the case where

the specular direction has zero prominence; the reflected energy is scattered uniformly in all directions, including the specular. This is the definition commonly used by designers of specialist diffusers[46] and is concordant with Schroeder's original work[30] in designing surfaces which produce diffraction lobes with uniform magnitudes. In some applications it may be more desirable for the diffuser to direct the reflected energy away from the specular direction completely, i.e. to create a notch in the polar response. Cox[8] has used this definition to evaluate the quality of small to medium sized diffusers mounted on large baffles, as discussed in Section 3.10. In fact for many polar response diffusion coefficients, the shape of the response defined as complete diffusion is of no great consequence because they can be adapted, usually by incorporating a weighting function, to rate diffusion accordingly. To avoid any confusion, uniform scattered intensity is the definition of complete diffusion used throughout this thesis when considering quantifying diffusion using polar responses, unless it is stated otherwise. The corresponding response shapes are a semicircle for single-plane scattering and a hemisphere in the three-dimensional case.

3.2.4 Zero diffusion.

Defining zero diffusion is more straightforward. Theoretically, zero diffusion is the case where no scattering occurs and all the incident energy is reflected in a single direction. This is essentially what happens in a ray-tracing model that does not include diffusion; at each reflection all the reflected energy is contained in one ray which propagates in the specular direction. This definition translates into practice as a polar response containing a single delta function, equal in extent to the dynamic range of the measurement system and of width dependent on the angular resolution with which the response is measured.

3.3 Introduction to polar response diffusion parameters and their principal limitation.

Practical surfaces have polar responses with shapes which lie somewhere between the two extremes of uniformity and a delta function. Establishing exactly

where in this range they lie and hence indicating the diffusion efficacy of the surfaces, is the purpose of a diffusion parameter. Most polar response diffusion parameters accomplish this by using one particular characteristic of the response corresponding to complete diffusion to evaluate the degree of similarity between any given response and the complete case, the larger this is, the greater the diffusion. It should be noted that although many of these metrics are defined in terms of energy, strictly speaking the true outward propagating energy is not obtained unless the polar response is measured in the far field. Since this is not always the case, the metrics are in reality based on squared pressure.

As discussed in Section 2.7, the shape of the polar response of a surface is dependent on the source and receiver distances unless the measurement is performed in the far field. An important consequence of this is that the value of any parameter which evaluates the diffusion efficacy of a surface from its polar response shape is similarly dependent on the source and receiver distances. For example, Figure 3.2 shows how the shape of the single-plane, normal incidence, polar response of a plane surface changes as the receiver distance decreases, the source remaining in the far field.

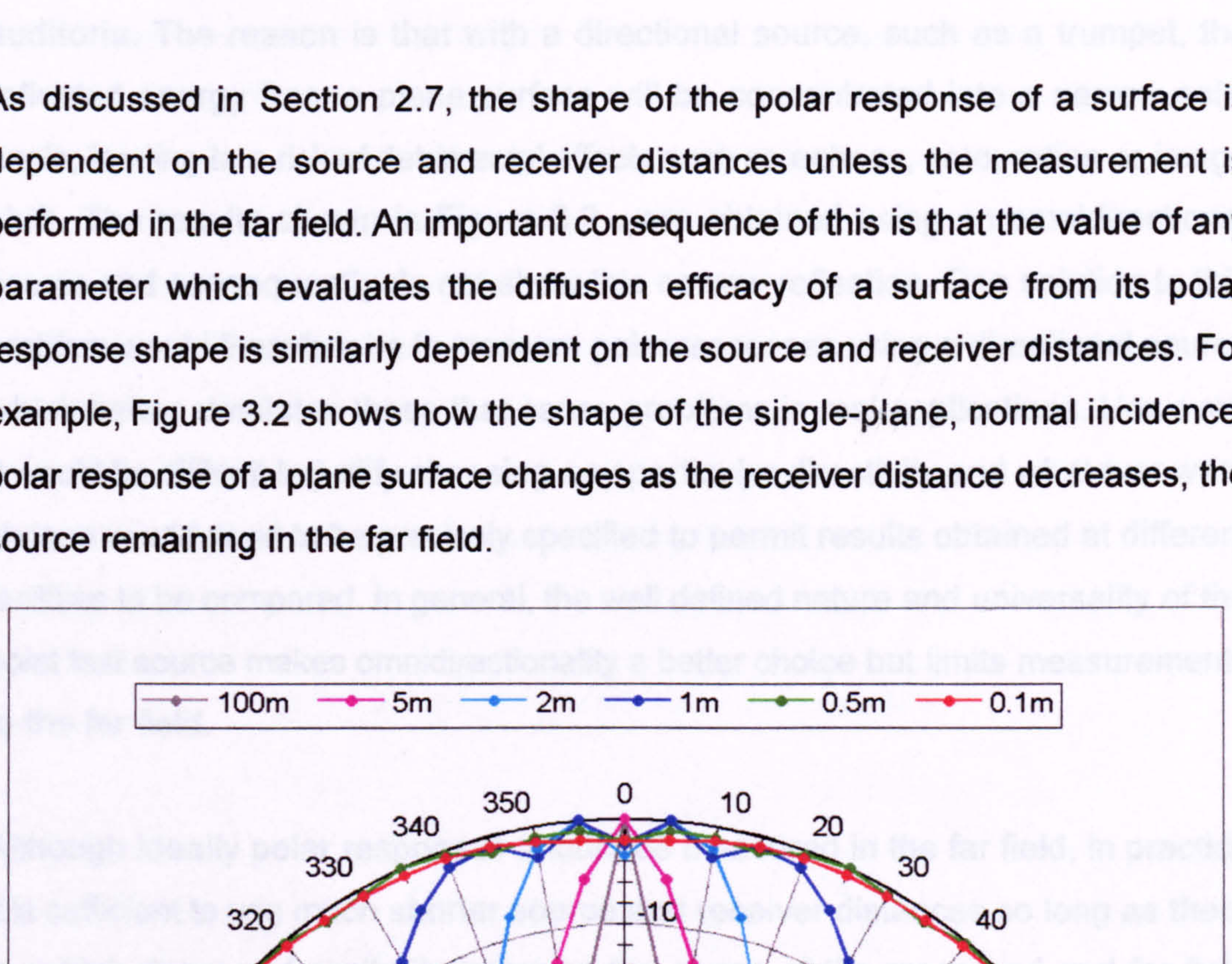

Figure 3.2: Effect of receiver distance on the shape of the normal incidence 5kHz polar response of a 1m square plane panel. BEM predictions.

The salient point is that the response becomes more uniform as the receiver distance decreases and would therefore be interpreted as becoming more diffuse. Using the responses measured at the shortest distances, the plane surface would be rated as a very good diffuser. (In fact, close enough to the surface, the reflection is provided by a simple image source that radiates the same energy to all receiver positions except for any minor effects due to spherical spreading). This contradicts experience acquired from room design, where plane surfaces are considered to be poor diffusers. To understand this contradiction, it is necessary to examine why plane surfaces are problematic in real applications such as auditoria. The reason is that with a directional source, such as a trumpet, the reflected energy from a plane surface will be concentrated into a narrow solid angle, leading to a risk of detrimental effects such as echoes, colouration or image shift. The results shown in Figure 3.2 were obtained using an omnidirectional source and consequently do not show this narrow reflection. One solution to this problem would therefore be to measure polar responses using a directional source which better simulates those that cause problems in real applications. However, it would be difficult to justify choosing any particular directivity and whatever were chosen would need to be precisely specified to permit results obtained at different facilities to be compared. In general, the well defined nature and universality of the point test source makes omnidirectionality a better choice but limits measurements to the far field.

Although ideally polar responses should be measured in the far field, in practice it is sufficient to use much shorter source and receiver distances so long as there is a high degree of similarity between the shape of the measured and far field responses. This far field measurement approach is necessary to ensure that the diffusion efficacy of samples is consistently rated and that different samples are therefore consistently ranked but unfortunately it is not representative of the many practical situations in which listeners are positioned in the near field of surfaces such as walls. Consequently, it would be prudent to additionally examine the polar response at typical listener distances to verify that there are no adverse near field effects. As discussed above, for essentially plane surfaces the polar response becomes more uniform as the receiver distance decreases. This is not of any real

consequence because the effect is well understood and known to be a false representation of their behaviour in practical applications with directional sources.

Of more concern are surfaces which would be overrated by a far field measurement, i.e. produce less diffusion at listener distances than expected. An extreme example of this can occur with concave surfaces because these focus the reflected sound and if it is focussed to a listener position then the sound quality at this position will be seriously degraded. Whether or not a concave surface will be problematic in a particular situation depends principally upon the distance at which it focusses sound, the focal length. This is in turn determined by exactly how concave the surface is. For highly concave surfaces such as hemispherical or semicylindrical shells, the focal length will be so short that focussing will occur very close to the surface and is therefore unlikely to cause a problem. Similarly, concave surfaces which are only slightly non-planar are unlikely to be problematic because their focal lengths will probably exceed the distances at which listeners are situated. It is those surfaces in between these two extremes which are the most likely to cause problems, one example being the concave sample described in Section 2.3.6 which was measured during this research.

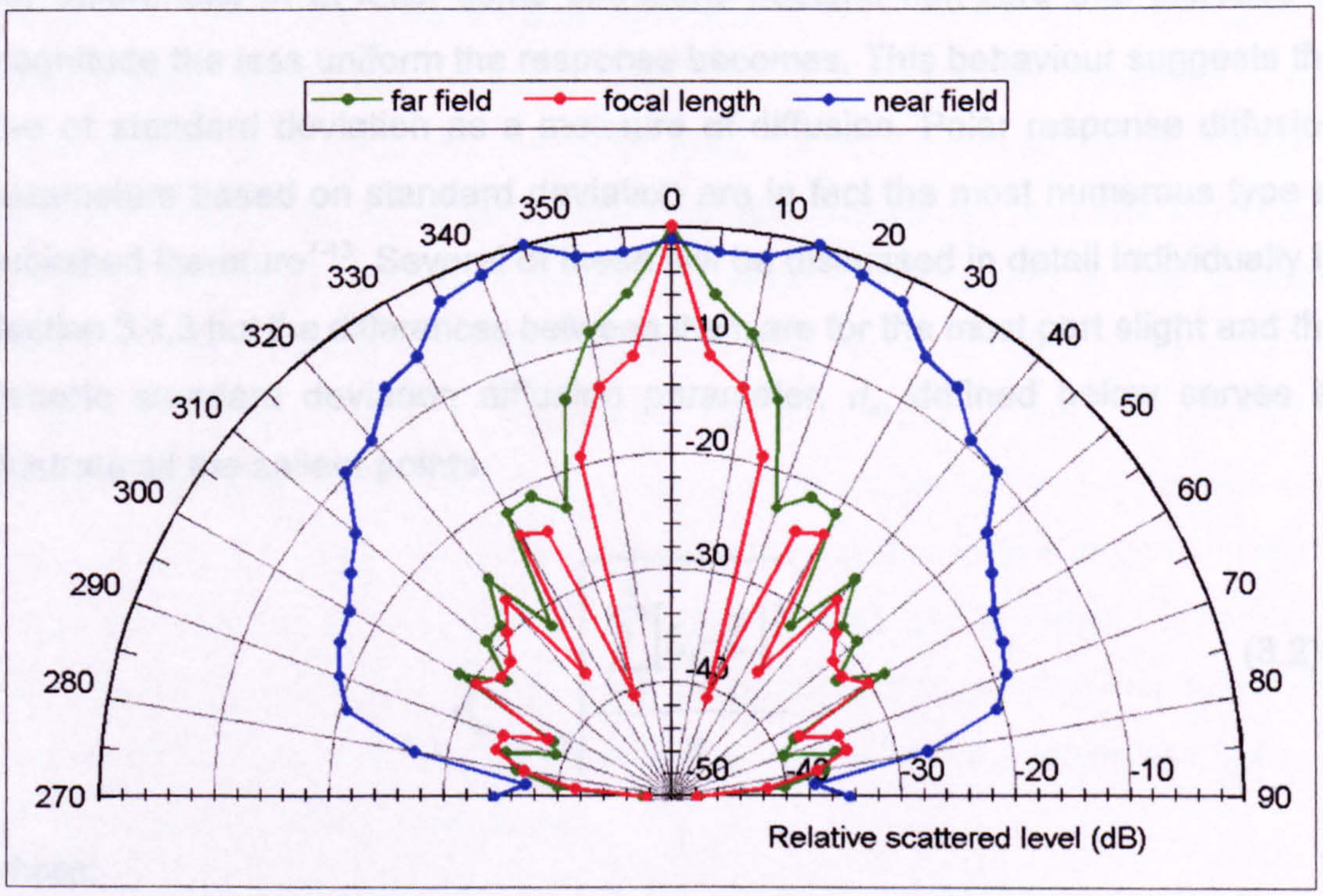

Figure 3.3: Effect of receiver distance on the shape of the normal incidence 2kHz polar response of the concave prism.

Figure 3.3 on the preceding page shows BEM predictions of the single-plane polar response of this sample when the receiver distance is equal to the focal length and also in the far and near fields.

Although in this case the focussing effect is small, Figure 3.3 does demonstrate that there are surfaces which will not perform as well in some practical applications as might be expected from their far field diffusion efficacy. Identifying whether a particular surface will exhibit any adverse behaviour in a particular application requires its polar response at listener distances to be obtained. This can be predicted if measurement is impractical.

3.4 Standard deviation type diffusion parameters.

3.4.1 Introduction and definition.

One property of the polar response corresponding to complete diffusion is that the difference between the scattered pressure in any direction and the mean value is zero. Any departure from the case of complete diffusion causes this not to be so, the differences in at least some directions become non-zero and increase in magnitude the less uniform the response becomes. This behaviour suggests the use of standard deviation as a measure of diffusion. Polar response diffusion parameters based on standard deviation are in fact the most numerous type in published literature[7-13]. Several of these will be discussed in detail individually in Section 3.4.3 but the differences between them are for the most part slight and the generic standard deviation diffusion parameter, d_σ, defined below serves to illustrate all the salient points.

$$d_\sigma = \sqrt{\frac{\sum_{i=1}^{n}\left[L_i - \bar{L}\right]^2}{n}} \qquad (3.2)$$

where:

L_i = SPL at receiver position i

$\bar{L}$ = Mean SPL

n = Number of receiver positions

3.4.2 **Appraisal.**

Standard deviation diffusion parameters are simple in concept and straightforward to calculate. The value of d_σ is zero in the case of complete diffusion and increases as the polar response becomes less diffuse. However, although standard deviation is a common statistical measure of spread, values of d_σ cannot be interpreted in the usual manner because, as discussed in Section 3.9.4, the distribution of levels in polar responses is generally not normal. Even if the distribution were normal and the value of d_σ could therefore be used to define the range over which x% of the levels in the polar response were spread, this would be of only limited benefit because it would not indicate the presence of extreme values much greater than the mean which could be problematic distinct reflections.

As will be shown in Section 3.4.3, the standard deviation of both the scattered sound pressure levels and energies have been proposed as measures of diffusion. Sound pressure level is a more linear perceptual scale to listeners than energy but, unfortunately, quantifying diffusion using simply the standard deviation of the levels fails for poor diffusers. This is because the sound pressure level standard deviation takes its maximum value when the reflected energy is scattered equally to half of the measurement positions, not when it is non-zero at only a single position. It therefore fails to identify the worst case and although it ranks surfaces which are moderate or good diffusers in the right order, it does not rank poor diffusers correctly. In fact using the standard deviation of the sound pressure levels, a very poor diffuser with a polar response similar to that shown in Figure 3.4 on the following page - a strong specular reflection but low level scattering in the majority of directions - will be rated as good. The reason for this is that the mean level is close to the low level scattering, resulting in the majority of the $(L_i - \bar{L})^2$ terms in (3.2) being close to zero.

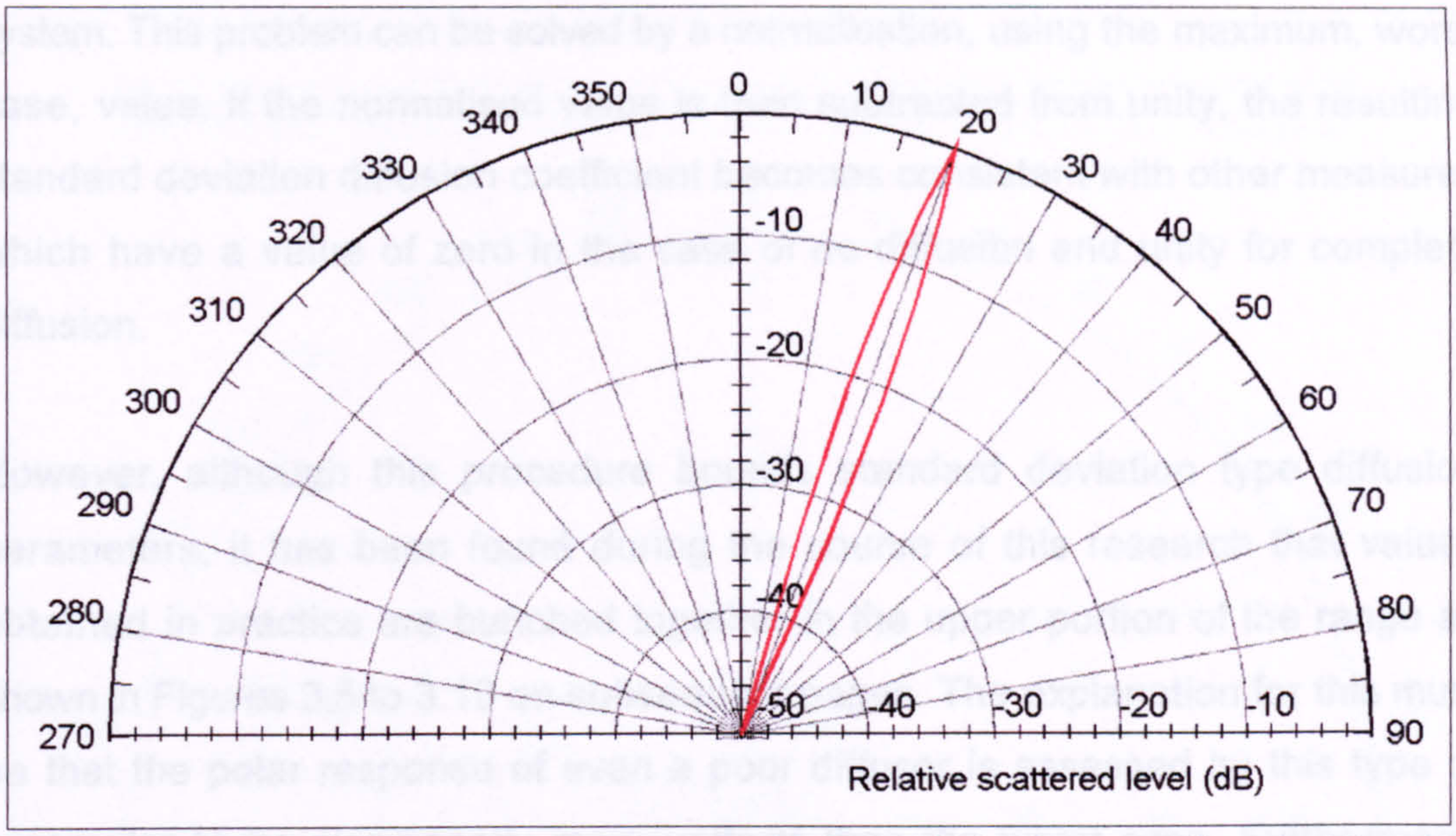

Figure 3.4: Example of a polar response which would be incorrectly rated by d_o.

A simple solution, suggested by Cox[9], is to calculate the mean level via energy as shown in (3.3) instead of simply taking the arithmetic mean of the levels.

$$\bar{L} = 10\log\left(\frac{\sum_{i=1}^{n} 10^{L_i/10}}{n}\right) \tag{3.3}$$

This shifts the mean level upwards, so penalising poor diffusers but does not completely solve the problem. For example, for single-plane measurements using an angular resolution of 5° and a dynamic range of 70dB, the standard deviation is a maximum when the reflected energy is scattered equally to five out of the thirty-seven measurement positions. Although calculating the mean level using (3.3) is not a complete solution to the improper evaluation of poor diffusers using standard deviation, it does reduce the problem to the point where it is more of a philosophical concern than a practical difficulty.

More problematic is the fact that standard deviation diffusion parameters such as (3.2) are not bounded between zero and unity. Although their minimum value is zero, their maximum value is a function of the dynamic range of the measurement

system. This problem can be solved by a normalisation, using the maximum, worst case, value. If the normalised value is then subtracted from unity, the resulting standard deviation diffusion coefficient becomes consistent with other measures which have a value of zero in the case of no diffusion and unity for complete diffusion.

However, although this procedure bounds standard deviation type diffusion parameters, it has been found during the course of this research that values obtained in practice are bunched together in the upper portion of the range as shown in Figures 3.5 to 3.10 on subsequent pages. The explanation for this must be that the polar response of even a poor diffuser is assessed by this type of parameter to be significantly more uniform than the worst case. Furthermore, although calculating the mean level using (3.3) appears at first to give a better spread of results, the bunching problem is in fact worse.

One possible solution to this bunching problem is to normalise to a practical - instead of the theoretical - worst case. The problem with this is deciding upon the worst practical diffuser: this could perhaps be a plane surface or maybe a concave surface. Whatever is chosen, there is a risk that something will later be encountered which is an even worse diffuser and so has a diffusion parameter greater than unity, negating the purpose of the normalisation.

One further problem with standard deviation type parameters is that interpreting the physical significance of values other than the extremes is difficult. Although values close to zero mean that the reflected energy is essentially uniformly scattered and values approaching unity indicate that energy is reflected in only a few directions, the meaning of intermediate values, e.g. 0.5, is unclear. If the levels comprising polar responses were normally distributed then these parameters would be quantitative measures of spread. However, since normal distribution is not typical, they provide only a qualitative assessment. Despite these problems, standard deviation parameters have been successfully utilised to rate diffusion when designing optimised diffusers and they do rank many practical surfaces which are effective diffusers correctly.

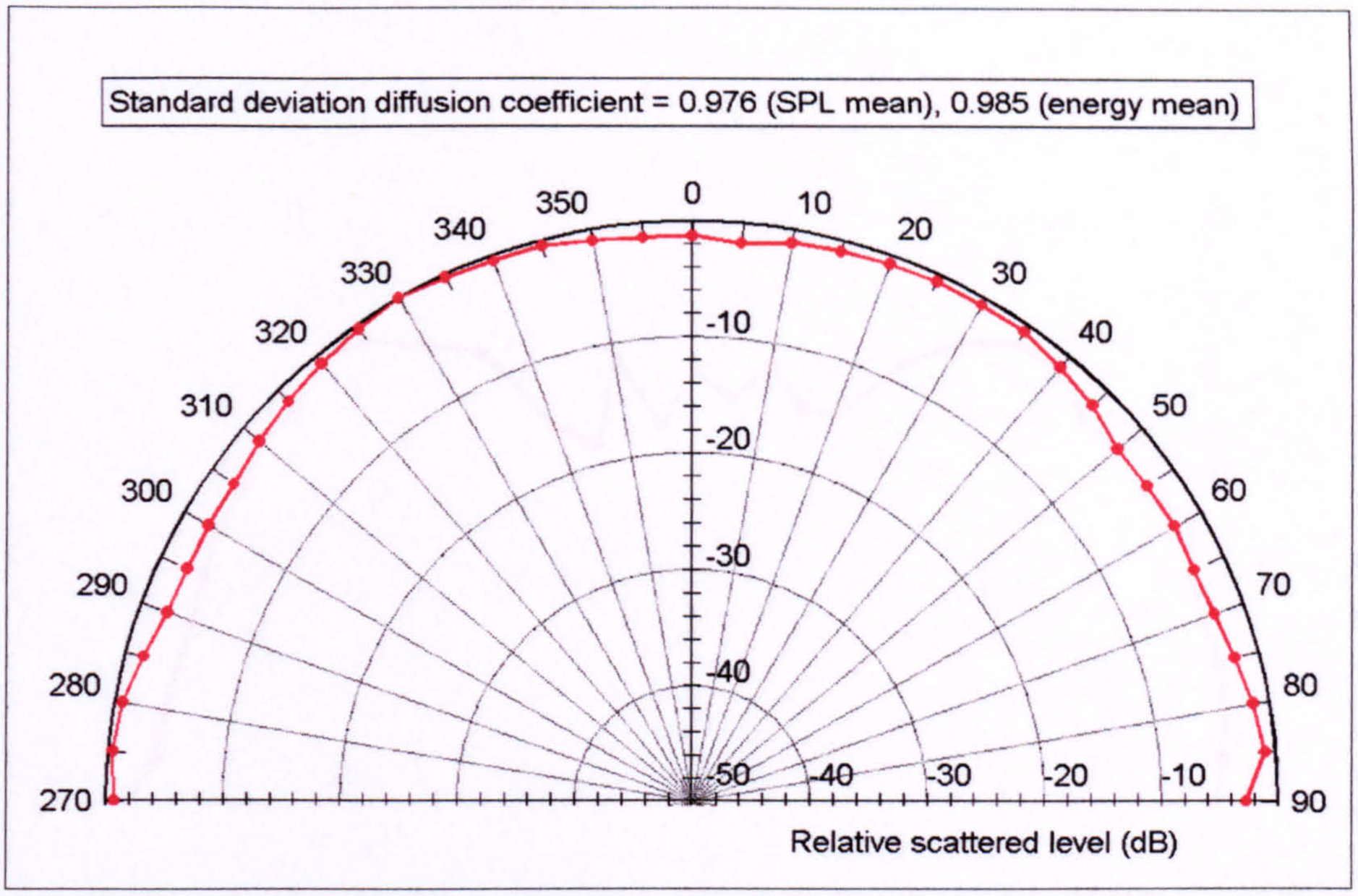

Figure 3.5: 1kHz normal incidence polar response of the semicylinder, measured at RPG.

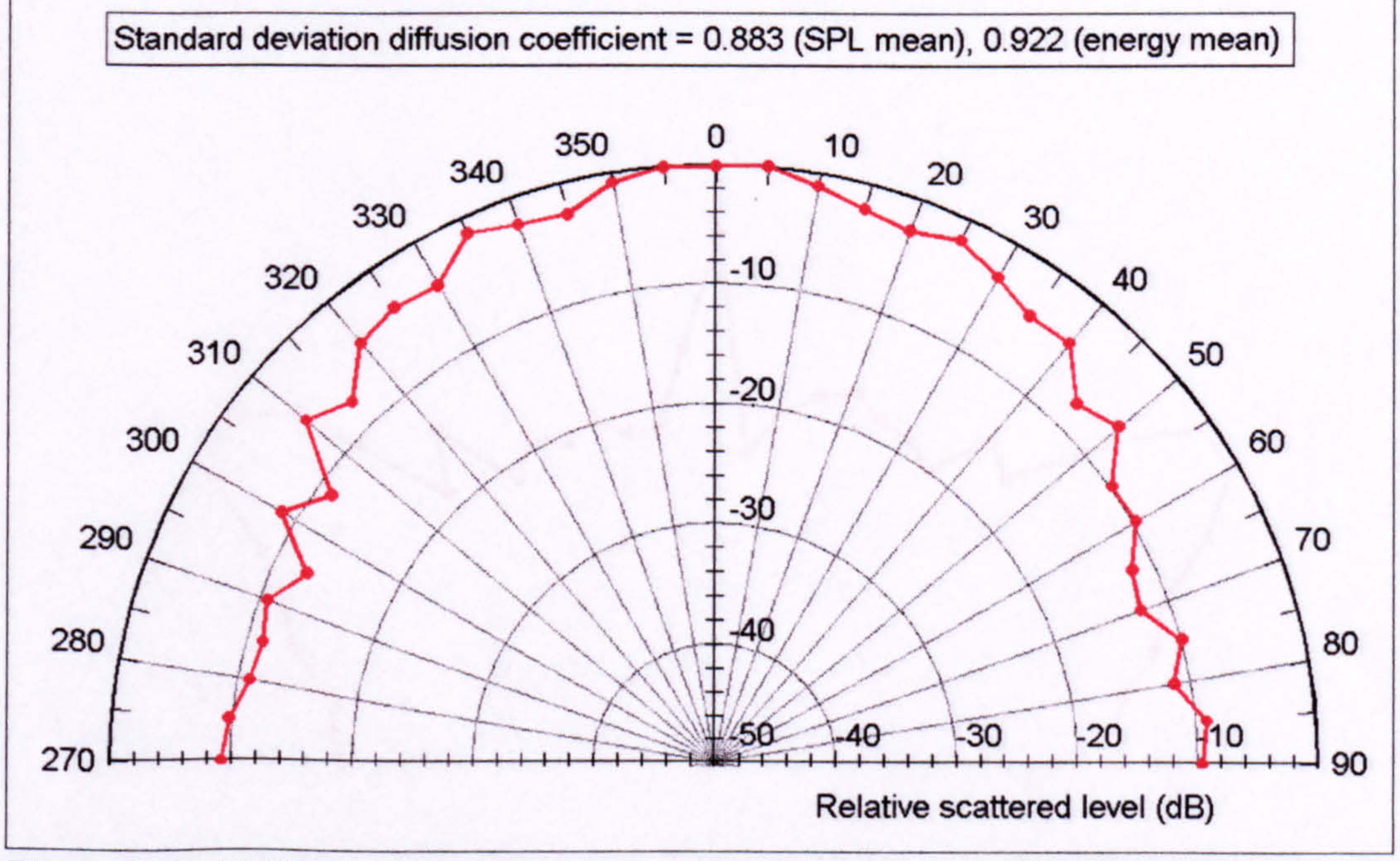

Figure 3.6: 400Hz normal incidence polar response of the QRD, measured at RPG.

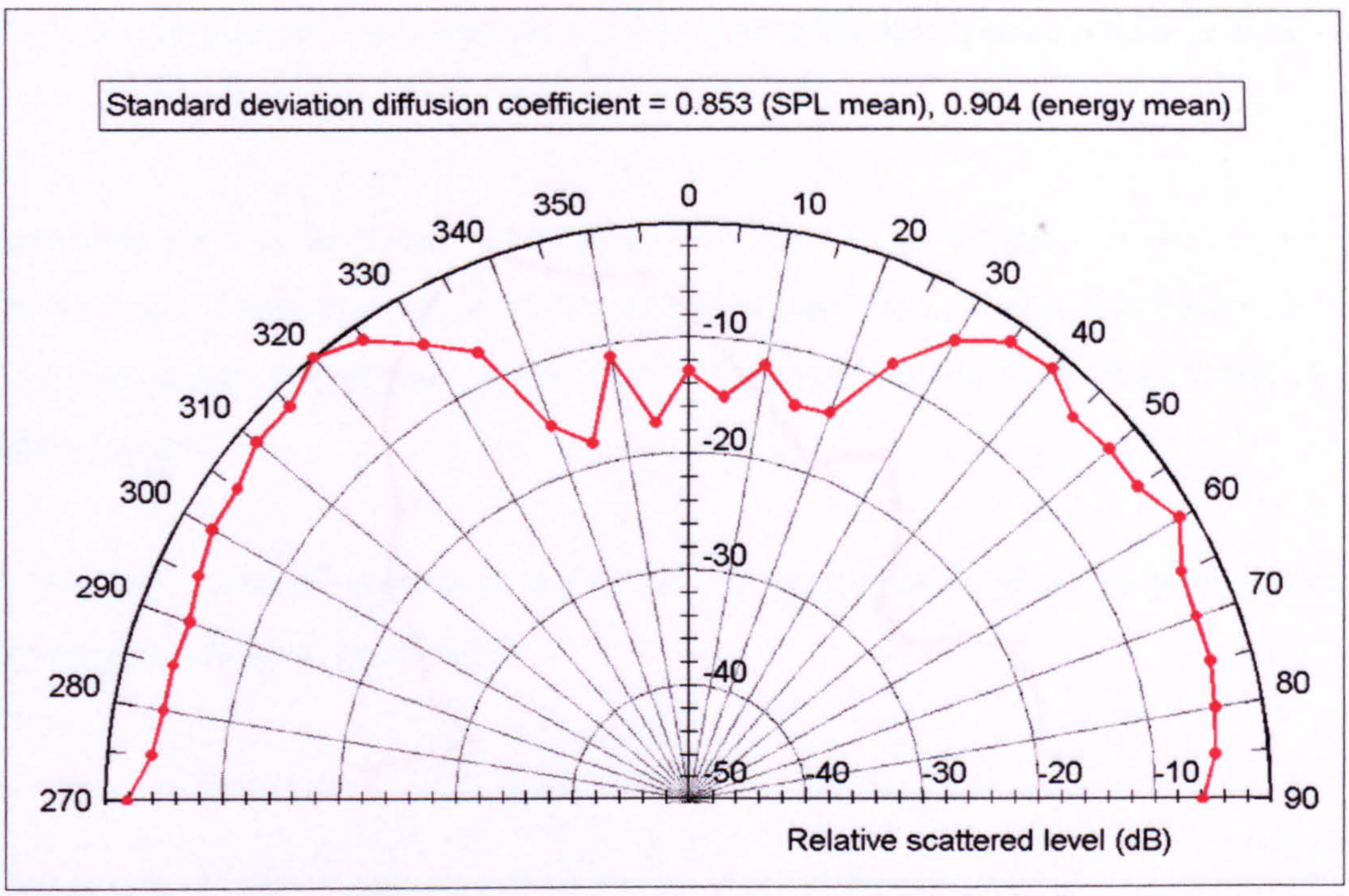

Figure 3.7: 2kHz normal incidence polar response of the seating, measured at RPG.

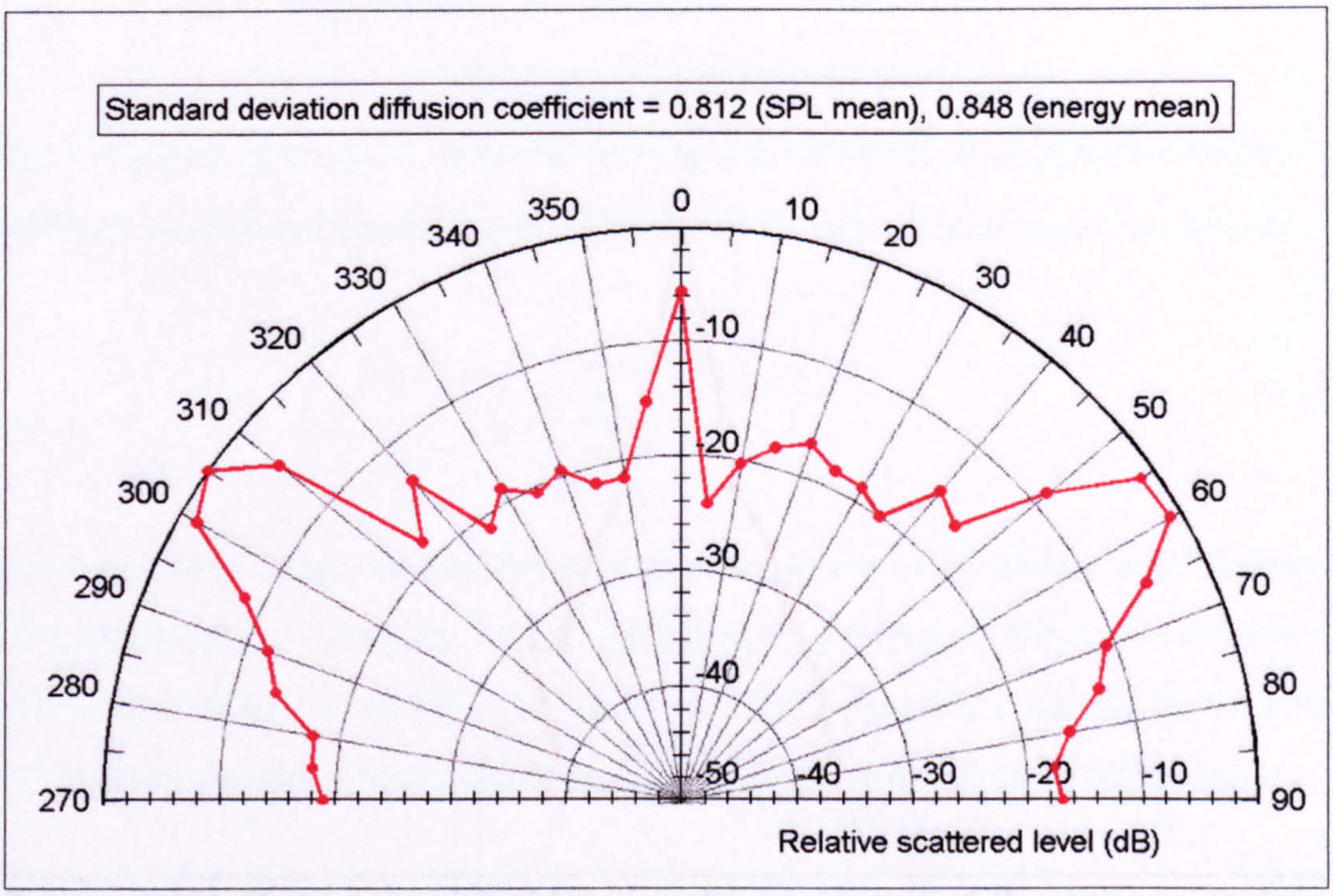

Figure 3.8: 2.5kHz normal incidence polar response of the cone, measured at RPG.

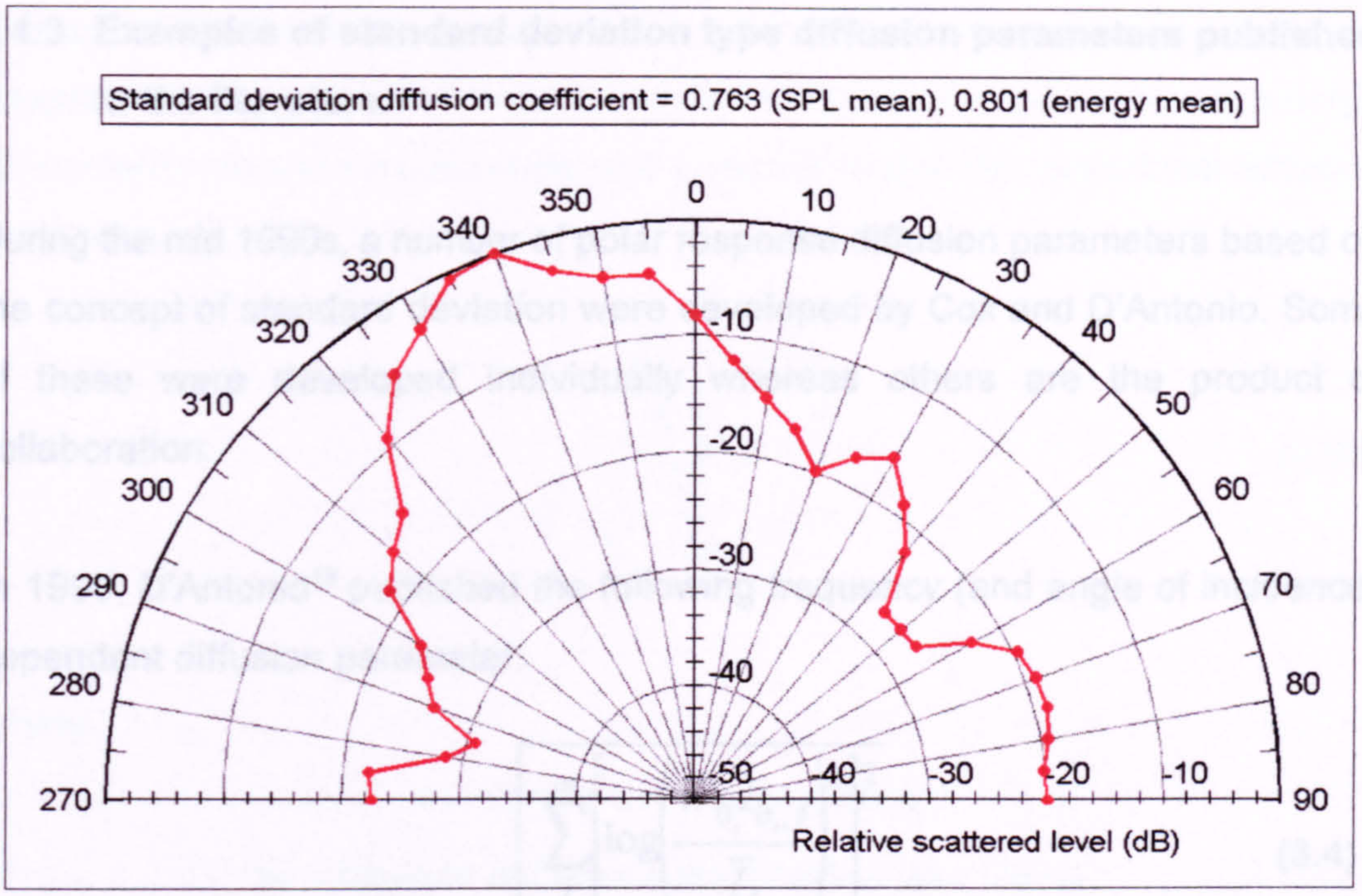

Figure 3.9: 3.15kHz 20° incidence polar response of the BAD Panel, measured at RPG.

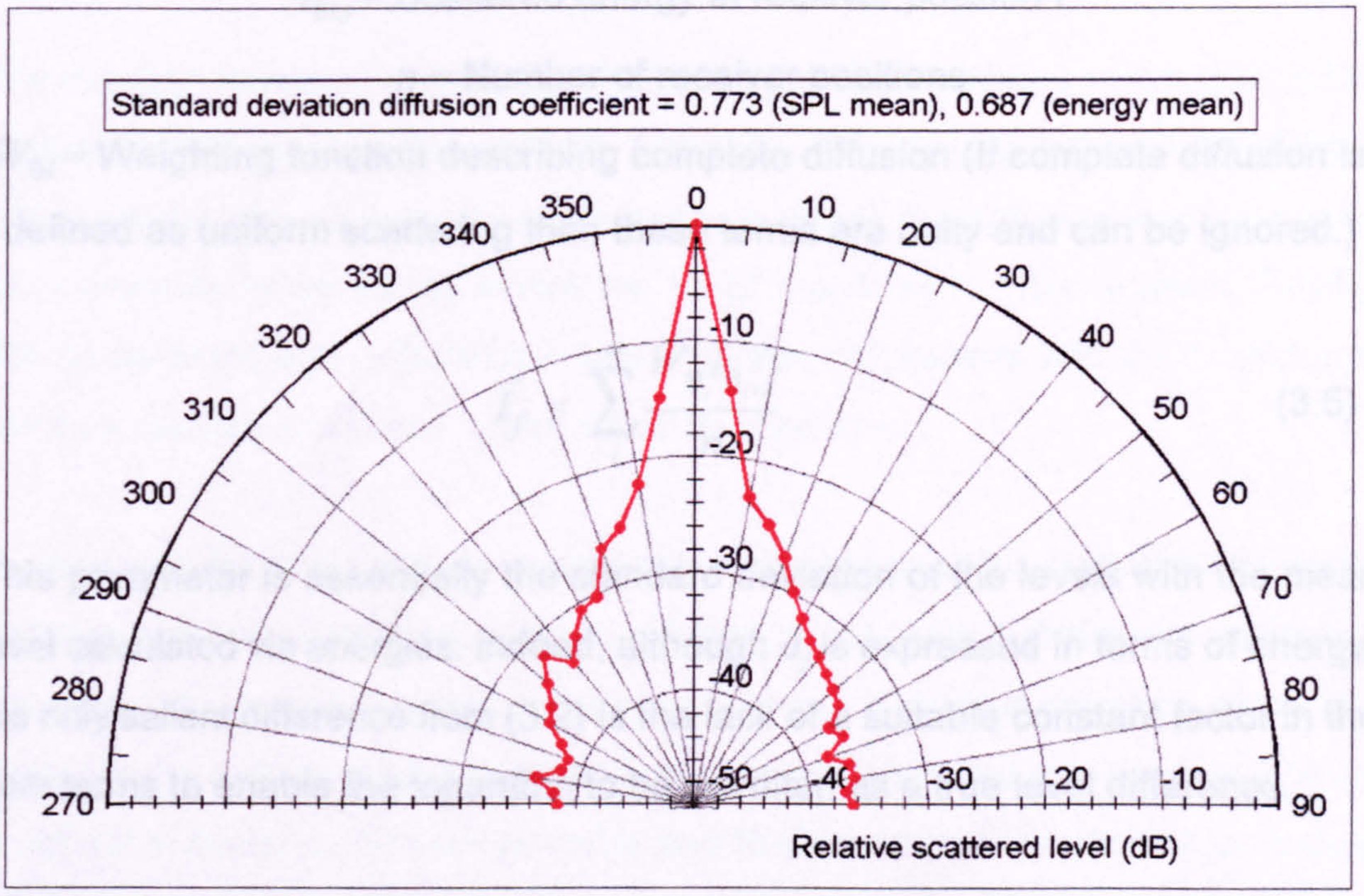

Figure 3.10: 4kHz normal incidence polar response of the concave prism, measured at RPG.

3.4.3 Examples of standard deviation type diffusion parameters published in the literature.

During the mid 1990s, a number of polar response diffusion parameters based on the concept of standard deviation were developed by Cox and D'Antonio. Some of these were developed individually whereas others are the product of collaboration.

In 1995, D'Antonio[13] published the following frequency (and angle of incidence) dependent diffusion parameter:

$$\sigma_f = \sqrt{\frac{\sum_i^n \left[\log\left(\frac{W_{\theta_i} I_{\theta_i,f}}{\overline{I}_f}\right)^2\right]^2}{(n-1)}} \tag{3.4}$$

where:

$I_{\theta i,f}$ = Scattered energy at receiver position i

n = Number of receiver positions

$W_{\theta i}$ = Weighting function describing complete diffusion (If complete diffusion is defined as uniform scattering then these terms are unity and can be ignored.)

$$\overline{I}_f = \sum_i^n \frac{W_{\theta_i} I_{\theta_i,f}}{n} \tag{3.5}$$

This parameter is essentially the standard deviation of the levels with the mean level calculated via energies. Indeed, although σ_f is expressed in terms of energy, the only salient difference from (3.2) is the lack of a suitable constant factor in the sum terms to enable the logarithm to be rewritten as a true level difference.

D'Antonio[13] and Cox[7] state that it is necessary to smooth polar responses before calculating a value of σ_f because of the numerous maxima and minima in single frequency responses which cause the standard deviation to be misleadingly large.

This smoothing is normally performed over a third-octave. D'Antonio and Cox then suggest that the mean and standard deviation of the set of σ_f values for each angle of incidence should be calculated and summed to give the 'directional diffusion parameter', D:

$$D = \overline{\sigma} + \sqrt{\frac{\sum_{i}^{m}\left[\sigma_{f_i} - \overline{\sigma}\right]^2}{(m-1)}} \qquad (3.6)$$

where:

σ_{fi} = Value of σ_f at frequency i

m = Number of frequencies (third-octave bands)

$$\overline{\sigma} = \sum_{i}^{m}\frac{\sigma_{f_i}}{m} \qquad (3.7)$$

The standard deviation is included in (3.6) to penalise surfaces which have polar responses that vary significantly with frequency. Simply taking the mean of the σ_f values would allow any third-octave bands in which the diffusion was poor to be compensated for by bands where the polar response is more uniform. Finally, D'Antonio proposes performing a similar averaging process with the D values to obtain a random incidence 'mean diffusion parameter'.

A problem with polar response diffusion parameters which D'Antonio does not address directly but which is nicely illustrated by his work is that when defining a parameter, it is necessary to compromise between providing too much detail and reducing the data to such an extent that all the detail is lost and the end product is difficult to interpret. This compromise and the associated question of averaging are addressed in Section 3.12. Some data reduction is required because it would be impractical for a general use diffusion parameter to be dependent on both frequency and angle of incidence, let alone anything else. However, as is the case

with absorption coefficients, it is likely that to be of any practical use, a diffusion coefficient will have to be expressed as a function of frequency. It is therefore curious as to why D'Antonio proposes to average over frequency as the first step in his data reduction process but the reason is likely to be that a single figure of merit was required by Cox for use in his optimisation procedures[7]. Although the single figure 'mean diffusion parameter' is the end result of his data reduction, D'Antonio does additionally demonstrate the utility of the intermediate σ_f and D values in expressing the diffusion efficacy of surfaces for particular frequencies and angles of incidence.

In a second paper, D'Antonio[12] states that the following parameter can be used to rate the diffusion produced by a surface for a particular frequency (third-octave band) and angle of incidence:

$$\sigma_f = \sqrt{\frac{\sum_i^n \left[10\log\left(\frac{I_{\theta_i,f}}{\overline{I}_f}\right)\right]^2}{(n-1)}} \qquad (3.8)$$

where:

$I_{\theta i,f}$ = Intensity for the observation angle θ_i and frequency f

$\overline{I}_f$ = Mean intensity averaged over the n observation positions

It is readily evident that this parameter differs from (3.4) only by the factor of ten multiplying the logarithm and the absence of the square on its argument. The effect of this is that (3.8) can be expressed in terms of sound pressure levels as:

$$\sigma_f = \sqrt{\frac{\sum_{i=1}^n \left[L_{\theta_i,f} - \overline{L}_f\right]^2}{(n-1)}} \qquad (3.9)$$

This is essentially the same as the generic standard deviation parameter, (3.2).

D'Antonio and Cox[7] go on to state that the standard error, ϵ_f, of the n intensity values comprising the polar response is given by:

$$\epsilon_f = \frac{\sigma_f}{\sqrt{n}} \approx \frac{10}{\ln(10)\bar{I}_f}\sqrt{\frac{\sum_{i=1}^{n}\left[I_{\theta_i,f}-\bar{I}_f\right]^2}{n(n-1)}} \tag{3.10}$$

This expression is obtained from (3.8) by converting the logarithm from base ten to natural and then taking the first term of its series expansion. A full derivation is given in Appendix B. However, since the series expansion is only valid if certain conditions are satisfied (for details see Appendix B), the validity of (3.10) is limited to cases where no individual intensity level in the polar response exceeds the mean by more than 3dB. This is a severe constraint and restricts the application of (3.10), which in any case is only an approximation, to good diffusers.

It is difficult to understand the reason why Cox proposes using standard error to quantify diffusion rather than standard deviation. The standard deviation of a set of data is a measure of spread; a quantitative measure if the data is normally distributed. The standard error, however, expresses the degree of confidence that the calculated value of the mean is accurate. If a number of sample data sets are taken from a population and their means calculated, it is highly likely that different values will be obtained. With normally distributed data there is approximately 68% confidence that the true mean, that of the population, is within one standard error of a calculated sample mean and approximately 95% confidence that it lies within two. The relevance of this to the characterisation of diffusion is unclear. Furthermore, it can be seen from (3.10) that the value of ϵ_f is, by definition, dependent on n and hence the angular resolution. As discussed in Section 2.8.2, this is an undesirable property for a diffusion parameter. It is pointless to circumvent the problem by specifying that the measurement should be made with a particular resolution; the standard deviation may as well be used instead.

Despite these reservations, Cox has used a standard error parameter to quantify diffusion in an optimisation process for designing diffusers[7]. In this application n is fixed and standard error will be superficially satisfactory in rating diffusion but has no benefits over standard deviation. The specific parameter used by Cox is shown below, it differs from (3.10) only in nomenclature and by a factor of two.

$$\epsilon = \frac{20}{\ln(10)\overline{I_\theta}}\sqrt{\frac{\sum_{\theta=-90}^{+90}\left[I_\theta - \overline{I_\theta}\right]^2}{n(n-1)}} \qquad (3.11)$$

Cox states that this parameter "*monitors the diffusion satisfactorily*" and that since the standard error is calculated via the intensities it "*penalizes nonuniform* [sic] *diffusion more than if decibel values were used.*" However, as discussed above, the derivation of this parameter is valid only for polar responses which approach uniformity.

Cox goes on to discuss averaging over frequency and states that "*A simple average of the standard errors for many frequencies allowed any poor frequency ranges for diffusion to be compensated for by other good frequency ranges. To prevent such compensation from occurring, after the standard errors were averaged... one standard error of the standard errors was added.*" Cox's resulting diffusion parameter, ϵ', for n frequencies each having a standard error of ϵ_{fi} is:

$$\epsilon' = \overline{\epsilon} + \frac{2}{\sqrt{(n(n-1)}}\sqrt{\sum_{i=1}^{n}\left[\epsilon_{fi} - \overline{\epsilon}\right]^2} \qquad (3.12)$$

where:

$$\overline{\epsilon} = \frac{1}{n}\sum_{i=1}^{n}\epsilon_{fi} \qquad (3.13)$$

Since each ϵ_{fi} value is two standard errors, Cox's description is strictly speaking not commensurate with (3.12) and (3.13), although the concept is clear and varies from that suggested by D'Antonio[12] only in that the use of standard error as opposed to standard deviation is suggested.

In a later work[9], Cox defines a slightly revised parameter:

$$\epsilon(r_s,\ r,\ f)\ = 2\sqrt{\frac{\sum_{\theta=-85}^{+85}\left[L_p(r,\theta)-\overline{L}_p(r,\theta)\right]^2}{n(n-1)}} \qquad (3.14)$$

where:

r_s = Vector from source to sample which defines the angle of incidence

r = Distance from sample to receiver points

f = Frequency

θ = Scattering angle

n = Number of receiver points between θ = -85° and θ = +85°

$L_p(r,\theta)$ = Scattered SPL at distance r and angle θ from the sample

$$\overline{L}_p(r,\theta)\ =\ \log\left[\frac{1}{n}\sum_{\theta=-85}^{85}10^{L_p(r,\theta)}\right] \qquad (3.15)$$

It has been established that (3.15) is erroneous[46] and should read:

$$\overline{L}_p(r,\theta)\ =\ 10\log\left[\frac{1}{n}\sum_{\theta=-85}^{85}10^{\frac{L_p(r,\theta)}{10}}\right] \qquad (3.16)$$

In (3.14), ϵ is defined explicitly as a function of incident angle, receiver distance and frequency. Cox makes no mention of performing any averaging and explains that the range of θ is limited to ±85° because "*It seems unnecessary for performance spaces to try and produce a diffuser that will work for the very extreme grazing angles, and so these have been excluded from the evaluation.*" This reduction in the range of θ may be justified for the particular application which Cox was addressing but generally it is not. In fact Cox now uses the range ±90° in diffuser design[46]. Except for the limits of the summation, (3.14) differs from the generic standard deviation diffusion parameter, (3.2), only in that it is an evaluation of the standard error as opposed to the standard deviation.

To summarise, although standard deviation type parameters evaluate the diffusion efficacy of good diffusers in a credible manner and are simple to calculate, they can overrate poor diffusers. A further problem is that they are unbounded and bounding them by normalisation causes values for practical surfaces to be bunched together into a small section of the range. It is also difficult to interpret the physical significance of intermediate values. Therefore although standard deviation parameters have been successfully utilised to monitor diffusion quality in optimisation algorithms, they are far from ideal for general use.

3.4.4 **Diffusion gain.**

A refinement of the standard deviation type of diffusion parameter is the concept of diffusion gain suggested by Angus[53]. The diffusion gain, in decibels, is defined as the ratio between the value of a standard deviation parameter for the surface being assessed and that for a plane surface of identical size. Angus used this measure to evaluate the performance of large arrays of Schroeder diffusers and his results neatly illustrate their superiority over a plane surface. However, this measure continues to be afflicted by all the drawbacks of standard deviation parameters discussed above.

3.5 Directivity type diffusion parameters.

3.5.1 Introduction and definition.

Some other suggested metrics[14,15] which quantify diffusion by reducing polar responses to single figures can be grouped together under the heading of 'directivity' because they rate diffusion according to what fraction of the total reflected energy is scattered in each direction. As is the case with measures based on standard deviation, published examples of these directivity type parameters exhibit minor variations but originate from a generic parameter, d_{dir}, shown below:

$$d_{dir} = 1 - \sqrt{\sum_{i=1}^{n}\left[\frac{E_i}{E_{total}} - \frac{1}{n}\right]^2} \qquad (3.17)$$

where:

E_i = Scattered energy (squared pressure) at receiver position i

$E_{total} = \sum E_i$

n = Number of receiver positions

The concept from which (3.17) is derived is that in the case of complete diffusion (defined as uniform scattering), the fraction of the total reflected energy measured at each receiver is equal to the reciprocal of the number of receivers. In this case, each term of the summation is zero and d_{dir} is unity. Any deviation from uniformity causes some of the summation terms to become non-zero and hence reduces the value of d_{dir}. In the theoretical worst case of all the energy reflected in a single direction, d_{dir} has value $1/n$. This directivity parameter is therefore bounded, a significant advantage over the parameters based on standard deviation discussed previously. Although the bounds are unity and $1/n$, these can readily be adjusted to unity and zero by the application of a simple correction to form a modified parameter, d_{dir}':

$$d_{dir}' = \frac{nd_{dir} - 1}{n-1} \qquad (3.18)$$

3.5.2 **Appraisal.**

In addition to being bounded, directivity type parameters possess the same benefits as standard deviation types; straightforward calculation and independence from the measurement distance so long as the receivers are in the far field, suggesting that they are superior. However, as shown in Figures 3.11 to 3.16 on subsequent pages, it has been found that practical values of this type of parameter for all but the poorest diffusers are bunched together in the upper half of the range, a similar phenomena to that observed with normalised values of the standard deviation parameter d_σ. Although initially surprising, there is a simple explanation: d_{dir} is in fact almost identical to the normalised standard deviation of energies.

If the standard deviation of energies is represented by $d_{\sigma E}$ then:

$$d_{\sigma E} = \sqrt{\frac{\sum_{i=1}^{n}\left[E_i - \overline{E}\right]^2}{n}} \qquad (3.19)$$

where:

$$\overline{E} = \frac{E_{total}}{n} \qquad (3.20)$$

Other symbols have the same meaning as in (3.17)

For the energy standard deviation, the worst case is when all the energy is reflected in a single direction:

$$d_{\sigma E_{worst}} = \sqrt{\frac{(E_{total} - \overline{E})^2 + (n-1)\overline{E}^2}{n}} \qquad (3.21)$$

Substituting for E_{total} using (3.20) and expanding the numerator gives:

$$d_{\sigma E_{worst}} = \overline{E}\sqrt{n-1} \qquad (3.22)$$

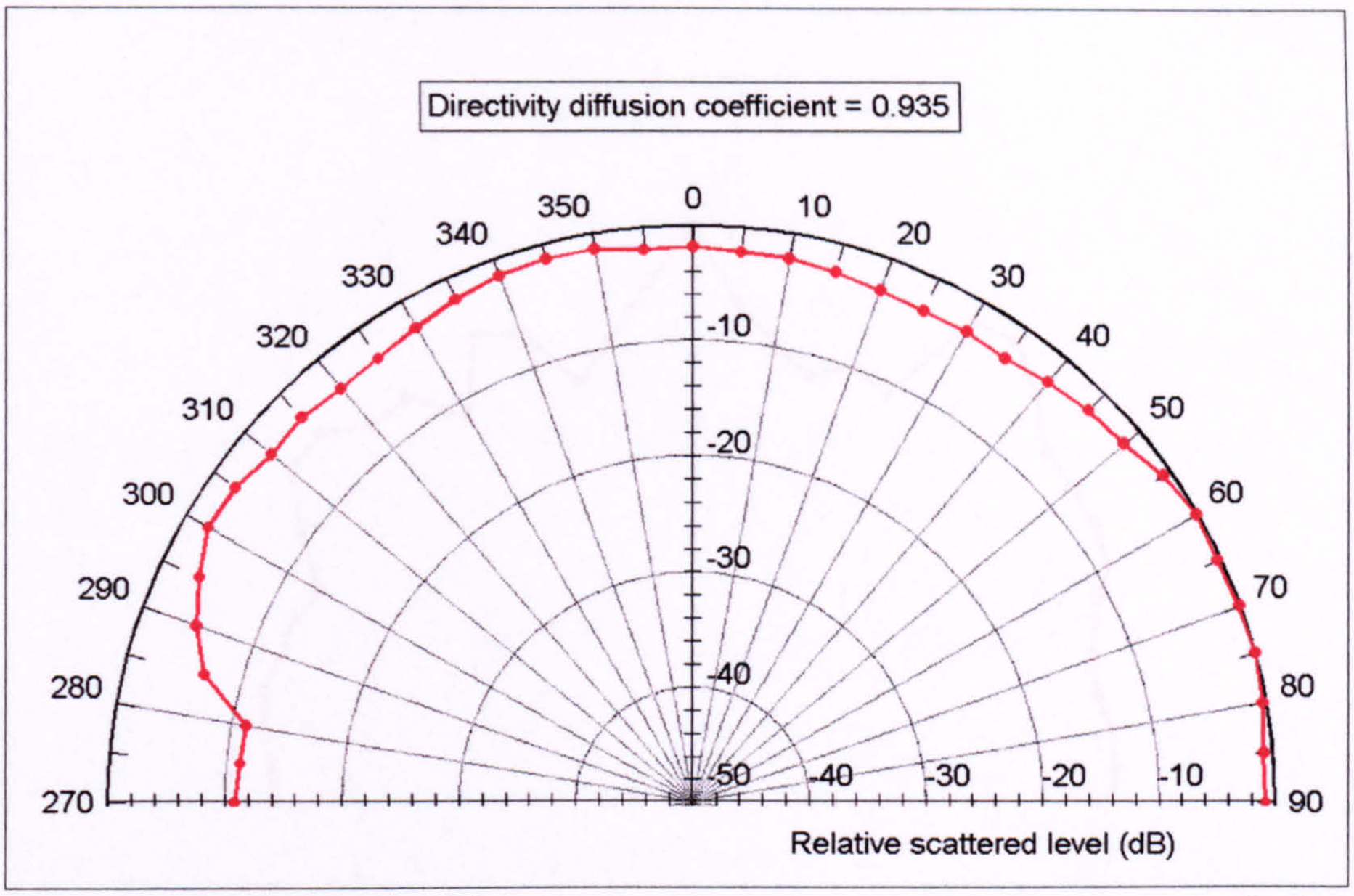

Figure 3.11: 1.25kHz 45° incidence polar response of the semicylinder, measured at RPG.

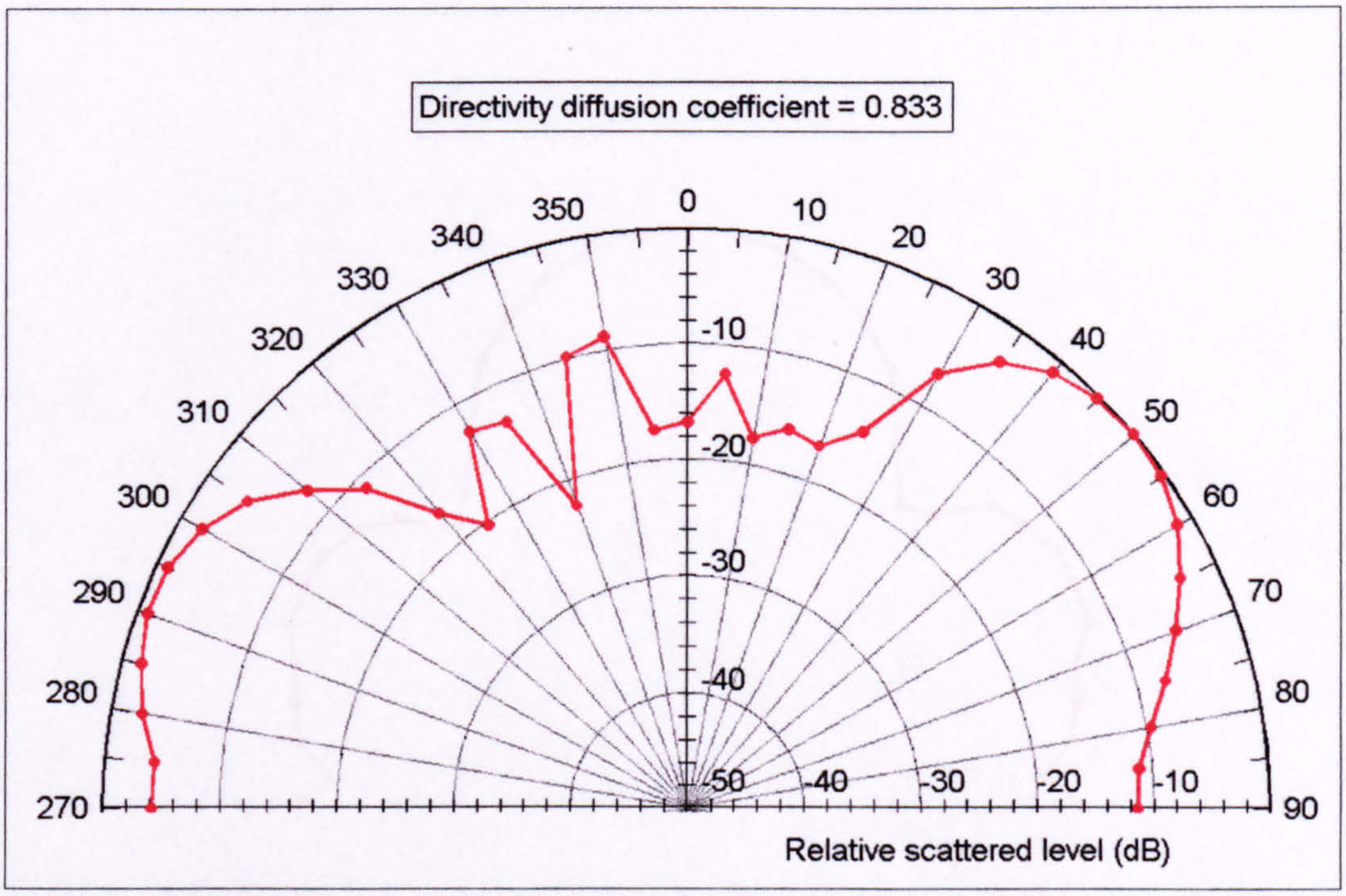

Figure 3.12: 1kHz 10° incidence polar response of the square-based pyramid, measured at RPG.

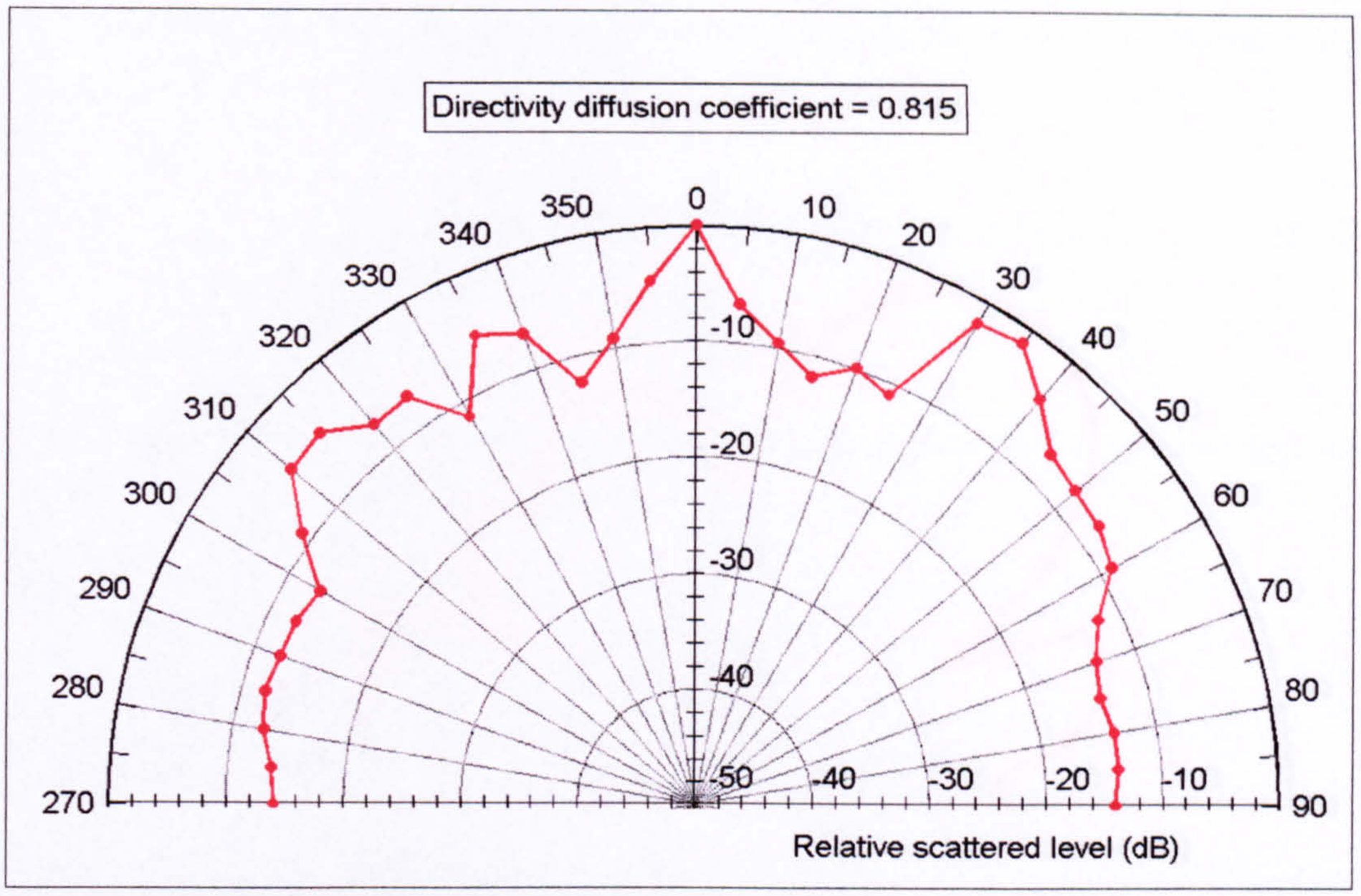

Figure 3.13: 2kHz normal incidence polar response of the Skyline, measured at RPG.

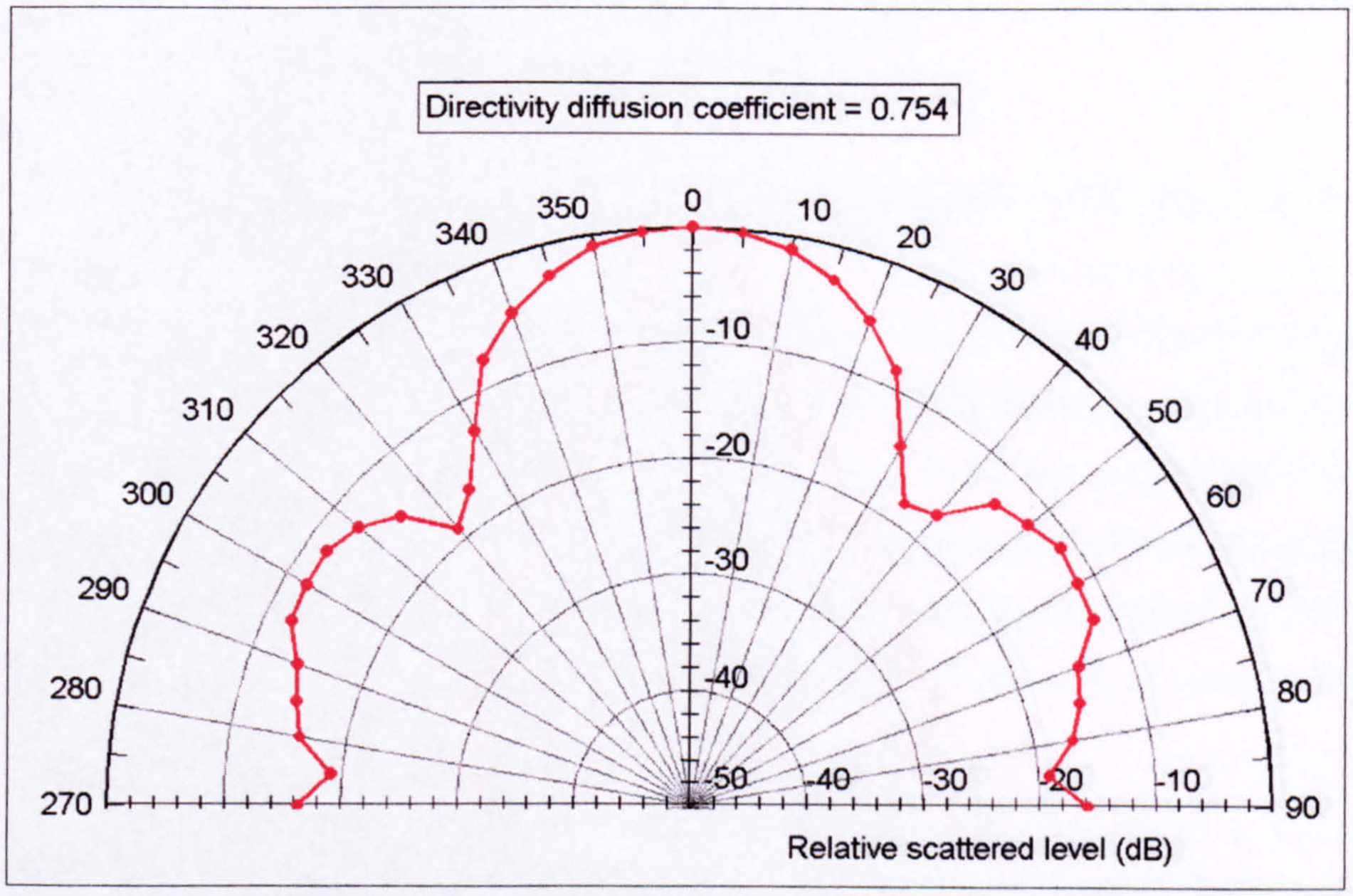

Figure 3.14: 500Hz normal incidence polar response of the Skyline, measured at RPG.

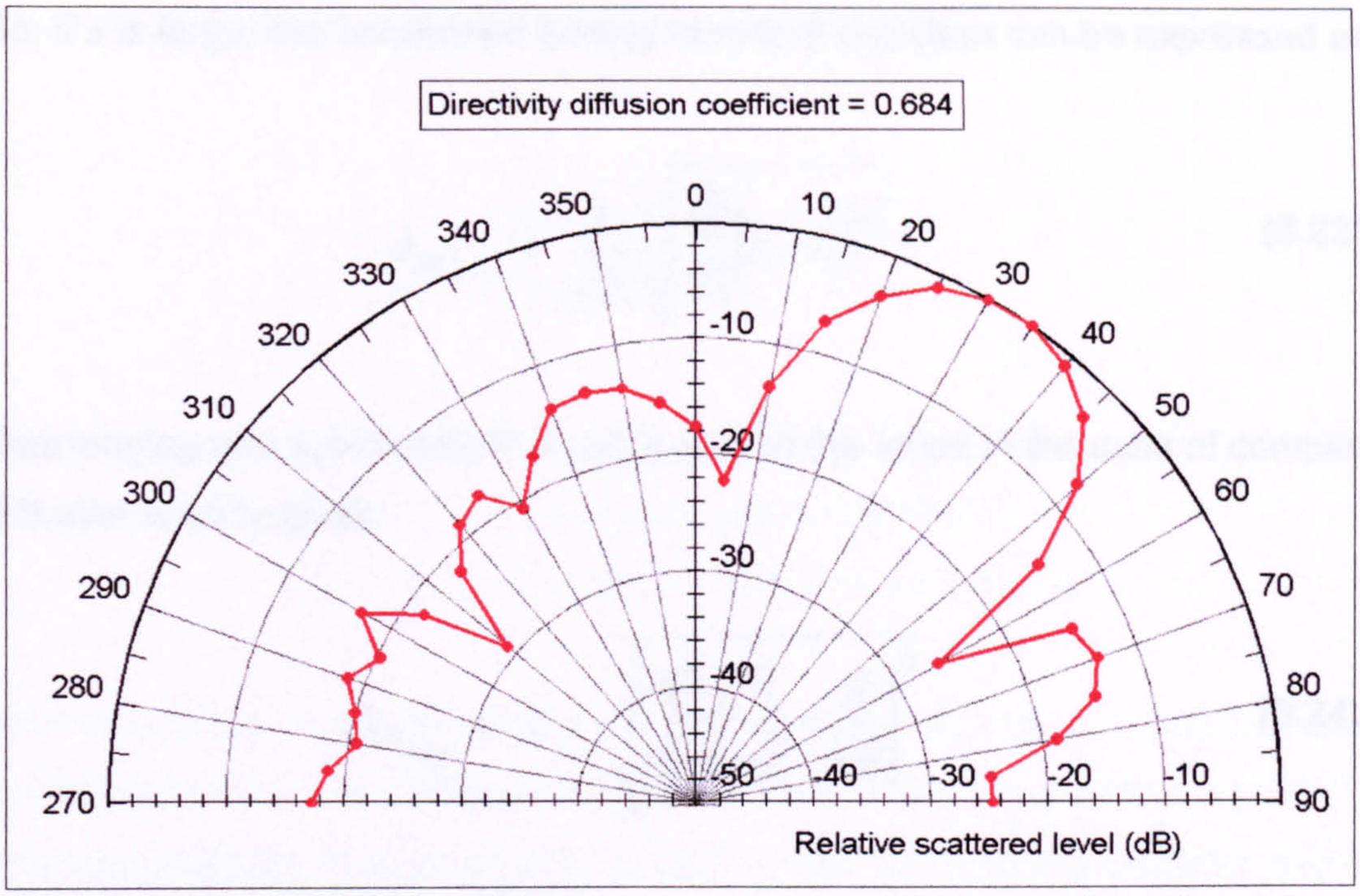

Figure 3.15: 2kHz 60° incidence polar response of the triangular prism, measured at RPG.

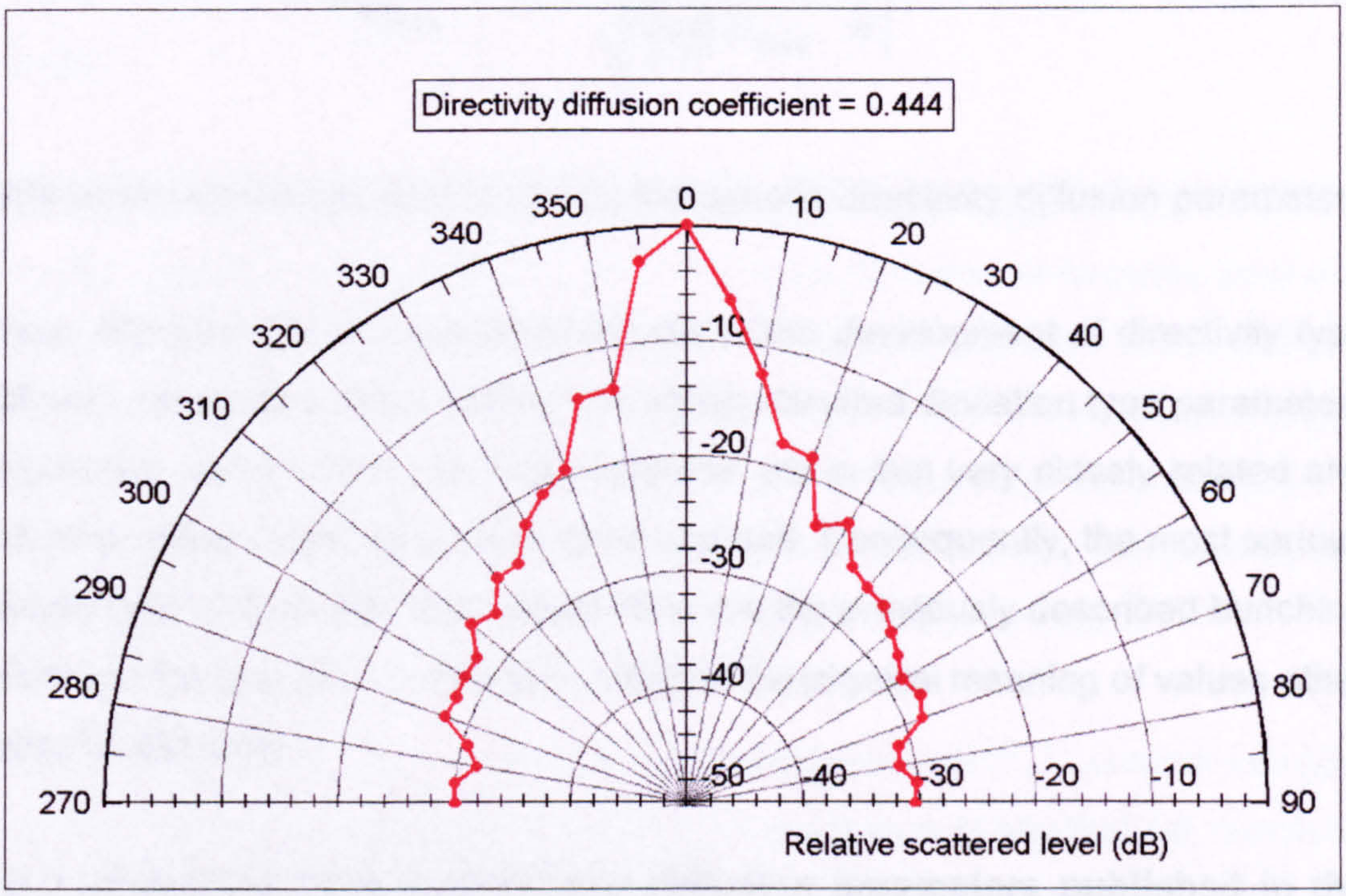

Figure 3.16: 4kHz normal incidence polar response of a 570mm wide plane panel, measured at RPG.

So, if n is large, the normalised energy standard deviation can be expressed as:

$$d_{\sigma E_{norm}} \approx \frac{1}{n\overline{E}}\sqrt{\sum_{i=1}^{n}\left[E_i-\overline{E}\right]^2} \tag{3.23}$$

Rearranging and subtracting from unity so that the value in the case of complete diffusion is unity gives:

$$d_{\sigma E_{norm}} \approx 1 - \sqrt{\sum_{i=1}^{n}\left[\frac{E_i}{n\overline{E}}-\frac{\overline{E}}{n\overline{E}}\right]^2} \tag{3.24}$$

Using (3.20), this can be written as:

$$d_{\sigma E_{norm}} \approx 1 - \sqrt{\sum_{i=1}^{n}\left[\frac{E_i}{E_{total}}-\frac{1}{n}\right]^2} \tag{3.25}$$

This expression is identical to (3.17), the generic directivity diffusion parameter.

Thus, although the philosophy which led to the development of directivity type diffusion parameters differs to that from which standard deviation type parameters originated, some of the resulting measures are in fact very closely related and therefore share similar properties, good and bad. Consequently, the most serious deficiencies of directivity type parameters are the previously described bunching effect and the fact that it is difficult to interpret the physical meaning of values other than the extremes.

3.5.3 Examples of directivity type diffusion parameters published in the literature.

The generic directivity diffusion parameter, d_{dir}, defined above is based on the

"*frequency dependent diffusion quality metric*", S_f^2, published by Angus[14] in 1995:

$$S_f^2 = \sum_{\theta=-90^\circ}^{\theta=90^\circ} \left\{ \frac{P_f(\theta)}{\sum_\theta P_f(\theta)} - \frac{1}{181} \right\}^2 \qquad (3.26)$$

where:

$P_f(\theta)$ = Power scattered in direction θ

$\sum_\theta P_f(\theta)$ = Total power radiated by the sample

This formulation assumes an angular resolution of 1° but can be generalised by replacing the constant being subtracted with the reciprocal of the number of receiver positions. The value of S_f^2 would be zero for complete diffusion and for other cases Angus states that, "S_f^2 *measures how far from a constant value it is by summing the squares of the difference between* $P_f(\theta)$ *and the amount of power at angle* θ *if the power were spread equally. Therefore surfaces which reflect strongly in only a few directions will have a higher value than those which scatter more evenly.*"

Although S_f^2 is bounded between zero and unity, Angus suggests summing over frequency to obtain the quantity S^2, which will thus be bounded between zero and the number of values of S_f^2 summed. Apart from data reduction, the benefits of this proposal are unclear and would seem to be outweighed by the drawbacks of losing the zero to unity bounding and the fact that the resulting value can be difficult to interpret and possibly misleading if the values of S_f^2 differ widely and poor values at some frequencies are compensated for by good values at others.

In appraising his parameter, Angus states that the value of S^2, "*...does in fact give a valid indication as to the diffusing quality...*". He goes on to say that, "*If, however, there were a sequence such that the values of* $P_f(\theta)$ *oscillated very quickly and evenly around a constant value then the size of* S^2 *would be relatively large. If the power is being scattered in a very large number of directions with equal intensity then we would consider the sequence to be a good diffuser but, since* S^2 *sums the*

difference between $P_f(\theta)$ and the average constant, then S^2 would be quite large in this case. This situation does not seem to occur in practice though, and is therefore not considered to be a real problem to the usefulness of S^2." In fact the case referred to by Angus of a polar response which is clearly diffuse but contains large numbers of maxima and minima and is therefore underrated by S_f^2 is unlikely to occur if frequency smoothing over at least a third-octave is performed.

The observation by Angus that there is a theoretical circumstance in which the parameter will fail but that this is unlikely to occur in practice and is therefore of no real concern is important because it is a situation commonly encountered during this type of research. Thought experiments will often reveal cases in which parameters will fail and in order to judge whether such failures are serious deficiencies or academic trifles it is necessary to know the behaviour of a wide variety of practical surfaces, in this case the shapes of the polar responses they produce. A beneficial by-product of this research is that the large number of polar responses which have been measured for many surfaces, frequencies and angles of incidence, partly to enable such judgements to be made, will continue to be of use in any future similar work.

In 1993, D'Antonio[10] suggested the following parameter to quantify diffusion as a function of frequency and angle of incidence:

$$D(f,v_i) = \frac{1}{N}\sum_{j=1}^{N}\frac{I_j}{I_{spec}} = \frac{1}{N}\sum_{j=1}^{N}10^{\left[\frac{dB_j - dB_{spec}}{10}\right]} \qquad (3.27)$$

where:

f = Frequency

v_i = Incident direction cosine

N = Number of receiver positions

I_j and dB_j = Scattered intensity and SPL at receiver position j

I_{spec} and dB_{spec} = Intensity and SPL at the specular receiver position

The 'specular receiver position' is defined as the point on the receiver arc through which a ray from the source that is specularly reflected at the centre of the sample would pass.

Although this parameter exhibits substantial differences from the generic directivity parameter defined in (3.17), it is included here because D'Antonio derives it from the definition of directivity index, using the philosophy that diffusion is the reciprocal of directivity. Provided that I_{spec} is the maximum scattered intensity in the polar response, it is likely that this parameter would rank (but not necessarily rate) responses correctly. However, it is commonplace for the maximum intensity not to occur at the 'specular receiver position' - an extreme example of this is shown in Figure 3.17 - and in these cases the parameter fails; its value is meaningless.

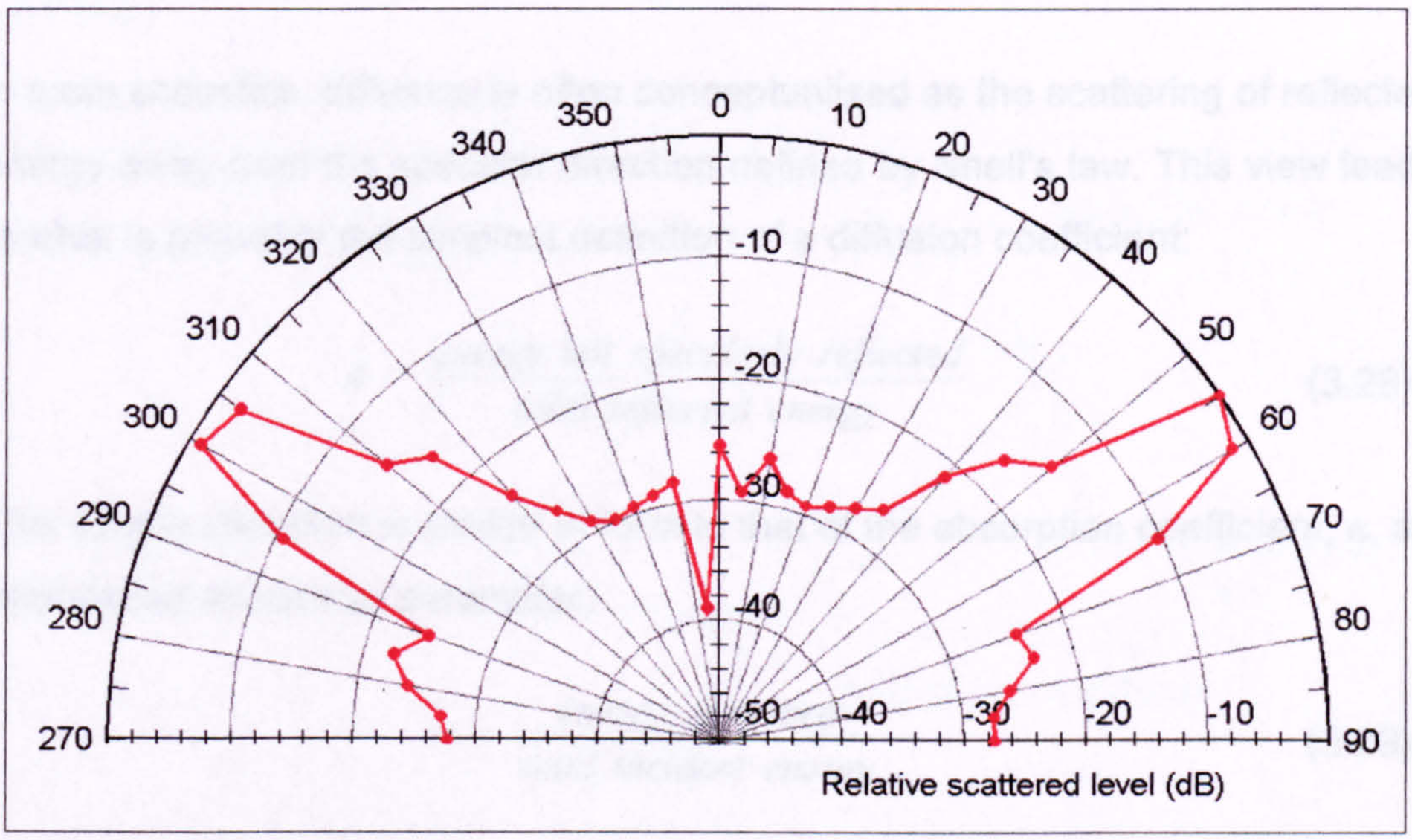

Figure 3.17: 4kHz normal incidence polar response of the square-based pyramid, measured at RPG.

If I_{spec} is replaced with the maximum value of intensity, regardless of where in the polar response this occurs, then the parameter is more generally applicable and will be bounded between zero and unity whatever the shape of the polar response. However, comparing the intensity at each receiver position to the maximum intensity causes the value of this parameter to be prone to error and any measured

aberration in a polar response would require investigation to determine whether it were a true feature of the scattered field or an artifice of the measurement. For example, a response which is uniform except at one or two positions where the measured sound pressure level is 6dB above the constant level would have a parameter value of approximately 0.5. If the raised levels are measurement glitches then the value should instead be unity, corresponding to complete diffusion. Parameters which quantify diffusion by comparing individual measured quantities to means or totals of a number of measurements are more tolerant of such glitches.

3.6 **Diffusion parameters based on the specular zone concept.**

3.6.1 **Introduction.**

In room acoustics, diffusion is often conceptualised as the scattering of reflected energy away from the specular direction defined by Snell's law. This view leads to what is probably the simplest definition of a diffusion coefficient:

$$d = \frac{energy\ not\ specularly\ reflected}{total\ reflected\ energy} \tag{3.28}$$

This simple definition is similar in form to that of the absorption coefficient, α, an established acoustical parameter:

$$\alpha = \frac{energy\ absorbed}{total\ incident\ energy} \tag{3.29}$$

In common with the absorption coefficient, the physical meaning of all values of this diffusion coefficient can be readily understood and it is bounded between zero and unity[†]. It also links to some of the styles of diffusion modelling used in prediction models. The main problem with this theoretically simple parameter is that its evaluation from a polar response requires the non-specularly reflected energy to be separated from the total, a procedure which is not straightforward.

[†] The upper bound of the absorption coefficient as defined in (3.29) should be unity but it is well known that when measuring absorption using the ISO 354 method, values in excess of this are regularly obtained.

3.6.2 **Definition of the specular zone.**

A common but crude attempt at achieving this separation is based on geometry and illustrated in Figure 3.18. It involves firstly determining the scattering directions in which a specular reflection is possible, given the position of the source. This in itself would prove to be a challenging task for samples with anything other than the simplest topography. Therefore to simplify the process, the sample being evaluated is assumed to be plane and identical in size to its normal incidence projection, regardless of what its actual form may be. This permits the image source method to be used to define the specular directions and once these are known, the portion of the receiver semicircle or hemisphere that they intersect can be determined. This arc length or surface area is termed the specular zone, energy within it is assumed to have been specularly reflected and energy outside it, scattered.

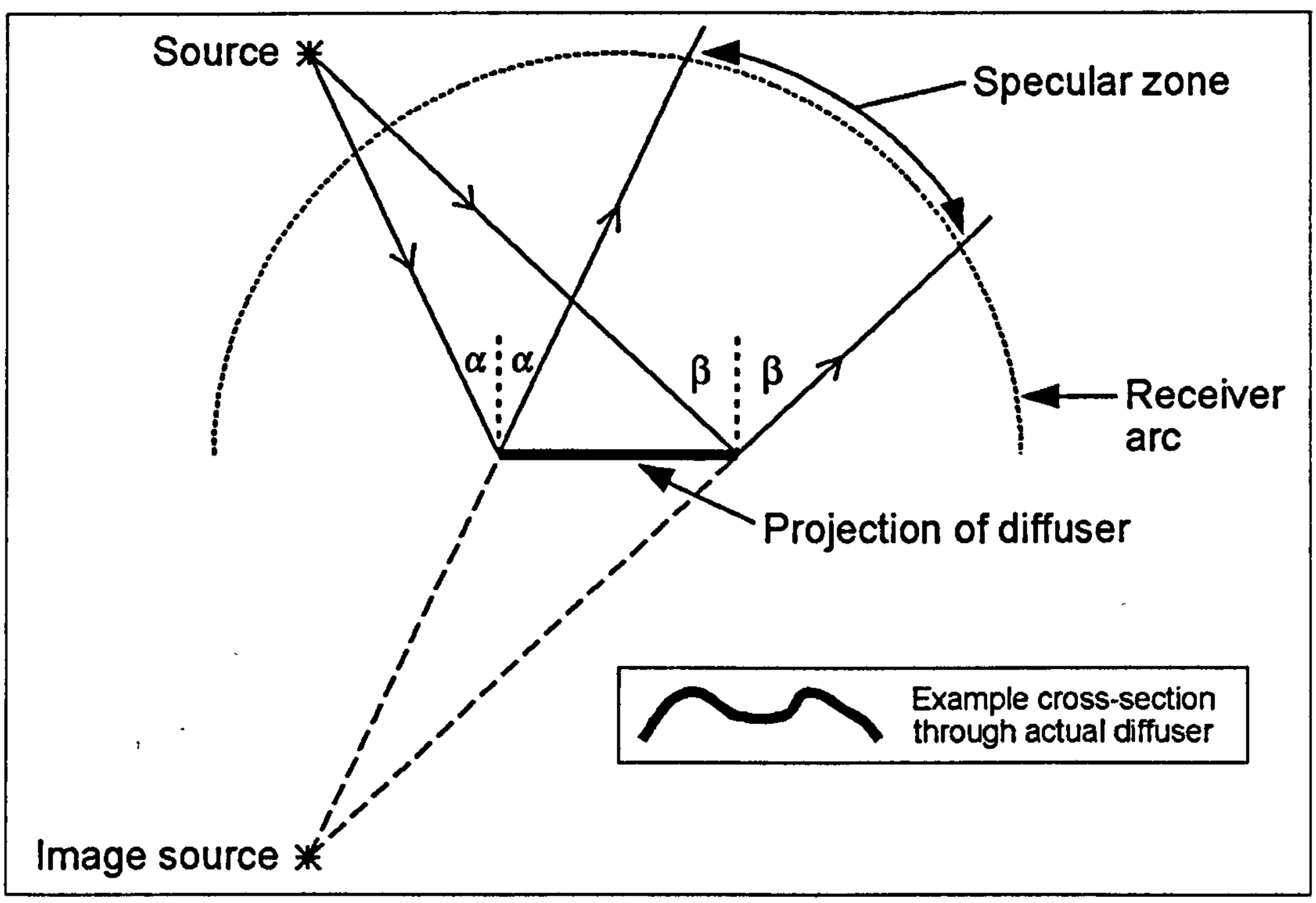

Figure 3.18: Definition of the specular zone (two dimensions).

3.6.3 **Definition and appraisal of diffusion parameters.**

Establishing the concept of the specular zone permits (3.28) to be expressed more formally:

$$d_{specl} = 1 - \frac{\sum_{i=1,(\theta_i,\varphi_i)\in s_z}^{n_z} E_i}{\sum_{i=1}^{n} E_i} \qquad (3.30)$$

where:

E_i = Energy at receiver position i

n_z = Number of receiver positions in the specular zone

n = Total number of receiver positions

The summation in the numerator is taken over only those receiver positions which have angles of elevation, θ_i, and azimuth, φ_i, such that they are members of the set of positions inside the specular zone, s_z.

This coefficient is similar in philosophy to one defined by Lam[16] and in addition to possessing the benefits identified previously, it relates to the commonly perceived role of diffusers in room acoustics, that of moving reflected energy away from the specular directions. It does, however, have two principal drawbacks.

The first is that according to (3.30), complete diffusion would be the case where there is zero energy in the specular zone, corresponding to a polar response which contains a notch as shown in Figure 3.19 on the following page. This conflicts with the definition of complete diffusion as uniform scattering and in any case there is no known surface that can produce such a shape of polar response over any significant bandwidth and for random incidence. Primitive root diffusers and modified forms[31,54,55] can generate notches at specific frequencies and by using

optimisation[55] surfaces which produce broader band notches can be designed but these only work for single specified angles of incidence.

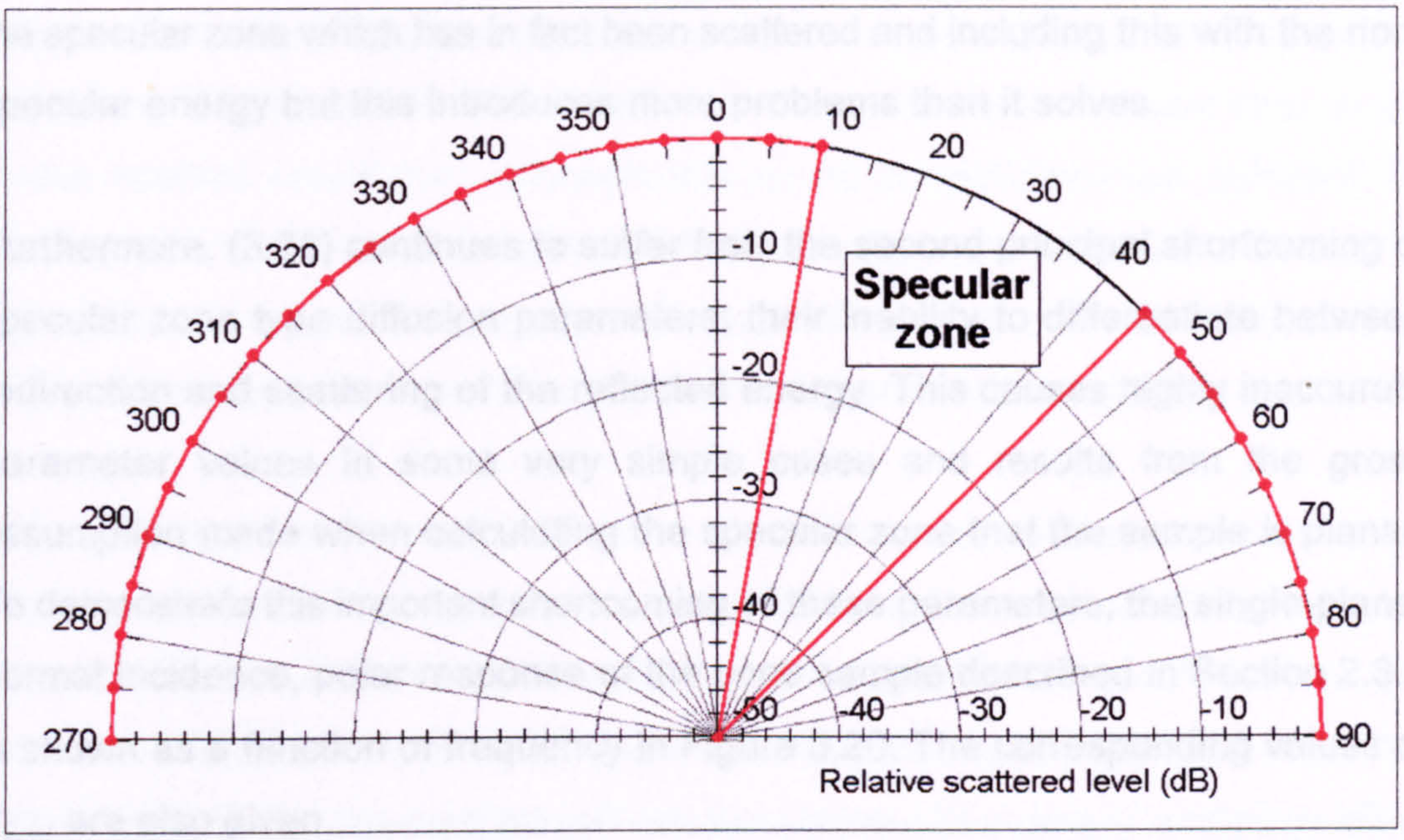

Figure 3.19: Polar response representing complete diffusion, according to (3.30).

One solution to this problem, suggested by Lam[56], is to incorporate a correction factor into (3.30) to make the value of the coefficient unity in the case of even scattering:

$$d_{spec2} = \left[1 - \frac{\sum_{i=1,(\theta_i,\varphi_i)\in s_z}^{n_z} E_i}{\sum_{i=1}^{n} E_i} \right] \frac{n}{n-n_z} \qquad (3.31)$$

However, although the introduction of this 'correction' factor solves one problem, it causes others. Firstly, the upper bound of the coefficient is no longer unity; a value in excess of this is now obtained if the level inside the specular zone is lower than that outside. Secondly, the physical meaning of values is more difficult to interpret because they no longer express the simple ratio given by (3.28).

Attempts have been made to further develop (3.30) with the aim of producing a specular zone diffusion coefficient without these deficiencies but there has been little success. One approach[56] involves estimating the proportion of the energy in the specular zone which has in fact been scattered and including this with the non-specular energy but this introduces more problems than it solves.

Furthermore, (3.31) continues to suffer from the second principal shortcoming of specular zone type diffusion parameters; their inability to differentiate between redirection and scattering of the reflected energy. This causes highly inaccurate parameter values in some very simple cases and results from the gross assumption made when calculating the specular zone that the sample is planar. To demonstrate this important shortcoming of these parameters, the single-plane, normal incidence, polar response of the cone sample described in Section 2.3.9 is shown as a function of frequency in Figure 3.20. The corresponding values of d_{specl} are also given.

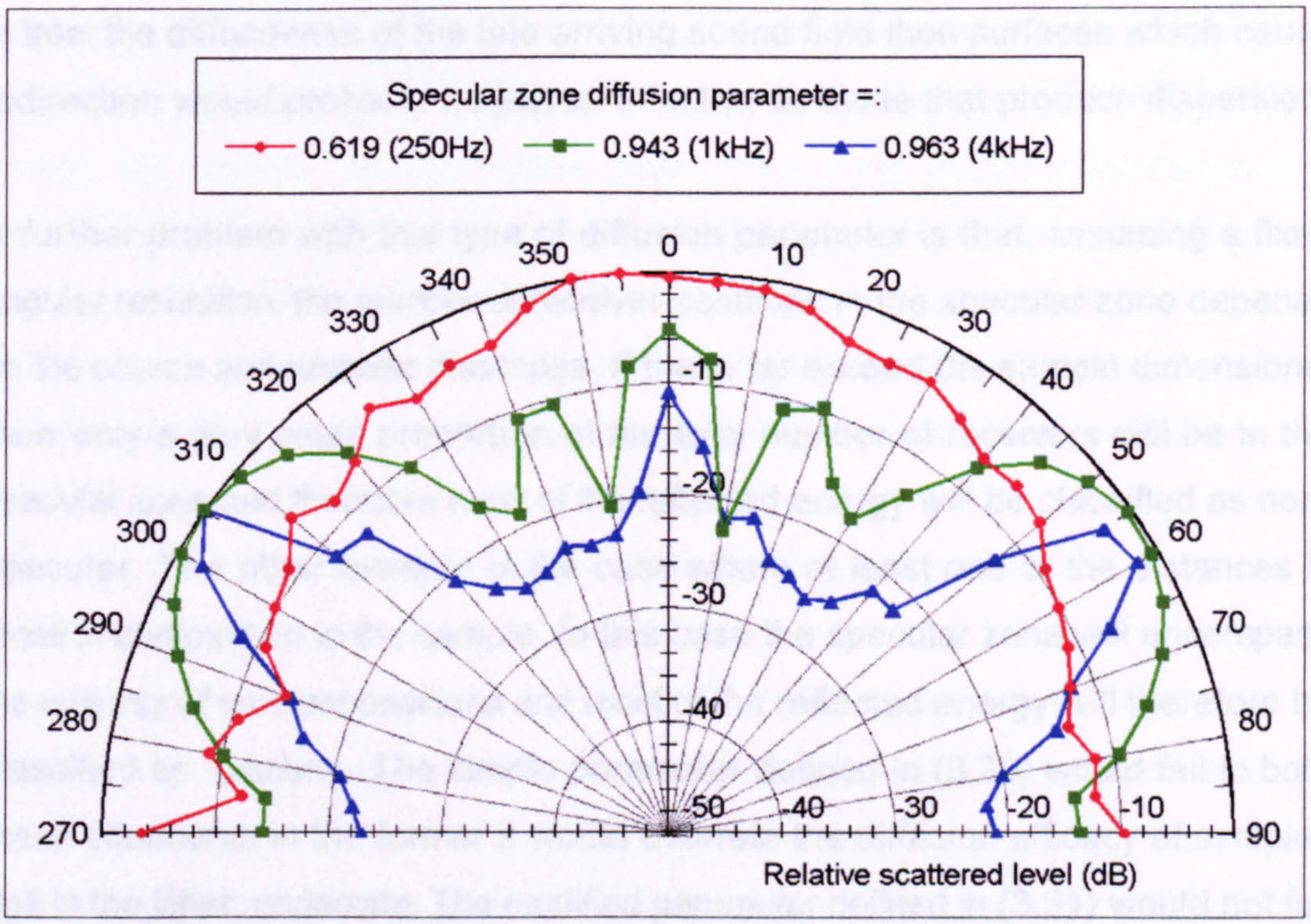

Figure 3.20: Illustration that specular zone type diffusion parameters fail to correctly rate the diffusion efficacy of surfaces which redirect as opposed to scatter the reflected energy.

From the polar responses it can be seen that the scattering becomes less diffuse as the frequency increases because the reflections from the cone sides become increasingly specular-like. However, the values of d_{specl} do not express this, in fact they indicate that the polar responses become more diffuse with increasing frequency. The reason for this is that since the sides of the cone are at an angle to the incident sound then although this sound is specularly-like reflected, its propagation direction after reflection is outside the specular zone defined by Figure 3.18. As a result, specular zone type diffusion parameters interpret this energy as non-specular even though it has not been scattered, merely redirected.

Although in both cases energy is moved out of the specular zone, surfaces which redirect the reflected energy as opposed to dispersing it are not usually considered to be diffusers. This is because an important application of diffusers is the treatment of first order reflections and if these are redirected instead of scattered then it is likely that the problem will not be eliminated but simply shifted to affect a different set of receiver positions. However, if the only purpose of diffusers was to treat the diffuseness of the late arriving sound field then surfaces which cause redirection would probably be just as effective as those that produce dispersion.

A further problem with this type of diffusion parameter is that, assuming a fixed angular resolution, the number of receiver positions in the specular zone depends on the source and receiver distances. If these far exceed the sample dimensions, then only a very small proportion of the total number of receivers will be in the specular zone and therefore most of the reflected energy will be classified as non-specular. The other extreme is the case where at least one of the distances is small in comparison to the sample. In this case the specular zone will encompass the majority of receiver positions and most of the reflected energy will therefore be classified as specular. The simple parameter defined in (3.30) would fail in both these situations; in the former it would overrate the diffusion efficacy of samples and in the latter, underrate. The modified parameter defined in (3.31) would not fail in this manner because the correction factor allows for changes in the size of the specular zone. However, both parameters would suffer from signal to noise problems if the number of receivers in the specular zone was very low.

Hence, in order for specular zone type diffusion parameters to have any prospect of providing a realistic assessment of diffusion efficacy, the source and receiver distances must be such that there are a significant number of receiver positions both inside and outside the specular zone. This requirement conflicts somewhat with the need for polar responses to be obtained in the far field; in the far field there may be too few receiver positions in the specular zone. The optimum specular to non-specular ratio of receiver positions is not known and has not been addressed by this research due to the limited applicability of this type of diffusion parameter. However, for most of the single-plane measurements about 15-20% of the receiver positions were in the specular zone.

To summarize, the conceptual simplicity and the firm physical basis of quantifying diffusion from the ratio of the non-specularly reflected energy and the total reflected energy are appealing. However, evaluating this quantity from a polar distribution using the specular zone idea is problematic and frequently produces incorrect results, particularly for samples which redirect rather than scatter the reflected energy. Alternative methods of dividing the reflected energy into specular and non-specular components have been proposed by Mommertz and Vörlander[22]. These approaches do not involve either measuring polar responses or the specular zone concept and are discussed in Chapters 4 and 5. However, Farina[57] has recently argued that the difficulty of separating the specular and non-specular energy is in fact too great and has proposed an alternative empirical technique for quantifying diffusion. Farina's work should be considered in future research.

3.7 Quantifying diffusion using surface spherical harmonics.

Angus[20] has demonstrated that three-dimensional polar responses can be modelled mathematically as continuous functions of direction on the surface of a sphere using the concept of surface spherical harmonics. The primary benefit of representing polar responses in this manner is efficiency; the amount of data which must be stored is reduced without compromising accuracy. An important subsidiary benefit is that from the mathematical model, the uniformity of the response, and hence the diffusion efficacy of the surface producing it, can be readily quantified.

Surface spherical harmonics are a hierarchical set of basis functions which are orthogonal upon the surface of a sphere. Therefore a three-dimensional polar response can be represented as a weighted sum of these harmonics in a similar manner to the more conventional one-dimensional case of Fourier analysis where the basis functions are sinusoidal harmonics.

Since surface spherical harmonics are hierarchical, the polar response model progressively increases in accuracy with the number of harmonics included. Higher order harmonics express more rapid variation of the polar response with respect to angle in an analogous fashion to the higher frequency Fourier components of conventional audio signals. The model also has a meaningful physical structure because particular surface spherical harmonic weights express particular patterns of directional variation in the polar response as shown in Figure 3.21.

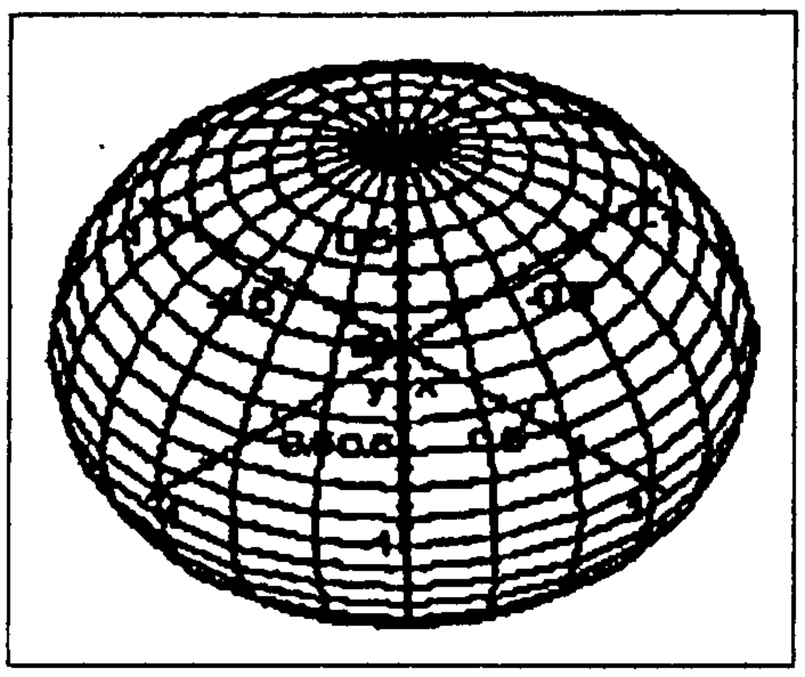

Figure 3.21a: The degree zero spherical harmonic. (Angus[20])

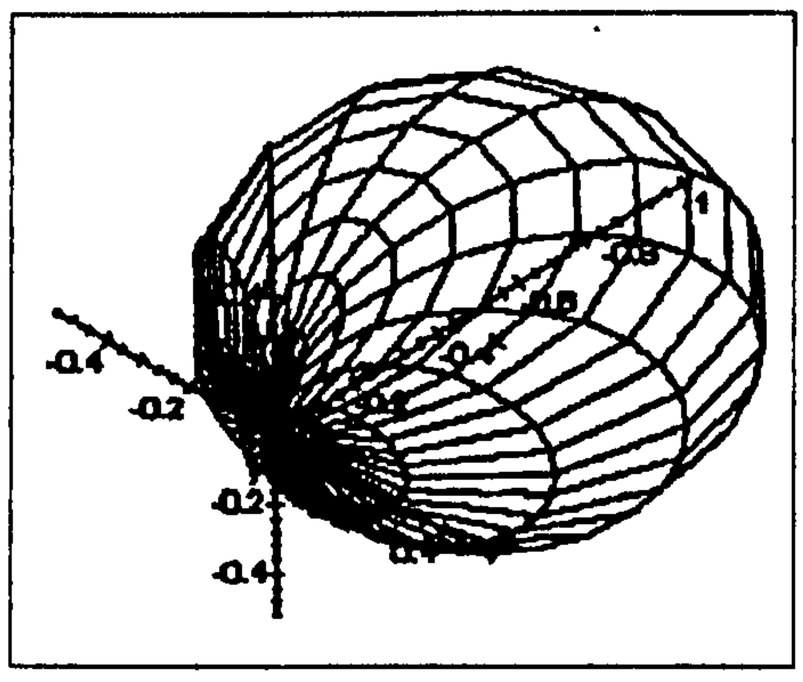

Figure 3.21b: A first degree spherical harmonic. (Angus[20])

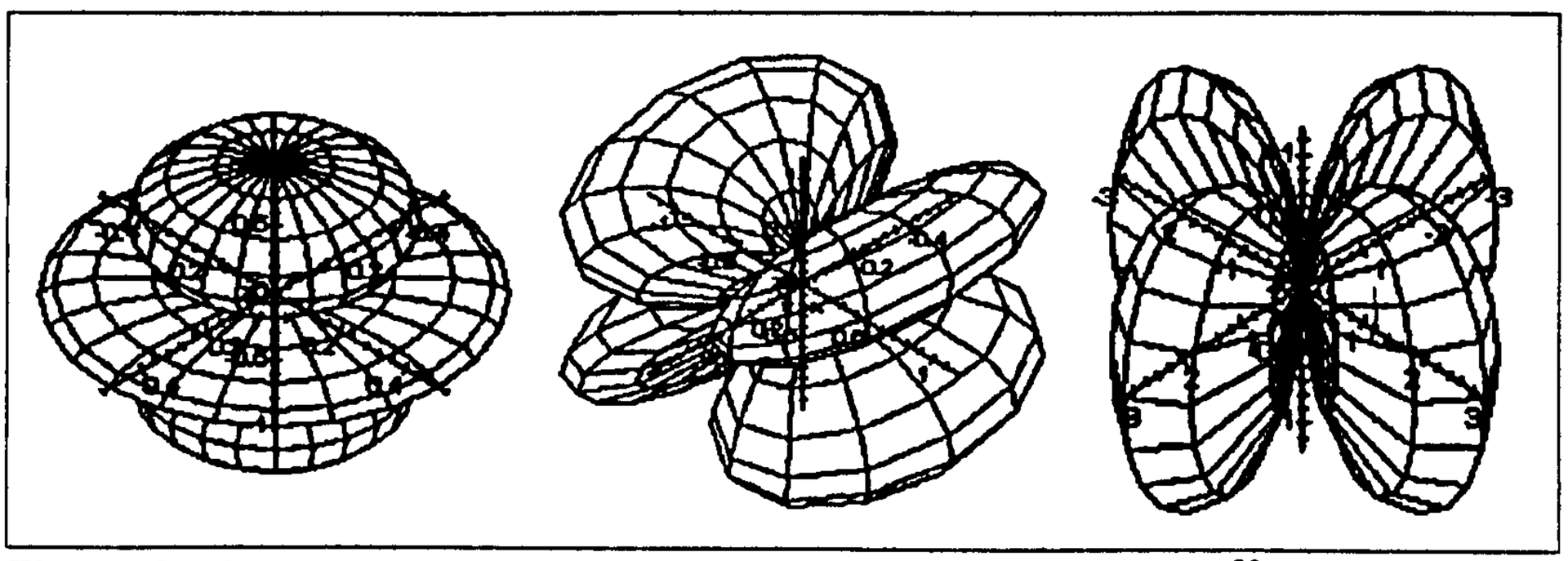

Figure 3.21c: Some degree two spherical harmonics. (Angus[20])

From Figure 3.21 it can be seen that the fundamental (degree zero) surface spherical harmonic is a sphere centred on the origin and thus corresponds to the omnidirectional component of the response. There are three first degree harmonics and these are spheres which lie along one of each of the Cartesian axes and intersect at the origin. Higher order harmonics have more complex shapes.

To evaluate the weights of the individual harmonics, the polar response must be sampled at a number of points but it is not necessary to measure over the complete sphere with an angular resolution of n^{o}, although the weights can be obtained from such a measurement. In fact the required number of measurements is greatly reduced, less than one hundred are required for evaluation of the surface spherical harmonics up to degree six. However, these measurement positions have different angles of azimuth and elevation so an automated measurement system is required to achieve the maximum benefit from their reduced number. It is possible to use a set of positions which are more regularly spaced, which makes the measurement more systematic, but a larger number are required.

To quantify diffusion, Angus suggests using the fraction of the total energy contained in the fundamental. In the case of uniform scattering this would be unity and would decrease for progressively less omnidirectional responses. It has not been possible to evaluate this diffusion parameter during the course of this research but it would be very interesting to do so and this is suggested as a priority for future work.

The process by which this diffusion parameter is obtained is possibly too complex for it to be suitable for general use but the concept of representing a polar response using surface spherical harmonics has the potential to be useful to researchers and in computer models. For example, modern loudspeaker CAD packages require a full specification of the polar response as a function of frequency in order to provide an accurate prediction of their likely performance in a given space. Future room models may require the polar response of surfaces to be specified to a similar degree of accuracy and this could be accomplished very efficiently using surface spherical harmonics.

3.8 New '90% energy' diffusion parameter.

3.8.1 Introduction and definition.

In the case of complete diffusion, energy is scattered in every direction whereas in the theoretical worst case, the reflected energy is non-zero in only a single direction. These features of the two extreme polar responses initiated an investigation into whether the diffusion efficacy of a sample could be quantified from the number of directions into which it scatters the reflected energy. However, since in practice it is rarely the case that zero energy is measured at any receiver position, even when the reflection is specular, it was necessary to develop a criterion which enabled the directions in which very little energy was reflected to be excluded.

One possibility was to count only those directions in which the reflected energy was above a certain threshold, ignoring those where the energy was, for example, in excess of kdB below either the maximum or mean level. However, this proved unsatisfactory because it results in insufficient discrimination between responses of dissimilar shape, whatever the value of k.

A second idea was to use a cumulative probability type approach and count the directions in decreasing order, starting with that in which the reflected energy is a maximum, simultaneously summing the energy until the sum reaches a certain percentage, x, of the total energy reflected. If the value of x is close to 100% then the number of directions counted, n_x, is that into which 'most' of the energy is reflected. This quantity is a diffusion metric (for a fixed number of receiver positions) with the beneficial property of having a straightforward and useful physical interpretation because it is similar in concept to a percentile measure. x cannot be actually equal to 100% because all directions would usually have to be included to account for the entire reflected energy, hence n_{100} would simply be equal to the total number of receiver positions.

It has been found that the purely pragmatic choice of x=90% results in an

acceptable variation in n_{90} for polar response shapes ranging from specular reflection to uniform scattering. For higher values the discrimination becomes increasingly poorer and for lower values the proportion of the reflected energy accounted for cannot be reasonably referred to as 'most' and therefore the measure loses its physical utility. Consequently an original measure, the '90% energy' diffusion parameter, $d_{90\%}$, was formulated:

$$d_{90\%} = \frac{n_{90}}{0.9n} \tag{3.32}$$

where:

n_{90} = Number of directions accounting for 90% of the total reflected energy

n = Number of directions (receiver positions)

The division by $0.9n$ is a normalisation which bounds the value of $d_{90\%}$ between zero (actually $1/0.9n$) and unity because $0.9n$ is the value of n_{90} in the case of uniform scattering.

The physical meaning of values of $d_{90\%}$ can be interpreted on two levels of sophistication; the simplest is to approximate and interpret a value of, say, 0.6 as meaning that all the reflected energy is scattered into 60% of the directions. The more accurate interpretation is that a value of 0.6 in fact means that 90% of the reflected energy is scattered into 54% of the directions but whether in practice this is any more useful than the approximation is doubtful. Neither interpretation gives any indication of which directions the energy is scattered into.

3.8.2 **Appraisal.**

This new diffusion coefficient goes a long way towards satisfying the criteria for the ideal; it has a firm physical basis, is bounded between zero and unity and, as shown in Figures 3.22 to 3.27, practical values are spread over the entire range.

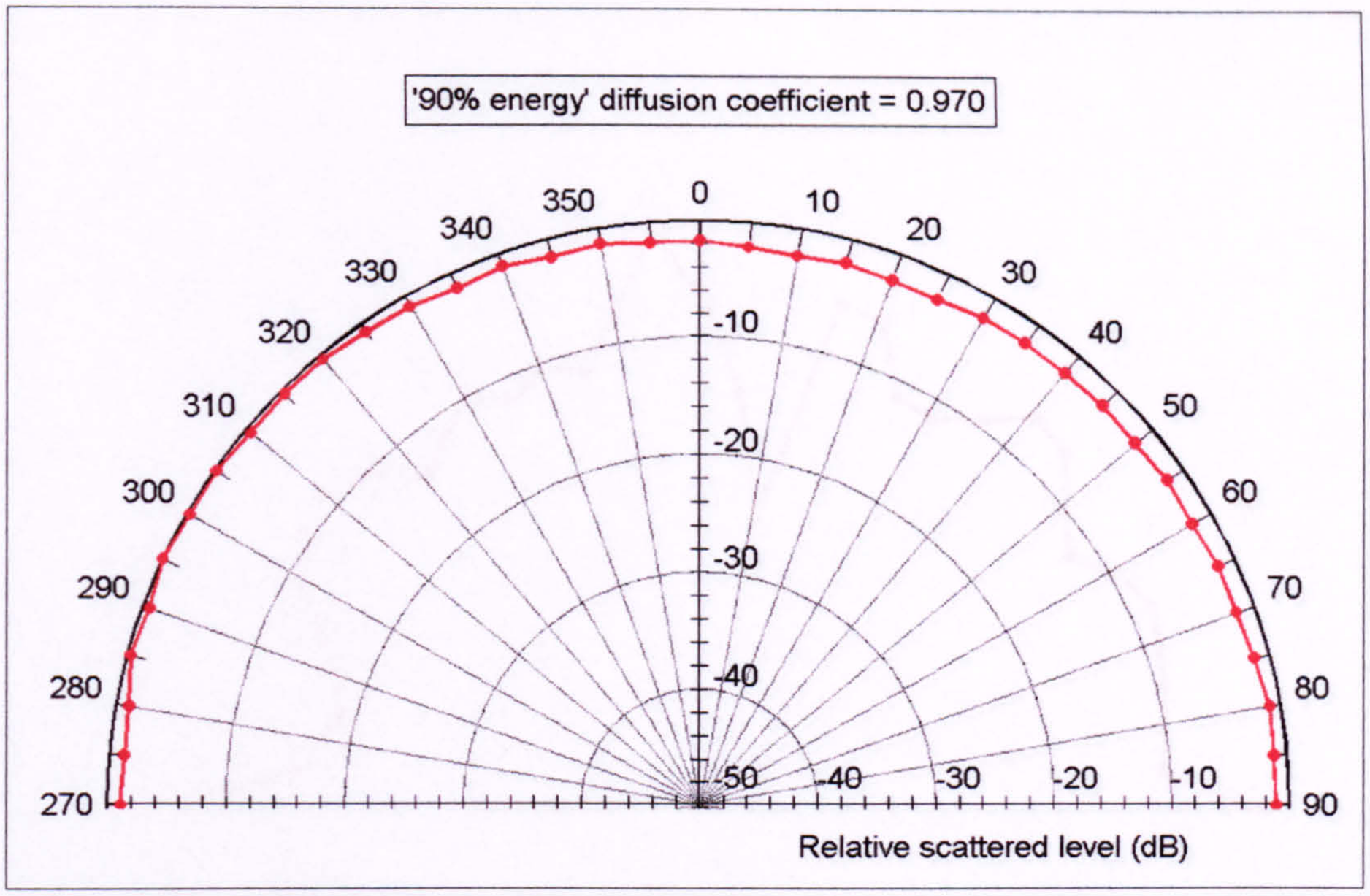

Figure 3.22: 500Hz 45° incidence polar response of the QRD, measured at RPG.

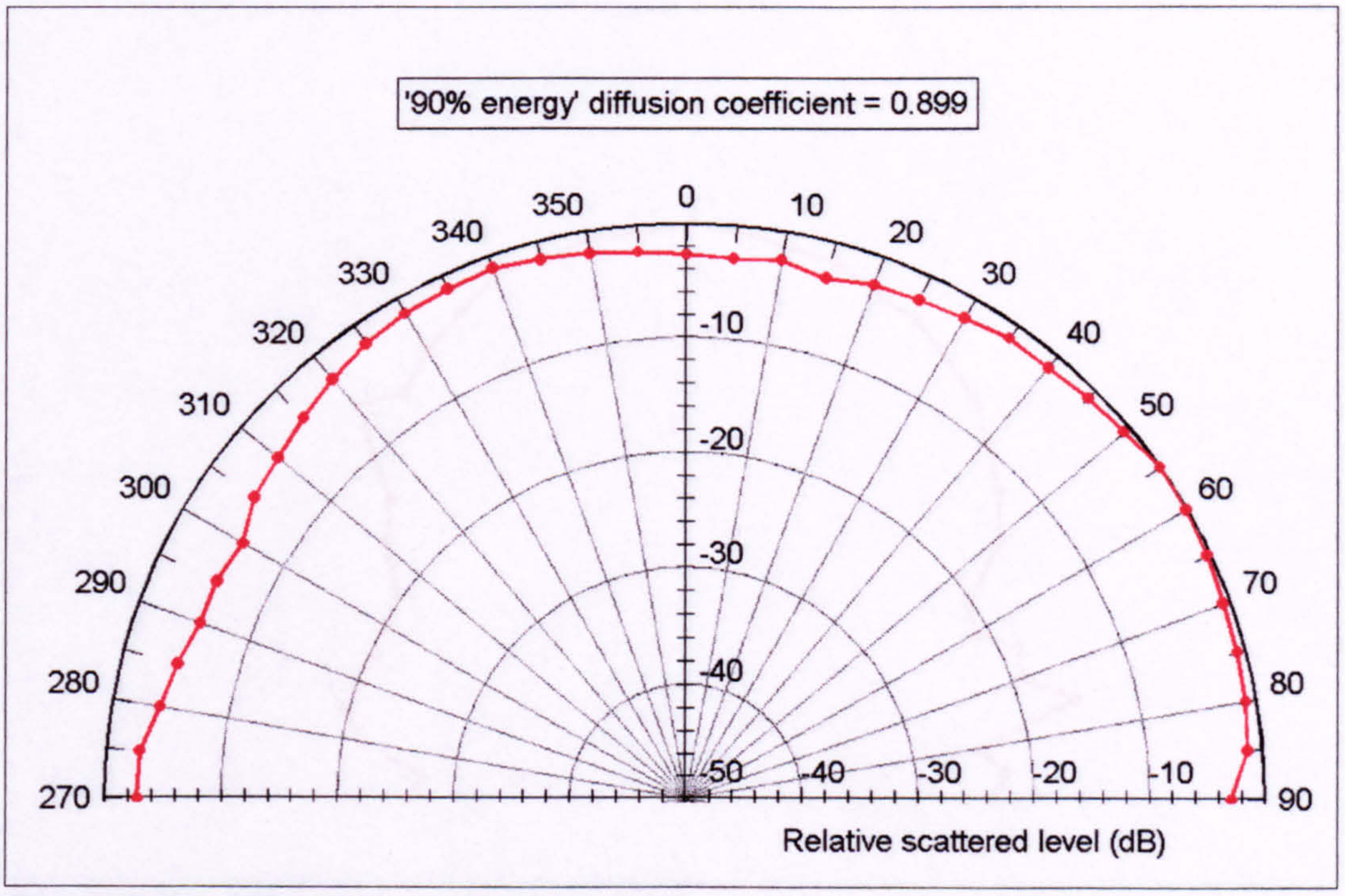

Figure 3.23: 800Hz 30° incidence polar response of the semicylinder, measured at RPG.

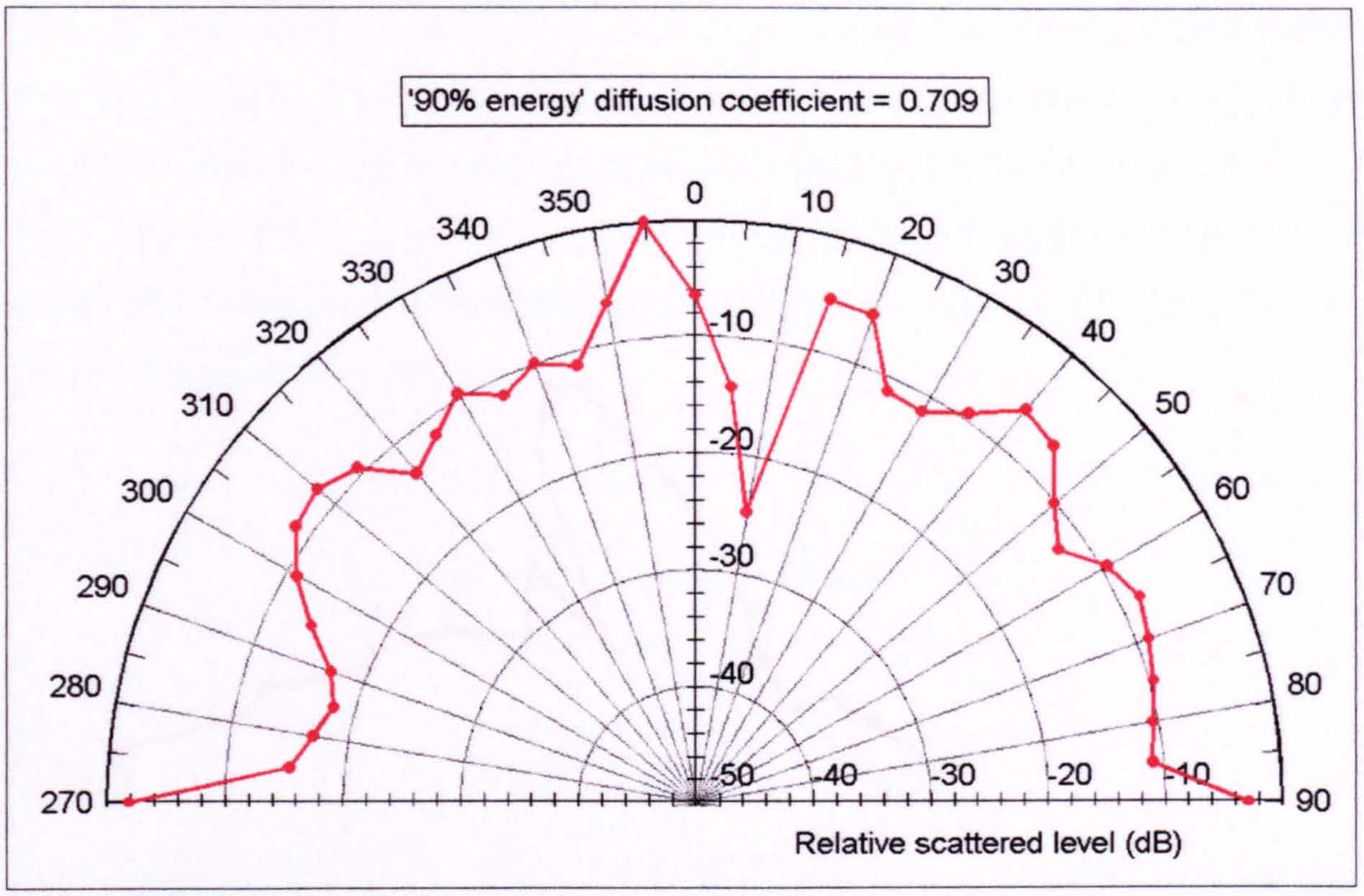

Figure 3.24: 1kHz normal incidence polar response of the random battens, in the plane perpendicular to the battens, measured at RPG.

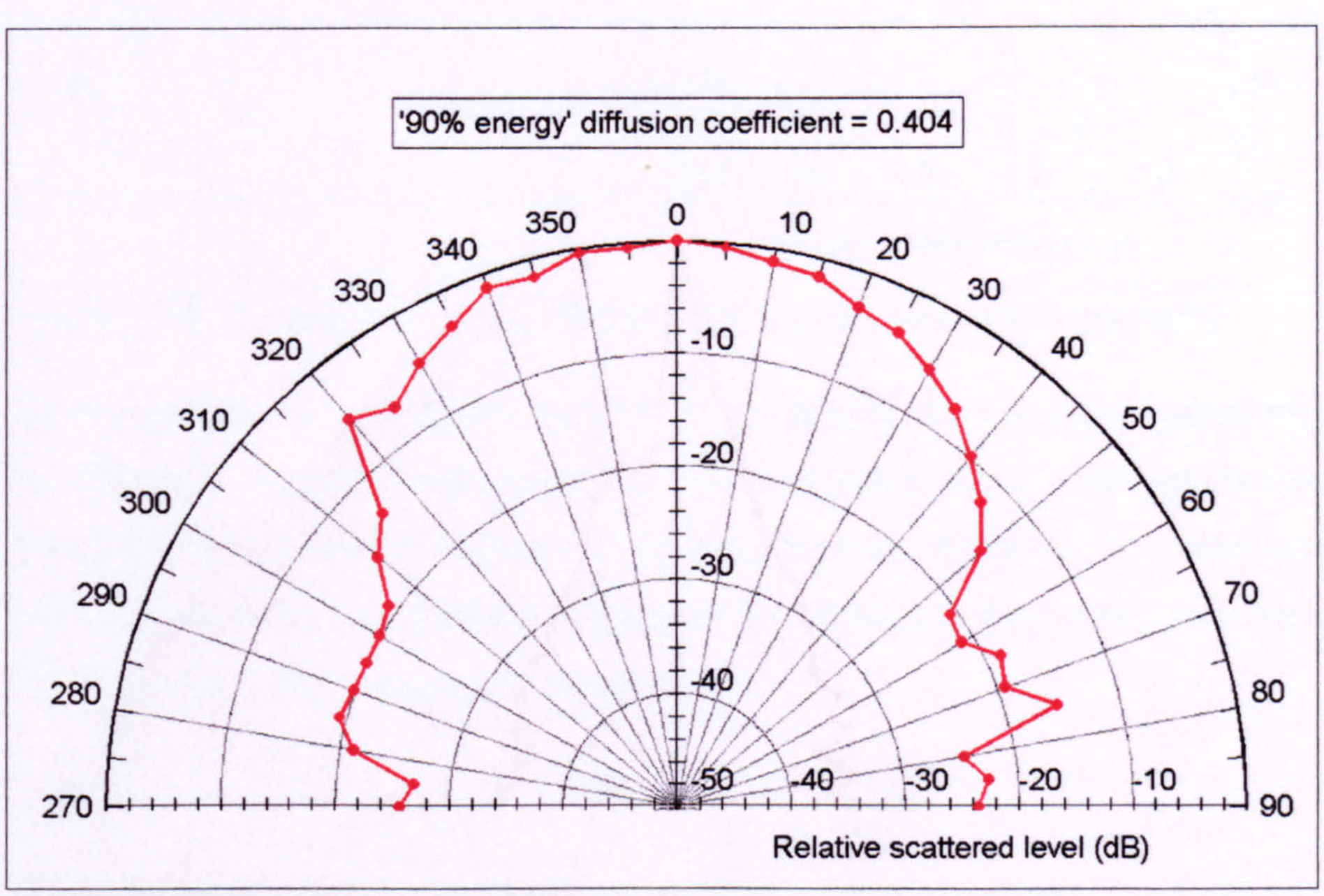

Figure 3.25: 630Hz normal incidence polar response of a BAD Panel, measured at RPG.

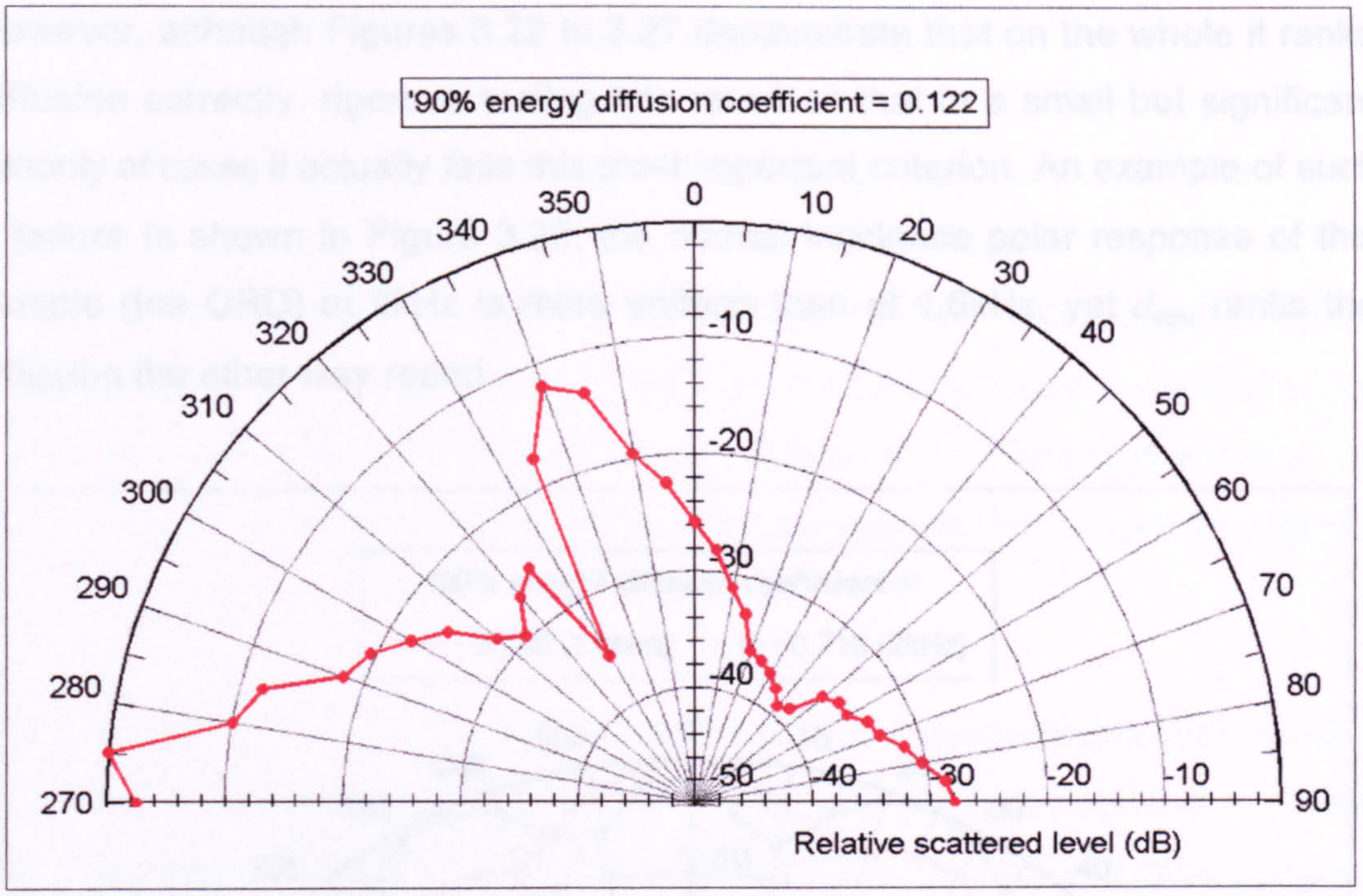

Figure 3.26: 4kHz 75° incidence polar response of the cone, measured at RPG.

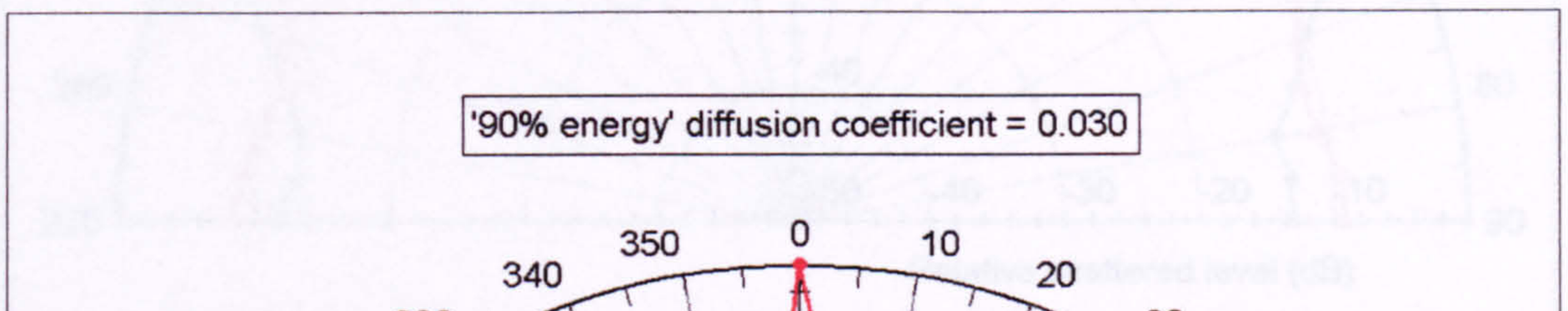

Figure 3.27: 3.15kHz normal incidence polar response of the concave prism, measured at RPG.

However, although Figures 3.22 to 3.27 demonstrate that on the whole it ranks diffusion correctly, rigorous testing has revealed that in a small but significant minority of cases it actually fails this most important criterion. An example of such a failure is shown in Figure 3.28, the normal incidence polar response of this sample (the QRD) at 2kHz is more uniform than at 1.6kHz, yet $d_{90\%}$ ranks the diffusion the other way round.

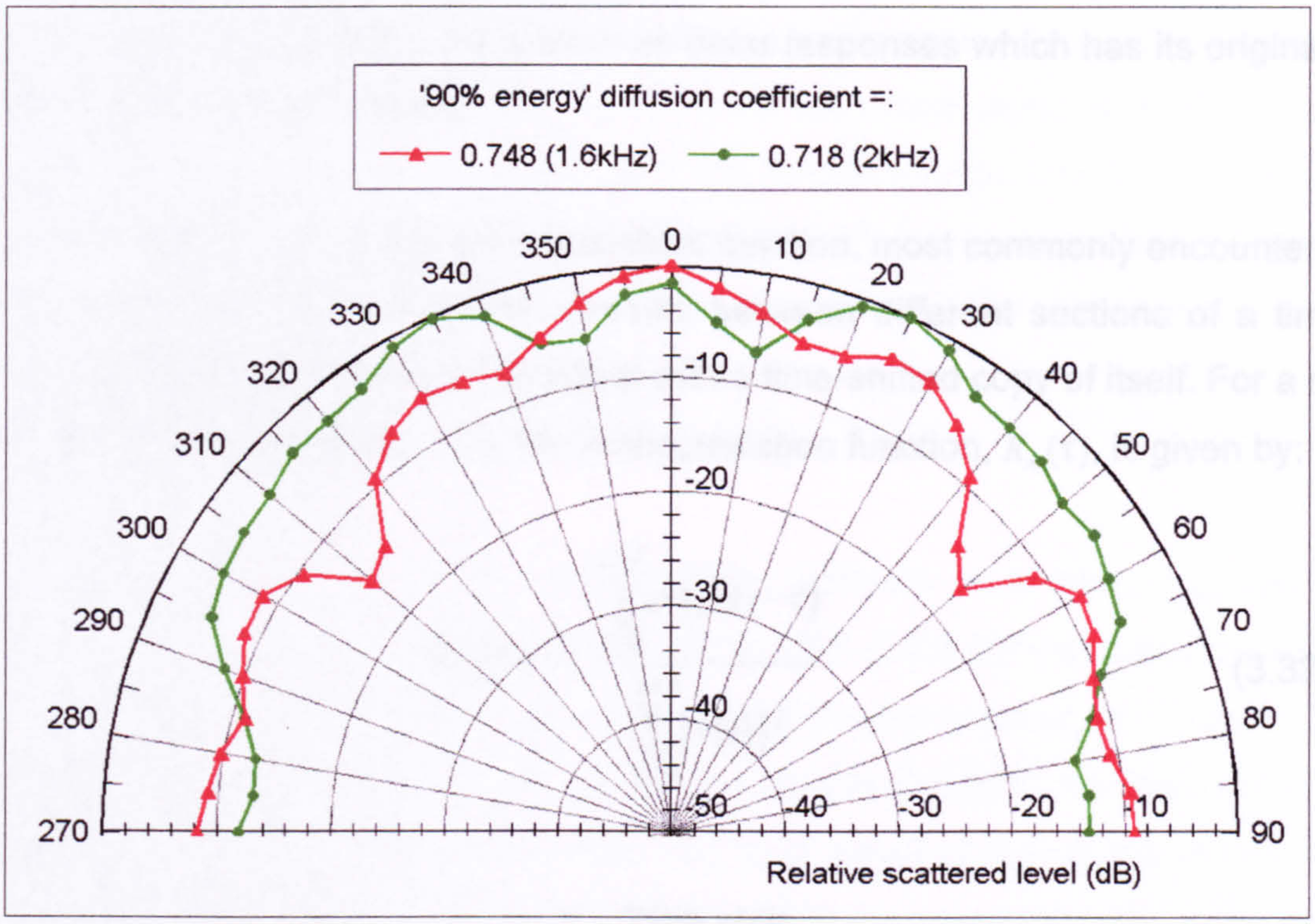

Figure 3.28: An example of $d_{90\%}$ failing to rank polar responses correctly.

In summary, this novel diffusion parameter possesses the significant advantage over standard deviation and directivity types of there being a straightforward physical interpretation of all values, not just the extremes. However, no matter how useful this property, it cannot be justified at the expense of incorrect ranking of diffusion, even if this occurs only occasionally.

3.9 New 'autocorrelation' diffusion parameter.

3.9.1 Introduction to the concept of autocorrelation.

One feature of complete diffusion (defined as uniform scattering) is that the magnitude of the reflected energy is independent of direction; it is the same at all receiver positions. This feature has been utilised in the development of a new parameter for quantifying diffusion from polar responses which has its origins in the autocorrelation function.

Autocorrelation is a well known statistical function, most commonly encountered in acoustics for assessing the similarity between different sections of a time-varying signal by comparing the signal with a time-shifted copy of itself. For a set of sampled signal values, $x(t)$, the autocorrelation function, $R_{xx}(\tau)$, is given by:

$$R_{xx}(\tau) = \frac{\sum_{t=0}^{t=T} x(t)x(t-\tau)}{\sum_{t=0}^{t=T} [x(t)]^2} \qquad (3.33)$$

where:

τ = Time shift

However when calculating this new parameter, which quantifies diffusion by assessing the similarity between different sections of a polar response, the autocorrelation function is evaluated in the spatial as opposed to time domain because a polar response is a function of angle. Consequently, although this autocorrelation is calculated using a formulation very similar to (3.33), τ represents a shift in angle rather than time. A single-plane polar response can be considered analogous to $x(t)$ in (3.33) because although they are actually continuous functions, measuring them at equally spaced receiver positions is a sampling process analogous to that of examining the value of a time-varying signal at regular intervals. The only significant difference between (3.33) and the polar response autocorrelation function utilised in the definition of this new parameter

is that the latter is evaluated circularly; when shifting the response by τ, the samples obtained at -90° and +90° are considered to be adjacent.

The concept underpinning the parameter is that for complete diffusion, the value of the circular autocorrelation function of the polar response is unity for all angle shifts whereas in all other cases its value for non-zero shifts varies between zero and unity depending on the shape of the response, as illustrated by Figures 3.29 to 3.36. The less uniform the response, the lower the value of the autocorrelation function, particularly for large angle shifts. In the theoretical worst case of non-zero reflected energy in only a single direction, the autocorrelation function is non-zero only when the angle shift is zero. For zero angle shift, the autocorrelation function is always equal to unity, regardless of the shape of the polar response.

3.9.2 **Definition.**

In the single-plane case, the autocorrelation diffusion parameter, d_{auto}, can be defined as the mean over angle shifts of -90° to +90° of the circular autocorrelation function of a polar response, i.e. the mean of the functions shown in Figures 3.30, 3.32, 3.34 and 3.36. Initially, it might appear from this definition that calculation of d_{auto} would be rather time-consuming but as a result of taking the mean, the parameter reduces to a simple formulation which bypasses the need to actually calculate any autocorrelation functions:

$$d_{auto} = \frac{\left[\sum_{i=1}^{n} E_i\right]^2}{n\sum_{i=1}^{n} E_i^2} \qquad (3.34)$$

where:

E_i = Scattered energy (squared pressure) at receiver position i

n = Number of receiver positions

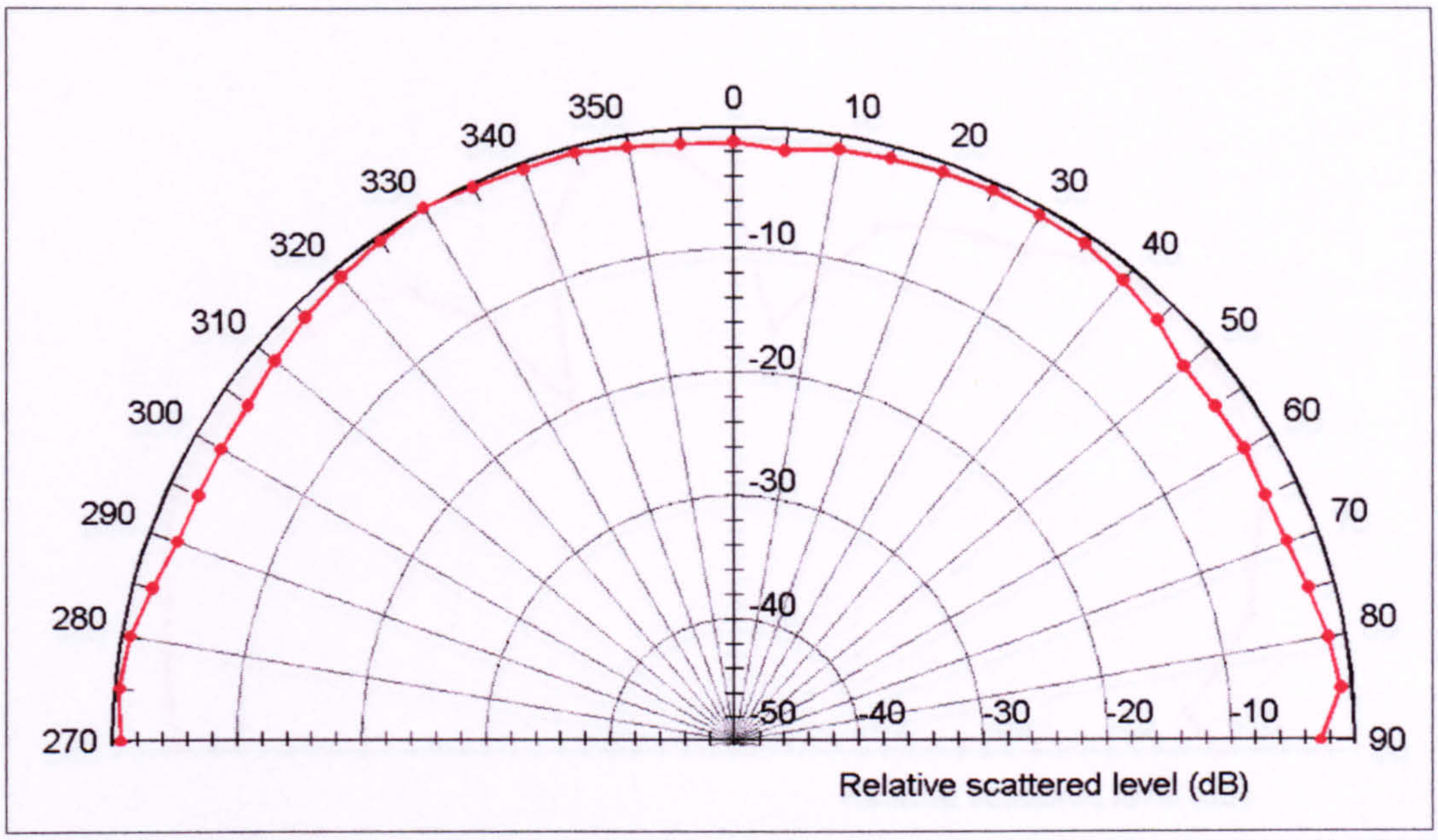

Figure 3.29: 1kHz normal incidence polar response of the semicylinder, measured at RPG.

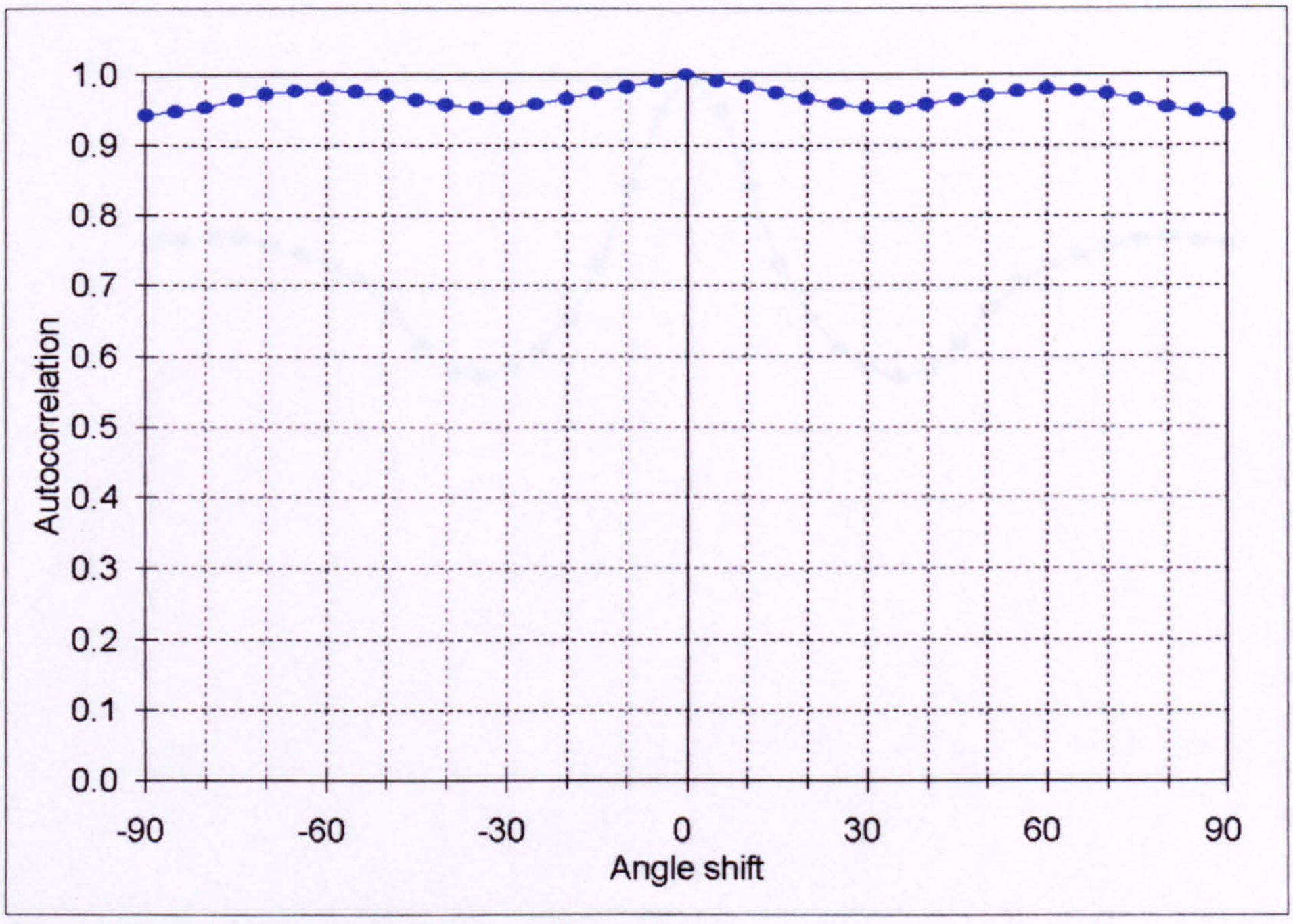

Figure 3.30: Autocorrelation function of polar response shown in Figure 3.29.

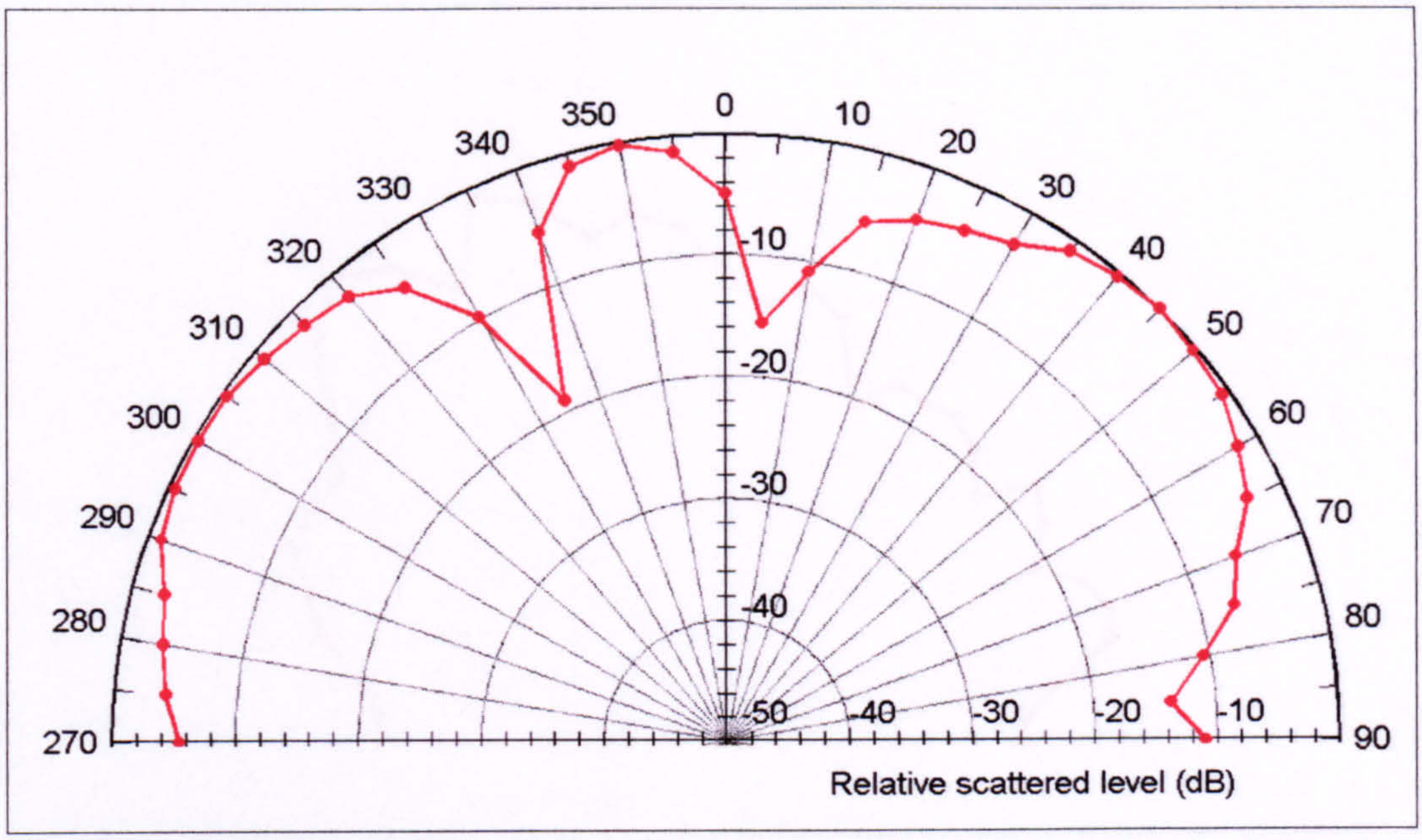

Figure 3.31: 630Hz 10° incidence polar response of the cone, measured at RPG.

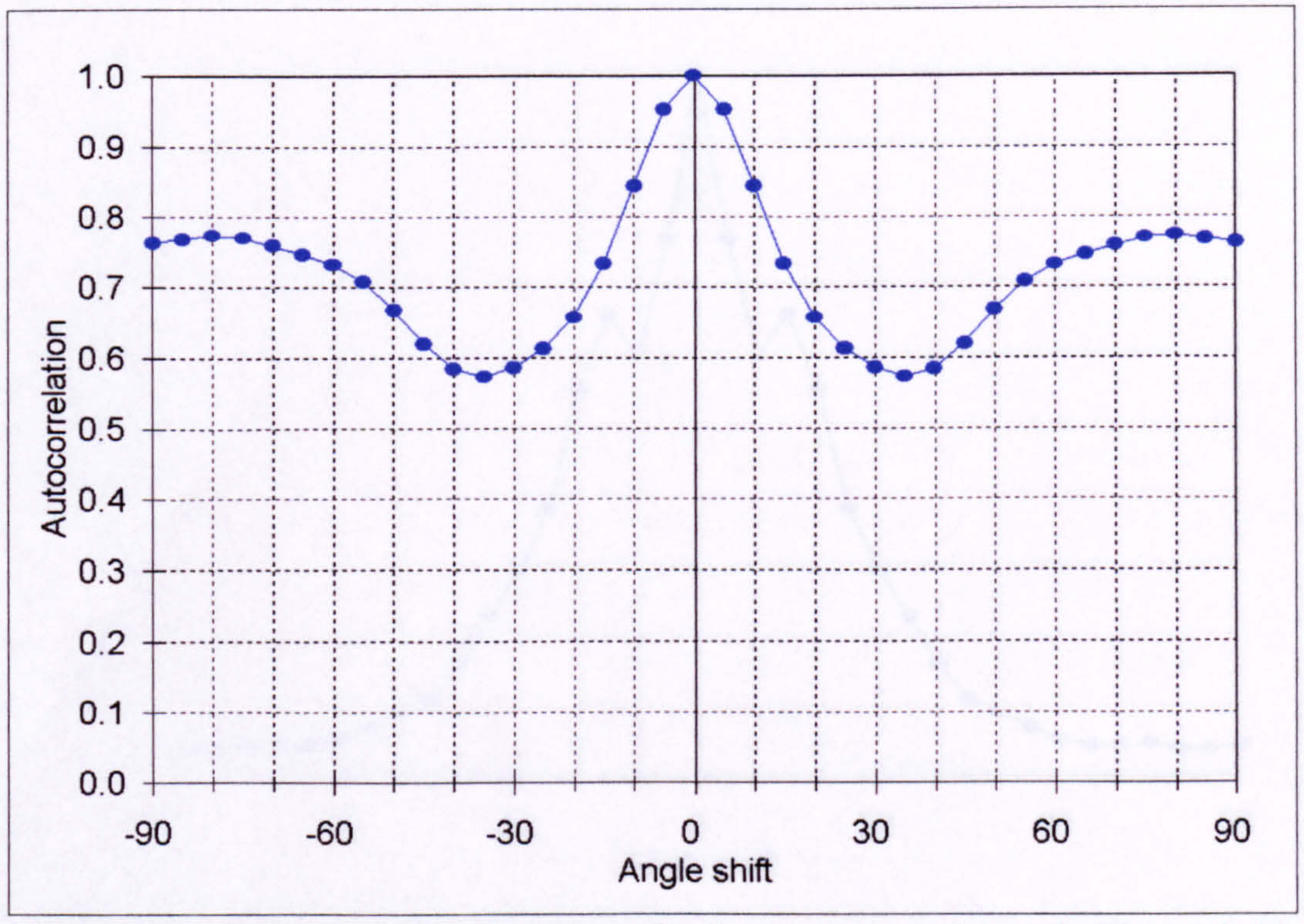

Figure 3.32: Autocorrelation function of polar response shown in Figure 3.31.

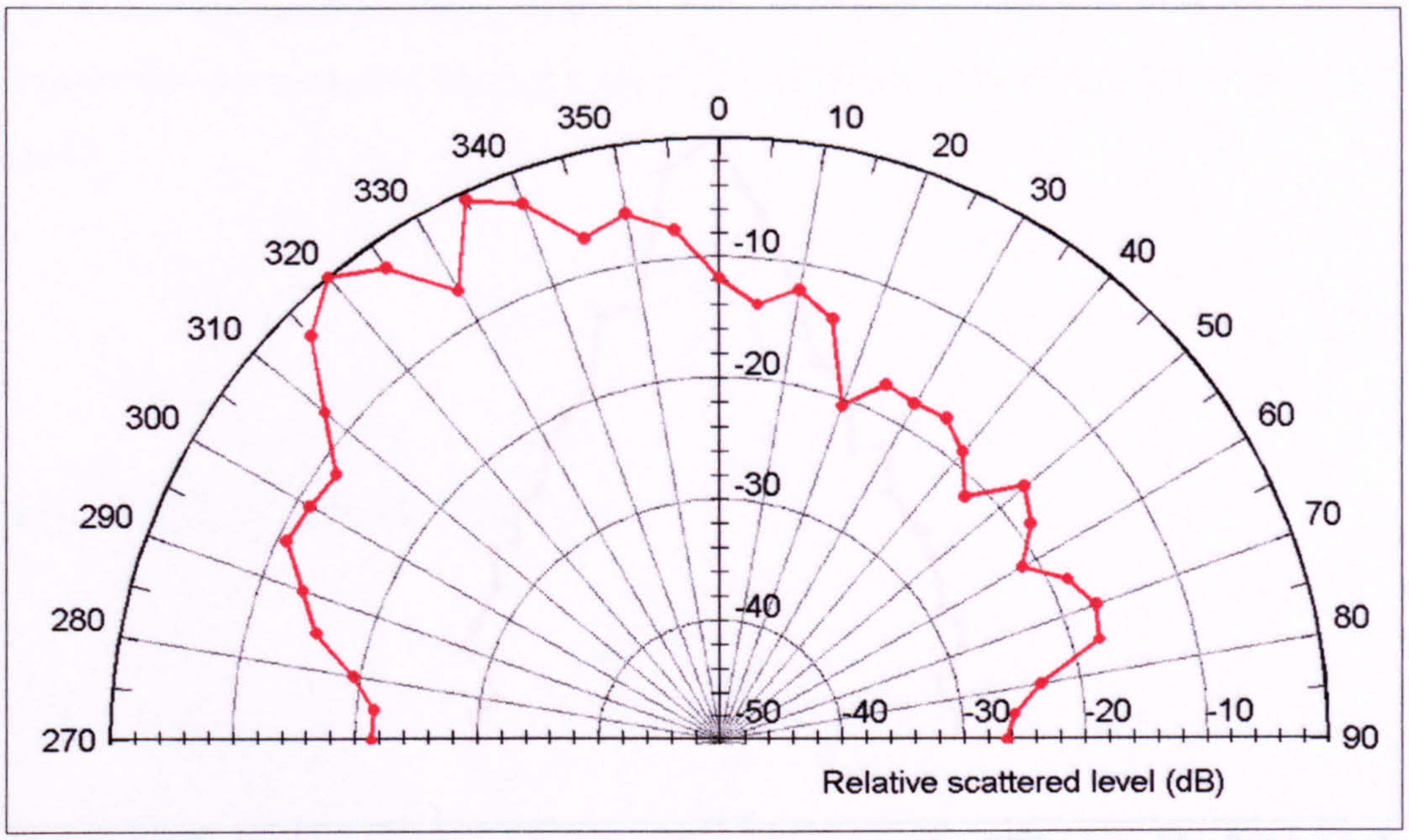

Figure 3.33: 6.3kHz 30° incidence polar response of a BAD Panel, measured at RPG.

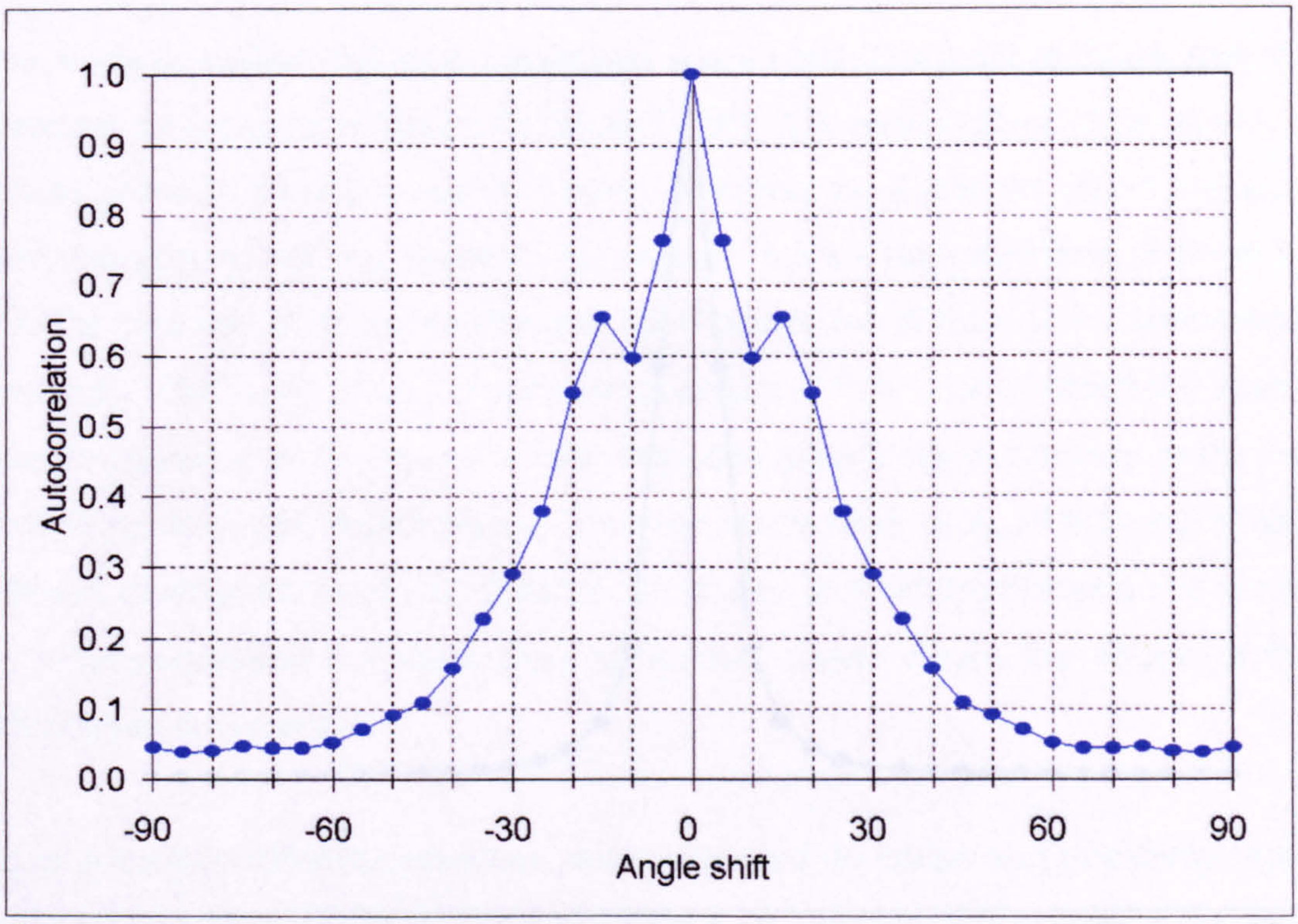

Figure 3.34: Autocorrelation function of polar response shown in Figure 3.33.

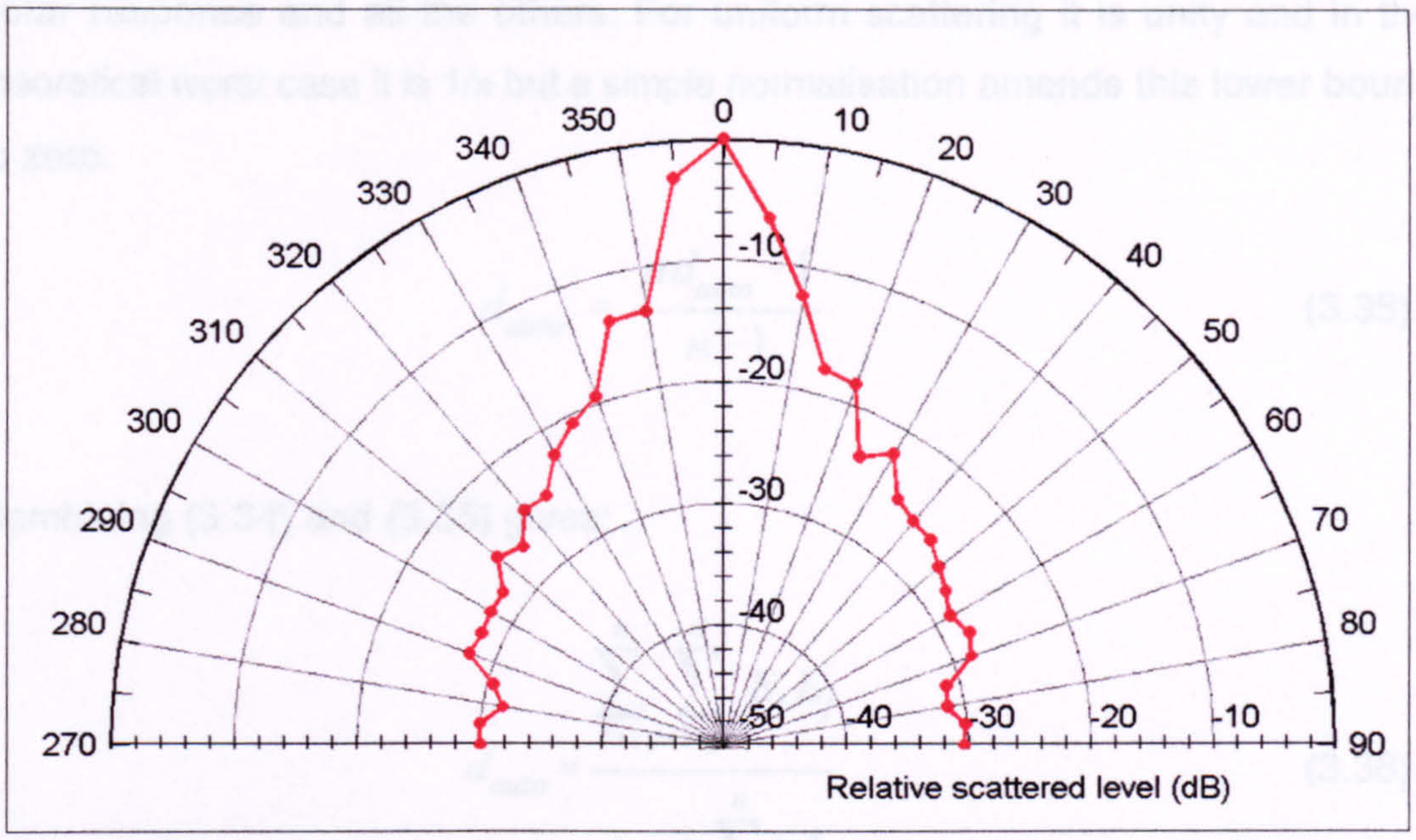

Figure 3.35: 4kHz normal incidence polar response of a 570mm wide flat panel, measured at RPG.

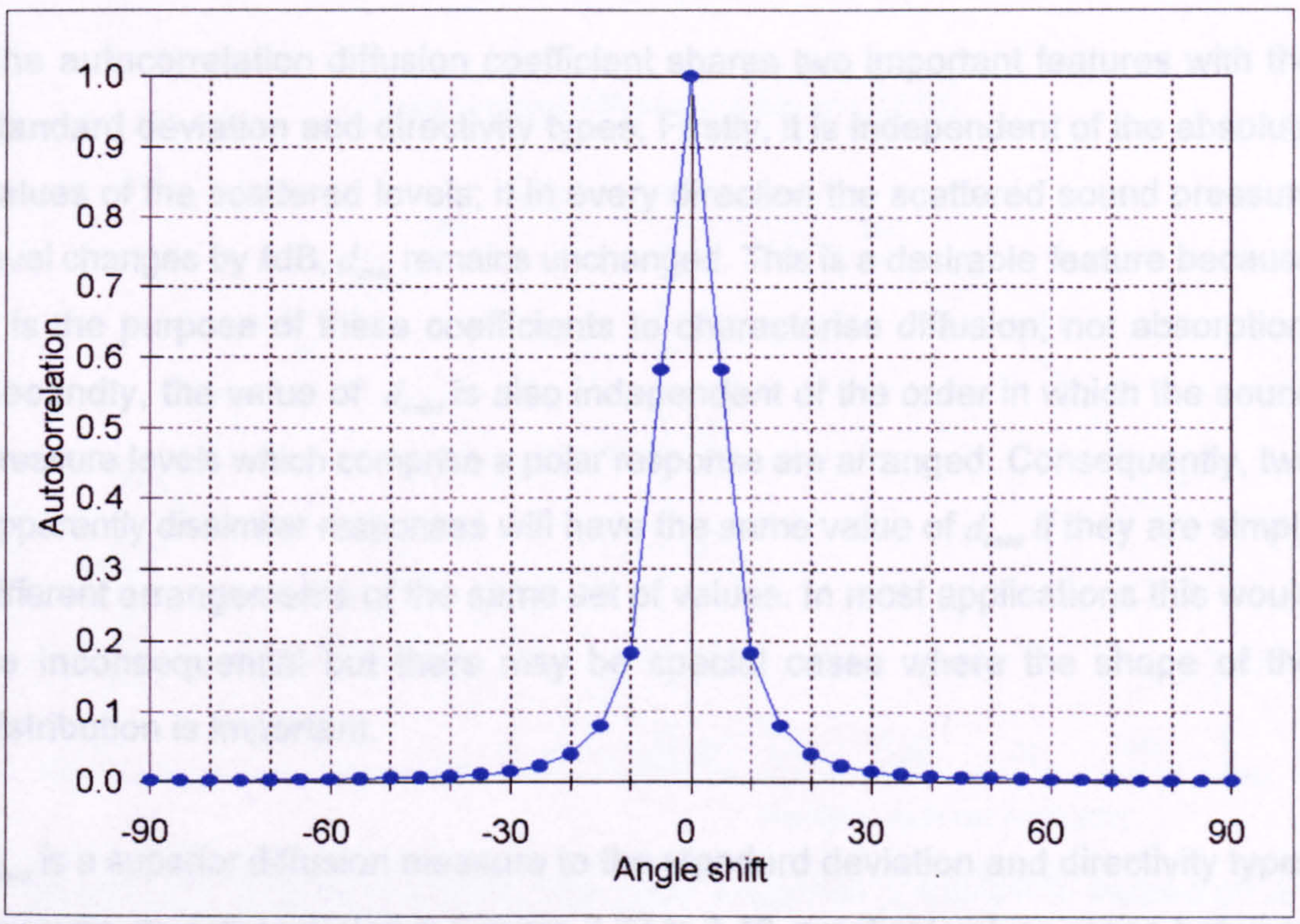

Figure 3.36: Autocorrelation function of polar response shown in Figure 3.35.

The value of d_{auto} quantifies diffusion from the similarity between each point in the polar response and all the others. For uniform scattering it is unity and in the theoretical worst case it is 1/n but a simple normalisation amends this lower bound to zero:

$$d_{auto} = \frac{n d_{auto} - 1}{n - 1} \tag{3.35}$$

Combining (3.34) and (3.35) gives:

$$d_{auto} = \frac{\sum_{i=1}^{n} \sum_{j=1, j \neq i}^{n} E_i E_j}{(n-1) \sum_{i=1}^{n} E_i^2} \tag{3.36}$$

3.9.3 Appraisal.

The autocorrelation diffusion coefficient shares two important features with the standard deviation and directivity types. Firstly, it is independent of the absolute values of the scattered levels; if in every direction the scattered sound pressure level changes by kdB, d_{auto} remains unchanged. This is a desirable feature because it is the purpose of these coefficients to characterise diffusion, not absorption. Secondly, the value of d_{auto} is also independent of the order in which the sound pressure levels which comprise a polar response are arranged. Consequently, two apparently dissimilar responses will have the same value of d_{auto} if they are simply different arrangements of the same set of values. In most applications this would be inconsequential but there may be special cases where the shape of the distribution is important.

d_{auto} is a superior diffusion measure to the standard deviation and directivity types because, as demonstrated in Figures 3.37 to 3.46, practical values range between zero and unity instead of being bunched together. d_{auto} enhances the discrimination between good diffusers and rates practical poor diffusers accordingly.

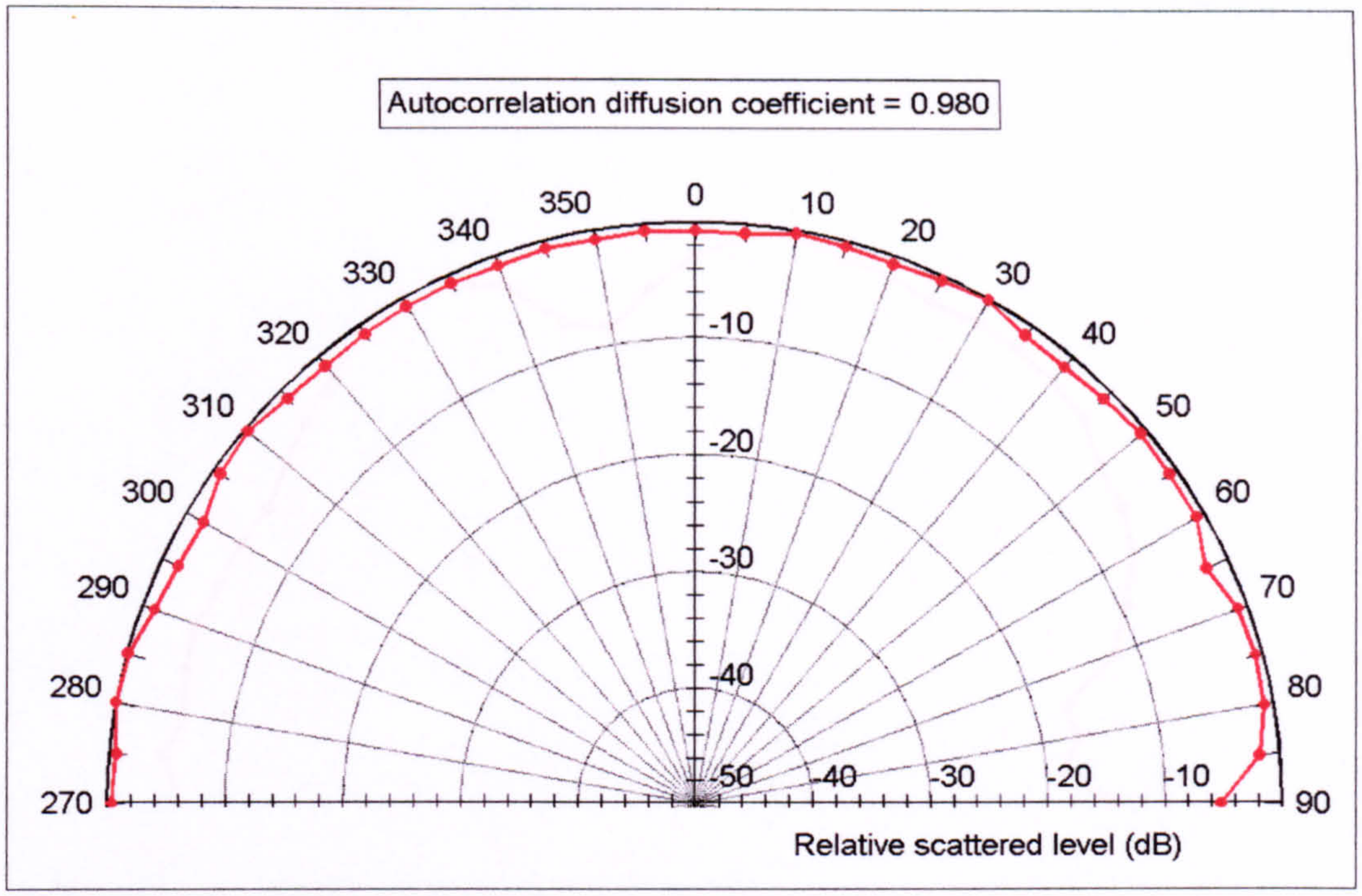

Figure 3.37: 2.5kHz normal incidence polar response of the semicylinder, measured at RPG.

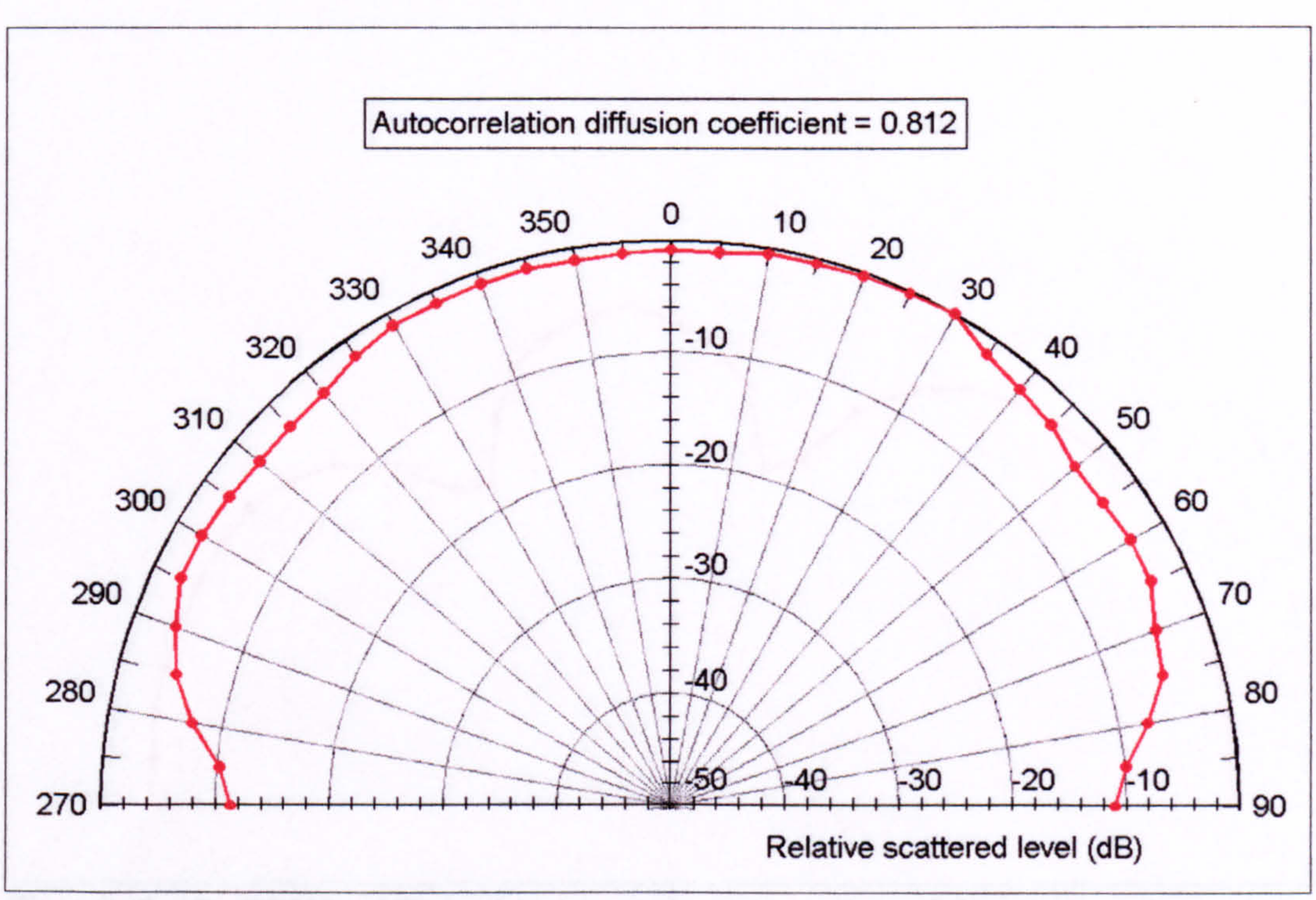

Figure 3.38: 1kHz normal incidence polar response of the QRD, measured at RPG.

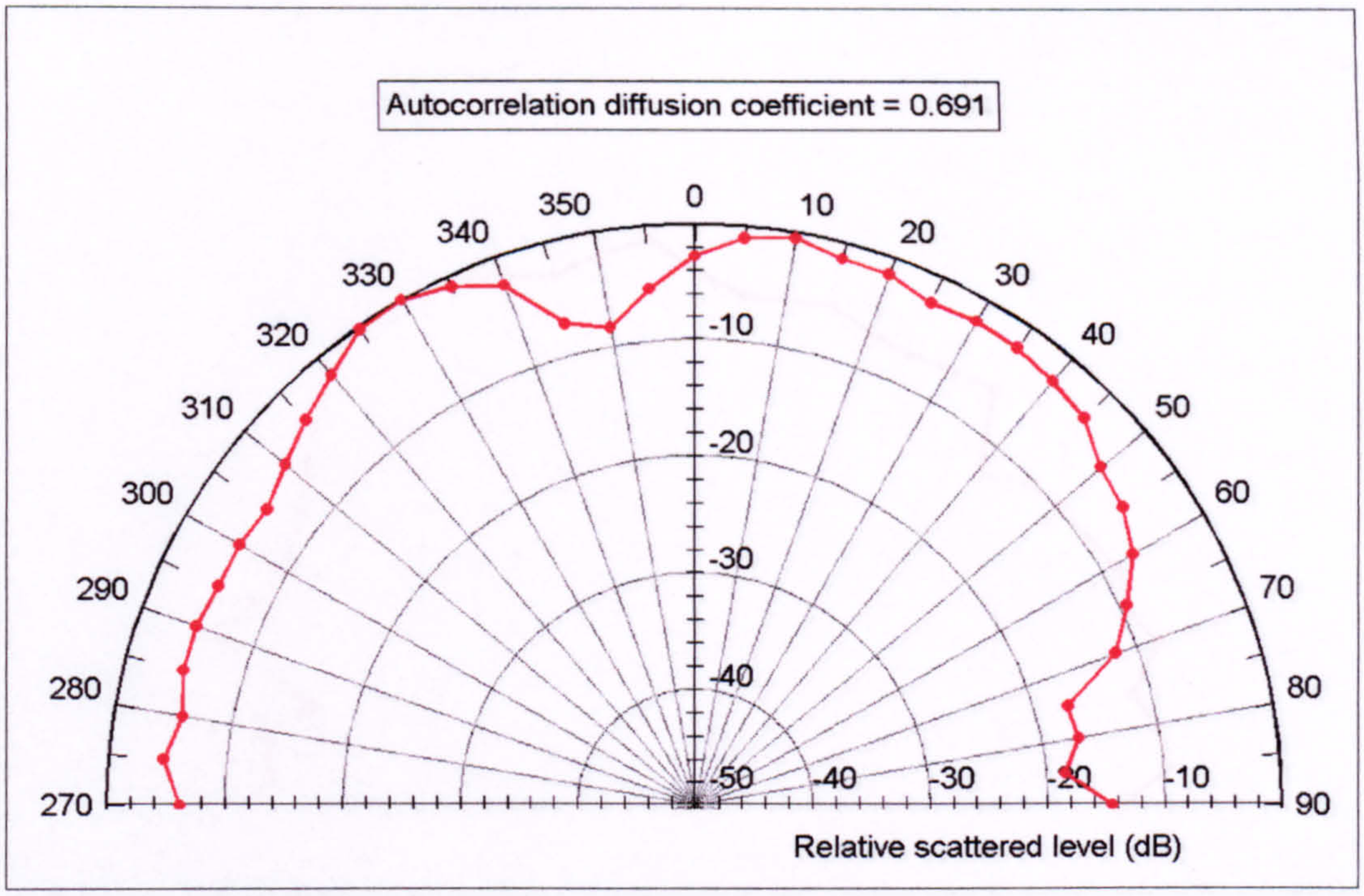

Figure 3.39: 500Hz 30° incidence polar response of the cone, measured at RPG.

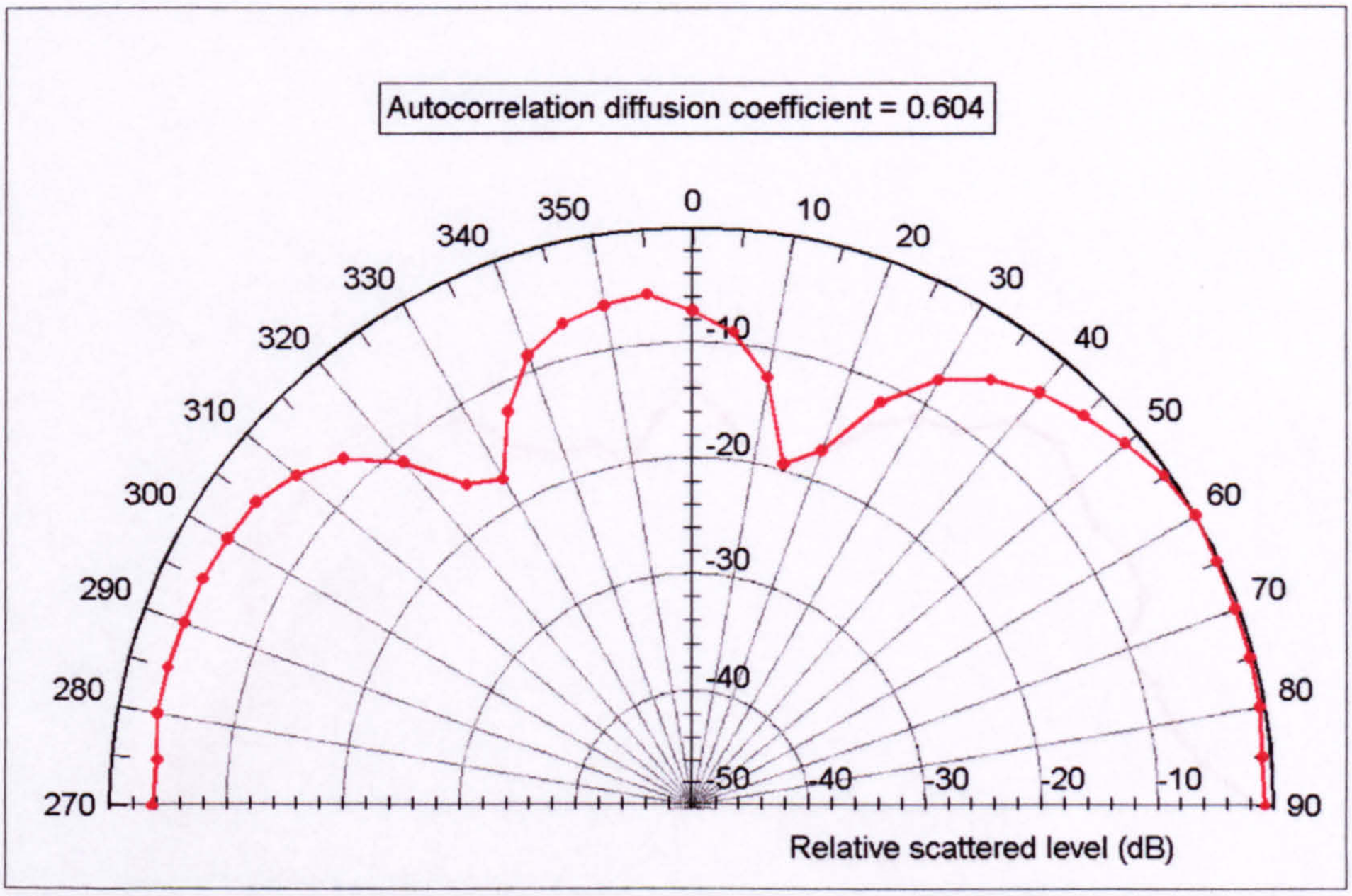

Figure 3.40: 800Hz 10° incidence polar response of the triangular prism, measured at RPG.

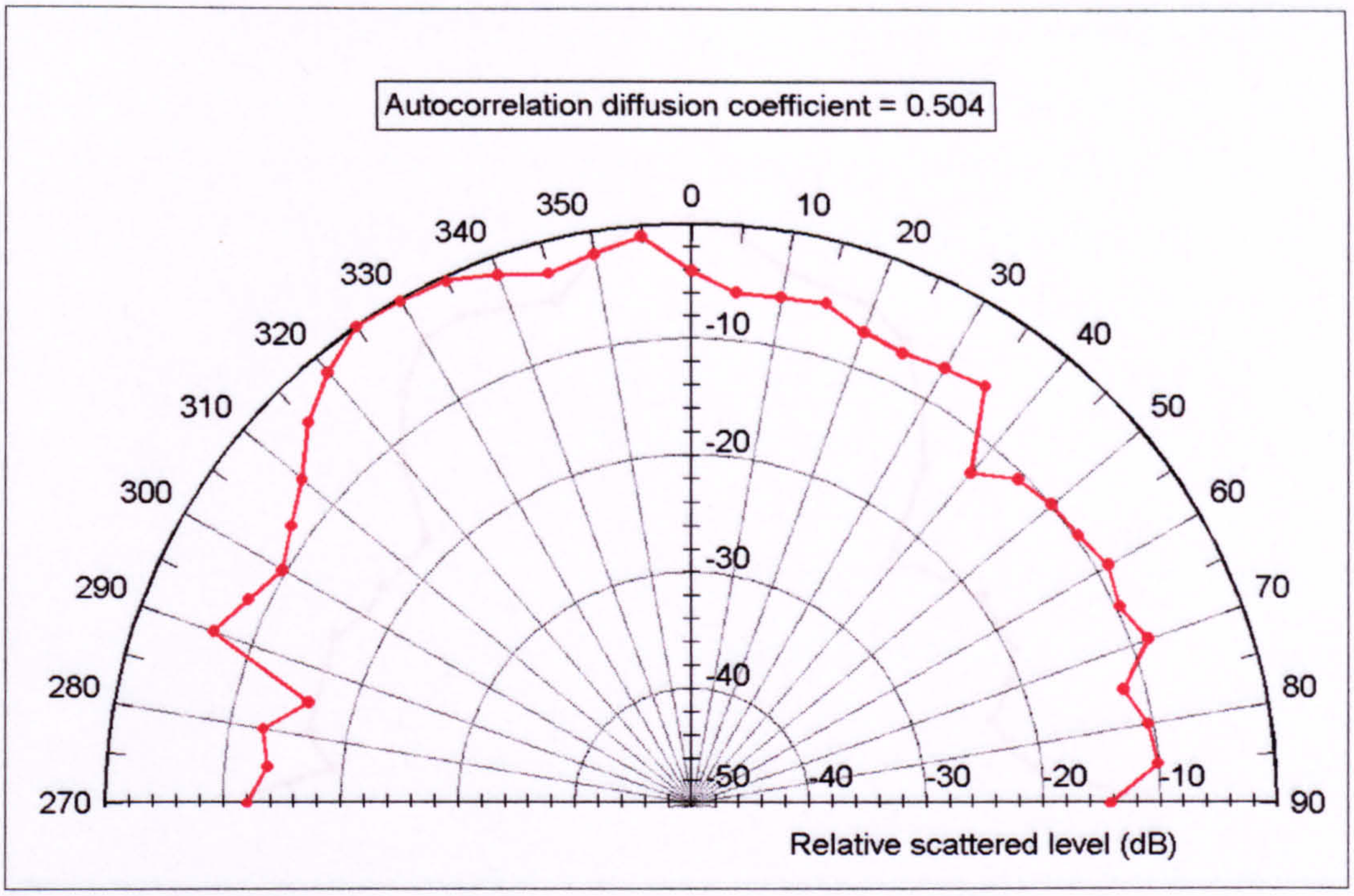

Figure 3.41: 400Hz 60° incidence polar response of a BAD Panel, measured at RPG.

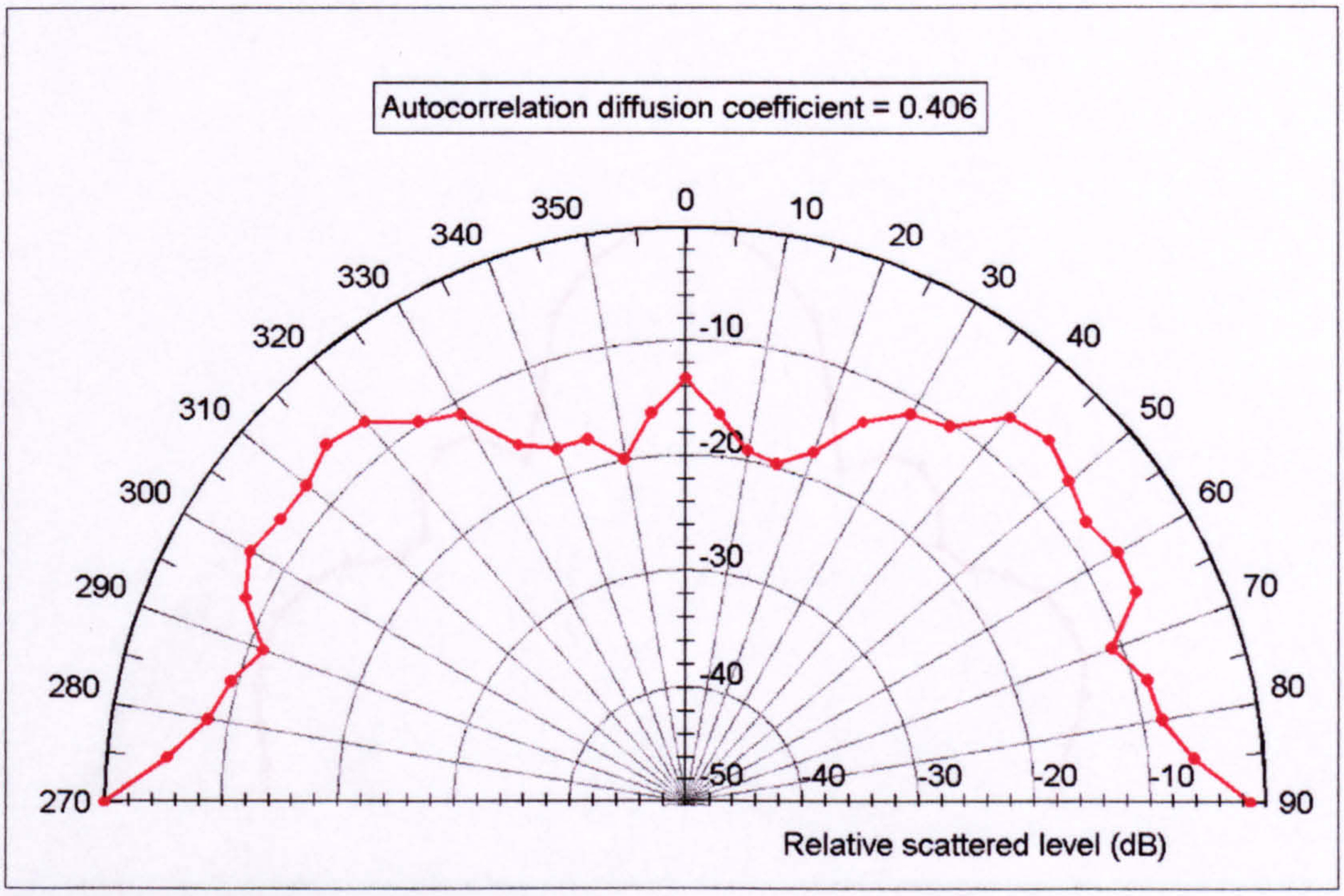

Figure 3.42: 400Hz normal incidence polar response of the seating, measured at RPG.

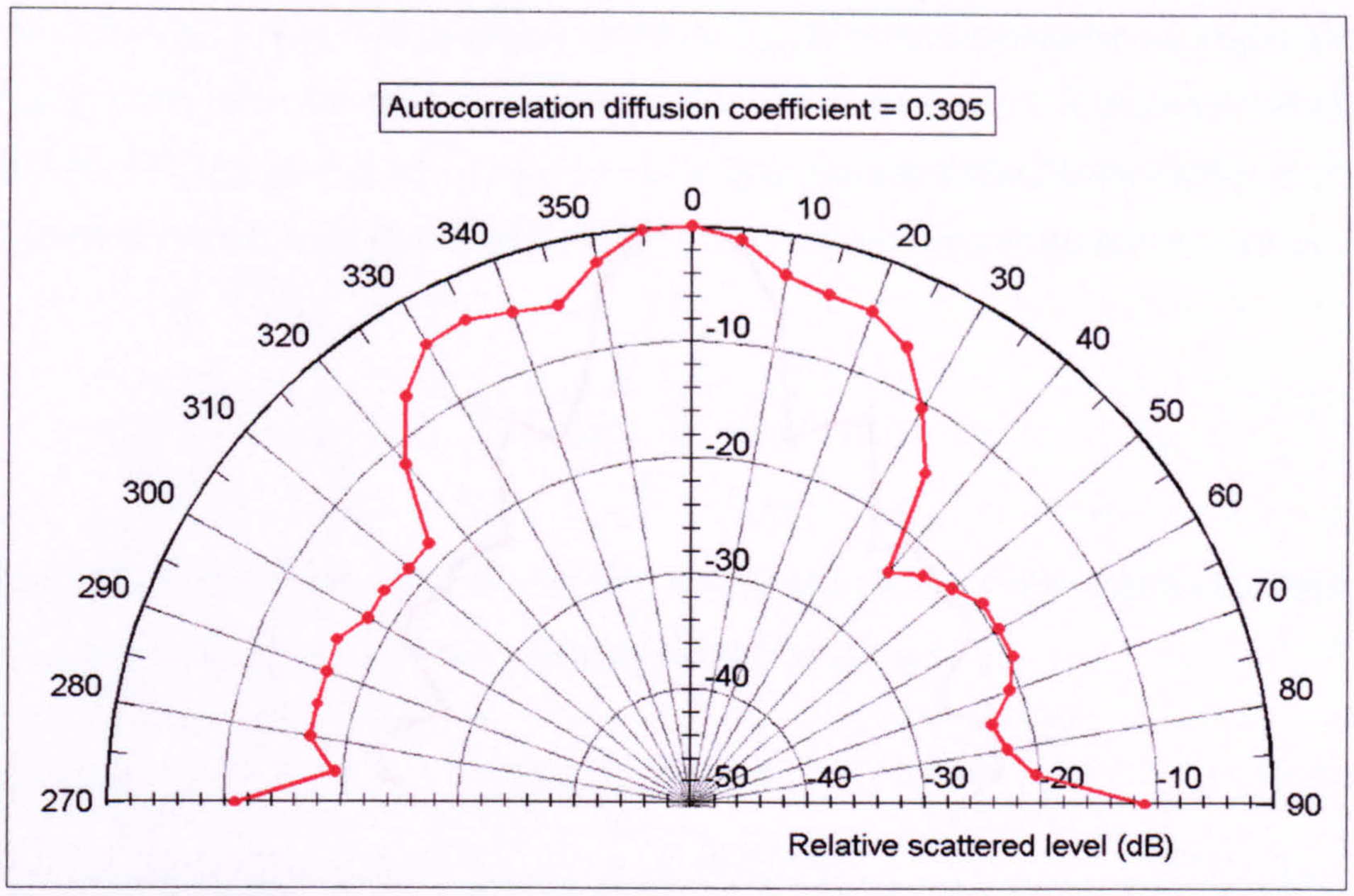

Figure 3.43: 400Hz normal incidence polar response of the random battens, in the plane perpendicular to the battens, measured at RPG.

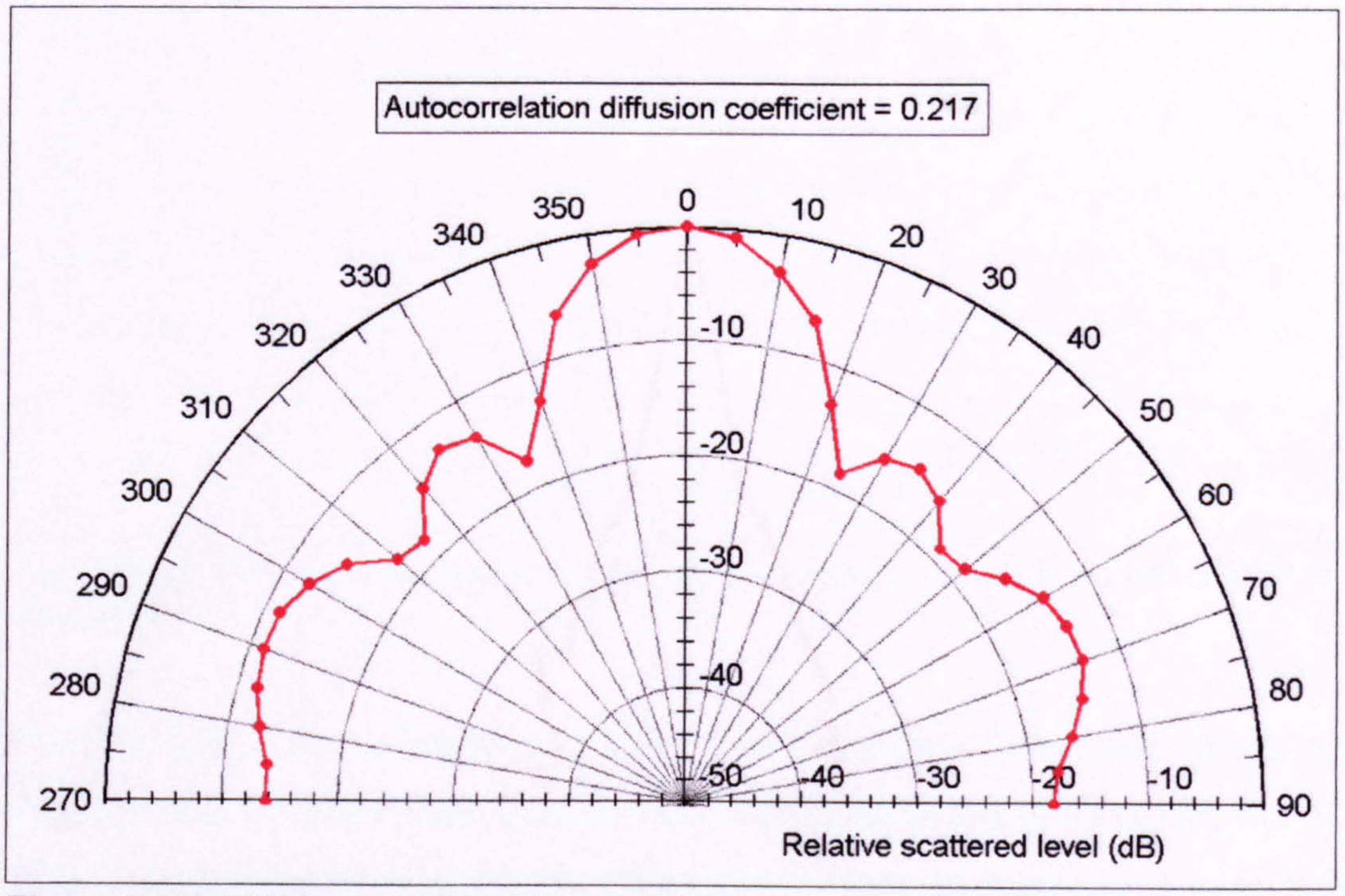

Figure 3.44: 800Hz normal incidence polar response of the Skyline, measured at RPG.

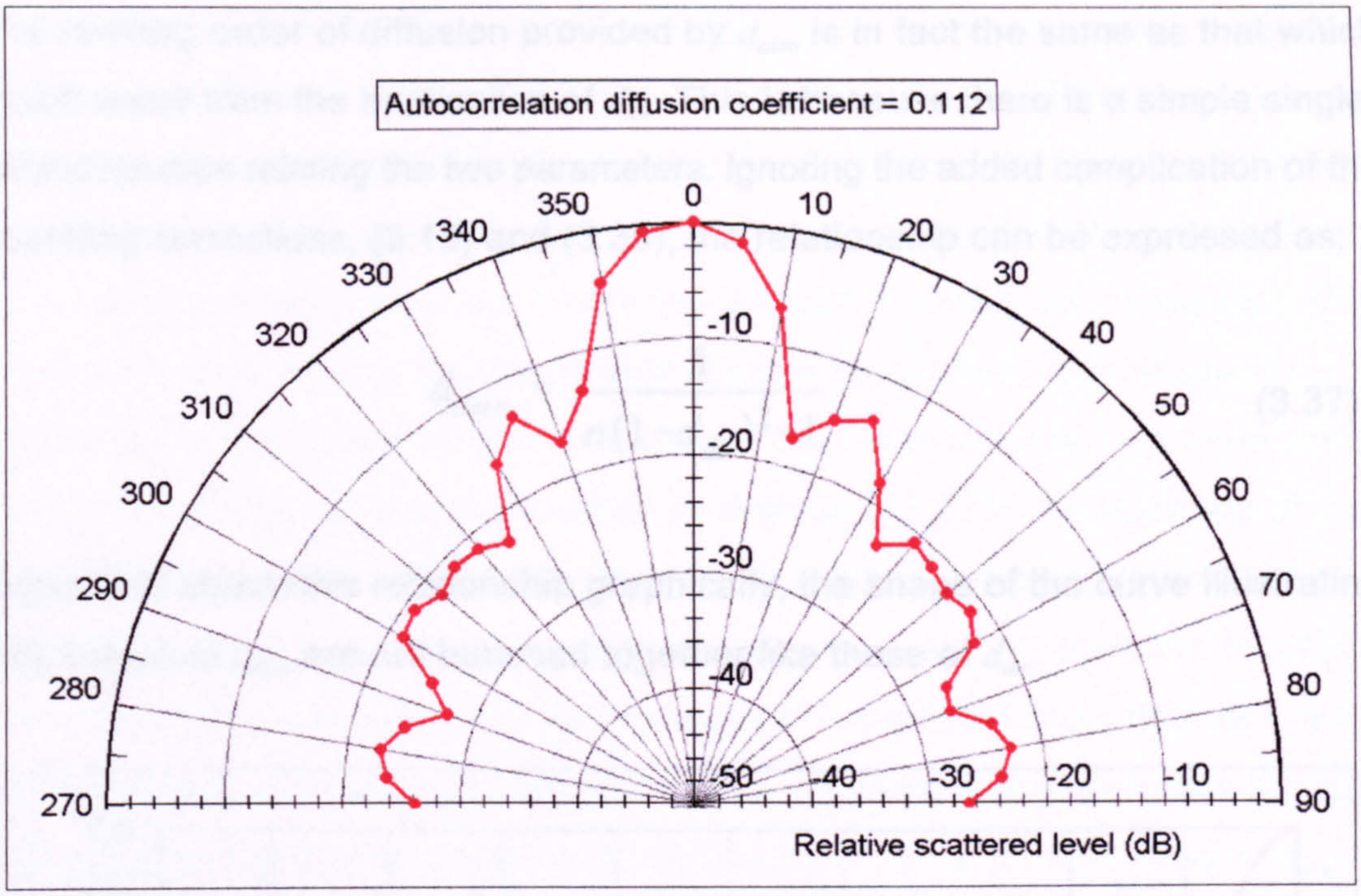

Figure 3.45: 2kHz normal incidence polar response of a 570mm wide flat panel, measured at RPG.

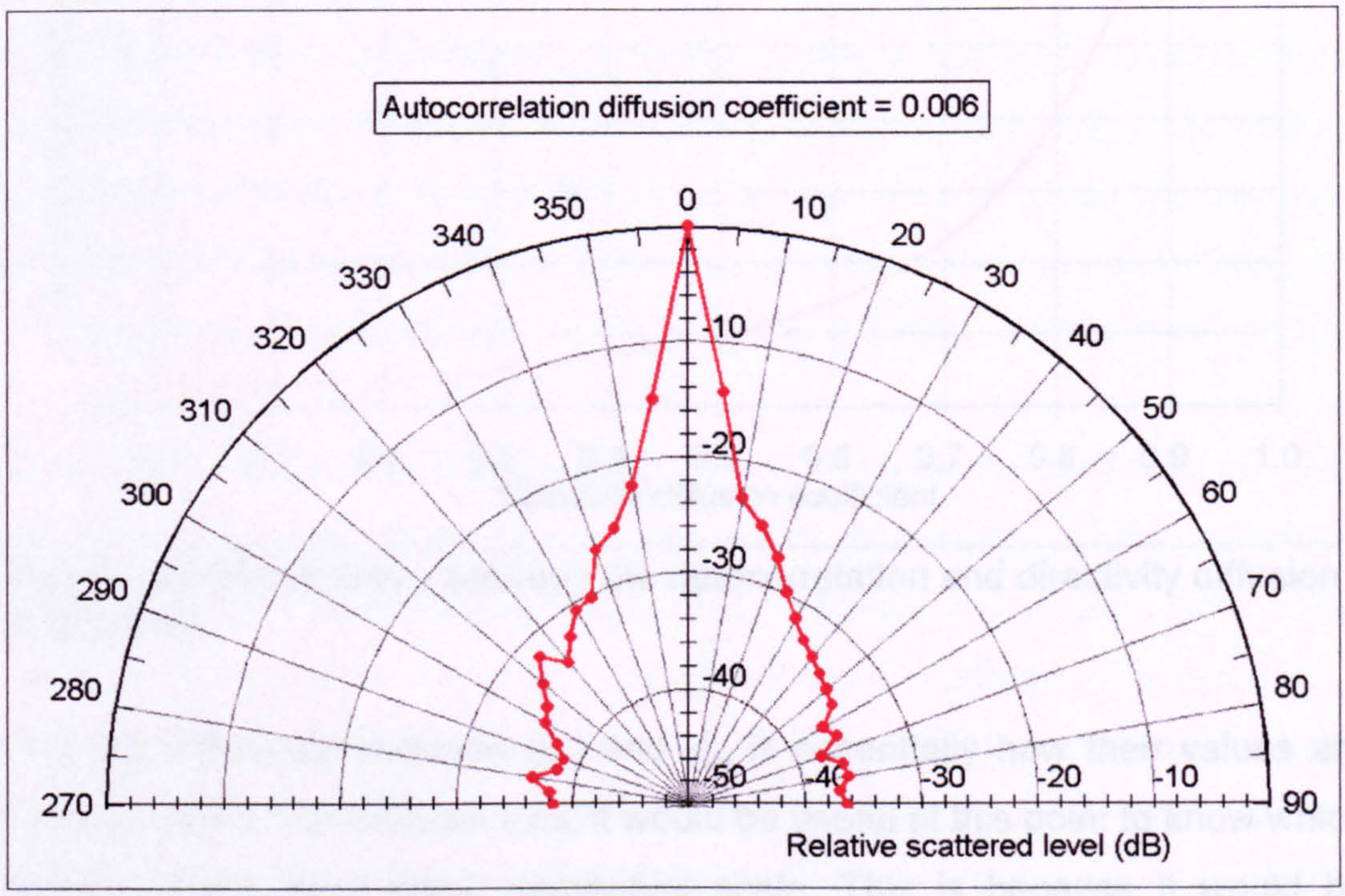

Figure 3.46: 4kHz normal incidence polar response of the concave prism, measured at RPG.

The ranking order of diffusion provided by d_{auto} is in fact the same as that which would result from the application of d_{dir}. This is because there is a simple single-valued function relating the two parameters. Ignoring the added complication of the bounding corrections, (3.18) and (3.35), the relationship can be expressed as:

$$d_{auto} = \frac{1}{n(1-d_{dir})^2+1} \tag{3.37}$$

Figure 3.47 shows this relationship graphically, the shape of the curve illustrating why values of d_{auto} are not bunched together like those of d_{dir}.

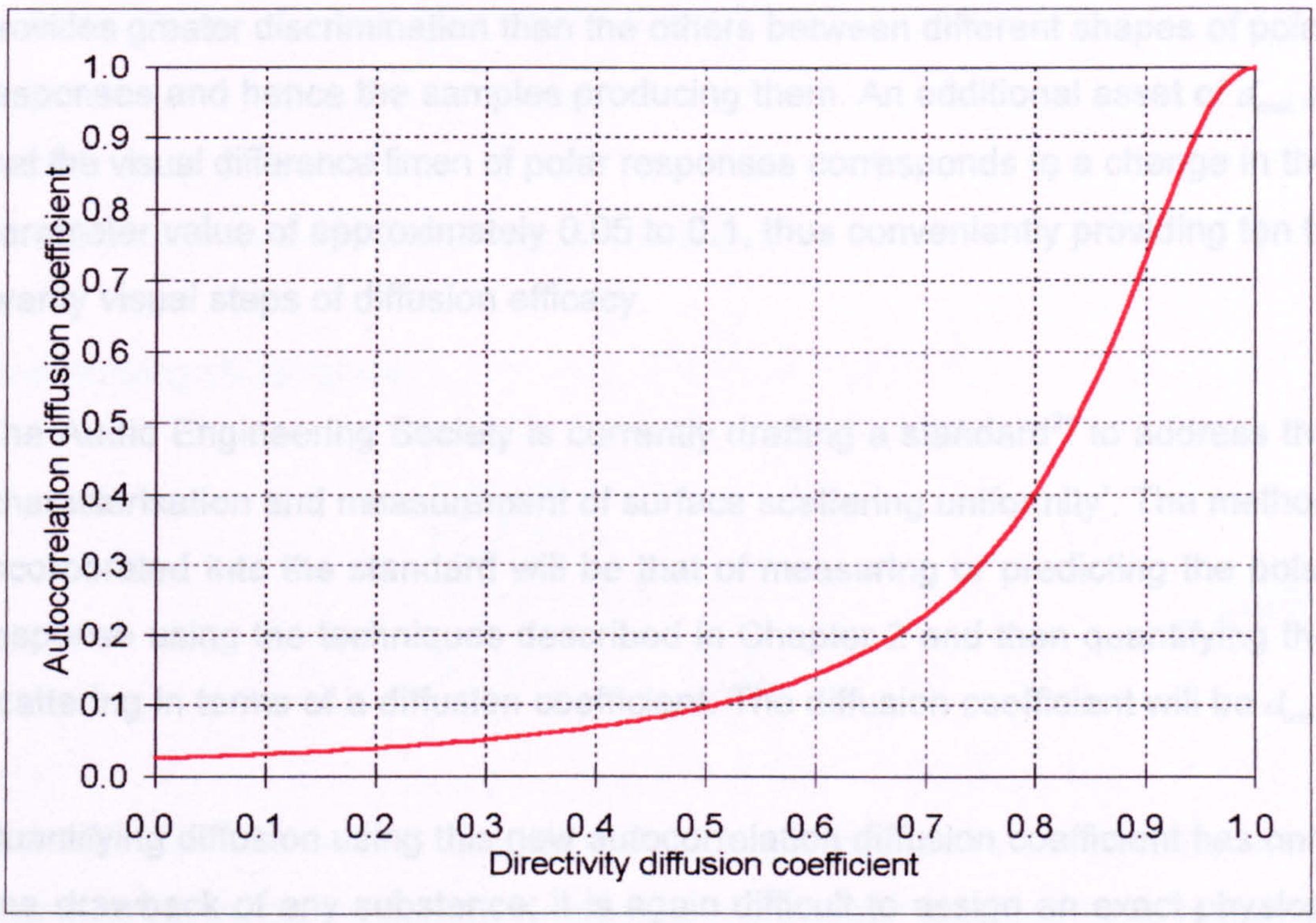

Figure 3.47: Relationship between the autocorrelation and directivity diffusion coefficients.

Since the difference between d_{auto} and d_{dir} is essentially how their values are distributed along the diffusion axis, it would be useful at this point to know which measure is the more linear perceptual scale. This is because it would be advantageous for the difference in the subjective perception of diffusion efficacy between surfaces with coefficients of, say, 0.2 and 0.3 to be the same as that between those whose coefficient values are, say, 0.8 and 0.9. However,

ascertaining this would not be possible without more knowledge of the subjective response to diffusion. It would also be beneficial to know the difference limen for diffusion because it is pointless to develop a measure which objectively appears to satisfy many of the ideal criteria if subjectively no difference between surfaces with coefficient values of, for example, 0.1 and 0.9 can be perceived. This information is also currently unavailable but is a likely area of future research. A preliminary investigation into the subjective response to diffusion has been made by Lee[26] and this is briefly discussed in Section 7.3.1. In the absence of any knowledge as to which of the parameters is the more linear perceptual scale, d_{auto} is assumed to be superior because practical values are not bunched together. Since practical values of d_{auto} are distributed over the whole range, this parameter provides greater discrimination than the others between different shapes of polar responses and hence the samples producing them. An additional asset of d_{auto} is that the visual difference limen of polar responses corresponds to a change in the parameter value of approximately 0.05 to 0.1, thus conveniently providing ten to twenty visual steps of diffusion efficacy.

The Audio Engineering Society is currently drafting a standard[21] to address the 'characterisation and measurement of surface scattering uniformity'. The method incorporated into the standard will be that of measuring or predicting the polar response using the techniques described in Chapter 2 and then quantifying the scattering in terms of a diffusion coefficient. The diffusion coefficient will be d_{auto}.

Quantifying diffusion using this new autocorrelation diffusion coefficient has only one drawback of any substance; it is again difficult to assign an exact physical meaning to intermediate values such as 0.5. Although d_{auto} satisfies more of the criteria for an ideal diffusion coefficient than those published in the literature, it does not directly provide any quantitative information about the shape of the polar response. As discussed in the following section, attempts have been made to relate d_{auto} values to spread but these relationships are either too vague to be of much benefit and/or the necessary assumption that the values comprising polar responses are normally distributed is generally incorrect.

3.9.4 Physical interpretation of d_{auto}.

As a consequence of the relationship between d_{auto} and d_{dir} shown in (3.37), d_{auto} can be expressed in terms of the mean and standard deviation of the energy (squared pressure) values which form the polar response. This enables a limited amount of information about the spread of these values to be obtained.

Firstly, the variance, σ^2, of the energies is formulated as the difference of the mean square energy and the square of the mean energy:

$$\sigma^2 = \frac{\sum_{i=1}^{n} E_i^2}{n} - \frac{\left[\sum_{i=1}^{n} E_i\right]^2}{n^2} \tag{3.38}$$

where the symbols have their usual meanings.

Rearranging (3.38) gives:

$$\frac{\left[\sum_{i=1}^{n} E_i\right]^2}{n\sum_{i=1}^{n} E_i^2} = 1 - \frac{n\sigma^2}{\sum_{i=1}^{n} E_i^2} \tag{3.39}$$

The left-hand side is now the expression for d_{auto} without the complication of the bounding correction. Further rearrangement of the right-hand side enables it to be written in terms of the mean, $\overline{E}$, and standard deviation, σ, directly:

$$d_{auto} = \frac{1}{1 + \dfrac{n^2\sigma^2}{\left[\sum_{i=1}^{n} E_i\right]^2}} = \frac{1}{1 + \left[\dfrac{\sigma}{\overline{E}}\right]^2} \tag{3.40}$$

The ratio of the standard deviation to the mean, found in the denominator of (3.40),

is known as the 'coefficient of variance'[58] and expresses the relative importance of the standard deviation referred to the mean. (3.40) explicitly shows that the reason the value of d_{auto} increases as polar responses become more uniform is that the coefficient of variance decreases; the standard deviation of the energies becomes smaller in comparison to the mean energy.

If the values of energy comprising polar responses were normally distributed about the mean then the standard deviation would be a quantitative measure of spread; 95% of the energies would lie within two standard deviations of the mean. It would be more useful, however, to be able to relate the value of d_{auto} to the spread of the sound pressure level values because these form a more linear perceptual scale. This can be achieved to a limited extent because from the value of d_{auto} it is possible to calculate the difference between the sound pressure level corresponding to the mean energy (the mean sound pressure level evaluated via energy) and that corresponding to the mean plus, or minus, k standard deviations.

Making the standard deviation the subject of (3.40) and incorporating the bounding correction for d_{auto}, (3.35), gives:

$$\sigma = \overline{E}\sqrt{\frac{n}{(n-1)d_{auto}+1}-1} \qquad (3.41)$$

The difference, ΔSPL, between the mean sound pressure level and that corresponding to the mean energy plus k standard deviations is therefore given by:

$$\begin{aligned}\Delta SPL &= 10\log(\overline{E}+k\sigma) - 10\log(\overline{E}) \\ &= 10\log\left[1+k\sqrt{\frac{n}{(n-1)d_{auto}+1}-1}\right]\end{aligned} \qquad (3.42)$$

This relationship between d_{auto} and ΔSPL is shown graphically in Figure 3.48 for different values of k. If the energy values comprising polar responses were

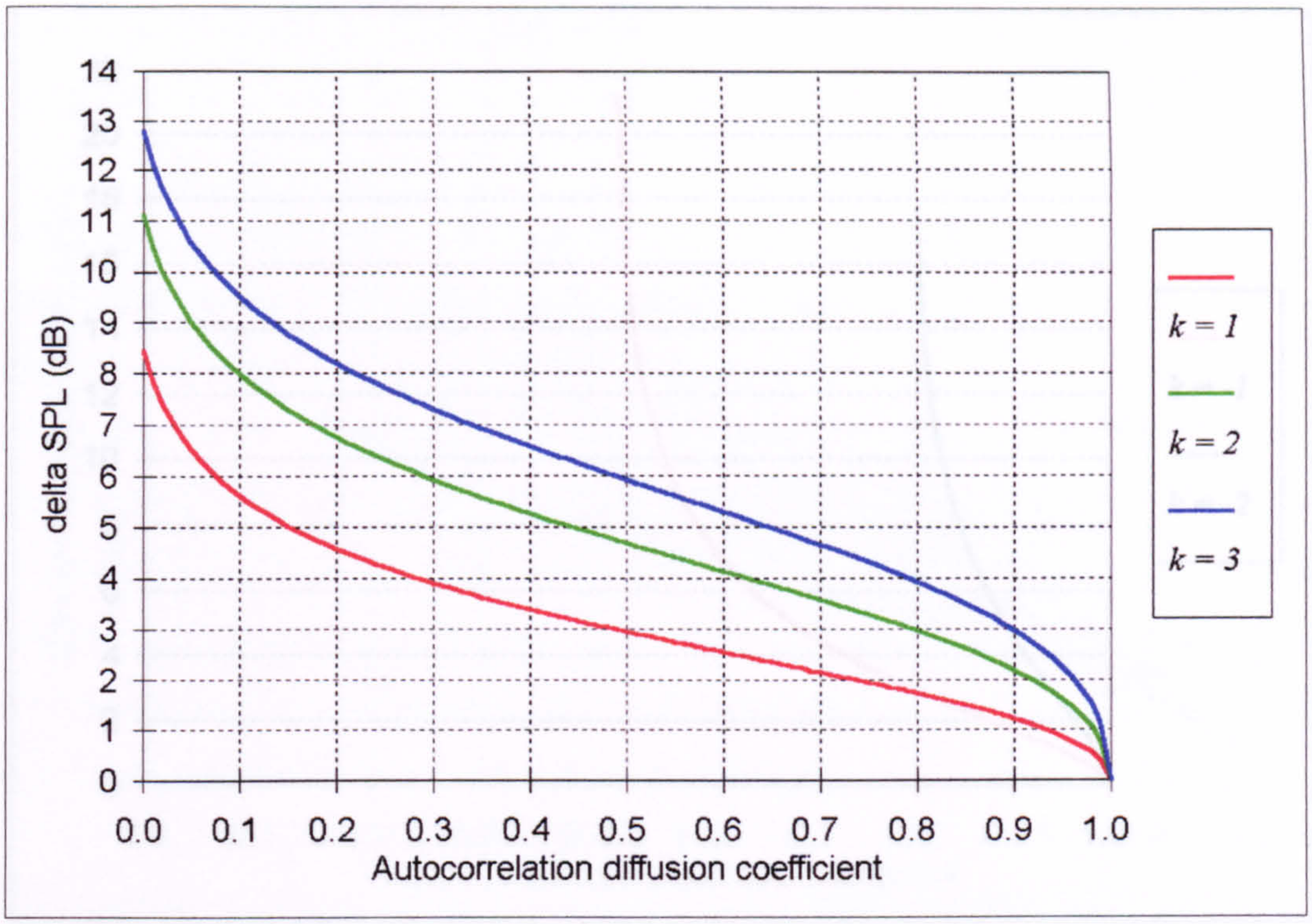

Figure 3.48: Relationship between d_{auto} and ΔSPL for positive values of k.

normally distributed then (3.42) or Figure 3.48 could be used to quantify the spread of sound pressure level values above the mean. For example, if the value of d_{auto} were 0.5 then it would be highly unlikely that any value of sound pressure level would exceed the mean by more than 6dB. However, during the course of this research it has been determined that the distribution of energies in polar responses is not usually normal and so this quantitative assessment does not hold. In any case, for most values of d_{auto} it would only be possible to quantify spread above the mean because (3.42) readily breaks down for negative values of k; if $k\sigma$ is negative and its magnitude exceeds the mean then the argument of the first logarithm becomes negative. For k=-1 this breakdown occurs for values of d_{auto} below 0.5 and for k=-2 below approximately 0.8. The physical significance of the breakdown is that the limiting energy value corresponding to the mean minus k standard deviations is less than zero. Since in practice this is an impossibility, the limit is instead zero and this result provides no information about the spread of energy values below the mean other than that they all exceed zero. Figure 3.49 on the following page illustrates the relationship between d_{auto} and ΔSPL for negative values of k.

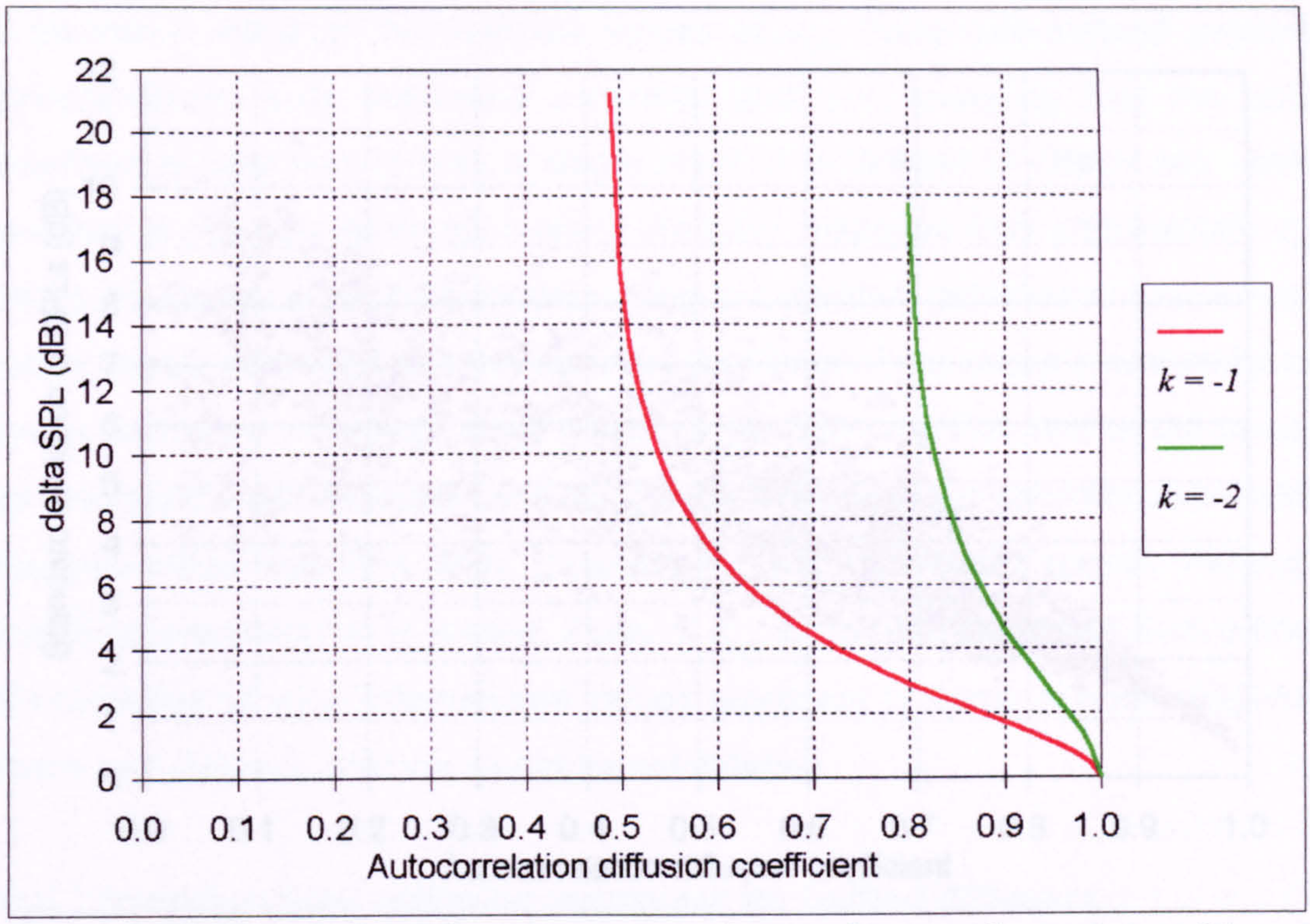

Figure 3.49: Relationship between d_{auto} and ΔSPL for negative values of k.

ΔSPL is not the standard deviation of the sound pressure levels comprising the polar response, this cannot be calculated from d_{auto}. However, since both d_{auto} and the standard deviation of the sound pressure levels are measures of uniformity, a degree of correlation between them would be expected. Figure 3.50 is an empirical illustration of the relationship between the d_{auto} values of a large number of single-plane polar responses and the corresponding values of the standard deviation of the sound pressure levels. If in every case the distribution of the sound pressure levels comprising the polar responses was normal then an estimate of the range in decibels, centred on the mean, over which a certain percentage of these sound pressure levels would be spread could be obtained from the value of d_{auto} by simply multiplying the corresponding standard deviation by the appropriate factor, eg four for 95% and six for 99%. Obtaining an accurate estimate of spread would be more difficult for low values of d_{auto} because as the value of d_{auto} decreases, the mapping between the two parameters becomes increasingly vague. However, all this is of little practical consequence because just as the distribution of the energy values in polar responses is not normal, neither, generally, is the distribution of the sound pressure levels.

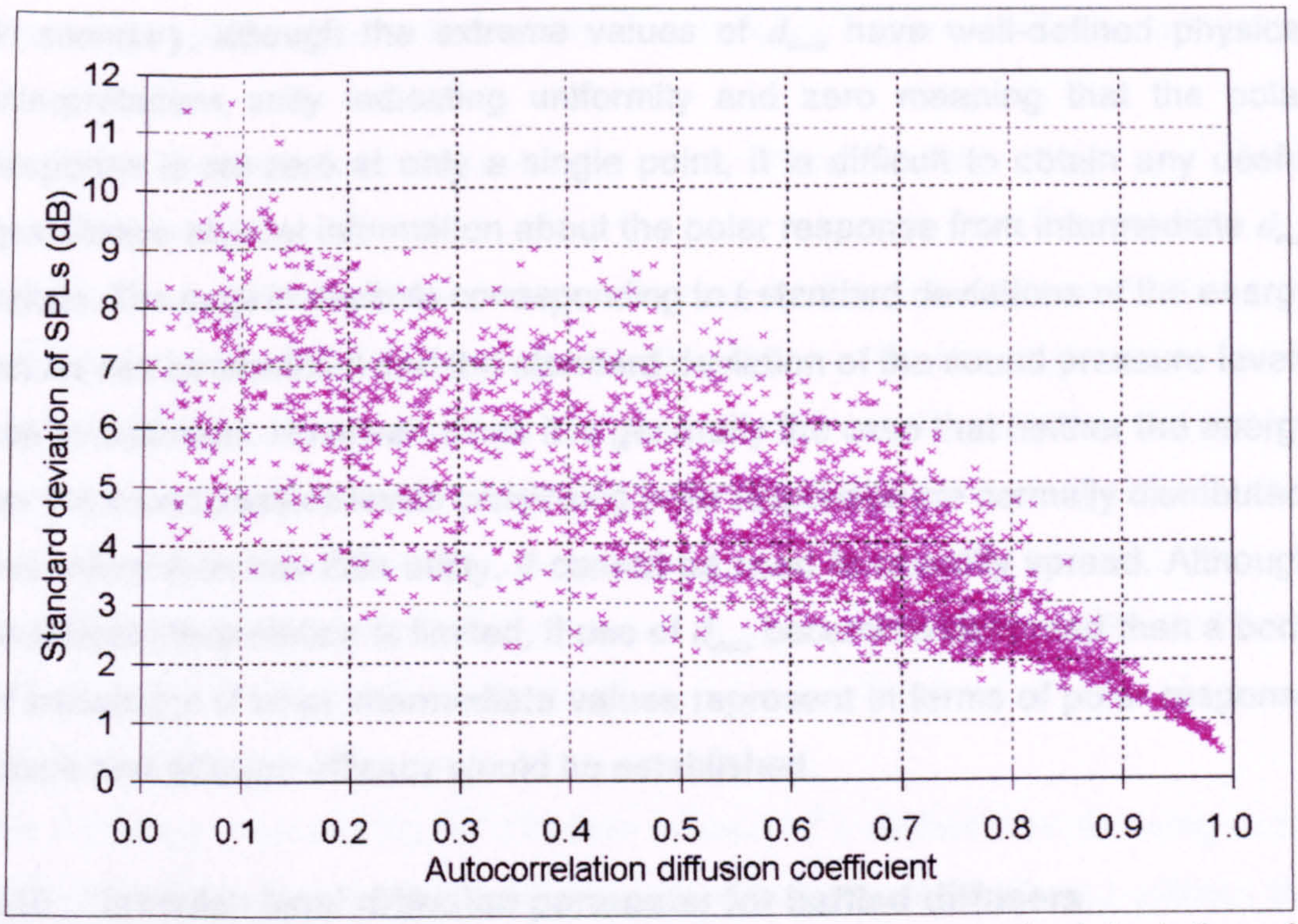

Figure 3.50: Empirical relationship between d_{auto} and the standard deviation of sound pressure level polar responses.

Investigations have revealed that although the sound pressure levels in polar responses which have middle-of-the-range d_{auto} values are sometimes distributed in a manner which approaches normality, in more uniform responses the distribution is skewed towards the maximum and for poor diffusers it is skewed towards the minimum. This absence of normality means that the spread of the sound pressure level values cannot be quantified from the standard deviation of the polar response. Therefore in order to obtain an estimate of this spread from the d_{auto} value, a direct mapping of the two quantities would be required, i.e. a chart similar to Figure 3.50 but with the y-axis directly quantifying spread as opposed to standard deviation. The most informative spread to relate to d_{auto} would be that which encompasses 95% or 99% of the values but this could not be accurately determined from polar responses containing only thirty-seven points. For the single-plane case it would thus be necessary to use responses measured with a finer angular resolution and although such measurements could be incorporated into future research, it is likely that the result would be a mapping resembling Figure 3.50 and therefore provide only vague information for most values of d_{auto}.

In summary, although the extreme values of d_{auto} have well-defined physical interpretations, unity indicating uniformity and zero meaning that the polar response is non-zero at only a single point, it is difficult to obtain any useful quantitative physical information about the polar response from intermediate d_{auto} values. The range in decibels corresponding to k standard deviations of the energy values can be calculated and the standard deviation of the sound pressure levels can be estimated. However, since it is generally the case that neither the energy nor the sound pressure levels comprising polar responses are normally distributed, this information has little utility, it cannot be used to quantify spread. Although analytical interpretation is limited, if use of d_{auto} became widespread then a body of knowledge of what intermediate values represent in terms of polar response shape and diffusion efficacy would be established.

3.10 **'Insertion loss' diffusion parameter for baffled diffusers**.

3.10.1 **Introduction**.

It has been discussed elsewhere that if the diffusion efficacy of a sample is to be quantified from its polar response, then ideally this should be measured in the far field where its shape is independent of the measurement distance. It has been recognised that in practice this ideal is often not achievable and that it is therefore acceptable to measure the polar response at sufficient a distance that the shape is not significantly dependent on it. This is a satisfactory state of affairs for samples that are designed to be situated in the free field but in some applications, particularly in performance spaces and studios, diffusing samples are often mounted on or in large plane surfaces such as walls. In these cases, the purpose of the diffuser is to move the reflected energy away from the specular zone (as defined in Section 3.6.2), either to prevent detrimental effects such as echoes or image shift or to create a reflection free zone. Theoretically, many of the diffusion parameters discussed in this chapter can be applied to this case of a baffled sample if a weighting function is incorporated into their formulation to account for the fact that complete diffusion is no longer defined as uniform scattering. However, even if the size of the surface on which the sample is mounted is

relatively small, the required measurement distance is likely to be impractical.

3.10.2 **Measurement procedure and parameter definition.**

Cox[8] has published a different approach to quantifying the diffusion efficacy of baffled samples which overcomes this problem. The method he proposes is based on the difference observed in the scattering from the baffle with and without the sample present; the decrease in level over the specular zone is used as the measure of diffusion quality. The advantage of this method is that it is not necessary to measure the polar response in the far field of the baffle, in theory samples could even be measured in-situ.

The first stage in quantifying the diffusion efficacy of a baffled sample using Cox's approach is to measure the polar response of the baffle with and without the sample present. These measurements do not need to be made in the far field. For the reasons discussed in Section 3.3, the response without the sample present will be uniform if measured in the near field, except for slight variations resulting from the different path lengths from the image source to each receiver position. From this, the response with the sample present is subtracted. The result is the 'insertion loss' obtained when the sample is added to the baffle.

It is difficult to determine how much insertion loss is required for any particular application because this depends on factors such as the angle and time of arrival of the reflections at the listeners and the number of other reflections present which may mask the image shift, colouration or echo. The safest approach is thus simply to assume that the more energy removed from the specular zone, the better. Cox suggests using the parameter defined on the following page to quantify this; the sum of the mean and one standard deviation of the insertion losses at receiver positions in the specular zone for all frequencies and source positions being considered. He states that adding a standard deviation to the mean of the insertion losses produces better results than using the mean alone because uneven responses are penalised.

$$\epsilon = \overline{L}_p + \sqrt{\frac{\sum_{m=1}^{n}\left[L_{p,m} - \overline{L}_p\right]^2}{n-1}} \tag{3.43}$$

where:

$$\overline{L}_p = \frac{1}{n}\sum_{m=1}^{n} L_{p,m} \tag{3.44}$$

$L_{p,m}$ = Insertion loss for a particular frequency, source position and receiver position (receiver positions limited to those within the specular zone)

n = total number of insertion losses measured

3.10.3 **Appraisal.**

One problem with this diffusion parameter is that it does not monitor the scattering outside the specular zone and therefore, like the specular zone type parameters discussed in Section 3.6, does not differentiate between scattering and redirection. It is also not bounded between zero and unity. A further problem is that this parameter is specifically for quantifying the diffusion efficacy of samples mounted on or in baffles, the evaluation procedure differs to that used for unbaffled samples. Cox expresses the concern that in practice this would present difficulties because for medium sized samples or baffles it would be unclear whether a baffled or unbaffled parameter should be used. He goes on to state that, "*A unified parameter would be more useful and less prone to arbitrary use.*"

Cox has used this parameter to quantify the diffusion produced by a small number of surfaces and the ranking order was as expected. However, since it fails in the case of samples which redirect as opposed to scatter the reflected energy, its application is limited and it has not been considered further in this research. It has, however, been successfully used by Cox as a cost function in designing optimised diffusers[7] where it was known that redirection was not occurring.

3.11 Quantifying diffusion from three-dimensional polar responses.

As stated in the introduction to this chapter, it is conceptually straightforward to extend the diffusion parameters discussed here into three dimensions. However, there is a practical problem with quantifying three-dimensional polar responses measured using the technique described in Section 2.9; although the scattered field is sampled at points spaced equally in azimuth and elevation, the density of these points on the surface of the hemisphere they describe is not uniform. The surface density is independent of azimuth but decreases with decreasing elevation, i.e. it is maximum around the normal direction and minimum at grazing angles. The consequence of this is that the sampling of the scattered field is spatially biased and if complete diffusion is defined as uniform scattered intensity (squared pressure) over the surface of the measurement hemisphere then the preponderance of measurement points around the surface normal places undue emphasis on this direction when quantifying diffusion from the polar response.

The effect of this bias can be annulled, but it is firstly necessary to conceive that each point at which the polar response is sampled represents an area of surface on the measurement hemisphere. These surface area elements vary in size inversely to the surface density; they are largest at grazing angles and become smaller with increasing elevation. To annul the bias, imaginary additional measurement points are introduced into each element so that the surface area represented by each point (real or imaginary) is constant over the whole hemisphere. The magnitude of the scattered field at the imaginary points is assumed to be the same as the measured value at the real point which represents the element into which they are introduced. The number of imaginary points that it is necessary to add into each surface area element, n_{imag}, is approximately equal to the ratio of the size of the particular element under consideration to the smallest, as shown below:

$$n_{imag} = \frac{Area\ of\ surface\ represented\ by\ real\ point}{Smallest\ area\ of\ surface\ represented\ by\ a\ real\ point} - 1 \qquad (3.45)$$

Apart from in the normal reflection direction (elevation=90°), the surface areas represented by the real measurement points are approximately trapezoidal in shape and, for angles of elevation other than 0°, can be evaluated using the following formula[††]:

$$S_\theta \approx r^2 \Delta\theta \, \Delta\varphi \cos\theta \cos\left(\frac{\Delta\theta}{2}\right) \qquad (3.46)$$

where:

r = Radius of measurement hemisphere (1.47m)

$\Delta\theta$ = Elevation angular resolution ($\pi/36$)

$\Delta\varphi$ = Azimuthal angular resolution ($\pi/36$)

θ = Angle of elevation

The smallest of these trapezia are those associated with the measurement points closest to the normal incidence direction, i.e. at an elevation of 85°. n_{imag} is therefore given by:

$$n_{imag} = \frac{S_\theta}{S_{85}} - 1 = \frac{\cos\theta}{\cos 85°} - 1 \qquad (3.47)$$

Since the number of imaginary points added to each surface area element must be an integer but, in general, n_{imag} is not, the value calculated using (3.47) was rounded to the nearest integer. The resulting n_{imag} values, as a function of elevation, are given in the following table:

Table 3.1: Values of n_{imag} as a function of elevation, θ.

θ°	5	10	15	20	25	30	35	40	45	50	55	60	65	70	75	80	85
n_{imag}	10	10	10	10	9	9	8	8	7	6	6	5	4	3	2	1	0

†† The derivation of this expression is contained in Appendix C. As discussed in Section 2.9, the three-dimensional polar responses measured during the course of this research do not include points at 0° elevation; the minimum elevation used was 5°.

The receiver point at an elevation of 90° (the normal incidence direction) is assumed to represent the circular area atop the measurement hemisphere and this surface area, S_{90}, is given by:

$$S_{90} \approx \pi\left[r\sin\left(\frac{\Delta\theta}{2}\right)\right]^2 \tag{3.48}$$

where the symbols have the same meaning as in (3.46).

This is considerably larger than S_{85} and the corresponding integer value of n_{imag} is in fact eight.

Incorporating the imaginary points (and the bounding correction) into the expression for the autocorrelation coefficient, d_{auto}, yields the following formulation:

$$d_{auto3D} = \frac{\left[\sum_{i=1}^{n} n_i 10^{L_i/10}\right]^2 - \sum_{i=1}^{n} n_i\left(10^{L_i/10}\right)^2}{\left[\sum_{i=1}^{n} n_i - 1\right]\sum_{i=1}^{n} n_i\left(10^{L_i/10}\right)^2} \tag{3.49}$$

where:

L_i = Scattered sound pressure level at receiver position i

n_i = Total number of points (real and imaginary) in the element of surface area represented by receiver position i, i.e. n_{imag} plus one

n = Number of receiver positions

Selected three-dimensional polar responses measured or predicted during the course of this research are shown, along with their corresponding values of the autocorrelation diffusion coefficient, in Figures 3.51 to 3.60. To enable visual comparison of these 'balloons', the maximum distance between the origin and the balloon surface is 50dB in all cases.

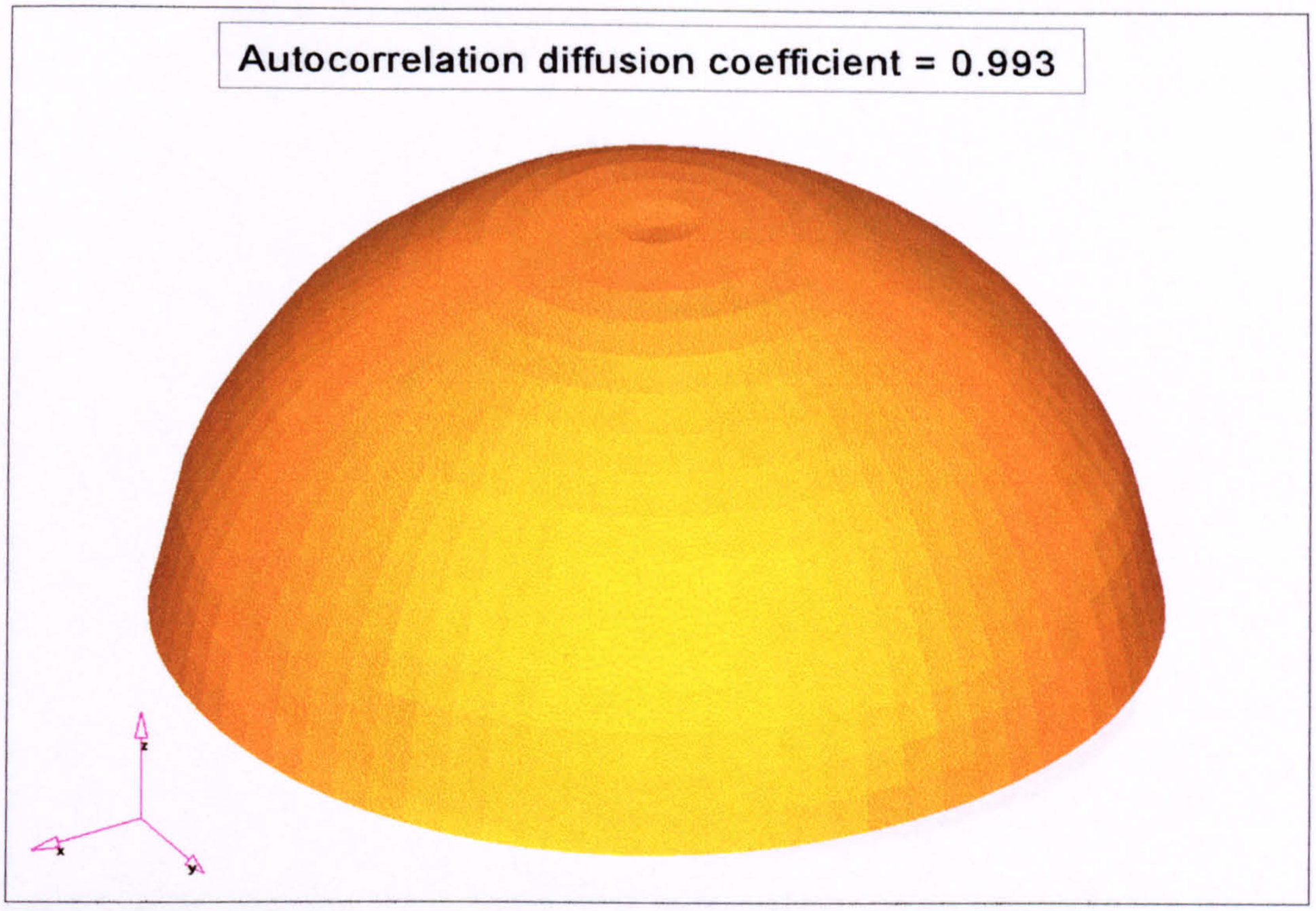

Figure 3.51: 1kHz normal incidence polar response of a small sphere, predicted using BEM.

Figure 3.52: 125Hz normal incidence polar response of the Skyline on a 15m (full scale) baffle, measured at Salford. (Essentially the response of the baffle.)

Figure 3.53: 800Hz normal incidence polar response of the Skyline on a 15m (full scale) baffle, measured at Salford. (Essentially the response of the baffle.)

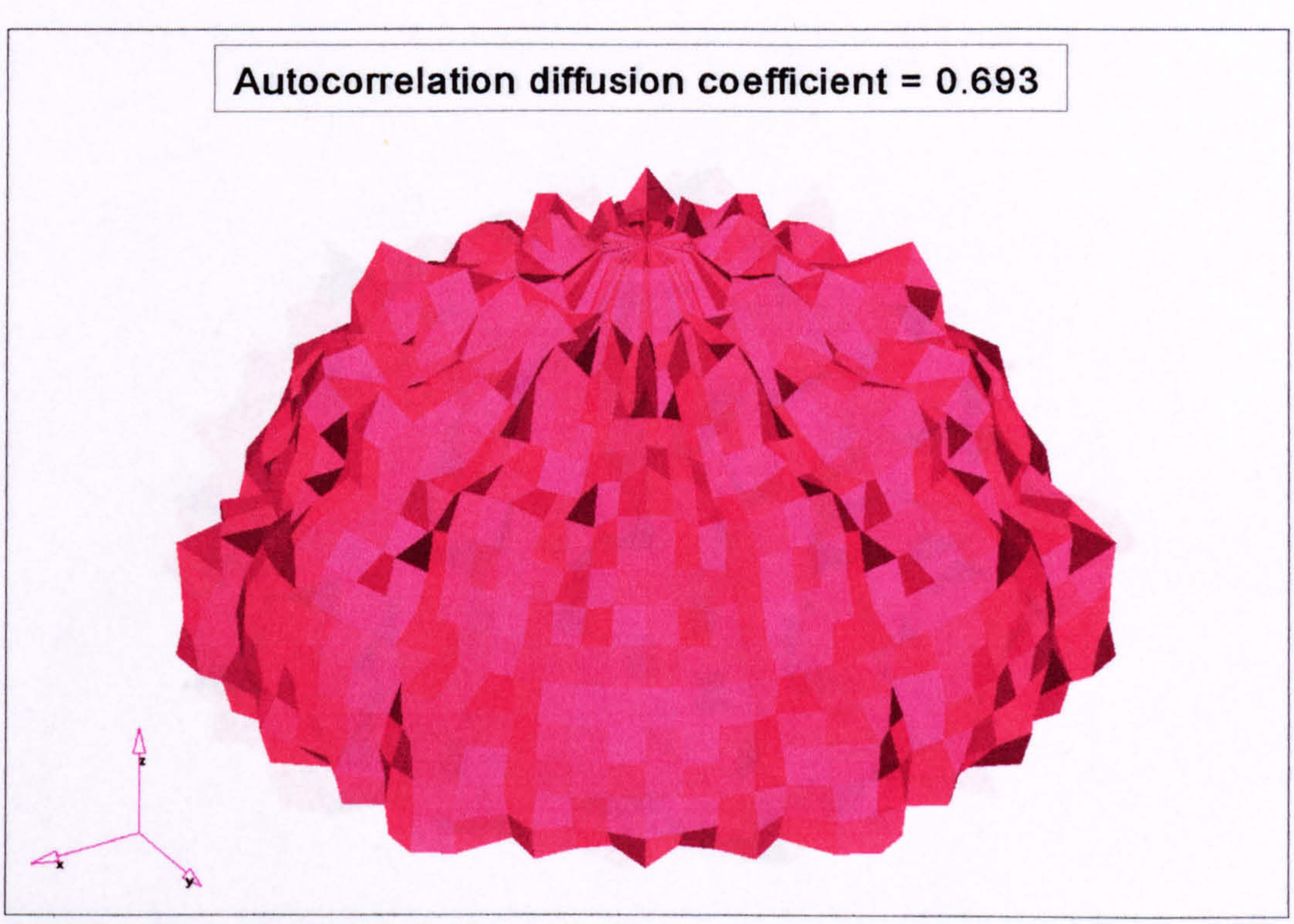

Figure 3.54: 3.15kHz normal incidence polar response of the periodic hemispheres, measured at Salford.

Figure 3.55: 500Hz normal incidence polar response of the square-based pyramid, measured at Salford.

Figure 3.56: 2.5kHz 45° incidence polar response of the Skyline, measured at Salford.

Figure 3.57: 160Hz normal incidence polar response of the plane hexagon, measured at Salford.

Figure 3.58: 1.6kHz normal incidence polar response of the Skyline, measured at Salford.

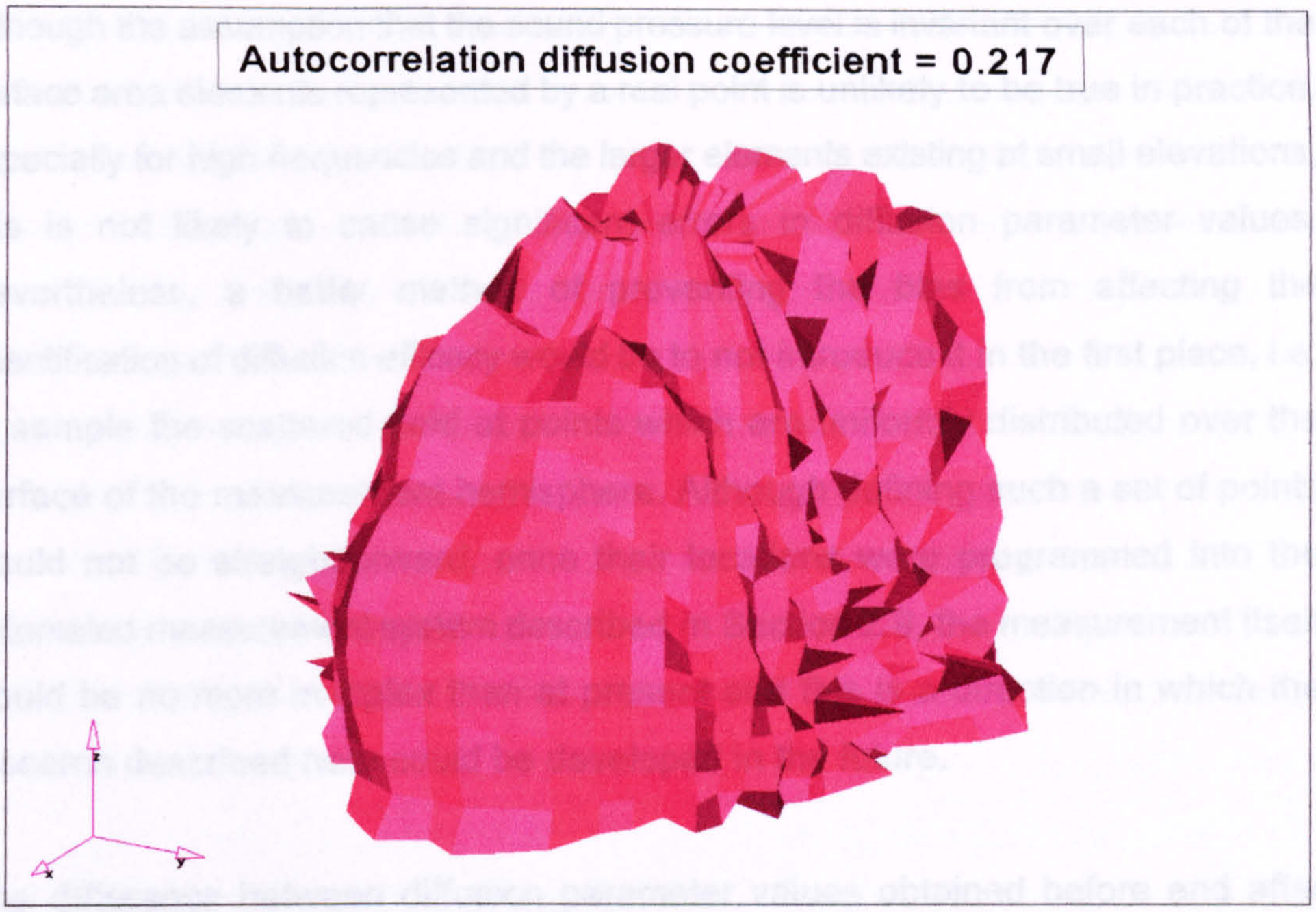

Figure 3.59: 1kHz 30° incidence polar response of the random battens (battens parallel to the y-axis), measured at Salford.

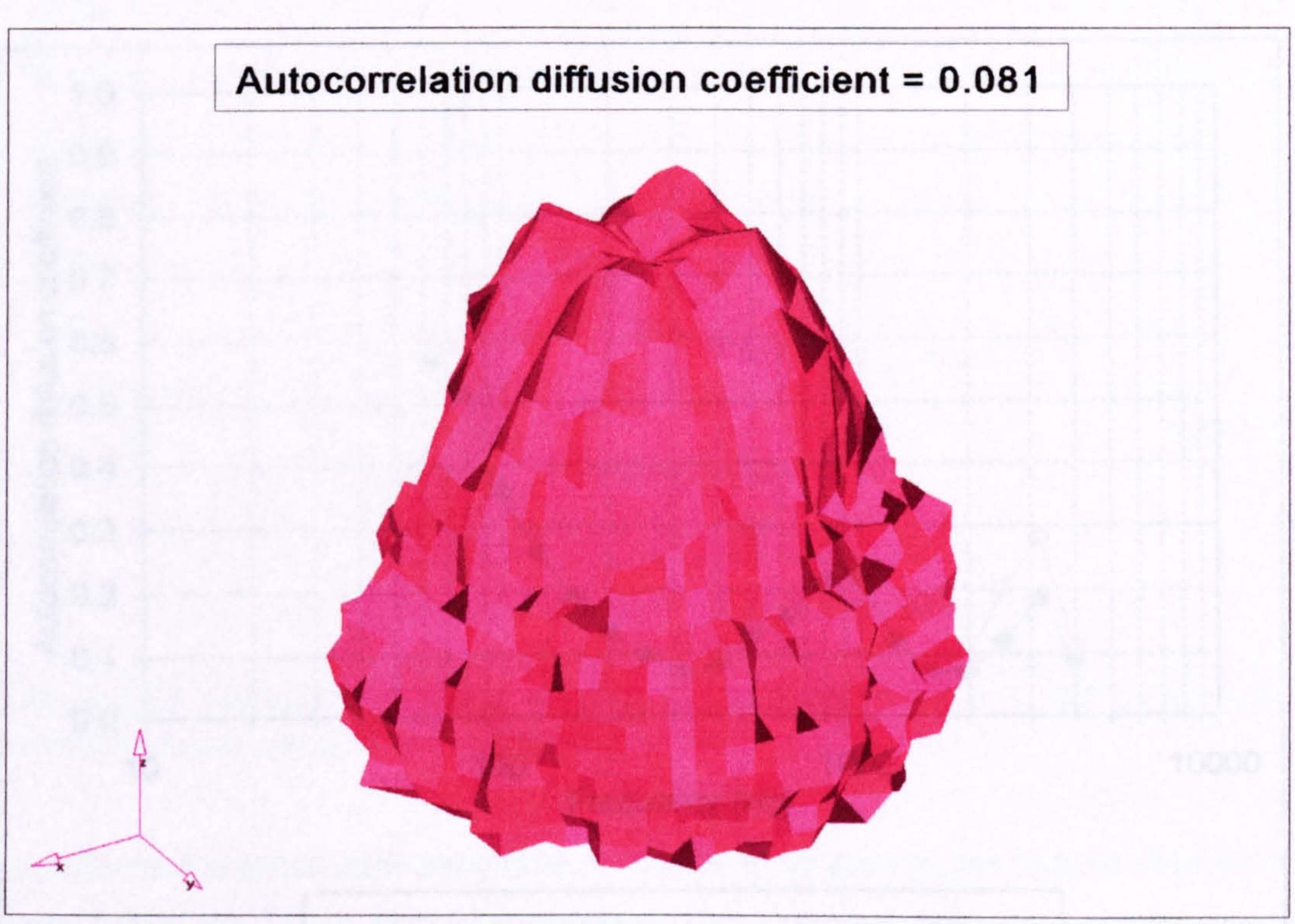

Figure 3.60: 5kHz normal incidence polar response of a BAD Panel, measured at Salford.

Although the assumption that the sound pressure level is invariant over each of the surface area elements represented by a real point is unlikely to be true in practice, especially for high frequencies and the larger elements existing at small elevations, this is not likely to cause significant errors in diffusion parameter values. Nevertheless, a better method of preventing the bias from affecting the quantification of diffusion efficacy would be to not introduce it in the first place, i.e. to sample the scattered field at points which are uniformly distributed over the surface of the measurement hemisphere. Although defining such a set of points would not be straightforward, once their locations were programmed into the automated measurement system described in Section 2.9, the measurement itself would be no more complex than at present and this is a direction in which the research described here could be developed in the future.

The difference between diffusion parameter values obtained before and after implementation of the bias correction is usually small, an example of this is shown in Figure 3.61.

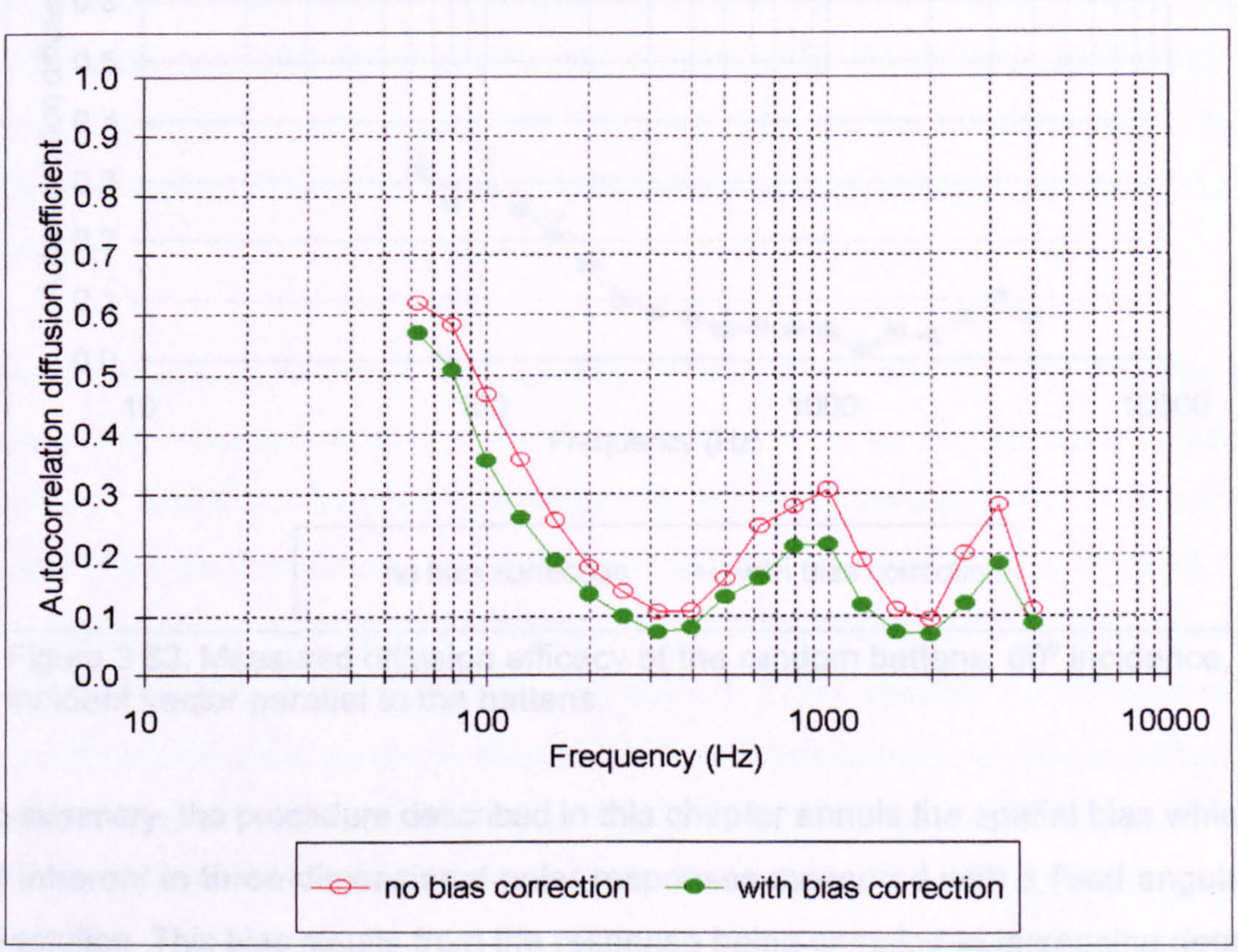

Figure 3.61: Measured diffusion efficacy of the random battens. 30° incidence, incident vector perpendicular to the battens.

As is the case in Figure 3.61, introducing the imaginary points normally lowers the parameter value, indicating that the presence of these additional points makes the polar response less uniform. This is perhaps the opposite of the expected result, especially since many of the additional points have identical values. However, the majority of the imaginary points are added at large scattering angles, where the sound pressure level is routinely lower than in directions close to the normal, especially if the angle of incidence is normal or close to it. Consequently, any non-uniformity in the polar response at large scattering angles is magnified by the bias correction, it assumes a much greater importance in the response as a whole. Only if the incident angle is itself large, as in the example shown in Figure 3.62, is it likely that adding the imaginary points will increase the uniformity of the response.

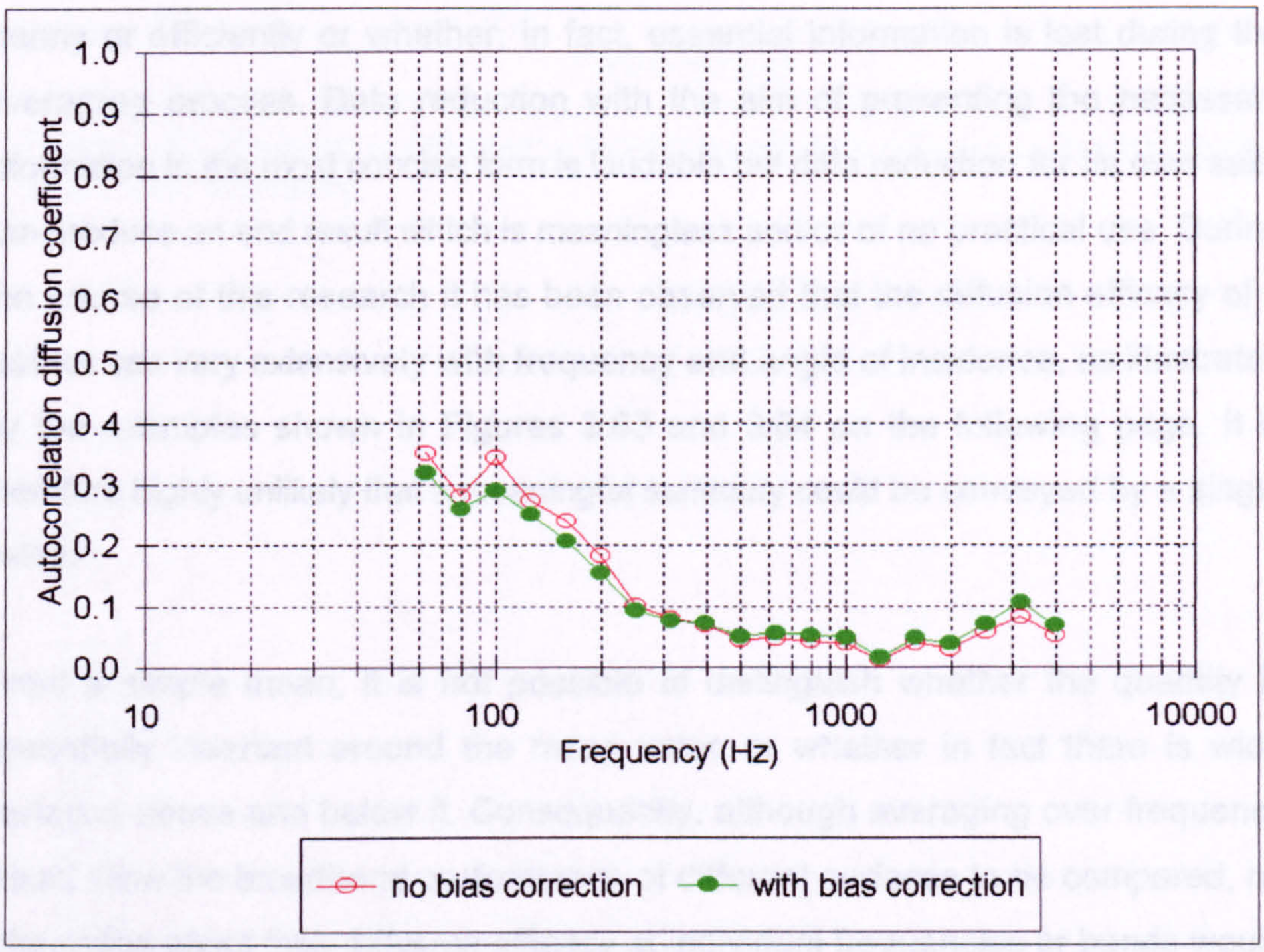

Figure 3.62: Measured diffusion efficacy of the random battens. 60° incidence, incident vector parallel to the battens.

In summary, the procedure described in this chapter annuls the spatial bias which is inherent in three-dimensional polar responses measured with a fixed angular resolution. This bias results from the response being sampled in increasing detail as the scattering angle approaches the normal incidence direction.

3.12 Averaging polar response diffusion coefficient values over frequency and angle of incidence.

It is well known that the polar response of a surface has a shape which, in general, is dependent on the source and receiver distances, the angle of incidence and the frequency. The dependence on the source and receiver distances is removed by measuring the response in the far field but the dependence on frequency and angle of incidence remains. Whatever measure for quantifying diffusion from polar responses is employed, it is therefore necessary to consider whether values should be averaged over frequency and/or angles of incidence. Both the concept and procedure of averaging over these quantities is simple, what must be considered is whether the result conveys the diffusion efficacy of the surface more clearly or efficiently or whether, in fact, essential information is lost during the averaging process. Data reduction with the aim of presenting the necessary information in the most concise form is laudable but data reduction for its own sake can produce an end result which is meaningless and/or of no practical use. During the course of this research it has been observed that the diffusion efficacy of a surface can vary extensively with frequency and angle of incidence, as illustrated by the examples shown in Figures 3.63 and 3.64 on the following page. It is therefore highly unlikely that a meaningful summary could be conveyed by a single value.

From a simple mean, it is not possible to distinguish whether the quantity is essentially invariant around the mean value or whether in fact there is wide variation above and below it. Consequently, although averaging over frequency would allow the broadband performance of different surfaces to be compared, no information about their diffusion efficacy at individual frequencies or bands would be provided. This is not satisfactory because in many applications diffusers are required to operate at particular frequencies so an assessment of their broadband performance is insufficient. Previous work[7,12,13] has addressed this deficiency by proposing that the standard deviation should be stated in addition to the mean. However, if the standard deviation is large then this still does not provide any information about the diffusion efficacy at a particular frequency.

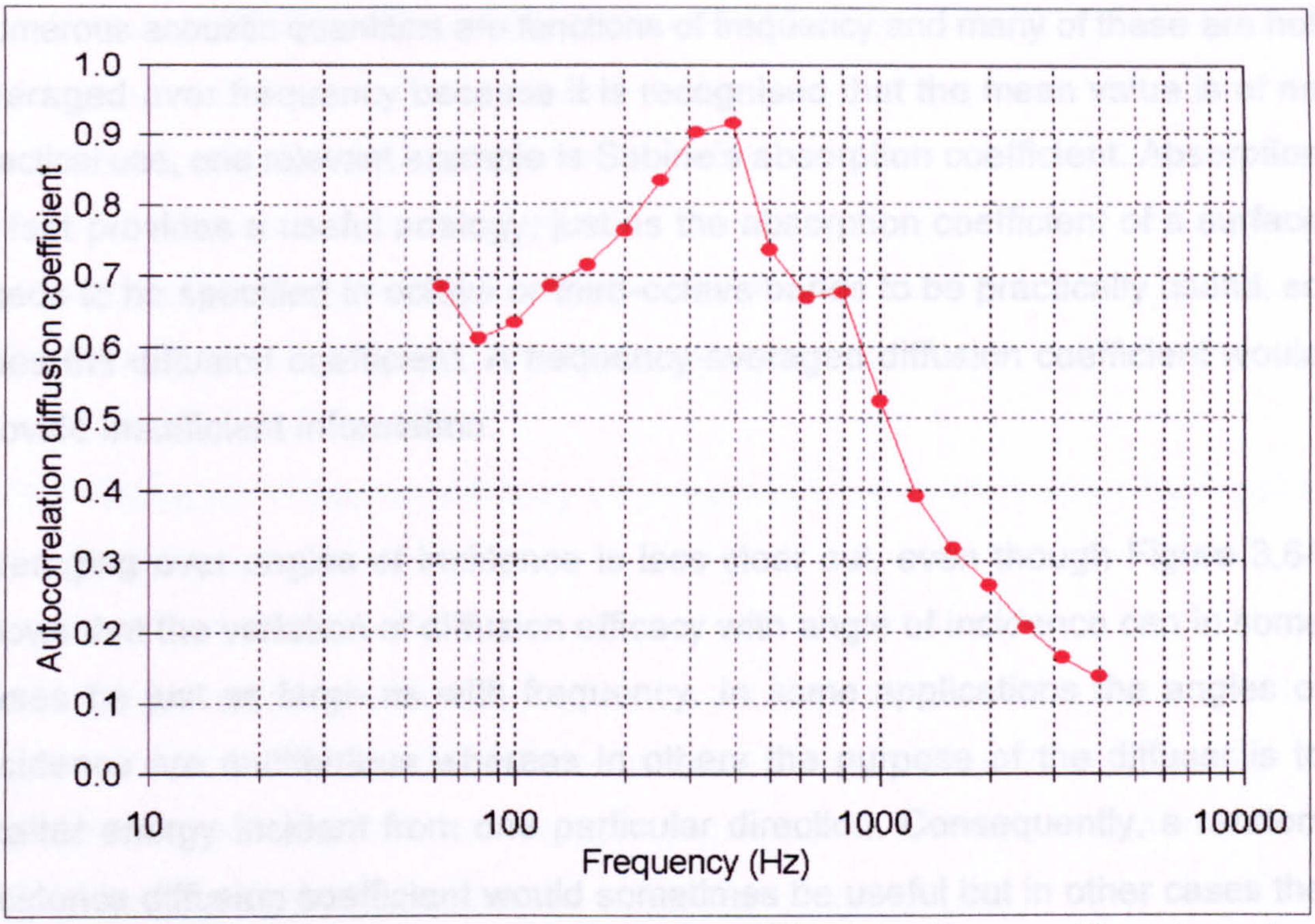

Figure 3.63: Variation of the normal incidence diffusion efficacy of the triangular prism with frequency.

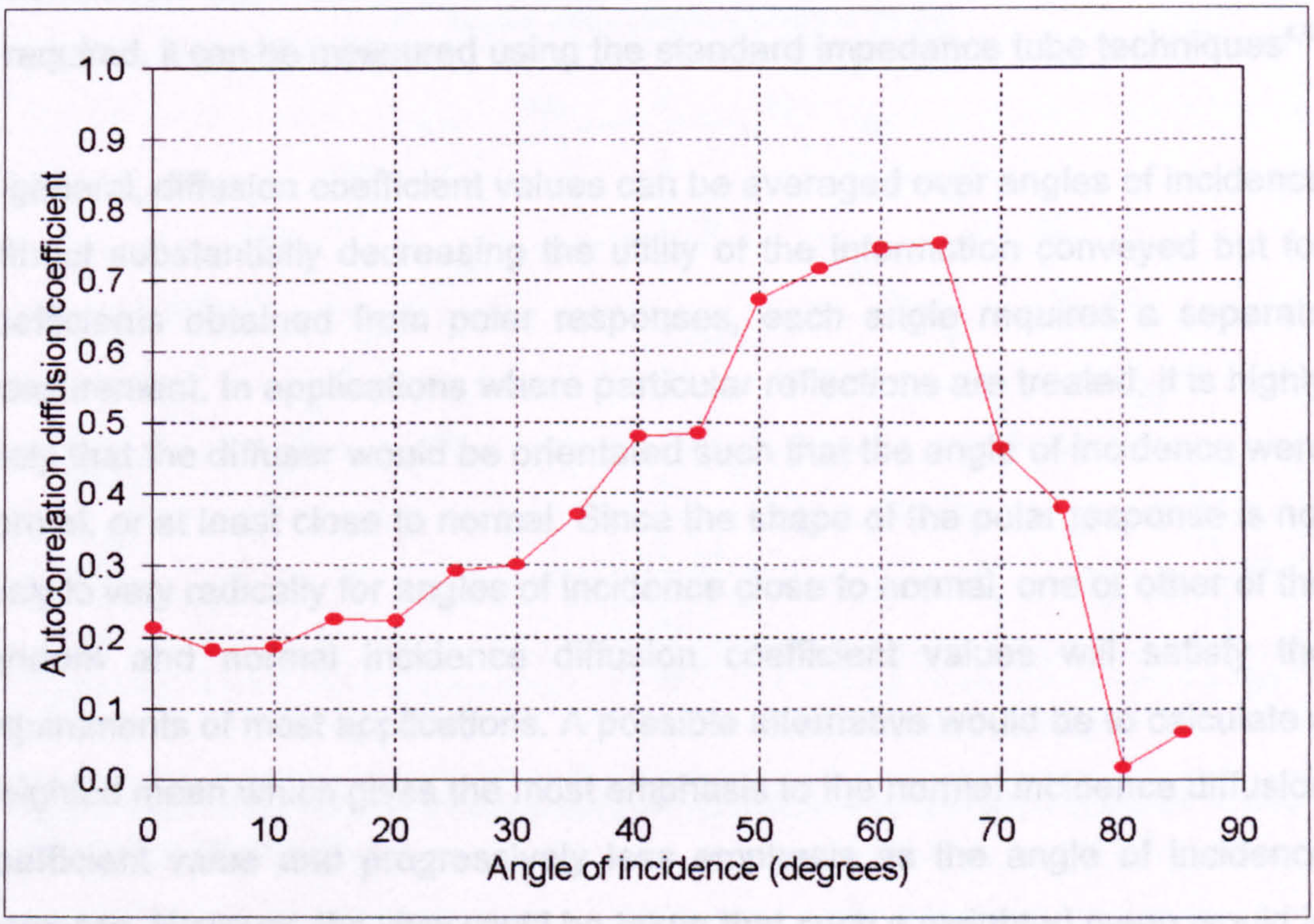

Figure 3.64: Variation of the 3.15kHz diffusion efficacy of the QRD with angle of incidence.

Numerous acoustic quantities are functions of frequency and many of these are not averaged over frequency because it is recognised that the mean value is of no practical use, one relevant example is Sabine's absorption coefficient. Absorption in fact provides a useful analogy; just as the absorption coefficient of a surface needs to be specified in octave or third-octave bands to be practically useful, so does the diffusion coefficient. A frequency-averaged diffusion coefficient would provide insufficient information.

Averaging over angles of incidence is less clear cut, even though Figure 3.64 shows that the variation of diffusion efficacy with angle of incidence can in some cases be just as large as with frequency. In some applications the angles of incidence are multifarious whereas in others the purpose of the diffuser is to scatter energy incident from one particular direction. Consequently, a random incidence diffusion coefficient would sometimes be useful but in other cases the value for a particular angle would suffice. Again there exists some analogy with absorption; random incidence values measured using the standard reverberation room method[6] are in this case the norm but if the value for a specific incident angle is required, it can be measured using the standard impedance tube techniques[4,5].

In general, diffusion coefficient values can be averaged over angles of incidence without substantially decreasing the utility of the information conveyed but for coefficients obtained from polar responses, each angle requires a separate measurement. In applications where particular reflections are treated, it is highly likely that the diffuser would be orientated such that the angle of incidence were normal, or at least close to normal. Since the shape of the polar response is not likely to vary radically for angles of incidence close to normal, one or other of the random and normal incidence diffusion coefficient values will satisfy the requirements of most applications. A possible alternative would be to calculate a weighted mean which gives the most emphasis to the normal incidence diffusion coefficient value and progressively less emphasis as the angle of incidence increases. However, the view could be taken that such a weighted mean would in fact be too much of a compromise and that greater practical utility would result from keeping the random and normal incidence values separate.

The merits or otherwise of averaging diffusion coefficient values over frequency and angle of incidence could be debated at length but a sensible conclusion is that the diffusion efficacy of a surface is expressed in a practically useful manner by normal incidence octave band values. More information can be conveyed by using third-octave bands and additionally quoting the random incidence coefficient values for but this would be excessive for many applications.

3.13 **Rating the diffusion efficacy of anisotropic scatterers from their polar response**.

Quantifying the diffusion efficacy of a sample from its three-dimensional polar response can be misleading if the scattering is significantly anisotropic. A semicylinder is one surface which produces anisotropic scattering, as demonstrated for the case of normal incidence in Figure 3.65.

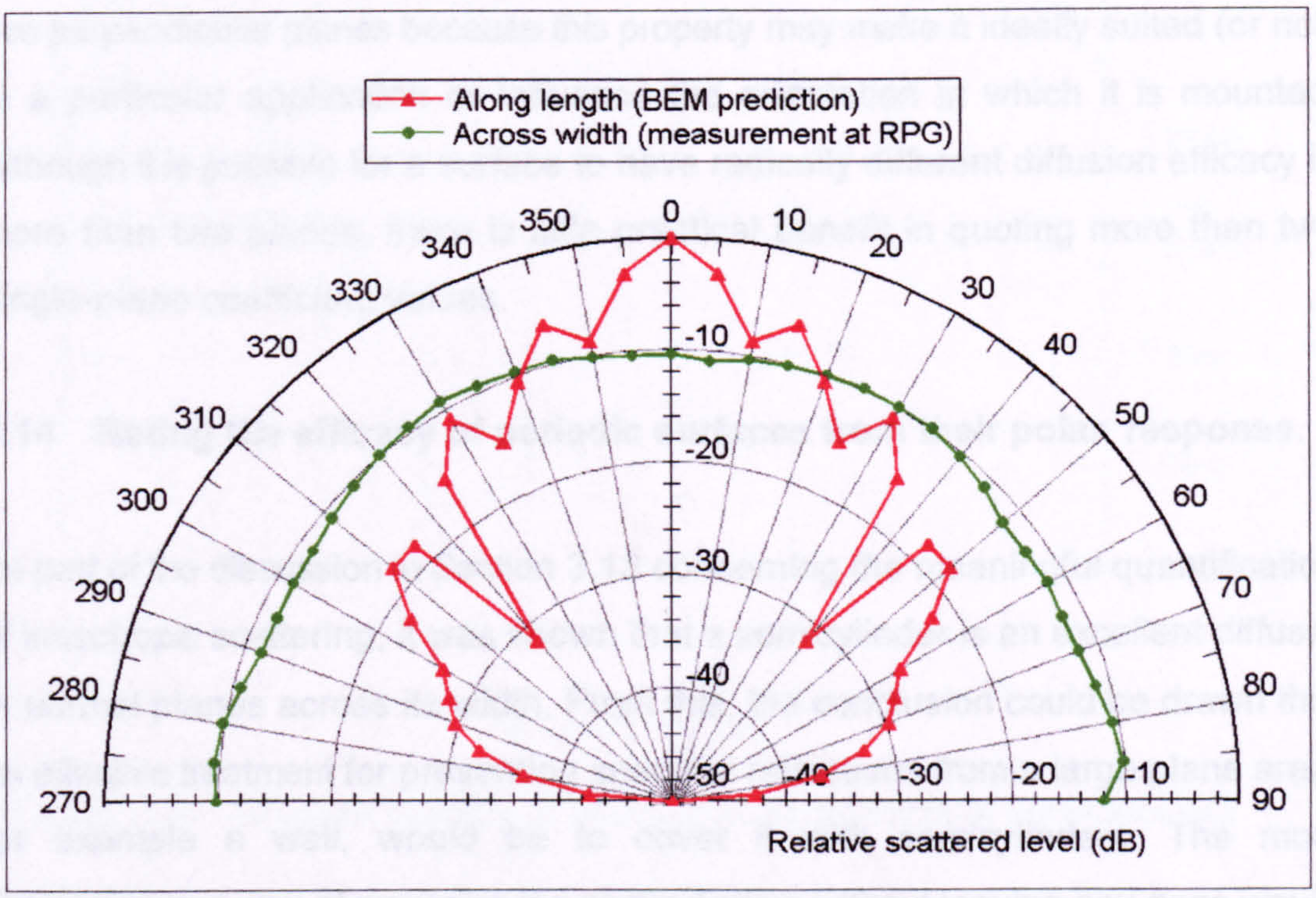

Figure 3.65: 1kHz normal incidence polar responses of the semicylinder in two perpendicular planes.

Figure 3.65 shows that along its length (i.e. in the normal plane containing its axis), a semicylinder is a poor diffuser because the reflection is essentially specular but

that across its width (in the perpendicular normal plane), the reflection is highly diffuse. When a polar response has this type of shape, the diffusion coefficient value calculated from the three-dimensional response is not representative of the scattering in either plane and therefore of little practical use. The reason for this is that the value of the diffusion coefficient is effectively an average over all normal planes and by definition an average value will not be representative of the extremes. The effect is similar to that which occurs when coefficient values are averaged over frequency and the method of presenting the diffusion efficacy in a practically useful manner is therefore also similar; separate coefficient values for the two planes must be quoted. However, unlike with frequency, not quoting an average value is the exception as opposed to the rule because most surfaces have polar responses which exhibit at least a reasonable degree of rotational symmetry about the surface normal.

It is practically useful to know if a surface has very different diffusion efficacy in two perpendicular planes because this property may make it ideally suited (or not) to a particular application or influence the orientation in which it is mounted. Although it is possible for a surface to have radically different diffusion efficacy in more than two planes, there is little practical benefit in quoting more than two single-plane coefficient values.

3.14 Rating the efficacy of periodic surfaces from their polar response.

As part of the discussion in Section 3.13 concerning the meaningful quantification of anisotropic scattering, it was shown that a semicylinder is an excellent diffuser in normal planes across its width. From this, the conclusion could be drawn that an effective treatment for preventing specular reflections from a large plane area, for example a wall, would be to cover it with semicylinders. The most straightforward way of arranging the semicylinders without leaving any gaps would be to place them side by side, as shown in Figure 3.66. However, this conclusion is flawed because, as a consequence of interference effects, the resultant polar response of a periodic arrangement of semicylinders (or indeed any unit) is not simply the sum of the individual sound pressure level responses.

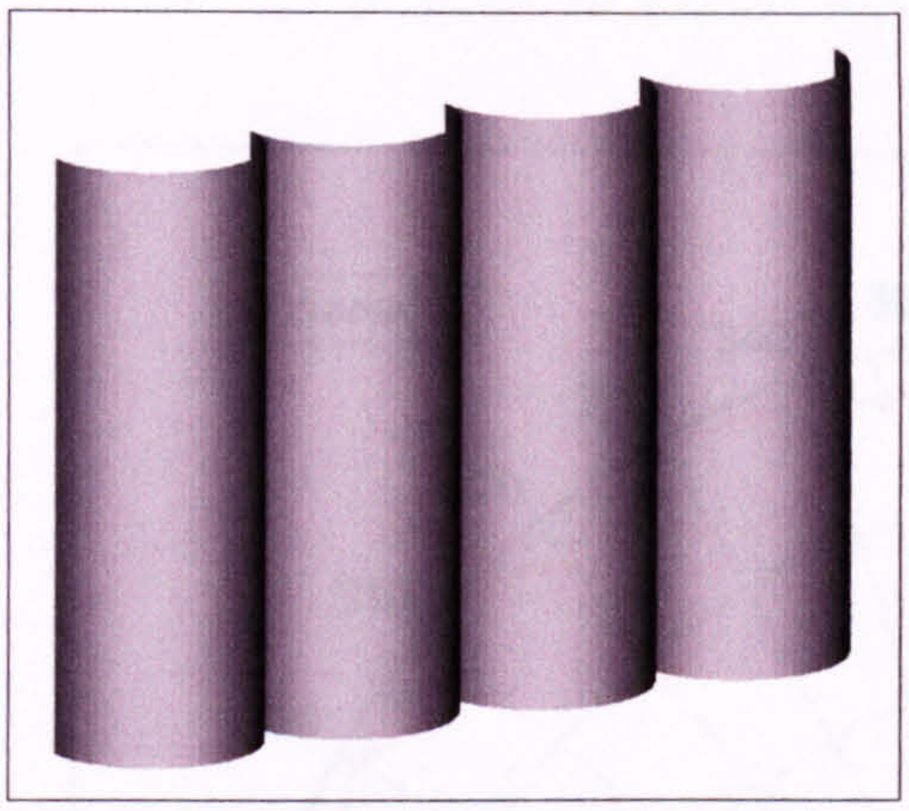

Figure 3.66: A periodic array of semicylinders.

To investigate how the shape of the resultant response is affected by the number of periods, single-plane measurements were made using periodic arrangements of between two and eighteen semicylinders of the type described in Section 2.33. Semicylinders were chosen because since they are such effective individual diffusers, the effect of the periodicity was expected to be large at some frequencies. Figure 3.67 shows how the autocorrelation diffusion coefficient varies with the number of periods and Figures 3.68 to 3.73 show selected 250Hz polar responses.

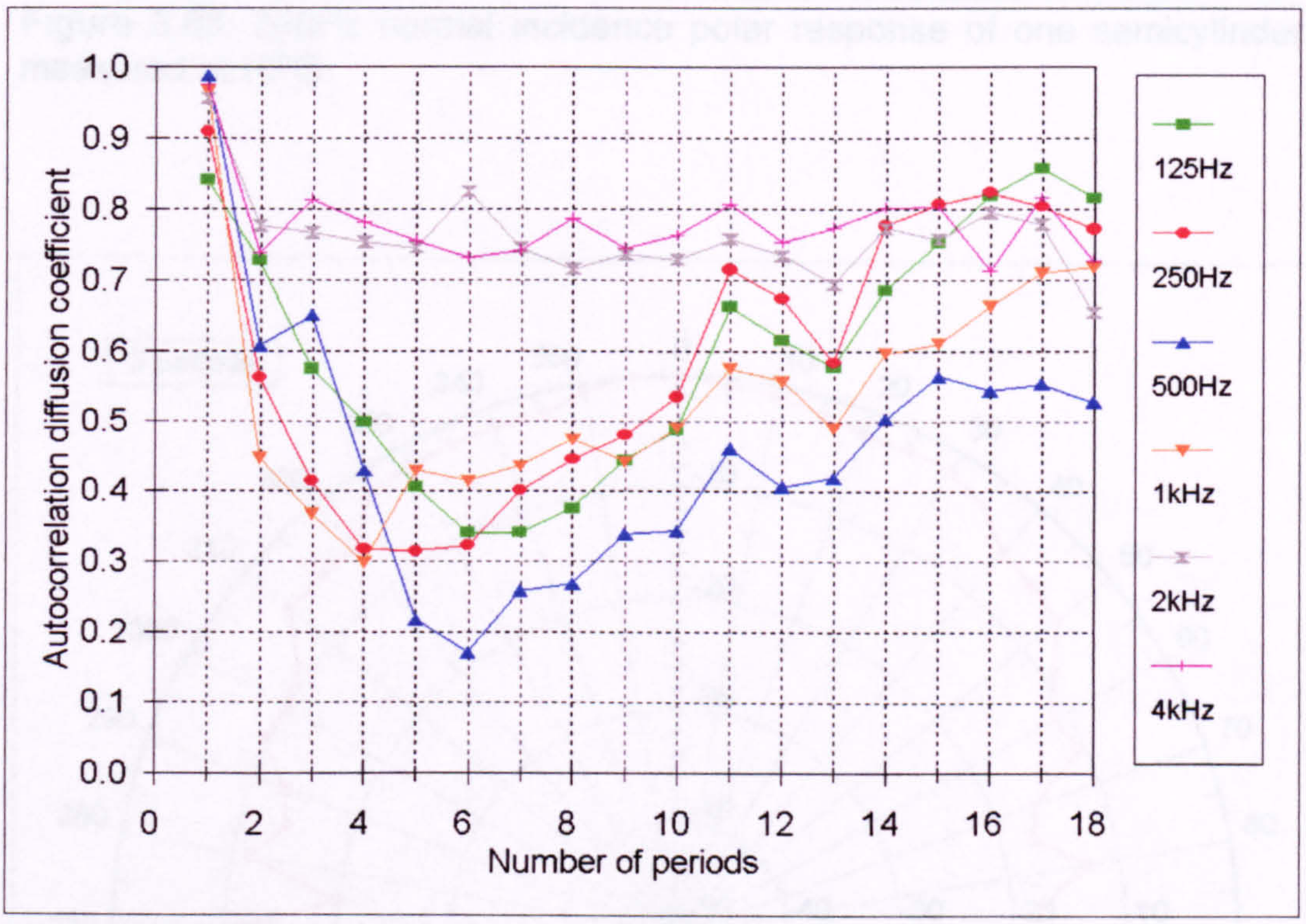

Figure 3.67: Diffusion efficacy of periodic arrangements of semicylinders.

From Figure 3.67, it can be seen that when two semicylinders are placed side by side, the resulting diffusion efficacy is lower than that of a single semicylinder at all frequencies. At frequencies below 2kHz, adding more periods to the array initially decreases the diffusion efficacy still further, although by smaller amounts.

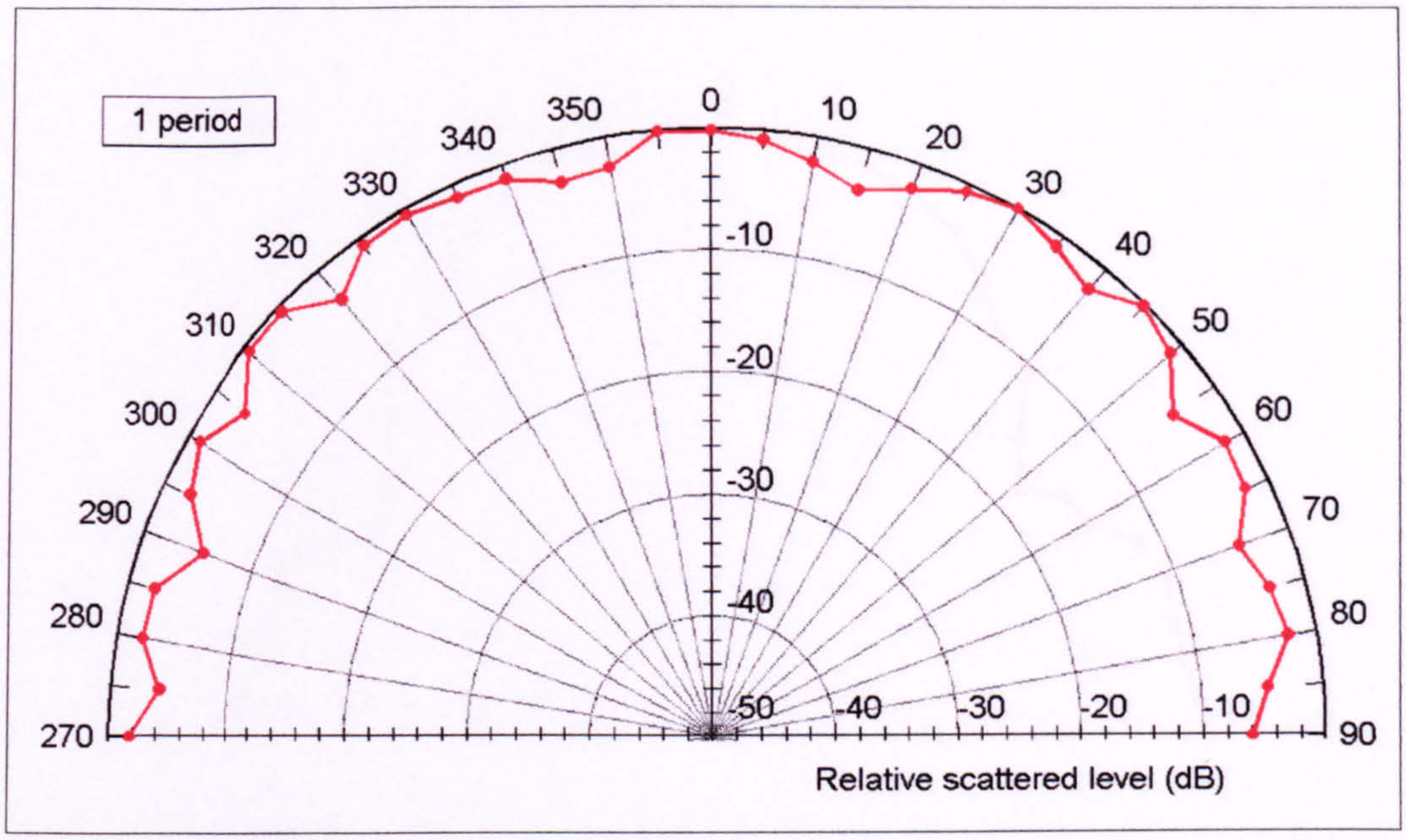

Figure 3.68: 250Hz normal incidence polar response of one semicylinder, measured at RPG.

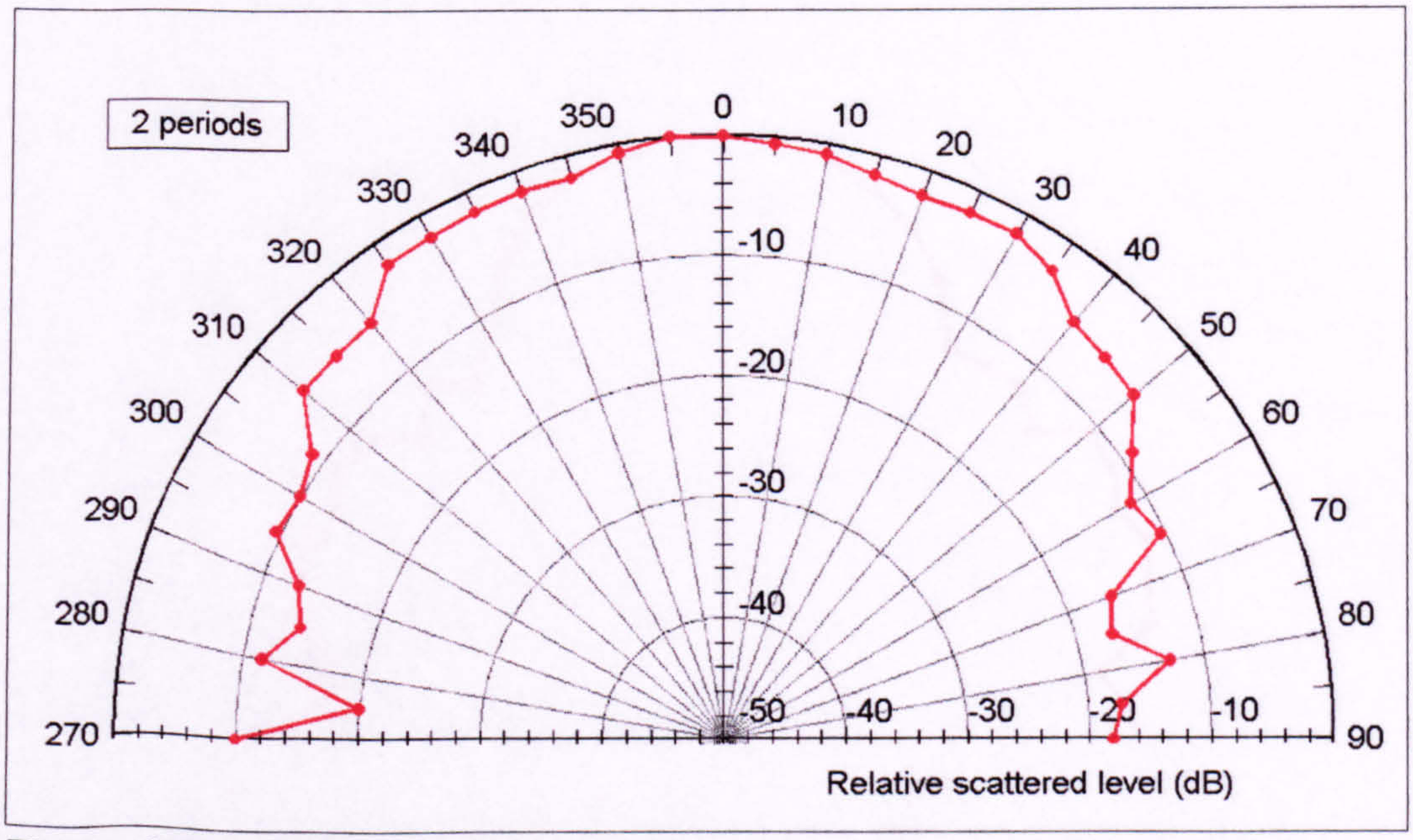

Figure 3.69: 250Hz normal incidence polar response of two semicylinders, measured at RPG.

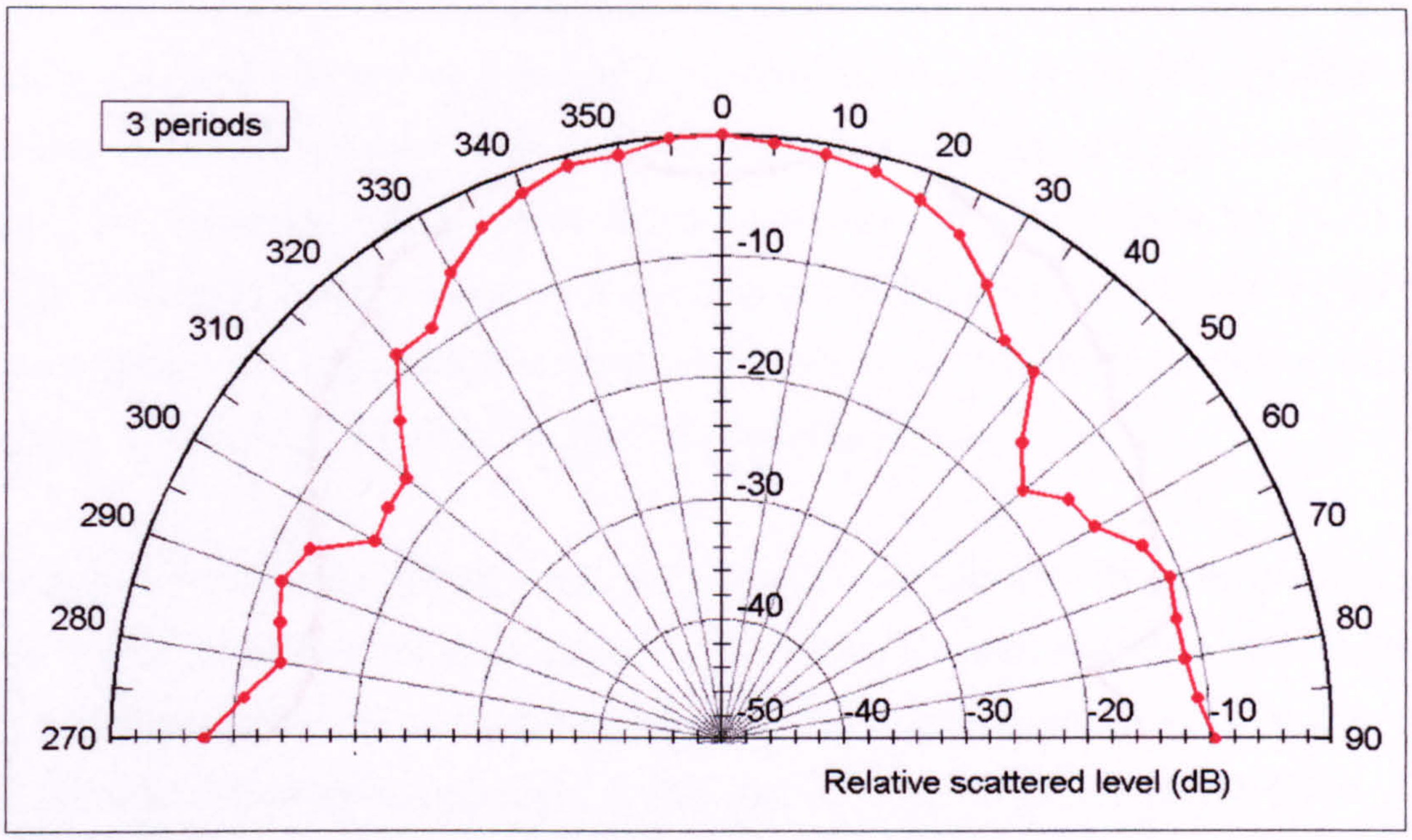

Figure 3.70: 250Hz normal incidence polar response of three semicylinders, measured at RPG.

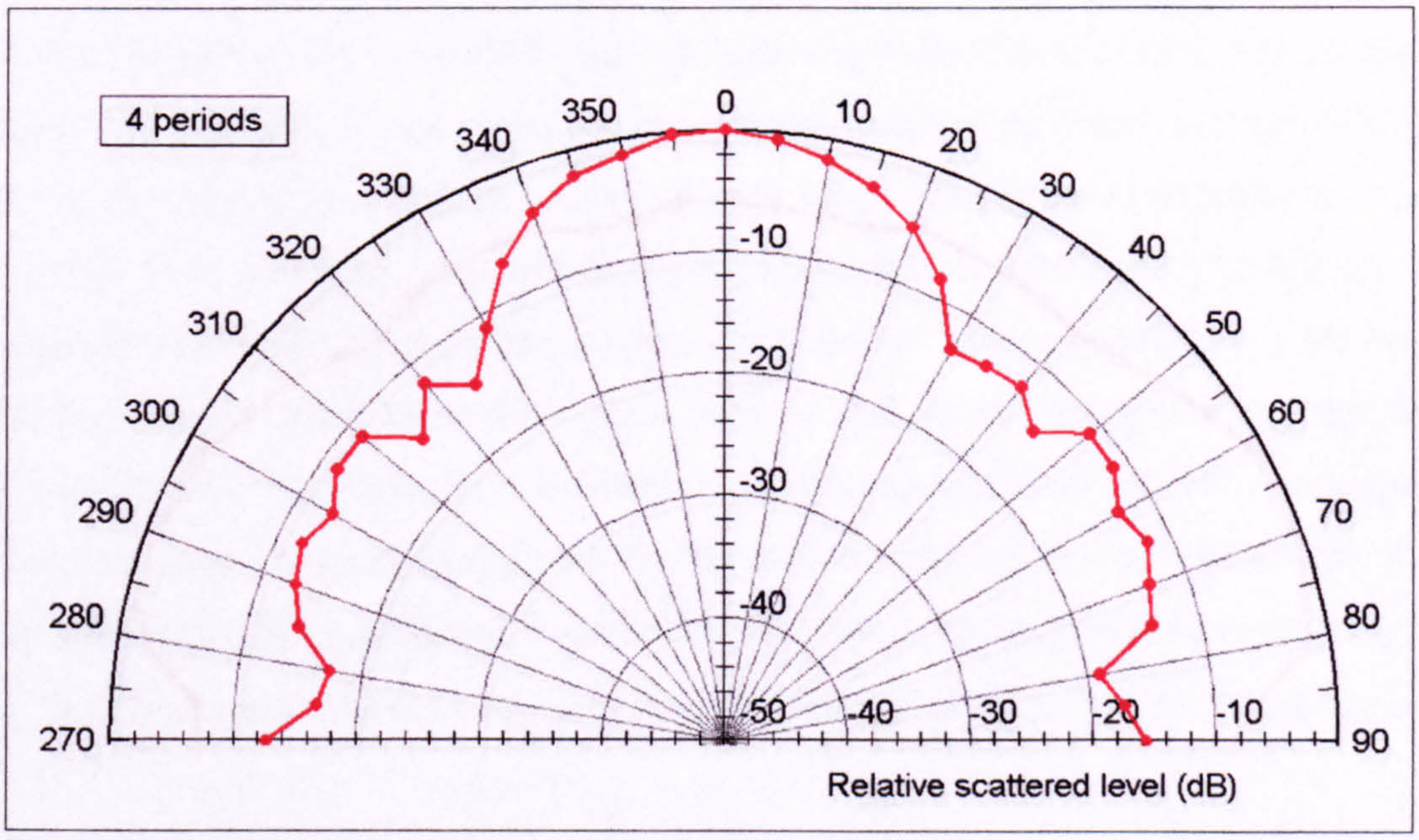

Figure 3.71: 250Hz normal incidence polar response of four semicylinders, measured at RPG.

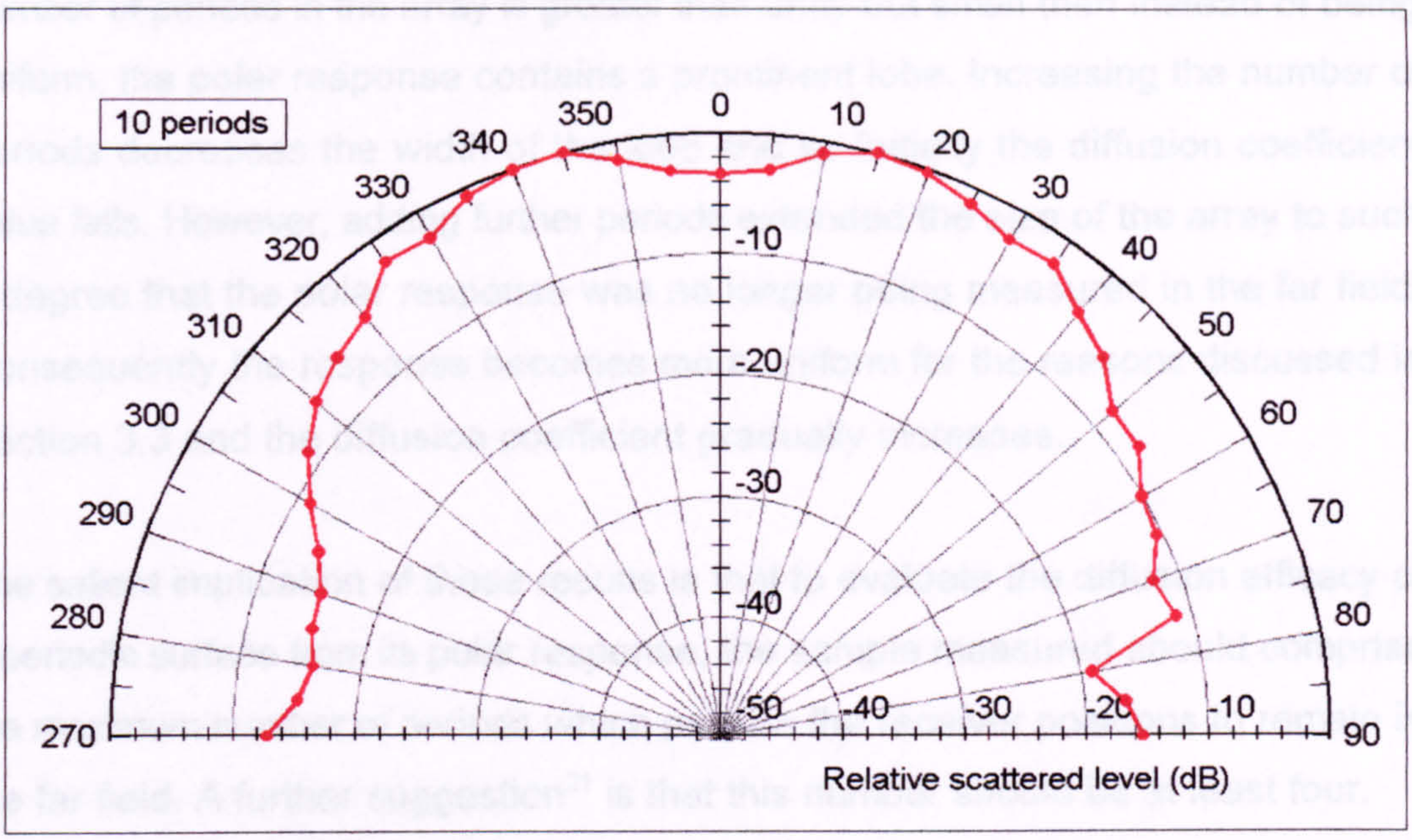

Figure 3.72: 250Hz normal incidence polar response of ten semicylinders, measured at RPG.

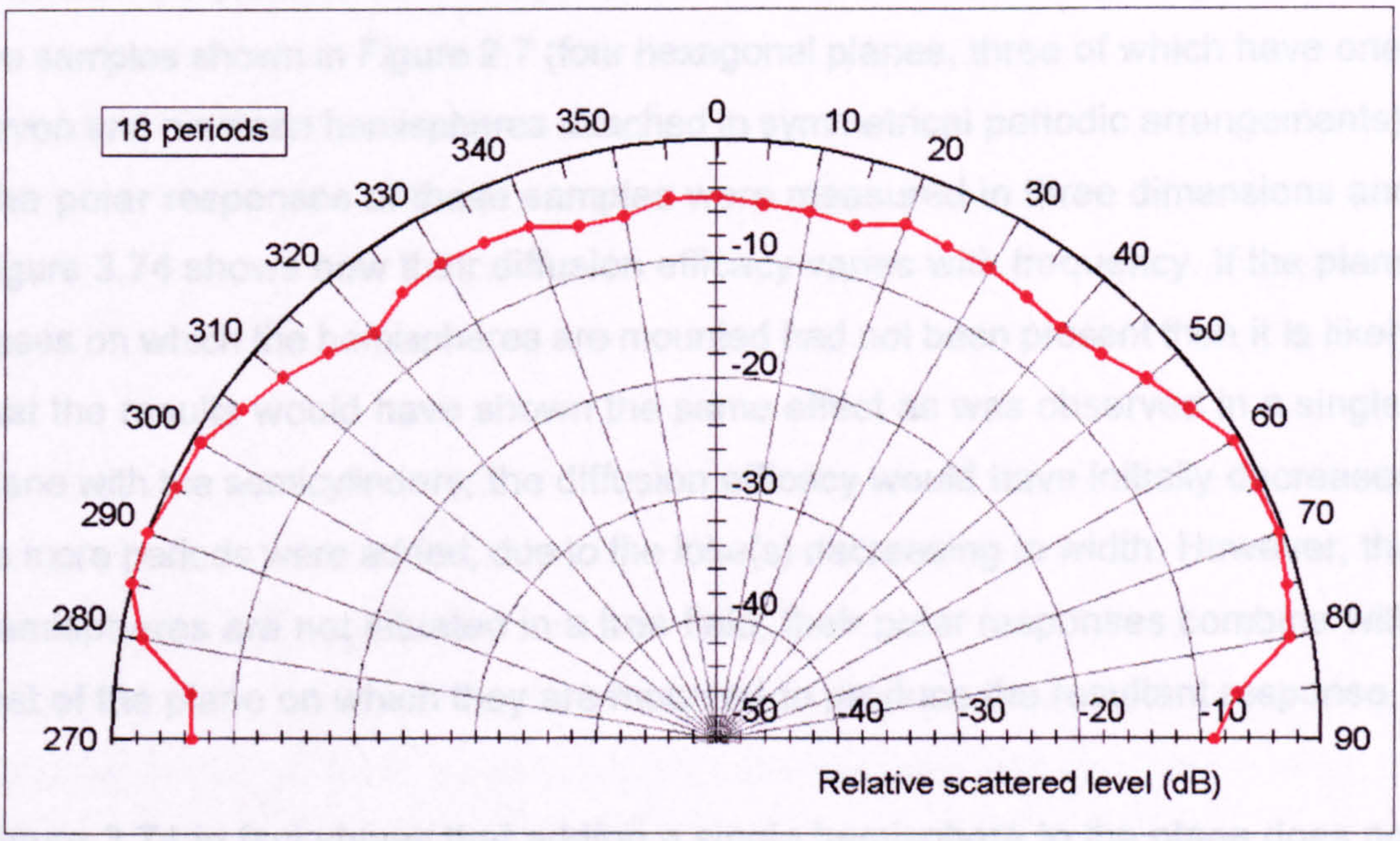

Figure 3.73: 250Hz normal incidence polar response of eighteen semicylinders, measured at RPG.

The explanation of this effect can be reasoned from Figures 3.68 to 3.73; when the number of periods in the array is greater than unity but small then instead of being uniform, the polar response contains a prominent lobe. Increasing the number of periods decreases the width of the lobe and so initially the diffusion coefficient value falls. However, adding further periods extended the size of the array to such a degree that the polar response was no longer being measured in the far field. Consequently the response becomes more uniform for the reasons discussed in Section 3.3 and the diffusion coefficient gradually increases.

The salient implication of these results is that to evaluate the diffusion efficacy of a periodic surface from its polar response, the sample measured should comprise the maximum number of periods which permits the receiver positions to remain in the far field. A further suggestion[21] is that this number should be at least four.

In addition to determining how the diffusion efficacy of a periodic surface varies with the number of periods measured, the effect of progressively adding diffusing elements to a plane surface in a periodic manner has also been investigated, using the samples shown in Figure 2.7 (four hexagonal planes, three of which have one, seven and nineteen hemispheres attached in symmetrical periodic arrangements). The polar responses of these samples were measured in three dimensions and Figure 3.74 shows how their diffusion efficacy varies with frequency. If the plane bases on which the hemispheres are mounted had not been present then it is likely that the results would have shown the same effect as was observed in a single-plane with the semicylinders; the diffusion efficacy would have initially decreased as more periods were added, due to the lobe(s) decreasing in width. However, the hemispheres are not situated in a free field, their polar responses combine with that of the plane on which they are mounted to produce the resultant response.

Figure 3.74 in fact shows that adding a single hemisphere to the plane does not significantly change its diffusion efficacy, the reflection remains specular. This is because the amount of energy incident on the hemisphere is small in comparison to that incident on the surrounding plane. Therefore even though the hemisphere is an effective diffuser, the majority of the energy is still specularly reflected.

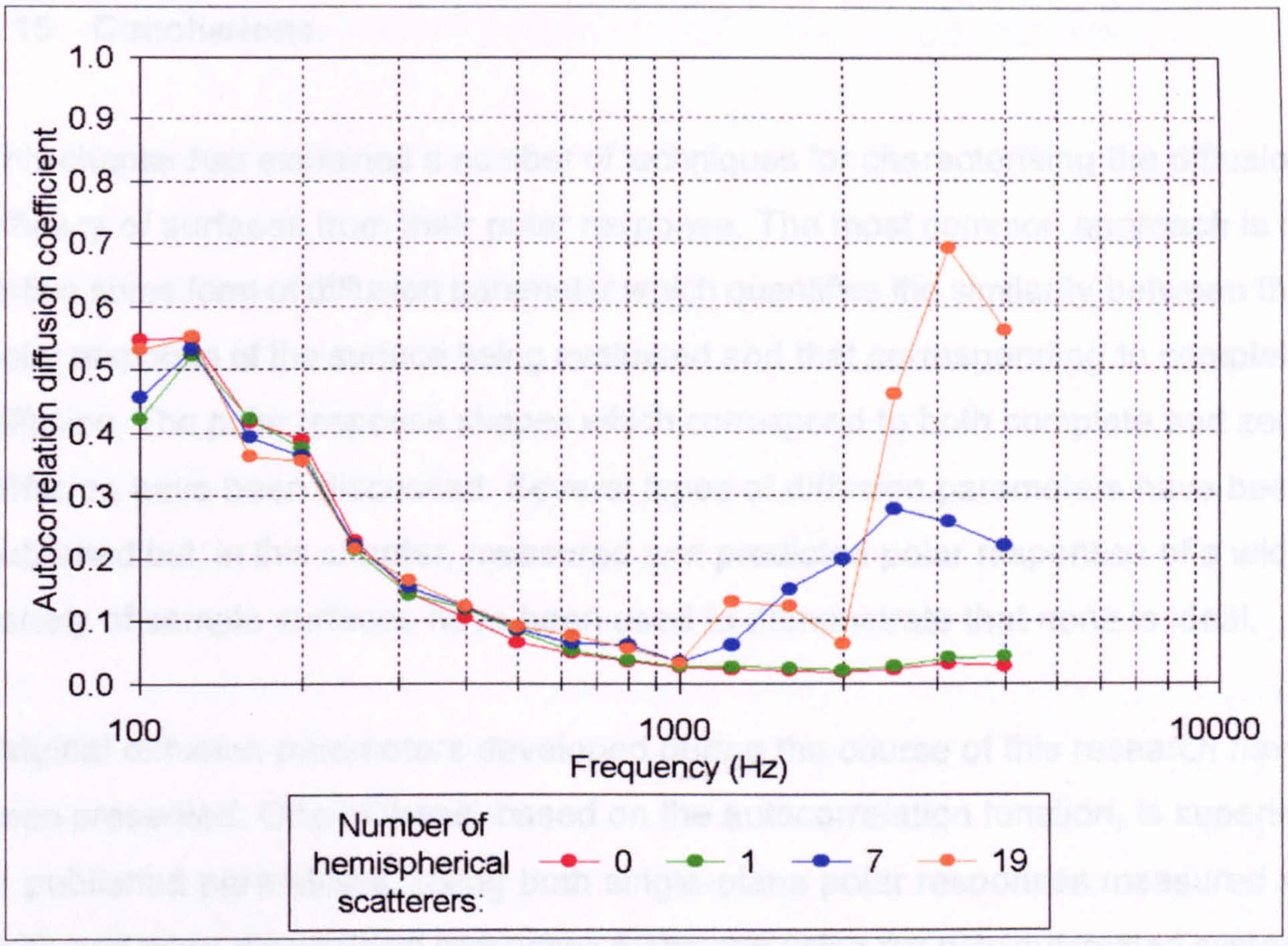

Figure 3.74: Diffusion efficacy of the periodic hemispheres samples.

As the proportion of the plane surface covered with hemispheres increases, the diffusion efficacy starts to increase at frequencies above 1kHz. When the plane base is completely covered with hemispheres, the diffusion efficacy at high frequencies - where the hemispheres are comparable in size to a wavelength - is greatly increased.

The case of the plane completely covered with hemispheres is analogous to the array of semicylinders discussed above and these results confirm that the scattering from a periodic arrangement of elements which are effective individual diffusers is less uniform than that from an isolated element. However, such an arrangement does have considerably greater diffusion efficacy than a similarly sized plane surface at frequencies where the wavelength is comparable to the dimensions of the scattering elements. For this reason, periodic surfaces are a common feature in performance spaces, often being preferred for visual aesthetic reasons to an aperiodic equivalent, even though the presence of lobes in the polar response means that their diffusion efficacy is inferior.

3.15 Conclusions.

This chapter has examined a number of techniques for characterising the diffusion efficacy of surfaces from their polar response. The most common approach is to define some form of diffusion parameter which quantifies the similarity between the polar response of the surface being evaluated and that corresponding to complete diffusion. The polar response shapes which correspond to both complete and zero diffusion have been discussed. Several types of diffusion parameters have been published but, in this chapter, measured and predicted polar responses of a wide variety of sample surfaces have been used to demonstrate that none is ideal.

Original diffusion parameters developed during the course of this research have been presented. One of these, based on the autocorrelation function, is superior to published parameters. Using both single-plane polar responses measured at RPG and three-dimensional responses measured using the new automated system at the University of Salford, it has been demonstrated that this autocorrelation diffusion coefficient ranks the diffusion efficacy of surfaces in an appropriate manner. In addition, the coefficient is simple to evaluate, is bounded between zero and unity and for practical surfaces has values which are spread between these bounds. Its only deficiency is the difficulty of interpreting the physical significance of intermediate values but a greater understanding of the relationship between values and response shapes will develop as its use becomes more widespread.

There is, however, a problem which limits the application of any polar response diffusion parameter: the shape of the response is dependent on the measurement distance unless both source and receivers are in the far field. Although in practice a response with approximately the same shape, and hence diffusion coefficient value, can often be obtained at a much shorter distance, in many applications this is still not representative of the distances at which listeners are situated. Characterising diffusion efficacy from the polar response is therefore a technique best suited to individual objects such as suspended reflectors rather than large surfaces. For large surfaces, the approach proposed by Mommertz and Vorländer[22] and discussed in the following two chapters may be more appropriate.

4. THE MOMMERTZ AND VORLANDER FREE FIELD METHOD.

4.1 Introduction.

One of the conclusions of the previous chapter is that an attractive measure for quantifying the diffusion efficacy of surfaces is the ratio of the scattered energy to the total energy reflected. This parameter is conceptually simple and the physical significance of all values is straightforward to interpret. However, its evaluation from polar responses necessitates deciding for each receiver position whether the measured energy has been scattered or specularly reflected. In practice this is not possible but attempts have been made using the specular zone concept described in Section 3.6. Although this concept enables the specular and non-specular energies to be evaluated, in many cases the resulting parameter value is inaccurate because gross assumptions in the specular zone definition cause there to be no discrimination between dispersion of the reflected energy and specular redirection. Ensuring that a significant proportion of the receiver positions are in the specular zone is a further problem because it conflicts with the requirement to measure the polar response in the far field.

Mommertz and Vorländer have proposed two new methods[22] for quantifying the scattering produced by surfaces, both of which utilise the diffusion concept referred to above - the proportion of the total reflected energy which is scattered. However, neither technique requires use of the specular zone concept or indeed the measurement of polar responses. One of the methods involves free field measurements and will be discussed in this chapter. The second method requires reverberant conditions and will be examined in Chapter 5.

4.2 Theory, measurement technique and parameter evaluation.

The crux of the Mommertz and Vorländer free field method is to determine the portions of the scattered energy which are variant and invariant to movement of the sample. In common with quantifying diffusion from three-dimensional polar responses, this involves making numerous impulse response measurements.

However, instead of the sample remaining fixed relative to the source whilst the reflected energy is measured, as described in Section 2.9, the source and receiver are positioned diametrically opposite one another at equal angles of elevation, θ, above the sample, as illustrated in Figure 4.1. The sample is then rotated stepwise in angular increments of azimuth $\Delta\varphi$ and a single measurement made at each step.

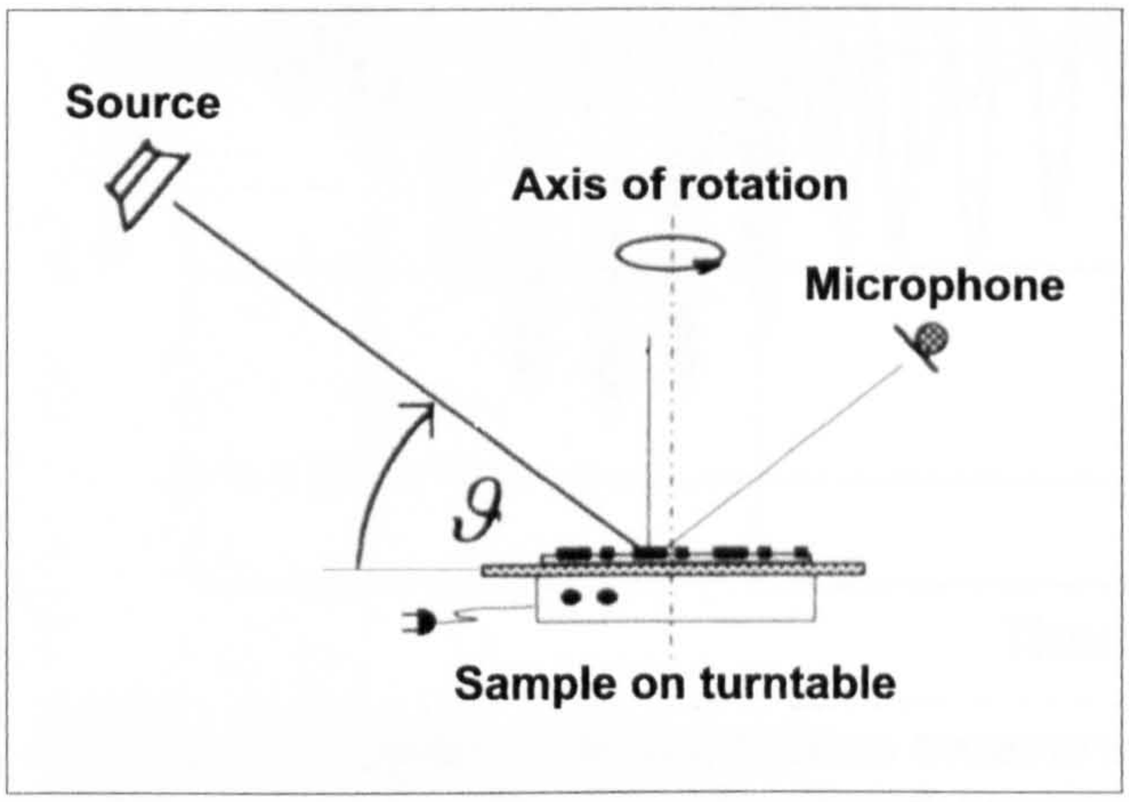

Figure 4.1: Measurement geometry.
(Mommertz and Vorländer[59])

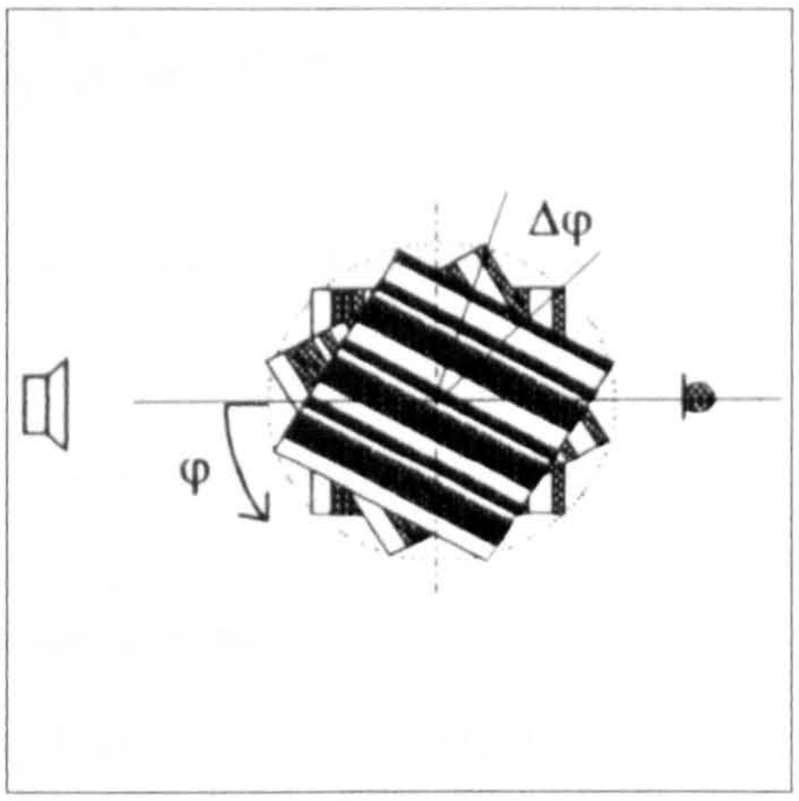

Plan view.
(Mommertz and Vorländer[59])

The principle of quantifying diffusion efficacy from these measurements is best illustrated in the time domain. Figure 4.2 on the following page shows three reflected band-limited pulses measured by Mommertz and Vorländer using the geometry shown in Figure 4.1. Each of these reflected pulses was obtained for a different orientation of the test sample, a plane surface covered with randomly spaced parallel rectangular battens, similar to that shown in Figure 2.12b. It can be seen that the initial portions of each reflection are strongly correlated whereas the later portions are not in phase; the shape of these 'tails' depends on the orientation of the sample. The reason for this is that the first part of each reflection propagates from source to receiver, via the sample, by the shortest possible path and thus corresponds to the specularly reflected energy. This specular component of the reflection is independent of the sample orientation, hence the observed correlation. In contrast, the tails contain energy which is delayed with respect to the specular because, instead of propagating by the shortest path, it has been scattered. This scattered energy, and hence the shapes of the tails, is dependent on the sample orientation because it is determined by the surface irregularities. In fact, the scattered components of each reflection are assumed to be incoherent.

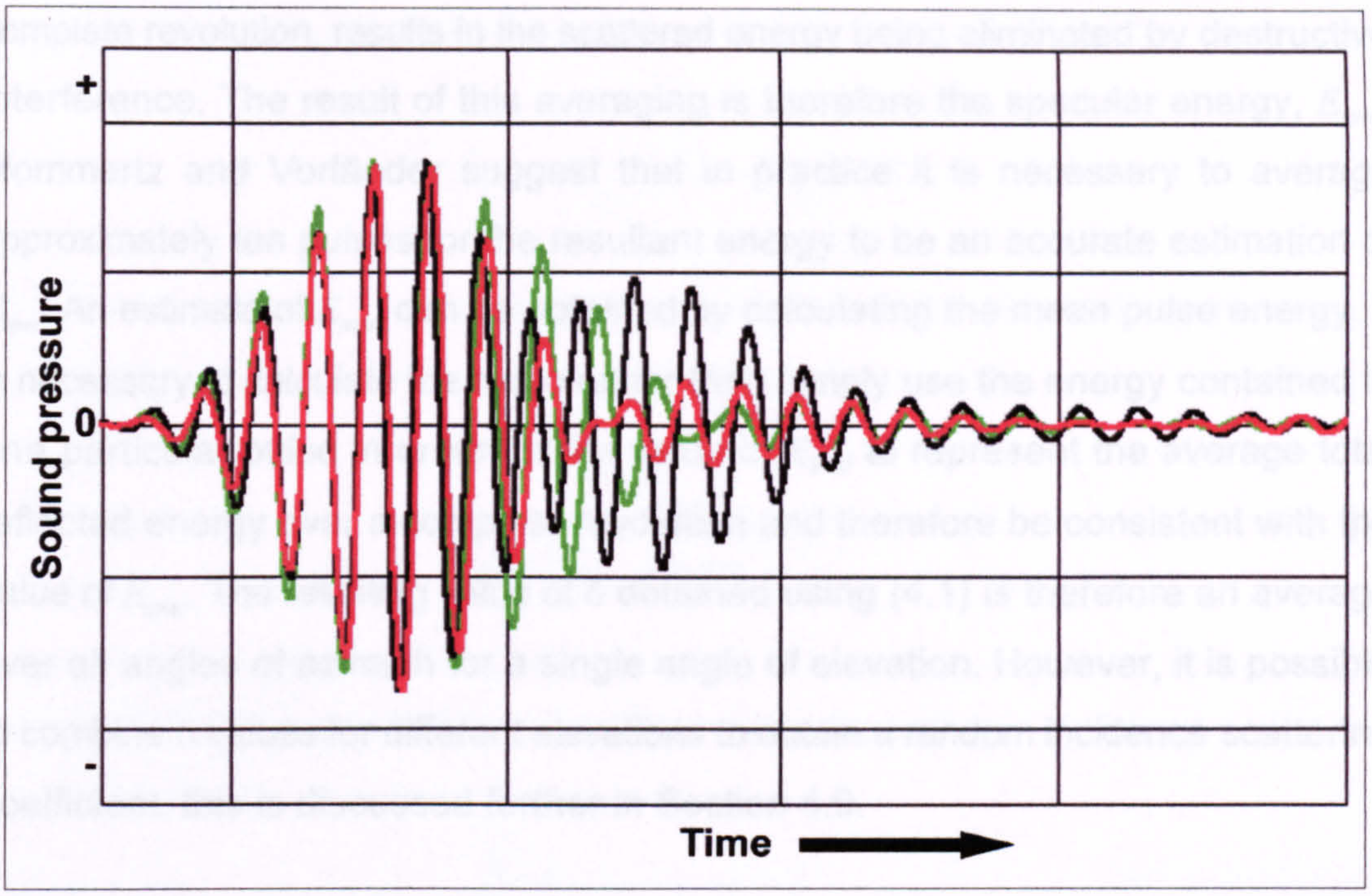

Figure 4.2: Typical reflected pulses measured by Mommertz and Vorländer for different orientations of a structured sample. (Mommertz and Vorländer[59])

The scattering coefficient, δ, of the test sample has the same definition as (3.28) - the ratio of the energy scattered to the total reflected energy. However, since the total reflected energy must be the sum of the specularly reflected and scattered energies, the formulation for δ most often used by Mommertz and Vorländer is:

$$\delta = 1 - \frac{E_{spec}}{E_{total}} \tag{4.1}$$

where:

E_{spec} = Specularly reflected energy

E_{total} = Total reflected energy

Determination of δ is therefore straightforward once E_{spec} and E_{total} have been evaluated. The most noteworthy aspect of this method for quantifying diffusion is the technique by which E_{spec} is extracted from the reflected pulses. Since the reflection tails are incoherent, phase-locked averaging of a sufficient number of pulses obtained for different sample orientations, spaced equally in angle over a

complete revolution, results in the scattered energy being eliminated by destructive interference. The result of this averaging is therefore the specular energy, E_{spec}. Mommertz and Vorländer suggest that in practice it is necessary to average approximately ten pulses for the resultant energy to be an accurate estimation of E_{spec}. An estimate of E_{total} can be obtained by calculating the mean pulse energy. It is necessary to calculate the mean rather than simply use the energy contained in one particular pulse in order for the value of E_{total} to represent the average total reflected energy over a complete revolution and therefore be consistent with the value of E_{spec}. The resulting value of δ obtained using (4.1) is therefore an average over all angles of azimuth for a single angle of elevation. However, it is possible to combine δ values for different elevations to obtain a random incidence scattering coefficient, this is discussed further in Section 4.9.

Although the principle of quantifying scattering by this method is most easily demonstrated in the time domain, Mommertz and Vorländer employed a broadband MLS stimulus instead of band-limited pulses for their practical measurements. As a consequence of measuring the impulse responses broadband, evaluation of δ is more easily performed in the frequency as opposed to the time domain. The first step is to isolate the reflection from the direct sound in each impulse response by applying a window which has unity gain in the appropriate section and zero elsewhere. A Fourier transform is then applied to obtain the complex reflected pressure as a function of frequency as opposed to time, $P(f)$, for each orientation of the sample. To calculate the scattering coefficient, δ, the complex reflected pressures will suffice but it is possible as a by-product to additionally calculate both the regular absorption coefficient, α, of the sample and a parameter termed by Mommertz and Vorländer the 'specular absorption coefficient' if the complex reflection coefficients are used instead[22].

Each of the reflected pressures can be considered to comprise a specular and a diffuse component. For any angle of elevation, θ, it is assumed that the specular component is independent of the azimuthal angle of incidence, φ, and that the diffuse components are incoherent.

$\underline{P}(f)$ can therefore be expressed as:

$$\underline{P}_i(f) = \underline{P}_{spec}(f) + \underline{P}_{diff,i}(f) \tag{4.2}$$

Since the specular component is invariant, it can be obtained by coherently averaging a large number, n, of complex pressures:

$$\underline{P}_{spec}(f) \approx \frac{1}{n}\sum_{i=1}^{n}\underline{P}_i(f) \tag{4.3}$$

The number of averages must be sufficient to ensure that:

$$\sum_{i=1}^{n}\underline{P}_{diff,i}(f) \longrightarrow 0 \tag{4.4}$$

The specularly reflected energy, E_{spec}, is therefore given by:

$$E_{spec} = \left|\underline{P}_{spec}(f)\right|^2 = \frac{1}{n^2}\left|\sum_{i=1}^{n}\underline{P}_i(f)\right|^2 \tag{4.5}$$

As stated previously, the mean total reflected energy can be calculated by averaging the quadratic summation of the complex pressures measured at each increment of azimuth:

$$E_{total} = \frac{1}{n}\sum_{i=1}^{n}\left|\underline{P}_i(f)\right|^2 \tag{4.6}$$

Substituting (4.5) and (4.6) into (4.1) gives an expression for δ as a function of frequency explicitly in terms of the complex pressures:

$$\delta = 1 - \frac{\left|\sum_{i=1}^{n} \underline{P}_i(f)\right|^2}{n\sum_{i=1}^{n}\left|\underline{P}_i(f)\right|^2} \qquad (4.7)$$

This formulation for δ bears a strong resemblance to (3.34), the expression for the autocorrelation diffusion coefficient d_{auto}. The relationship between these two parameters is explored in Section 4.10.

4.3 The limiting values of δ and their physical interpretation.

For a circular plane sample, the complex reflected pressure is independent of its orientation. From (4.2), the value of $\underline{P}_{diff,i}(f)$ must therefore be constant. If the sample is large and edge diffraction is ignored, $\underline{P}_{diff,i}(f)$ can be assumed to be zero. $\underline{P}_i(f)$ is thus equal to the constant value $\underline{P}_{spec}(f)$ and the expression for δ reduces to:

$$\delta = 1 - \frac{\left|n\,\underline{P}_{spec}(f)\right|^2}{n.n\left|\underline{P}_{spec}(f)\right|^2} = 0 \qquad (4.8)$$

Even if $\underline{P}_{diff,i}(f)$ is non-zero, so long as it is invariant $\underline{P}_i(f)$ will be constant and δ will be zero. Any sample which when rotated has no effect on the complex reflected pressure will therefore be rated as having a diffusion efficacy of zero.

For surfaces which scatter the reflected energy to any degree, some destructive interference will occur when the complex reflected pressures are summed. Therefore E_{spec} will be less than E_{total} and the value of δ will lie between zero and unity. With this measure of scattering, complete diffusion is the case where the destructive interference is total and the resultant therefore zero. From (4.7) it can be seen that if the sum of the pressures is zero then the value of δ is unity. δ is thus bounded between zero and unity and so satisfies at least one of the criteria for the ideal diffusion coefficient.

4.4 **Measurements**.

In order to appraise this method further, new practical measurements were made to investigate how δ quantifies the diffusion efficacy of different surfaces. No results of measurements made using this method, other than those performed by Mommertz and Vorländer, have been published. The surfaces measured were the random battens shown in Figure 2.12b, the cone shown in Figure 2.8 and the sample shown in Figure 4.3.

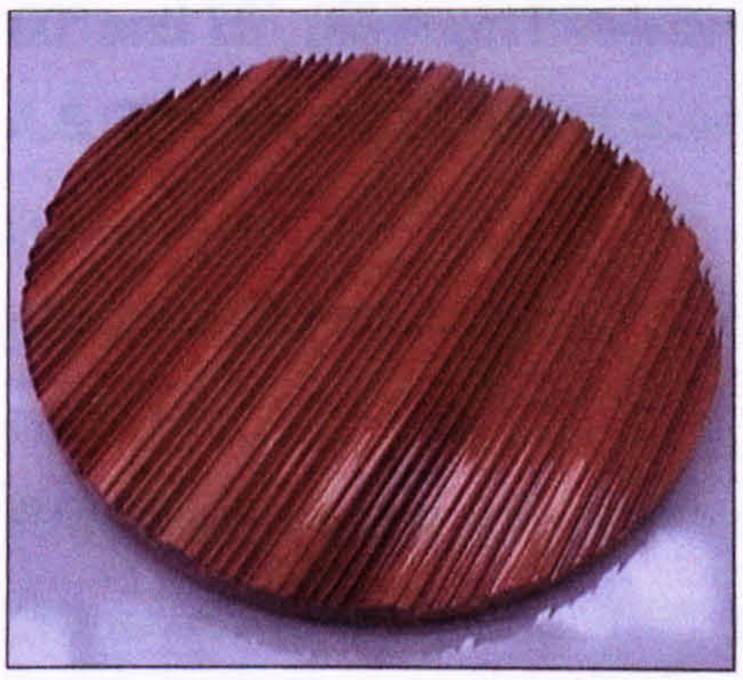

Figure 4.3: FlutterFree®.

This third sample comprises several periods of an RPG product called FlutterFree® which is a Schroeder type diffuser designed to treat high frequency flutter echoes. The reason for measuring this sample was that it had previously been measured by Mommertz and Vorländer, albeit using their reverberation chamber method discussed in Chapter 5.

4.4.1 **Modifications to the method described by Mommertz and Vorländer**.

As outlined in Section 4.2 and illustrated in Figure 4.1, the measurement procedure involves mounting the source and receiver at equal angles of elevation and rotating the sample. An equivalent procedure is to keep the sample stationary and rotate both the source and receiver around it because the relative motion is identical. This would normally be the more complex option but since the existing automated system for measuring three-dimensional polar responses described in Section 2.9 can be programmed to simply rotate a receiver at any elevation around a stationary sample, it was easier to modify this apparatus to additionally carry the source than construct something new for rotating the samples. Apart from some changes to the control software, all that was required was to mount the source on the semicircular microphone frame at the desired angle of elevation. However, the loudspeaker used for polar response measurements was too bulky to be attached to the lattice frame so it was necessary to find an alternative. A sensible choice

was the much smaller and lighter loudspeaker successfully used by RPG in their polar response measurements, a Bose Acoustimass® cube.

Mommertz and Vorländer suggest that about ten sample orientations are sufficient for the incoherent scattered energy to be removed by destructive interference, corresponding to an azimuthal angular resolution of 36°. However, in order to verify this, it was necessary to use a finer resolution for these new measurements so that the effect of reducing it could be observed. For this reason an azimuthal resolution of 5° was chosen. Measurements were made at elevation angles of 15°, 30°, 45°, 60° and 75°, although this was not necessary for the cone, as discussed in Section 4.5. The elevation of the source was changed manually.

4.4.2 Data processing.

Processing the measured impulse responses to obtain the complex scattered pressures as functions of frequency, $P(f)$, involved using a similar technique to that described in Section 2.9.12 for extracting the polar response. Before applying a unity gain window to isolate the portion of the response corresponding to the reflected sound, a reference measurement made with no sample present was subtracted to remove the direct sound. This step was more important here than when extracting polar responses because whereas in that case there was usually a gap between the direct and reflected sound, in this case, particularly for small elevations, the path difference is small and they consequently become superposed. An associated problem is that, as a result of the directivity of the source, for large elevations the direct sound has less magnitude than the reflected. The consequence of this was that the measurement and reference responses could not always be aligned simply on their maximum values, it was necessary to examine only the portion of the response corresponding to the direct sound and this varies with the angle of elevation. After isolating the reflected sound by windowing, a Fourier transform was applied to generate the complex reflected pressure as a function of frequency. Once this process had been performed for all orientations to obtain the values of $P(f)$, the energies E_{spec} and E_{total} were evaluated in third-octave bands and then used to calculate δ.

4.4.3 **Results.**

Figures 4.4 and 4.5 show how δ varies with frequency and angle of elevation, θ, for the random battens and FlutterFree samples respectively. In order to be consistent with the polar response measurements and allow results to be compared, it was assumed that both samples are 1:5 scale models, therefore the frequency axes have been scaled accordingly. For both samples, the scattering coefficient is negligible below about 200Hz, except for the angle of incidence closest to grazing. The reason for this is that at low frequencies the irregularities on both samples are small in comparison to a wavelength so the incident energy will be reflected in essentially the same manner as if the samples were plane, i.e. specularly. When the angle of elevation is small, it may be that a significant proportion of the incident energy is scattered or otherwise non-specularly reflected from the side of the sample, resulting in disproportionately large values of δ. Although these δ values are not representative of the scattering efficacy of the sample faces, it is very difficult when measuring diffusion from finite surfaces to separate the scattering caused by irregularities in the surface structure from edge diffraction, although a method has recently been proposed by Mommertz[60].

As the frequency increases, the value of δ initially increases also, the rate of increase decreasing with increasing angle of elevation. For the random battens, the increase is steady up to a frequency of about 1kHz, except for 15° elevation, where δ increases much more sharply and the peak is a little lower in frequency. It is unsurprising that the scattering is a maximum at frequencies around 1kHz because it is in this range that the cross-sectional dimensions of the battens are approximately a quarter of a wavelength. For the FlutterFree sample, the increase in δ is more rapid, the maximum value greater and the peak slightly higher in frequency, again except for when the elevation is 15°. These results are also unsurprising because the irregularities in the surface of this sample are smaller than the battens and FlutterFree units are designed to be effective diffusers. Above the peak frequency, the value of δ decreases but not as far as its low frequency value. Above 2kHz the scattering behaviour of both samples is somewhat erratic, δ continuing to decrease for some angles of elevation but increasing at others.

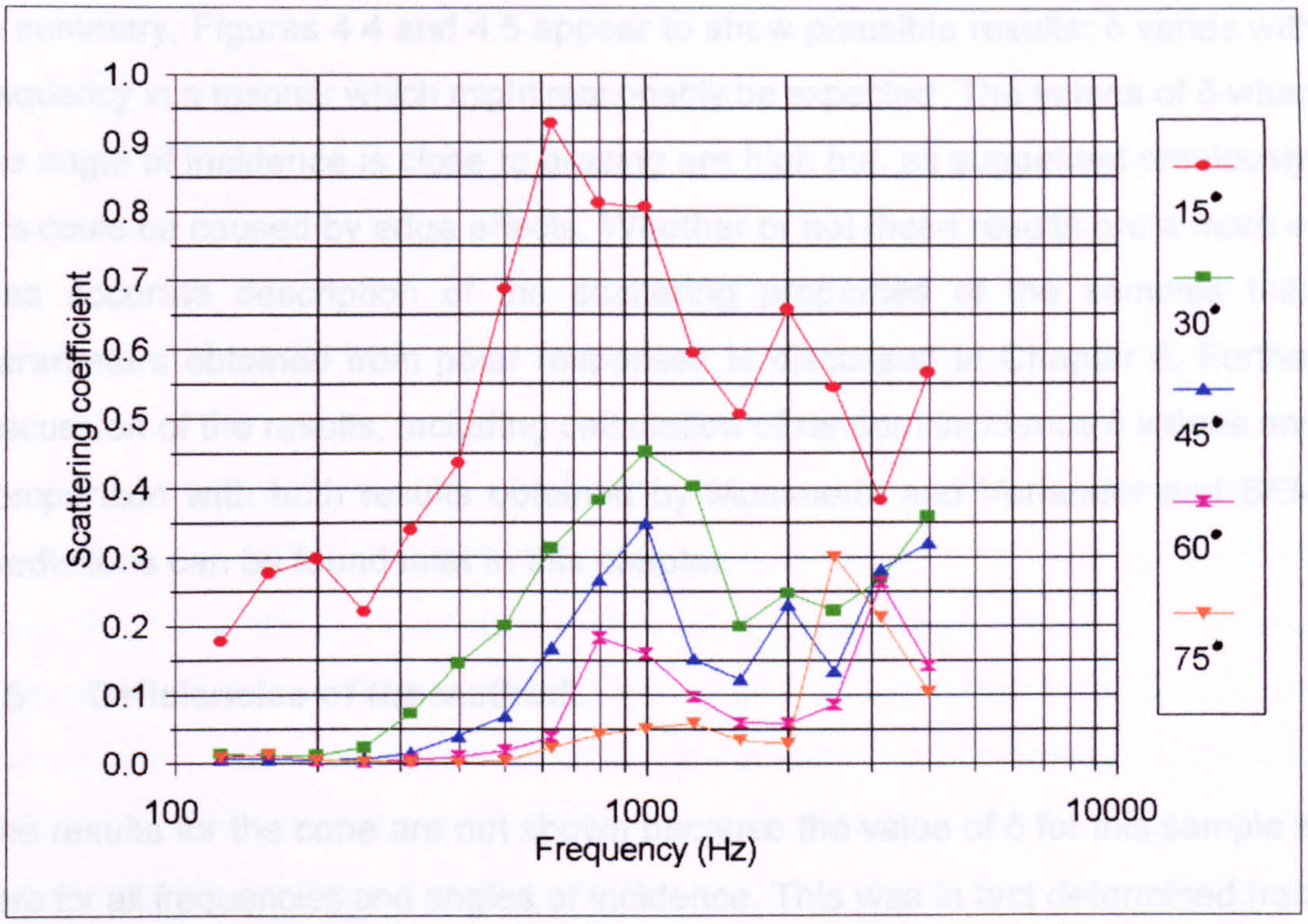

Figure 4.4: Variation of δ with frequency and elevation angle for the random battens.

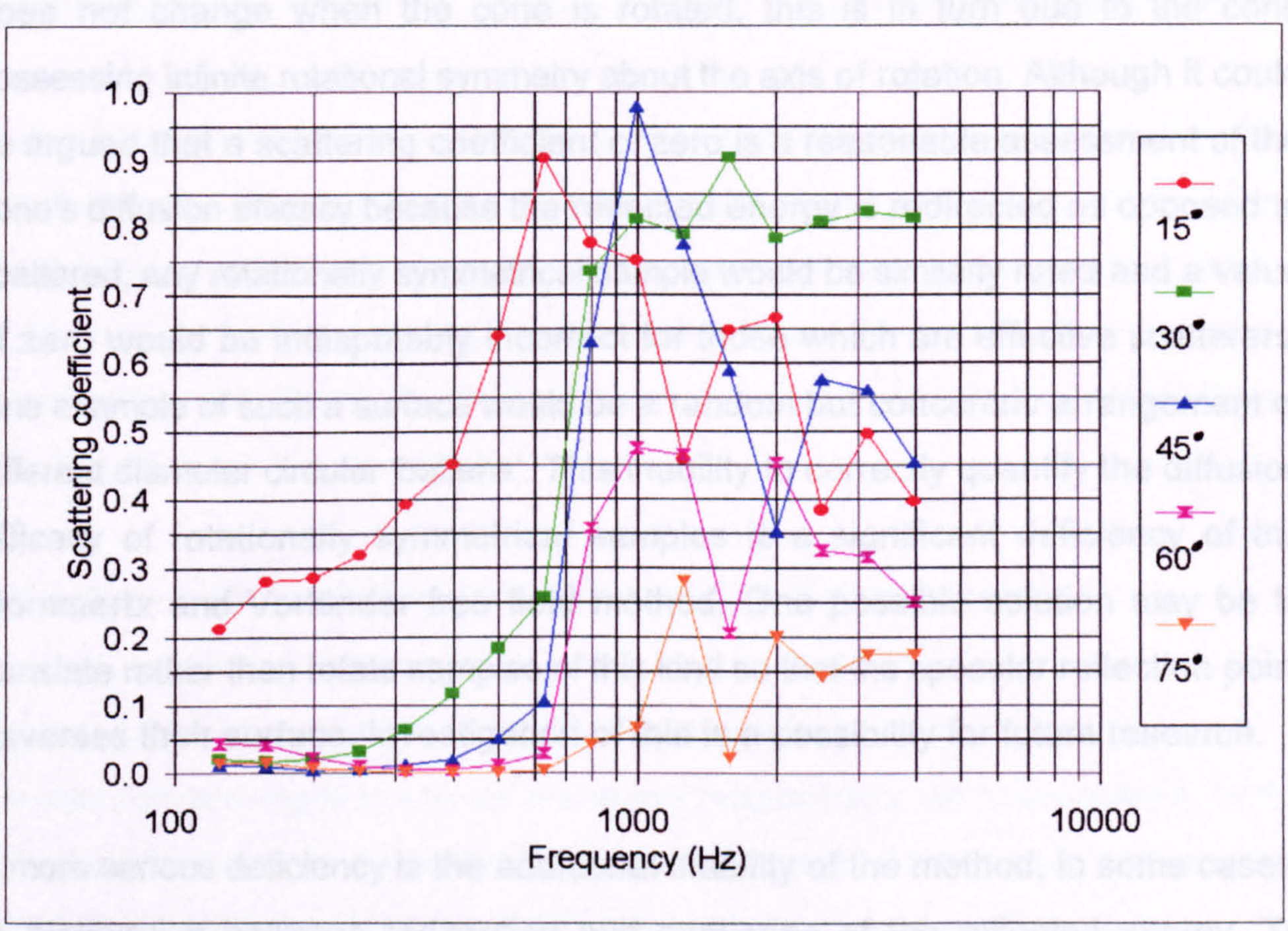

Figure 4.5: Variation of δ with frequency and elevation angle for the FlutterFree.

In summary, Figures 4.4 and 4.5 appear to show plausible results; δ varies with frequency in a manner which might reasonably be expected. The values of δ when the angle of incidence is close to grazing are high but, as suggested previously, this could be caused by edge effects. Whether or not these results are a more or less accurate description of the scattering properties of the samples than parameters obtained from polar responses is discussed in Chapter 8. Further discussion of the results, including calculation of random incidence δ values and comparison with both results obtained by Mommertz and Vorländer and BEM predictions can be found later in this chapter.

4.5 Deficiencies of the method.

The results for the cone are not shown because the value of δ for this sample is zero for all frequencies and angles of incidence. This was in fact determined from the theory but a measurement using one angle of elevation was performed for confirmation. The reason that δ is zero is that the measured impulse response does not change when the cone is rotated, this is in turn due to the cone possessing infinite rotational symmetry about the axis of rotation. Although it could be argued that a scattering coefficient of zero is a reasonable assessment of the cone's diffusion efficacy because the reflected energy is redirected as opposed to scattered, any rotationally symmetrical sample would be similarly rated and a value of zero would be indisputably incorrect for those which are effective scatterers. One example of such a surface would be a random but concentric arrangement of different diameter circular 'battens'. This inability to correctly quantify the diffusion efficacy of rotationally symmetrical samples is a significant deficiency of the Mommertz and Vorländer free field method. One possible solution may be to translate rather than rotate samples of this kind so that the specular reflection point traverses their surface. Investigation of this is a possibility for future research.

A more serious deficiency is the additional inability of the method, in some cases, to distinguish between redirection and scattering of the reflected energy. To illustrate this, consider the sample shown in Figure 4.6: a cylinder cut obliquely so that the top face is not parallel to the base. Since the top face is plane, a reflection

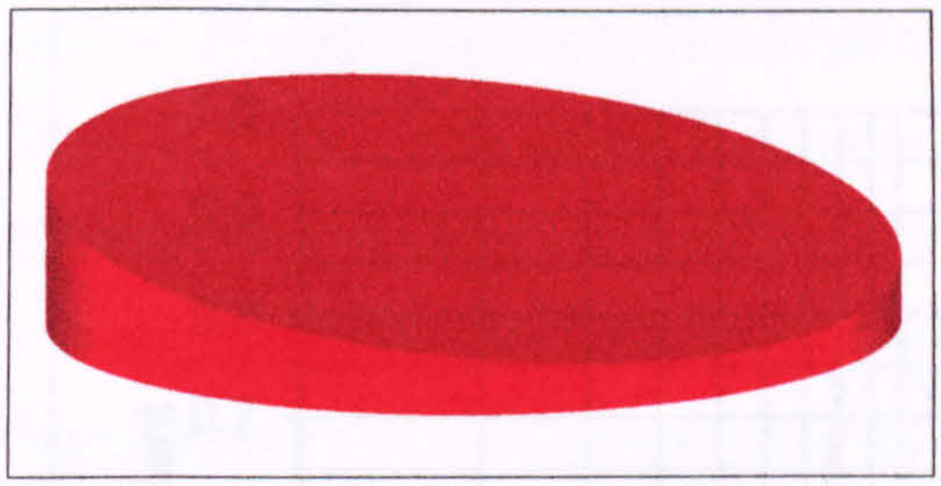

Figure 4.6: Redirecting surface.

from it will be specular, whatever the angle of incidence. However, if the diffusion efficacy of this sample were evaluated using the Mommertz and Vorländer free field method, the pressure measured would vary as it was rotated and the value of δ would consequently be non-zero. This would indicate that the sample is a more effective diffuser than a plane surface when, in fact, it is simply a plane surface tilted at an angle. In contrast, polar response diffusion measures will rate a plane surface as a poor diffuser regardless of its orientation, so long as the source and receiver distances are appropriate. For a universal diffusion parameter, this deficiency would be substantial but Mommertz and Vorländer make no reference to it. Although it is not stated explicitly, the reason for this is likely to be that their methods are designed to quantify scattering from extensive rough surfaces, i.e. those which are covered with numerous irregularities that are small in size compared to the dimensions of the surface, rather than simple geometric shapes constructed from plane surfaces.

Further important deficiencies of this method are that samples must be circular if the value of δ is not to be increased by edge effects and that surfaces which scatter the reflected energy more effectively in one plane than another are too highly rated. These are also deficiencies of the Mommertz and Vorländer reverberation chamber method discussed in Chapter 5 and are examined in more detail in Sections 5.4.5 and 5.5.

4.6 Dependence of δ on the azimuthal angular resolution.

Figures 4.7 and 4.8 show, for two of the measurements discussed in Section 4.4, the effect of reducing the number of impulse responses used to evaluate δ. In the first example, it can be seen that the calculated value of δ becomes erroneous at higher frequencies when the number of responses summed falls to eight, although lesser errors are evident at some frequencies when eighteen responses are used. However at frequencies below 800Hz, δ does not change significantly until the

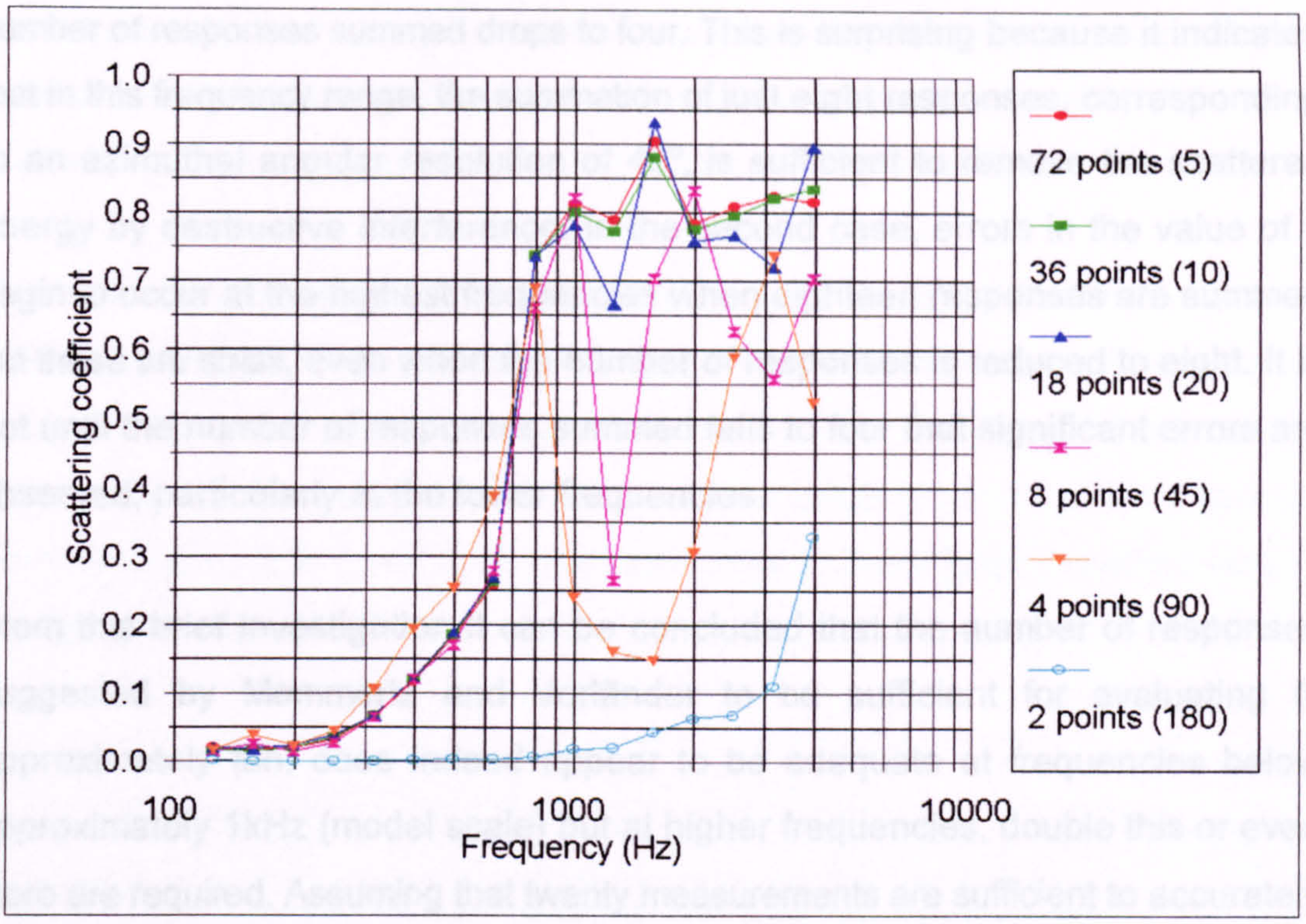

Figure 4.7: Effect of the azimuthal angular resolution on the δ value for the FlutterFree. 30° elevation.

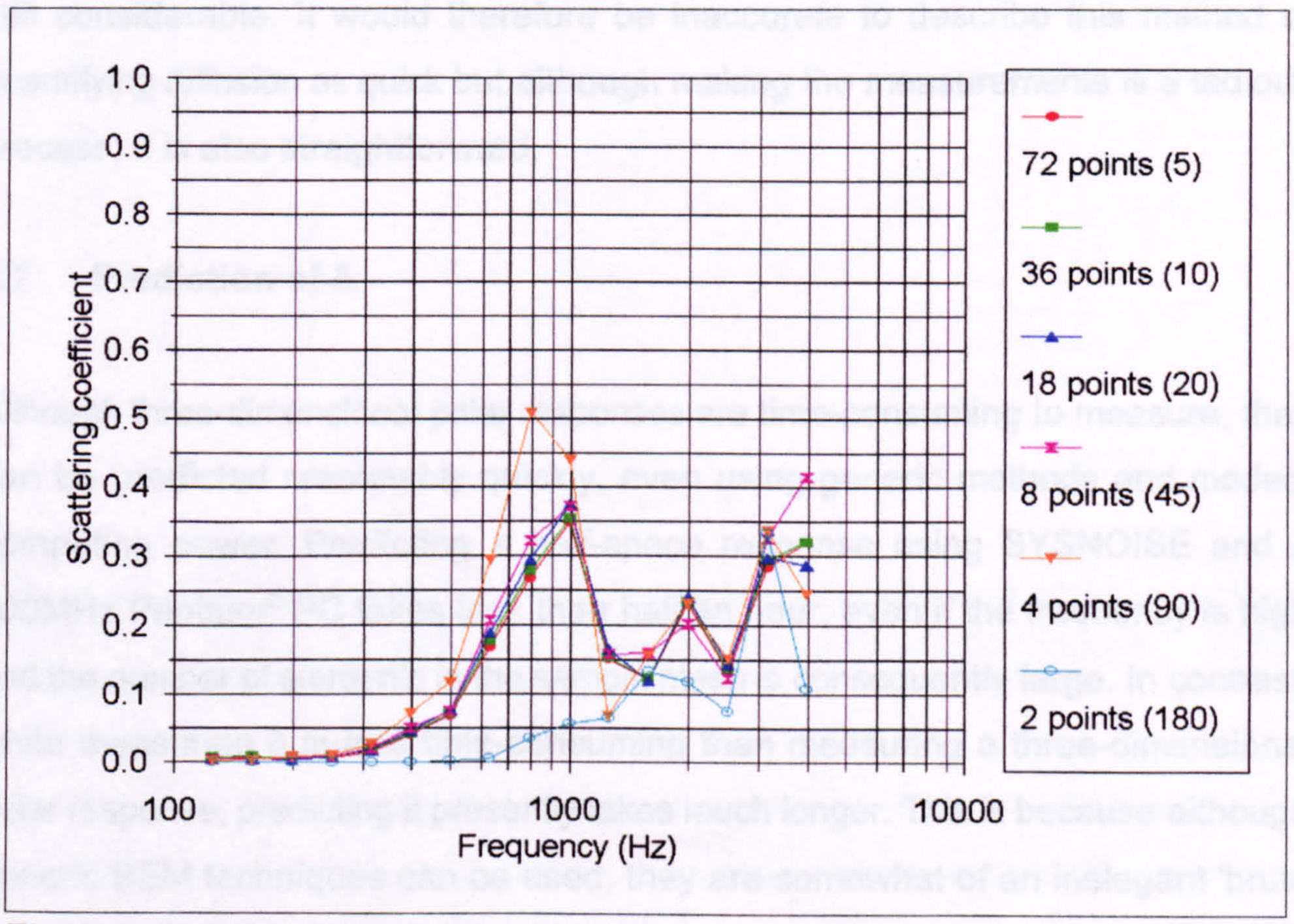

Figure 4.8: Effect of the azimuthal angular resolution on the δ value for the random battens. 45° elevation.

number of responses summed drops to four. This is surprising because it indicates that in this frequency range, the summation of just eight responses, corresponding to an azimuthal angular resolution of 45°, is sufficient to remove the scattered energy by destructive interference. In the second case, errors in the value of δ begin to occur at the highest frequencies when eighteen responses are summed but these are small, even when the number of responses is reduced to eight. It is not until the number of responses summed falls to four that significant errors are observed, particularly at the lower frequencies.

From this brief investigation it can be concluded that the number of responses suggested by Mommertz and Vorländer to be sufficient for evaluating δ, approximately ten, does indeed appear to be adequate at frequencies below approximately 1kHz (model scale) but at higher frequencies, double this or even more are required. Assuming that twenty measurements are sufficient to accurately evaluate δ at all frequencies of interest, the number required to obtain a random incidence value, although significantly less than for polar response measures, is still considerable. It would therefore be inaccurate to describe this method of quantifying diffusion as quick but although making the measurements is a tedious process, it is also straightforward.

4.7 Prediction of δ.

Although three-dimensional polar responses are time-consuming to measure, they can be predicted reasonably quickly, even using generic methods and modest computing power. Predicting a half-space response using SYSNOISE and a 200MHz Pentium® PC takes less than half an hour, even if the frequency is high and the number of elements in the sample mesh is consequently large. In contrast, while measuring δ is less time-consuming than measuring a three-dimensional polar response, predicting it presently takes much longer. This is because although generic BEM techniques can be used, they are somewhat of an inelegant 'brute force' approach because since the source moves relative to the sample between each measurement, the surface pressures must be recalculated each time. Consequently, predicting δ for just a single angle of elevation takes several hours,

even if the azimuthal angular resolution is coarse. It is likely that a more efficient prediction method than the brute force approach employed here could be devised, particularly if a more approximate technique than BEM is utilised.

Since predicting values of δ is so time-consuming, it was not possible to compare measured and predicted results thoroughly. However, a number of individual δ values for the random battens sample were predicted to enable spot comparisons to be made with the measurements discussed in Section 4.4; these are shown in black on Figure 4.9. Predictions were also used to investigate the effect on δ of changing the source and receiver distances; this is examined in Section 4.8.

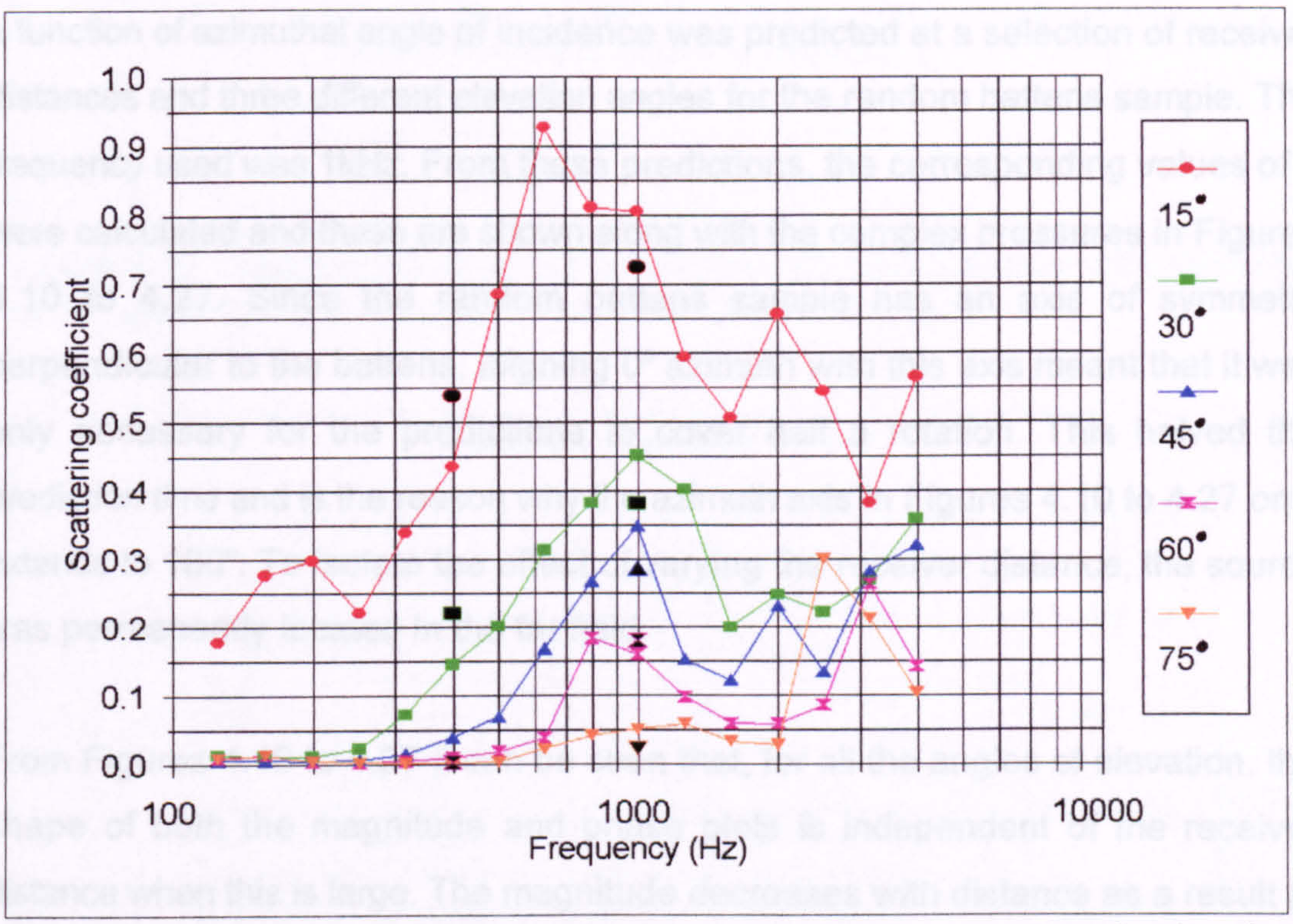

Figure 4.9: Comparison of δ values for the random battens measured using the Mommertz and Vorländer free field method with single-frequency BEM predictions (in black).

From Figure 4.9 it can be seen that the spot comparisons at 400Hz and 1kHz between predicted and measured δ values are close, especially when it is considered that the predictions are at single frequencies whereas the measurements are in third-octave bands. It is therefore reasonable to assume that the measurements are also accurate at the other frequencies.

4.8 Dependence of δ on the source and receiver distances.

In previous chapters it has been discussed at some length that the polar response of a sample is only independent of the source and receiver distances when both the source and all the receiver positions are in the far field. It has also been discussed that the primary consequence of this is that full-scale polar response measurements are generally impractical due to the large size of anechoic test facility required. It was expected that this method for quantifying diffusion proposed by Mommertz and Vorländer would be similarly afflicted because it also involves sampling the scattered pressure in free field conditions, even though only one sample is taken for each source position. To verify this, the complex pressure as a function of azimuthal angle of incidence was predicted at a selection of receiver distances and three different elevation angles for the random battens sample. The frequency used was 1kHz. From these predictions, the corresponding values of δ were calculated and these are shown along with the complex pressures in Figures 4.10 to 4.27. Since the random battens sample has an axis of symmetry perpendicular to the battens, aligning 0° azimuth with this axis meant that it was only necessary for the predictions to cover half a rotation. This halved the prediction time and is the reason why the azimuth axis in Figures 4.10 to 4.27 only extends to 180°. To isolate the effect of varying the receiver distance, the source was permanently located in the far field.

From Figures 4.10 to 4.27 it can be seen that, for all the angles of elevation, the shape of both the magnitude and phase plots is independent of the receiver distance when this is large. The magnitude decreases with distance as a result of spherical spreading and the absolute values of phase change, causing in some cases the phase plot to be wrapped around the y-axis, but the manner in which both quantities vary with the sample orientation remains unchanged. The value of δ is therefore independent of the receiver distance in the far field. However as the receiver distance decreases so that it is no longer large in comparison to the (full scale) sample dimensions, the shape of both the magnitude and phase plots changes. In addition to changing in envelope, they also become less smooth and, particularly in the case of the magnitude, exhibit many local maxima and minima.

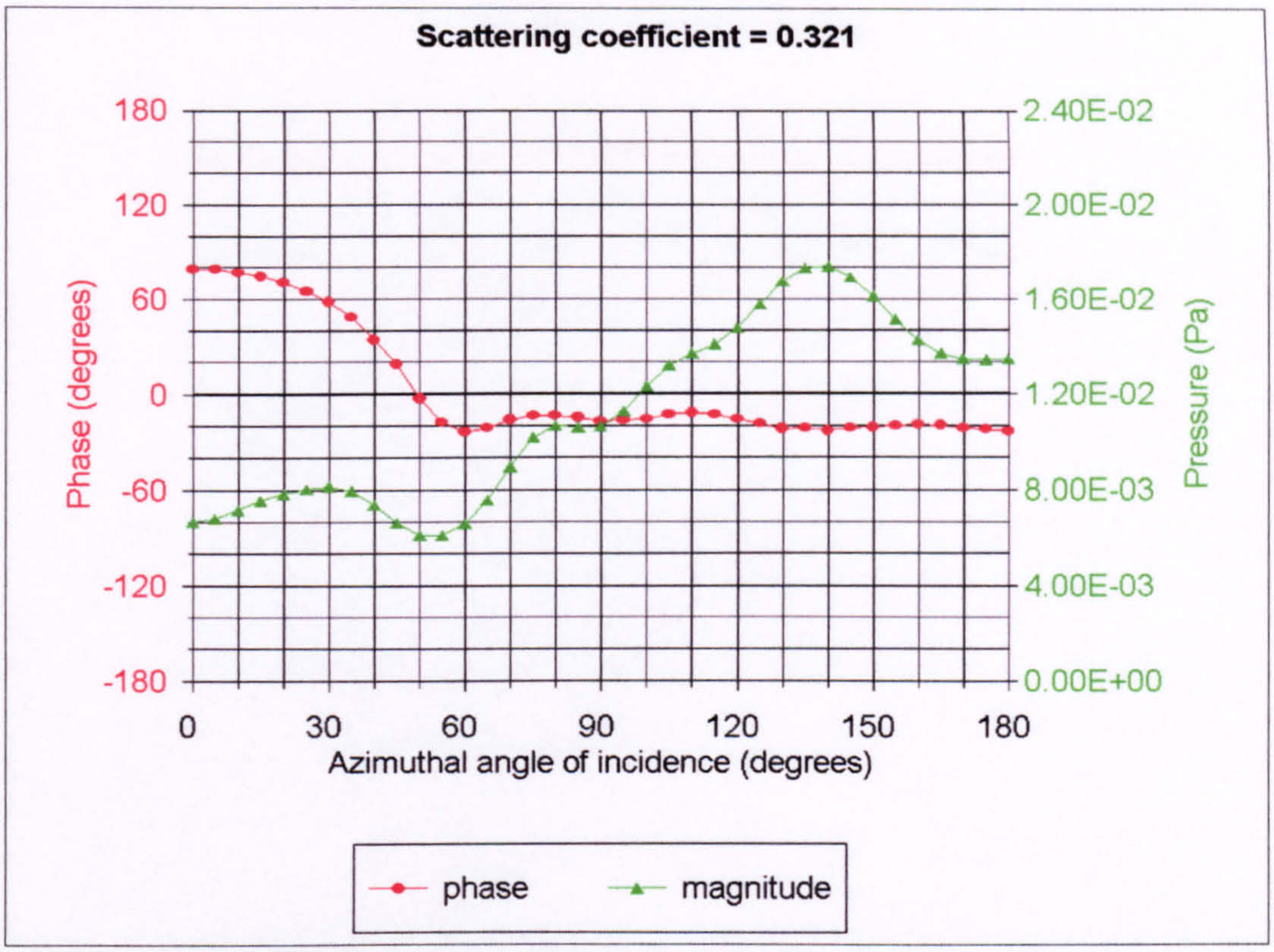

Figure 4.10: Predicted variation of the complex reflected pressure with azimuth at **75°** elevation and **1.4m** (full scale) from the random battens.

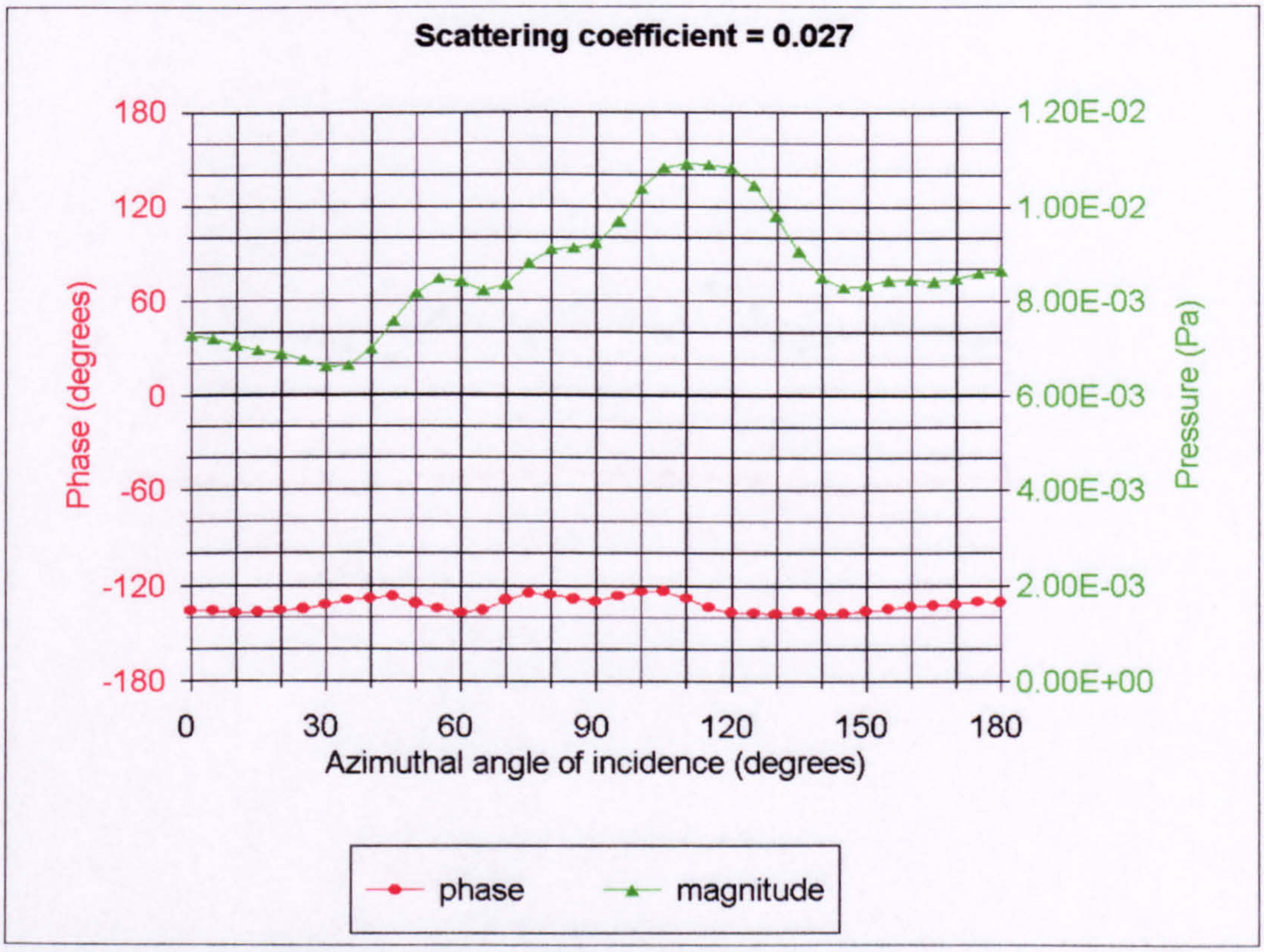

Figure 4.11: Predicted variation of the complex reflected pressure with azimuth at **75°** elevation and **7.35m** (full scale) from the random battens.

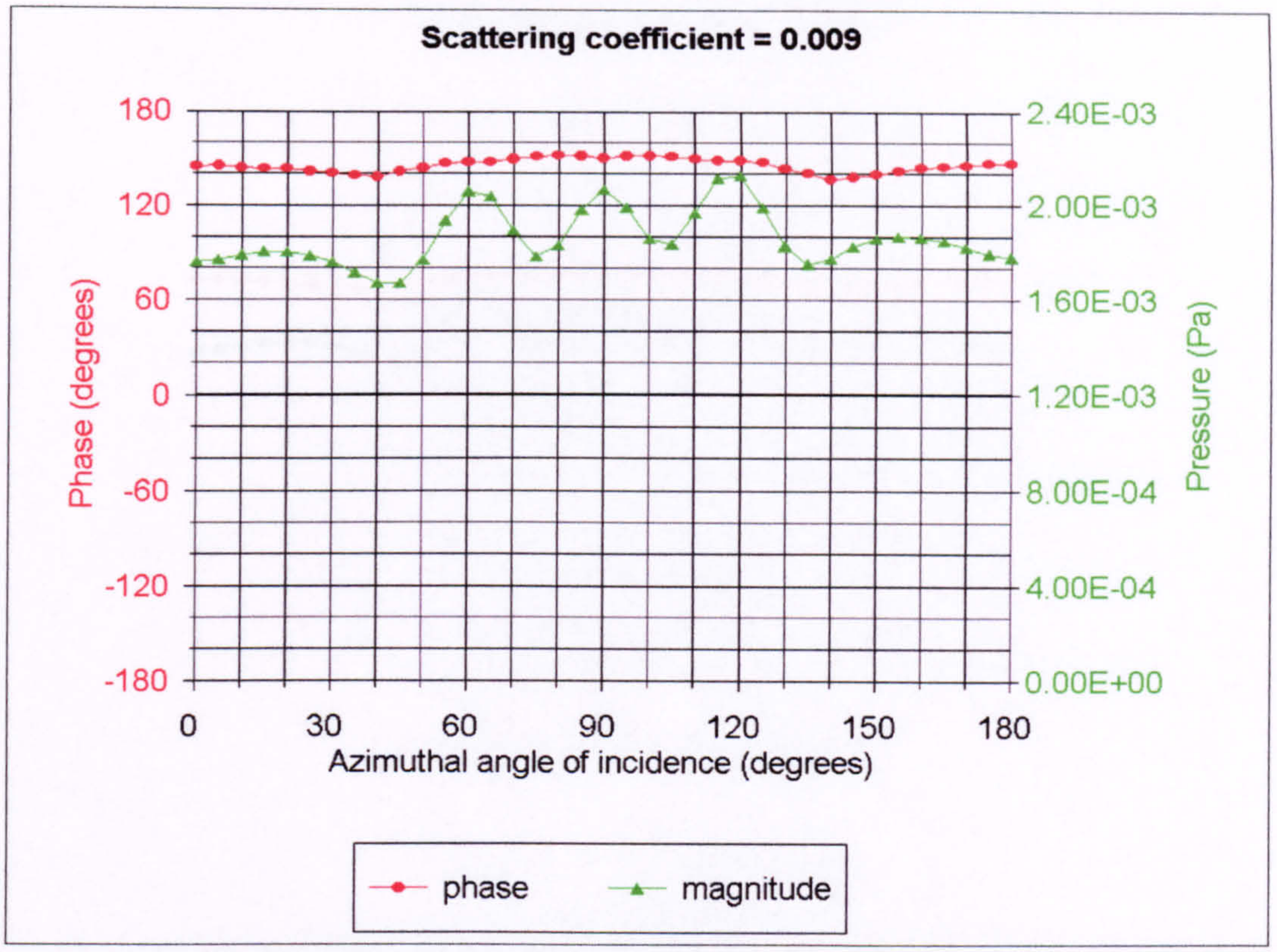

Figure 4.12: Predicted variation of the complex reflected pressure with azimuth at **75°** elevation and **50m** (full scale) from the random battens.

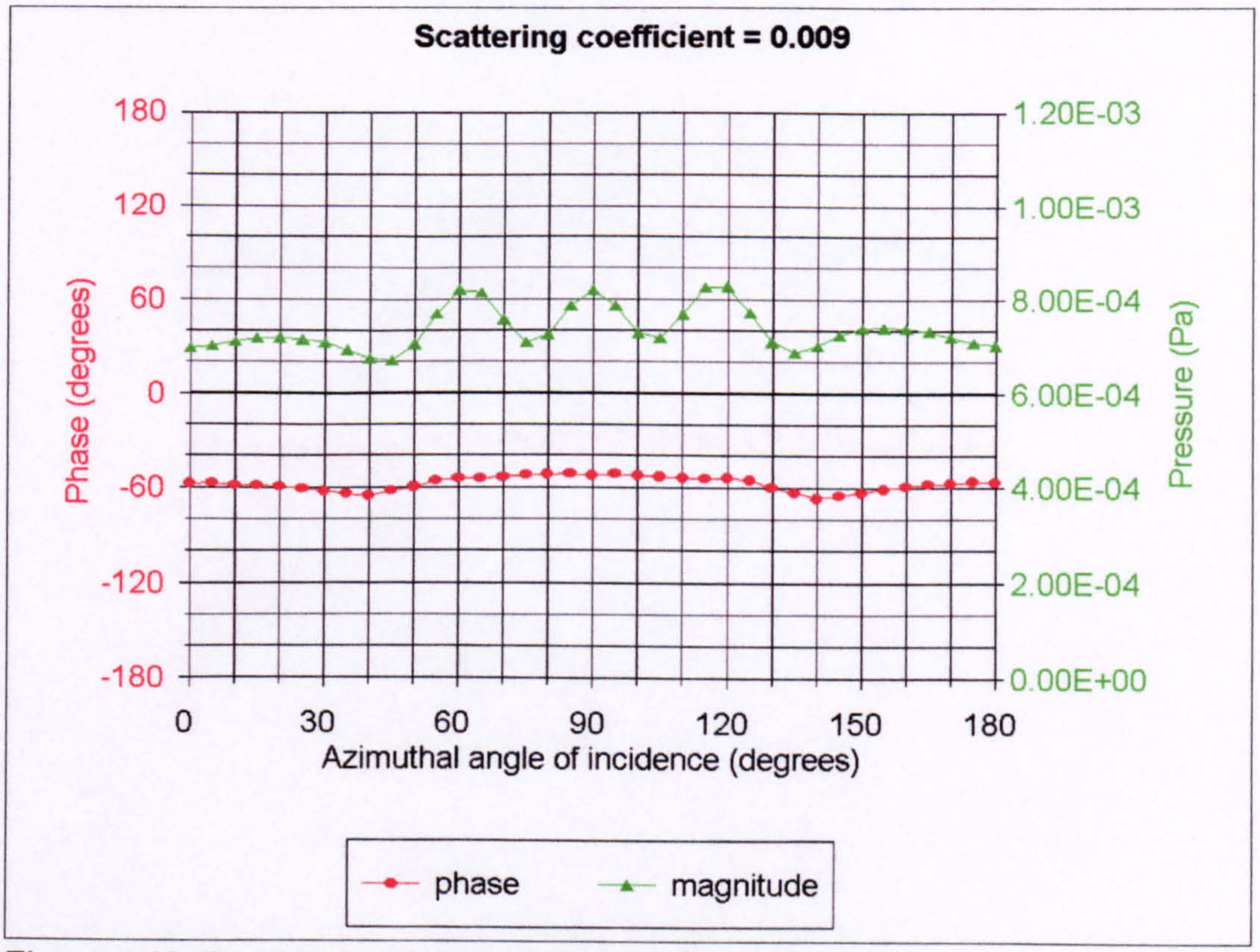

Figure 4.13: Predicted variation of the complex reflected pressure with azimuth at **75°** elevation and **125m** (full scale) from the random battens.

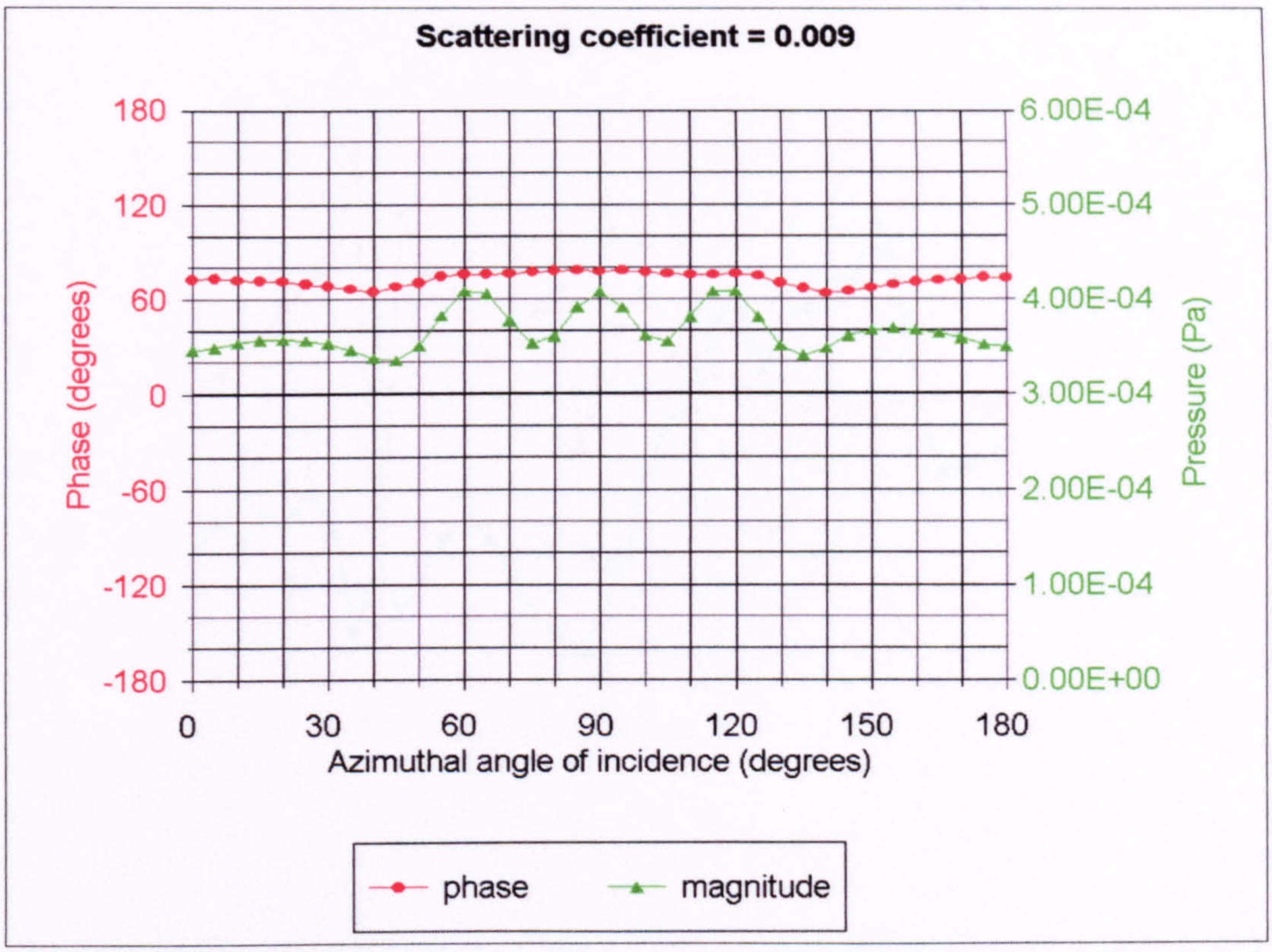

Figure 4.14: Predicted variation of the complex reflected pressure with azimuth at **75°** elevation and **250m** (full scale) from the random battens.

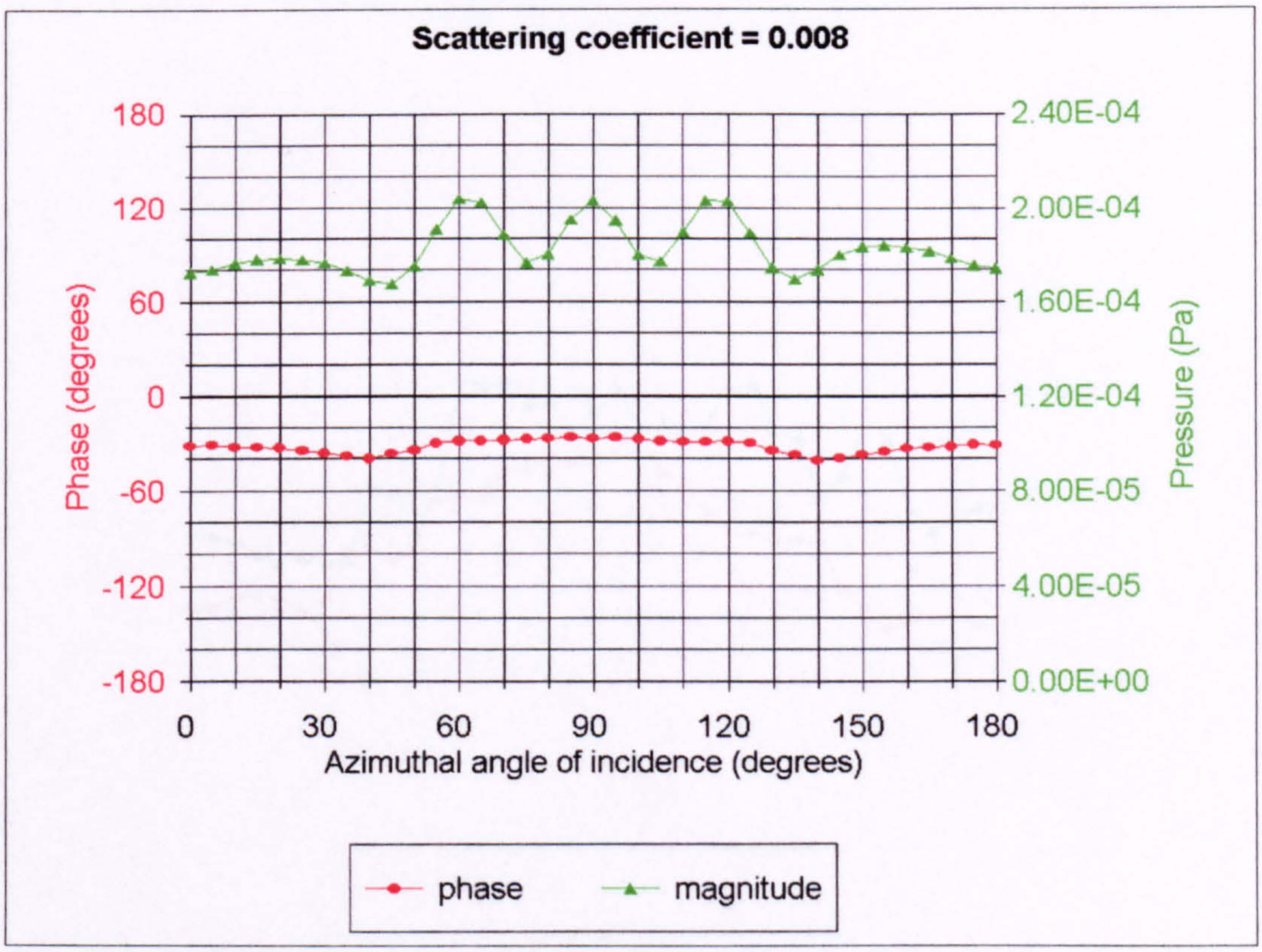

Figure 4.15: Predicted variation of the complex reflected pressure with azimuth at **75°** elevation and **500m** (full scale) from the random battens.

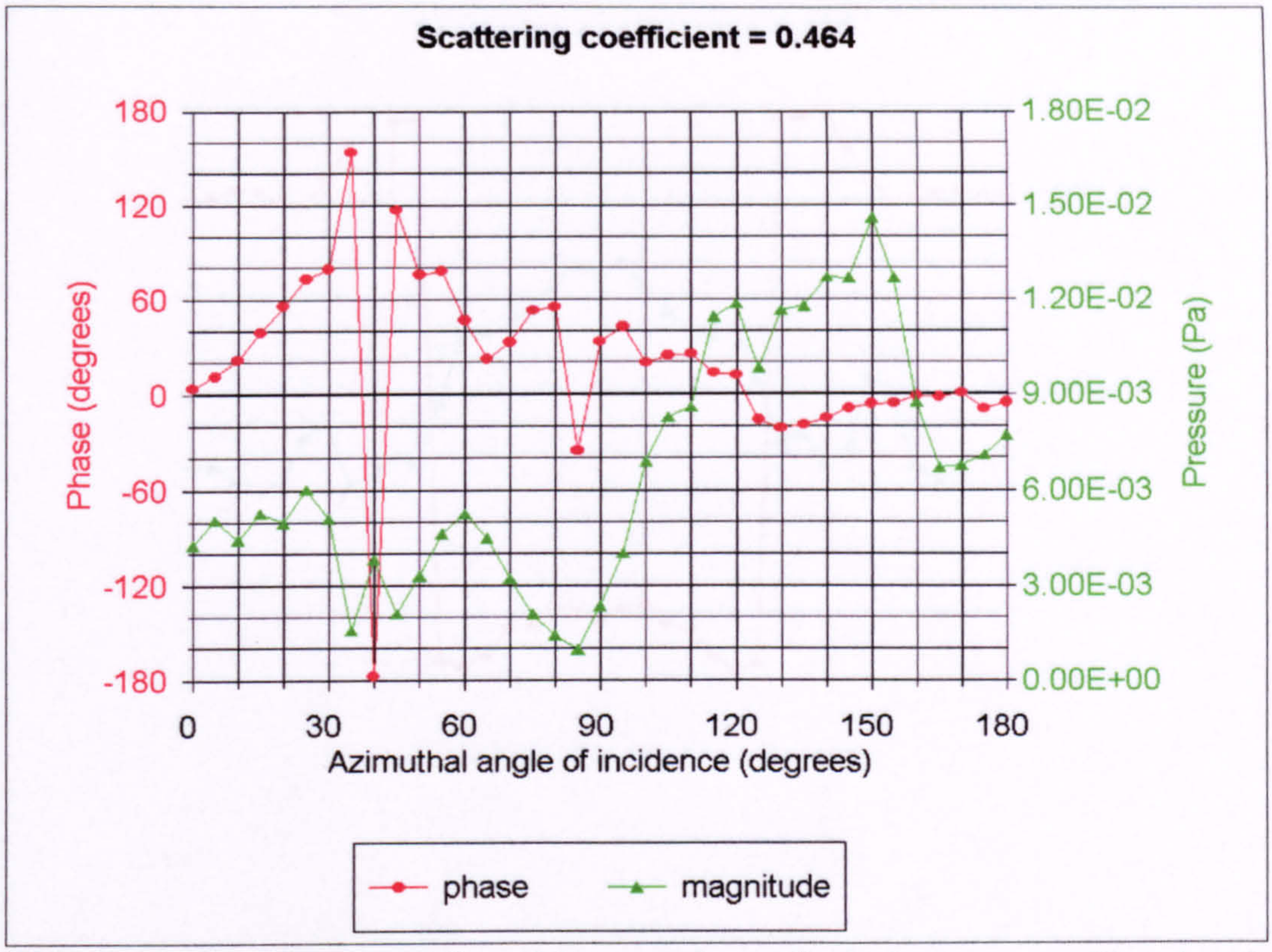

Figure 4.16: Predicted variation of the complex reflected pressure with azimuth at **45°** elevation and **1.4m** (full scale) from the random battens.

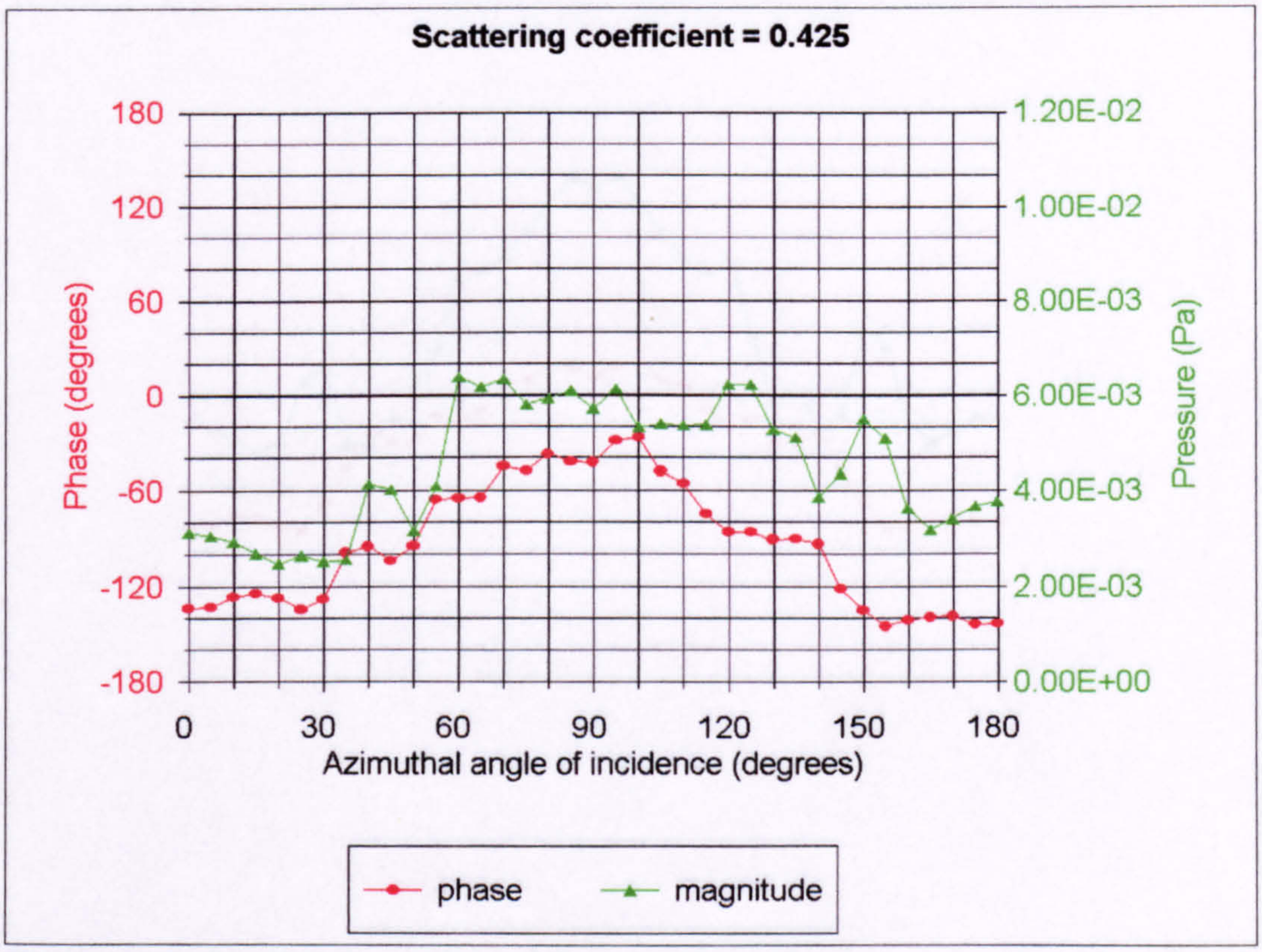

Figure 4.17: Predicted variation of the complex reflected pressure with azimuth at **45°** elevation and **7.35m** (full scale) from the random battens.

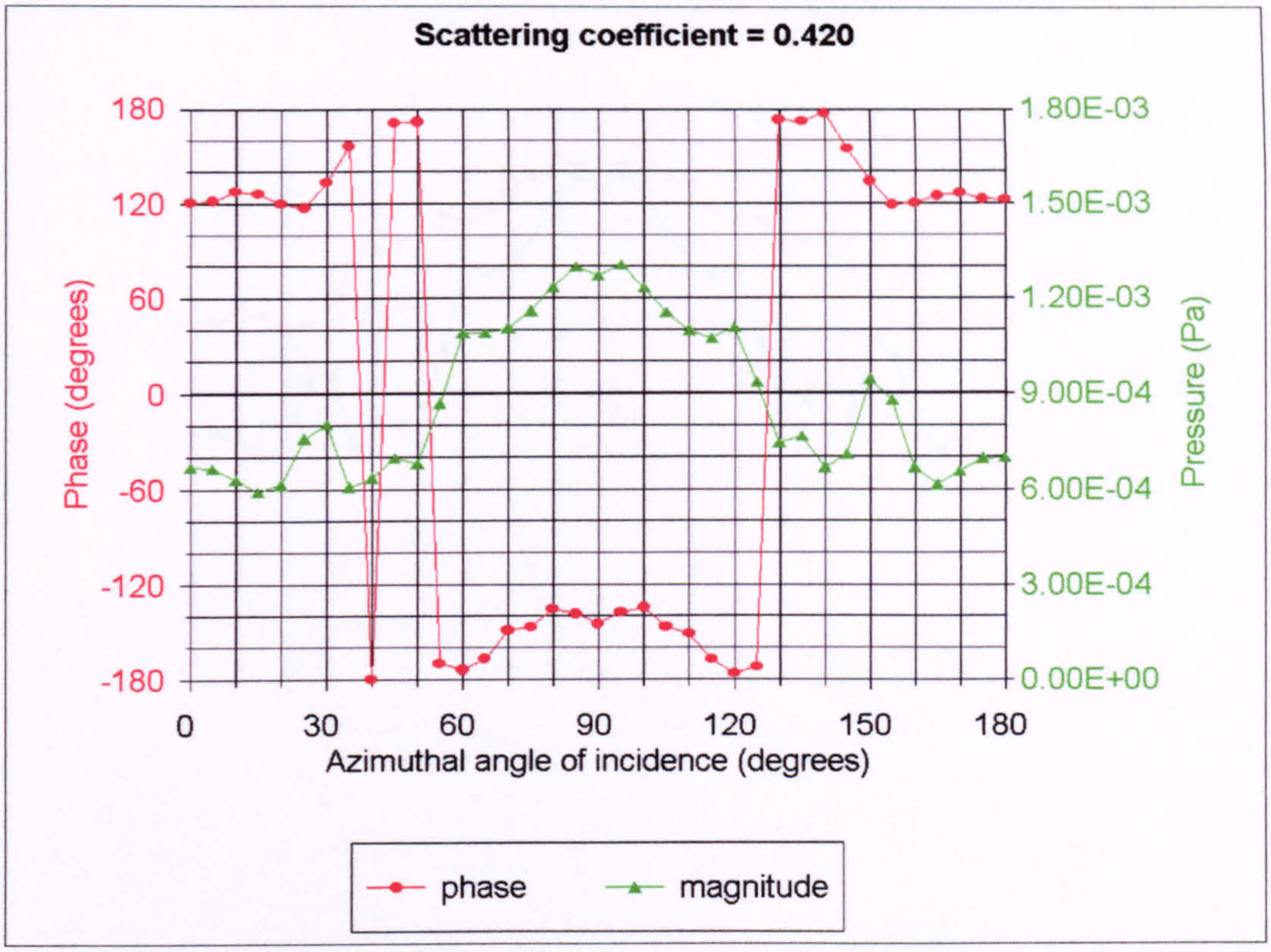

Figure 4.18: Predicted variation of the complex reflected pressure with azimuth at **45°** elevation and **50m** (full scale) from the random battens.

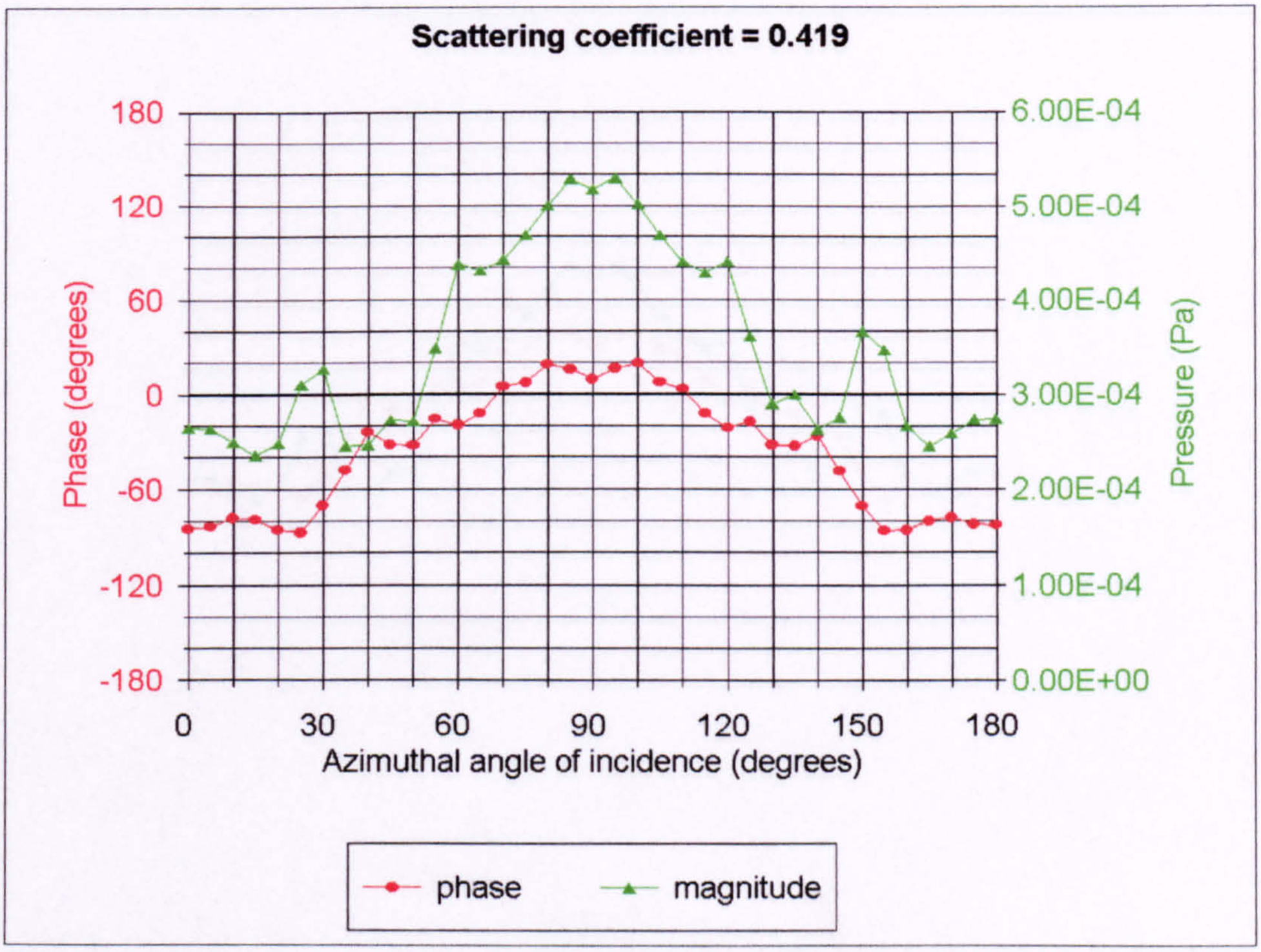

Figure 4.19: Predicted variation of the complex reflected pressure with azimuth at **45°** elevation and **125m** (full scale) from the random battens.

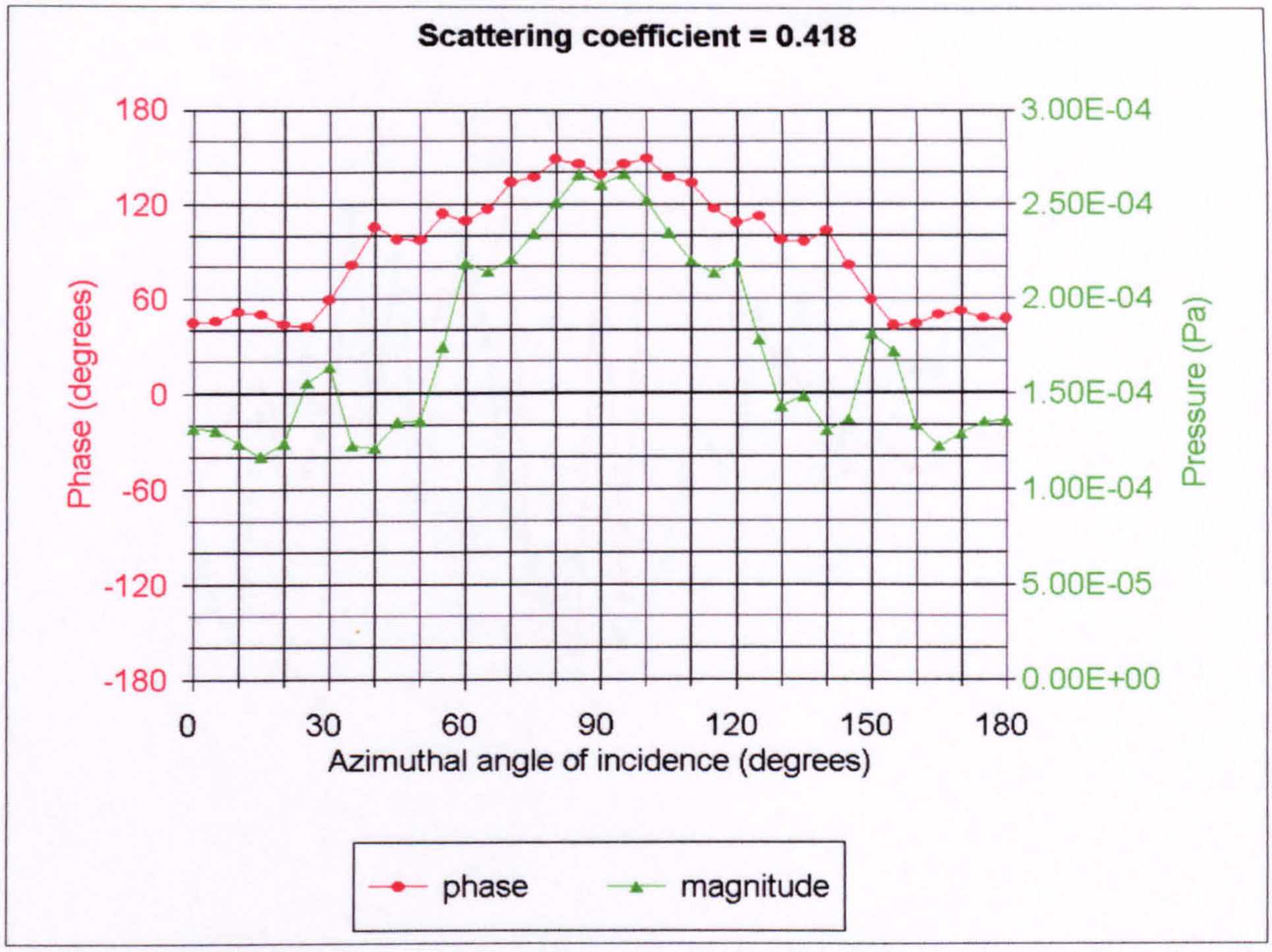

Figure 4.20: Predicted variation of the complex reflected pressure with azimuth at **45°** elevation and **250m** (full scale) from the random battens.

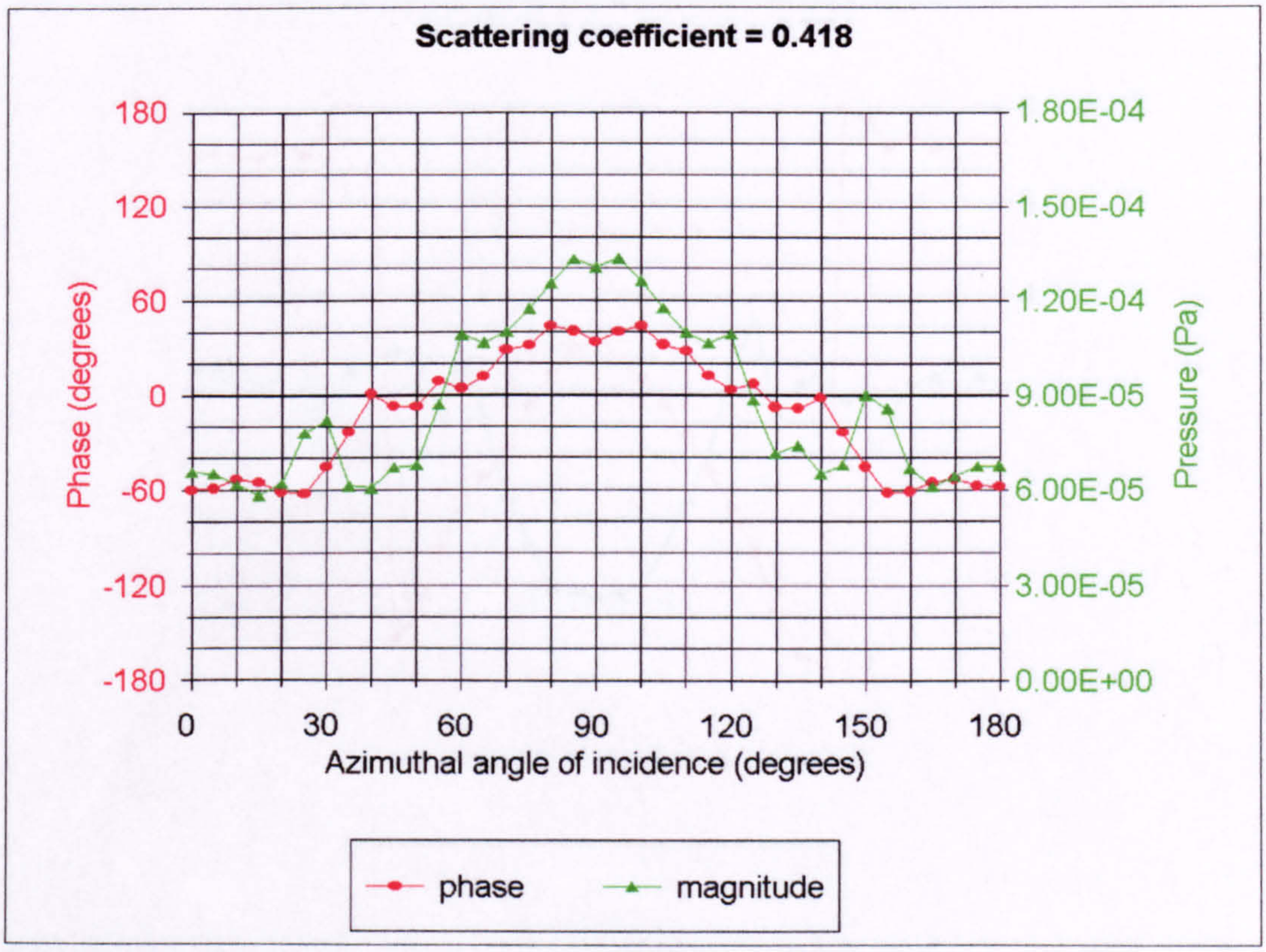

Figure 4.21: Predicted variation of the complex reflected pressure with azimuth at **45°** elevation and **500m** (full scale) from the random battens.

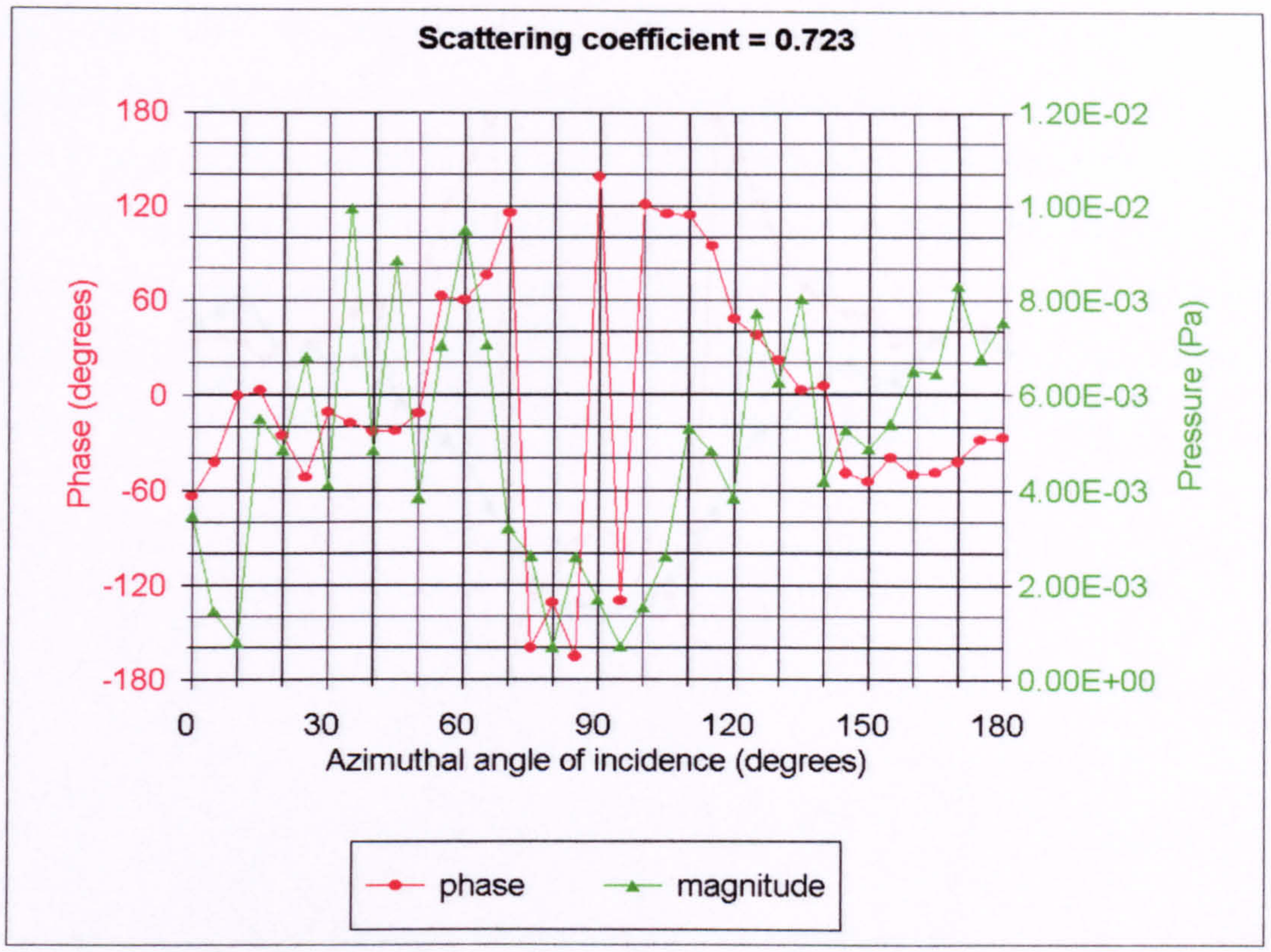

Figure 4.22: Predicted variation of the complex reflected pressure with azimuth at **15°** elevation and **1.4m** (full scale) from the random battens.

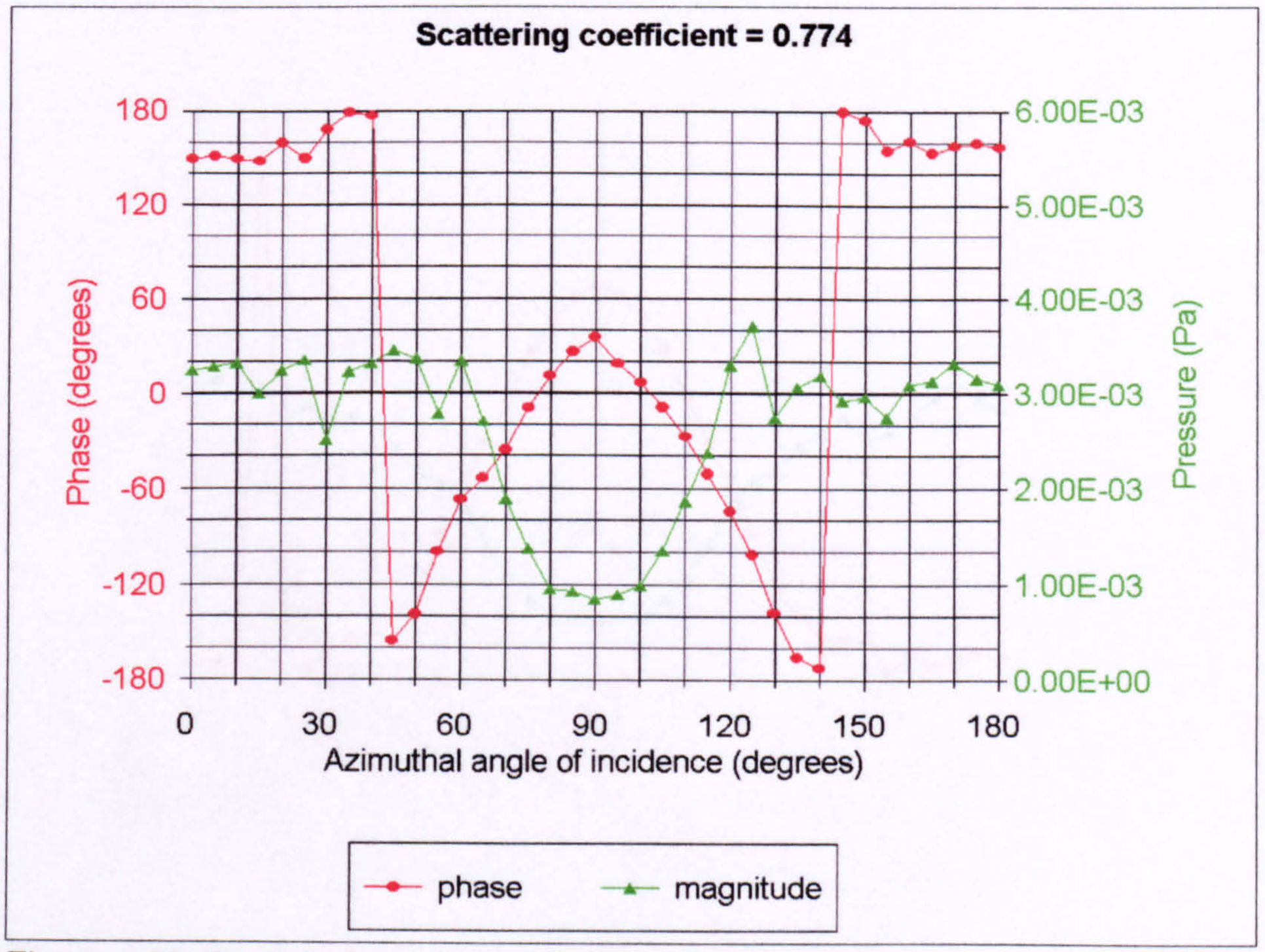

Figure 4.23: Predicted variation of the complex reflected pressure with azimuth at **15°** elevation and **7.35m** (full scale) from the random battens.

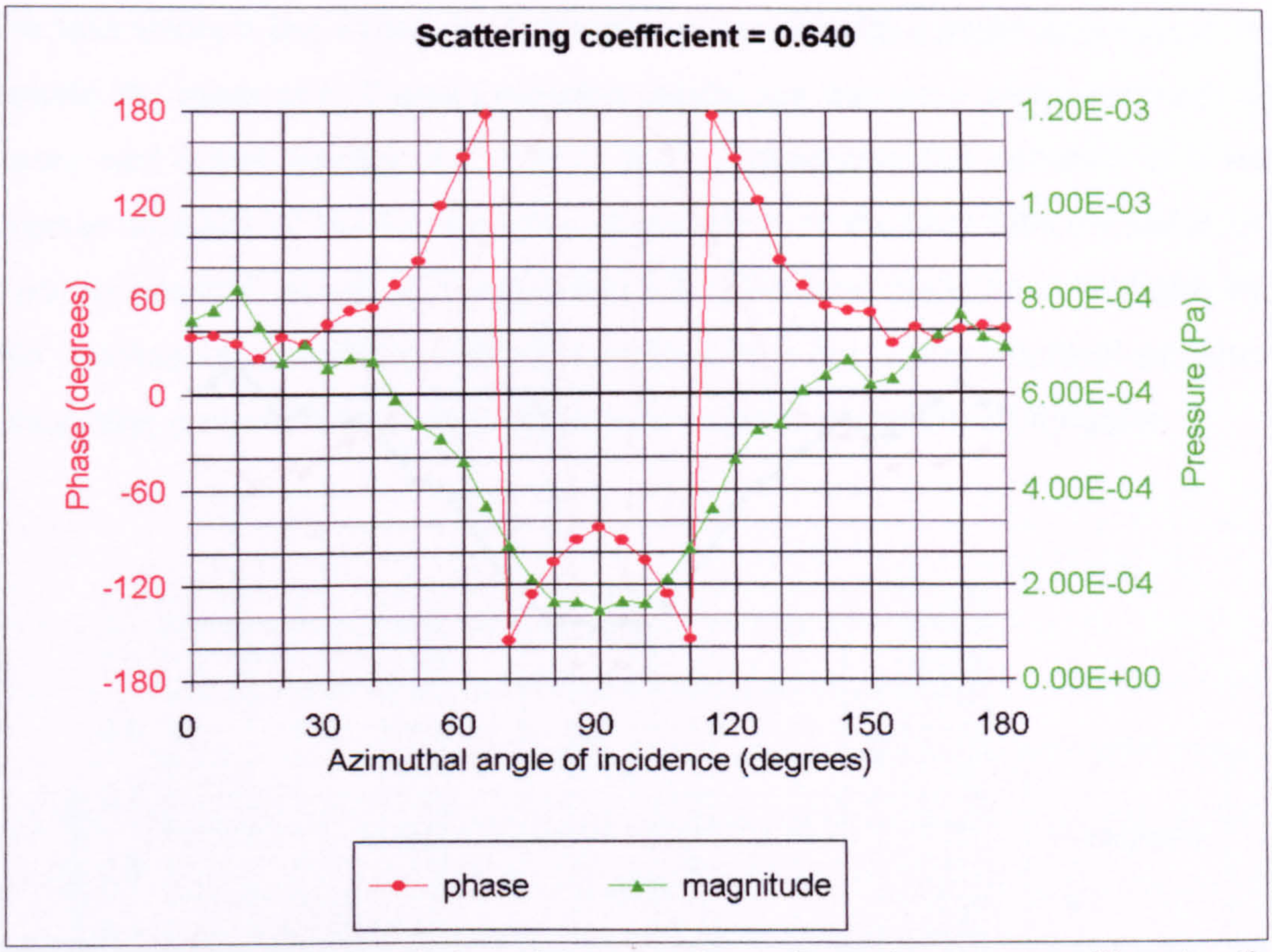

Figure 4.24: Predicted variation of the complex reflected pressure with azimuth at **15°** elevation and **50m** (full scale) from the random battens.

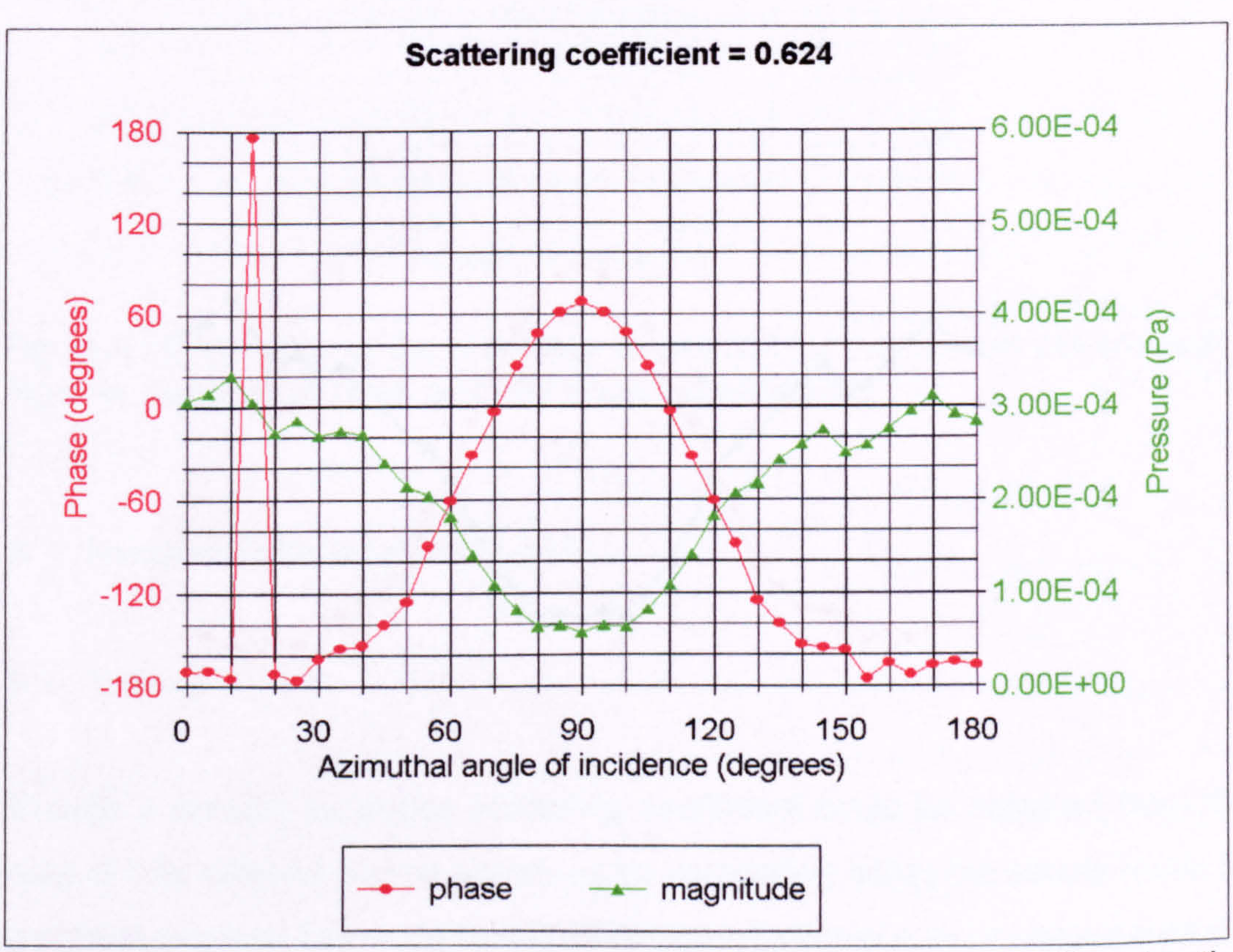

Figure 4.25: Predicted variation of the complex reflected pressure with azimuth at **15°** elevation and **125m** (full scale) from the random battens.

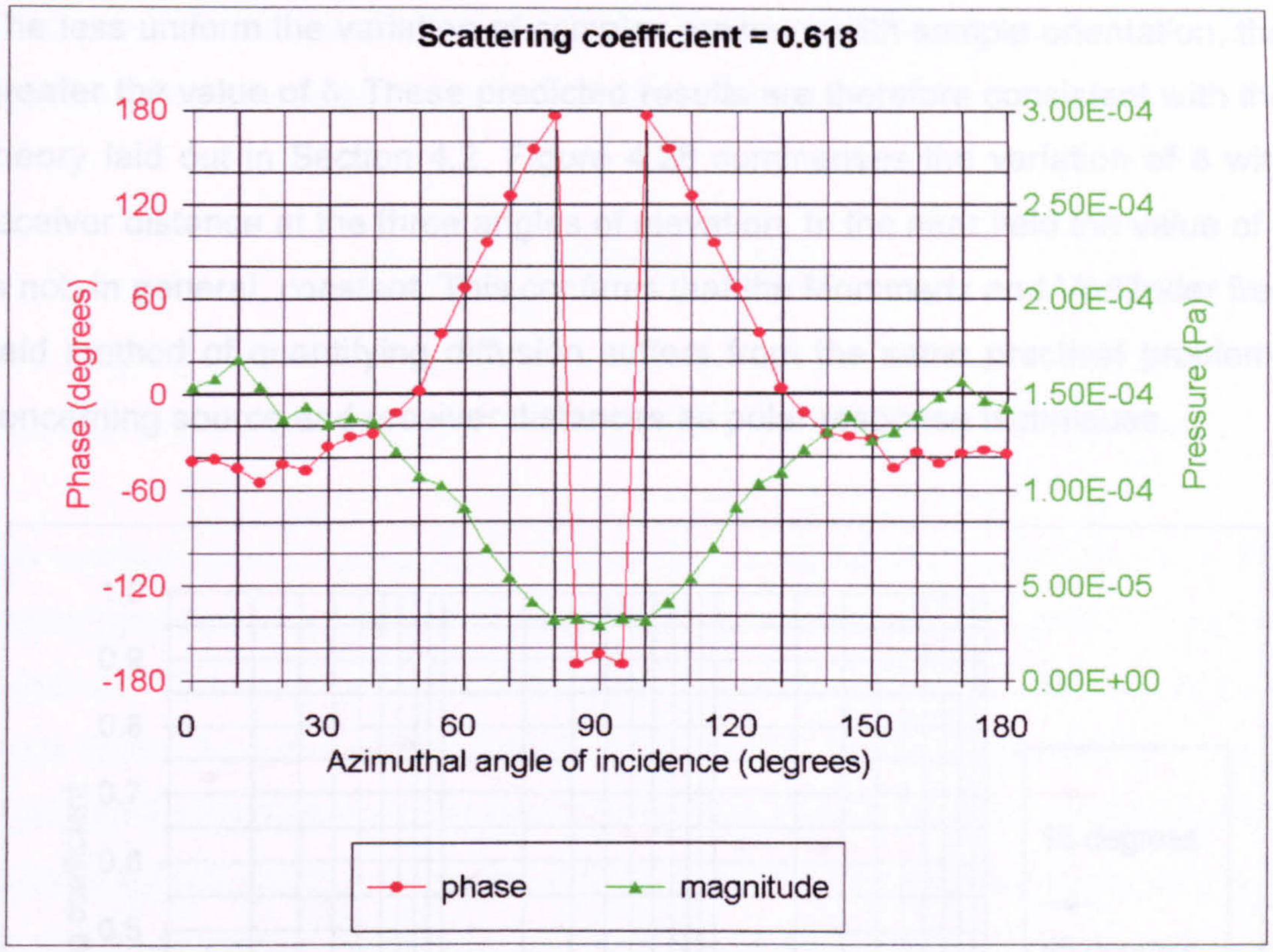

Figure 4.26: Predicted variation of the complex reflected pressure with azimuth at **15°** elevation and **250m** (full scale) from the random battens.

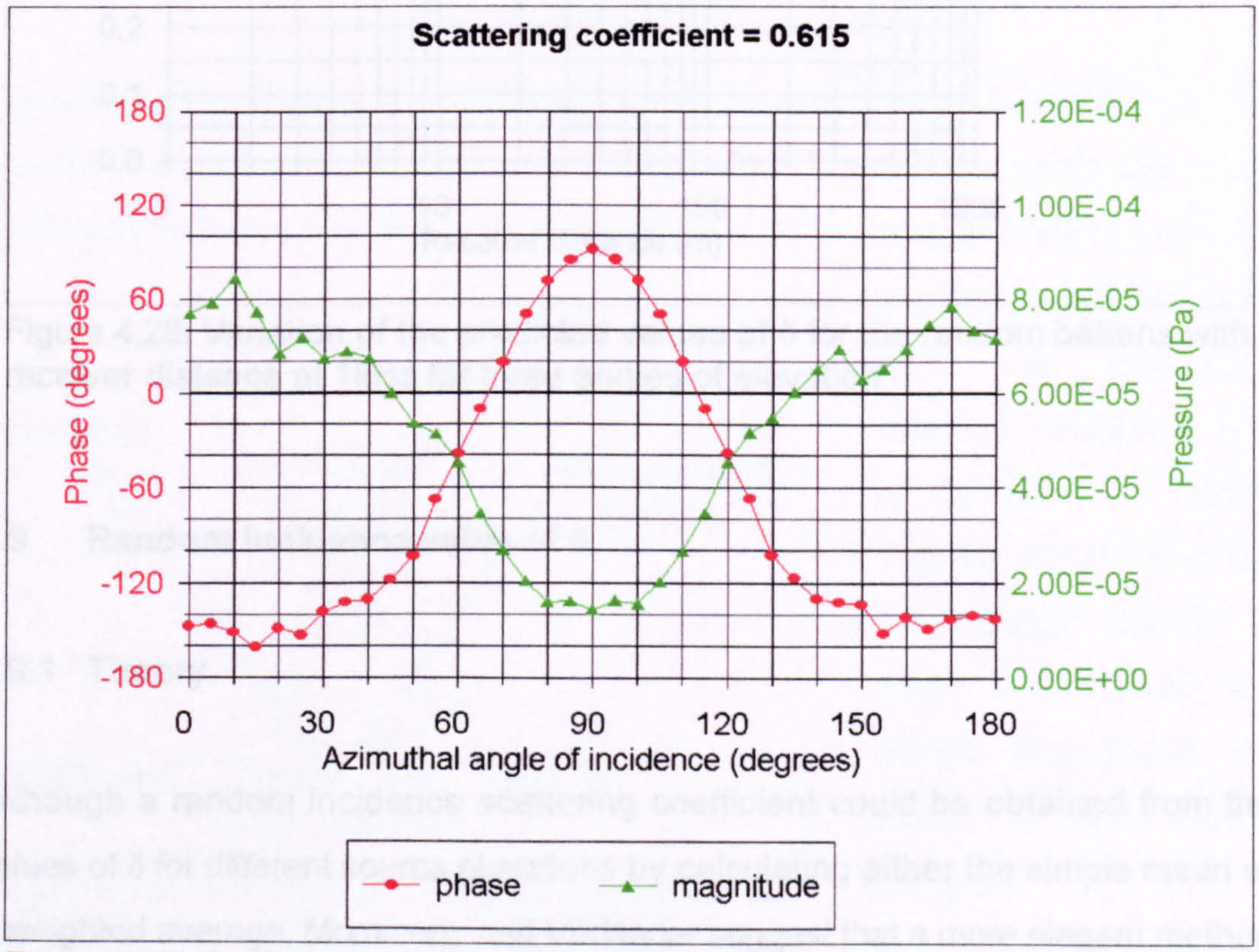

Figure 4.27: Predicted variation of the complex reflected pressure with azimuth at **15°** elevation and **500m** (full scale) from the random battens.

The less uniform the variation of complex pressure with sample orientation, the greater the value of δ. These predicted results are therefore consistent with the theory laid out in Section 4.2. Figure 4.28 summarises the variation of δ with receiver distance at the three angles of elevation. In the near field the value of δ is not, in general, constant. This confirms that the Mommertz and Vorländer free field method of quantifying diffusion suffers from the same practical problems concerning source and receiver distances as polar response techniques.

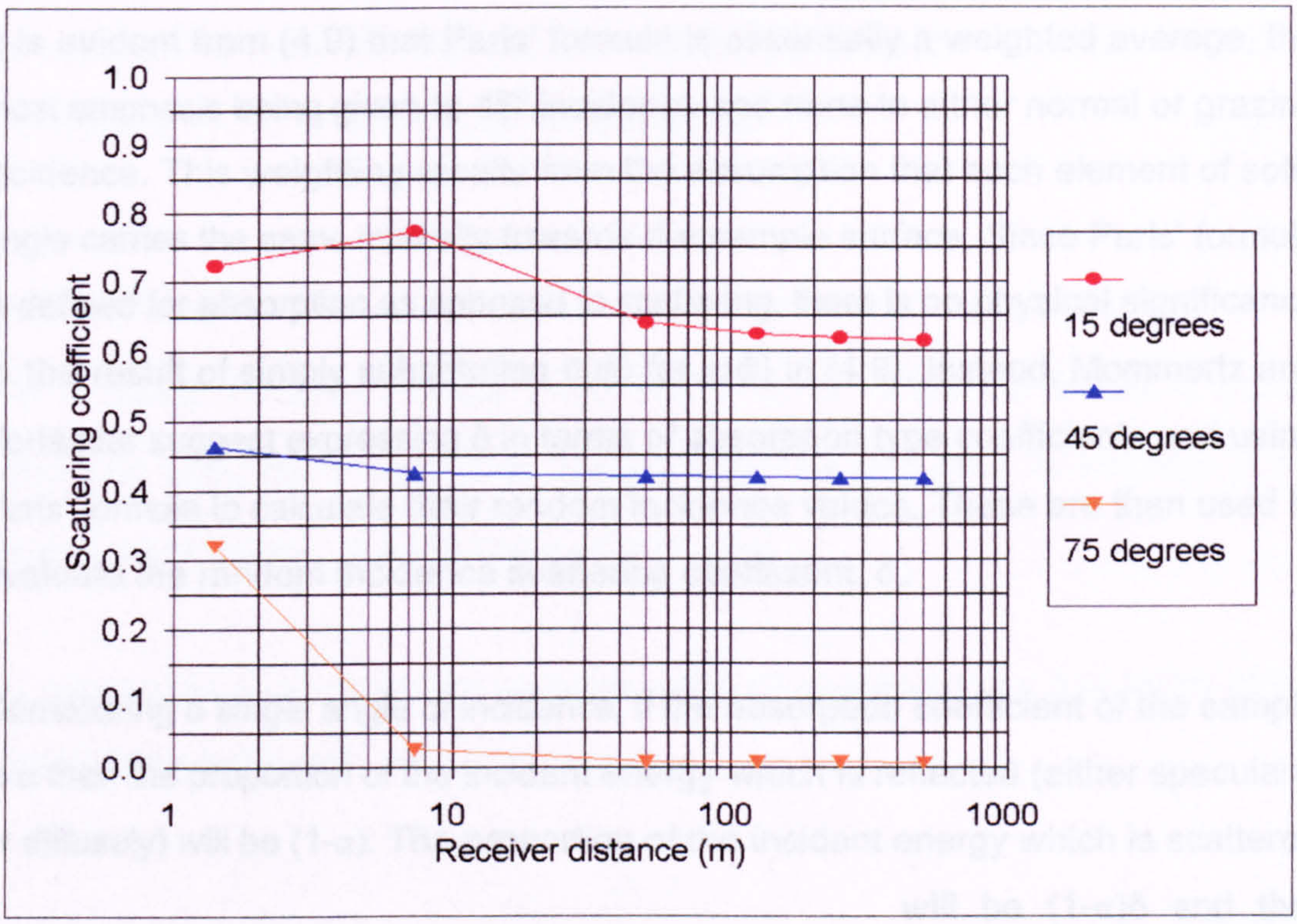

Figure 4.28: Variation of the predicted values of δ for the random battens with receiver distance at 1kHz for three angles of elevation.

4.9 **Random incidence value of δ.**

4.9.1 **Theory**.

Although a random incidence scattering coefficient could be obtained from the values of δ for different source elevations by calculating either the simple mean or a weighted average, Mommertz and Vorländer suggest that a more elegant method is to apply Paris' formula[61]. Paris' formula is normally used to evaluate the

absorption coefficient value for uniformly distributed incidence, α_{uni}, from angle-dependent results, $\alpha(\phi)$, and can be expressed as:

$$\alpha_{uni} = \int_0^{\pi/2} \alpha(\phi)\sin(2\phi)\,d\phi \qquad (4.9)$$

where ϕ is the angle of incidence measured from the surface normal.

It is evident from (4.9) that Paris' formula is essentially a weighted average, the most emphasis being given to 45° incidence and none to either normal or grazing incidence. This weighting results from the assumption that each element of solid angle carries the same intensity towards the sample surface. Since Paris' formula is defined for absorption as opposed to scattering, there is no physical significance to the result of simply substituting $\delta(\phi)$ for $\alpha(\phi)$ in (4.9). Instead, Mommertz and Vorländer suggest expressing δ in terms of absorption type coefficients and using Paris' formula to calculate their random incidence values. These are then used to evaluate the random incidence scattering coefficient, δ_r.

Considering a single angle of incidence, if the absorption coefficient of the sample is α then the proportion of the incident energy which is reflected (either specularly or diffusely) will be $(1-\alpha)$. The proportion of the incident energy which is scattered will be $(1-\alpha)\delta$ and that which is specularly reflected, $(1-\alpha)(1-\delta)$. This is illustrated in Figure 4.29 for the case where the incident energy is unity; in this case the energy proportions are equal to the actual energies.

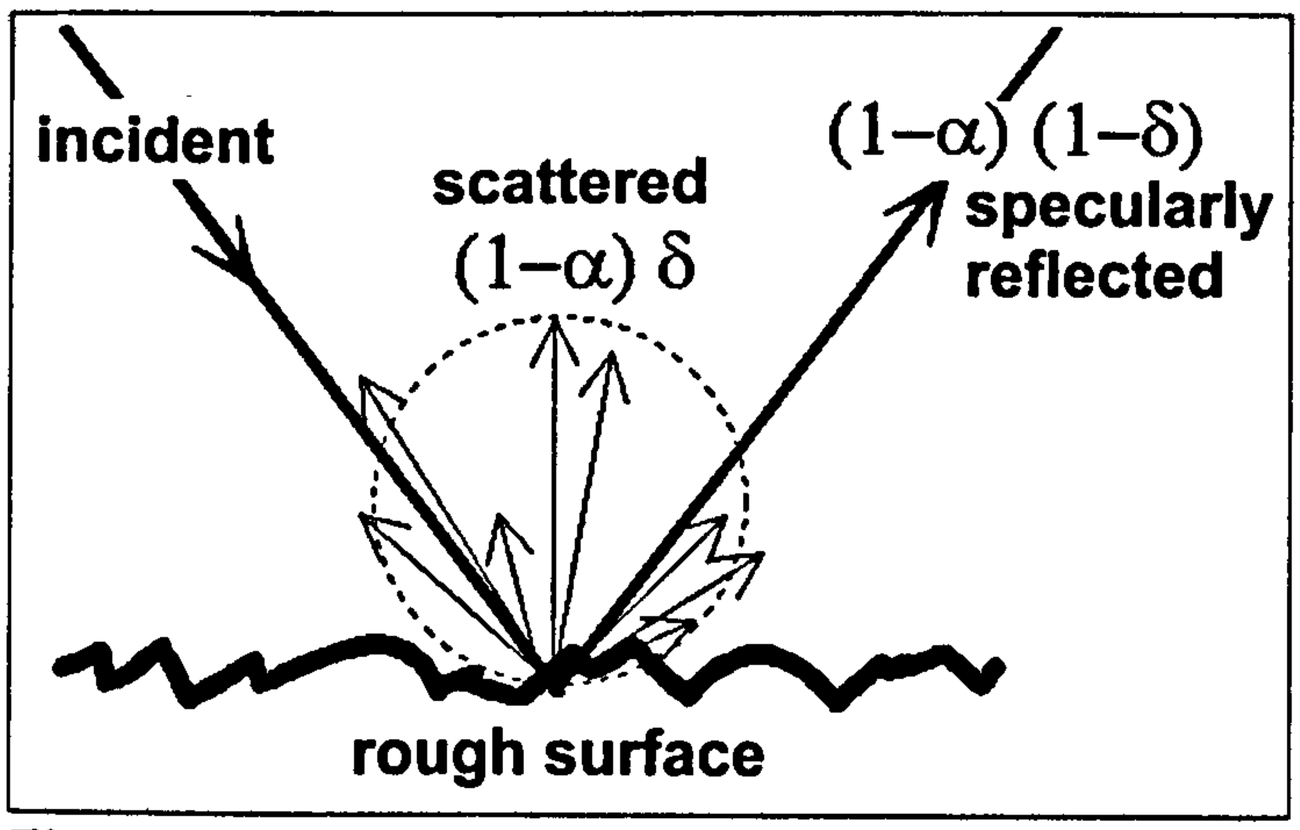

Figure 4.29: Definition of scattered and specularly reflected energies in terms of α and δ. (Mommertz and Vorländer[59])

Mommertz and Vorländer define the quantity a, which they term the 'specular absorption coefficient', using the expression:

$$1-a = (1-\alpha)(1-\delta) \tag{4.10}$$

From Figure 4.29, it can be seen that a is the proportion of the incident energy which is not specularly reflected. It is not a true absorption coefficient because it takes into account energy which is both absorbed and scattered. Therefore it will be referred to here as the pseudo specular absorption coefficient. In fact, rearranging (4.10) to make a the subject gives:

$$a = \alpha+\delta-\alpha\delta \tag{4.11}$$

For a totally reflective sample, α=0 and a=δ; for a sample which is purely specularly reflecting, δ=0 and a=α. Only if α and δ are both zero, for example in the case of a rigid plane, will the value of a be zero.

An alternative rearrangement of (4.10) gives an expression for δ in terms of the 'absorption coefficients' a and α.

$$\delta = \frac{a-\alpha}{1-\alpha} \tag{4.12}$$

Although it is not shown explicitly, all of the quantities in (4.12) are functions of both frequency, f and angle of incidence, ϕ. This is the form of expression for δ which is required for evaluating the random incidence scattering coefficient, δ_r, using Paris' formula.

Since α is the proportion of the incident energy which is not reflected, it can be defined in terms of the measured complex pressures, $P(f)$, as follows:

$$\alpha(f) \approx 1-\frac{1}{n}\sum_{i=1}^{n}\left|\underline{R}_i(f)\right|^2 \tag{4.13}$$

where $\underline{R}_i(f)$ is the complex reflection factor obtained by normalising the measured complex pressure, $\underline{P}_i(f)$, with respect to that which would be reflected if the sample were replaced with a rigid plane, $\underline{P}_{ref}(f)$. The values of α and δ (and hence a) for this reference plane must be zero.

$$\underline{R}_i(f) = \frac{\underline{P}_i(f)}{\underline{P}_{ref}(f)} \tag{4.14}$$

For the purposes of this analysis it is assumed that $\underline{P}_{ref}(f)$ is independent of both the sample orientation and the angle of elevation. Although this should be true theoretically, in a practical measurement it is likely that some variation with azimuth would be unavoidable for the reasons discussed in Section 5.4.5. In addition, diffraction from the sample edges cannot be eliminated (for a finite sample) and this would result in $\underline{P}_{ref}(f)$ varying with elevation.

Substituting for $\underline{R}_i(f)$ in (4.13) using (4.14) results in an expression for α explicitly in terms of the measured and reference pressures:

$$\alpha(f) \approx 1-\frac{\sum_{i=1}^{n}\left|\underline{P}_i(f)\right|^2}{n\left|\underline{P}_{ref}(f)\right|^2} \tag{4.15}$$

To define a in a similar manner it is first necessary to express the complex reflection factor as a sum of specular and diffuse components, i.e. in the same form as the complex pressure in (4.2):

$$\underline{R}_i(f) = \underline{R}_{spec}(f)+\underline{R}_{diff,i}(f) \tag{4.16}$$

Since a is the proportion of the incident energy which is not specularly reflected, it can be defined in terms of $\underline{R}_{spec}(f)$:

$$a(f) = 1 - \left|\underline{R}_{spec}(f)\right|^2 \tag{4.17}$$

$\underline{R}_{spec}(f)$ can be obtained from $\underline{R}_i(f)$ using the same coherent averaging process used to extract $\underline{P}_{spec}(f)$ from $\underline{P}_i(f)$. Consequently (4.17) can be written as:

$$a(f) \approx 1 - \frac{1}{n^2}\left|\sum_{i=1}^{n}\underline{R}_i(f)\right|^2 \tag{4.18}$$

Substituting for $\underline{R}_i(f)$ using (4.14) gives a explicitly in terms of the measured and reference pressures:

$$a(f) = 1 - \frac{\left|\sum_{i=1}^{n}\underline{P}_i(f)\right|^2}{n^2\left|\underline{P}_{ref}(f)\right|^2} \tag{4.19}$$

To obtain δ_r, Paris' formula is applied to the 'absorption coefficients' in (4.12). The result of this and the additional substitution of a and α using (4.13) and (4.18) is:

$$\delta_r(f) = \frac{\int_0^{\pi/2}\left[1 - \frac{1}{n^2}\left|\sum_{i=1}^{n}\underline{R}_i(f)\right|^2\right]_\phi \sin(2\phi)d\phi \; - \int_0^{\pi/2}\left[1 - \frac{1}{n}\sum_{i=1}^{n}\left|\underline{R}_i(f)\right|^2\right]_\phi \sin(2\phi)d\phi}{1 \; - \int_0^{\pi/2}\left[1 - \frac{1}{n}\sum_{i=1}^{n}\left|\underline{R}_i(f)\right|^2\right]_\phi \sin(2\phi)d\phi} \tag{4.20}$$

The contents of each pair of square brackets in (4.20) are a function of angle of incidence, ϕ (and frequency) but their values can be calculated only at the discrete elevations where measurements are made. For each elevation, the summations include all sample orientations but only those measurements which are made at

the particular elevation; the value of n is the number of azimuthal increments in one revolution of the sample, not the total number of measurements made. Expanding the square brackets and evaluating the resulting analytical integrals enables (4.20) to be reduced to:

$$\delta_r(f) = 1 - \frac{\int_0^{\pi/2} \left[\left| \sum_{i=1}^{n} \underline{R}_i(f) \right|^2 \right]_\phi \sin(2\phi)\, d\phi}{n \int_0^{\pi/2} \left[\sum_{i=1}^{n} \left| \underline{R}_i(f) \right|^2 \right]_\phi \sin(2\phi)\, d\phi} \qquad (4.21)$$

Substituting for $\underline{R}(f)$ using (4.14) gives δ_r as a function of the measured pressures, $\underline{P}(f)$, and the reference, $\underline{P}_{ref}(f)$. Since $\underline{P}_{ref}(f)$ is independent of both the sample orientation and the angle of incidence, a factor of $1/|\underline{P}_{ref}(f)|^2$ can be removed from both integrals and cancelled to leave δ_r in terms of the measured pressures only:

$$\delta_r(f) = 1 - \frac{\int_0^{\pi/2} \left[\left| \sum_{i=1}^{n} \underline{P}_i(f) \right|^2 \right]_\phi \sin(2\phi)\, d\phi}{n \int_0^{\pi/2} \left[\sum_{i=1}^{n} \left| \underline{P}_i(f) \right|^2 \right]_\phi \sin(2\phi)\, d\phi} \qquad (4.22)$$

The important consequence of this is that although, as can be seen from (4.15) and (4.19), evaluation of a or α requires $\underline{P}_{ref}(f)$ to be determined, the random incidence scattering coefficient, δ_r, can be calculated from the measured pressures alone.

4.9.2 Calculation of δ_r from measured results.

δ_r was evaluated for both the random battens and FlutterFree samples, the integrals being evaluated numerically. Figure 4.30 on the following page shows how these random incidence scattering coefficients vary with frequency.

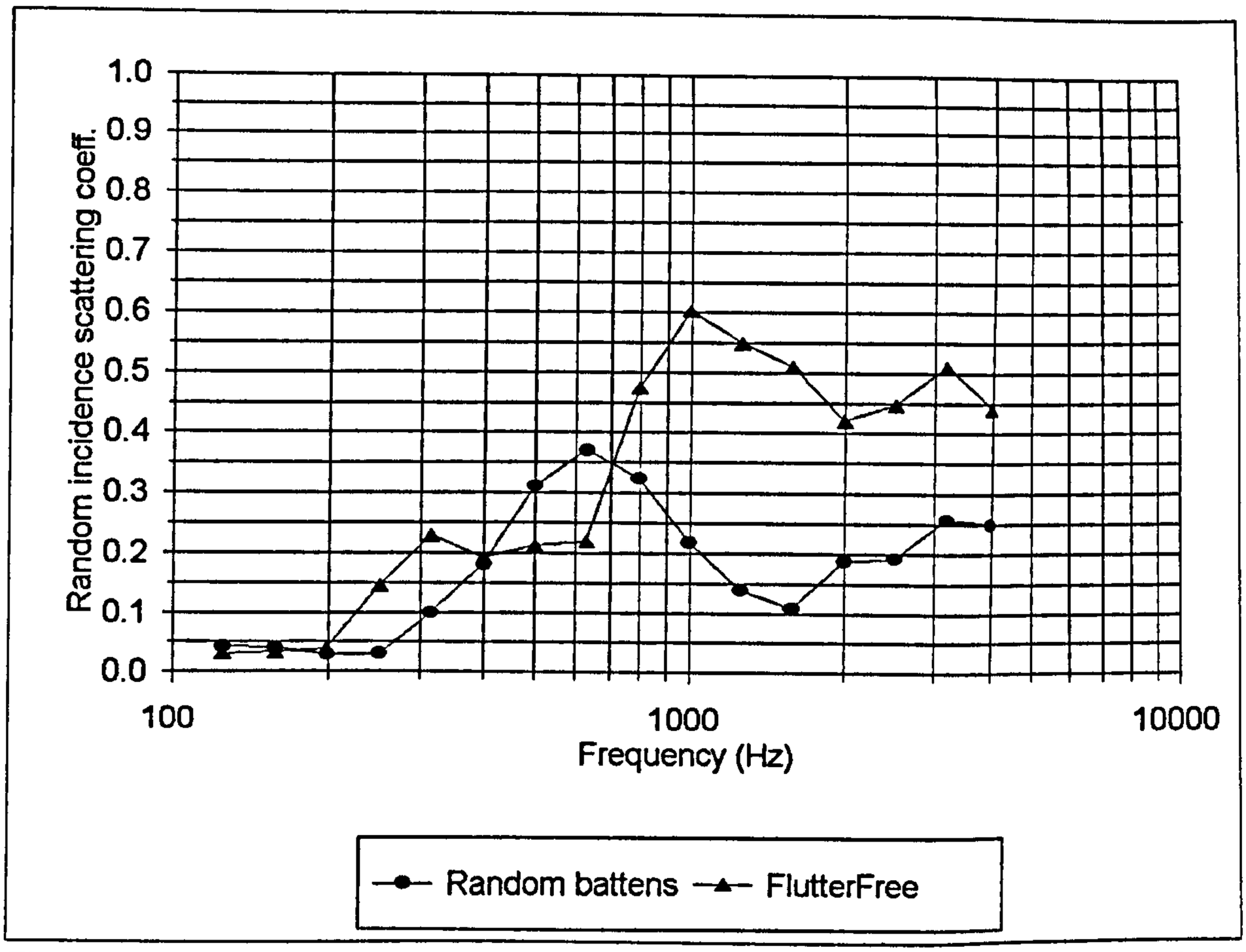

Figure 4.30: δ_r values for the random battens and FlutterFree calculated from measurements.

It is evident that the FlutterFree sample is a considerably more effective scatterer at the higher frequencies than the random battens, peaking at a value of 0.6 at 1kHz. However the random battens are superior at frequencies around 500 - 600Hz, where their value of δ_r peaks at approximately 0.37. As mentioned previously in Section 4.4.3, the reason that the FlutterFree sample generally produces more scattering is likely to be that it was specifically designed to be an effective diffuser whereas the random battens sample was not. With the random battens, the expectation was that a significant amount of scattering would occur in the range of frequencies where a quarter of a wavelength is similar to the cross-sectional dimensions of the battens and the sound is incident perpendicular to them. However, the arrangement of the battens was not optimised in any way to maximise the scattering.

4.9.3 Comparison with results obtained by Mommertz and Vorländer.

Figure 4.31 shows the variation of δ_r with frequency for both the random battens and a similar sample measured by Mommertz and Vorländer[22].

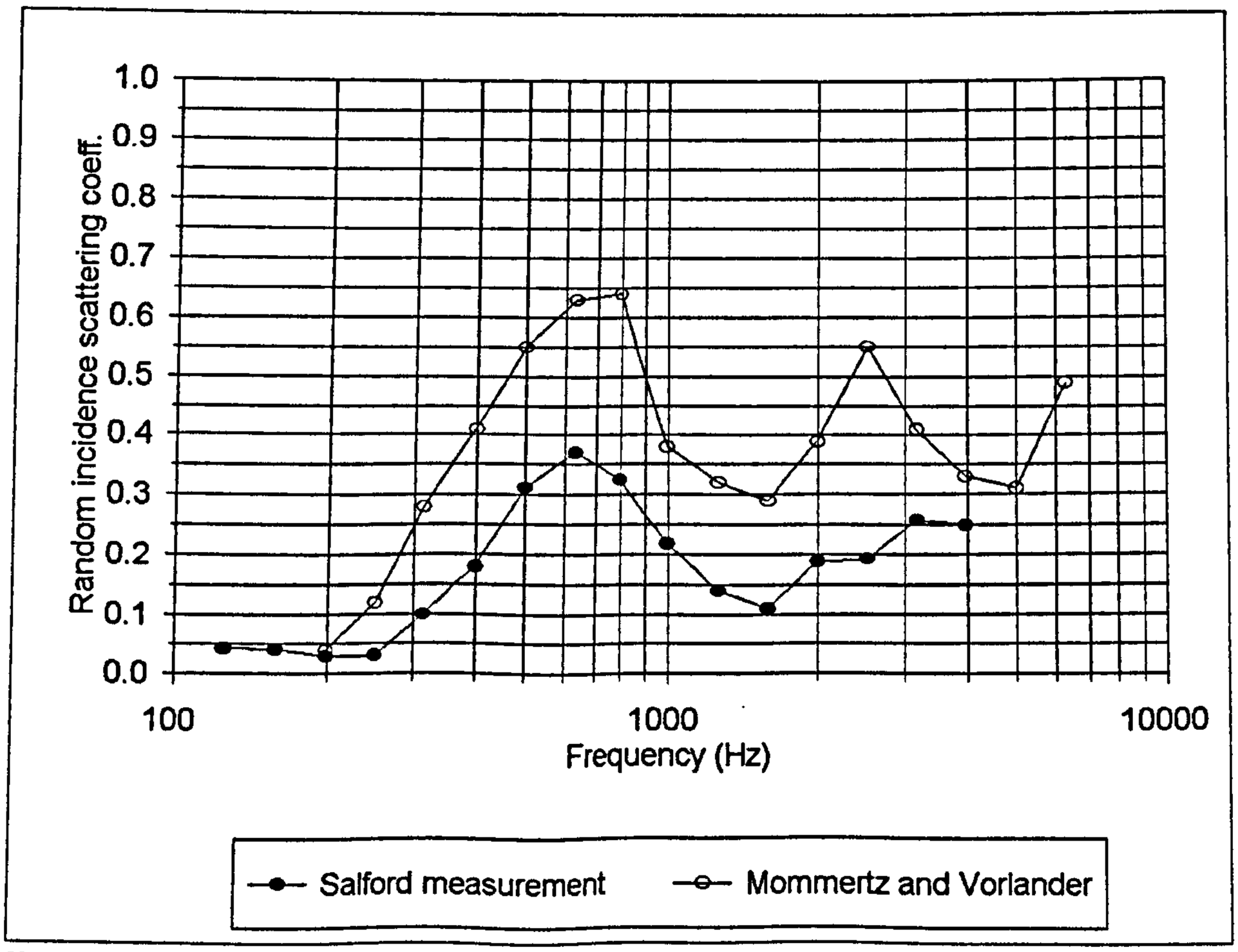

Figure 4.31: Comparison of the δ_r values for random battens obtained at Salford and by Mommertz and Vorländer.

Although in both cases the surfaces and battens are similar in size and shape, the manner in which the battens are arranged on the surfaces is quite different. For the sample measured by Mommertz and Vorländer, instead of the presence or absence of a batten at a particular position being determined by a random binary sequence, the distance between adjacent battens is random and has a mean value equal to twice the batten width. The purpose of Figure 4.31 is therefore to compare the manner in which δ_r varies with frequency for these two similar samples, not to compare individual values because no meaningful comparison can be made unless the measurements are of exactly the same sample. The arrangement of battens used by Mommertz and Vorländer is clearly the more effective at generating

scattering and the higher frequency peak is noticeably absent from the new measurement with the random battens sample. However, it can be seen that the value of δ_r does vary in a similar manner for both samples up to a frequency of approximately 2kHz.

Figure 4.32 compares the δ_r values for the FlutterFree sample evaluated from the new measurements with some calculated previously for exactly the same sample by Mommertz and Vorländer[22]. However, the measurement performed by Mommertz and Vorländer utilised the reverberation chamber technique discussed in Chapter 5 so although both measurements are of the same sample, the methods used are different. As discussed further in Chapter 8, Mommertz and Vorländer have found that values of δ_r obtained using the reverberation chamber method are in general significantly greater at higher frequencies than those measured using the free field technique but at lower frequencies both methods yield similar results[22]. This is borne out by Figure 4.32.

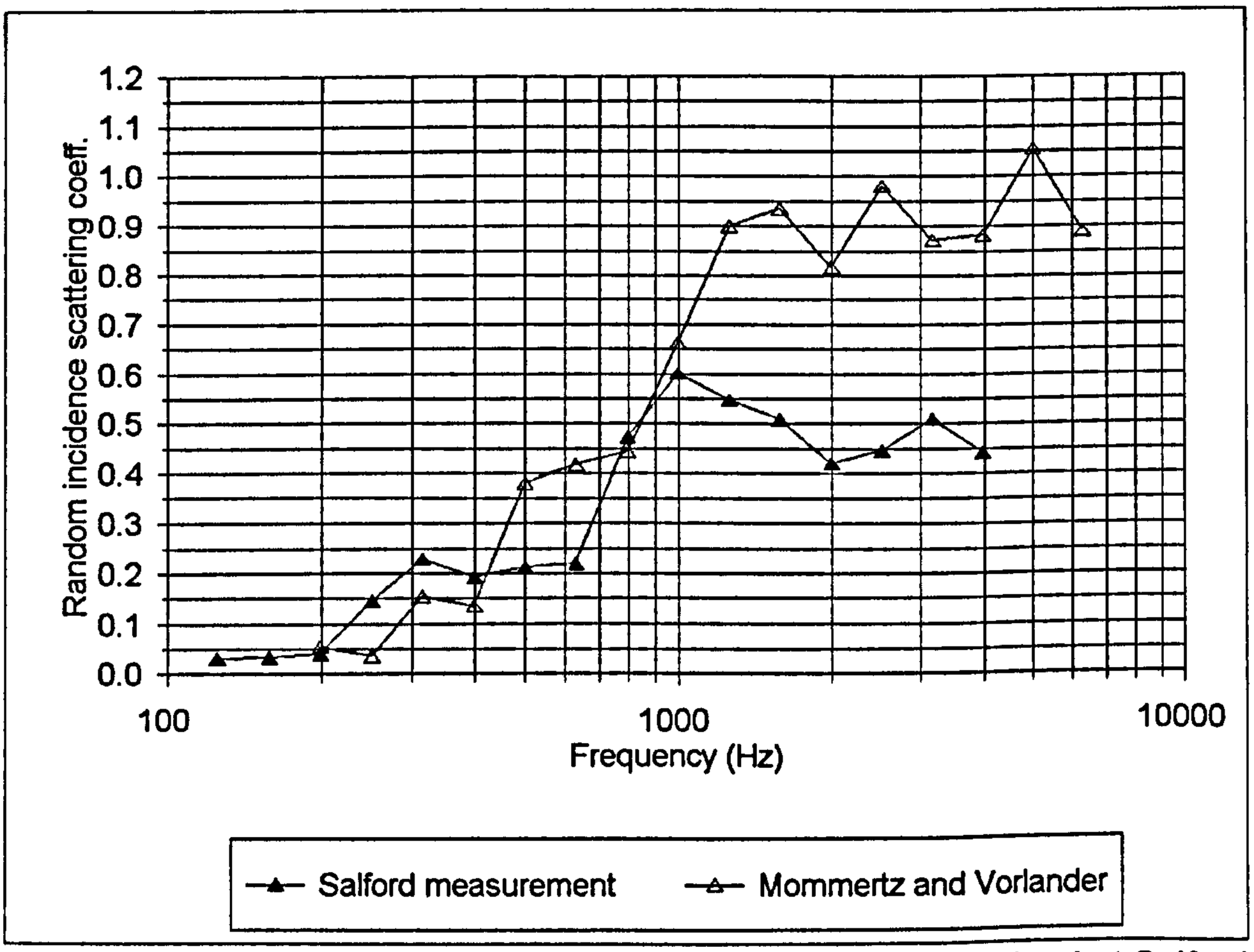

Figure 4.32: Comparison of the δ_r values for the FlutterFree obtained at Salford (free field) and by Mommertz and Vorländer (reverberation chamber).

4.9.4 Discussions.

The δ and δ_r results presented in this chapter are the only measurements of diffusion efficacy using the Mommertz and Vorländer free field method which have been performed by an independent laboratory. They are discussed further and compared to those obtained using other methods for quantifying diffusion in Chapter 8. It can be concluded that calculating δ_r is a tedious and time consuming process although no more so than obtaining a random incidence diffusion coefficient by measuring polar responses. However, whereas in the case of polar response diffusion measures the normal incidence value is sufficient for many applications, there is no equivalent with the Mommertz and Vorländer free field method. The only alternative to calculating the random incidence scattering coefficient would be to quote a value for one particular elevation angle and this would be of little practical use. A further complication is that although Paris' formula is well known, its validity has been called into question by a number of authors, particularly Makita and Hidaka[62]. However, Makita and Hidaka do suggest an alternative formulation for α_{uni} which, although more complex, could replace Paris' formula in the evaluation of δ_r.

4.10 Mathematical similarities between δ and the autocorrelation diffusion coefficient, d_{auto}.

In Section 4.2 it was remarked that the expression for the scattering coefficient, δ, resembles that for the autocorrelation diffusion coefficient discussed in Section 3.9, d_{auto}, without the complication of the bounding correction. Although δ has a clear physical definition and there is little to be gained from analysis of its mathematical expression, it is interesting to examine the extent of the similarity between the formulations for these two apparently quite different parameters for quantifying diffusion. To recapitulate, the two relevant expressions are shown on the following page:

$$\delta = 1 - \frac{\left|\sum_{i=1}^{n} \underline{P}_i(f)\right|^2}{n\sum_{i=1}^{n}\left|\underline{P}_i(f)\right|^2} \tag{4.7}$$

and:

$$d_{auto} = \frac{\left[\sum_{i=1}^{n} E_i\right]^2}{n\sum_{i=1}^{n} E_i^2} \tag{3.34}$$

One obvious difference between the expressions is the '1-' in (4.7) which is not present in (3.34). However, this dissimilarity has a simple explanation and is inconsequential: The value of d_{auto} increases as the scattered energies (squared pressures) comprising the polar response, E_i, become increasingly similar. This is because increased similarity between the E_i values corresponds to increased polar response uniformity and hence increased diffusion efficacy of the sample. In contrast, increased similarity between the complex pressures, $\underline{P}(f)$, in the expression for δ corresponds to a decrease in the proportion of the reflected energy which is scattered and hence to a decrease in diffusion efficacy. This is the reason for the '1-' in (4.7).

Disregarding this trifle, the only remaining difference between the expressions are the modulus signs in (4.7). However since these serve only to avoid ambiguity, it is valid to alternatively define δ as the mean of the circular autocorrelation function of the measured complex pressures. Although the expressions for δ and d_{auto} are essentially identical in form, their physical interpretations are in contrast highly disparate because E_i and $\underline{P}_i(f)$ are different quantities measured using different techniques. d_{auto} quantifies the directional invariance of the energy scattered from a sample for a particular source position and measurements are made both inside

and outside the specular zone. It is a measure of the uniformity of the reflected sound field. δ on the other hand measures the invariance of the scattered complex pressure in the specular reflection direction to movement of the sample. It quantifies the ratio of the scattered energy to the total energy reflected but does not convey any information about the directions in which energy is scattered or the uniformity of the resultant reflected field.

4.11 Conclusions.

The scattering coefficient defined by Mommertz and Vorländer is attractive because it has a simple physical interpretation. However, measurement using their free field method is tedious and time consuming, especially if a random incidence value is required. Prediction of the coefficient value is even more time consuming using existing methods. This coefficient is most suited to quantifying the scattering from extensive rough surfaces, it fails for those samples which simply redirect the reflected energy away from the specular direction. It is also unsuited to samples that scatter anisotropically because it is not possible to assign δ values to different planes; the value of δ takes all azimuthal directions into account and this can result in such surfaces being overrated. For samples which possess complete rotational symmetry, the measurement method would need to be modified. In common with the various techniques of quantifying diffusion from polar responses discussed in the previous chapter, the Mommertz and Vorländer free field method suffers from the problem that the reflected pressure is dependent on the measurement distance except in the far field. This problem afflicts any method involving free field measurement of the reflected sound field. One solution, discussed in subsequent chapters, is to employ a reverberation chamber approach to quantify diffusion.

5. THE MOMMERTZ AND VORLANDER REVERBERATION CHAMBER METHOD.

5.1 Introduction.

The scattering coefficient, δ, proposed by Mommertz and Vorländer becomes much more attractive when measured using their reverberation chamber method[22,59]. This is because the technique yields the random incidence value, δ_r, directly and is therefore much less time consuming than the free field method discussed in the previous chapter. In this chapter the concept of the Mommertz and Vorländer reverberation chamber method for measuring δ_r is presented and its practical implementation considered. New measurements of δ_r for a variety of test samples are described and the results discussed. The chapter concludes with an appraisal of the method as a technique for quantifying diffusion.

5.2 Theory.

The concept of this reverberation chamber technique for determining δ_r is fundamentally the same as that of the free field method; the specular and diffuse components of the energy reflected from a test sample are separated by coherent averaging of a number of measured impulse responses. However, in addition to the impulse responses being measured in reverberant as opposed to anechoic conditions, the source and receiver can be positioned anywhere inside the chamber, it is not necessary to use the geometry shown in Figure 4.1. Despite these experimental differences, the measurement procedure is identical to the free field case; the sample is rotated stepwise through a complete revolution by increments $\Delta\varphi$ and the impulse response of the chamber is measured for each orientation. If the sample reflects energy purely specularly (and is circular) then all the impulse responses will be perfectly correlated, regardless of the source and receiver positions or the shape of the reverberation chamber. However, if a proportion of the reflected energy is scattered differently with different orientations then there will be slight changes in the fine structure of individual responses, although the average energy decay will be unchanged. The greatest differences

are observed in the tails of the responses because the longer a reflection is delayed relative to the direct sound, the more times it is likely to have been scattered by the sample. It is shown below that in common with the free field method, phase-locked averaging of the impulse responses obtained for different orientations of the sample results in the incoherent diffuse components of the reflected energy being eliminated by destructive superposition, the remainder being the coherent specularly reflected component.

Each (bandpass filtered) impulse response, $h_i(t)$, measured for a particular orientation of the sample can be expressed as the sum of an invariant specular component, $h_{spec}(t)$ and a diffuse component, $h_{diff,i}(t)$, which is a function of the orientation:

$$h_i(t) = h_{spec}(t) + h_{diff,i}(t) \tag{5.1}$$

The resultant energy impulse response after coherent addition of n of these individual responses is therefore given by:

$$\left|\sum_{i=1}^{n} h_i(t)\right|^2 = \left|n h_{spec}(t) + \sum_{i=1}^{n} h_{diff,i}(t)\right|^2 \tag{5.2}$$

Provided that the specular and diffuse components are statistically independent, (5.2) can be written as shown below because the cross terms drop out:

$$\left|\sum_{i=1}^{n} h_i(t)\right|^2 \approx \left|n h_{spec}(t)\right|^2 + \left|\sum_{i=1}^{n} h_{diff,i}(t)\right|^2 \tag{5.3}$$

The expectation value of the resultant energy impulse response can be expressed as:

$$\left|\sum_{i=1}^{n} h_i(t)\right|^2 \approx n^2 \left|h_{spec}(t)\right|^2 + n\left\langle\left|h_{diff}(t)\right|^2\right\rangle \tag{5.4}$$

where:

$$<\left|h_{diff}(t)\right|^2> \;=\; \frac{1}{n}\sum_{i=1}^{n}\left|h_{diff,i}(t)\right|^2 \qquad (5.5)$$

So long as the diffuse components are sufficiently decorrelated that statistical independence can be assumed, (5.5) can alternatively be written as:

$$<\left|h_{diff}(t)\right|^2> \;\approx\; \frac{1}{n}\left|\sum_{i=1}^{n}h_{diff,i}(t)\right|^2 \qquad (5.6)$$

Substitution of (5.6) into (5.4) yields (5.3), demonstrating that (5.3) and (5.4) are equivalent subject to the above condition. Therefore, referring to (5.4), if n is sufficiently large then the diffuse components are insignificant and the resultant decay contains only the specularly reflected energy.

5.3 Practical implementation of the theory.

Although the scattering coefficient is still defined as the ratio of the non-specularly reflected energy to the total energy reflected by the sample, using this reverberation chamber method it is more straightforward to evaluate δ_r from its alternative definition in terms of the regular and pseudo specular absorption coefficients, derived in the previous chapter:

$$\delta_r \;=\; \frac{a-\alpha_{sample}}{1-\alpha_{sample}} \qquad (5.7)$$

where:

a = Random incidence pseudo specular absorption coefficient of the sample

α_{sample} = Random incidence regular absorption coefficient of the sample†

† The 'sample' subscript is necessary here to distinguish between the absorption coefficient of the sample and that of the reverberation chamber surfaces.

These absorption coefficients are calculated using the standard method[6] which involves measuring the reverberation time of the chamber with and without the sample present. However, determination of a requires the 'reverberation time' of solely the specularly reflected energy; this is obtained from the result of the coherent averaging process described in Section 5.2.

Using Sabine's well-known formulation[63], the reverberation time of the specularly reflected energy, T_{spec}, can be expressed as:

$$T_{spec} = \frac{0.161\,V}{S\bar{a}} \tag{5.8}$$

where:

V = Volume of reverberation chamber

S = Surface area of reverberation chamber

$$\bar{a} = \frac{1}{S}\left[S_{sample}a + (S - S_{sample})\alpha_{rev}\right] \tag{5.9}$$

α_{rev} = Random incidence absorption coefficient of rev. chamber surfaces

S_{sample} = Surface area of sample

In order to evaluate a, it is necessary to additionally measure the reverberation time of the empty chamber, T_{empty} and express this in the same form as T_{spec}:

$$T_{empty} = \frac{0.161\,V}{S\alpha_{rev}} \tag{5.10}$$

Neglecting the quantity $S_{sample}\alpha_{rev}$, which will in any case be small because the surfaces of a reverberation chamber are highly reflective, combination of (5.8), (5.9) and (5.10) yields this familiar form of expression for a:

$$a = \frac{0.161\,V}{S_{sample}}\left[\frac{1}{T_{spec}} - \frac{1}{T_{empty}}\right] \qquad (5.11)$$

Referring to (5.7), in order to calculate δ_r, it is also necessary to determine α_{sample}, the random incidence regular absorption coefficient of the sample. The only additional quantity which it is necessary to measure in order to accomplish this is the reverberation time of the chamber with the sample present but stationary, T_{sample}. This reverberation time is independent of the orientation of the sample and can be expressed as:

$$T_{sample} = \frac{0.161\,V}{S\overline{\alpha}} \qquad (5.12)$$

where:

$$\overline{\alpha} = \frac{1}{S}\left[S_{sample}\alpha_{sample} + (S - S_{sample})\alpha_{rev}\right] \qquad (5.13)$$

Again neglecting the quantity $S_{sample}\alpha_{rev}$, combination of (5.10), (5.12) and (5.13) enables α_{sample} to be expressed as:

$$\alpha_{sample} = \frac{0.161\,V}{S_{sample}}\left[\frac{1}{T_{sample}} - \frac{1}{T_{empty}}\right] \qquad (5.14)$$

Determination of δ_r using this reverberation chamber method thus essentially requires the measurement of three reverberation times.

5.4 New measurements of δ_r using the reverberation chamber method.

5.4.1 Introduction.

Since only Mommertz and Vorländer[22,59] have published any results of using this method to quantify the diffusion efficacy of surfaces, a number of original

measurements were performed as part of this research to provide new data. The purpose of these measurements was to both examine how the diffusion efficacy of different surfaces is rated and ranked and to appraise the method from a practical perspective.

The reverberation chamber in which these new measurements were performed has a volume of $30m^3$ and is therefore approximately half-scale in comparison to the size stipulated in ISO 354. Consequently, it was necessary to design and construct some larger sample surfaces; the 1:5 samples described in Section 2.3 would not effect sufficient change in the impulse response of this chamber for either a or α_{sample} to be measured accurately. Some of the new samples were specifically designed to investigate particular attributes of this method for quantifying scattering, whereas others were essentially larger versions of those used in previous measurements, to be able to compare results. Although the samples are all approximately 1:2 scale, it was necessary to vary the exact scale factor slightly between differently shaped samples to ensure that as they rotated, the minimum distance between the sample and a chamber boundary surface did not fall below that permitted by ISO 354. This is a much larger scale than that employed by Mommertz and Vorländer for the majority of their measurements[22]; they used a model reverberation chamber with a volume of approximately $1m^3$.

5.4.2 **Test samples**.

Figures 5.1 to 5.6 show the six sample surfaces.

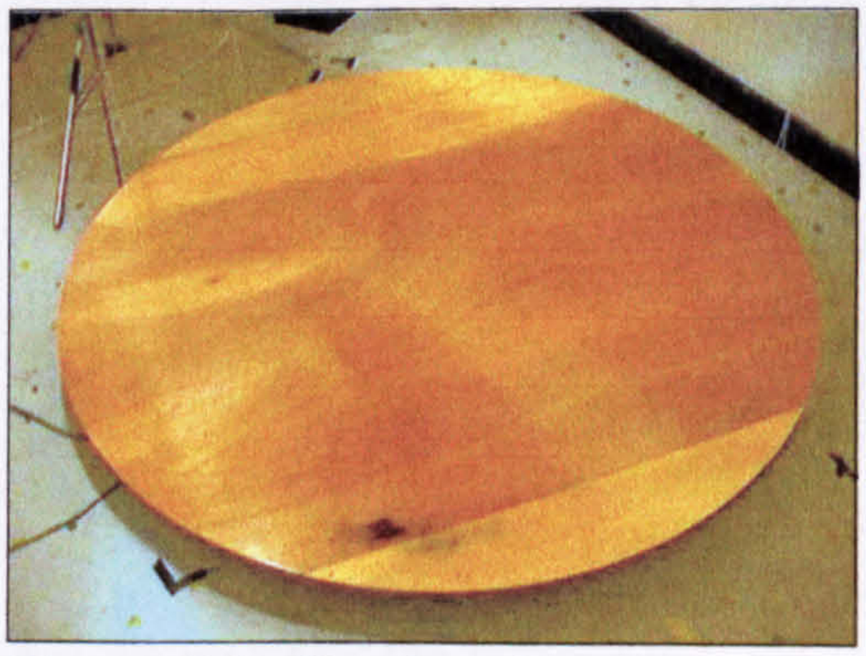

Figure 5.1: Circular plane.

- 1.55m diameter.
- Material: Varnished 12.5mm plywood with bracing on the underside to prevent deformation.

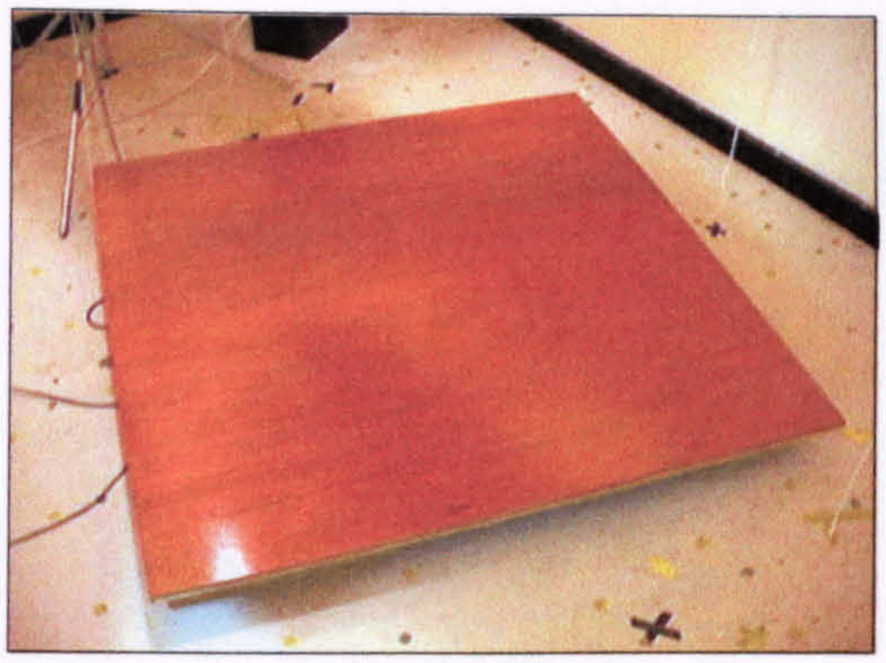

Figure 5.2: Square plane.

- 1.35m square.
- Material: Varnished 12.5mm plywood with bracing on the underside to prevent deformation.

The purpose of the circular plane was to examine how close its practical value of δ_r approached the theoretical value of zero for such a surface. The square plane was included for comparison, to examine the effect of sample shape on δ_r.

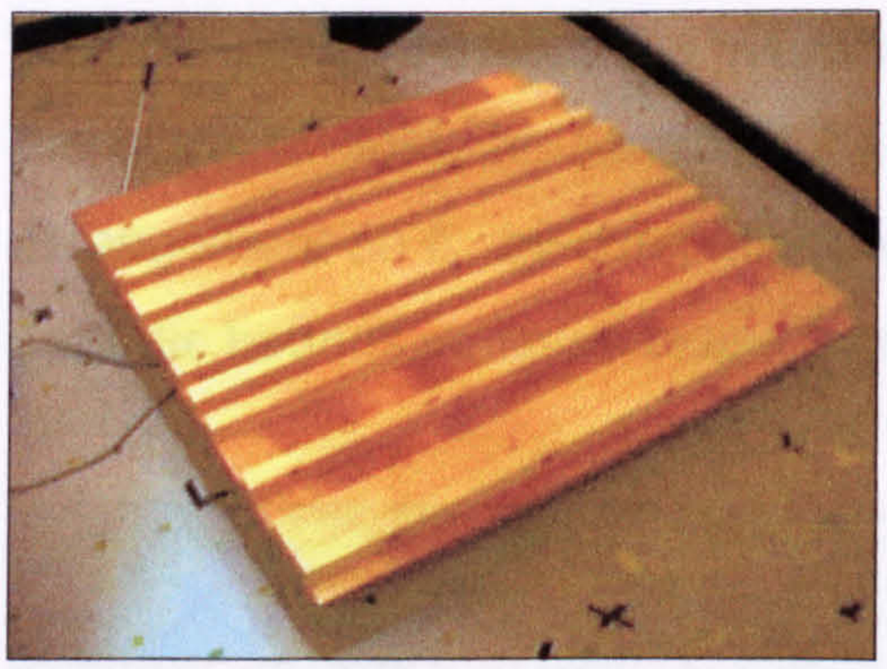

Figure 5.3: Square random battens.

- 1.35m square.
- Cross-section of battens = 43mm.
- Material: Battens are varnished hardwood. Base is varnished 12.5mm plywood.

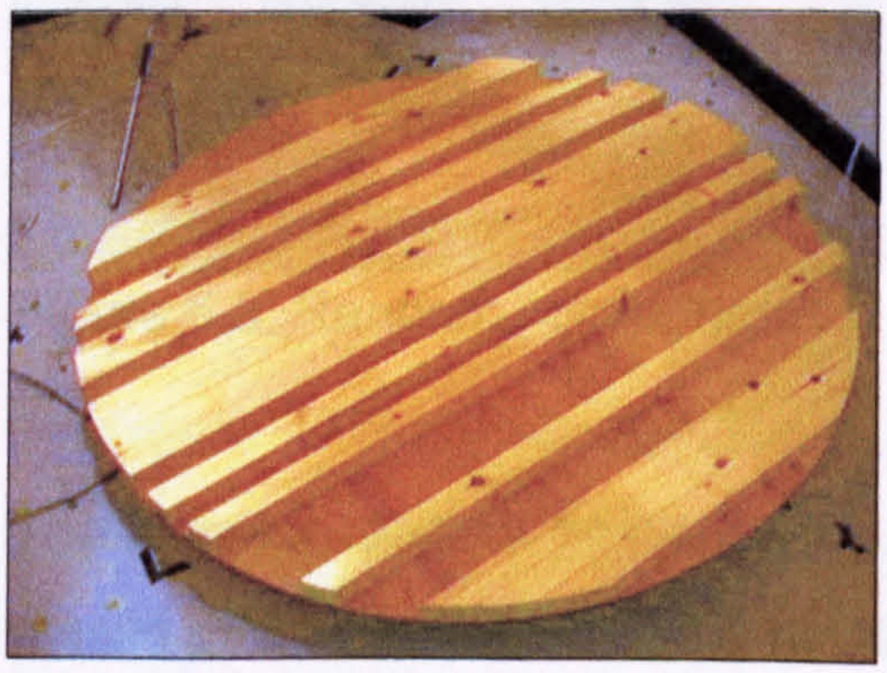

Figure 5.4: Circular random battens.

- 1.55m diameter.
- Cross-section of battens = 50mm.
- Material: Battens are varnished hardwood. Base is varnished 12.5mm plywood.

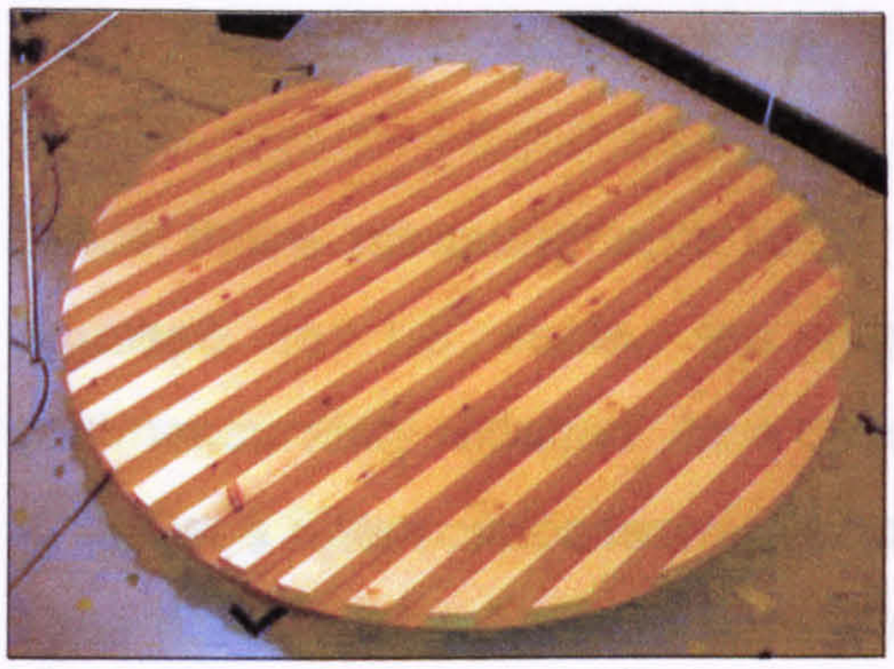

- 1.55m diameter.
- Cross-section of battens = 50mm.
- Material: Battens are varnished hardwood. Base is varnished 12.5mm plywood.

Figure 5.5: Circular periodic battens.

The square random battens sample is essentially a scaled-up version of that shown in Figure 2.12b, a value of δ_r for which was determined using the free field technique. This is the only sample whose diffusion efficacy has been measured using both of the Mommertz and Vorländer methods. Both of the random battens samples have identical structures and the same number of battens as the circular periodic battens sample. The purpose of the circular random battens sample was therefore twofold; to examine the effect of both sample shape and batten arrangement on δ_r, by comparison with the square random battens and circular periodic battens samples respectively.

- Diameter of base = 1.55m.
- Diameter of hemispheres = 0.20m.
- Material: Hemispheres are 1.5mm ABS. Base is varnished 12.5mm plywood with bracing on the underside to prevent deformation.

Figure 5.6: Random hemispheres.

The circular random hemispheres sample was included in the set because it should produce more isotropic scattering than the battens samples and at some frequencies it has significant absorption, unlike any of the others. It was also one of the samples measured using Lam's method of quantifying diffusion which is discussed in Chapter 6.

5.4.3 **Practical considerations.**

Since these measurements were carried out in approximately 1:2 scale as opposed to 1:5 scale, the highest measurement frequency could be commensurately reduced. As a consequence of this decrease in bandwidth, the ¼" Brüel & Kjær condenser microphone Type 4135 was replaced with a ½" GRAS Type 40AF, which has the benefit of higher sensitivity. A different source was used also because neither the Visonik 6003 nor the Bose Acoustimass® Cube loudspeakers utilised in previous measurements have sufficient sensitivity at low frequencies to generate enough sound pressure level in the chamber for the reverberation time to be accurately extracted from the decay. Initially, a two-way ported loudspeaker with a 300mm low frequency driver, designed for the reproduction of music in large halls, was employed. However, using established MLS techniques for measuring reverberation time[64], it was found that only approximately 40dB of decay could be obtained in any third-octave band, even though band levels measured with and without the source active suggested that the decay should be in excess of 60dB over the measurement bandwidth. This was confirmed by using a Real-Time Analyser (RTA) to simply measure the third-octave band levels as functions of time immediately after switching off the source. While a 40dB decay is usually sufficient for obtaining an accurate estimate of reverberation time, the extent to which the fine structure of the tail of the response can be examined is limited. Although this problem could be solved by measuring the decay using an RTA, the amount of averaging required to ensure an accurate measurement would be tedious and time-consuming.

The reason why the entire decay was not obtained using the MLS method was brought to light by detailed examination of impulse responses measured using it. This revealed broadband noise extending over the complete analysis frame which, although normally invisible, was of sufficient magnitude to limit the decay obtained by Schroeder integration of the response. The noise was dependent on the signal level and was not reduced by averaging. Such noise can result from time-aliasing if the duration of the MLS stimulus is shorter than the reverberation time being measured[50], however this was not the case here. It was also ensured that the

input signal level with the source active was such that the full range of the 12-bit input analogue to digital converter was utilised, the theoretical dynamic range of this being about 70dB. Another possible cause of broadband noise in MLS measurements is non-linear distortion in the measurement chain[50]. By a process of elimination it was discovered that this was the cause here and that the source of the distortion was in fact the loudspeaker. Replacing the loudspeaker with a Mission Type 733 designed for high-fidelity reproduction of music in the domestic environment decreased this distortion and increased the maximum amount of decay which could be measured using the MLS technique to approximately 55dB.

In Section 5.2 it is stated that the procedure for obtaining the pseudo specular absorption coefficient, a, involves rotating the sample stepwise through one complete revolution and measuring the impulse response of the chamber for each of these n orientations. The impulse responses are then coherently averaged and the reverberation time, T_{spec}, of the resultant decay is used in the calculation of a. It has been shown[22,59] that so long as the specular and diffuse components of the individual impulse responses can be assumed to be statistically independent, the resultant can be modelled as an exponential decay, $E(t)$:

$$E(t) \approx (n-1)e^{\frac{cS}{4V}\ln(1-\bar{a})t} + e^{\frac{cS}{4V}\ln(1-\bar{\alpha})t} \qquad (5.15)$$

where the symbols have their previous meanings.

As illustrated in Figure 5.7 on the following page, $E(t)$ is in fact a superposition of two decays with different initial levels and decay constants, similar to that observed in coupled rooms. Mommertz and Vorländer have shown that the early, steeper, portion of this bended decay relates to the specular energy and is that from which T_{spec} is obtained whereas the later decay is related to the fixed sample and could therefore theoretically be used to obtain T_{sample}. The initial level of the late decay decreases by 3dB per doubling of n, so the greater the number of responses averaged, the longer the duration of the early portion of the decay and

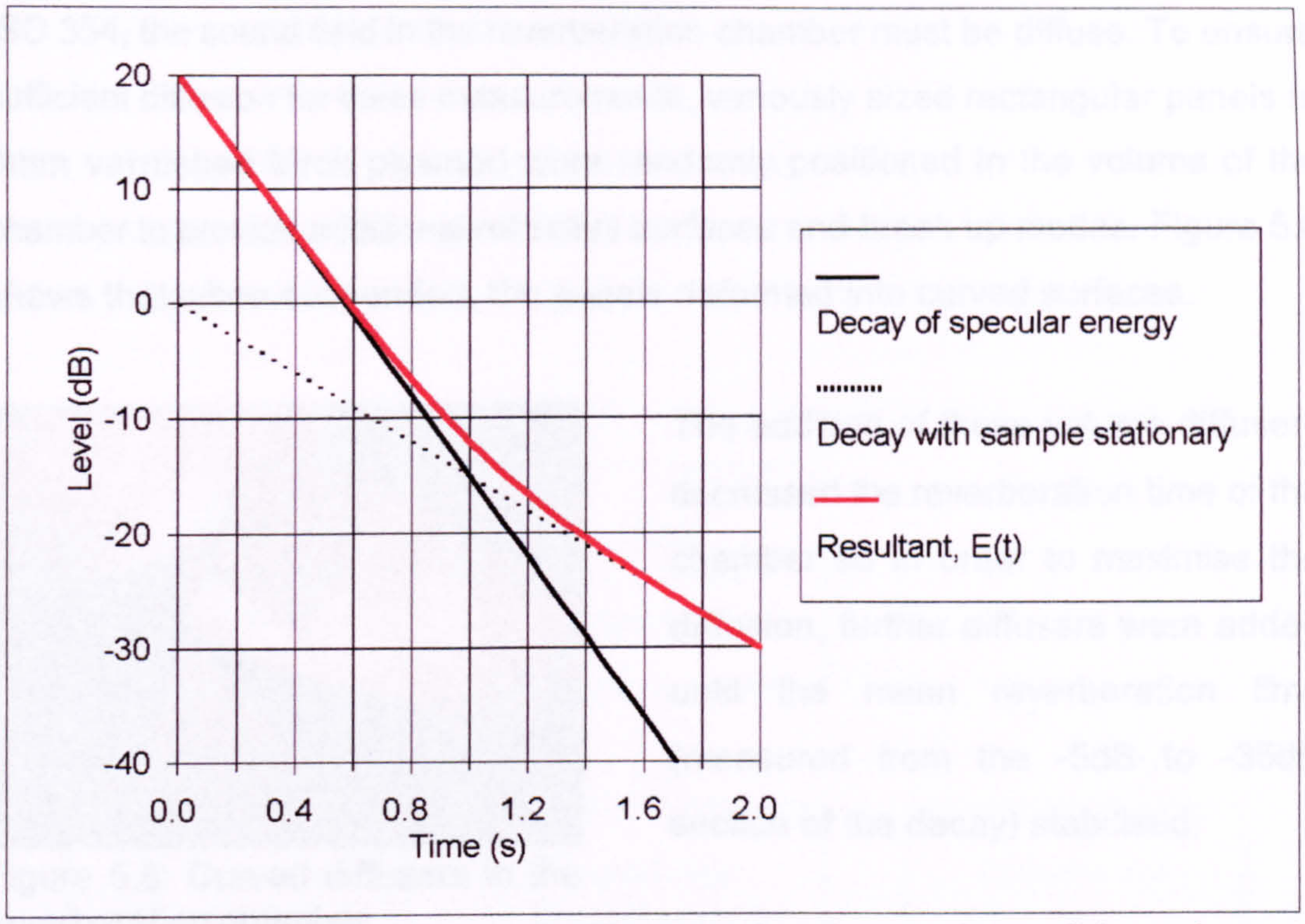

Figure 5.7: Schematic diagram to illustrate that the resultant of the coherent averaging process, $E(t)$, is a bended decay.

the easier it is to accurately determine T_{spec}. However in order to increase n, the angle through which the sample is rotated between measurements, $\Delta\varphi$, must be reduced and this reduces the decorrelation of the diffuse components of consecutively measured responses. There is therefore an upper limit to the duration of the early portion of the decay and Mommertz and Vorländer have demonstrated that this is reached when the sample is rotated continuously as opposed to stepwise, impulse responses being measured and averaged as the sample rotates through exactly one revolution[22]. This continuous measurement yields valid results because although the MLS technique assumes time-invariance, only the time-invariant component of the impulse response is being determined. In addition to providing the longest duration of decay from which to determine T_{spec}, measuring and averaging the n impulse responses continuously rather than stepwise is significantly quicker and was therefore the procedure used for the new measurements carried out as part of this research.

In order to accurately measure random incidence absorption coefficients using

ISO 354, the sound field in the reverberation chamber must be diffuse. To ensure sufficient diffusion for these measurements, variously sized rectangular panels of 3mm varnished birch plywood were randomly positioned in the volume of the chamber to provide additional reflective surfaces and break up modes. Figure 5.8 shows that when suspended, the panels deformed into curved surfaces.

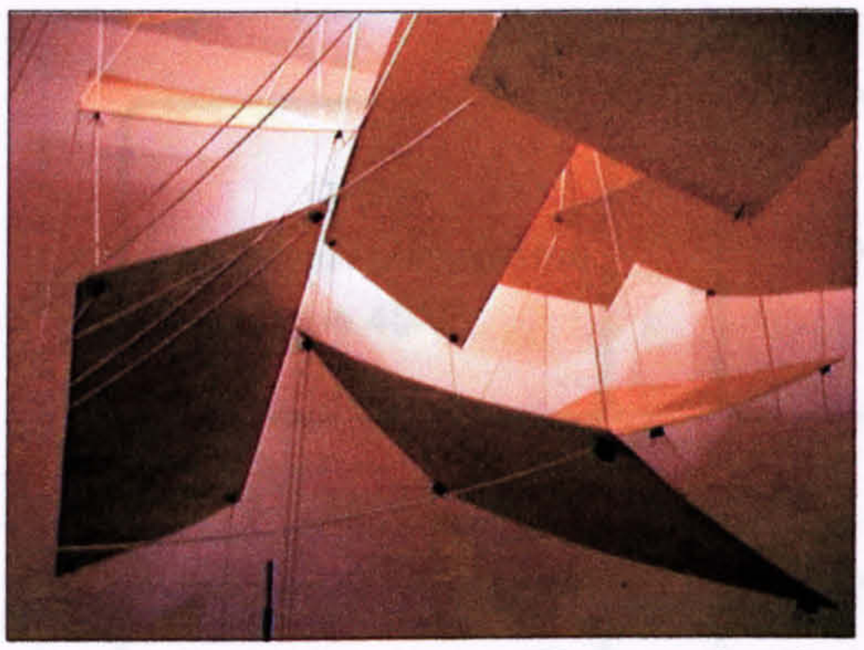

Figure 5.8: Curved diffusers in the reverberation chamber.

The addition of these volume diffusers decreased the reverberation time of the chamber so in order to maximise the diffusion, further diffusers were added until the mean reverberation time (measured from the -5dB to -35dB section of the decay) stabilised.

To enable the samples to be rotated, they were placed on the computer controlled turntable described in Section 2.9. This allowed full control of both the sample and the MLS measurement system from outside the reverberation chamber. An illustrative view of the experimental set-up inside the chamber is shown in Figure 5.9; the source and microphone were not positioned in such close proximity for actual measurements.

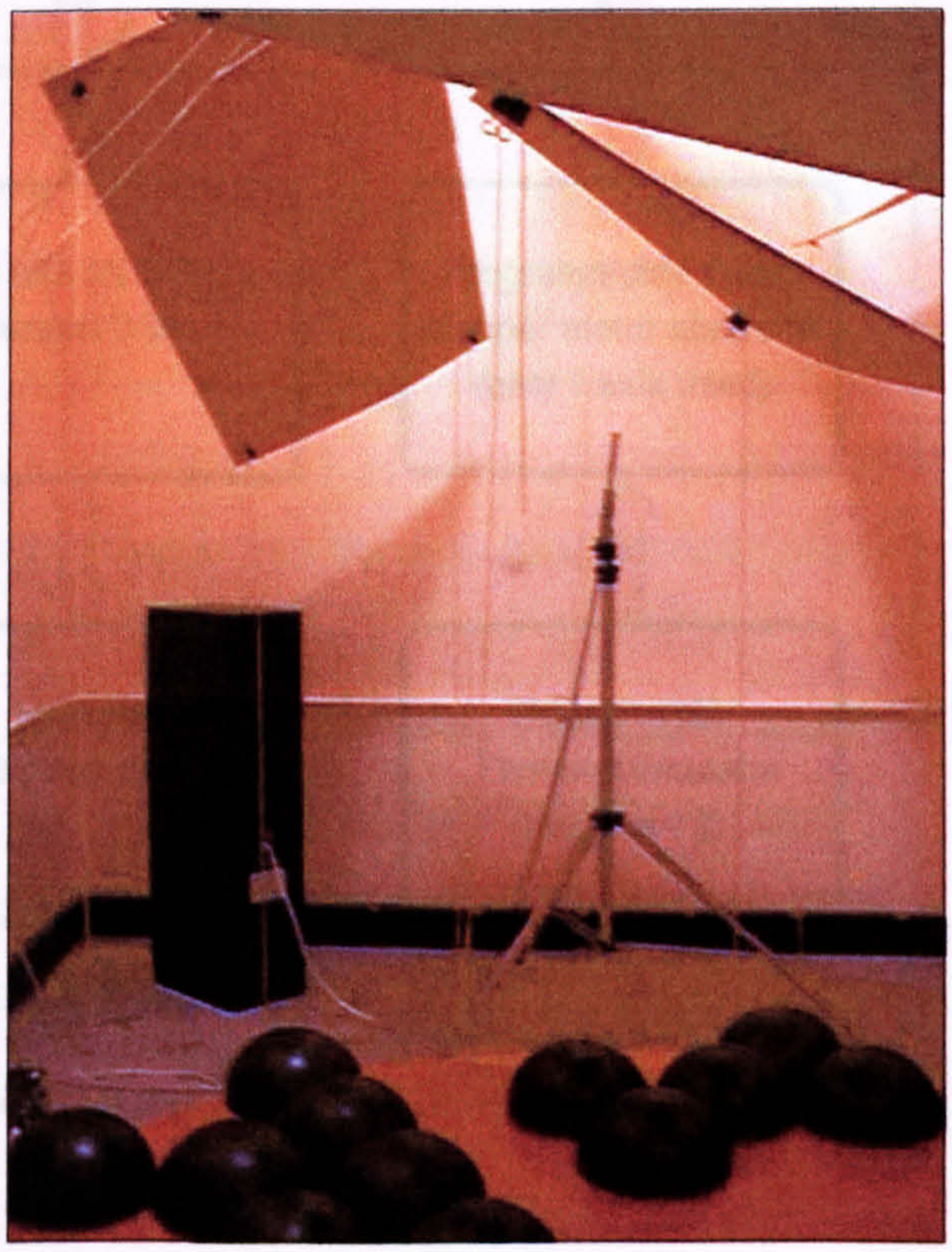

Figure 5.9: Interior view of the reverberation chamber.

5.4.4 **Measurement procedure**.

Figure 5.10 shows a block diagram of the apparatus used to determine the random incidence scattering coefficient, δ_r, of the samples shown in Figures 5.1 to 5.6 using the Mommertz and Vorländer reverberation chamber method.

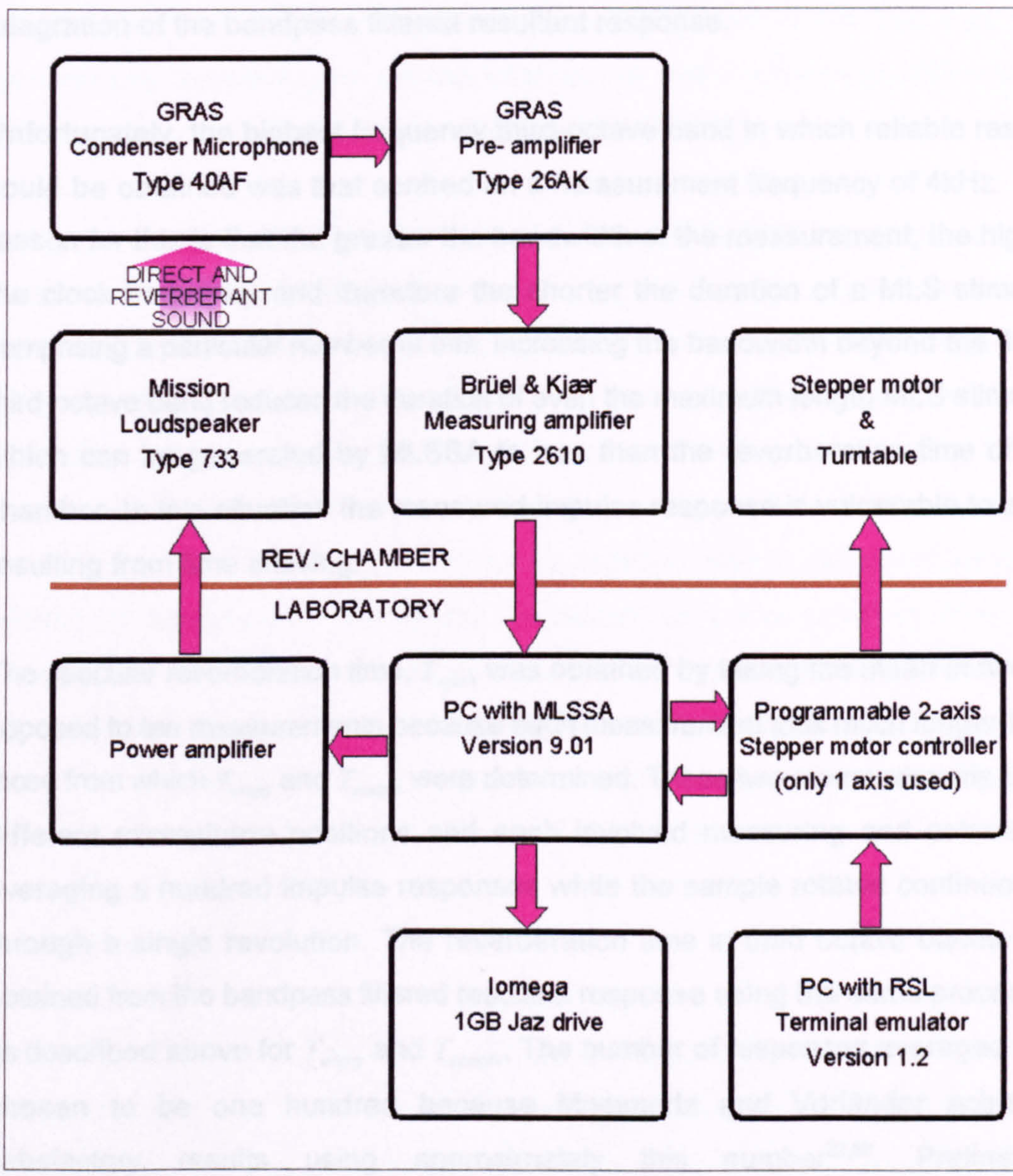

Figure 5.10: Block diagram of the apparatus used to determine the random incidence scattering coefficient, δ_r, using the Mommertz and Vorländer reverberation chamber method.

The reverberation times T_{empty} and T_{sample} were evaluated by taking the mean of ten individual measurements made at different positions in the chamber, five for each

of two source positions. It was ensured that none of these microphone positions were too close to either the source, the sample, a chamber boundary or a diffuser, although the minimum distance criteria stated in the ISO 354 were reduced by the scale factor of approximately two. At each position, sixteen impulse responses were pre-averaged and the reverberation time calculated in third-octave bands by extrapolating the -5dB to -35dB portion of the decay obtained from Schroeder integration of the bandpass filtered resultant response.

Unfortunately, the highest frequency third-octave band in which reliable results could be obtained was that centred on a measurement frequency of 4kHz. The reason for this is that the greater the bandwidth of the measurement, the higher the clock frequency and therefore the shorter the duration of a MLS stimulus comprising a particular number of bits. Increasing the bandwidth beyond the 4kHz third-octave band reduces the duration of even the maximum length MLS stimulus which can be generated by MLSSA to less than the reverberation time of the chamber. In this situation the measured impulse response is vulnerable to error resulting from time aliasing.

The specular reverberation time, T_{spec}, was obtained by taking the mean of two as opposed to ten measurements because each measurement took much longer than those from which T_{empty} and T_{sample} were determined. These two measurements used different microphone positions and each involved measuring and coherently averaging a hundred impulse responses while the sample rotated continuously through a single revolution. The reverberation time in third octave bands was obtained from the bandpass filtered resultant response using the same procedure as described above for T_{empty} and T_{sample}. The number of responses averaged was chosen to be one hundred because Mommertz and Vorländer achieved satisfactory results using approximately this number[22,59]. Preliminary measurements revealed that if the sample did not make exactly one revolution during the measurement then the reverberation time extracted from the resultant decay was usually shorter than that obtained if it did. The reason why it appears not to be equally probable that the reverberation time will be reduced or increased in such circumstances is unclear and further investigation is required.

In order to ensure that the sample performed precisely one revolution during the measurement, it was firstly necessary to determine the measurement duration in seconds, $t_{measure}$. Although the duration of the MLS stimulus is known, since $t_{measure}$ also includes the times between consecutive stimuli, when the impulse response is calculated from the acquired data and the running average updated, it has to be measured empirically. The rotational speed of the stepper motor in steps per second which causes the sample to rotate exactly once in this time was then calculated by considering the number of steps per motor revolution (200) and the reduction ratio between the motor and turntable (120:1).

Using a bandwidth of 5kHz and a stimulus length of 65535 bits (the maximum length available using MLSSA), the value of $t_{measure}$ if a hundred impulse responses are continuously measured and averaged is approximately 870 seconds, i.e. a little less than a quarter of an hour. The corresponding motor speed was calculated to be approximately 27 steps s^{-1} but at this low step rate the torque developed is insufficient to turn the sample. Since the number of steps per motor revolution is fixed and $t_{measure}$ could not be reduced without either reducing the number of averages or risking the introduction of errors resulting from time aliasing, the only solution was to increase the amount of reduction. Therefore a 25:1 gearbox was incorporated into the drive mechanism between the stepper motor and the turntable to enable the motor speed to be increased to 688 steps s^{-1}, a speed at which the torque developed is sufficient.

5.4.5 **Results**.

Once the reverberation times T_{empty}, T_{sample} and T_{spec} had been determined, the values of a, α_{sample} and finally δ_r could be calculated using (5.11), (5.14) and (5.7). The variation of these latter three quantities with frequency is shown for all six samples in Figures 5.11 to 5.13 respectively.

From Figure 5.12 it can be seen that the random incidence regular absorption coefficient, α_{sample}, of all the samples constructed solely from varnished wood is small, less than 0.1 at frequencies below 400Hz and almost always less than 0.15.

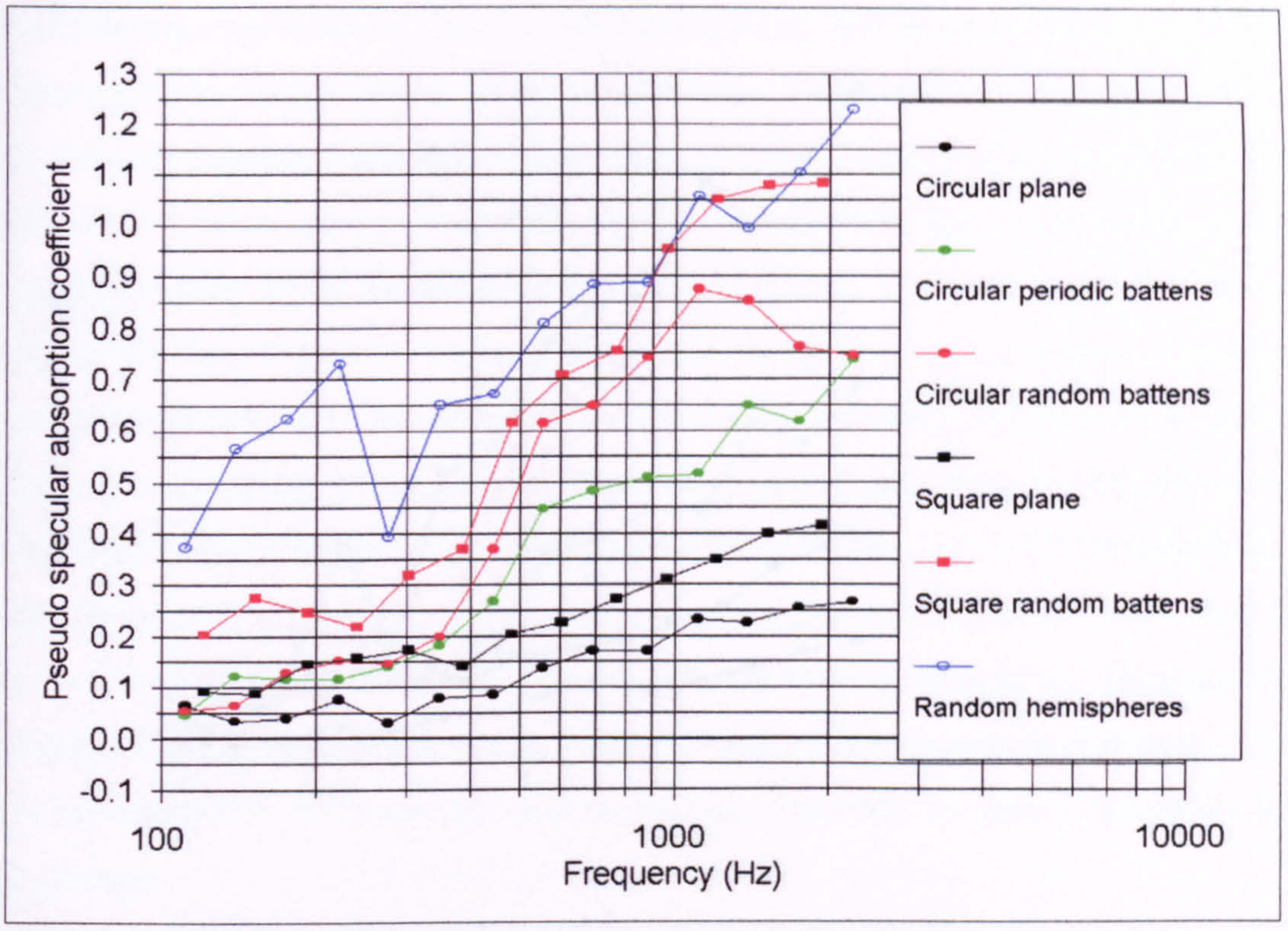

Figure 5.11: Variation of a with frequency.

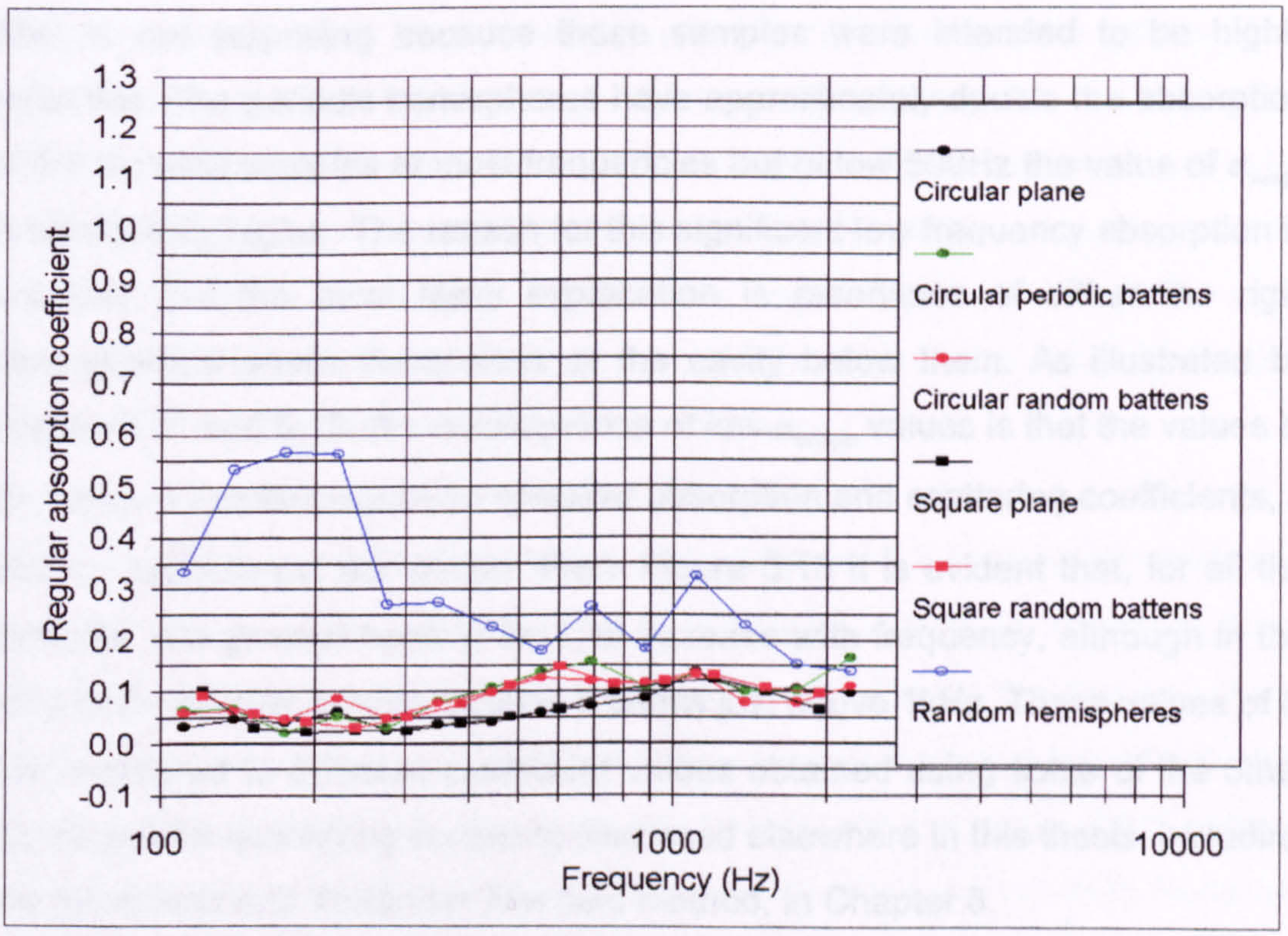

Figure 5.12: Variation of α_{sample} with frequency.

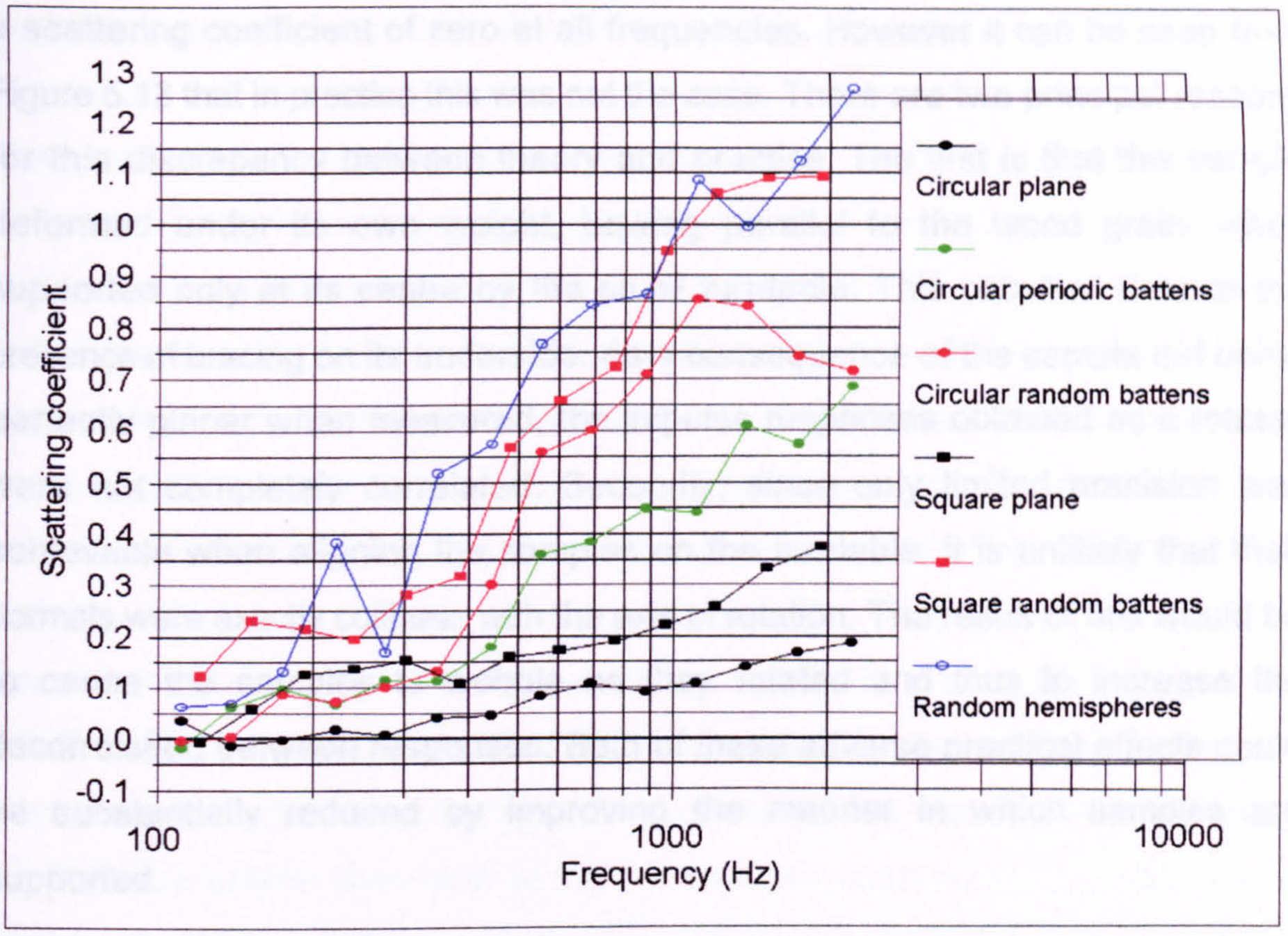

Figure 5.13: Variation of δ_r with frequency.

This is not surprising because these samples were intended to be highly reflective. The periodic hemispheres have approximately double the absorption of the wooden samples at most frequencies but below 500Hz the value of α_{sample} is significantly higher. The reason for this significant low frequency absorption is unknown but the most likely explanation is resonance of either the rigid hemispherical shells themselves or the cavity below them. As illustrated by Figures 5.11 and 5.13, the consequence of low α_{sample} values is that the values of the random incidence pseudo specular absorption and scattering coefficients, a and δ_r respectively, are similar. From Figure 5.13 it is evident that, for all the samples, the general trend is for δ_r to increase with frequency, although in the case of the circular random battens it peaks just above 1kHz. These values of δ_r are compared to diffusion coefficient values obtained using some of the other techniques for quantifying scattering discussed elsewhere in this thesis, including the Mommertz and Vorländer free field method, in Chapter 8.

According to the theory expounded in Section 5.2, the circular plane should have

a scattering coefficient of zero at all frequencies. However it can be seen from Figure 5.13 that in practice this was not the case. There are two principal reasons for this discrepancy between theory and practice. The first is that this sample deformed under its own weight, bowing parallel to the wood grain, when supported only at its centre by the small turntable. This occurred despite the presence of bracing on its underside. As a consequence of the sample not being perfectly planar when measured, the impulse responses obtained as it rotated were not completely correlated. Secondly, since only limited precision was achievable when aligning the samples on the turntable, it is unlikely that their normals were exactly collinear with the axis of rotation. The result of this would be to cause the samples to wobble as they rotated and thus to increase the decorrelation between responses. Both of these adverse practical effects could be substantially reduced by improving the manner in which samples are supported.

The value of δ_r is higher for the square plane than the circular, demonstrating that it is dependent on the shape of samples and not just their surface structure. Edge diffraction is the likely explanation. Scattering will occur at the edges of all samples measured and if they are not circular then the position of their edges within the chamber changes when they are rotated. This changes the impulse response in the same manner as surface scattering and therefore increases δ_r. Even in the case of circular samples, the edge diffraction is unlikely to be completely independent of their orientation unless the edge itself is uniform, especially if the sample has appreciable thickness.

Figure 5.13 also shows that the frequency at which all the 'battens' samples start to become diffusing, i.e. that at which their values of δ_r increase relative to those for the corresponding plane samples, is as expected given the cross-sectional dimensions of the battens. The circular random battens sample is a significantly more effective scatterer than its periodic equivalent over the range of frequencies from approximately 500Hz to 1.5kHz. Since the only difference between these two samples is the arrangement of the battens, this result provides further evidence that periodicity reduces the efficacy of diffusers. In Section 3.14 it was discussed

that the reason for this is that, as a result of interference effects, the polar responses of periodic surfaces contain prominent lobes. One interesting observation from Figure 5.13 is that the frequency range over which there is the greatest disparity between the scattering coefficient values for the circular random and periodic battens samples is approximately coincident with that where there is the greatest similarity between the values of δ_r for the circular and square random battens samples. Outside this range, the square sample is ranked the more effective scatterer but this could be as a result of edge diffraction rather than surface scattering being the dominant diffusion mechanism at these frequencies.

The random hemispheres sample is shown by Figure 5.13 to be a remarkably effective diffuser although perhaps this is not surprising because hemispheres are more isotropic scatterers than battens. However, the value of the scattering coefficient is greater than unity at high frequencies, as it is in fact in the case of the square random battens sample. From (5.7) it is evident that for δ_r to be in excess of unity then the pseudo specular absorption coefficient, a, must also exceed unity and Figure 5.11 confirms that this is indeed the case. The exact reason for this is presently unclear but (5.11) shows that if the effective sample area is in fact larger than the physical area, S_{sample}, as a result of the extra scattering resulting from edge diffraction then the value of a will be overestimated. a is determined using an essentially analogous method to Sabine's absorption coefficient and, although it is physically incorrect, values of this quantity greater than unity have been accepted by acousticians for many years. Furthermore, some of the results published by Mommertz and Vorländer[22] include values of δ_r exceeding unity.

It has recently been shown by Mommertz[65] that the error in the value of δ_r increases as α_{sample} increases and can be considerable; the absolute error can be as great as 0.3 when α_{sample} is 0.5. Therefore the peak at approximately 200Hz in the value of δ_r for the random hemispheres, evident in Figure 5.13, could be erroneous. In fact the ISO working group currently standardising a method for measuring the random incidence scattering coefficient of surfaces consider that

it would not be sensible to use the Mommertz and Vorländer reverberation chamber method for samples with absorption coefficients exceeding 0.5[66]. This is a serious limitation of the technique.

5.5 Appraisal.

The chief advantages of this method for determining the scattering coefficient are that the measurement procedure is familiar, existing reverberation chambers can be used and it is relatively quick. However it is even more critical than is the case with ISO 354 absorption coefficient measurements to keep the conditions in the reverberation chamber, such as temperature and humidity, constant throughout the duration of the measurement[67]. To minimise the influence of edge diffraction on the value of δ_r, samples measured should be circular and thin in comparison to their diameter. One consequence of edge effects is that although δ_r is theoretically bounded between zero and unity, in practice values greater than unity can be obtained. A further drawback is that, in common with the free field method, the value of δ_r for samples which possess complete rotational symmetry will be zero, even if they are effective scatterers such as a single hemisphere. The reason for this is that the impulse response of the chamber does not change when samples of this type are rotated. Whether or not translation instead of rotation is a solution to this problem, as was proposed in the case of the free field method, is again a possible subject for future investigation.

An additional deficiency of the technique is that although measurement of δ_r is uncomplicated, it is difficult, if not impossible, to predict. As mentioned previously, there exists an analogy here with the random incidence absorption coefficient because prediction of this is difficult for anything other than a planar locally reacting surface whereas measurement is straightforward.

Another difficulty with this method of quantifying diffusion is that anisotropic scatterers, such as the arrangements of parallel battens shown in Figures 5.3 to 5.5, are overrated. Although such structures disperse the reflected energy with reasonable uniformity in the plane perpendicular to the battens, in the plane

parallel to the battens the reflection is more specular, as shown in Figure 3.59. The values of δ_r shown in Figure 5.13 for these samples are therefore unjustifiably high, especially at high frequencies. In addition Mommertz and Vorländer have measured the value of δ_r for a QRD using this method and obtained similarly high results[22].

As has been discussed previously in the appraisal of the free field method, δ_r is best suited to quantifying the diffusion efficacy of samples which have surface irregularities that are small in comparison to their dimensions. Diffusion coefficients derived from the polar response are more appropriate for smaller samples with large surface irregularities. However, the Mommertz and Vorländer reverberation chamber method is likely to be standardised by ISO as a method for measuring scattering because their remit is to standardise a 'random incidence scattering coefficient of surfaces' and this is presently the only published technique which yields the random incidence value directly.

5.6 Minimum number of averages required to determine T_{spec}.

Although this method of measuring the random incidence scattering coefficient is much quicker than the free field technique, even less time would be required if n, the number of impulse responses coherently averaged to determine T_{spec}, could be reduced because this is the most time consuming part of the measurement. To determine the minimum value of n for which valid results are obtained, the relationship between n and the resulting T_{spec} values was investigated for the case of the circular random battens sample. This was not straightforward because changing n, without altering the duration of the MLS stimulus, changes the measurement duration and hence the angular velocity at which the sample must rotate.

When n was doubled from one hundred, approximately the number of responses averaged by Mommertz and Vorländer, to two hundred, there was no significant change in the value of T_{spec} in any of the third-octave bands. This verified that a hundred averages is sufficient for T_{spec} to be accurately determined. Having

confirmed this, the value of n was reduced to fifty and it was found that this had little effect on the values of T_{spec} but that it was more difficult to extract these values from the resultant decay because this was less extensive than before. The reason for this reduction in the extent of the resultant decay was that the reduced number of averages was insufficient to eliminate the noise generated by the motor and drive mechanism. When the value of n was halved again, to twenty-five, the resultant decay was limited by motor noise to such a degree that it was not possible to accurately measure the reverberation time, despite the fact that the amount of reduction in the drive train had been increased to reduce the motor speed. To circumvent this problem, the averaging process was performed over two revolutions as opposed to one, the total number of impulse responses averaged therefore being fifty. Although this provided no benefit in terms of time compared with the previous case of averaging fifty responses over a single revolution, the purpose of this measurement was to produce the resultant response which would be obtained when averaging twenty-five responses if motor noise was not an issue. However, because the sample was now taking only approximately 3.6 minutes to perform a revolution, it was more difficult to synchronise its rotation with MLSSA to ensure that the responses were measured with it in exactly the same positions during both revolutions. Although it was difficult to obtain reliable results, especially at the higher frequencies, it did appear as though there was no appreciable change in the decay rates but this result must be treated with scepticism. An attempt was made to reduce the number of responses averaged to ten but, because of its speed, it proved impossible to synchronise the sample with MLSSA for the number of revolutions required to sufficiently reduce the motor noise.

The conclusion of this limited investigation is that the minimum number of responses which must be averaged in order to yield reliable values of T_{spec} is (in the case of the circular random battens sample) less than a hundred but to be any more precise, a means of rotating the sample more quietly would have to be developed.

5.7 Conclusion.

A second method proposed by Mommertz and Vorländer for measuring the scattering coefficient, δ, of surfaces has been presented and discussed. Its concept is similar to that of their free field method examined in the previous chapter but in this case the measurements are made in reverberant conditions. This method yields the value of the random incidence scattering coefficient, δ_r, directly and is thus much less time consuming than the free field method. The measurement procedure is similar to the standard method for measuring random incidence absorption coefficients (ISO 354); it therefore shares many of the benefits and drawbacks of that technique.

Results of the first measurements carried out at an independent laboratory using this method have been presented. These measurements had a dual purpose; to determine the value of δ_r for a variety of test samples and to investigate various practical aspects of the technique. The samples were ranked in the expected manner but some were overrated, especially at high frequencies. This method is best suited to quantifying the diffusion efficacy of surfaces with irregularities that are small in comparison to their dimensions. It is not ideal and would fail to rate some types of surfaces correctly, including those which have complete rotational symmetry, those which redirect as opposed to disperse the reflected energy and those which scatter the reflected energy in a highly anisotropic manner. Nevertheless, this method is likely to be standardised by ISO as the technique for measuring the random incidence scattering coefficient of surfaces.

6. LAM'S METHOD.

6.1 Introduction.

The Mommertz and Vorländer method discussed in the previous chapter was the first of several 'reverberation chamber' techniques for measuring the diffusion efficacy of surfaces which were investigated during this research. Over the course of the next two chapters more of these techniques will be discussed, all of which share the concept of quantifying the diffusion efficacy of surfaces by the indirect approach of measuring their effect on the diffuseness of a sound field in an enclosed space. This contrasts with the free field approach of sampling the reflected field directly.

Although the Mommertz and Vorländer reverberation chamber method does require diffuse conditions, it is misleading to categorise these other measurement techniques as 'diffuse field' because in order for it to be possible that the addition of a sample surface can increase the diffuseness of a sound field, it must in fact be non-diffuse beforehand. Such a non-diffuse sound field can be created in a normal reverberation chamber if one of the surfaces is made absorptive. The diffuseness of a sound field can be evaluated by measuring any one of a number of different properties, examples are the directional distribution of intensity, the spatial variation of sound pressure level and the linearity of the reverberant level decay. Whether a parameter which quantifies the diffusion efficacy of the sample can be elicited from such measurements is the question addressed in Chapter 7.

This chapter, however, is concerned with an alternative approach to quantifying the diffusion efficacy of surfaces from their effect on the diffuseness of a non-diffuse field, suggested by Lam[23]. Lam's method involves comparing the reverberation time measured in a real non-diffuse space with that predicted by a computer model of it which includes diffusion. The diffusion coefficient of the sample is obtained by the trial and error process of adjusting its value in the model until the predicted reverberation time matches the measurement. The definition of this diffusion coefficient depends on how the model implements diffuse reflection.

After presenting the theoretical basis of Lam's method, the chapter continues with a detailed description of a new practical realisation which has enabled this method to be used to evaluate the diffusion efficacy of several sample surfaces for the purposes of this research. Included in this is an examination of how diffuse reflection is implemented in one particular computer model. This new work contributes a practical perspective to the appraisal of Lam's method as a technique for quantifying the diffusion efficacy of surfaces which concludes the chapter.

6.2 Theory.

Since reverberation chambers are simple in shape, it should be possible to accurately predict the sound field within them using computer models. To quantify the diffusion efficacy of a sample using Lam's method, any model in which some form of diffusion coefficient is assigned to each surface can be used but different models often yield different values for the same surface if the manner in which they implement diffusion differs[68]. This does not mean that the method is inaccurate because the physical interpretation of the values will also be different. Obtaining the diffusion coefficient of the sample, d, is a simple but tedious (if not automated) empirical process which requires only that the regular absorption coefficient of the boundary surfaces of the empty chamber (which are all assumed to possess the same absorption and diffusion characteristics), $\alpha_{chamber}$, is either known or can be estimated. Figures 6.1 to 6.3 on the following pages show the process graphically.

The first step is to determine the diffusion coefficient of the boundary surfaces, $d_{chamber}$. This is accomplished by adjusting its value in the model until the predicted reverberation time is equal to that measured in the empty chamber. This trial and error process must be repeated for every frequency band of interest.

The space is now made non-diffuse by making one of the boundary surfaces absorptive as opposed to reflective. The absorption coefficient of this absorbent surface, α_{absorb}, can be measured using ISO 354 and its diffusion coefficient, d_{absorb}, then determined in the same way as $d_{chamber}$. Again, the process must be repeated for every frequency band of interest.

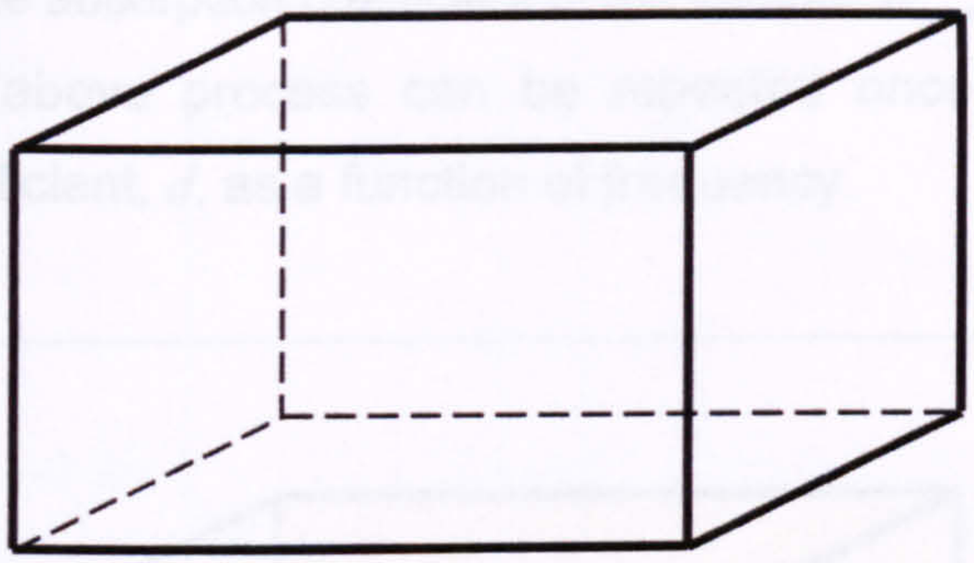

- Assume $\alpha_{chamber}$
- Determine $d_{chamber}$ by trial and error.

Chamber boundary surfaces, $\alpha_{chamber}$, $d_{chamber}$.

Figure 6.1: Step 1 of Lam's method for calculating the diffusion coefficient, d, of a sample surface.

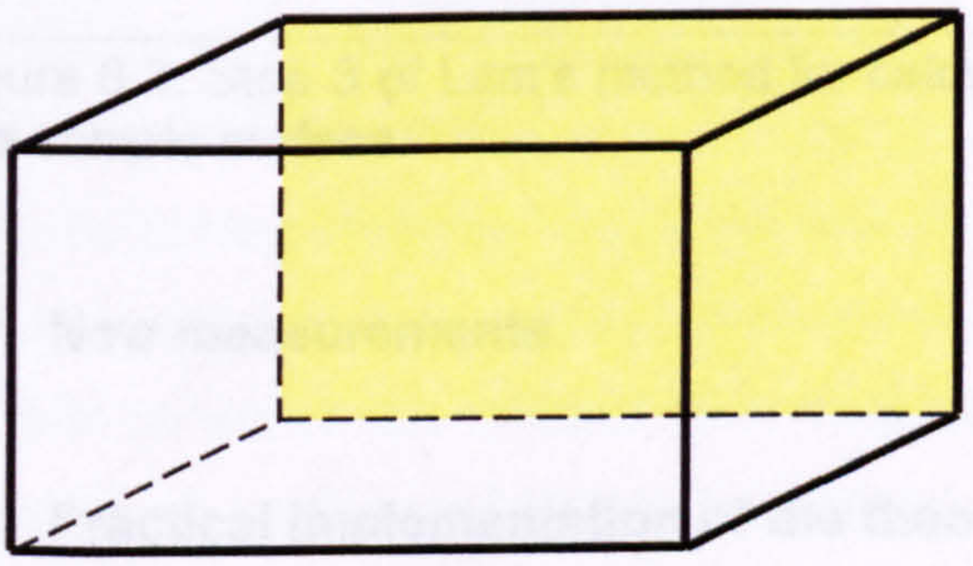

- Introduce absorptive wall with known α_{absorb}.
- Determine d_{absorb} by trial and error.

Chamber boundary surfaces, $\alpha_{chamber}$, $d_{chamber}$.

Absorptive wall, α_{absorb}, d_{absorb}.

Figure 6.2: Step 2 of Lam's method for calculating the diffusion coefficient, d, of a sample surface.

One of the remaining reflective surfaces is now replaced with the sample. So long as the absorption coefficient of the sample, α_{sample}, has been previously determined, the above process can be repeated once again to determine its diffusion coefficient, d, as a function of frequency.

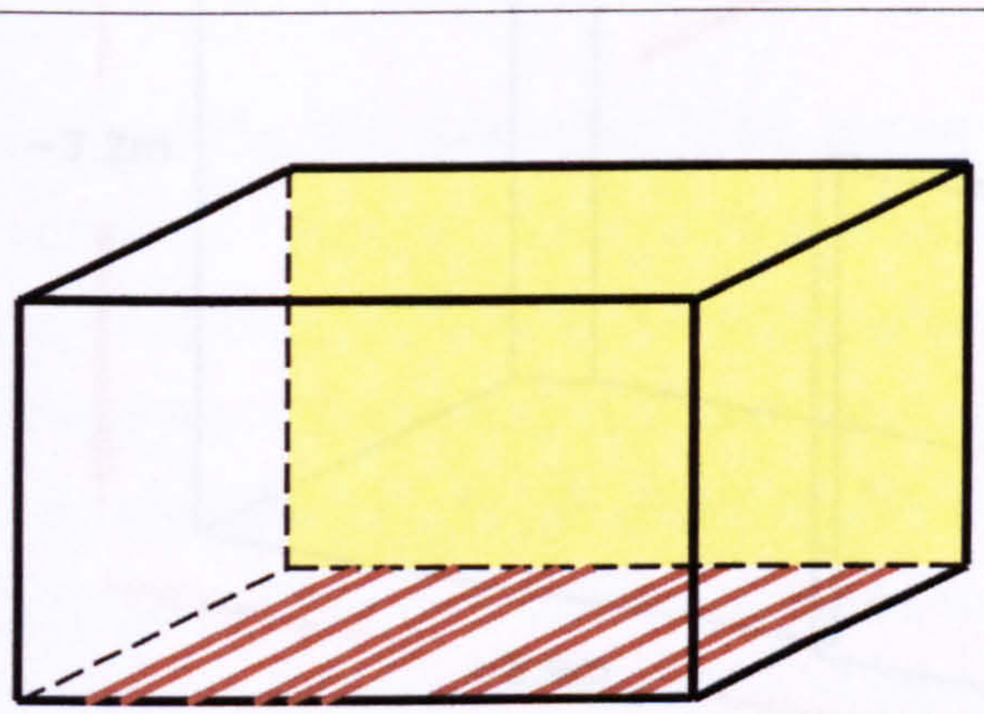

Figure 6.3: Step 3 of Lam's method for calculating the diffusion coefficient, d, of a sample surface.

6.3 **New measurements**.

6.3.1 **Practical implementation of the theory**.

Although this method of quantifying the diffusion efficacy of surfaces is theoretically simple, only a single set of results, obtained in 1:10 scale using a model reverberation chamber, have been published previously[23]. Therefore in order to appraise the method from a practical perspective, some new measurements were carried out as part of this research. These measurements were performed in the same $30m^3$ reverberation chamber utilised for the diffuse field Mommertz and Vorländer measurements, the geometry of which is shown in Figure 6.4 on the following page.

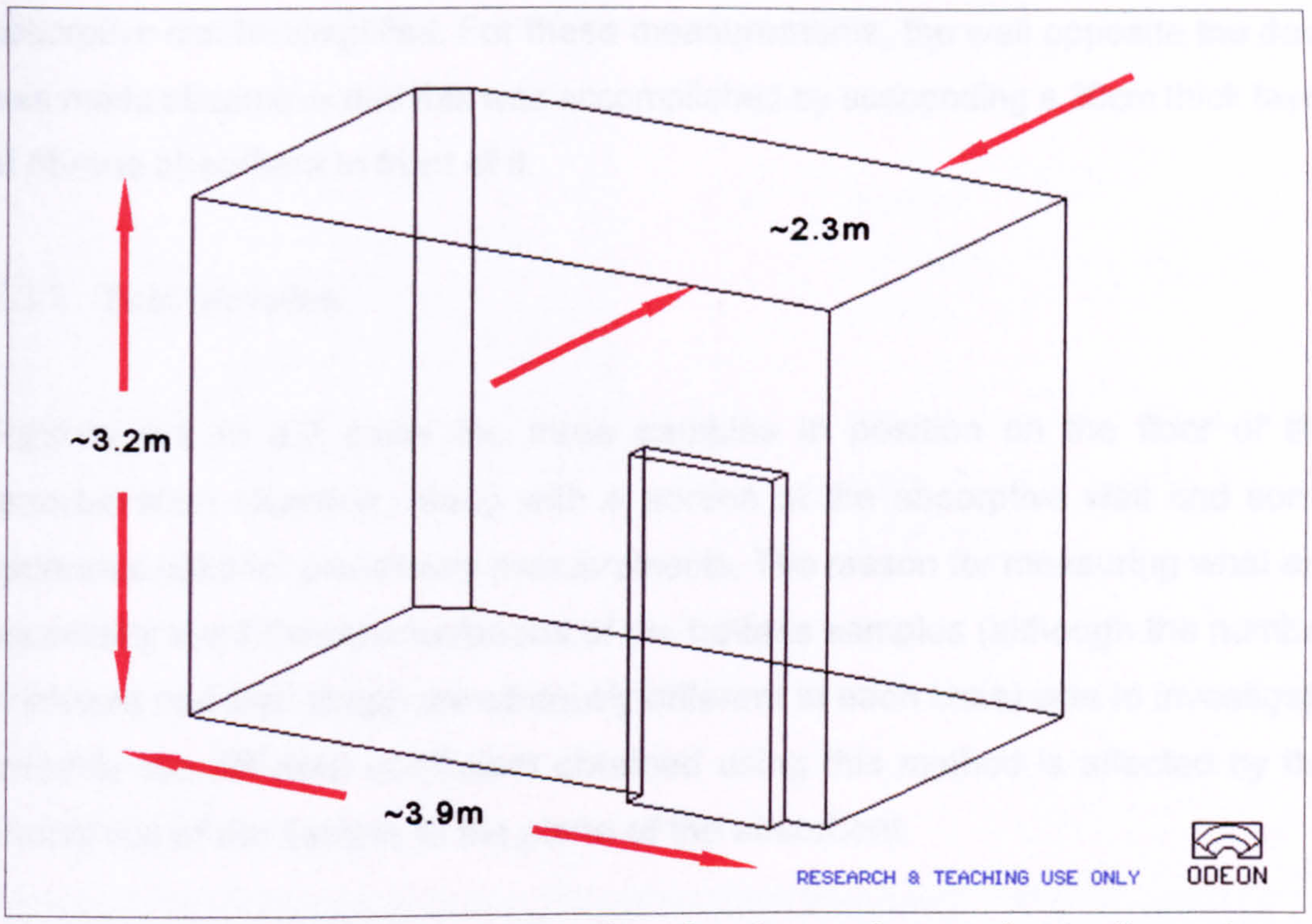

Figure 6.4: Diagram of the reverberation chamber and approximate dimensions.

The samples measured are described in Section 6.3.2 below; they were similar arrangements of battens and hemispheres to those measured using the Mommertz and Vorländer reverberation chamber method but their dimensions are larger because for Lam's method it is necessary for the sample to completely cover one of the boundary surfaces of the reverberation chamber. The nature of these samples meant that the easiest surface to cover was the floor because this is the only one on which the battens or hemispheres could simply be placed in the desired configuration and held in position by gravity. Covering the floor with the sample meant that one of the walls had to be made absorptive. (Although covering the ceiling is an alternative, it is likely that this would affect the value of d obtained because since the action of a diffuser is to spread the reflected energy away from the specular direction, the increase in incident energy resulting from the presence of the sample on the floor will not be as great for the ceiling as for the walls[46].) However, once the reverberation time of the empty chamber has been measured, this surface can remain absorptive whilst the diffusion coefficients of the various samples are evaluated. Since it is not necessary for this surface to be readily interchangeable between absorptive and reflective, the method used to make it

absorptive can be simplified. For these measurements, the wall opposite the door was made absorptive and this was accomplished by suspending a 30cm thick layer of fibrous absorbent in front of it.

6.3.2 **Test samples**.

Figures 6.5 to 6.7 show the three samples in position on the floor of the reverberation chamber, along with a portion of the absorptive wall and some apparatus used for preliminary measurements. The reason for measuring what are essentially two different orientations of the battens samples (although the number of battens and their length are obviously different in each case) was to investigate whether the diffusion coefficient obtained using this method is affected by the orientation of the sample to the plane of the absorbent.

Figure 6.5a: Random battens. (Perpendicular to absorptive wall)

Figure 6.5b: Random battens. (Parallel to absorptive wall)

Figure 6.6a: Periodic battens. (Perpendicular to absorptive wall)

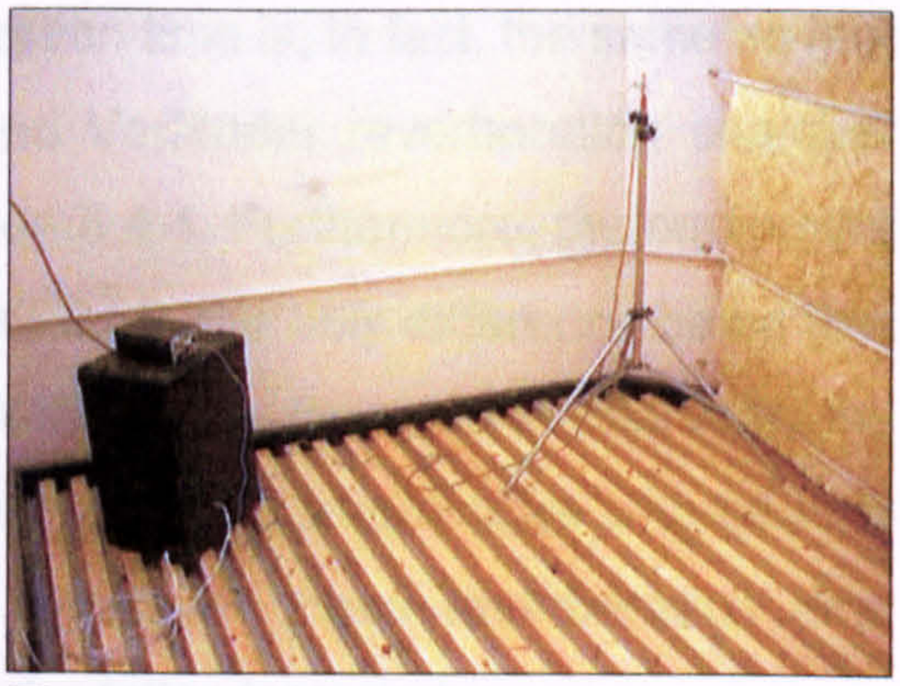

Figure 6.6b: Periodic battens. (Parallel to absorptive wall)

Figure 6.7: Random hemispheres.

- All samples are assumed to be 1:2 scale.
- Battens are varnished hardwood, 50mm in cross-section.
- Hemispheres are 20cm in diameter and formed from 1.5mm ABS.

6.3.3 **Determining the reverberation time of the non-diffuse space by measurement**.

The first step in quantifying the diffusion efficacy of these samples using Lam's method was to determine the reverberation time of the chamber both with and without them present. Since the space is non-diffuse, the reverberation time is not completely independent of position. Therefore in each case a spatial mean over ten microphone positions, five for each of two source positions was evaluated. At each microphone position, sixteen individual impulse responses were pre-averaged and the resultant response bandpass filtered and then Schroeder integrated to yield the energy decay in third-octave bands. The reverberation time at the position was then obtained by extrapolating the -5dB to -35dB section of these decays.

This procedure for determining the reverberation time is, in fact, the same as that followed in the case of the Mommertz and Vorländer reverberation chamber method measurements, described in Section 5.4.4. Furthermore, the equipment used was the same as that shown in Figure 5.10, the only difference being that since the absorptive wall reduced the reverberation time of the chamber, the measurement bandwidth could be extended to higher frequencies without time aliasing compromising the results. The results of these reverberation time measurements are shown in Figure 6.8 on the following page.

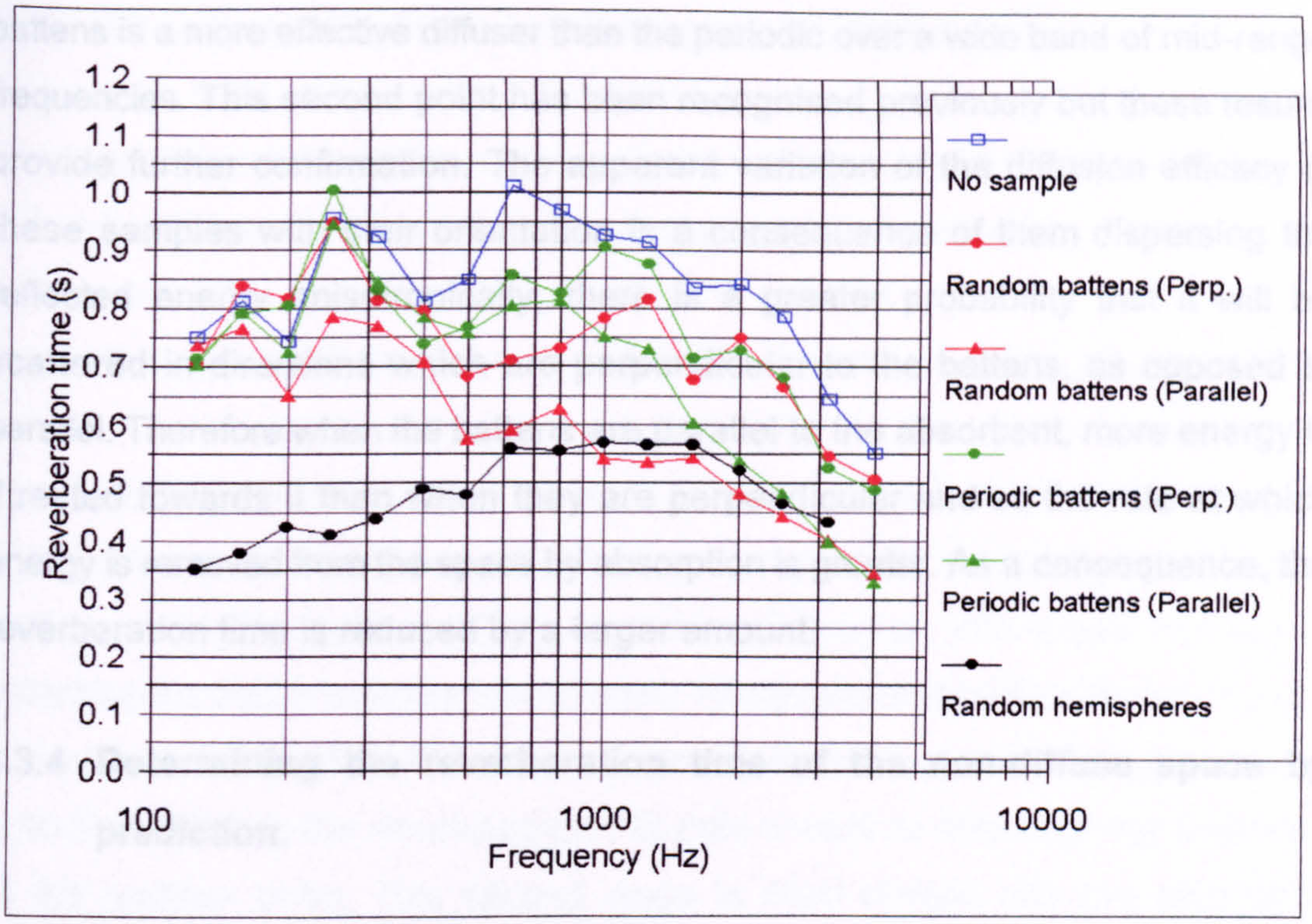

Figure 6.8: Effect of each of the samples on the reverberation time of the non-diffuse space.

It can be seen that the broad effect of all the samples is to reduce the reverberation time, although most arrangements of the battens have little effect below approximately 400Hz. In general, this reduction of the reverberation time will be caused by a combination of both absorption and diffusion so it would not be possible to deduce anything about the diffusion efficacy of the samples from these results alone. However, the absorption coefficient of the battens is small and can be assumed to be independent of their arrangement[†]. Thus in the case of these samples any reduction of the reverberation time is predominantly a result of diffusion and Figure 6.8 therefore ranks their diffusion efficacy.

From Figure 6.8, two conclusions regarding the amount of scattering produced by the battens samples can be drawn: When the battens are orientated parallel to the absorptive wall, the diffusion efficacy of the sample is rated as greater than when they are perpendicular and, for both orientations, the random arrangement of

---

† Although the absorption coefficient of varnished wood is very small[69], since neither the battens nor the chamber floor were geometrically perfect, it is likely that these samples did have some absorption as a result of viscous losses in the small gaps between adjacent battens and between battens and the floor.

battens is a more effective diffuser than the periodic over a wide band of mid-range frequencies. This second point has been recognised previously but these results provide further confirmation. The apparent variation of the diffusion efficacy of these samples with their orientation is a consequence of them dispersing the reflected energy anisotropically; there is a greater probability that it will be scattered in directions which are perpendicular to the battens, as opposed to parallel. Therefore when the battens are parallel to the absorbent, more energy is directed towards it than when they are perpendicular and so the rate at which energy is removed from the space by absorption is greater. As a consequence, the reverberation time is reduced by a larger amount.

6.3.4 Determining the reverberation time of the non-diffuse space by prediction.

Simply measuring the effect of a sample on the reverberation time of a non-diffuse space does allow some qualitative evaluation of its diffusion efficacy if it is essentially non-absorptive. However, in order to evaluate a diffusion coefficient which quantifies the scattering produced by any sample, it is necessary to proceed to the second step of Lam's method and use a computer model to predict the reverberation time of the space. The model suggested by Lam and which was used in the determination of the only published results obtained using this method[23] is the ODEON room acoustics program developed at the Acoustics Laboratory of the Technical University of Denmark[70]. All work with ODEON conducted during this research utilised version 2.6 of the software.

ODEON 2.6 is a hybrid ray tracing prediction model which can be used to investigate many aspects of room acoustics. At the present time, simplifications of acoustic phenomena have to be made in order for any computer model to be practically useful. In this particular model this is accomplished by making the following assumptions:

- The laws of geometrical acoustics hold, i.e. sound energy travels in straight lines and wave phenomena are absent.

- All surfaces are plane and infinite as far as diffraction is concerned.
- Surfaces absorb sound energy according to an energy absorption coefficient which is independent of angle of incidence.
- Sound is treated as an energy function, i.e. phase effects are neglected.

The salient parameters which must be specified in order to predict the energy decay are the room geometry, the absorption and diffusion coefficients of all its surfaces and the position of the source and receiver. The actual process of predicting the decay comprises two stages: Firstly rays emitted from the source are traced around the room in a purely geometrical process, 'discovering' potential reflection paths. In the second stage this data is used to determine the response at the receiver point. This second stage is itself divided into two algorithms because finding all the reflections which would be received at any point is a hopelessly large task, the number is so enormous. Therefore up to a certain (user specified) reflection order, known as the early-reverberant transition order, the rays are used to discover the location of image sources[71] and it is these which produce the early reflections, although only those image sources which are visible from the receiver actually contribute to the response. Above this reflection order the purpose of the ray tracing is instead to generate secondary sources on the room surfaces. These secondary sources produce the later reflections, the contributions of which at the receiver ensure that the energy decay is approximately correct and the reflection density adequately high. This hybrid method thus fulfils the demands of the image source theory up to an arbitrary (but limited) time in the response and does not require vast amounts of time to estimate the reverberant decay.

In ODEON 2.6, diffusion is understood to be, "*the process whereby the transport of sound energy in a room gradually becomes more and more chaotic with time*"[70]. This concept encompasses all phenomena which cause the energy incident on a surface to be spread into a larger solid angle after reflection and so includes edge diffraction in addition to effects caused by surface irregularities and impedance changes.

Early reflections in the model are unaffected by diffusion; the diffusion coefficients of surfaces are irrelevant for these reflections. Therefore during ray tracing, rays are specularly reflected up to and including the early-reverberant transition order, which for this application was set to two because lower values resulted in flawed predictions of the decay; the early decay time exceeded the reverberation time. At subsequent reflections diffusion is implemented by determining the direction of the reflected ray according to the following process: A random number between zero and unity is generated; if this exceeds the diffusion coefficient of the surface then the ray is specularly reflected, otherwise the reflection direction is chosen at random from a Lambertian distribution[27]. The diffusion coefficient of a surface is therefore the probability that a ray will not be specularly reflected from it during the ray tracing process (when the order of the reflection exceeds the early-reverberant transition order).

The first step in predicting the reverberation time of the non-diffuse space using the computer model was to determine the absorption and diffusion coefficients of the plane, reflective, boundary surfaces. Their diffusion coefficient was assumed to be 0.1 at all frequencies because this is the value suggested by Naylor and Rindel for plane surfaces[70]. They add that values of less than 0.1 should probably be avoided. The absorption coefficient was evaluated empirically by the iterative process of adjusting its value until the predicted reverberation time was the same as that measured in the completely empty chamber. Just as was the case with the measurements, this predicted reverberation time was a spatial mean evaluated over ten receiver positions, although only a single source position was used. Figure 6.9 on the following page shows their locations within the space.

Since the model predicts reverberation times in octave as opposed to third-octave bands, it was necessary to calculate octave band values from the measured data in addition to the third-octave results shown in Figure 6.8. Table 6.1 shows the measured octave band reverberation times of the completely empty chamber[††].

---

†† The centre frequencies have been scaled to enable the diffusion coefficient values determined using this method to be compared with those obtained for the same samples by other techniques. However, the scaling is not exactly correct because a scale factor of two has been used for simplicity whereas the true value is slightly greater than this.

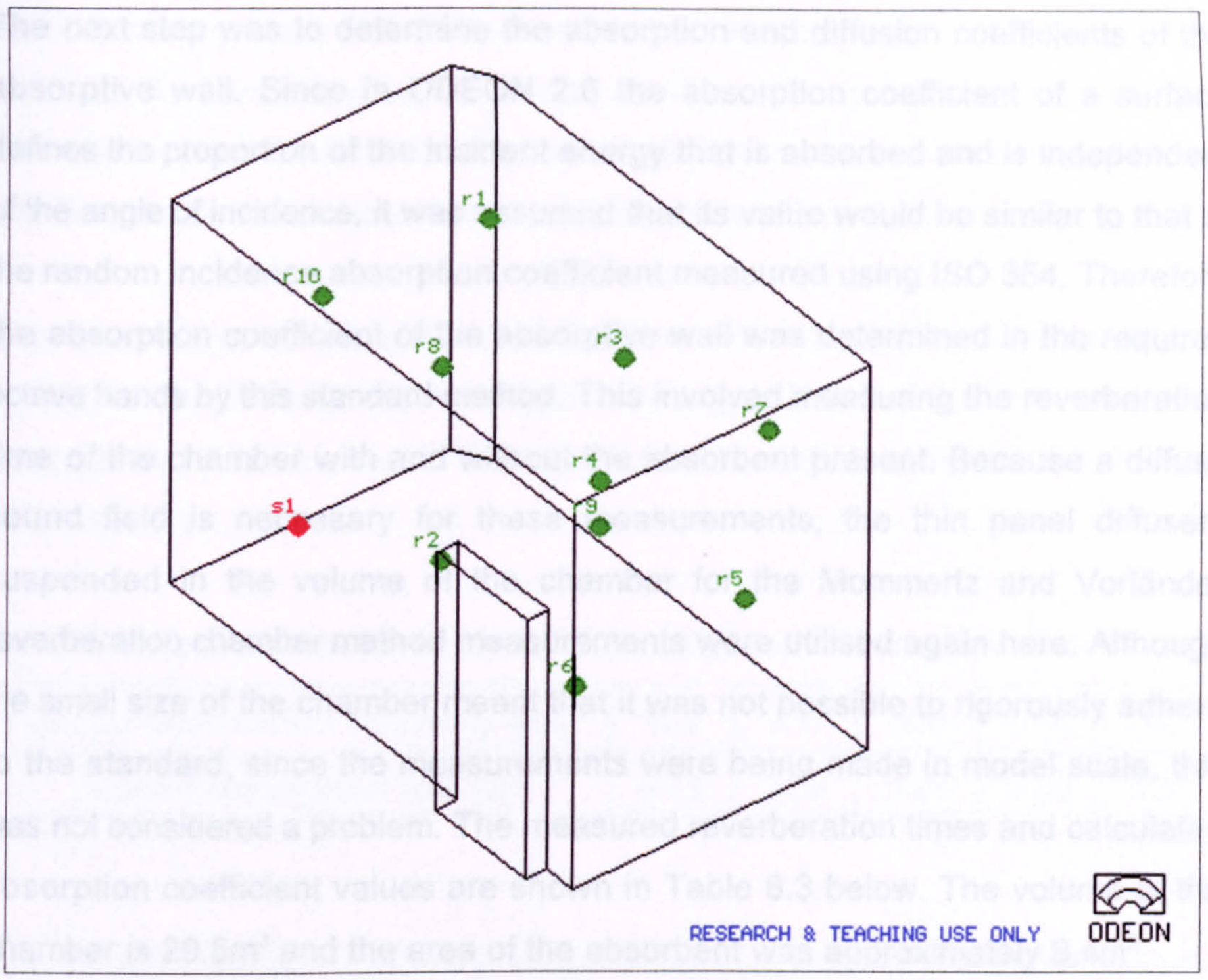

Figure 6.9: Source and receiver positions within the reverberation chamber.

Table 6.1: Measured mean reverberation time of the completely empty chamber.

Octave band centre frequency (Hz)	125	250	500	1000	2000
Mean reverberation time (s)	3.75	3.89	3.52	2.94	2.09

The octave band absorption coefficient values for the reflective boundary surfaces which resulted in the reverberation time of the completely empty chamber predicted by the model being the same in all bands as the measured values in Table 6.1 are given, to two decimal places, in Table 6.2. These absorption coefficient values are reasonable for a plane, reflective, surface.

Table 6.2: Calculated absorption coefficient of the reflective boundary surfaces.

Octave band centre frequency (Hz)	125	250	500	1000	2000
Absorption coefficient	0.02	0.02	0.02	0.02	0.02

The next step was to determine the absorption and diffusion coefficients of the absorptive wall. Since in ODEON 2.6 the absorption coefficient of a surface defines the proportion of the incident energy that is absorbed and is independent of the angle of incidence, it was assumed that its value would be similar to that of the random incidence absorption coefficient measured using ISO 354. Therefore the absorption coefficient of the absorptive wall was determined in the required octave bands by this standard method. This involved measuring the reverberation time of the chamber with and without the absorbent present. Because a diffuse sound field is necessary for these measurements, the thin panel diffusers suspended in the volume of the chamber for the Mommertz and Vorländer reverberation chamber method measurements were utilised again here. Although the small size of the chamber meant that it was not possible to rigorously adhere to the standard, since the measurements were being made in model scale, this was not considered a problem. The measured reverberation times and calculated absorption coefficient values are shown in Table 6.3 below. The volume of the chamber is 29.5m^3 and the area of the absorbent was approximately 9.4m^2.

Table 6.3: Calculation of the absorption coefficient of the absorptive wall.

Octave band centre frequency (Hz)	125	250	500	1000	2000
Mean RT without absorptive wall	3.19	3.22	2.89	2.45	1.38
Mean RT with absorptive wall	0.45	0.36	0.33	0.31	0.28
Absorption coefficient	0.95	1.26	1.36	1.39	1.42

These results were not entirely unexpected because absorption coefficients greater than unity are often obtained for effective absorbers. However, the maximum value of absorption coefficient accepted by the model is unity and so this was the value ascribed to the absorptive wall for those bands in which the measured coefficient exceeded unity. It was hoped that by assigning these absorption coefficients to the model absorptive wall, its diffusion coefficient could be determined by the empirical iterative comparison method. However, the resulting predicted reverberation times of the non-diffuse space were in fact much shorter than those measured, whatever the diffusion coefficient of the absorptive

wall. Even changing the early-reverberant transition ratio did not solve the problem. The only way forward was to abandon this approach and revert to the procedure followed for the reflective boundary surfaces; assume a diffusion coefficient value and determine the absorption coefficients empirically.

The measured octave band reverberation times of the non-diffuse space are given in Table 6.4. The reason that these are longer than the corresponding 'with absorptive wall' times stated in Table 6.3 is that those were obtained with diffusers in the space.

Table 6.4: Measured mean reverberation time of the chamber with absorptive wall.

Octave band centre frequency (Hz)	125	250	500	1000	2000
Mean reverberation time (s)	0.73	0.88	0.88	0.93	0.82

The diffusion coefficient of the absorptive wall was arbitrarily assumed to be 0.1 at all frequencies. The absorption coefficient values which then caused the predicted reverberation times of the non-diffuse space to be the same as the measured values in Table 6.4 are shown in Table 6.5.

Table 6.5: Empirically calculated absorption coefficient of the absorptive wall.

Octave band centre frequency (Hz)	125	250	500	1000	2000
Absorption coefficient	0.57	0.42	0.41	0.35	0.35

Although the layer of absorbent is rigidly backed, considering its thickness these absorption coefficient values are low, especially at the higher frequencies[69]. Nevertheless they are the values which equalised the predicted and measured reverberation times. They were not significantly altered by changing the value of the diffusion coefficient so this was left as 0.1.

6.3.5 **Results.**

Having assigned absorption and diffusion coefficients to all the boundary surfaces of the non-diffuse space, albeit not quite in the manner intended, the diffusion coefficients of the samples could be evaluated. The battens samples were assumed to have absorption coefficients of zero at all frequencies, therefore their diffusion coefficients, d, could be directly determined by the now familiar process of iteratively adjusting the diffusion coefficient of the appropriate model surface until the predicted reverberation time matches that obtained by measurement. The results for the battens samples, in terms of reverberation times and diffusion coefficients, are presented in Tables 6.6 to 6.9.

Table 6.6: Diffusion coefficient of random battens perpendicular to absorptive wall.

OBCF (Hz)	125	250	500	1000	2000
RT (s)	0.71	0.85	0.74	0.76	0.70
d	0.19 - 0.20	0.20 - 0.21	>1.00	>1.00	>1.00

Table 6.7: Diffusion coefficient of random battens parallel to absorptive wall.

OBCF (Hz)	125	250	500	1000	2000
RT (s)	0.65	0.73	0.64	0.57	0.46
d	0.28 - 0.29	>1.00	>1.00	>1.00	>1.00

Table 6.8: Diffusion coefficient of periodic battens perpendicular to absorptive wall.

OBCF (Hz)	125	250	500	1000	2000
RT (s)	0.69	0.86	0.79	0.86	0.70
d	0.20 - 0.21	0.19 - 0.20	0.71 - 0.72	0.64 - 0.65	>1.00

Table 6.9: Diffusion coefficient of periodic battens parallel to absorptive wall.

OBCF (Hz)	125	250	500	1000	2000
RT (s)	0.66	0.85	0.78	0.76	0.53
d	0.27 - 0.28	0.20 - 0.21	0.86 - 0.87	>1.00	>1.00

In the cases where d is given as '>1.00', the predicted reverberation time could not be reduced to the corresponding measured value, even if the diffusion coefficient of the sample was set to unity.

Figure 6.10 shows how the predicted reverberation time of the non-diffuse space varies with the diffusion coefficient assigned to the floor in each of the five octave bands considered here. The absorption coefficient of the floor is assumed to be zero at all frequencies.

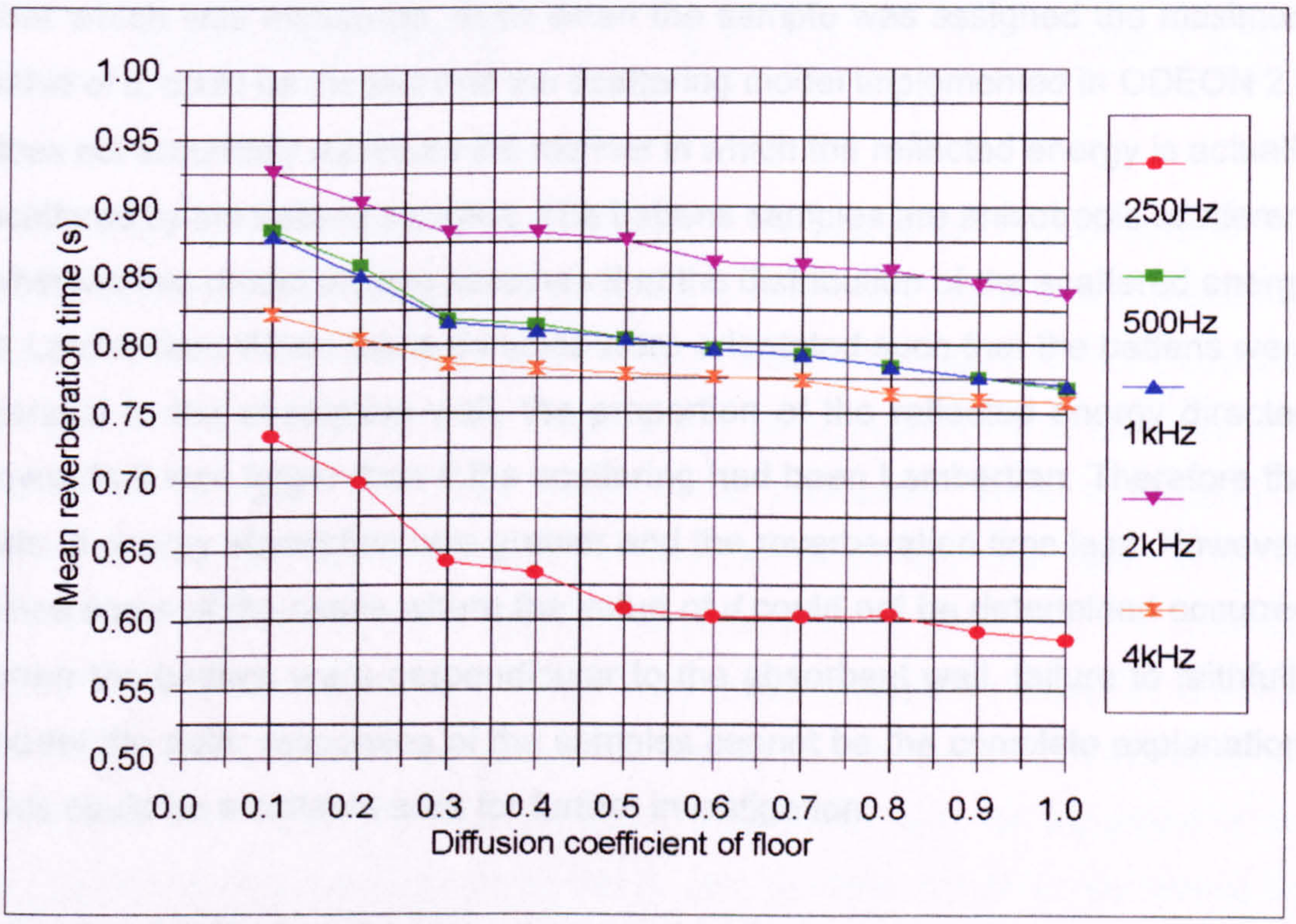

Figure 6.10: Effect of the value of d assigned to the floor on the mean predicted reverberation time of the non-diffuse space.

In addition to observing that increasing d decreases the reverberation time, the

most distinct features are that the effect of d on the reverberation time is small and decreases with increasing frequency and that the magnitude of this change is greater in the lower half of the range of d values than the upper.

From the values of d which could be determined, it can be seen from Tables 6.6 to 6.9 that this method of quantifying diffusion rates the efficacy of these samples as higher in the 500Hz octave band and above than at lower frequencies. This is concordant with the cross-sectional dimensions of the (full-scale) battens. Although the amount of useful data in the results is limited, they do substantiate the conclusion drawn previously from other measurements that a random arrangement of battens is a more effective diffuser than a periodic arrangement. They also demonstrate that, for these samples, the diffusion coefficient values obtained using this method are dependent on their orientation to the absorptive wall.

The reason why the predicted reverberation time frequently remained longer than that which was measured, even when the sample was assigned the maximum value of d, could be the fact that the scattering model implemented in ODEON 2.6 does not accurately represent the manner in which the reflected energy is actually scattered by the battens samples. The battens samples are anisotropic scatterers whereas this model always assumes that the distribution of the scattered energy is Lambertian. When these samples were orientated such that the battens were parallel to the absorptive wall, the proportion of the reflected energy directed towards it was larger than if the scattering had been Lambertian. Therefore the rate of energy absorption was greater and the reverberation time less. However, since some of the cases where the value of d could not be determined occurred when the battens were perpendicular to the absorbent wall, failure to faithfully model the polar responses of the samples cannot be the complete explanation. This could be a suitable area for further investigation.

Since the distribution of scattered energy from a hemisphere is more Lambertian than that from battens, it was reasonable to assume that the diffusion coefficient of the random hemispheres sample would be better suited to determination by this method than those of the battens samples. However, during the course of the

Mommertz and Vorländer reverberation chamber method measurements discussed in the previous chapter, it was established that the random hemispheres sample has significant absorption. Consequently, before ODEON 2.6 could be used to evaluate its diffusion coefficient, it was necessary to assign the absorption of the sample to the appropriate model surface. Obtaining the required octave band absorption coefficients involved reprocessing some of the data obtained during the Mommertz and Vorländer reverberation chamber method measurements because the absorption coefficient values evaluated previously and presented in Figure 5.12 were for third-octave bands. The resulting octave band values are shown along with the reverberation times in Table 6.10.

Table 6.10: Random hemispheres sample - calculated absorption coefficient and measured reverberation time of the chamber.

Octave band centre frequency (Hz)	125	250	500	1000	2000
Absorption coefficient	0.43	0.30	0.22	0.23	0.17
Reverberation time (s)	0.37	0.44	0.53	0.56	0.50

After assigning these absorption coefficients to the appropriate model surface, the usual technique was employed to attempt to determine the diffusion coefficient values. However, the predicted reverberation time was longer than the measured values shown in Table 6.10 for every octave band, regardless of the value of d. Since this problem had been encountered previously, when attempting to parameterise the absorptive wall, it was not surprising that again a set of absorption coefficient values determined essentially by using ISO 354 were not those required by ODEON 2.6 to accurately model the space. However, whereas the measured values for the absorptive wall had to be reduced, in this case the predicted and measured reverberation times could only be equalised if the absorption coefficients were increased. In fact, in order to sufficiently reduce the predicted reverberation time, the random hemispheres sample had to be made more absorbent than the absorptive wall, even if its diffusion coefficient was set to unity. Since this is absurd, using Lam's method to quantify the diffusion efficacy of this sample was abandoned.

6.4 Appraisal.

Lam's method has one principal advantage over the other techniques for quantifying diffusion investigated during this research; the diffusion coefficient values it yields can, in theory, be directly incorporated into the computer model used for their determination, in this case ODEON 2.6. Diffusion coefficients evaluated by any of the other methods discussed in previous chapters cannot be utilised in computer models unless either the implementation of diffusion in the model is the same as the definition of the measured coefficient or the relationship between the measured value and that required by the model has first been established. However this advantage is not as great as may initially be expected because Lam himself has shown that in addition to different models requiring different diffusion coefficient values for the same surface, for some models the diffusion coefficient of a surface is application dependent[3]. The consequence of this second finding is that the values for a sample surface obtained using a simple non-diffuse space may not be the same at all frequencies as those required for the same surface when it is incorporated in a model of an actual space, even if the prediction model is unchanged.

Both the physical interpretation and the properties of a diffusion coefficient evaluated using Lam's method are determined by how diffusion is implemented in the particular model used. In the case of ODEON 2.6, the diffusion coefficient of a surface is simply the probability that a ray will not be specularly reflected (if the order of reflection exceeds the early-reverberant transition order, otherwise its value is inconsequential) and is therefore bounded between zero and unity. Establishing whether or not the value of this coefficient has any physical significance outside the model would require further investigation but it does enable the diffusion efficacy of different surfaces to be compared and ranked.

Although the empirical process which forms the foundation of this method for quantifying the diffusion efficacy of surfaces is theoretically simple, it is tedious and difficult to implement in practice. One practical difficulty is that the random incidence absorption coefficient of a surface measured using ISO 354 is not strictly

the proportion of the total incident energy it absorbs, the quantity usually required by a computer model. If it were then values greater than unity would not be obtained. The absorption coefficients of both the absorptive boundary surface of the non-diffuse space and the samples must be determined accurately because the diffusion coefficient value assigned to a sample has in comparison a much smaller effect on the reverberation time of the space. Although the absorption coefficient of some surfaces could be measured using the standard impedance tube methods[4,5], determining a random incidence value using this technique is tedious and would be practically difficult for rough surfaces such as the random hemispheres sample measured here. A further undesirable practical feature of Lam's method is that the sample must cover the whole of one of the reflective surfaces of the non-diffuse space, making it unsuitable for rating individual diffusers.

This method is therefore best suited to quantifying the diffusion efficacy of extensive surfaces which are non-absorbent and which also scatter the reflected energy in at least approximately the same manner as scattering is implemented in the model. The implicit requirement of this final criterion is that the scattered sound field must be reasonably isotropic because current room acoustics prediction models which include diffusion assume that the polar response of any surface which is not specularly reflective is either uniform or Lambertian. Although in some cases this assumption causes flawed prediction of early reflections, in most 'normal' rooms it does not introduce any significant error into the predicted reverberant field because the number of reflections involved is so large. However in contrived situations such as the non-diffuse space utilised here, where the distribution of absorption on the boundary surfaces is highly uneven, the reverberation time is not independent of the sample's polar response. As a consequence the efficacy of surfaces which scatter the reflected energy anisotropically, such as arrangements of parallel battens, will fail to be correctly rated by this method of quantifying diffusion.

With the benefit of hindsight, better results might have been obtained if the efficiency of the absorptive wall had been reduced because this might have

improved the matching between ISO 354 α_{sample} values and those required by the prediction model. If, as appears to have happened here, the model fails to accurately model the chamber as soon as the absorptive wall is introduced, this method is unlikely to quantify the diffusion efficacy of samples in a meaningful manner.

6.5 Conclusions.

A method for quantifying the diffusion efficacy of surfaces from their effect on the reverberation time of a non-diffuse space has been presented. In addition to measurements, predictions obtained using a computer model are an integral component of this technique. The ODEON 2.6 model is outlined, particular attention being given to the manner in which it implements diffusion. The application of this method to quantify the diffusion efficacy of several sample surfaces is described. The success of these new measurements/predictions was limited by experimental difficulties. Although the method is straightforward in principle, in practice it is tedious, appropriate only for certain types of surfaces and the resulting diffusion coefficient values are specific to the particular computer model used. Therefore it is currently unsuitable for general use but has potential if better computer models become available.

7. OTHER METHODS OF QUANTIFYING DIFFUSION.

7.1 Introduction.

One of the drawbacks of Lam's method for quantifying the diffusion efficacy of surfaces is that the value of the resulting diffusion coefficient is dependent on the prediction model used and may also be affected by the geometry of the non-diffuse space. In Section 6.3.3 it was demonstrated that replacing a specularly reflective boundary surface of a non-diffuse space with one which is equally reflective but instead scatters the reflected sound, decreases the reverberation time of the space, indicating that the diffuseness of the sound field is increased[72]. This suggests that it may be possible to quantify the diffusion efficacy of a surface by measuring its effect on the diffuseness of a non-diffuse sound field.

In the first part of this chapter, several measures of sound field diffuseness are examined and practical investigation of how their value in a non-diffuse space changes with the introduction of different scattering surfaces is described. It is then discussed whether, in general, the diffusion efficacy of surfaces could be determined from any of these changes. The chapter concludes by considering some alternative free field methods for quantifying diffusion and discussing why a comprehensive investigation into its subjective aspects is required.

7.2 Reverberation chamber techniques.

There are a number of approaches to evaluating the diffuseness of a sound field but no standard technique. The most familiar method is probably that developed by Thiele[73] in the 1950s. Thiele's method involves using a highly directional microphone to measure the intensity incident at a point in the sound field from directions uniformly distributed around it. Plotting this intensity as a function of direction yields a polar response similar in form to those considered in previous chapters but representing the variation with direction of the incident as opposed to reflected energy. In an analogous manner to quantifying the diffusion efficacy of surfaces by examining their polar response, as discussed in Chapter 3, the

diffuseness of the sound field (at the measurement point) can be evaluated from the similarity between this response and the uniform case corresponding to an ideal diffuse field. This similarity could be evaluated using any of the parameters discussed in Chapter 3. However, since a large amount of information is lost when a polar response is represented by a single figure, although Thiele did initially suggest reducing the polar response to the parameter defined in (7.1), he later, in conjunction with Meyer, considered the graphical representation to be superior[74].

$$d = 1 - \frac{\sum_{i=1}^{n} |E_i - \overline{E}|}{n\overline{E}} \cdot \frac{n\overline{E}_0}{\sum_{i=1}^{n} |E_{0,i} - \overline{E}_0|} \qquad (7.1)$$

where:

E_i = Energy incident from direction i

$E_{0,i}$ = Energy incident from direction i in free field conditions

$$\overline{E} = \frac{1}{n}\sum_{i=1}^{n} E_i \quad , \quad \overline{E}_0 = \frac{1}{n}\sum_{i=1}^{n} E_{0,i}$$

n = number of equally spaced incident directions

Although quantifying the diffuseness of a space by sampling the directional uniformity of the incident energy at various points is a straightforward concept, practically measuring the required intensities is not a simple task, even today. Since one of the criteria of the ideal diffusion coefficient is that it should be easy to measure, it was investigated whether the change in diffuseness of a non-diffuse space resulting from the introduction of a sample surface could alternatively be observed by measuring any of the following properties:

- Mean reverberation time.

- Spatial variation of reverberation time.

- Spatial variation of sound pressure level.

- Linearity of the reverberant level decay, via the mean correlation coefficient.

The ultimate objective of these investigations was to assess the feasibility of quantifying the diffusion efficacy of surfaces by measuring their effect on these properties. It will be shown that the issue is not how the diffuseness is measured but defining quantifiable limits.

7.2.1 **Mean reverberation time.**

It is well known that introducing diffusing elements either onto the boundary surfaces or into the volume of a non-diffuse space decreases its reverberation time. Hodgson has demonstrated using a ray-tracing prediction model that the effect is similar regardless of how the diffusion is applied[75]. There is however a limit beyond which the reverberation time cannot be further reduced purely by means of diffusion. This limiting value, RT_{min}, is the reverberation time in the case when the sound field in the space is ideally diffuse and it can be predicted using the Eyring reverberation time formula shown below.

$$RT_{min} = -\frac{0.161\,V}{S\ln(1-\bar{\alpha})} \tag{7.2}$$

where:

V = Volume of the space

S = Total surface area of the space

$$\bar{\alpha} = \frac{1}{S}\sum_{i=1}^{n} S_i\alpha_i$$

S_i = Area of boundary surface i

α_i = Absorption coefficient of boundary surface i

n = Number of boundary surfaces

In Section 6.3.4, the measurements performed to determine the absorption coefficient of the absorptive wall which converted the reverberation chamber used during the course of this research into a non-diffuse space are described. The ISO 354 method was used and since this requires the sound field to be diffuse, volume diffusers were added to the chamber until the reverberation time in each octave band no longer decreased. It is therefore reasonable to assume that these minimum mean reverberation times are the RT_{min} values for the chamber when the rear wall is absorptive. However this cannot be verified using (7.2) because the absorption coefficients of the boundary surfaces are not known.

Since the difference between RT_{min} and the reverberation time measured when there are no diffusers present, RT_{empty}, is the maximum reduction that can be achieved by the addition of either volume or surface diffusers to the non-diffuse space, it can be used as a benchmark against which reductions in the mean reverberation time brought about by non-absorbent sample surfaces can be compared; the simple ratio of these reductions quantifying the diffusion efficacy of the sample. This measure of diffusion efficacy can thus be expressed in the form of a parameter, d, as shown below:

$$d = \frac{RT_{empty} - RT_{sample}}{RT_{empty} - RT_{min}} \tag{7.3}$$

where:

RT_{sample} = Mean reverberation time of the non-diffuse space when the sample replaces a reflective boundary surface.

In addition to RT_{min}, RT_{empty} was also determined during the Lam's method measurements, as of course were values of RT_{sample} for the samples shown in Figures 6.5 to 6.7. Therefore no further measurements were necessary to evaluate the above parameter for these samples but the value for the random hemispheres is meaningless because it has significant absorption. It may be possible to include absorption effects in (7.3) but no attempt was made to do so. This characterisation

technique is in fact essentially a variation on Lam's method which has the advantage that a diffusion coefficient can be assigned to non-absorbent surfaces without the need to use a prediction model. However since this coefficient is conceptually different to that implemented in ODEON 2.6, the values obtained differ from those yielded by Lam's method which are presented in Chapter 6.

Figure 7.1 shows how, in terms of the value of d defined in (7.3), the diffusion efficacy of the battens samples varies with frequency. A table of results containing the measured third-octave values of RT_{empty}, RT_{min} and RT_{sample} from which these values of d were calculated can be found in Appendix D.

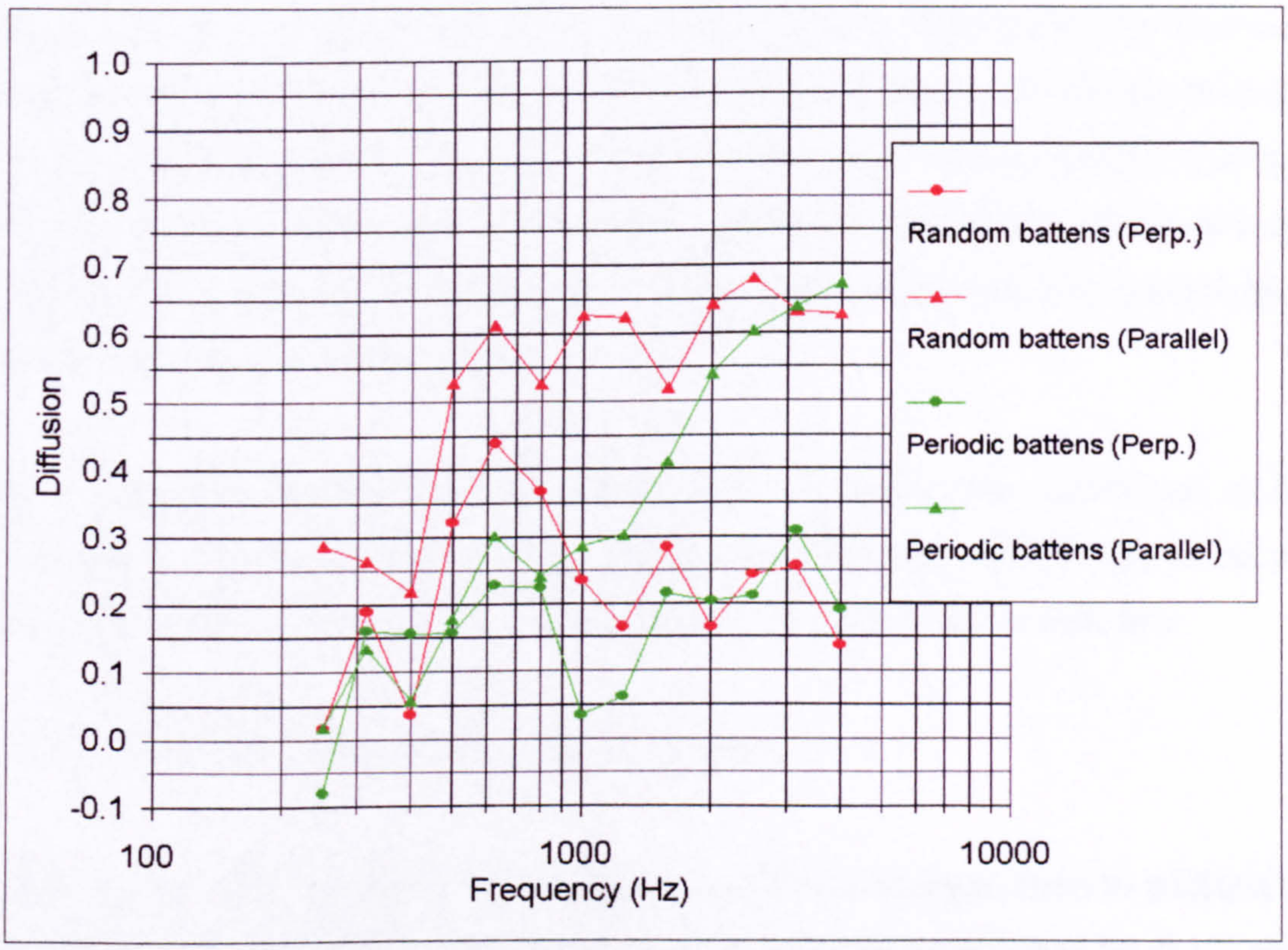

Figure 7.1: Values of d (defined in (7.3)) for the battens samples.

Figure 7.1 illustrates that d is a useful measure of the diffusion produced by (non-absorbent) surfaces and substantiates the following previously drawn conclusions about how these battens samples scatter the reflected energy: A random arrangement of battens is a more effective diffuser over a wide range of frequencies than a periodic arrangement and in both cases the scattering is predominantly in directions perpendicular to the battens.

Although this technique for quantifying the diffusion efficacy of surfaces has its merits, for example it is simple, uses standard facilities and the value of the resulting coefficient is theoretically bounded between zero and unity, the fact that it is limited to those which are non-absorbent is a substantial drawback and it is therefore far from ideal. In fact before it could even be recommended as suitable for non-absorbent surfaces, it would be necessary to verify by measurement that it does in fact rank the diffusion efficacy of other samples correctly. One aspect of the technique which would require some consideration if it were to be further developed is the number of reflective boundary surfaces of the non-diffuse space that it is necessary to cover with the sample surface. Since the results shown in Figure 7.1 are calculated from Lam's method measurements, the sample surface formed only one boundary of the space. However it is improbable that the mean reverberation time could be reduced to the value predicted by the Eyring formula, (7.2), by applying diffusion to just a single surface. Cox[46] has suggested that one of the surfaces comprising each opposing pair should be covered, i.e three in total. However, covering any surface other than the floor would increase the practical complexity of the measurement.

To enable diffusion coefficient values obtained using this technique to be compared, the amount of boundary surface covered with sample has to be the same in all cases. It is therefore unsuitable for rating individual diffusers.

7.2.2 Spatial variation of reverberation time.

When the diffuseness of the sound field in a space increases, then in addition to the reverberation time itself decreasing towards the value predicted by the Eyring reverberation time formula, a decrease should theoretically also be observed in its spatial variation because an ideally diffuse space has a reverberation time which is independent of the measurement position. It was therefore investigated whether the spatial variation of the reverberation time of the non-diffuse space changed when one of its reflective boundary surfaces was replaced with each of the samples shown in Figures 6.5 to 6.7 and whether, consequently, the diffusion efficacy of these samples could be quantified from this change. To accomplish this,

the standard deviations of the reverberation times measured at different positions in the non-diffuse space, for each sample, were calculated. As discussed in Section 6.3.3, ten different microphone positions were used, five for each of two source positions. The standard deviation of the ten reverberation times measured in the absence of any sample was also calculated. Figure 7.2 shows all these standard deviations as functions of frequency.

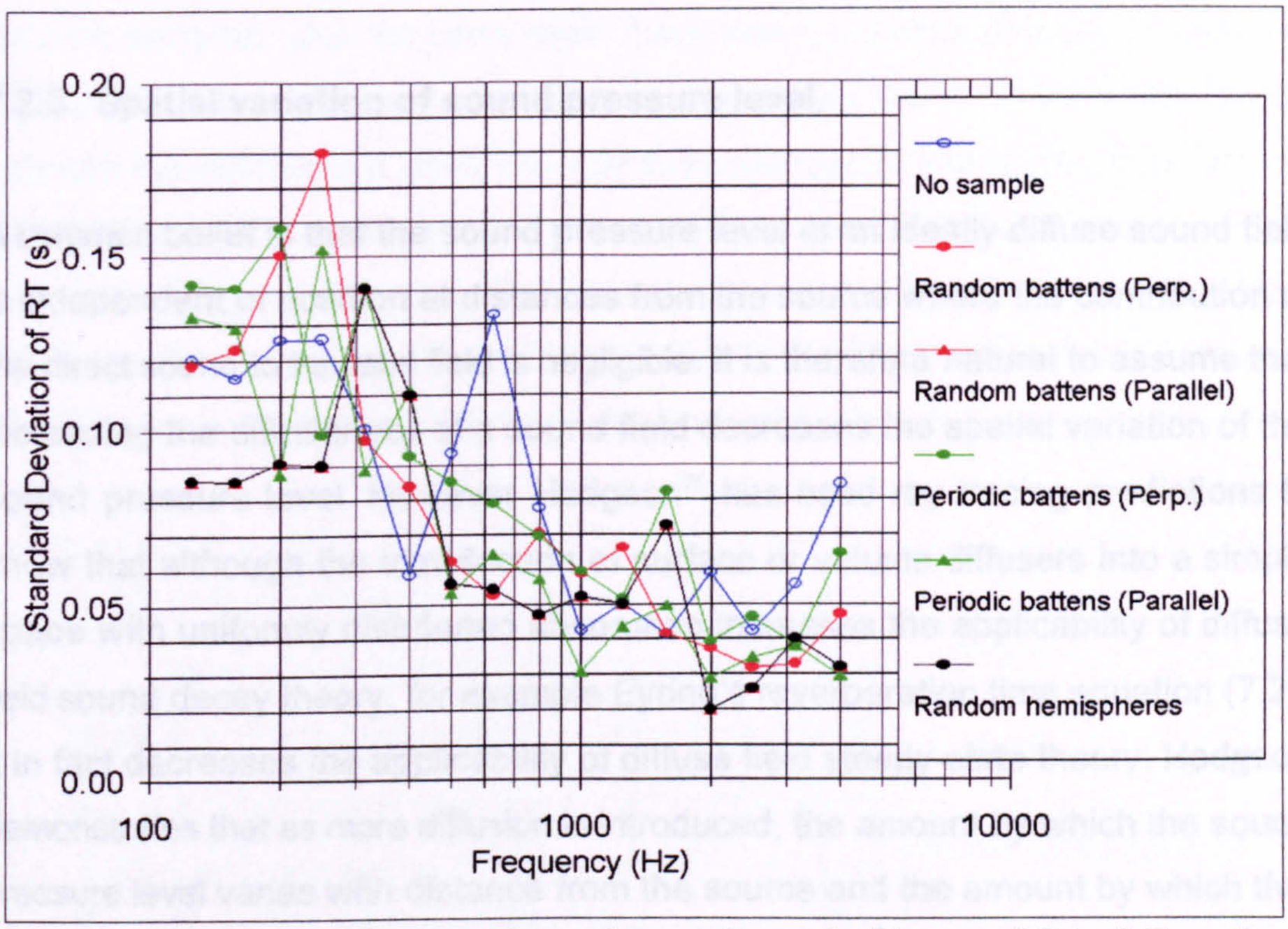

Figure 7.2: Effect of the sample surfaces shown in Figures 6.5 to 6.7 on the standard deviation of the reverberation time of the non-diffuse space.

The salient characteristic conveyed by Figure 7.2 is that although the spatial variation of the reverberation time generally decreases with frequency, it does not consistently decrease when any of the samples are introduced into the space; for all the samples it increases at some frequencies and decreases at others. Furthermore, there are only small differences between all the standard deviations in each third-octave band and the ordering of the samples is inconsistent. The two most plausible explanations of these results are that either the samples do not increase the diffuseness of the space, or they do but this increase is not reflected in the spatial variation of its reverberation time measured using the method

described. Since, as discussed in Section 7.2.1, the presence of the non-absorbent samples reduced the mean reverberation time of the space, the former possibility is unlikely. It is much more probable that the diffuseness of the space is increased but that because the associated change in the spatial variation of its reverberation time is small, it is difficult to measure accurately. The conclusion is that this measure of sound field diffuseness is not that from which the diffusion efficacy of sample surfaces can be most easily quantified.

7.2.3 Spatial variation of sound pressure level.

A common belief is that the sound pressure level in an ideally diffuse sound field is independent of position at distances from the source where the contribution of the direct sound to the total field is negligible. It is therefore natural to assume that increasing the diffuseness of a sound field decreases the spatial variation of the sound pressure level. However Hodgson[75] has used ray tracing predictions to show that although the introduction of surface or volume diffusers into a simple space with uniformly distributed absorption increases the applicability of diffuse field sound decay theory, for example Eyring's reverberation time equation (7.2), it in fact decreases the applicability of diffuse field steady-state theory. Hodgson demonstrates that as more diffusion is introduced, the amount by which the sound pressure level varies with distance from the source and the amount by which this variation with distance deviates from that predicted by the Eyring steady-state formula given below both increase.

$$SPL(r) = L_w + 10\log\left[\frac{1}{4\pi r^2} + \frac{4(1-\bar{\alpha})}{-\ln(1-\bar{\alpha})S}\right] \qquad (7.4)$$

where:

r = Distance from source

L_w = Sound power level of source

Other symbols have the same meaning as in (7.2)

As a consequence, the variation of the sound pressure level over the entire space

may actually increase with increasing diffuseness, exactly the opposite of what is commonly assumed. It was therefore investigated whether introducing the battens samples shown in Figures 6.5 and 6.6 into the non-diffuse space increased or decreased the spatial variation of the sound pressure level in the sound field and whether this change could be used to quantify their diffusion efficacy.

The variation of the standard deviation of the octave band levels with frequency for both samples, plus the case when there was no sample present, is shown in Figure 7.3. Although there are one or two spurious points and the differences between the samples are small, the indication provided by these results is that the standard deviation of the levels increases when the diffuseness of the space is increased. However because both the standard deviations themselves and the differences between them are small, it is difficult to conclude whether this indicated effect is real or whether it is in fact a measurement artifact or simply chance.

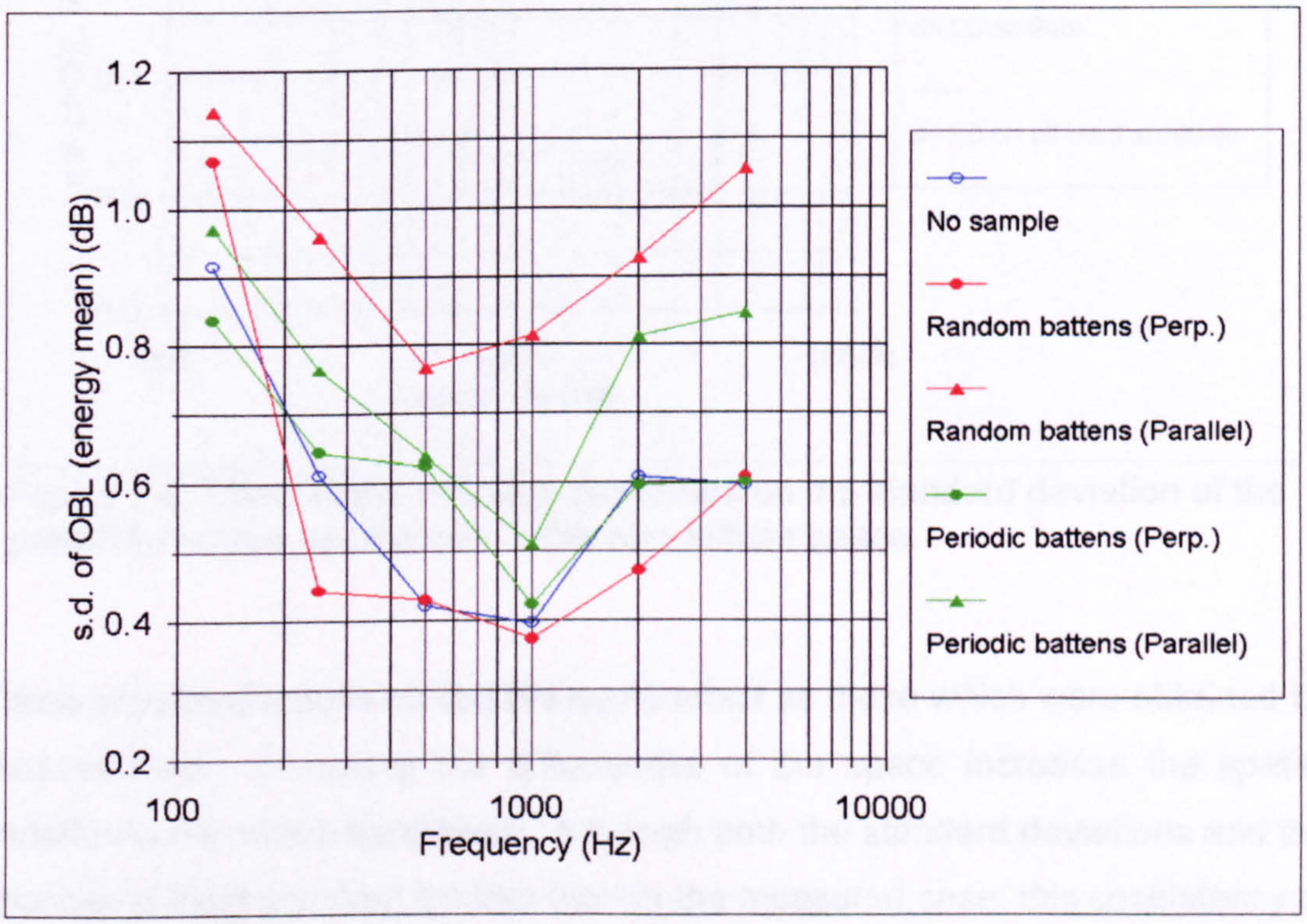

Figure 7.3: Effect of the battens samples on the standard deviation of the octave band levels measured in the non-diffuse space.

To attempt to resolve this, it was decided to ascertain whether and how the spatial variation of the octave band levels predicted by ODEON 2.6 varied when the

diffusion coefficient of the floor of the non-diffuse space was changed. The same source position and ten receiver positions shown in Figure 6.9 were used and the standard deviation of the predicted levels at these receiver positions was evaluated when the floor was assigned diffusion coefficient values of 0.1, 0.5 and unity. Figure 7.4 shows these standard deviations as functions of frequency and includes an additional case where the diffusion coefficient of all the boundary surfaces except the absorptive wall was set to unity.

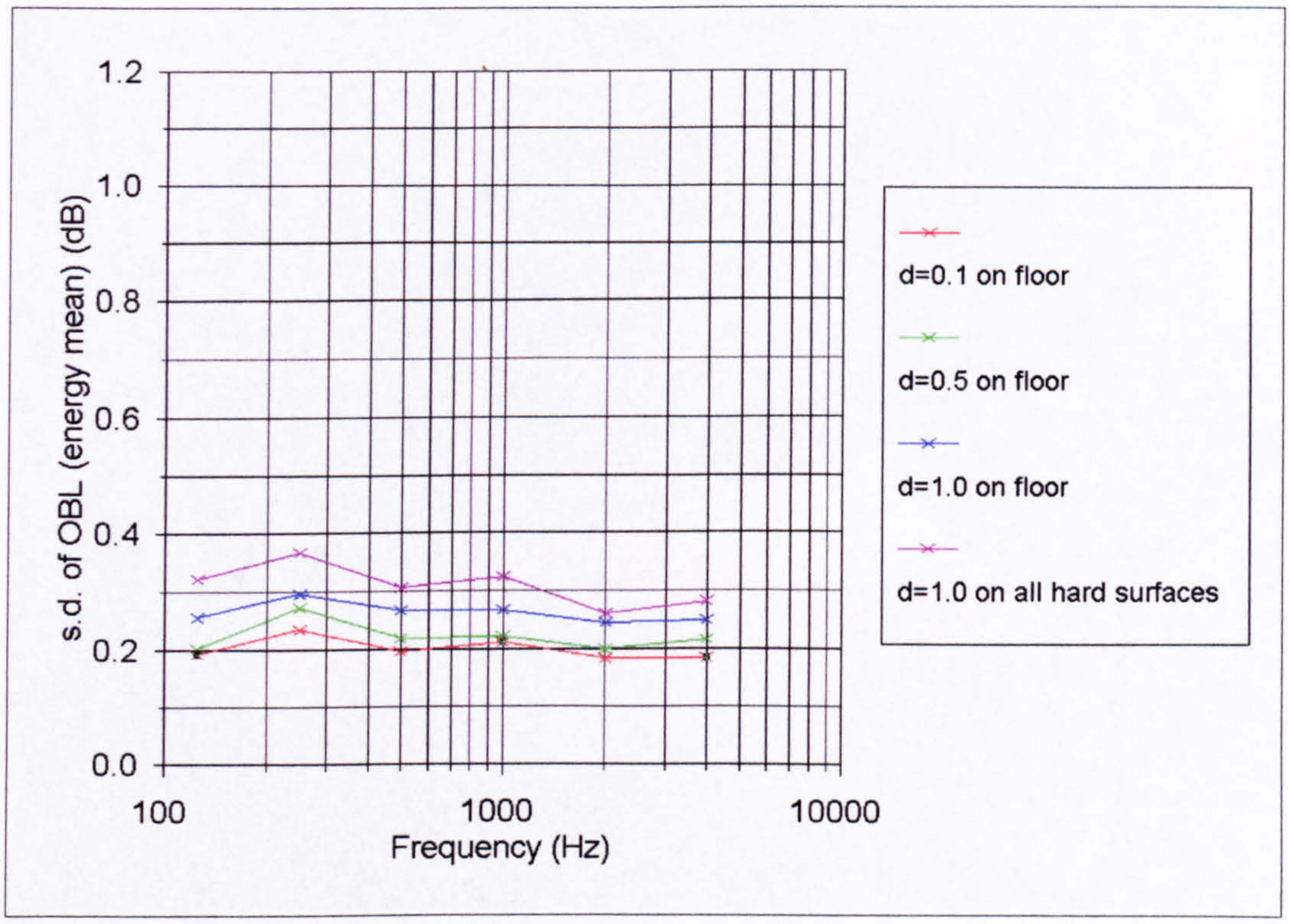

Figure 7.4: Effect of the diffusion coefficient on the standard deviation of the predicted octave band levels in the non-diffuse space.

These predicted results exhibit the same effect as those which were obtained by measurement; increasing the diffuseness of the space increases the spatial variation in the octave band levels. Although both the standard deviations and the changes in them are even smaller than in the measured case, this consistency of the measured and predicted results strongly suggests that the effect is real. However since the effect is so slight, it would in practice be very difficult to use the spatial variation of the levels in a non-diffuse space to quantify the diffusion efficacy of surfaces.

Although the effect is too small to be of any practical use, to gain more understanding of the reason why the standard deviation of the octave band levels in the non-diffuse space increases when the diffusion efficacy of the floor is increased, ODEON 2.6 was used to predict the level in the 500Hz (full scale) octave band throughout the space when, as before, diffusion coefficient values of 0.1, 0.5 and unity were assigned to the floor. The results are shown in Figures 7.5 to 7.14 on this and following pages.

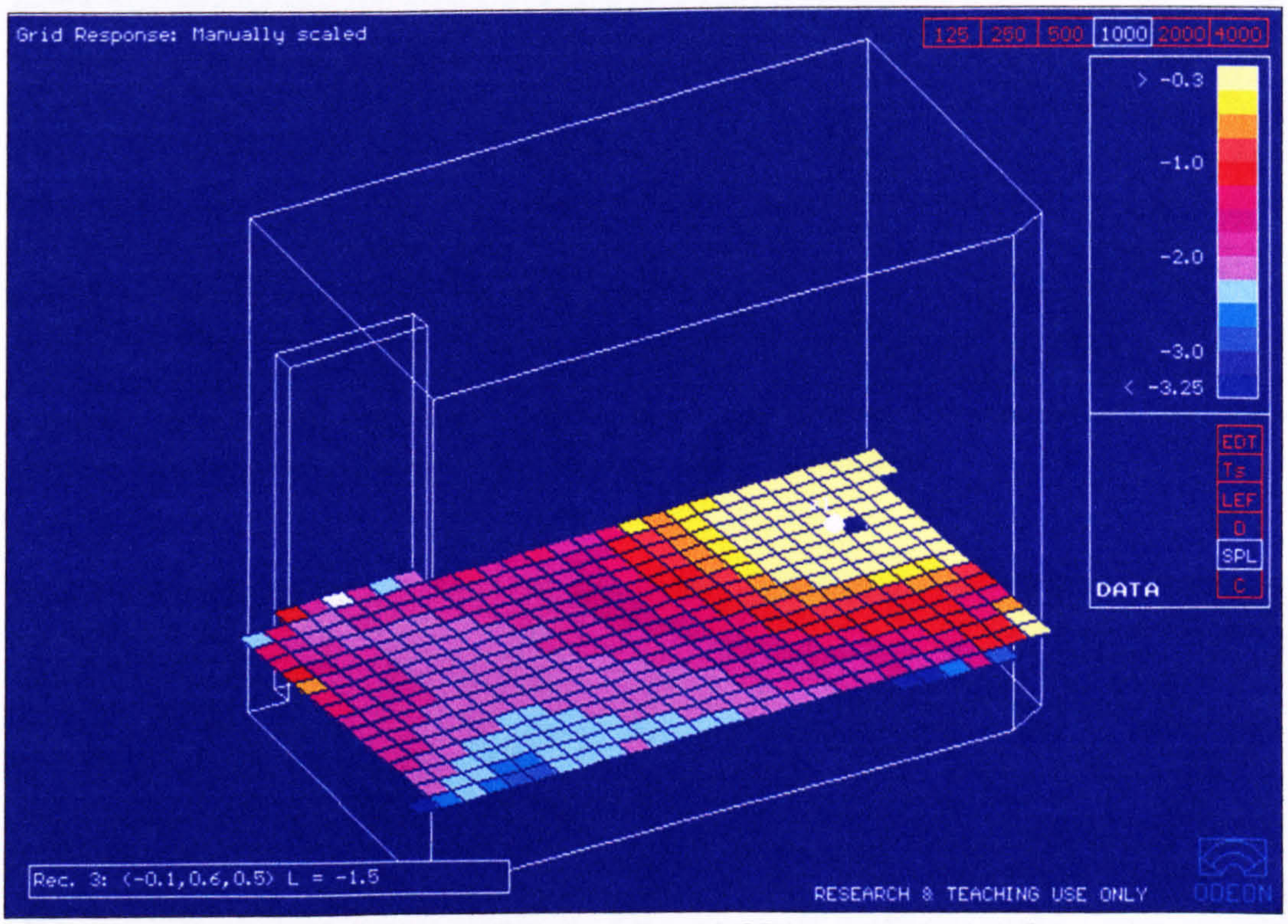

Figure 7.5: Spatial variation of the predicted SPL close to the floor of the non-diffuse space when the value of d is 0.1 for all surfaces.

The most striking feature of the results is the increase in extent of the blue areas, which represent low level, as the diffusion coefficient of the floor is increased. It is this increase in the prevalence of low level which increases the standard deviation because it results in the spatial distribution becoming more polarised. The reason for this decrease in the octave band level in certain areas is unclear but it could be due to an increase in the amount of reverberant energy directed towards the absorptive wall and thus removed from the space. Since close to the source the direct field dominates and a reduction in the reverberant energy does

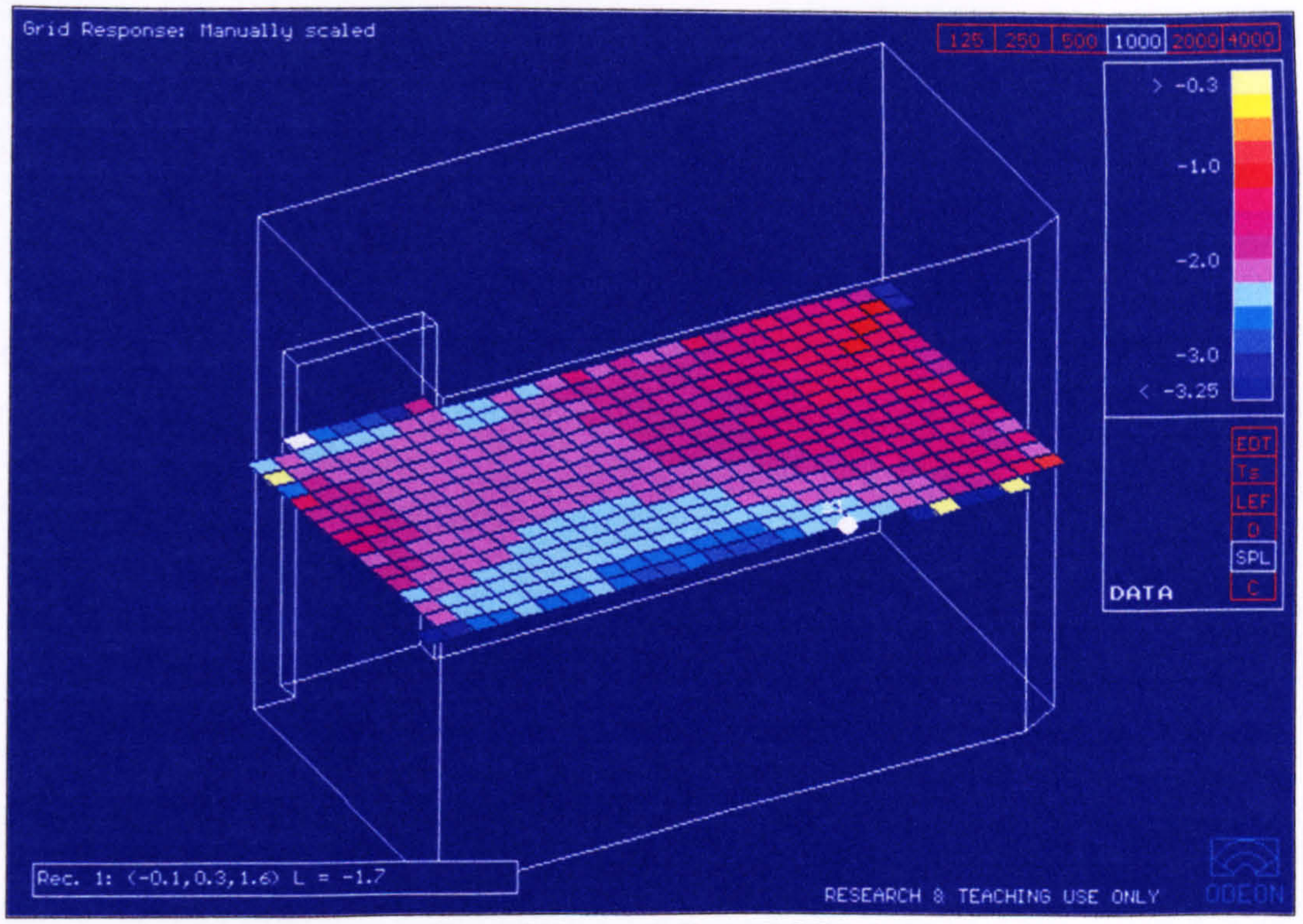

Figure 7.6: Spatial variation of the predicted SPL in the centre of the non-diffuse space when the value of d is 0.1 for all surfaces.

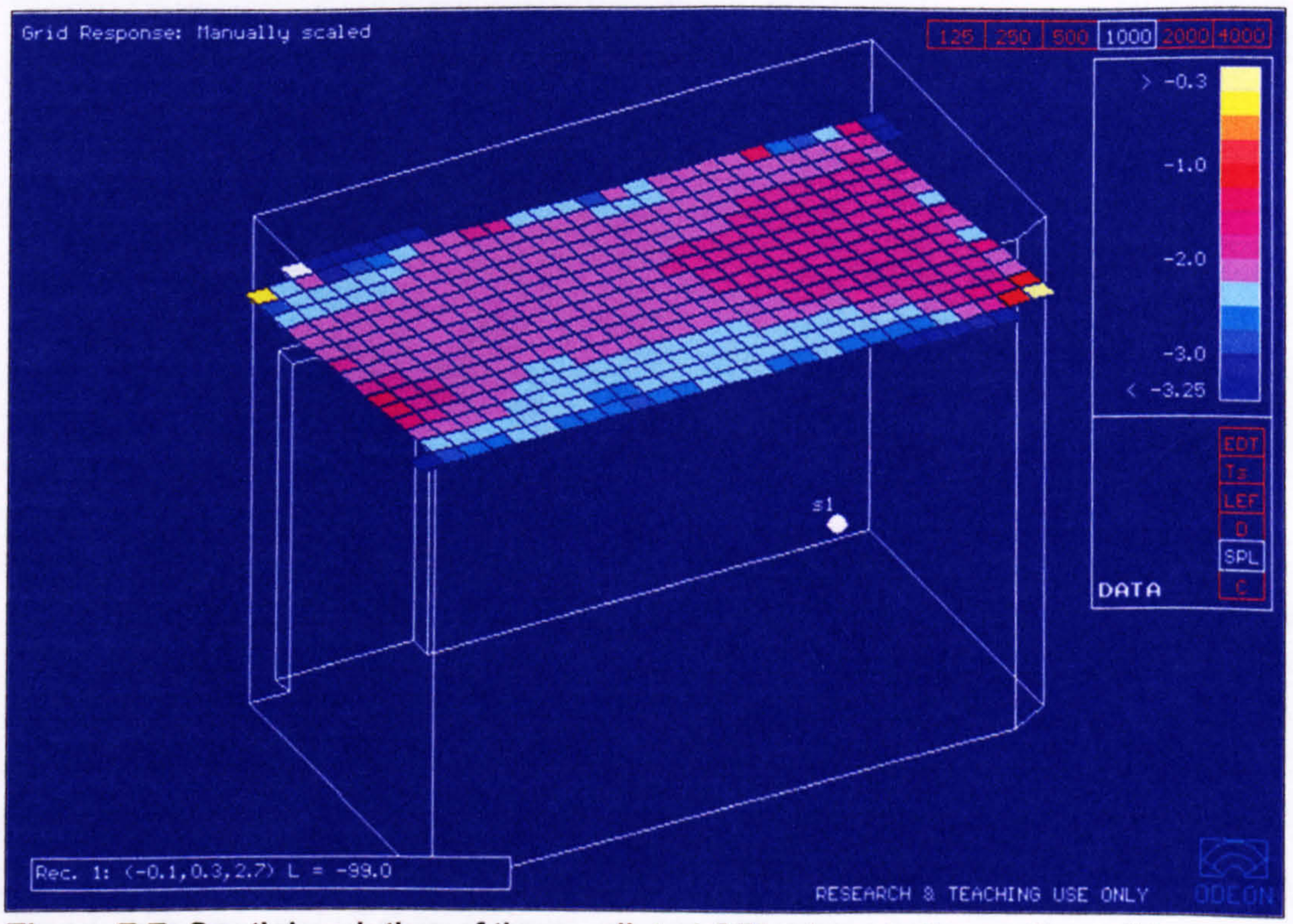

Figure 7.7: Spatial variation of the predicted SPL close to the ceiling of the non-diffuse space when the value of d is 0.1 for all surfaces.

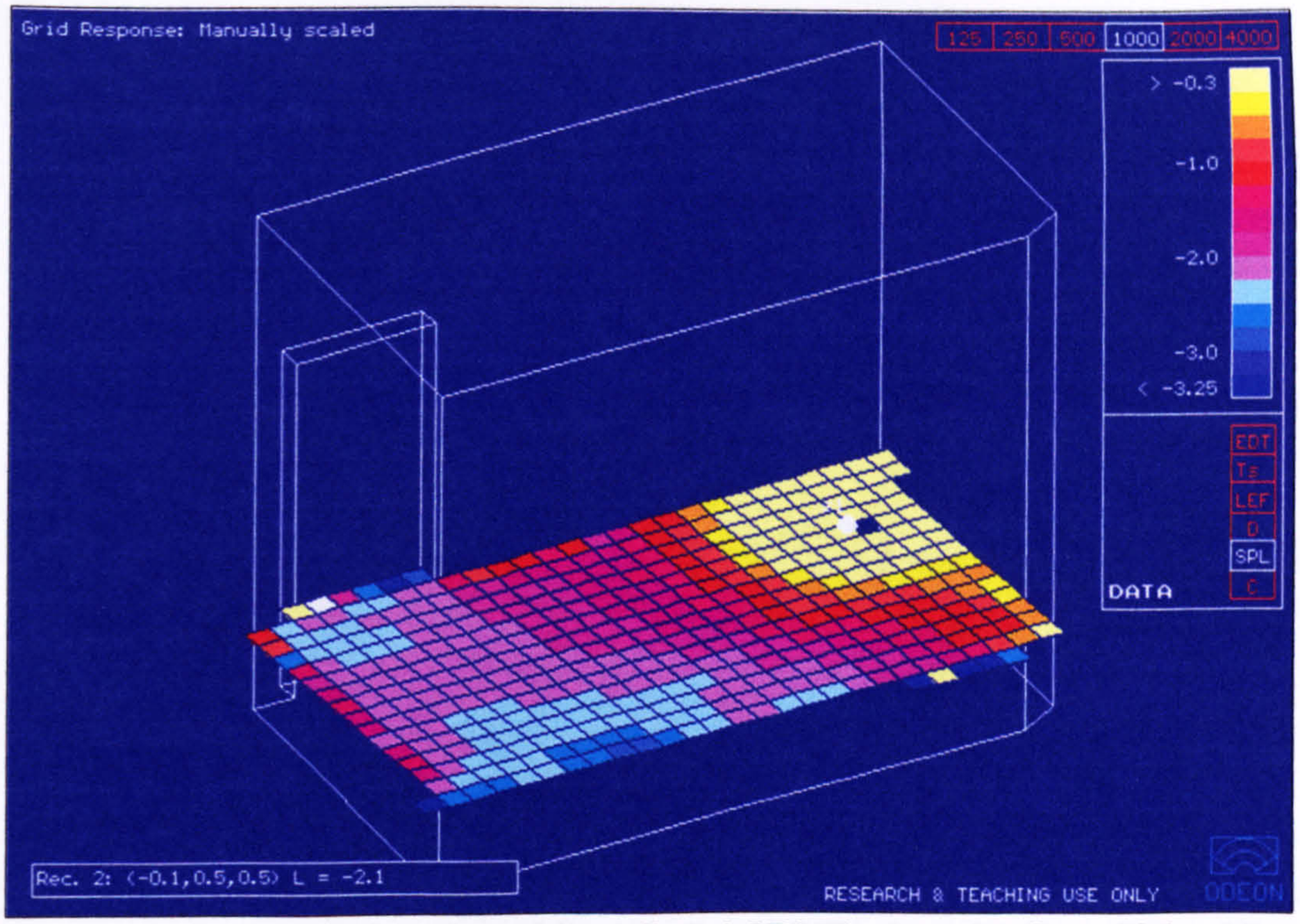

Figure 7.8: Spatial variation of the predicted SPL close to the floor of the non-diffuse space when the value of d is 0.5 for the floor and 0.1 for other surfaces.

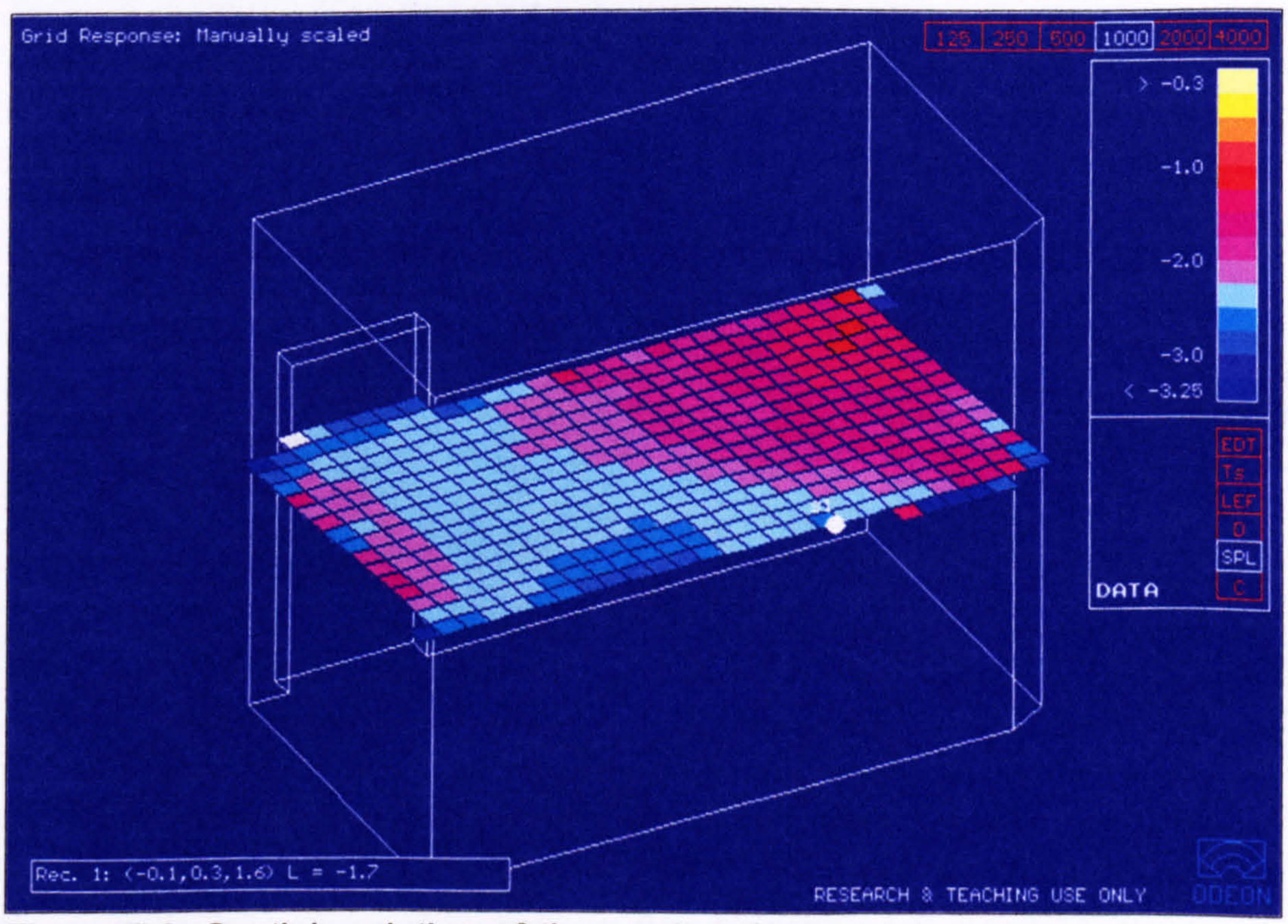

Figure 7.9: Spatial variation of the predicted SPL in the centre of the non-diffuse space when the value of d is 0.5 for the floor and 0.1 for other surfaces.

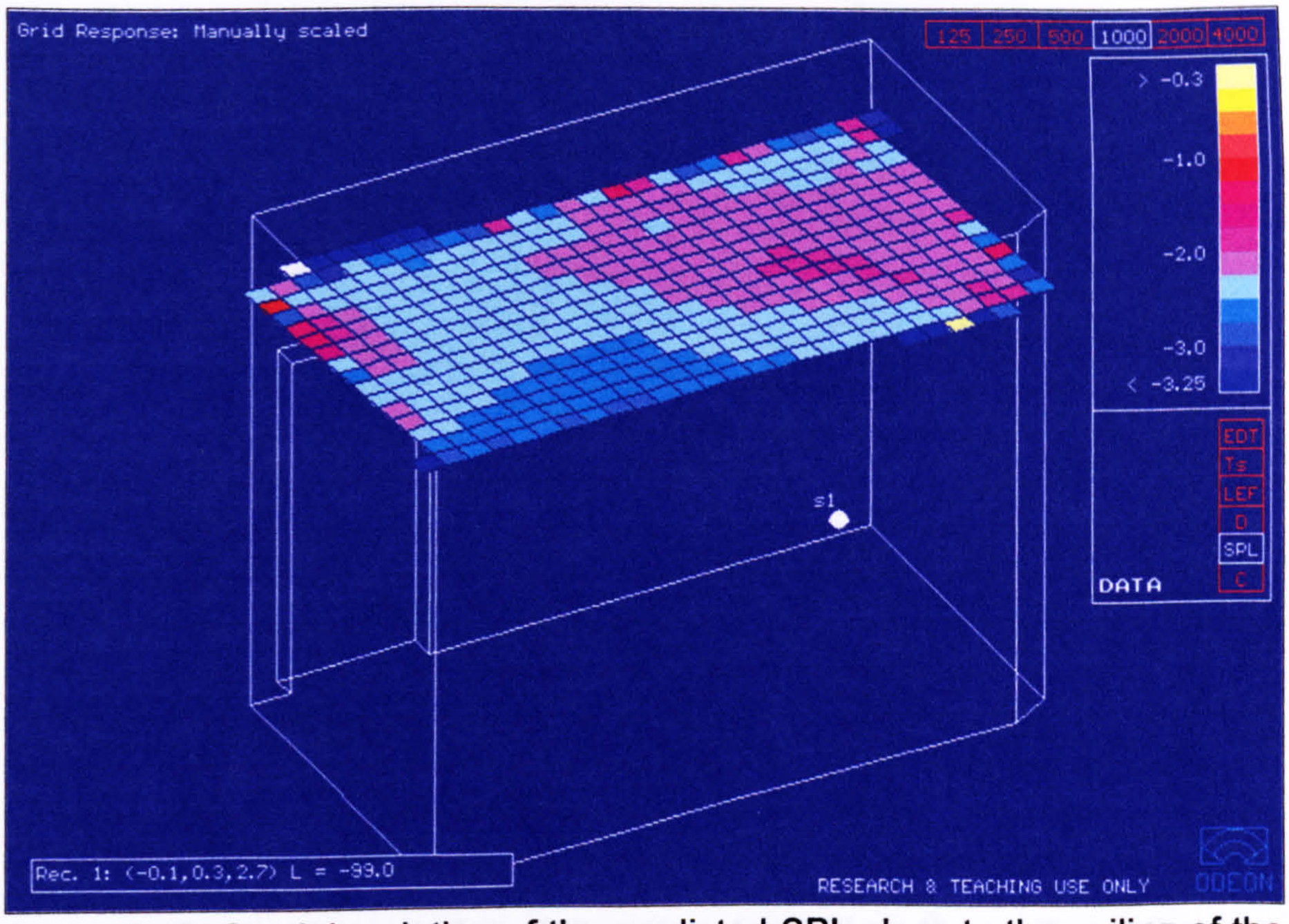

Figure 7.10: Spatial variation of the predicted SPL close to the ceiling of the non-diffuse space when the value of d is 0.5 for the floor and 0.1 for other surfaces.

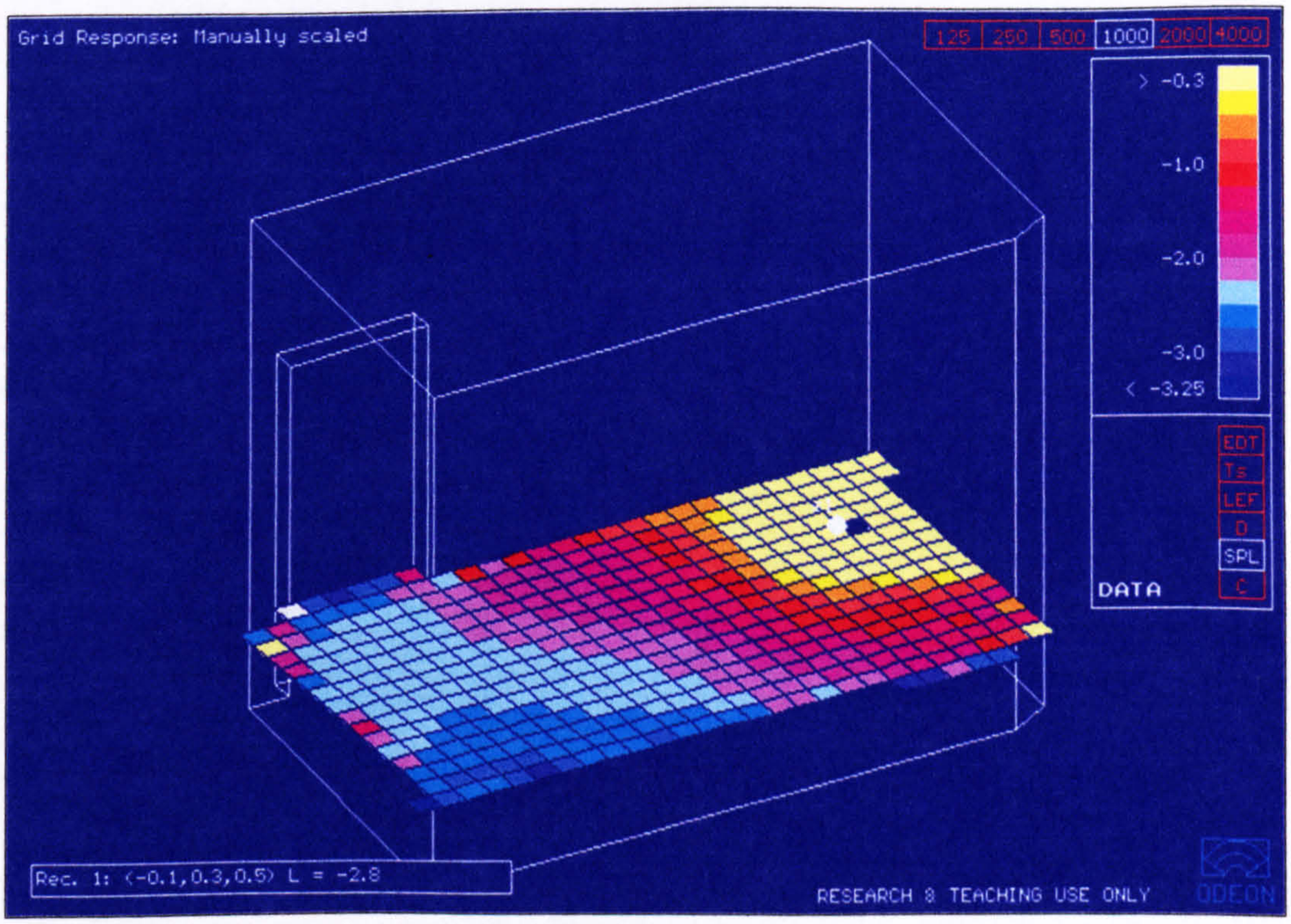

Figure 7.11: Spatial variation of the predicted SPL close to the floor of the non-diffuse space when the value of d is 1.0 for the floor and 0.1 for other surfaces.

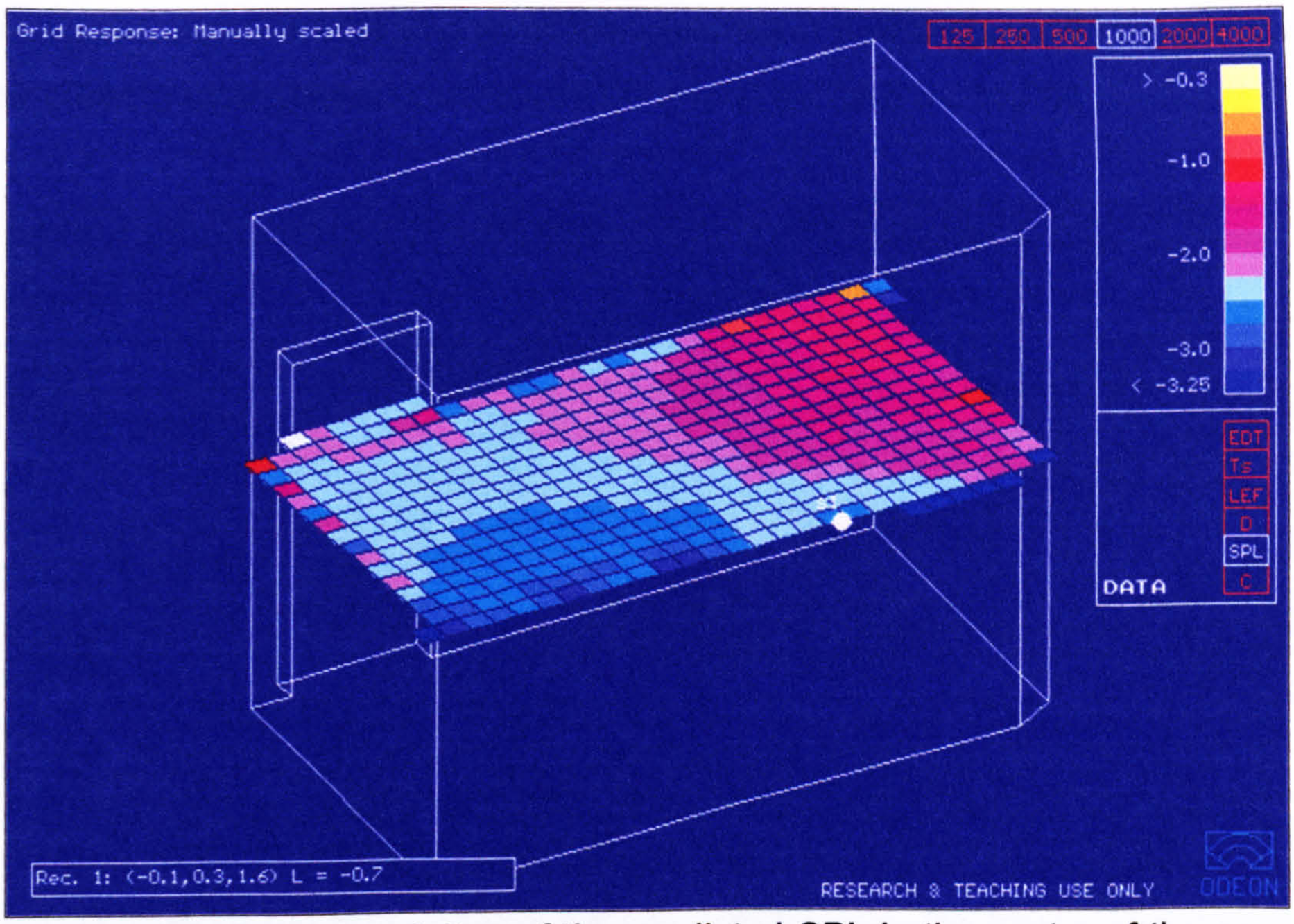

Figure 7.12: Spatial variation of the predicted SPL in the centre of the non-diffuse space when the value of d is 1.0 for the floor and 0.1 for other surfaces.

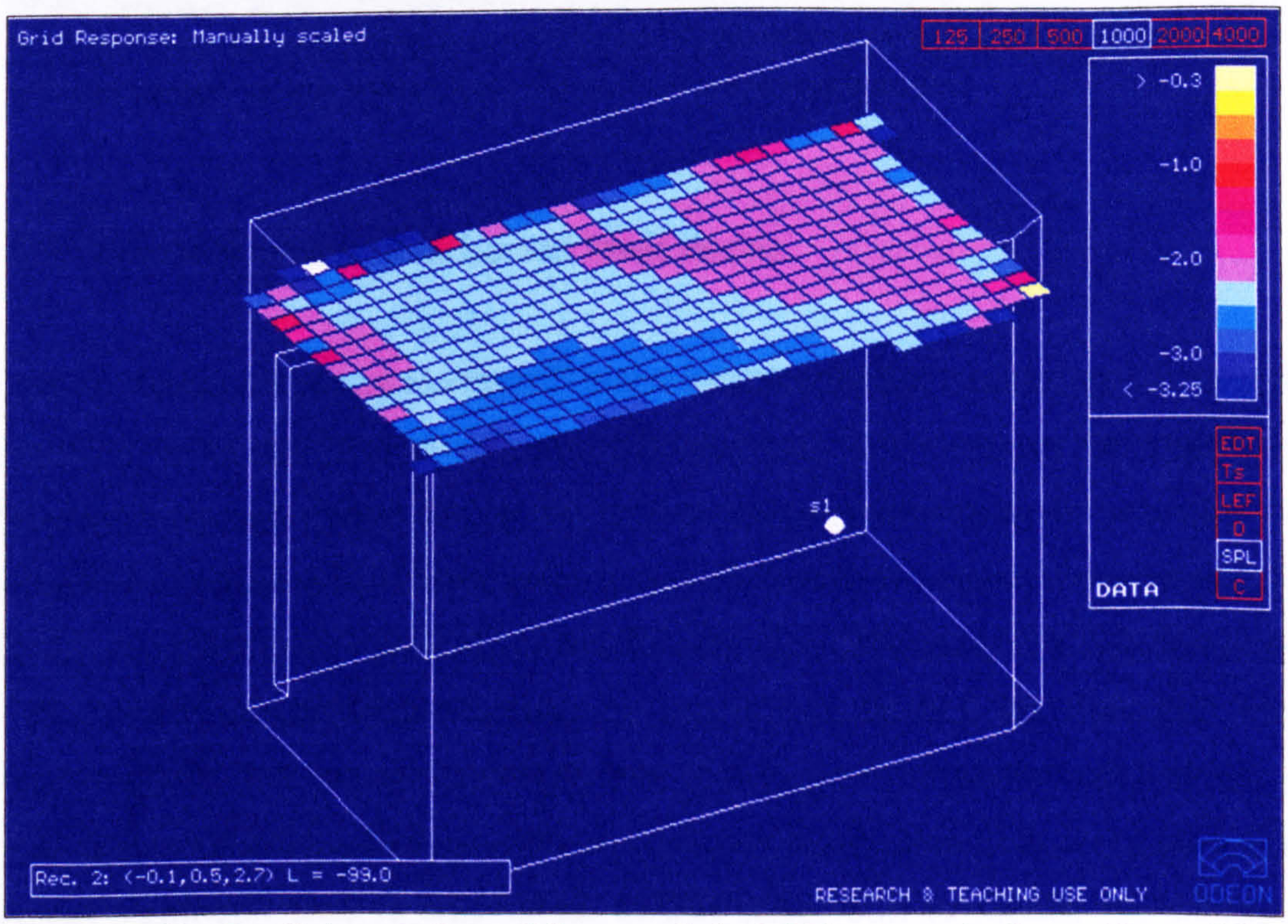

Figure 7.13: Spatial variation of the predicted SPL close to the ceiling of the non-diffuse space when the value of d is 1.0 for the floor and 0.1 for other surfaces.

not significantly affect the total level, this explanation is consistent with the fact that the effect is most pronounced at positions furthest from the source.

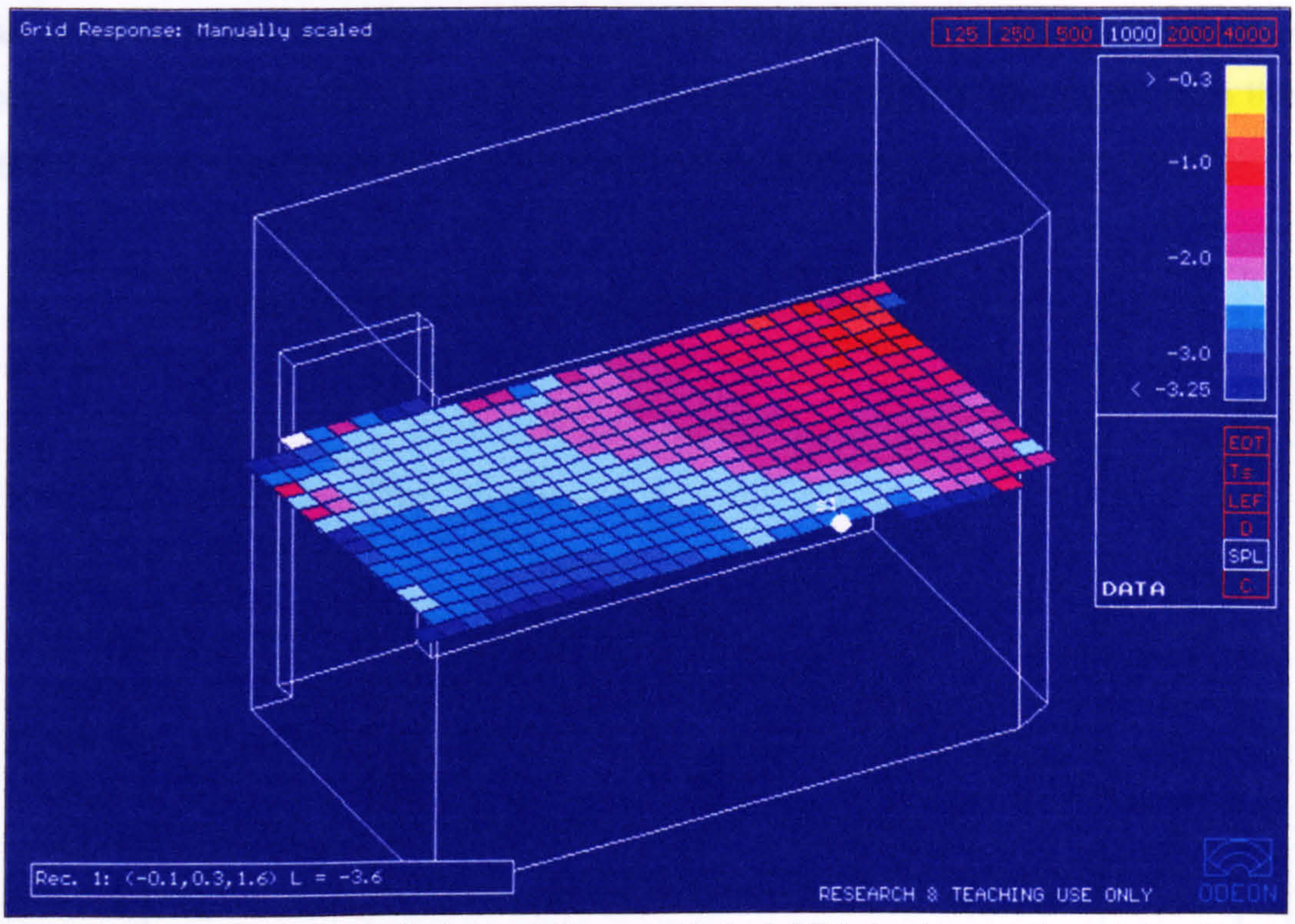

Figure 7.14: Spatial variation of the predicted SPL in the centre of the 'non-diffuse' space when the value of d is 1.0 for all surfaces.

7.2.4 **Linearity of the reverberant level decay.**

It has also been shown by Hodgson[75] that a further effect of increasing the amount of surface or volume diffusion in a non-diffuse space is to increase the linearity of the sound pressure level decay, i.e. to increase the resemblance between the decay of the reverberant energy and a true exponential. However it is evident from the results of Hodgson's predictions that this change in linearity is small, therefore it has been investigated whether or not it can in fact be detected from measurements. This was achieved by investigating the correlation coefficients, r, calculated by MLSSA (which quantify how closely the section of decay from which the reverberation time is calculated, in this case -5dB to -35dB, resembles a straight line) of the sound pressure level decays obtained from previous impulse response measurements. It was found that the magnitude of these correlation

coefficients invariably exceeded 0.995; an example decay is shown in Figure 7.15. Since the individual magnitudes were all so close to unity, the mean correlation coefficients were essentially the same and did not enable the different samples to be distinguished, let alone placed in any sort of ranking order. It was thus concluded that the diffusion efficacy of surfaces cannot be calculated from their effect on the linearity of the reverberant level decay in a non-diffuse space.

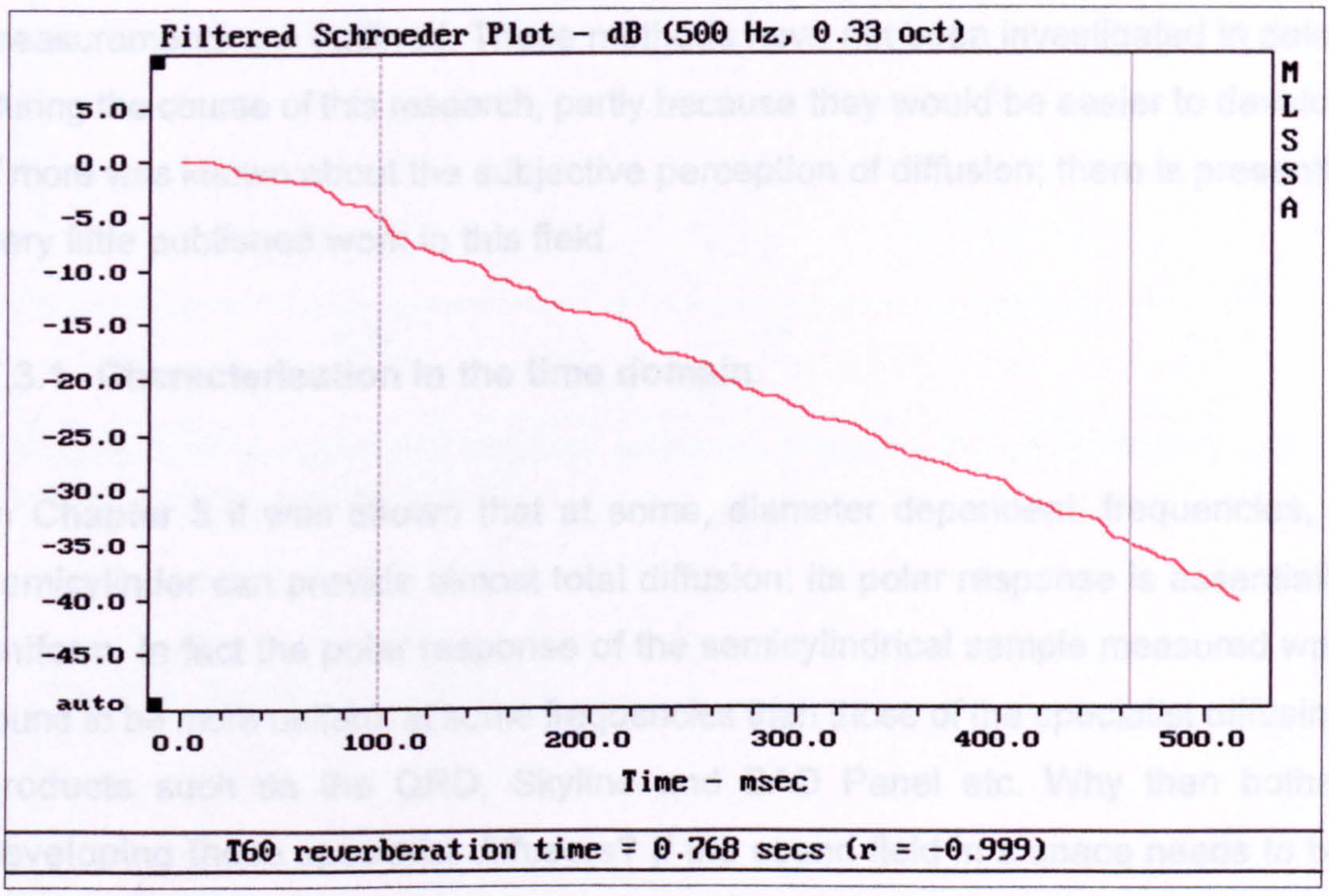

Figure 7.15: Example of a measured reverberant level decay.

To summarise, although the concept of these reverberation chamber techniques for quantifying the diffusion efficacy of surfaces is valid, the measured changes in the sound field parameters investigated are generally too small to be practically useful. The only parameter which changes significantly is the mean reverberation time but since this is affected by both absorption and diffusion, such a measurement can only be used to evaluate the diffusion efficacy of non-absorbent samples. Larger changes in some of the other parameters may be observed if more than a single boundary surface of the reverberation chamber is covered with the sample; this is a possibility for future investigation.

7.3 Free field techniques.

In previous chapters, a number of techniques for quantifying the diffusion efficacy of surfaces from free field measurements of the reflected sound have been discussed, examples include inspection of the polar response, spherical harmonics and the Mommertz and Vorländer free field method. In this section one or two other possible methods for quantifying diffusion which would require free field measurements are outlined. These methods have not been investigated in detail during the course of this research, partly because they would be easier to develop if more was known about the subjective perception of diffusion; there is presently very little published work in this field.

7.3.1 Characterisation in the time domain.

In Chapter 3 it was shown that at some, diameter dependent, frequencies, a semicylinder can provide almost total diffusion; its polar response is essentially uniform. In fact the polar response of the semicylindrical sample measured was found to be more uniform at some frequencies than those of the specialist diffusing products such as the QRD, Skyline and BAD Panel etc. Why then bother developing these specialist diffusers? If the sound field in a space needs to be made more diffuse then why not simply cover the boundary surfaces with variously sized semicylinders and hemispheres (the three-dimensional equivalent) ?

It has been suggested that the answer to these questions is that the subjective response to reflections from such surfaces is unfavourable, they are perceived as harsh[76]. The reason for this could be that although semicylinders etc. spread the reflected energy uniformly, because their surfaces are smooth they do not actually scatter the energy in the manner that an irregular surface such as a QRD does. The reflected energy received by a listener emanates from just one particular area of the surface and propagates via a single path. It is therefore short in duration, as shown in Figure 7.16. Such a reflection exhibits many of the characteristics of one which is specular, in fact it could be argued that it is specular. Consequently it would be unsurprising if the subjective response is unfavourable.

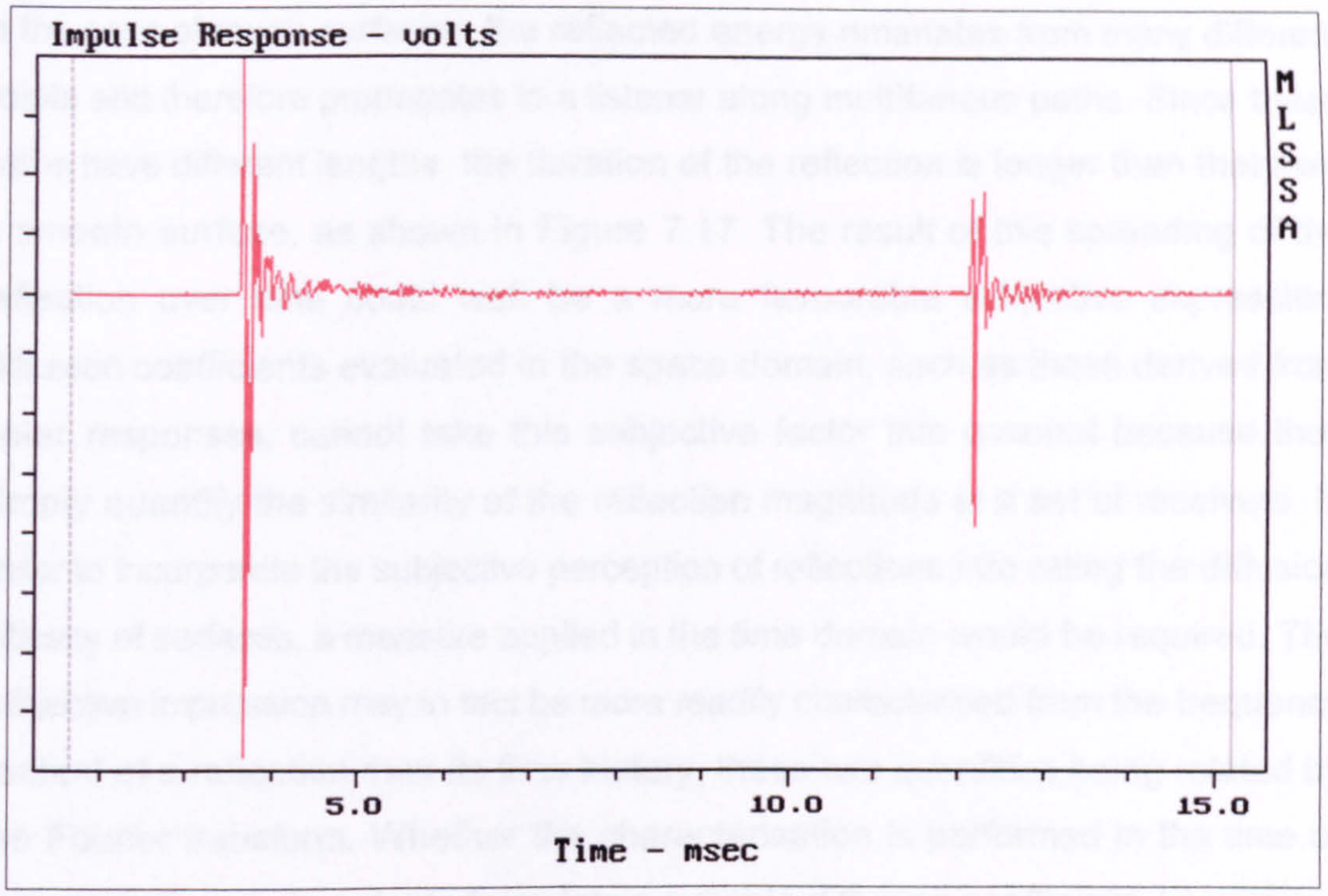

Figure 7.16: A measured impulse response showing the direct sound and a reflection from a semicylinder.

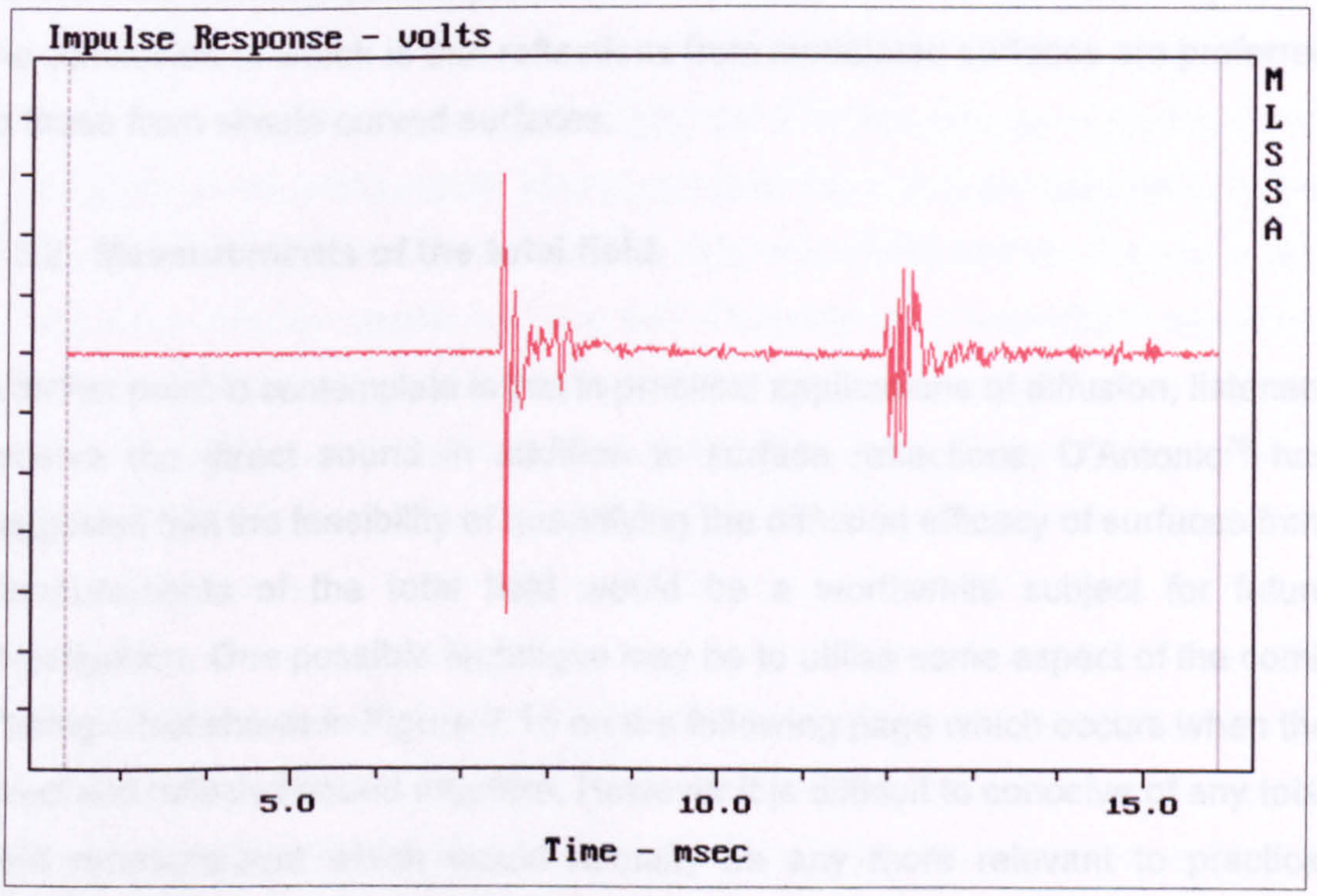

Figure 7.17: A measured impulse response showing the direct sound and a reflection from a rough surface.

In the case of rough surfaces, the reflected energy emanates from many different points and therefore propagates to a listener along multifarious paths. Since these paths have different lengths, the duration of the reflection is longer than that from a smooth surface, as shown in Figure 7.17. The result of this spreading of the reflection over time could well be a more favourable subjective impression. Diffusion coefficients evaluated in the space domain, such as those derived from polar responses, cannot take this subjective factor into account because they simply quantify the similarity of the reflection magnitude at a set of receivers. In order to incorporate the subjective perception of reflections into rating the diffusion efficacy of surfaces, a measure applied in the time domain would be required. The subjective impression may in fact be more readily characterised from the frequency content of a reflection than its time history, these two quantities being related by the Fourier transform. Whether the characterisation is performed in the time or frequency domain, in order to formulate a suitable diffusion coefficient, knowledge of the subjective response to a wide variety of reflection shapes would be required and this is currently unavailable. Furthermore, the value of such a coefficient would be dependent on the receiver position. A small study has been conducted by Lee[26], the conclusion of which is that reflections from modulated surfaces are preferred to those from simple curved surfaces.

7.3.2 **Measurements of the total field.**

A further point to contemplate is that in practical applications of diffusion, listeners receive the direct sound in addition to surface reflections. D'Antonio[76] has suggested that the feasibility of quantifying the diffusion efficacy of surfaces from measurements of the total field would be a worthwhile subject for future investigation. One possible technique may be to utilise some aspect of the comb filtering effect shown in Figure 7.18 on the following page which occurs when the direct and reflected sound interfere. However it is difficult to conceive of any total field measurement which would actually be any more relevant to practical applications of diffusion than the measurements of the reflected field alone which have been discussed elsewhere.

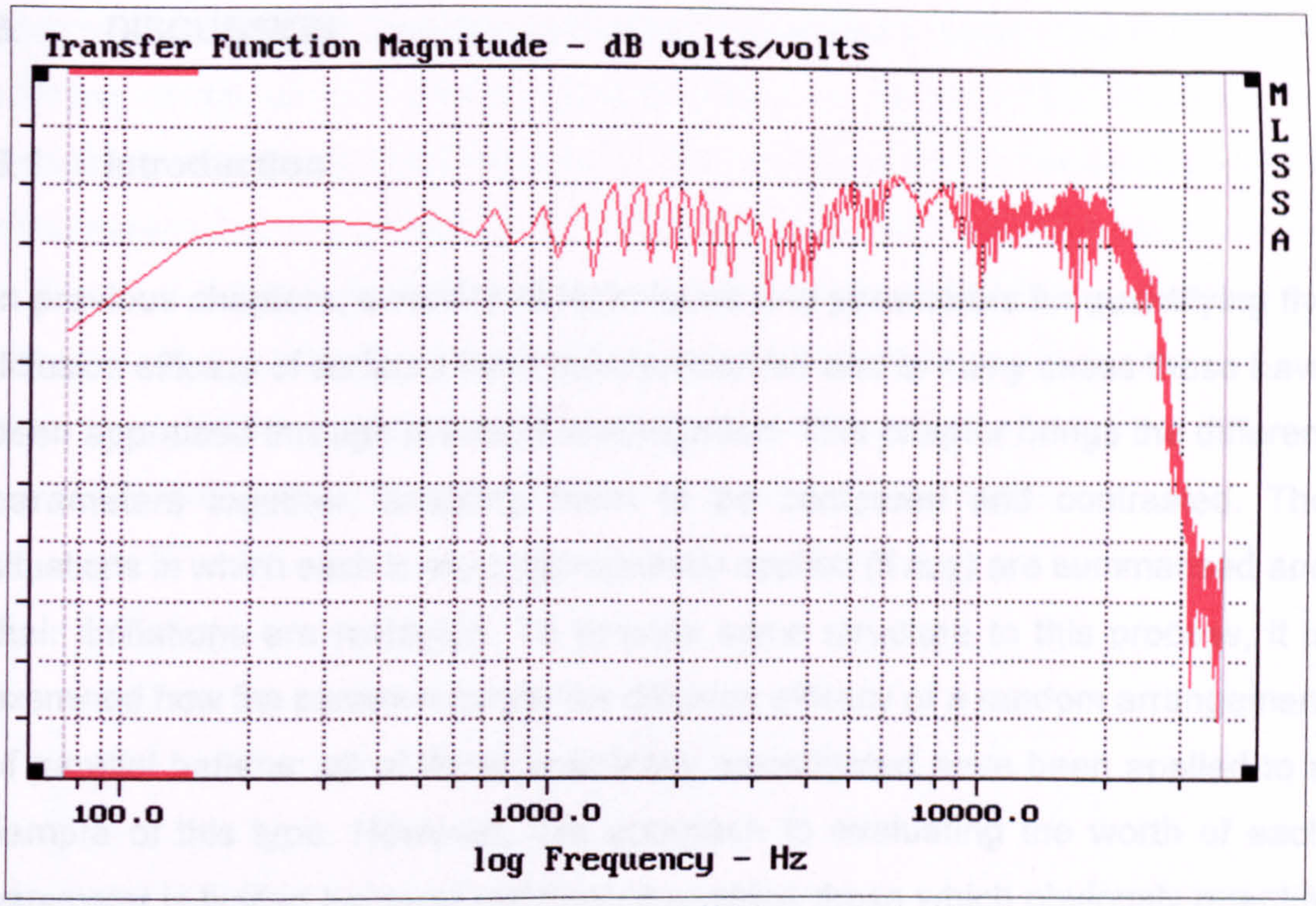

Figure 7.18: A frequency response exhibiting comb filtering. (Obtained by Fourier transformation of the impulse response shown in Figure 7.17.)

7.4 **Conclusions**.

In this chapter, the technique of quantifying the diffusion efficacy of surfaces from their effect on the diffuseness of a sound field has been investigated. Several measures of sound field diffuseness have been described and the change in their values when different sample surfaces are introduced into a non-diffuse space has been measured. Of these measures, only the mean reverberation time has any potential and in order not to be limited to non-absorbent samples, the problem of separating the effects of absorption and diffusion on the reverberation time would have to be overcome.

A second conclusion is that many of the diffusion coefficients examined during the course of this research do not take into account how diffusion is perceived by listeners. A parameter which does consider the subjective response would most likely be defined in the time/frequency domain and may be evaluated in critical bands[77] instead of the conventional octave or third-octave bands. Formulating such a measure will require more knowledge of the subjective aspects of diffusion.

8. DISCUSSION.

8.1 Introduction.

In previous chapters, a variety of techniques and parameters for quantifying the diffusion efficacy of surfaces have been presented and in many cases these have been appraised through practical investigation. This chapter brings the different parameters together, enabling them to be compared and contrasted. The situations in which each is most appropriately applied (if any) are summarised and their limitations are reviewed. To provide some structure to this process, it is examined how the parameters rate the diffusion efficacy of a random arrangement of parallel battens; all of those practically investigated have been applied to a sample of this type. However, this approach to evaluating the worth of each parameter is limited because although it enables those which obviously quantify the diffusion efficacy incorrectly to be dismissed (at least for the type of surface being considered), it is difficult to place parameters which yield values that could be interpreted as 'reasonable' in a ranking order of merit. Whether or not a parameter value is 'reasonable' is a subjective decision usually taken on the bases of visually inspecting the appropriate polar response, even in cases where the parameter itself is nothing to do with the polar response, and experience. The reason for this difficulty in ranking the worth of parameters is that there is no benchmark value for the diffusion efficacy of a surface against which to compare their values; establishing such a benchmark is the principal objective of this research.

8.2 Comparison of approaches to quantifying the diffusion efficacy of room surfaces.

Considering firstly the polar response approach, it has been established in Chapter 3 that the autocorrelation diffusion coefficient developed during this research is superior to previously published measures. By way of recapitulation, Figure 8.1 on the following page illustrates how both this new coefficient and examples of the three principal types of published polar response diffusion

parameters - standard deviation, directivity and specular zone - rate the diffusion efficacy of the random battens sample shown in Figure 2.12b. The standard deviation parameter is that defined by (3.2) and normalised to the worst case, the other parameters are defined by (3.18) and (3.30) respectively. The values shown in Figure 8.1 were obtained from normal incidence, single-plane, third-octave polar responses measured at RPG in the plane perpendicular to the battens, i.e. that in which the greatest amount of scattering occurs. A selection of these responses is shown in Figures 8.2 to 8.9 on subsequent pages.

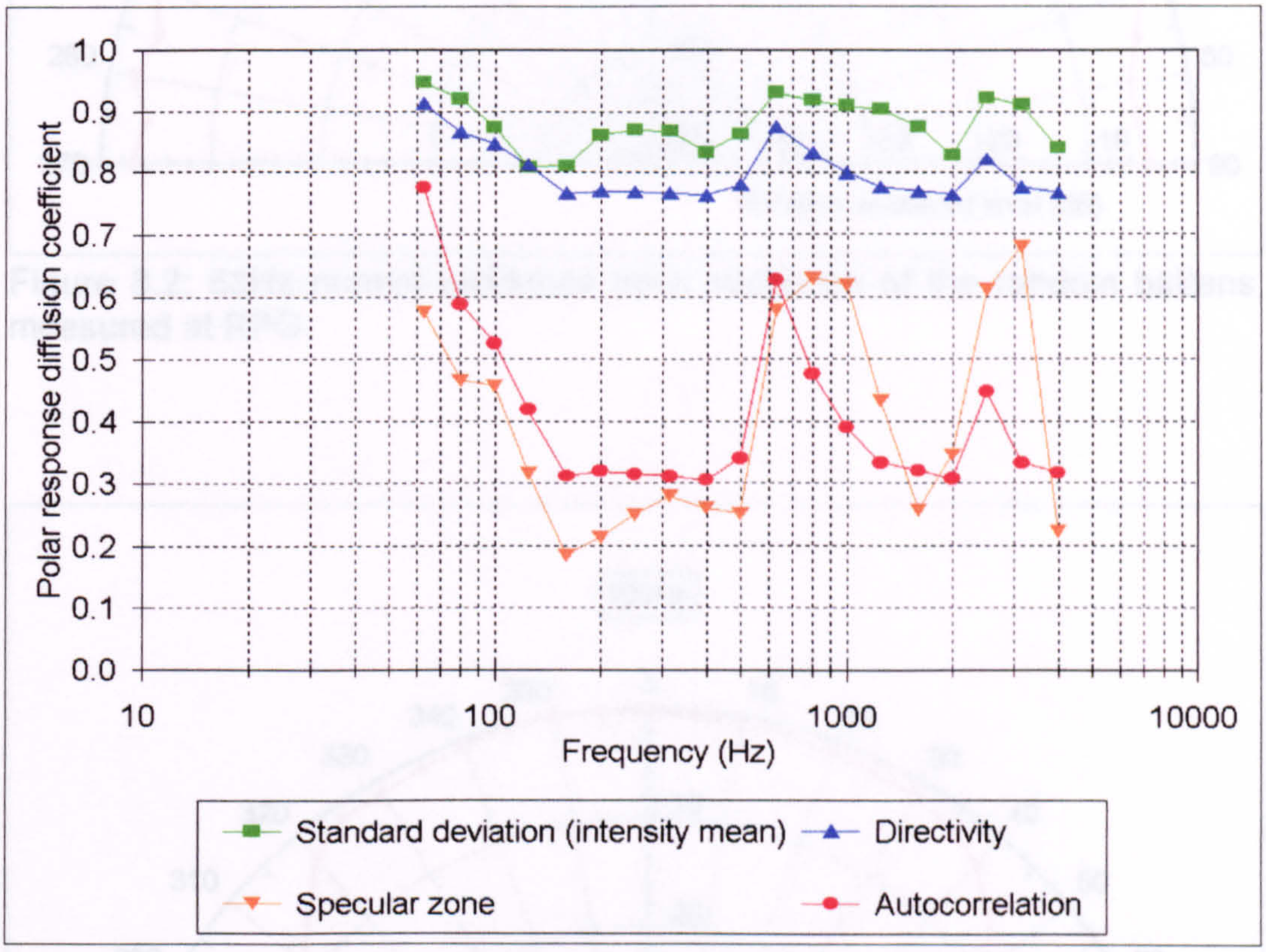

Figure 8.1: Comparison of polar response diffusion coefficients.

From Figure 8.1 it can be observed that the variation with frequency of the autocorrelation, standard deviation and directivity parameter values is similar - they increase and decrease in unison and their local maxima and minima occur at coincident frequencies. Reference to Figures 8.2 to 8.9 should confirm that this pattern of parameter values correctly ranks the diffusion efficacy of the sample at the various frequencies but the subjective evaluation of diffusion efficacy from visual inspection of polar responses is open to some variation.

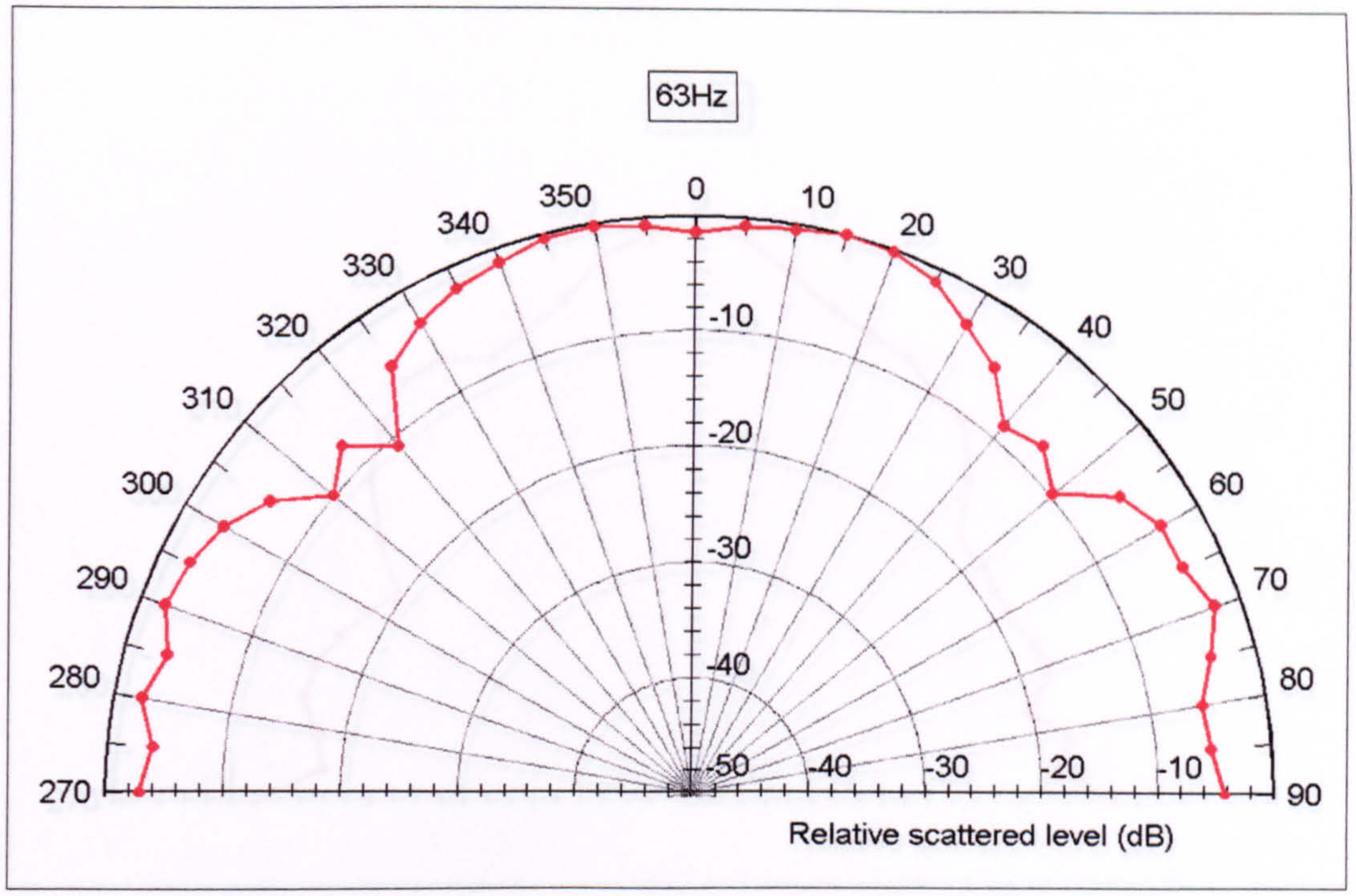

Figure 8.2: 63Hz normal incidence polar response of the random battens, measured at RPG.

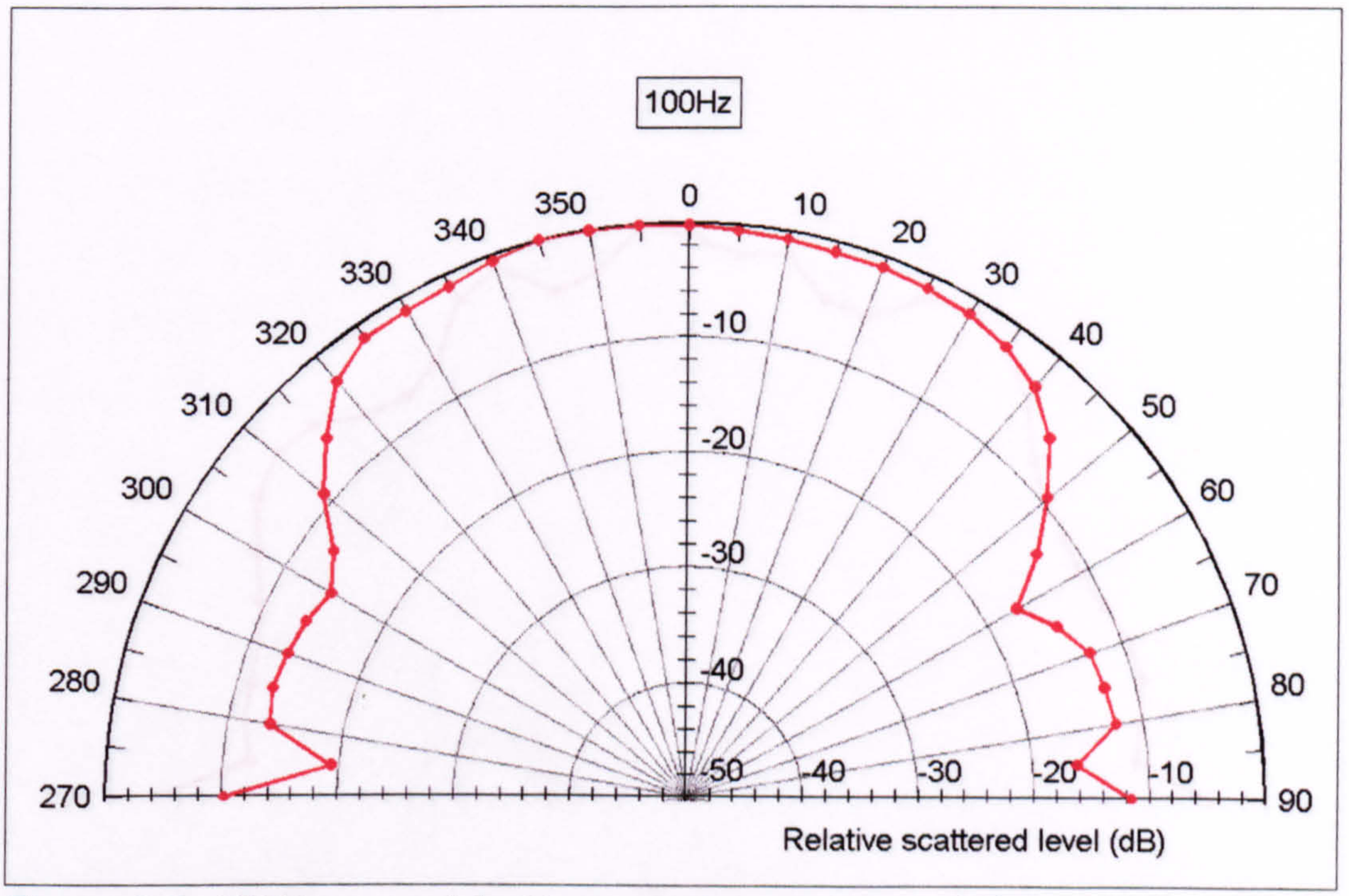

Figure 8.3: 100Hz normal incidence polar response of the random battens, measured at RPG.

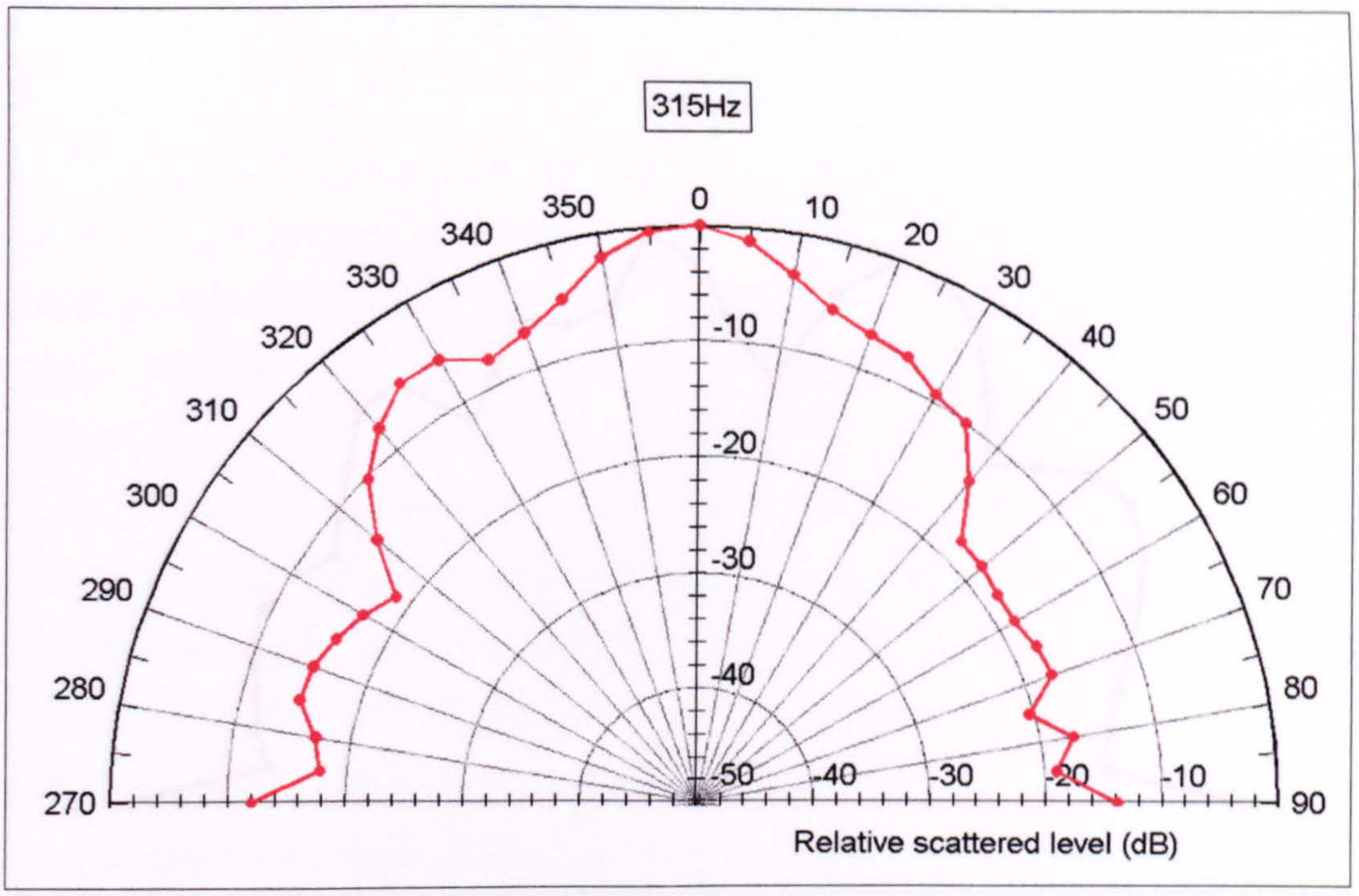

Figure 8.4: 315Hz normal incidence polar response of the random battens, measured at RPG.

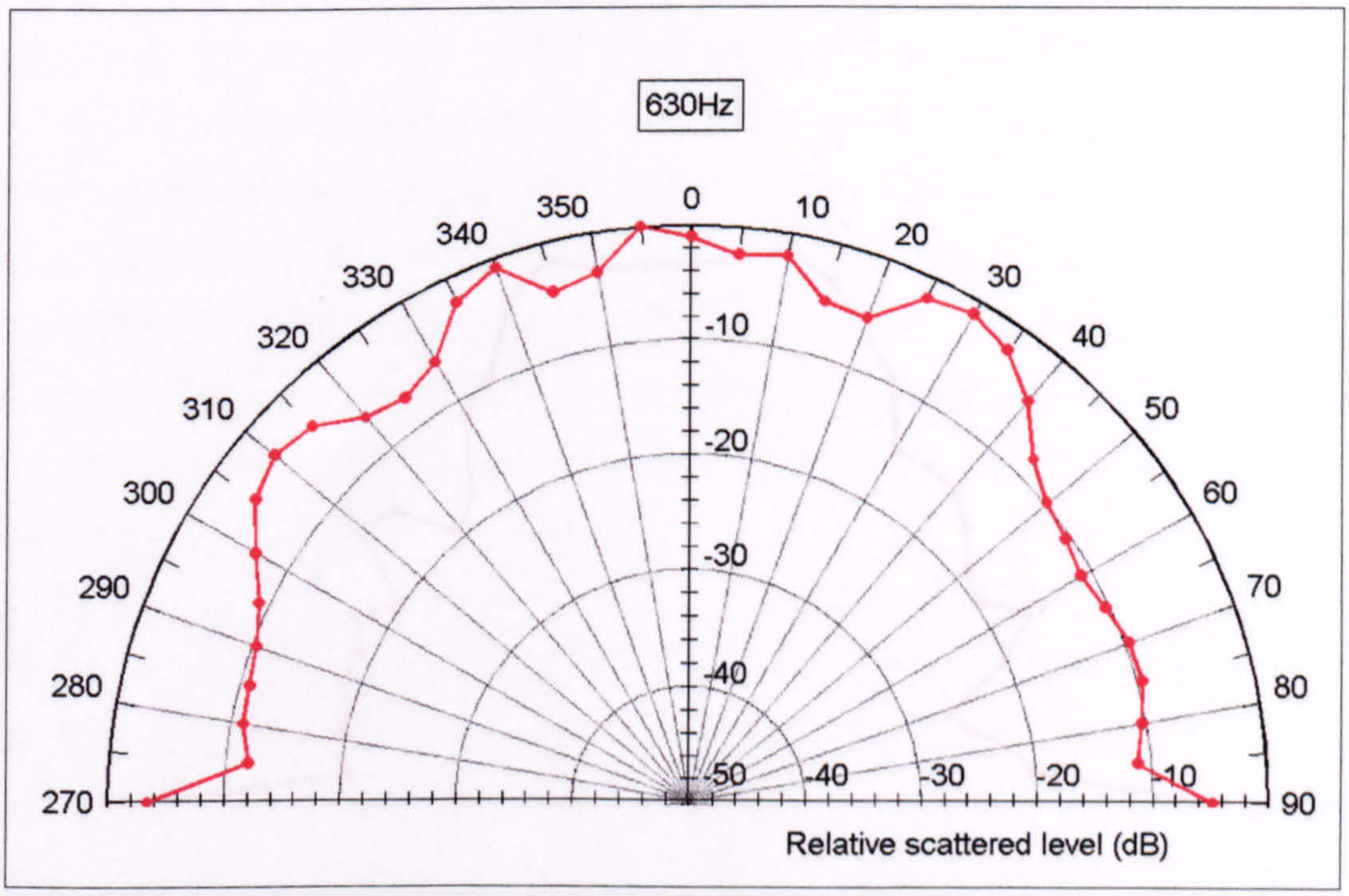

Figure 8.5: 630Hz normal incidence polar response of the random battens, measured at RPG.

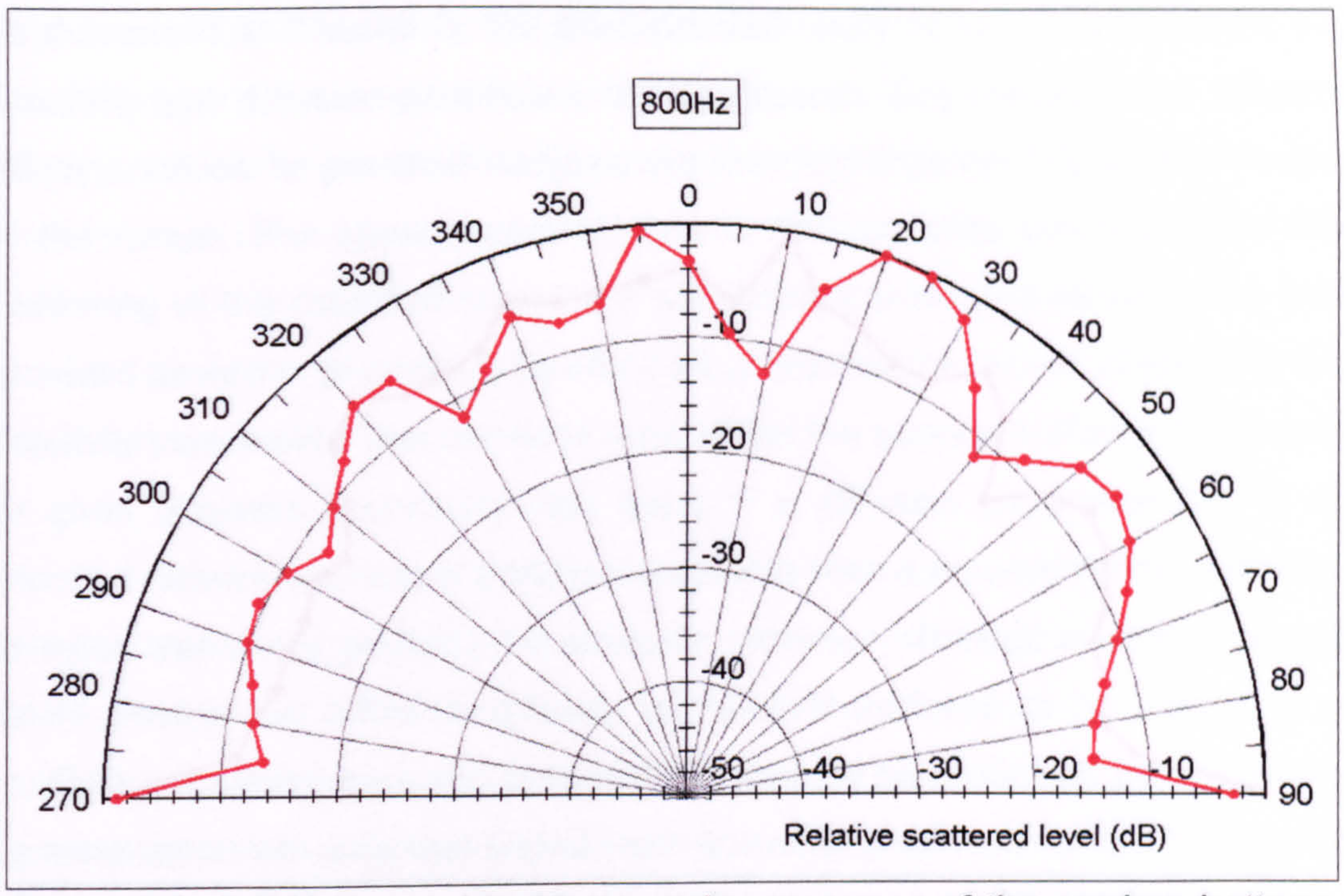

Figure 8.6: 800Hz normal incidence polar response of the random battens, measured at RPG.

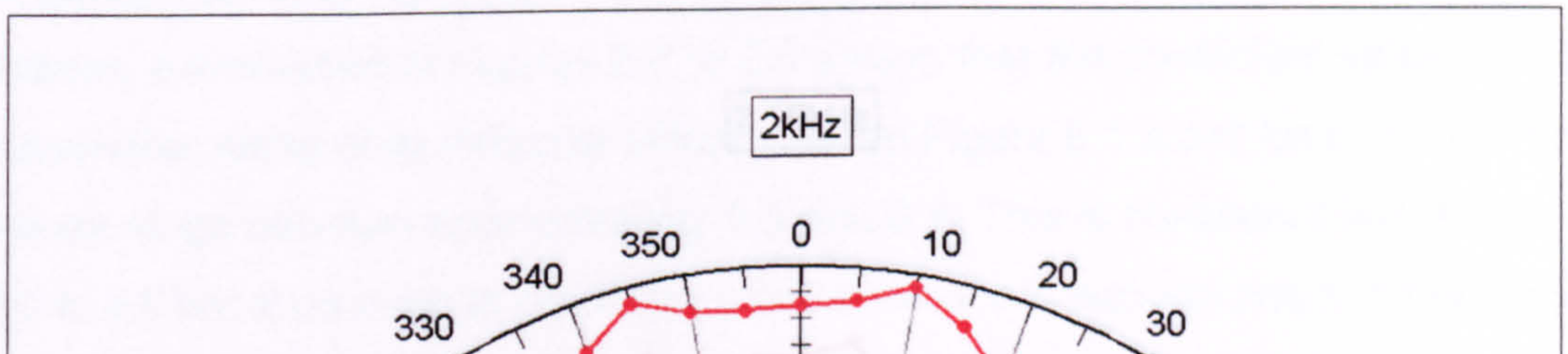

Figure 8.7: 2kHz normal incidence polar response of the random battens, measured at RPG.

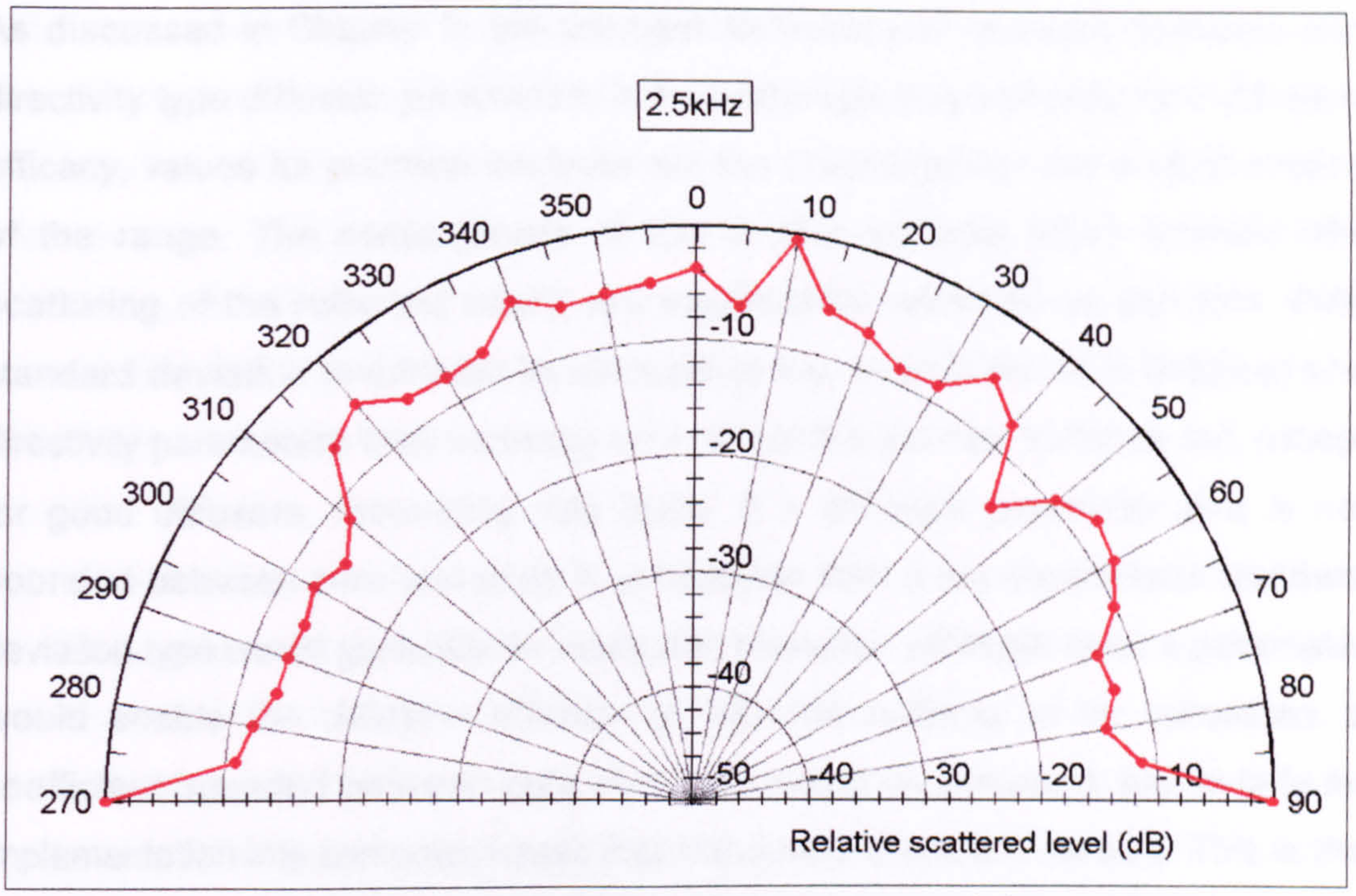

Figure 8.8: 2.5kHz normal incidence polar response of the random battens, measured at RPG.

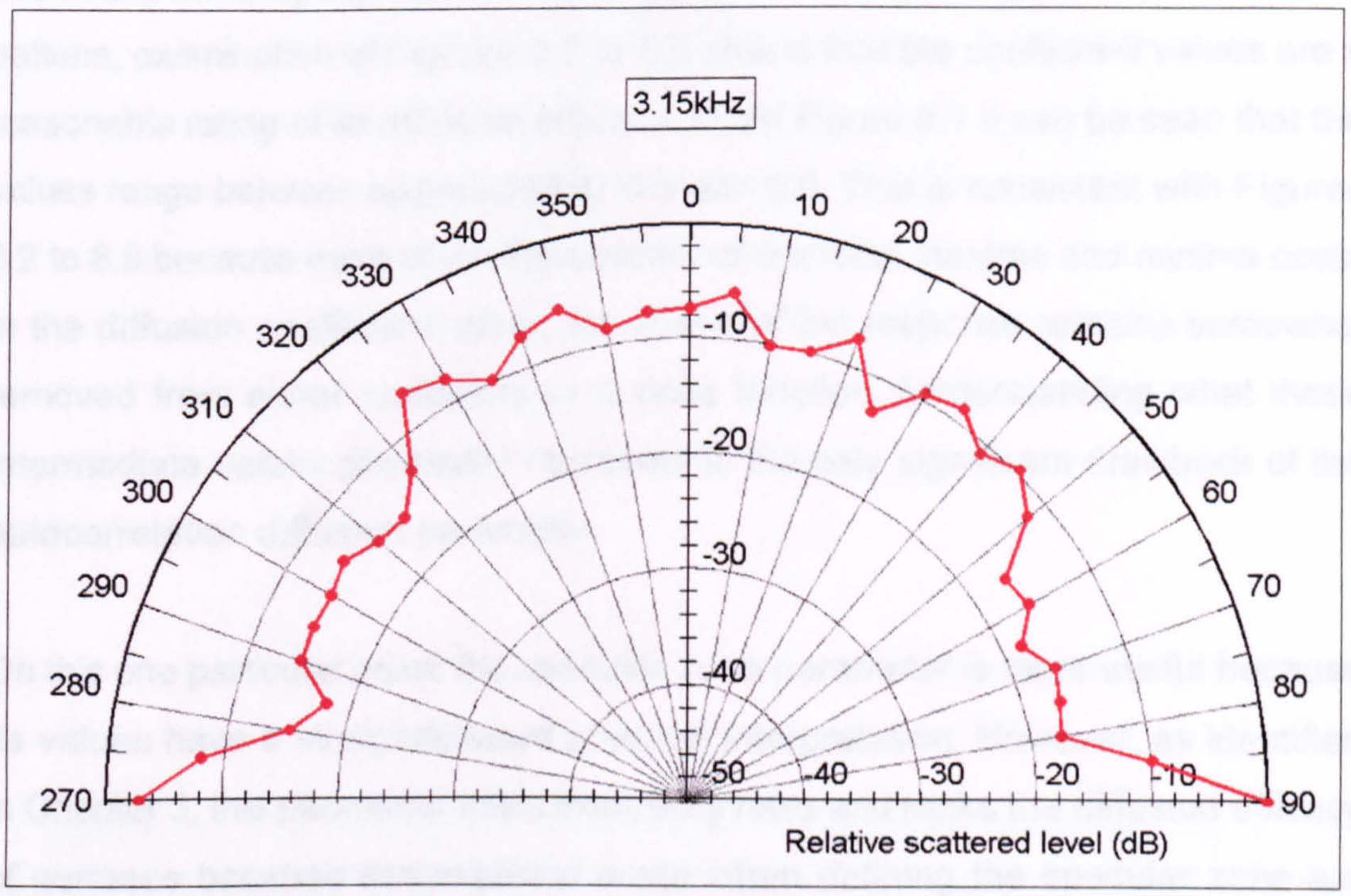

Figure 8.9: 3.15kHz normal incidence polar response of the random battens, measured at RPG.

As discussed in Chapter 3, the principal deficiency of standard deviation and directivity type diffusion parameters is that although they correctly rank diffusion efficacy, values for practical surfaces are bunched together into a small section of the range. The consequence of this is that surfaces which provide little scattering of the reflected sound are significantly overrated as diffusers. Both standard deviation (evaluated by calculating the mean level via intensities) and directivity parameters thus correctly rank all but the poorest surfaces but, except for good diffusers, incorrectly rate them. If a diffusion parameter that is not bounded between zero and unity is acceptable then a non-normalised standard deviation type would generally be adequate. However, although such a parameter would enable the diffusion efficacy of different surfaces to be compared, a coefficient bounded between zero and unity would be preferred, particularly for implementation into computer-based room acoustics prediction models. This is the primary reason why the autocorrelation diffusion parameter is superior.

In addition to demonstrating that the variation with frequency of the autocorrelation coefficient correctly represents the changes in the diffusion efficacy of the random battens, examination of Figures 8.2 to 8.9 shows that the coefficient values are a reasonable rating of its diffusion efficacy. From Figure 8.1 it can be seen that the values range between approximately 0.3 and 0.8. This is consistent with Figures 8.2 to 8.9 because even at the frequencies where local maxima and minima occur in the diffusion coefficient value, the shape of the response remains somewhat removed from either uniformity or a delta function. Understanding what these intermediate values physically represent is the only significant drawback of the autocorrelation diffusion parameter.

On this one particular point, the specular zone parameter is more useful because its values have a straightforward physical interpretation. However, as identified in Chapter 3, this parameter often incorrectly rates and ranks the diffusion efficacy of surfaces because assumptions made when defining the specular zone are frequently false. Specific examples of this can be identified in Figure 8.1, where the specular zone parameter ranks the diffusion efficacy of the random battens at some adjacent frequencies in the reverse order to the three other parameters. The

only type of samples which are likely to be consistently correctly rated by the specular zone parameter are those with a featureless topography. This includes flat samples which generate diffusion by virtue of having a non-uniform surface impedance, such as the BAD Panel, in addition to rigid planes. The parameter fails most dramatically in the case of profiled samples, such as a cone, which redirect the reflected energy away from the specular zone in specular-like reflections rather than dispersing it.

When these polar response diffusion parameters are applied to the three-dimensional as opposed to single-plane response of a surface, their value is usually reduced. The reason for this is that in the three-dimensional case, the parameters evaluate the uniformity of the response with azimuth as well as with elevation and few surfaces scatter the reflected energy with complete rotational symmetry. The random battens sample is an extreme example of this; its polar response is highly anisotropic, as shown in Figure 8.10.

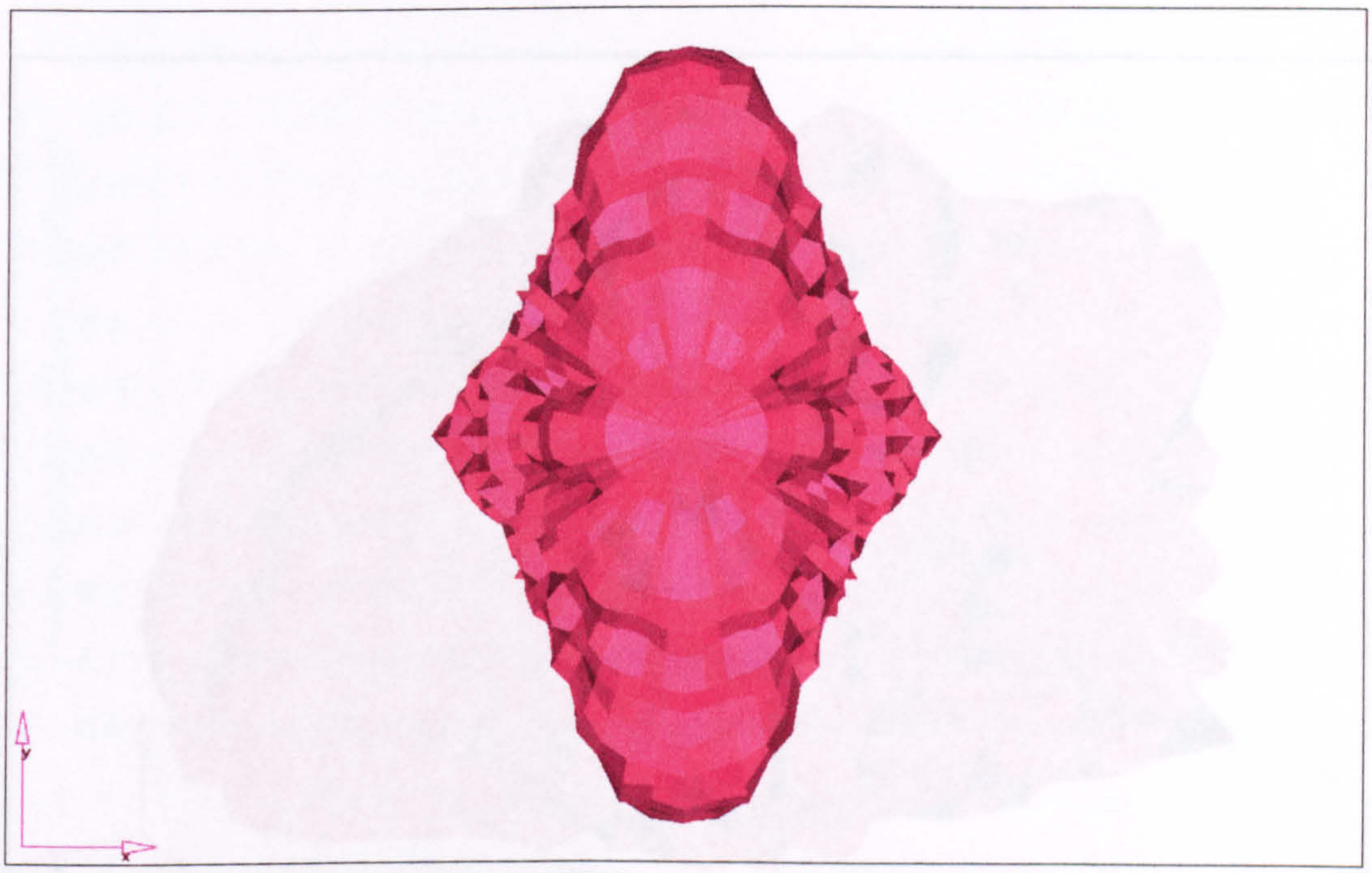

Figure 8.10: Top view of the 800Hz normal incidence polar response of the random battens, measured at Salford. The battens are parallel to the x-axis.

Figure 8.10 shows that there is much more scattering in the plane perpendicular to the battens than in the plane parallel to them. If the three-dimensional response

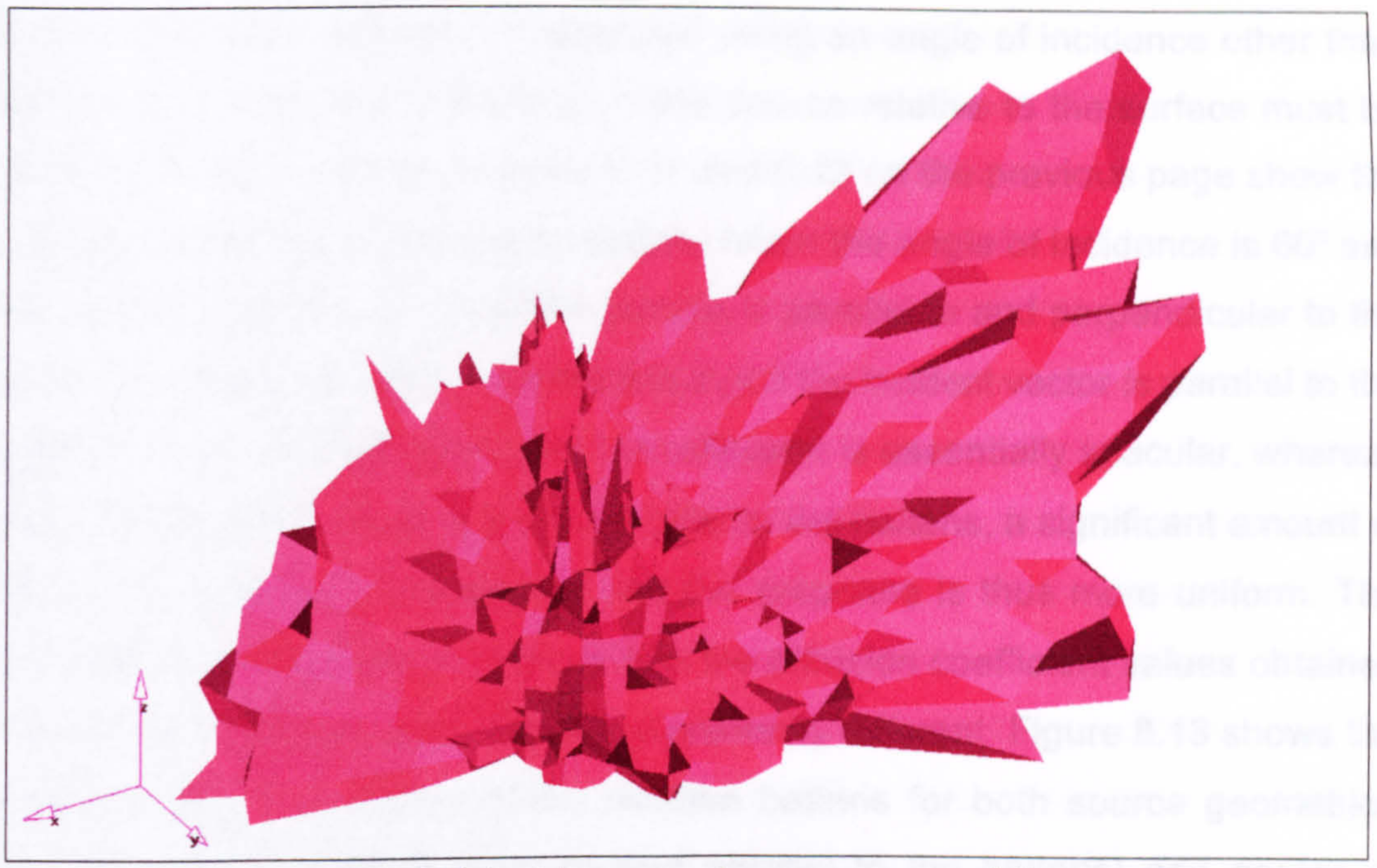

Figure 8.11: 1.25kHz 60° incidence polar response of the random battens (battens parallel to the x-axis), measured at Salford. Vector from sample to source is parallel to the x-axis and extends in the direction of positive x.

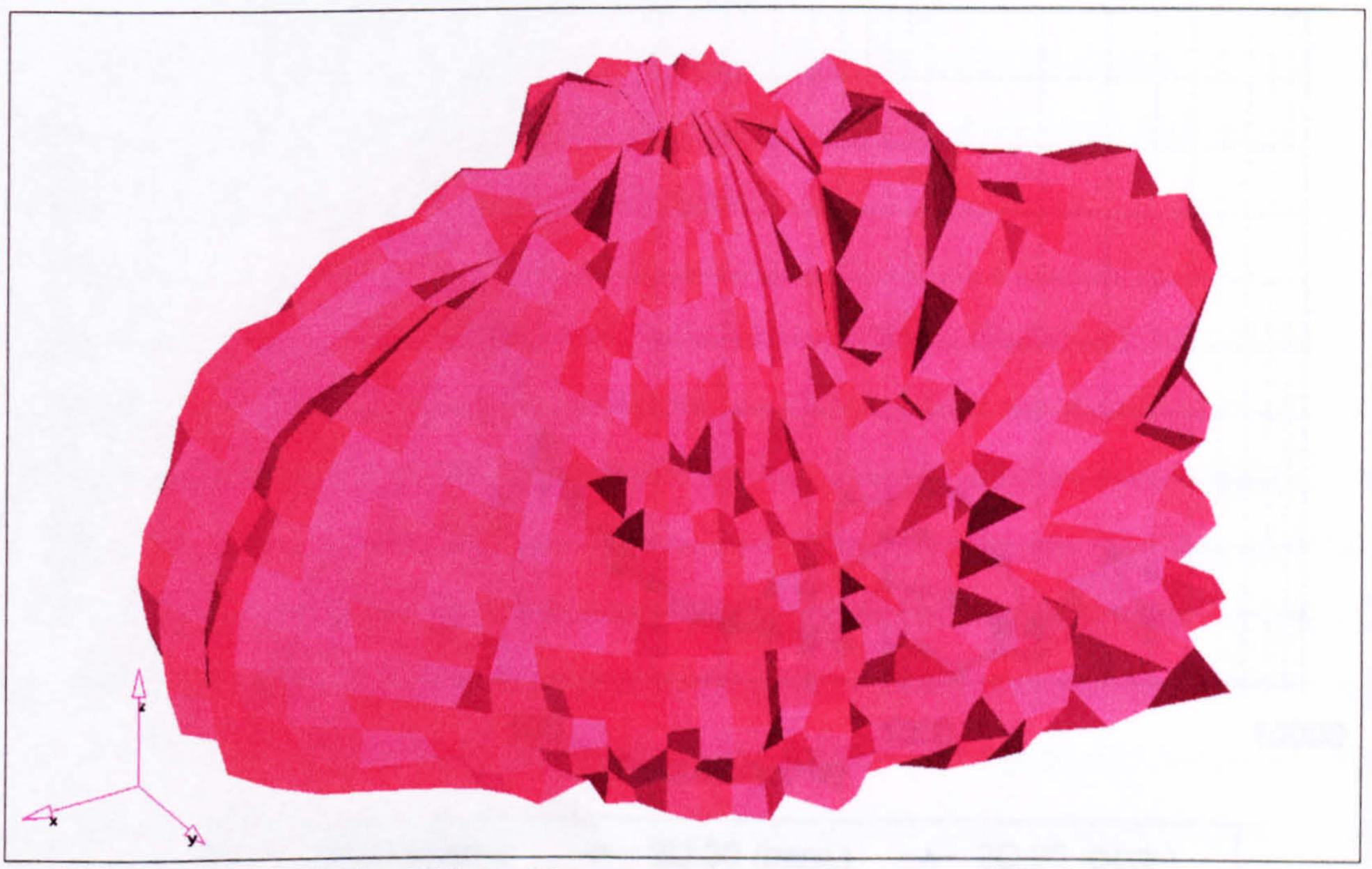

Figure 8.12: 1.25kHz 60° incidence polar response of the random battens (battens parallel to the y-axis), measured at Salford. Vector from sample to source is parallel to the x-axis and extends in the direction of positive x.

of an anisotropic scatterer is measured using an angle of incidence other than normal, the azimuthal orientation of the source relative to the surface must be considered. For example, Figures 8.11 and 8.12 on the previous page show the 1.25kHz responses of the random battens when the angle of incidence is 60° and the vector from the source to the sample is parallel to and perpendicular to the battens, respectively. This demonstrates that if the incident vector is parallel to the battens, they have little effect and the reflection is essentially specular, whereas when the incident vector is perpendicular to the battens, a significant amount of the reflected energy is scattered and the response is thus more uniform. The unsurprising consequence of this is that the diffusion coefficient values obtained using these two source geometries are markedly different. Figure 8.13 shows the autocorrelation coefficient of the random battens for both source geometries (incident vector perpendicular to and parallel to the battens) and angles of incidence of 30° and 60°. Also shown are normal incidence values, calculated from both three-dimensional and single-plane (perpendicular to the battens) responses.

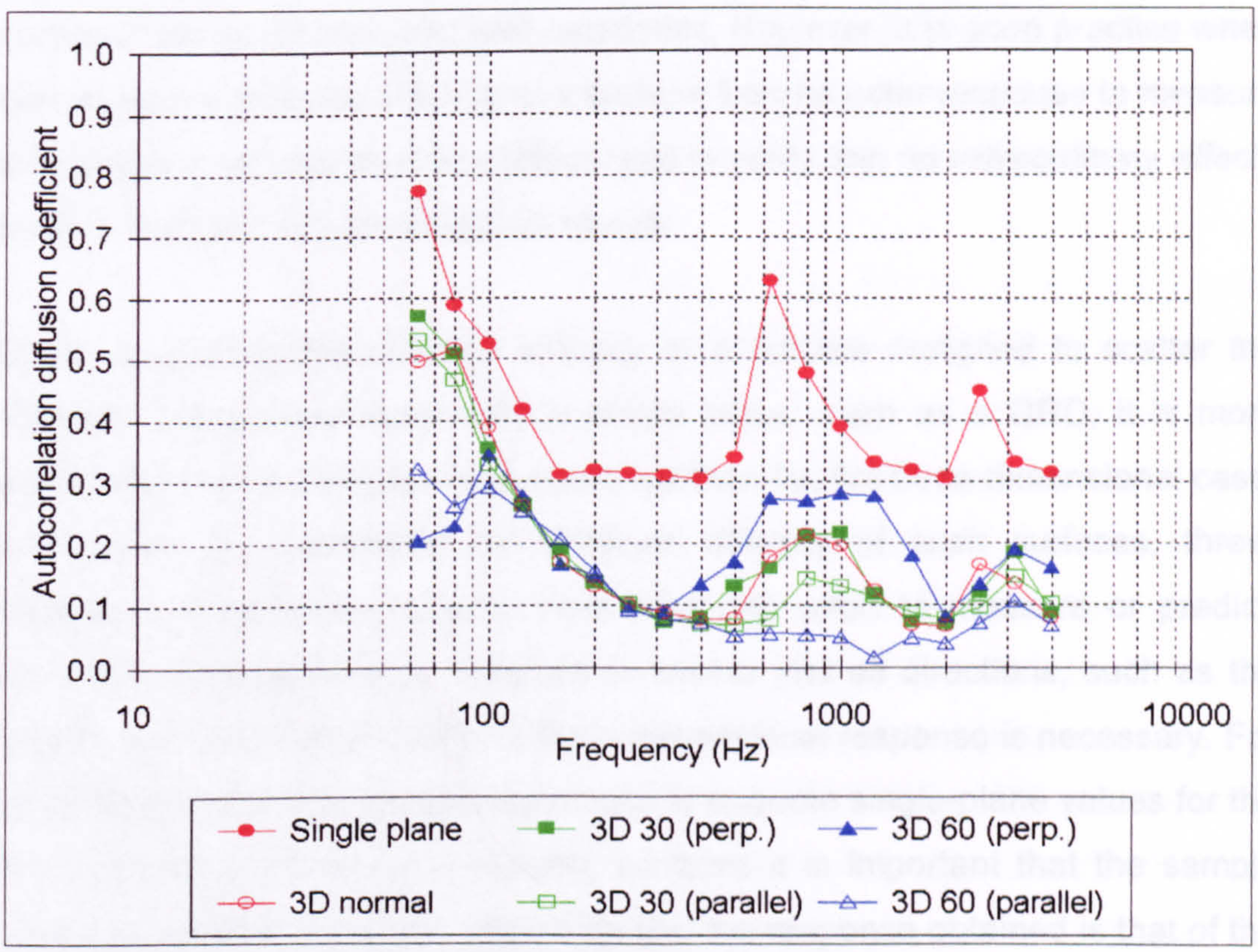

Figure 8.13: Autocorrelation diffusion coefficient of the random battens.

The salient point conveyed by Figure 8.13 is that if the diffusion efficacy of a surface is to be quantified from its polar response, then in order to obtain a meaningful value, the geometry of the measurement or prediction must be appropriate to both the surface and the application to which it is being put. For example, if the purpose of the surface is to scatter the energy contained in a particular specular reflection then the angle of incidence can be determined and used when obtaining the polar response. Such cases are simplified if the surface can be aligned for normal incidence because the diffusion parameter value is then independent of the azimuthal orientation of the sample. If the angle of incidence is either unknown or multifarious then it may appear necessary to evaluate a random incidence value. However, for most surfaces this is unlikely to differ markedly from the normal incidence value and is much more time consuming to determine using polar responses, especially for anisotropic scatterers where it is additionally necessary to consider the azimuthal position of the source. In practice, a random incidence value obtained from polar responses is not likely to be significantly more useful than the normal incidence value, any increase in 'accuracy' being, for the most part, academic. However, it is good practice when evaluating the diffusion efficacy of a surface from its polar response to measure for a couple of off-axis source positions, just to verify that no extraordinary effects occur in the case of non-normal incidence.

When evaluating the diffusion efficacy of a surface designed to scatter the reflected energy into essentially a single plane, such as a QRD, it is more appropriate to use a single-plane response than the full three-dimensional case. In addition to underrating the diffusion efficacy of such surfaces, three-dimensional responses require more time and effort to measure or predict. However, if the surface is designed to scatter into all directions, such as the Skyline, then evaluation from the three-dimensional response is necessary. For anisotropic scatterers, the best approach is to quote single-plane values for the two orthogonal planes. For periodic surfaces it is important that the sample comprises a sufficient number of periods that the response obtained is that of the surface rather than the individual repeat units. As stated in Section 3.14, it has been suggested that this number should be at least four.

At numerous points throughout this thesis, it has been stated that all polar response diffusion parameters are afflicted by the problem that the shape of the polar response of any surface is dependent on the distance from it of both the source and receivers, unless the source and all the receivers are situated in the far field. The reason that this is a problem is that the dimensions of many room surfaces are such that the distance from them at which the far field begins is so large that full-scale measurements are generally impractical. In practice, however, it has been found that the measurement distance can be reduced, so long as the measured polar response remains sufficiently similar in shape to that which would be obtained in the far field that the difference in the diffusion parameter values is not significant. This, in conjunction with the use of scale modelling techniques, enables the polar responses of many types of surfaces to be measured in standard test facilities. However, there are practical limits on the maximum scale factor which can be used and this means that quantifying the diffusion efficacy of surfaces from the shape of their polar responses is an approach best suited to small individual surfaces situated in free space, such as specialist diffusers and suspended reflectors in concert halls. For larger architectural surfaces, the reverberation chamber techniques proposed by Mommertz and Vorländer[22,59] or Lam[23] and discussed in Chapters 5 and 6 may be more appropriate.

Figure 8.14 on the following page shows values of the random incidence scattering coefficient, δ_r, for the random battens sample, obtained using both the free field and reverberation chamber Mommertz and Vorländer methods, and compares them with the autocorrelation diffusion coefficient evaluated from the three-dimensional, normal incidence, polar response. The most striking observation is that although there is some similarity between the manners in which the autocorrelation coefficient and the free field δ_r values vary with frequency, the variation of the reverberation chamber δ_r values, and at high frequencies the values themselves, are very different. The reason for this large difference between the reverberation chamber δ_r and autocorrelation coefficient values could be that although they are both intended to be measures of diffusion efficacy, they do not in fact quantify the same thing. The autocorrelation coefficient quantifies the uniformity of the scattering produced by surfaces from measurements or

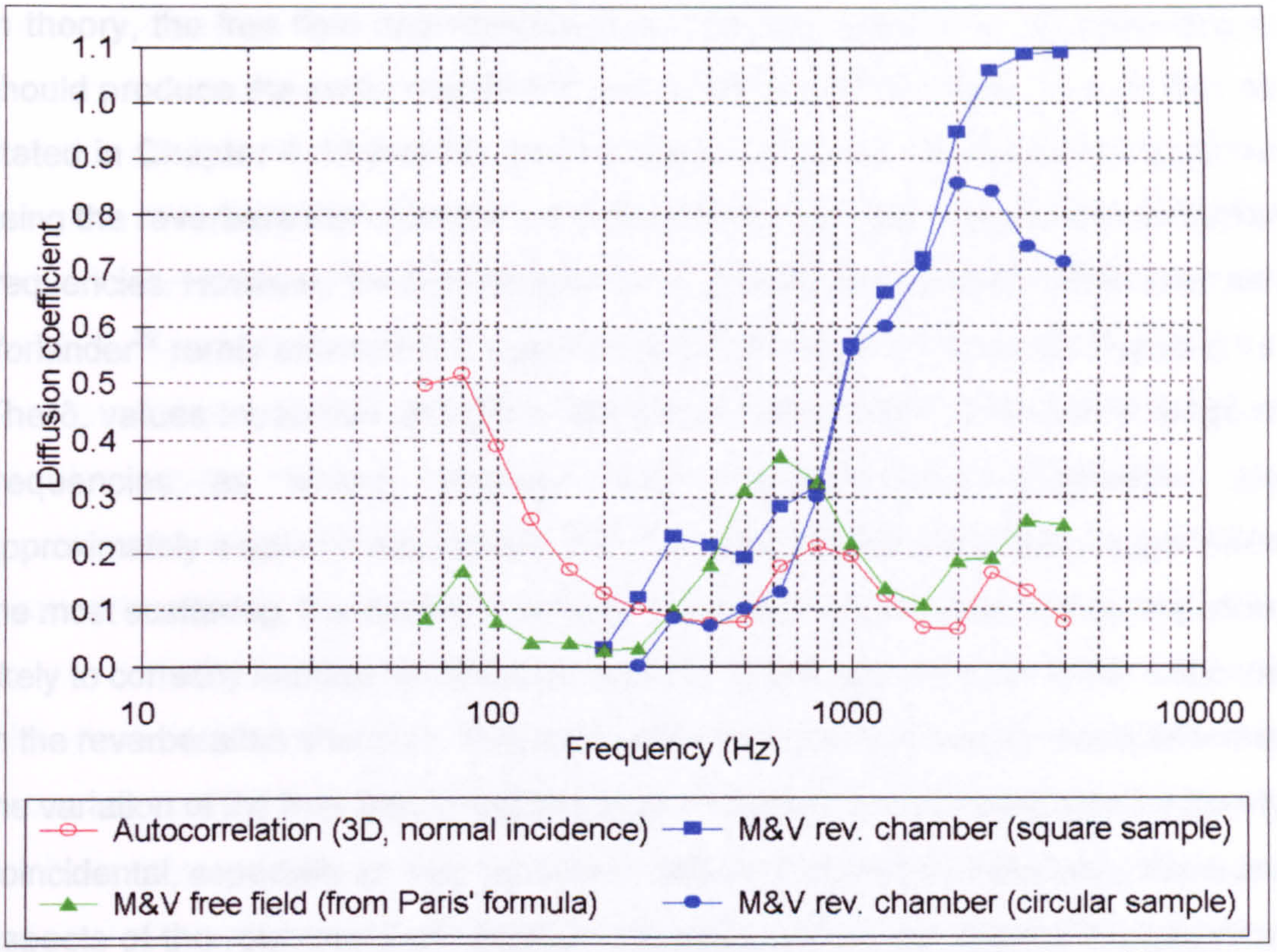

Figure 8.14: Comparison of different methods for rating the diffusion efficacy of the random battens.

predictions of their polar responses. It is a measure of quality designed to inform producers and users of surfaces that, either deliberately or accidentally, diffuse sound. In contrast, the scattering coefficient defined by Mommertz and Vorländer, δ_r, expresses the ratio of the non-specularly reflected energy to the total energy reflected by a surface, it does not measure the scattering uniformity, nor does it differentiate between dispersion of the reflected energy and redirection. Which of these two parameters most accurately describes the diffusion efficacy of a surface is therefore dependent on the user's definition of diffusion and the application to which the surface is to be put. For the treatment of individual reflections, for example, the autocorrelation coefficient is the more suitable measure because it is necessary to ensure that the reflection is not simply shifted to another listener position. A high autocorrelation coefficient indicates that the polar response of a surface does not contain any prominent lobes which could cause this problem. If, however, the purpose of the surface is to increase the diffuseness of the reverberant field in a room then the uniformity of the polar response is not of such great concern and in this case δ_r may quantify its diffusion efficacy satisfactorily.

In theory, the free field and reverberation chamber techniques of evaluating δ_r should produce the same results but that is clearly not the case here. In fact, as stated in Chapter 4, Mommertz and Vorländer have found that values obtained using the reverberation chamber method are often greater, particularly at higher frequencies. However, the difference in the δ_r values measured by Mommertz and Vorländer[22] rarely exceeds 0.3, significantly less than that shown in Figure 8.14. The δ_r values measured using the free field method peak in the same range of frequencies as where, because their cross-sectional dimensions are approximately a quarter wavelength, the (full scale) battens are likely to generate the most scattering. It is therefore tempting to assume that these values are more likely to correctly indicate the diffusion efficacy of the sample than those obtained in the reverberation chamber. This may not be true and the resemblance between the variation of the free field δ_r and the autocorrelation values could also be purely coincidental, especially as they represent different quantities. However, there are aspects of the reverberation chamber technique which still require investigation and which could cause the resulting δ_r values to be erroneous. One example is why values in excess of unity are sometimes obtained; according to the definition of the parameter this should not be possible. A likely contributing factor is that as a sample such as the random battens rotates, the profile of its edge changes and the resulting edge diffraction thus changes also. The measurement cannot distinguish between these changes in edge diffraction and changes in the scattering generated by the face of the sample. As a consequence, the value of δ_r is artificially inflated. This hypothesis is supported by the fact that, as shown in Figure 8.14, at many frequencies the circular sample has a significantly lower δ_r value than the square one. By virtue of its shape, edge diffraction from the circular sample will not be as dependent on its orientation as that from the square sample. However, edge effects are also present in the free field measurement of δ_r - although they may not have as great an influence on its value - and it is the opinion of some researchers[46,56] that edge diffraction alone is unlikely to account for the large differences between the values of δ_r obtained using the two methods.

The Mommertz and Vorländer reverberation chamber method is an appealing technique for quantifying the diffusion efficacy of surfaces because it gives a

random incidence value directly and this is tedious to obtain using either the free field method or the polar response approach. Although a random incidence diffusion coefficient is not ideal for some practical applications, it is what computer modellers desire. Another appealing property of the reverberation chamber method is that although there are practical limits on sample size[25], larger samples can be measured because there is not the need for the source and receiver positions to be in the far field. However, a significant drawback is that the values of polar response parameters can be predicted whereas reverberation chamber δ_r values cannot, using current techniques. Developing a suitable prediction method for this parameter would be a worthwhile area of future research.

The other reverberation chamber techniques examined during the course of this research also provide random incidence diffusion parameters. The empirical method proposed by Lam and discussed in Chapter 6 appears promising in theory but poor results were obtained when it was put into practice using the ODEON 2.6 computer model. With hindsight, the reason for this is likely to have been the choice of model and a worthwhile suggestion for future work would be to repeat the investigation using a model which is known to be accurate for small rooms containing surfaces with very different absorption characteristics. The most significant drawback of this technique is that Lam has discovered by investigation that different models often require different diffusion coefficient values for the same surface[3,68]. Furthermore, models can even require different values for the same surface in different rooms. This problem may be reduced by future improvements to the algorithms used to model (partially) diffuse reflections. At present, most computer models assign to each room surface a single figure random incidence diffusion coefficient which simply quantifies what proportion of the energy reflected from the surface is scattered. The directional distribution of this scattered energy is not considered, in fact many models assume Lambertian[27] scattering. In the future, as computing power increases, it is likely that directional scattering information will be implemented into models, possibly in the form of a look-up table containing polar responses. However, before developing models containing such look-up tables for different surface types, frequencies, angles of incidence etc, it must be established whether this massive increase in complexity

significantly improves the accuracy of the predicted sound field and, in the case of auralization, whether any difference can be subjectively perceived.

Of the reverberation chamber methods investigated in Chapter 7, which quantify the diffusion efficacy of surfaces by examining their effect on the diffuseness of a non-diffuse space, only measuring the effect on the mean reverberation time generated any useful results. At present, this technique is suitable only for non-absorbent surfaces but in the future more general application may be possible if a means is developed to separate the reductions in reverberation time caused by absorption and diffusion. Figure 8.15 shows, for the random battens sample, the results of this method, along with some of those obtained using the other techniques for quantifying diffusion efficacy.

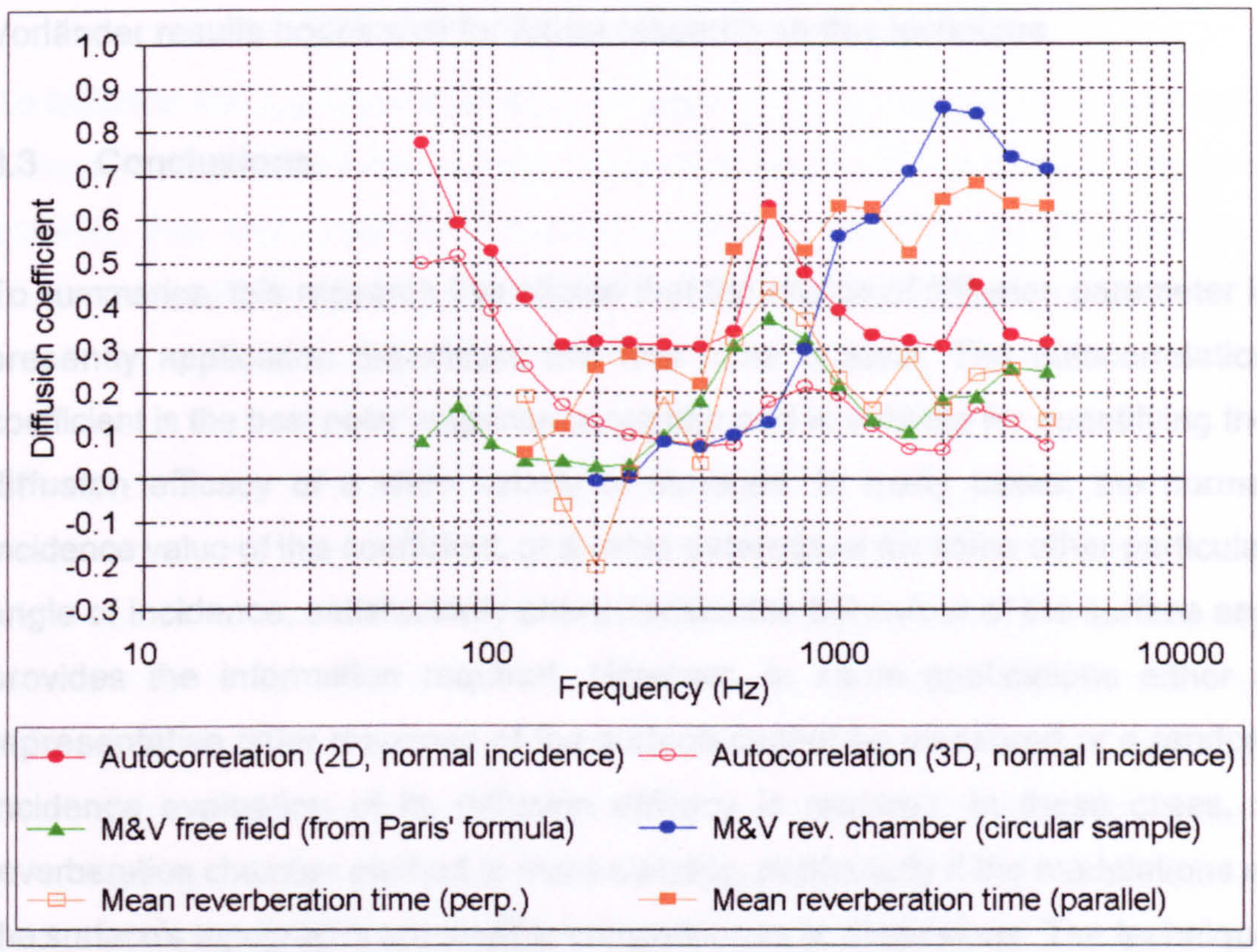

Figure 8.15: Further comparison of different methods for rating the diffusion efficacy of the random battens.

It is evident from Figure 8.15 that at many frequencies there is a significant difference between the diffusion coefficient values obtained using the 'mean reverberation time' method for the two different orientations of the sample: battens

perpendicular to the absorptive wall and battens parallel to the absorptive wall. In Chapter 7 it is discussed that the reason for this is likely to be that the sample scatters the reflected energy anisotropically; when the battens are parallel to the absorptive wall, more energy is scattered towards the absorbent, decreasing the reverberation time by a greater amount. This technique of quantifying the diffusion efficacy of surfaces requires a more thorough investigation, to determine, for example, whether or not it in fact ranks surfaces correctly and how many boundaries of the reverberation chamber should be covered with the sample. Consequently, there is presently little to be gained from quantitatively comparing the diffusion coefficient values obtained using this technique with those obtained using other methods that are shown in Figure 8.15. Nevertheless, the fact that for both orientations of the sample these preliminary results exhibit a peak at the same frequency as the single-plane autocorrelation and free field Mommertz and Vorländer results bodes well for future research on this technique.

8.3 **Conclusions**.

To summarise, this research has shown that the choice of diffusion parameter is presently application dependent and that none is ideal. The autocorrelation coefficient is the best polar response parameter and is suitable for quantifying the diffusion efficacy of a wide variety of surfaces. In many cases, the normal incidence value of this coefficient, or a value determined for some other particular angle of incidence, satisfactorily characterises the behaviour of the surface and provides the information required. However, in some applications either a representative polar response of the surface cannot be measured or a random incidence evaluation of its diffusion efficacy is required. In these cases, a reverberation chamber method is more suitable, particularly if the modulations of the surface's topography are small in comparison to its dimensions. The technique proposed by Mommertz and Vorländer is the most developed of the reverberation chamber methods but they all require further investigation.

9. CONCLUSIONS.

Diffuse reflections can play a key role in determining the sound field within a room and are therefore particularly important in acoustically critical spaces. Although their importance is now generally acknowledged, no standard or accepted parameter for quantifying the diffusion efficacy of surfaces currently exists. Without such a parameter, it is difficult to compare the performance of different architectural surfaces or develop design specifications for specialist diffusers. A diffusion parameter would also be of great benefit to developers of computer-based geometric room acoustic prediction models and, furthermore, should contribute to the future design and construction of rooms with better acoustics by improving the understanding of diffusion among practitioners in both the acoustics and building industries.

To facilitate the appraisal of existing diffusion parameters and the development of new ones, the ideal diffusion parameter has been defined in terms of a set of criteria. The most important criterion is usually assumed to be whether a parameter evaluates the diffusion efficacy of surfaces correctly. To ascertain this, a wide variety of different sample surfaces have been employed.

One approach to quantifying the diffusion efficacy of a surface is to examine the shape of its polar response. This method usually involves defining a parameter which quantifies the uniformity of the response; a number of such parameters have been previously published. To assist in the appraisal of these polar response diffusion parameters, polar responses of the sample surfaces were determined, either by measurement using maximum-length sequence techniques or prediction using boundary element methods. Two measurement facilities were employed, an existing one at RPG Diffusor Systems Inc. for measuring single-plane scattering and a new automated system for measuring three-dimensional responses built at the University of Salford. A combination of thought experiments and the polar responses of the diverse set of sample surfaces has enabled identification of both the situations in which each parameter can be most successfully applied and those in which they fail. It has been demonstrated that none is ideal.

Original polar response diffusion parameters developed during the course of this research have been presented. Measured and predicted responses of the sample surfaces have been used to demonstrate that one of these new parameters, based on the concept of autocorrelation, is superior to any of those previously published. This autocorrelation diffusion coefficient satisfies many criteria of the ideal coefficient. For example, it correctly ranks the diffusion efficacy of surfaces and is not confused by redirection, it is straightforward to evaluate from both measurements and predictions, it is bounded between zero and unity and values for practical surfaces are spread between these extremes. It is likely to be standardised by the Audio Engineering Society for "*characterisation of surface scattering uniformity*" and is currently being used by some diffuser designers. It does, however, have two significant deficiencies. One is that it is difficult to interpret the physical meaning of intermediate values, such as 0.5, but a greater understanding of this will develop as use of the coefficient becomes more widespread. The other difficulty, common to all polar response diffusion parameters, is the limitation of its application due to the shape of the polar response of a surface depending on the measurement distance, unless both the source and all the receivers are situated in the far field. It has been shown that, in practice, shorter measurement distances can often be used without seriously decreasing the accuracy of the resultant parameter value but in many cases these distances are still not representative of listener locations. Even if measurements are performed in model scale, the technique of characterising the diffusion efficacy of a surface from its polar response is therefore best suited to small surfaces situated in free space, such as specialist diffusers or suspended reflectors.

Another attractive measure of diffusion is the ratio of the energy scattered by a surface to the total energy it reflects; it is conceptually simple and the physical significance of all values is straightforward to interpret. However, evaluating this ratio from a polar response necessitates deciding whether the energy arriving at each receiver position has been scattered by the surface or specularly reflected. In practice this is not possible and although a 'specular zone' can be defined using geometrical considerations, for many surfaces the necessary assumptions are false and the resulting evaluation of diffusion efficacy consequently inaccurate.

The greatest inaccuracies occur with surfaces which redirect the reflected energy away from the specular zone in specular-like reflections instead of dispersing it.

Two alternative methods for evaluating this scattering coefficient - the ratio of the energy scattered by a surface to the total energy it reflects - have been proposed by Mommertz and Vorländer[22]. Neither technique requires the use of the specular zone concept or the determination of polar responses. Both methods derive the scattering coefficient from measurements of the invariance of the reflected energy to movement of the surface. One method is applied in the free field and the other requires reverberant conditions.

The free field method is tedious, especially if the random incidence scattering coefficient is required. Predictions were done but these are even more time consuming using existing methods. The reverberation chamber method is much quicker because it yields the random incidence scattering coefficient directly but this cannot be predicted using current techniques. However, it has the additional advantage of not suffering from the problem of having to measure in the far field of the sample surface and can therefore be used to evaluate the diffusion efficacy of larger samples.

Both methods have been practically investigated; the results obtained using the reverberation chamber approach are the first to be presented by an independent laboratory. Although the sample surfaces measured were ranked in the expected order, in some cases their diffusion efficacy appears to be overrated at high frequencies, possibly due to edge effects. The reverberation chamber method is most suited to quantifying the diffusion efficacy of large surfaces with topographical irregularities that are small in comparison to their dimensions but further investigation of certain practical aspects is required. Both methods fail for surfaces which simply redirect the reflected energy in a specular-like manner as opposed to dispersing it and overrate those which scatter anisotropically because the scattering coefficient is averaged over all directions. Furthermore, for samples possessing complete rotational symmetry, the measurement procedure would require modification. Despite these limitations, the Mommertz and Vorländer

reverberation chamber method is likely to be standardised by ISO for "*measuring the random incidence scattering coefficient of surfaces*".

Lam[23] has suggested a second reverberation chamber approach and this has also been practically investigated. Lam's method is empirical and involves comparing the change in the measured reverberation time of a real non-diffuse space caused by the introduction of a sample surface with that predicted by a computer model. The diffusion coefficient of the sample is obtained by an iterative trial and error process which involves adjusting its value in the model until the predicted reverberation time matches the measurement. The definition of this diffusion coefficient is dependent on exactly how the particular computer model used implements diffuse reflection.

Lam's method has been used to evaluate the diffusion efficacy of several sample surfaces, enabling it to be appraised from a practical perspective. However, the success of this work was limited by experimental difficulties. Although the method is straightforward in principle, in practice it is tedious and appropriate only for extensive surfaces, not individual diffusers. Furthermore, the resulting diffusion coefficient values are specific to the particular computer model used and may also be affected by the geometry of the non-diffuse space. This method is therefore currently unsuitable for general use but does have some potential if better computer models become available.

The possibility of quantifying the diffusion efficacy of surfaces from their effect on the diffuseness of a sound field has also been investigated. The change in several measures of sound field diffuseness when different sample surfaces were introduced into a non-diffuse space has been determined experimentally. It was found that only the mean reverberation time is of any potential use for quantifying diffusion efficacy and in order not to be limited to non-absorbent samples, it would be necessary to be able to separate the effects of absorption and diffusion on the reverberation time.

A common failing of most of the diffusion parameters examined during this

research is that they do not take into account how diffusion is perceived by listeners. The reason for this is primarily that there is little knowledge of the subjective aspects of diffusion. This is suggested as a priority for future work.

In summary, the primary conclusions of this research are that the choice of diffusion parameter is application dependent and none is ideal. Although at first it may appear possible to define a universal parameter, detailed examination has revealed this to be impossible. This should be a familiar situation to acousticians, who regularly deal with the absorption coefficient and the associated problems in measurement and application of this parameter. For many applications the normal incidence value of the autocorrelation polar response diffusion coefficient, developed during this research, is a satisfactory measure of the diffusion efficacy of a surface. However, this parameter is most usefully applied to individual diffusers used to treat particular reflections and if the surface to be quantified is large, or a random incidence scattering coefficient is required, the reverberation chamber method proposed by Mommertz and Vorländer is currently the best option but requires refinement.

APPENDICES

A. Details of how the plaster test samples were produced.

As stated in Section 2.3, some of the geometric shapes used as test samples, eg. cone and square-based pyramid, were fabricated by casting plaster in moulds rather than by shaping a block of solid material. There were two reasons for this: many samples could be produced from one mould (nearly thirty hemispheres were required) and it was in fact easier to make suitable moulds than to form the samples directly.

The material used was a strong mix of herculite plaster and the viscosity of this was such that care had to be taken when depositing it in the moulds not to trap any pockets of air. Once set and removed from the mould, any visible imperfections on a sample were removed using fine abrasive paper. A weak solution of PVA adhesive was then applied to seal the surface of the plaster and increase its reflectivity. When sealed, the samples were mounted on plywood bases and painted with gloss acrylic paint.

B. Derivation of (3.10) from (3.8).

D'Antonio[12] states that the parameter shown in (B1), σ_f, can be used to rate the diffusion efficacy of a surface for a particular frequency (third-octave band) and angle of incidence. This formulation of σ_f is (3.8) in Section 3.4.3.

$$\sigma_f = \sqrt{\frac{\sum_i^n \left[10\log\left(\frac{I_{\theta_i,f}}{\overline{I}_f}\right)\right]^2}{(n-1)}} \qquad \text{(B1)}$$

where:

$I_{\theta i,f}$ = Intensity for the observation angle θ_i and frequency f

$\overline{I}_f$ = Mean intensity averaged over the n observation positions

σ_f can alternatively be expressed in terms of natural logarithms as:

$$\sigma_f = \sqrt{\frac{\sum_i^n \left[\frac{10}{\ln(10)}\ln\left(\frac{I_{\theta_i,f}}{\overline{I}_f}\right)\right]^2}{(n-1)}} \qquad \text{(B2)}$$

The series expansion of $\ln(x)$ is[78]:

$$\ln(x) = (x-1) - \frac{(x-1)^2}{2} + \frac{(x-1)^3}{3} - \frac{(x-1)^4}{4} + \frac{(x-1)^5}{5} \ldots \qquad \text{(B3)}$$

Substituting the first term of this series expansion for the logarithm and moving the multiplying factor outside the square root produces an approximation for σ_f:

$$\sigma_f \approx \frac{10}{\ln(10)}\sqrt{\frac{\sum_i^n \left[\frac{I_{\theta_i,f}}{\overline{I}_f} - 1\right]^2}{(n-1)}} \qquad \text{(B4)}$$

A factor of $\overline{I}_f^2$ can now be removed from the denominator of the summation terms and then the square root to give:

$$\sigma_f \approx \frac{10}{\ln(10)\overline{I}_f}\sqrt{\frac{\sum_{i=1}^{n}\left[I_{\theta_i,f}-\overline{I}_f\right]^2}{(n-1)}} \qquad \text{(B5)}$$

This form of expression for σ_f is identical to (3.10), a parameter used by both D'Antonio and Cox[7].

The series expansion of $\ln(x)$ is valid only for $0<x<2$ because it is obtained from the expansion of $\ln(1+x)$ by replacing x with x-1 and the expansion of $\ln(1+x)$ is valid only for $|x|<1$.

(B5) is therefore only a valid approximation of σ_f if the following condition is satisfied:

$$\frac{I_{\theta_i,f}}{\overline{I}_f} < 2 \qquad \text{(B6)}$$

The practical significance of this condition is that for (B5) to be valid, the intensity at each receiver position must not exceed the mean intensity by more than 3dB. Application of (B5) is thus limited to polar responses which are approximately uniform, i.e. to good diffusers.

C. **Derivation of (3.46)**.

Figure C1 illustrates (in blue) the element of surface area on the measurement hemisphere represented by the receiver point at angle of elevation θ and angle of azimuth φ.

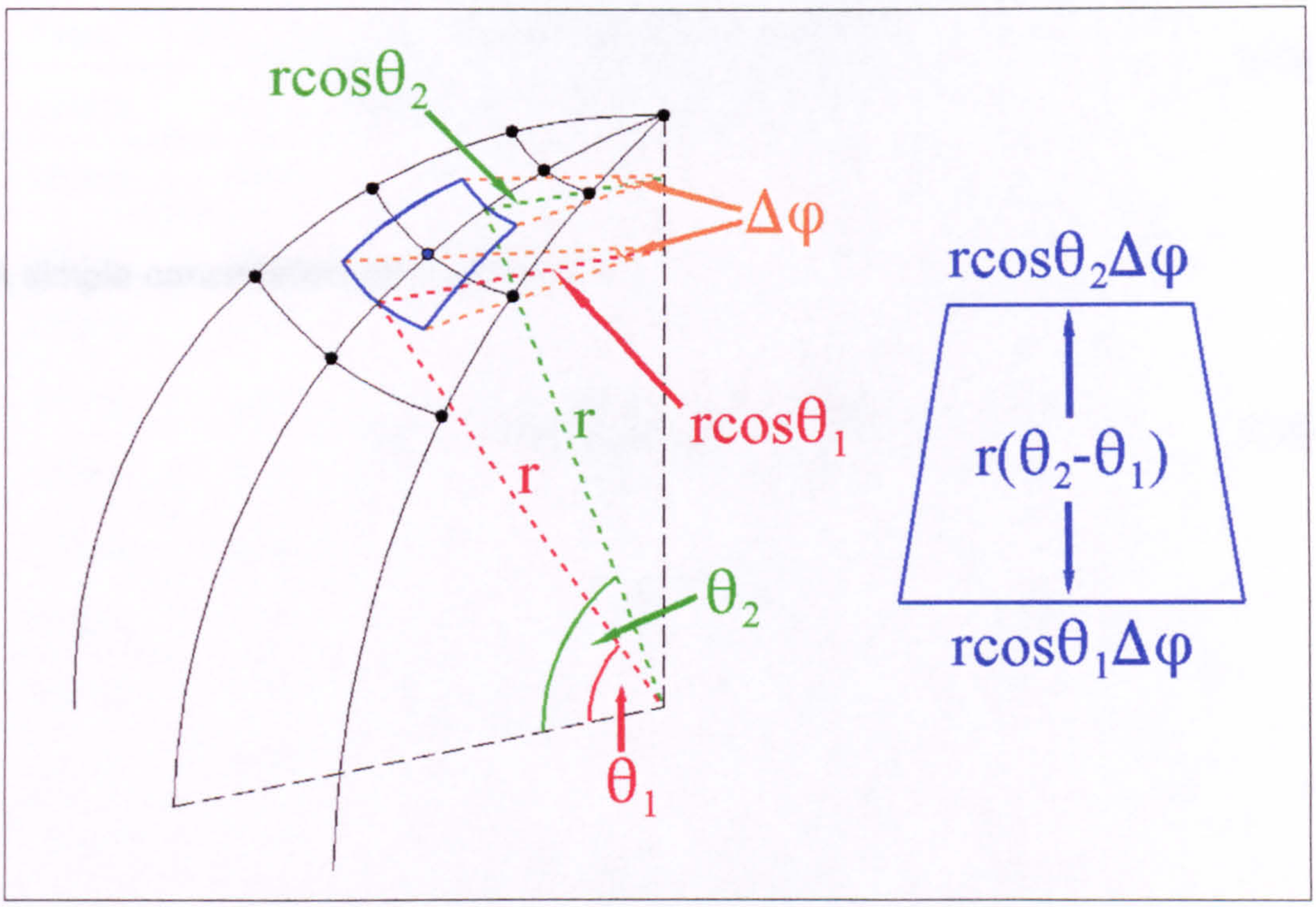

Figure C1: Element of surface area represented by receiver point (r, θ, φ).

These elements are approximately trapezoidal in shape, therefore their area, S_θ, can be approximated by:

$$S_\theta \approx \tfrac{1}{2} \times sum\ of\ parallel\ sides \times height \qquad \text{(C1)}$$

Substituting into (C1) using Figure C1 yields:

$$S_\theta \approx \frac{(r\cos\theta_1\Delta\varphi + r\cos\theta_2\Delta\varphi)\, r(\theta_2-\theta_1)}{2} \qquad \text{(C2)}$$

Since $\theta_2-\theta_1=\Delta\theta$, $\theta_1=\theta-\Delta\theta/2$ and $\theta_2=\theta+\Delta\theta/2$, where $\Delta\theta$ and $\Delta\varphi$ are the elevation and azimuthal angular resolutions respectively, (C2) can be rewritten as:

$$S_\theta \approx \frac{r^2 \Delta\theta \, \Delta\varphi \left(\cos\left(\theta - \frac{\Delta\theta}{2} \right) + \cos\left(\theta + \frac{\Delta\theta}{2} \right) \right)}{2} \qquad \text{(C3)}$$

Use of a trigonometric identity {REF} enables (C3) to be simplified:

$$S_\theta \approx \frac{r^2 \Delta\theta \, \Delta\varphi \left(2\cos\theta \cos\left(\frac{\Delta\theta}{2} \right) \right)}{2} \qquad \text{(C4)}$$

A simple cancellation then yields (3.46):

$$S_\theta \approx r^2 \Delta\theta \, \Delta\varphi \cos\theta \cos\left(\frac{\Delta\theta}{2} \right) \qquad \text{(C5)}$$

D. Measured data for Figure 7.1.

Table D1: Reverberation times used to calculate the values of d in Figure 7.1.

			Random battens (Perp.)	Random battens (Parallel)	Periodic battens (Perp.)	Periodic battens (Parallel)
Freq.	RT_{empty}(s)	RT_{min}(s)	RT_{sample}(s)	RT_{sample}(s)	RT_{sample}(s)	RT_{sample}(s)
125Hz	0.75	0.51	0.71	0.74	0.71	0.70
160Hz	0.81	0.41	0.84	0.77	0.79	0.79
200Hz	0.74	0.38	0.82	0.65	0.80	0.73
250Hz	0.96	0.36	0.95	0.79	1.00	0.95
315Hz	0.92	0.34	0.81	0.77	0.83	0.85
400Hz	0.81	0.34	0.79	0.71	0.74	0.78
500Hz	0.85	0.33	0.68	0.58	0.77	0.76
630Hz	1.01	0.32	0.71	0.59	0.86	0.81
800Hz	0.97	0.32	0.73	0.63	0.82	0.81
1kHz	0.93	0.31	0.78	0.54	0.91	0.75
1.25kHz	0.91	0.31	0.81	0.54	0.88	0.73
1.6kHz	0.84	0.27	0.68	0.54	0.71	0.60
2kHz	0.84	0.28	0.75	0.48	0.73	0.54
2.5kHz	0.79	0.28	0.66	0.44	0.68	0.48
3.15kHz	0.65	0.26	0.55	0.40	0.53	0.40
4kHz	0.55	0.22	0.51	0.34	0.49	0.33

REFERENCES

1. D'Antonio P, Cox T J, '*Diffusor Application in Rooms*', Applied Acoustics, (accepted for publication).

2. Vorländer M, '*International Round Robin on Room Acoustical Computer Simulations*', proc. 15th ICA, Trondheim, Norway, vol. II, pp689-692 (1995).

3. Lam Y W, '*The Dependence of Diffusion Parameters in a Room Acoustics Prediction Model on Auditorium Sizes and Shapes*', J. Acoust. Soc. Am., 100(4), pp2193-2203 (1996).

4. ISO 10534-1:1996 Acoustics - Determination of sound absorption coefficient and impedance in impedance tubes. Part 1: Method using standing wave ratio.

5. ISO 10534-2:1998 Acoustics - Determination of sound absorption coefficient and impedance in impedance tubes. Part 2: Transfer function method.

6. BS EN 20354:1993 (ISO 354 1985) Acoustics - Measurement of sound absorption in a reverberation room.

7. Cox T J, '*The Optimization of Profiled Diffusers*', J.Acoust.Soc.Am., 97(5), pp2928-2936 (1995).

8. Cox T J, '*Diffusion Parameters for Baffled Diffusers*', Presented at the 99th Audio Eng. Soc. Conv., Preprint #4115 (1995).

9. Cox T J, '*Designing Curved Diffusers for Performance Spaces*', J. Audio Eng. Soc., 44(5), pp354-364 (1996).

10. D'Antonio P, '*The DISC Project; Directional Scattering Coefficient Determination and Auralization of Virtual Environments*', proc. Noise-Con 93, Williamsburg VA, pp259-264 (1993).

11. D'Antonio P, Konnert J H, Kovitz P S, '*The DISC Project: Experimental Measurement of the Directional Scattering Properties of Architectural Acoustic Surfaces*', proc. W.C.Sabine Centennial Symposium, Cambridge MA, pp141-144 (1994)

12. D'Antonio P, '*Performance Evaluation of Optimized Diffusors*', J. Acoust. Soc. Am., 97(5), pp2937-2941 (1995).

13. D'Antonio P, '*Two Decades of Diffusor Design and Development*', Presented at the 99th Audio Eng. Soc. Conv., Preprint #4114 (1995).

14. Angus J A S, Marvin A C, Clegg J, Dawson J F, '*A Practical Metric for Evaluating Sound Diffusers*', Presented at the 98th Audio Eng. Soc. Conv., Preprint #3955 (1995).

15. Takahashi D, '*Development of Optimum Acoustic Diffusers*', J. Acoust. Soc. Jpn., 16(2), pp51-58 (1995).

16. Lam Y W, '*A Boundary Integral Formulation for the Prediction of Acoustic Scattering from Periodic Structures*', J. Acoust. Soc. Am., 105(2), pp762-769 (1999).

17. Cox T J, Lam Y W, '*Evaluation of Methods for Predicting the Scattering from Simple Rigid Panels*', Applied Acoustics, 40, pp123-140 (1993).

18. Cox T J, '*Predicting the Scattering from Reflectors and Diffusors using 2D Boundary Element Methods*', J. Acoust. Soc. Am., 96(2), pp874-878 (1994).

19. Cox T J, Lam Y W, '*Prediction and Evaluation of the Scattering from Quadratic Residue Diffusers*', J. Acoust. Soc. Am., 95(1), pp297-305 (1994).

20. Angus J A S, '*Diffuser Assessment Using Surface Spherical Harmonics*', J. Acoust. Soc. Am., 104(3), pp1857-1858 (1998).

21. '*Characterisation and Measurement of Surface Scattering Uniformity*', Audio Eng. Soc. information document for room acoustics and sound reinforcement systems, AES-4id-1999.

22. Vorländer M, Mommertz E, '*Definition and Measurement of Random-Incidence Scattering Coefficients*', Applied Acoustics, (accepted for publication).

23. Pantelides A C, '*The Effect of Absorbing and Diffusing Surfaces in a Rectangular Shaped Recording Studio*', M.Sc. thesis, University of Salford, UK (1995).

24. Rozsíval T, '*Description of Diffusing Surfaces Behaviour*', proc. 33rd Conference on Acoustics, Prague, Czech Republic, pp120-123 (1996).

25. ISO/TC 43/SC 2/WG '*Determination of Random Incidence Scattering Coefficients*'.

26. Lee E J, '*Effects of Surface Textures of Choral Reflectors*' proc. 16th ICA, Seattle WA, vol. III, pp2149-2150 (1998).

27. Kuttruff H, '*Room Acoustics*', Elsevier Applied Science, London UK, 3rd ed., p84 (1991).

28. Schroeder M R, '*Diffuse Sound Reflection by Maximum Length Sequences*', J. Acoust. Soc. Am., 57(1), pp144-150 (1975).

29. Schroeder M R, Gerlach R, '*Response to "Comments on Diffuse Sound Reflection by Maximum Length Sequences"*', J. Acoust. Soc. Am., 60(10), p954 (1976).

30. Schroeder M R, '*Binaural Dissimilarity and Optimum Ceilings for Concert Halls: More Lateral Sound Diffusion*', J. Acoust. Soc. Am., 65, pp958-963 (1979).

31. Schroeder M R, '*Toward Better Acoustics for Concert Halls*', Phys. Today, pp24-30 (1980 Oct.).

32. Schroeder M R, '*Acoustics in Human Communications: Room Acoustics, Music, and Speech*', J. Acoust. Soc. Am., 68(7), pp22-28 (1980).

33. Schroeder M R, '*Number Theory in Science and Communication*', Springer Series in Information Sciences, vol. 7, Springer, Berlin Germany (1984).

34. Schroeder M R, '*Fractals, Chaos, Power Laws: Minutes from an Infinite Paradise*', W. H. Freeman and Company, New York NY (1991).

35. D'Antonio P, Konnert J H, '*The Reflection Phase Grating Diffusor: Design Theory and Application*', J. Audio Eng. Soc., 32(4), pp228-238 (1984).

36. Davies W J, '*The Effects of Seating on the Acoustics of Auditoria*', Ph.D. thesis, University of Salford, UK (1992).

37. Beranek L L, '*Concert and Opera Halls: How They Sound*', Acoust. Soc. Am., Woodbury NY, chap.10 (1996).

38. D'Antonio P, Cox T J, '*Two Decades of Sound Diffusor Design and Development, Part 1: Applications and Design*', J. Audio Eng. Soc., 46(11), pp955-976 (1998).

39. Angus J A S, '*Amplitude Gratings as Acoustic Diffusors*', Proc. Inst. Acoust., 16(4), pp291-297 (1994).

40. Angus J A S, '*Sound Diffusors Using Reactive Absorption Gratings*', Presented at the 98th Audio Eng. Soc. Conv., Preprint #3953 (1995).

41. Rife D D, Vanderkooy J, '*Transfer-Function Measurement with Maximum-Length Sequences*', J. Audio Eng. Soc., 37(6), pp419-444 (1989).

42. Schenck H A, '*Improved Integral Formulation for Acoustic Radiation Problems*', J. Acoust. Soc. Am., 44, pp41-58 (1968).

43. Beranek L L, '*Acoustics*', Acoust. Soc. Am., Woodbury NY, 3rd ed., p100 (1990).

44. Kinsler L E, Frey A R, Coppens A B, Sanders J V, '*Fundamentals of Acoustics*', John Wiley & Sons, New York NY, 3rd ed., chap.8 (1982).

45. Bies D A, Hansen C H, '*Engineering Noise Control: Theory and Practice*', Unwin Hyman, London UK, p133 (1988).

46. Cox T J, Personal communication.

47. Hargreaves T J, Cox T J, Lam Y W, D'Antonio P, '*Diffusion Parameters for Auditorium Surfaces*', Proc. Inst. Acoust., 19(3), pp19-27 (1997).

48. BS EN 60268-5:1997 Sound System Equipment - Loudspeakers.

49. BS 6840-3:1992 (IEC 60268-3:1988) Sound System Equipment - Methods for Specifying and Measuring the Characteristics of Sound System Amplifiers.

50. Vanderkooy J, '*Aspects of MLS Measuring Systems*', J. Audio Eng. Soc., 42(4), pp219-231 (1994).

51. Kuttruff H, '*Room Acoustics*', Elsevier Applied Science, London UK, 3rd ed., chap.IV (1991).

52. Pierce A D, '*Acoustics: An Introduction to its Physical Principles and Applications*', McGraw-Hill, New York NY, pp293-294 (1981).

53. Angus J A S, '*Using Modulated Phase Reflection Gratings to Achieve Specific Diffusion Characteristics*', Presented at the 99th Audio Eng. Soc. Conv., Preprint #4117 (1995).

54. Feldman E, '*A Reflection Grating that Nullifies the Specular Reflection: A Cone of Silence*', J. Acoust. Soc. Am., 98(1), pp623-634 (1995).

55. Cox T J, '*Acoustic Phase Gratings for Reduced Specular Reflection*', Applied Acoustics, (accepted for publication).

56. Lam Y W, Personal communication.

57. Farina A, Personal communication.

58. Mulholland H, Jones C R, '*Fundamentals of Statistics*', Butterworths, London UK, pp104-105 (1968).

59. Mommertz E, Vorländer M, '*Measurement of Scattering Coefficients of Surfaces in the Reverberation Chamber and in the Free Field*', proc. 15th ICA, Trondheim, Norway, vol. II, pp577-580 (1995).

60. Mommertz E, '*Determination of Scattering Coefficients from the Reflection Directivity of Architectural Surfaces*', Applied Acoustics, (accepted for publication).

61. Kuttruff H, '*Room Acoustics*', Elsevier Applied Science, London UK, 3rd ed., p49 (1991).

62. Makita Y, Hidaka T, '*Revision of the Cos θ Law of Oblique Incident Sound Energy and Modification of the Fundamental Formulations in Geometrical Acoustics in Accordance with the Revised Law*', Acustica, 63(3), pp163-173 (1987).

63. Kinsler L E, Frey A R, Coppens A B, Sanders J V, '*Fundamentals of Acoustics*', John Wiley & Sons, New York NY, 3rd ed., chap.13 (1982).

64. Rife D D, '*MLSSA Reference Manual*', DRA Laboratories, Version 7.0, pp105-108 (1991).

65. Mommertz E, '*Measurement of Scattering Coefficients in the Reverberation Room - Some Precision Considerations*', ISO/TC 43/SC 2/WG 25 N 17, p3 (2000).

66. Rindel J-H et al., '*Acoustics - Measurement of the Random-Incidence Scattering Coefficient of Surfaces*', ISO/TC 43/SC 2/WG 25 N 18, p4 (2000).

67. Mommertz E, Personal communication.

68. Lam Y W, '*A Comparison of Three Diffuse Reflection Modeling Methods used in Room Acoustics Computer Models*', J. Acoust. Soc. Am., 100(4), pp2181-2192 (1996).

69. Bies D A, Hansen C H, '*Engineering Noise Control: Theory and Practice*', Unwin Hyman, London UK, p173 (1988).

70. Naylor G, Rindel J-H, '*ODEON Room Acoustics Program*', The Acoustics Laboratory, Technical University of Denmark, Lyngby Denmark (1994).

71. Kuttruff H, '*Room Acoustics*', Elsevier Applied Science, London UK, 3rd ed., p83 (1991).

72. Kuttruff H, '*Room Acoustics*', Elsevier Applied Science, London UK, 3rd ed., chap.V (1991).

73. Thiele R, '*Richtungsverteilung und Zeitfolge der Schallrückwurfe in Raumen*', Acustica, 3, pp291-303 (1953).

74. Meyer E, Thiele R, '*Raumakustische Untersuchungen in Zahlreichen Konzertsälen und Rundfunkstudios unter Anwendung Neuerer Messverfahren*', Acustica, 6, p425 (1956).

75. Hodgson M, '*On Measures to Increase Sound-Field Diffuseness and the Applicability of Diffuse-Field Theory*', J. Acoust. Soc. Am., 95(6), pp3651-3653 (1994).

76. D'Antonio P, Personal communication.

77. Bies D A, Hansen C H, '*Engineering Noise Control: Theory and Practice*', Unwin Hyman, London UK, pp43-46 (1988).

78. Stroud K A, '*Engineering Mathematics: Programmes and Problems*', Macmillan, Basingstoke UK, 3rd ed., p432 (1991).